

# Gas Phase Chemical Physics Program

DOE Principal Investigators'  
Abstracts

April, 2016

Chemical Sciences, Geosciences, and Biosciences Division  
Office of Basic Energy Sciences  
Office of Science  
U.S. Department of Energy

The research grants and contracts described in this document are supported by the U.S. DOE Office of Science, Office of Basic Energy Sciences, Chemical Sciences, Geosciences and Biosciences Division.

## Foreword

This collection of active research abstracts illustrates the breadth and depth of basic research supported by the Department of Energy's Office of Basic Energy Sciences (BES) and, in large measure, by the Gas Phase Chemical Physics program that contributes to the development of a predictive capability for combustion processes and addresses grand challenges in gas phase chemical physics. The long-term objective of this effort is the provision of theories, data, and procedures to enable the development of reliable computational models of combustion processes, systems, and devices.

We appreciate the privilege of serving in the management of this research program. In carrying out these tasks, we learn from the achievements and share the excitement of the research of the many sponsored scientists and students whose work is summarized in the abstracts published on the following pages.

We thank all of the researchers whose dedication and innovation have advanced DOE BES research. We look forward to our assembly in 2017 for our 37<sup>th</sup> annual meeting.

Jeffrey Krause  
Wade Sisk



# *Table of Contents*



# Table of Contents

Foreword.....	iii
Table of Contents.....	v
Abstracts .....	1
<b><u>Keynote Speaker Abstract</u></b>	
Dwayne Heard, School of Chemistry, University of Leeds - Hydroxyl and Peroxy Radicals: Quantitative Atmospheric Field Measurements and Unusual Temperature Dependent Kinetics.....	1
<b><u>Principal Investigators' Abstracts</u></b>	
Musahid Ahmed, Kevin Wilson, and Oleg Kostko – The Chemical Dynamics Beamline.....	3
Robert S. Barlow - Turbulence-Chemistry Interactions in Reacting Flows.....	7
Josette Bellan - Predictive Large-Eddy Simulation of Supercritical-Pressure Reactive Flows In the Cold Ignition Regime.....	11
Guillaume Blanquart - Towards predictive simulations of soot formation: from surrogate to turbulence.....	15
Laurie J. Butler - Dynamics of Product Branching from Radical Intermediates in Elementary Combustion Reactions:.....	19
David W. Chandler – Imaging Chemical Dynamics and Spectroscopy.....	23
Jacqueline H. Chen - Petascale Direct Numerical Simulation and Modeling of Turbulent Combustion.....	27
Robert E. Continetti - Dynamics and Energetics of Elementary Combustion Reactions and Transient Species.....	31
F.F. Crim - Vibrational Dynamics and Dissociation of Ground- and Excited-State Cluster.....	35
P. Dagdigian and Millard H. Alexander - Theoretical investigation of Kinetic Processes in Small Radicals” .....	39
Rainer Dahms - Theory and Modeling of Multiphase Reacting Flow Dynamics in Simulations and Experiments.....	43
H. Floyd Davis - Bimolecular Dynamics of Combustion Reactions.....	45
Michael J. Davis - Exploration and validation of chemical-kinetic mechanisms.....	49
Gary Douberly - Vibrational Spectroscopy of Transient Combustion Intermediates Trapped in Helium Nanodroplets.....	53
Robert W. Field - Spectroscopic and Dynamical Studies of Highly Energized Small Polyatomic Molecules.....	57
Jonathan H. Frank - Quantitative Imaging Diagnostics for Reacting Flows.....	61
William H. Green - Computer-Aided Construction of Chemical Kinetic Models.....	65

Gregory E. Hall - Gas-Phase Molecular Dynamics: High Resolution Spectroscopy and Collision Dynamics of Transient Species.....	69
Nils Hansen - Flame Chemistry and Diagnostics.....	73
Lawrence B. Harding - Theoretical Studies of Potential Energy Surfaces.....	77
Martin Head-Gordon, William H. Miller, and Eric Neuscamman – Theory of Electronic Structure and Chemical Dynamics.....	81
John F. Hershberger - Laser Studies of Combustion Chemistry.....	85
Ahren W. Jasper – Theoretical - Methods for Pressure Dependent Kinetics and Electronically Nonadiabatic Chemistry.....	89
Ralf I. Kaiser - Probing the Reaction Dynamics of Hydrogen-Deficient Hydrocarbon Molecules and Radical Intermediates via Crossed Molecular Beams.....	93
Christopher J. Kliewer - Time-Resolved nonlinear Optical Diagnostics.....	97
Stephen J. Klippenstein - Theoretical Chemical Kinetics.....	101
Stephen J. Klippenstein and Craig A. Taatjes et. al - Argonne-Sandia Consortium on High-Pressure Combustion Chemistry.....	105
Marsha I. Lester – spectroscopy and Dynamics of Reaction Intermediates in Combustion Chemistry.....	109
Tianfeng Lu - Computational Flame Diagnostics for Direct Numerical Simulations with Detailed Chemistry of Transportation Fuels.....	113
Robert P. Lucht - Advanced Nonlinear Optical Methods for Quantitative Measurements in Flames.....	117
H. A. Michelsen - Particle Diagnostics Development.....	121
William H. Miller - Reaction Dynamics in Polyatomic Molecular Systems.....	125
Amy S. Mullin - Dynamics of Activated Molecules.....	129
Habib N. Najm - Reacting Flow Modeling with Detailed Chemical Kinetics.....	133
David J. Nesbitt - Spectroscopy, Kinetics and Dynamics of Combustion Radicals.....	137
Daniel M. Neumark and Stephen Leone – Spectroscopy and Dynamics of Free Radicals.....	141
Joseph C. Oefelein - Large Eddy Simulation of Reacting Flow Physics.....	145
David L. Osborn - Kinetics and Dynamics of Combustion Chemistry.....	149
Carol A. Parish - A Theoretical Investigation of the Structure and Reactivity of the Molecular Constituents of Oil Sand and Oil Shale.....	153
William J. Pitz and Charles K. Westbrook – Chemical Kinetic Modeling of Combustion Chemistry.....	157
Stephen B. Pope and Perrine Pepiot - Investigation of Non-Premixed Turbulent Combustion.....	161
Stephen T. Pratt - Optical Probes of Atomic and Molecular Decay Processes.....	165
Kirill Prozument – Chirped-Pulse Fourier Transform Millimeter-Wave Spectroscopy for Dynamics and Kinetics Studies of Combustion-Related Reactions.....	169
Hanna Reisler - Photoinitiated Reactions of Radicals and Diradicals in Molecular Beams.....	173
Branko Ruscic - Active Thermochemical Tables.....	177
Trevor Sears - Gas-Phase Molecular Dynamics: High Resolution Spectroscopy and Collision Dynamics of Transient Species.....	181

Ron Shepard - Theoretical Studies of Potential Energy Surfaces and Computational Methods.....	185
Raghu Sivaramakrishnan - Mechanisms and Models for Combustion Simulations.....	189
John F. Stanton - Quantum Chemistry of Radicals and Reactive Intermediates.....	193
Arthur G. Suits - Universal and State-Resolved Imaging Studies of Chemical Dynamics.....	197
James Sutherland – An Update on the Implementation of a Novel Multi-scale Simulation Strategy for Turbulent Reacting Flows.....	201
Craig A. Taatjes - Elementary Reaction Kinetics of Combustion Species.....	205
Robert S. Tranter - Elementary Reactions of PAH Formation.....	209
Angela Violi - Developing a predictive model for the chemical composition of soot nanoparticles: Integrating Model and Experiment.....	213
Albert Wagner - Pressure Dependence of Combustion Reactions: Quantum Inelastic Dynamics On Automatically Generated Potential Energy Surfaces.....	217
Margaret S. Wooldridge - Low Temperature Combustion Chemistry and Fuel Component Interactions.....	221
Hua-Gen Yu - Gas-Phase Molecular Dynamics: Theoretical Studies in Spectroscopy and Chemical Dynamics.....	225
Judit Zádor - Chemical Kinetics of Elementary Reactions.....	229
Timothy S. Zwier - Isomer-specific Spectroscopy and Isomerization in Aromatic Fuels.....	233

*Keynote Speaker*



# Hydroxyl and Peroxy Radicals: Quantitative Atmospheric Field Measurements and Unusual Temperature Dependent Kinetics

Dwayne E. Heard

School of Chemistry, University of Leeds, Leeds, LS2 9JT, UK, [d.e.heard@leeds.ac.uk](mailto:d.e.heard@leeds.ac.uk)

## Introduction

Free-radicals are involved intimately in the oxidation chemistry of both combustion and atmospheric media. For example, the hydroxyl radical, OH, removes the majority of trace gases emitted into the atmosphere either naturally or via human activities, and is a key species in the development of auto-ignition. Atmospheric emissions include greenhouse gases and substances harmful to health, and OH initiates the formation of a wide range of secondary products, many of which are implicated in poor air quality, for example ozone and organic aerosols. Concentrations of OH in flames, which can reach ppm levels or higher, have been measured using a number of *in situ* laser-based diagnostic techniques, and are useful targets for models of combustion chemistry. However, *in situ* measurements of OH and other radical species in the atmosphere are extremely challenging, owing to their very low abundance ( $[\text{OH}] < 0.1$  ppt) and short lifetimes. Laser-induced fluorescence (LIF) spectroscopy is a very sensitive method that has enjoyed considerable success in the quantitative detection of radicals in combustion media [1] and the atmosphere [2, 3]. My presentation will be split into two main components.

## Field measurements of OH and other radicals in the atmosphere

In the first part of the presentation I will describe LIF detection of atmospheric OH, HO<sub>2</sub> and RO<sub>2</sub> radicals at low pressure using the so called FAGE (fluorescence assay by gas expansion) technique [2, 3] from ground and airborne platforms. At the heart of FAGE is a supersonic free-jet expansion which is crossed by a multi-kHz pulsed tunable laser at 308 nm, and combined with gated single-photon counting to collect fluorescence from OH present in the atmosphere at around 10<sup>6</sup> molecule cm<sup>-3</sup>. Accurate calibration of the instruments is crucial, and is achieved using 185 nm photolysis of water vapour, using a chemical actinometer to measure the radiation flux [2]. My group has also made measurements of OH reactivity, which is a kinetic parameter representing the total removal rate of OH via reaction with its atmospheric sinks [4]. The Leeds instruments have been operated in a number of locations worldwide, ranging from the Poles to the Tropics, and from rainforests to urban centres. Owing to their short lifetime, the abundance of radicals at a given point is determined solely by their rate of chemical production and loss, and not by bulk transport. Field measurements of the concentrations of radicals and comparison with calculations using a numerical model therefore constitutes one of the very best ways to test whether the chemistry in each of these locations is understood and accurately represented in the model. I will show a flavour of measurements from recent field campaigns in a range of environments (megacity, tropical rainforest, marine), together with comparisons with a detailed chemical box model which utilizes the Leeds *Master Chemical Mechanism* which contains up to ca. 6,700 chemical species and 17,000 reactions.

## Reaction kinetics studied at very low temperatures using a pulsed Laval nozzle apparatus

Reactions of OH with volatile organic compounds feature prominently in chemical mechanisms describing oxidation in combustion media and the atmosphere. The majority of reactions involve abstraction of a hydrogen atom to generate an alkyl radical, displaying normal Arrhenius kinetic behaviour owing to the presence of an activation barrier to reaction. Such reactions have largely been neglected in mechanisms describing interstellar chemistry as they

are assumed to be negligibly slow at the very low temperatures (10-100 K) of most interstellar environments. However, for reactions of OH with acetone, methyl ethyl ketone, methanol, ethanol, di-methyl ether and ammonia, all of which have an activation barrier to abstraction, we have observed a dramatic acceleration in the rate coefficient at very low temperatures (two examples shown in Figure 1) [5-7]. For example, for methanol the rate coefficient is almost two orders of magnitude larger at 63 K compared to 200 K [5]. We used a Laval nozzle apparatus to generate supersonic, thermalized flows at temperatures down to  $\sim 40$  K suitable for kinetic studies, and utilised laser-flash photolysis with LIF detection to measure rate coefficients. The enhancement of these rate coefficients at low temperatures is rationalised by the formation of a weakly bound van der Waals complex between OH and the VOC prior to the barrier to reaction. This complex, which has an enhanced lifetime at lower temperatures, has three possible fates: dissociation back to reactants, collisional stabilisation into the pre-barrier well or quantum mechanical tunnelling through the barrier to form products. Measurement of the pressure dependence (or not) of the rate coefficients, as well as direct observation of products by LIF, helps to unravel details of this mechanism. We have also used the Leeds MESMER (Master Equation Solver for Multi Energy well Reactions) programme [8] to calculate the pressure and temperature dependence of the rate coefficients, for comparison with measurements and to extrapolate to even lower temperatures.

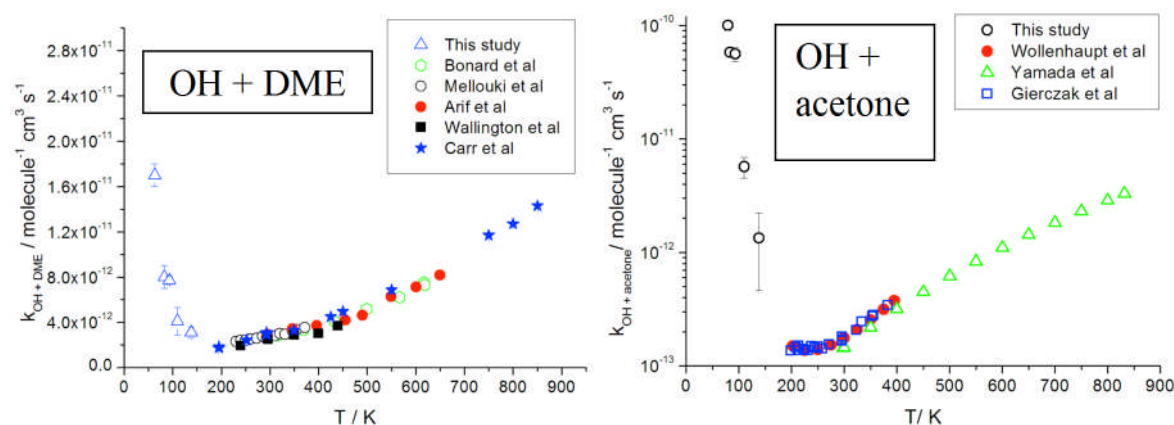


**Figure 1.** Temperature dependence of the rate coefficients for reaction of OH with di-methyl ether (left) and acetone (right). “This study” refers to the Laval nozzle experiments. Taken from ref. [6].

## References

- [1] D. E. Heard, J. B. Jeffries, G. P. Smith and D. R. Crosley, LIF Measurements in Methane/Air Flames of Radicals Important in Prompt-NO Formation, *Comb. Flame*, **88**, 137, 1992.
- [2] D. E. Heard and M. J. Pilling, Measurement of OH and HO<sub>2</sub> in the troposphere, *Chem. Rev.*, **103**, 5163 (2003).
- [3] D. Stone, L. K. Whalley, D. E. Heard, Tropospheric OH and HO<sub>2</sub> radicals: field measurements and model comparisons, *Chem. Soc. Rev.*, 41, 6348, 2012.
- [4] Whalley, et al., and Heard, D. E.: Atmospheric OH reactivity in central London: observations, model predictions and estimates of in situ ozone production, *Atmos. Chem. Phys.*, **16**, 2109, 2015.
- [5] R.J. Shannon, et al., and D.E. Heard, Accelerated chemistry in the reaction between the hydroxyl radical and methanol at interstellar temperatures facilitated by tunnelling, *Nature Chemistry*, **5**, 745, 2013.
- [6] R. J. Shannon, R. L. Caravan, M. A. Blitz, D. E. Heard, A combined experimental and theoretical study of reactions between the hydroxyl radical and oxygenated hydrocarbons relevant to astrochemical environments, *Phys. Chem. Chem. Phys.*, **16**, 3466, 2014.
- [7] R. L. Caravan, R. J. Shannon, T. Lewis, M. A. Blitz and D. E. Heard, Measurements of Rate Coefficients for Reactions of OH with Ethanol and Propan-2-ol at Very Low Temperatures, *J. Phys. Chem. A.*, doi:10.1021/jp505790m, 2014.
- [8] D. R. Glowacki, Liang, C.-H., Morley, C., Pilling, M. J. and Robertson, S. H. MESMER: an open-source master equation solver for multi-energy well reactions. *J. Phys. Chem. A* **116**, 9545-9560, 2012.

*Abstracts  
of  
Principal Investigator  
Presentations*



## The Chemical Dynamics Beamline

Musahid Ahmed, Kevin Wilson & Oleg Kostko

Chemical Sciences Division, Lawrence Berkeley National Laboratory  
MS 6R2100, 1 Cyclotron Road, Berkeley, CA-94720, [mahmed@lbl.gov](mailto:mahmed@lbl.gov)

**Program Scope:** The Chemical Dynamics Beamline, located in the Advanced Light Source (ALS) at Lawrence Berkeley National Laboratory (LBNL), is a national user facility providing state-of-the-art experimental resources for visiting scientists and staff to undertake studies of fundamental chemical processes. Much of the work is related to chemical physics, energy production and utilization via combustion, environmental science and chemical reactions on interfaces. Vacuum Ultraviolet (VUV) synchrotron photoionization mass spectrometry on two experimental platforms (molecular beam and aerosol sampling) are applied to a variety of problems of relevance to the Gas Phase Chemical Physics program. A vigorous user program from Sandia National Laboratory and Argonne National Laboratory at the beamline is exemplified in the work of Tranter, Osborn, Taatjes, Hansen, Michelsen & Sheps reported in their respective abstracts at this meeting.

### Recent Progress and Future Plans:

**Molecular growth processes in hydrocarbon chemistry-** The formation mechanisms of polycyclic aromatic hydrocarbons (PAHs) with indene and naphthalene cores in hydrocarbon-based combustion processes are being examined in collaboration with Ralf Kaiser (Hawaii). This is achieved by simulating the combustion relevant conditions (pressure, temperature, reactant molecules) in a high temperature ‘chemical reactor’. For almost half a century, polycyclic aromatic hydrocarbons (PAHs) have been proposed to play a key role in the astrochemical evolution of the interstellar medium (ISM) and in the chemistry of combustion systems. However, even the most fundamental reaction mechanism assumed to lead to the simplest PAH naphthalene—the hydrogen abstraction–acetylene addition (HACA) mechanism—has eluded experimental observation. Here, by probing the phenylacetylene ( $C_8H_6$ ) intermediate together with naphthalene ( $C_{10}H_8$ ) under combustion-like conditions by photo-ionization mass spectrometry, the very first direct experimental evidence for the validity of the HACA mechanism which so far had only been speculated theoretically is reported. Recently we showed that upon reaction of the naphthyl radical with acetylene, HACA effectively shuts down and does not lead to cyclization of the third aromatic ring, and a new pathway, via ethynyl substitution is operational. These findings indicate that – as predicted from electronic structure calculations - the HACA mechanism is less versatile toward the formation of more complex PAHs than previously postulated thus opening up alternative reaction pathways possibly via vinylacetylene-mediated synthesis of more complex PAHs in combustion flames.

A concerted effort is underway to understand the molecular mass growth processes involving small hydrocarbons and their aromatic (AR) as well as resonance stabilized free radicals (RSFRs) that lead to PAHs in order to successfully mitigate their formation in the combustion of fossil fuels. We are investigating the key reaction between the benzyl radicals ( $C_7H_7$ ) and acetylene ( $C_2H_2$ ) to ascertain the ability of this bimolecular reaction to form the prototypical PAH indene. Our investigation aims to elucidate the branching ratio between the PAH indene and alternative non-bicyclic isomers potentially formed in this process. Future work will be with propargyl ( $C_3H_3$ ) and allyl ( $C_3H_5$ ) RSFR’s with  $C_2$  to  $C_4$  hydrocarbons.

**Fundamental Processes in the Thermal Cracking of Biomass-** Thermochemical processing of biomass, with the goal of producing synthesis gas ( $CO$  and  $H_2$ ) is an important pathway towards the production of renewable fuels. Understanding of this process is incomplete, however, as even the thermolysis chemistry of many of the organic molecules encountered in these processes is poorly understood or completely unknown. To this end, we use a miniature, short residence time flow reactor coupled to synchrotron radiation, computational fluid dynamics and theoretical chemistry to determine the identity of the elementary decomposition pathways in collaboration with Barney Ellison (Colorado), John Daily (Colorado) & John Stanton (Texas). We have focused on a molecule that has proven to be a ubiquitous

biomass cracking and combustion intermediate – cyclopentadienone ( $C_5H_4=O$ ), as well as 2,5-dimethylfuran, which is the first legitimate biofuel that we have studied. Specifically, we have determined that  $C_5H_4=O$  yields acetylene and vinylacetylene upon thermolysis and its mechanism elucidated. Similarly, pyrolysis of 2,5-dimethylfuran leads to an observed set of products rather different from what might be expected based on our earlier work with furan, and indeed are inconsistent with some interpretations already in the literature. This work was extended to the furanic ether, 2-methoxyfuran, and a pressure-dependent kinetic model developed to model the decomposition. A comprehensive pyrolytic and photoionization study on the benzyl radical,  $C_6H_5CH_2$  was completed. Pyrolysis of the  $C_6H_5CD_2$ ,  $C_6D_5CH_2$ , and  $C_6H_5^{13}CH_2$  benzyl radicals produces a set of methyl radicals, cyclopentadienyl radicals, and benzynes that are not predicted by a fulvenallene pathway. Explicit searches for the cycloheptatrienyl radical were unsuccessful; there is no evidence for the isomerization of benzyl and cycloheptatrienyl radicals:  $C_6H_5CH_2 \leftrightarrow C_7H_7$ . The power of tunable synchrotron radiation, which can resolve isomers based upon ionization energy, was demonstrated during the pyrolysis of cyclohexanone, the simplest ketone, which can isomerize to its enol form under thermal conditions. Finally, a successful effort to understand the thermal decomposition of the simplest carbohydrate, glycolaldehyde, and glyoxal leads us to believe that the pyrolysis of complex sugars can be understood as well.

**Multiphase Chemistry of Aerosol Interfaces-** The overall goal of this work is to better elucidate interfacial reaction mechanisms and rates and to determine how surface reactions might differ from analogous processes in isolated gas phase molecules. OH reactions at organic surfaces produce a suite of free radical intermediates (peroxy and alkoxy radicals) whose overall reaction pathways govern molecular weight growth as well as decomposition. Alkoxy radical intermediates play important roles in breaking C-C bonds during a reaction. In addition, intermolecular hydrogen abstraction by alkoxy radicals is quite rapid leading to the potential of free radical chain chemistry. Both of these processes can play significant roles in determining the overall rate and oxidation mechanism of atmospheric organic aerosols. We have observed that in the presence of NO or  $SO_2$ , the effect heterogeneous oxidation rate of model organic particles is greatly accelerated to rates that are in excess of the OH-particle collision frequency. It is found that unlike reactions in the gas phase, peroxy radical reactions with NO and  $SO_2$  do not form stable reaction products (organic nitrates and sulfates), but rather exclusively alkoxy radicals. These alkoxy radicals efficiently abstract hydrogen atoms (like OH) and propagate chain reactions leading to oxidation rates that are 10-40 times the OH collision frequency. This new reaction mechanism (which is unexpected based upon analogous gas phase mechanisms) shows that heterogeneous oxidation reactions can potentially alter the chemical properties of organic aerosols within a matter of hours (rather than weeks) in urban environments such as megacities.

Initial studies have been completed of the heterogeneous reaction of OH with squalene particles. These measurements aim to understand how surface OH addition reactions to alkenes compare to analogous reactions in the gas phase. Measurements of the effective reaction probably over many orders of magnitude reveal facile chain propagation chemistry. At  $[OH] = 10^6$  molec.  $cm^{-3}$  the aerosol oxidation rate is ~100 times the OH collision frequency. In addition, there is evidence for the formation of higher molecular weight hydroperoxide species that may be formed via unimolecular H-transfer reactions. Modeling is currently underway to examine possible mechanisms to explain how the formation of hydroperoxides is ultimately connected to radical cycling reactions for aerosol phase alkenes.

**Development of new capabilities at the Chemical Dynamics Beamline-** The undulator servicing the beamline, has appreciable photon flux up to 1500 eV. This provides a rich source of soft X-rays and expands the beamline capabilities from VUV to soft X-rays. Plans are underway with support from ALS staff to prepare two terminals for photon energies up to 800 eV, which will allow access to C, N, and O soft X-ray spectroscopy. X-ray photoelectron spectroscopy of nanoparticles, aerosols and interfaces, X-ray absorption spectroscopy of size selected clusters, correlated multimodal probing of chemical reactions in solution with X-rays and mass spectrometry, and time-resolved pump probe dynamics on gas phase, liquids, interfaces and surfaces will be enabled at such a facility.

A new versatile photoelectron spectroscopy apparatus has been recently commissioned. The apparatus was designed for UPS, XPS, and NEXAFS types of measurements on gas-phase molecular, aerosol and nanoparticle samples. It will be utilized to probe the electronic properties of solvated species, surface chemistry and solid-liquid interfaces on nanoparticles and aerosols.

#### List of DOE sponsored research publications (2014-to date)

- B. Bandyopadhyay, T. Stein, Y. Fang, O. Kostko, A. White, M. Head-Gordon, and M. Ahmed, "[Probing Ionic Complexes of Ethylene and Acetylene with Vacuum Ultraviolet Radiation](#)," J. Phys. Chem. A., DOI: 10.1021/acs.jpca.6b00107, (2016, accepted)
- O. Kostko, B. Bandyopadhyay, and M. Ahmed, "[Vacuum Ultraviolet Photoionization of complex chemical systems](#)," Ann. Rev. Phys. Chem., Vol. 67, DOI: 10.1146/annurev-physchem-040215-112553 (2016, accepted)
- J. P. Porterfield, J. H. Baraban, T. P. Troy, M. Ahmed, M. C. McCarthy, K. M. Morgan, J. W. Daily, T. L. Nguyen, J. F. Stanton, and G. B. Ellison, "[Pyrolysis of the Simplest Carbohydrate, Glycolaldehyde \(CHO-CH<sub>2</sub>OH\), and Glyoxal in a Heated Micro-Reactor](#)," J. Phys. Chem. A., DOI: 10.1021/acs.jpca.6b00652 (2016, accepted)
- N. K. Richards-Henderson, A. H. Goldstein, and K. R. Wilson, "[Sulfur Dioxide Accelerates the Heterogeneous Oxidation Rate of Organic Aerosol by Hydroxyl Radicals](#)," Environ. Sci. Technol., DOI: 10.1021/acs.est.5b05369 (2016, accepted)
- J. P. Porterfield, T. L. Nguyen, J. H. Baraban, G. T. Buckingham, T. P. Troy, O. Kostko, M. Ahmed, J. F. Stanton, J. W. Dailey, and G. B. Ellison, "Isomerization and Fragmentation of Cyclohexanone in a Heated Micro-Reactor," J. Phys. Chem. A., **119**, 12635, DOI: 10.1021/acs.jpca.5b10984 (2015)
- D. S. N. Parker, R. I. Kaiser, O. Kostko, T. Troy, M. Ahmed, B. J. Sun, S. H. Chen, and A. H. Chang, "On the Formation of Pyridine in the Interstellar Medium," Phys. Chem. Chem. Phys., **17**, 32000, DOI: 10.1039/C5CP02960K (2015)
- N. K. Richards-Henderson, A. H. Goldstein, and K. R. Wilson, "Large Enhancement in the Heterogeneous Oxidation Rate of Organic Aerosols by Hydroxyl Radicals in the Presence of Nitric Oxide," J. Phys. Chem. Lett., **6**, 4451, DOI: 10.1021/acs.jpcclett.5b02121 (2015)
- D. R. Worton, H. Zhang, G. Isaacman-VanWertz, A. W. H. Chan, K. R. Wilson, and A. H. Goldstein, "Comprehensive chemical characterization of hydrocarbons in NIST standard reference material 2779 Gulf of Mexico crude oil," Environ. Sci. Technol., **49**, 13130, DOI: 10.1021/acs.est.5b03472 (2015)
- K. R. Kolesar, Z. Li, K. R. Wilson, C. D. Cappa, "Heating-Induced Evaporation of Nine Different Secondary Organic Aerosol Types," Environ. Sci. Technol., **49**, 12242, DOI: 10.1021/acs.est.5b03038 (2015)
- D. M. Popolan-Vaida, C.-L. Liu, T. Nah, K. R. Wilson, and S. R. Leone, "Reaction of chlorine molecules with unsaturated submicron organic particles," Z. Phys. Chem, **229**, 1521, DOI: 10.1515/zpch-2015-0662 (2015)
- J. H. Kroll, C. Y. Lim, S. H. Kessler, and K. R. Wilson, "Heterogeneous Oxidation of Atmospheric Organic Aerosol: Kinetics of Changes to the Amount and Oxidation State of Particle-Phase Organic Carbon," J. Phys. Chem. A., **119**, 10767, DOI: 10.1021/acs.jpca.5b06946 (2015)
- K. N. Urness, Q. Guan, T. P. Troy, M. Ahmed, J. W. Dailey, G. B. Ellison, and J. M. Simmie, "Pyrolysis Pathways of the Furanic Ether 2-Methoxyfuran," J. Phys. Chem. A., **119**, 9962, DOI: 10.1021/acs.jpca.5b06779 (2015)
- H. Zhang, D. R. Worton, S. Shen, T. Nah, G. Isaacman-VanWertz, K. R. Wilson, and A. H. Goldstein, "Fundamental Timescales Governing Organic Aerosol Multiphase Partitioning and Oxidative Aging," Environ. Sci. Technol. Lett., **49**, 9768, DOI: 10.1021/acs.est.5b02115 (2015)
- B. B. Kirk, J. D. Savee, A. Trevitt, D. L. Osborn and K. R. Wilson, "Molecular weight growth in Titan's atmosphere: branching pathways for the reaction of 1-propynyl radical (H<sub>3</sub>CC=C•) with small alkenes and alkynes," Phys. Chem. Chem. Phys., **17**, 20754, DOI: 10.1039/C5CP02589C (2015)
- D. S. N. Parker, R. I. Kaiser, O. Kostko, and M. Ahmed, "Selective Formation of Indene via the Reaction of Benzyl Radicals with Acetylene," Chem. Phys. Chem., **16**, 2091, DOI: 10.1002/cphc.201500313 (2015)
- B. Bandyopadhyay, O. Kostko, Y. Fang, and M. Ahmed, "Probing Methanol Cluster Growth by Vacuum Ultraviolet Ionization," J. Phys. Chem. A, **119**, 4083, DOI: 10.1021/acs.jpca.5b00912 (2015)
- T. K. Ormond, P. Hemberger, T. P. Troy, M. Ahmed, J. F. Stanton, and G. B. Ellison, "The Ionisation Energy of Cyclopentadienone: A Photoelectron-Photoion Coincidence Study," Mol. Phys., **113**, 2350, DOI: 10.1080/00268976.2015.1042936 (2015)

- D. S. N. Parker, R. I. Kaiser, B. Bandyopadhyay, O. Kostko, T. P. Troy, and M. Ahmed, "Unexpected Chemistry from the Reaction of Naphthyl and Acetylene at Combustion-Like Temperatures," *Angew. Chem. Int. Ed.*, **127**, 5511, DOI: 10.1002/anie.201411987 (2015)
- T. P. Troy, and M. Ahmed, "Rings of fire: Carbon combustion from soot to stars," *Phys. Today*, **68**, 62, DOI: 10.1063/PT.3.2729 (2015)
- D. S. N. Parker, R. I. Kaiser, O. Kostko, T. P. Troy, M. Ahmed, A. M. Mebel, and A. G. G. M. Tielens, "Gas Phase Synthesis of (Iso)Quinoline and Its Role in the Formation of Nucleobases in the Interstellar Medium," *Astrophys. J.*, **803**, 53, DOI: 10.1088/0004-637X/803/2/53 (2015)
- E. C. Browne, J. P. Franklin, M. R. Canagaratna, P. Massoli, T. W. Kirchstetter, D. R. Worsnop, K. R. Wilson, and J. H. Kroll, "Changes to the Chemical Composition of Soot from Heterogeneous Oxidation Reactions," *J. Phys. Chem. A*, **119**, 7222, DOI: 10.1021/jp511390f (2015)
- T. K. Ormond, A. M. Scheer, M. R. Nimlos, D. J. Robichaud, T. P. Troy, M. Ahmed, J. W. Daily, T. L. Nguyen, J. F. Stanton, and G. B. Ellison, "Pyrolysis of Cyclopentadienone: Mechanistic Insights From a Direct Measurement of Product Branching Ratios," *J. Phys. Chem. A*, **119**, 7222, DOI: 10.1021/jp511390f (2015)
- P. T. Lynch, T. P. Troy, M. Ahmed, and R.S. Tranter, "Probing Combustion Chemistry in a Miniature Shock Tube with Synchrotron VUV Photo Ionization Mass Spectrometry," *Anal. Chem.*, **87**, 2345, DOI: 10.1021/ac5041633 (2015)
- M. R. Canagaratna, P. Massoli, E. C. Browne, J. P. Franklin, K. R. Wilson, T. B. Onasch, T. W. Kirchstetter, E. C. Fortner, C. E. Kolb, J. T. Jayne, J. H. Kroll, and D. R. Worsnop, "Chemical Compositions of Black Carbon Particle Cores and Coatings via Soot Particle Aerosol Mass Spectrometry with Photoionization and Electron Ionization," *J. Phys. Chem. A.*, **119**, 4589, DOI: 10.1021/jp510711u (2015)
- G. T. Buckingham, T. K. Ormond, J. P. Porterfield, P. Hemberger, O. Kostko, M. Ahmed, D. J. Robichaud, M. R. Nimlos, J. W. Daily, and G. B. Ellison, "The thermal decomposition of the benzyl radical in a heated micro-reactor: I. Experimental findings," *J. Chem. Phys.*, **142**, 044307, DOI: 10.1063/1.4906156 (2015)
- D. S. N. Parker, R. I. Kaiser, T. P. Troy, O. Kostko, M. Ahmed, and A. M. Mebel, "Toward the Oxidation of the Phenyl Radical and Prevention of PAH Formation in Combustion Systems," *J. Phys. Chem. A.*, **119**, 7145, DOI: 10.1021/jp509170x (2015)
- K. O. Johansson, J. Y. W. Lai, S. A. Skeen, K. R. Wilson, N. Hansen, A. Violi, and H. A. Michelsen, "Soot Precursor Formation and Limitations of the Stabilomer Grid," *Proc. Combust. Inst.*, **35**, 1819, DOI: 10.1016/j.proci.2014.05.033 (2015)
- T. Nah, H. Zhang, D. R. Worton, C. Ruehl, B. B. Kirk, A. Goldstein, S. R. Leone, and K. R. Wilson, "Isomeric Product Detection in the Heterogeneous Reaction of Hydroxyl Radicals with Aerosol Composed of Branched and Linear Unsaturated Organic Molecules," *J. Phys. Chem. A*, **118**, 11555, DOI: 10.1021/jp508378z (2014)
- D. M. Popolan-Vaida, S. R. Leone, and K. R. Wilson, "Reaction of Iodine Atoms with Submicrometer Squalane and Squalene Droplets: Mechanistic Insights into Heterogeneous Reactions," *J. Phys. Chem. A*, **118**, 10688, DOI: 10.1021/jp5085247 (2014)
- M. R. Canagaratna, J. L. Jimenez, J. H. Kroll, Q. Chen, S. H. Kessler, P. Massoli, L. Hildebrandt Ruiz, E. Fortner, L. R. Williams, K. R. Wilson, J. D. Surratt, N. M. Donahue, J. T. Jayne, and D. R. Worsnop, "Elemental ratio measurements of organic compounds using aerosol mass spectrometry: characterization, improved calibration, and implications", *Atmos. Chem. Phys. Discuss*, **14**, 19791, DOI: 10.5194/acpd-14-19791-2014 (2014)
- D. S. N. Parker, R. I. Kaiser, T. P. Troy, and M. Ahmed, "Hydrogen Abstraction-Acetylene Addition Revealed," *Angew. Chem. Int. Ed.*, **53**, 7740, DOI: 10.1002/anie.201404537 (2014)
- T. Nah, S. H. Kessler, K. E. Daumit, J. H. Kroll, S. R. Leone, and K. R. Wilson, "The influence of molecular structure and chemical functionality on the heterogeneous OH-initiated oxidation of unsaturated organic particles," *J. Phys. Chem. A*, **118**, 4106, DOI: 10.1021/jp502666g (2014)
- D. R. Worton, G. Isaacman, D. R. Gentner, T. R. Dallmann, A. W. H. Chan, C. Ruehl, T. W. Kirchstetter, K. R. Wilson, R. A. Harley, and A. H. Goldstein, "Lubricating oil dominates primary organic aerosol emissions from motor vehicles," *Environ. Sci. Technol.*, **48**, 3698, DOI: 10.1021/es405375j (2014)
- N. Hansen, S. A. Skeen, H. A. Michelsen, K. R. Wilson, and K. Kohse-Höinghaus, "Flame Experiments at the Advanced Light Source: New Insights into Soot Formation Processes," *J. Vis. Exp.* **87**, doi:10.3791/51369 (2014)
- K. R. Kolesar, G. Buffaloe, K. R. Wilson, and C. D. Cappa, "OH-Initiated Heterogeneous Oxidation of Internally-Mixed Squalane and Secondary Organic Aerosol," *Environ. Sci. Technol.*, **48**, 3196 (2014)

## Turbulence-Chemistry Interactions in Reacting Flows

Robert S. Barlow  
Combustion Research Facility  
Sandia National Laboratories, MS 9051  
Livermore, California 94550  
barlow@sandia.gov

### Program Scope

This program is directed toward achieving a more complete understanding of turbulence-chemistry interactions in gaseous flames and providing detailed measurements for validation of combustion models. In the Turbulent Combustion Laboratory (TCL) simultaneous line imaging of spontaneous Raman scattering, Rayleigh scattering, and two-photon laser-induced fluorescence (LIF) of CO is applied to obtain spatially and temporally resolved measurements of temperature, the concentrations of all major species, mixture fraction, and reaction progress, as well as gradients in these quantities in hydrocarbon flames. The instantaneous three-dimensional orientation of the turbulent reaction zone is also measured by imaging of OH LIF or Rayleigh scattering at 355 nm in two crossed planes, which intersect along the laser axis for the multiscale measurements. These combined data characterize both the thermo-chemical state and the instantaneous flame structure, such that the influence of turbulent mixing and molecular transport on flame chemistry may be quantified. Our experimental work is closely coupled with international collaborative efforts to develop and validate predictive models for turbulent combustion. This is accomplished through our visitor program and through the TNF Workshop series. In recent years the workshop and this program have expanded their scope to address a range of combustion modes, including premixed, stratified, partially premixed, and nonpremixed flames. We are also working to extend our quantitative multiscale diagnostics to more complex hydrocarbon fuels, such as dimethyl ether. Entry into these new research areas has prompted developments in both hardware and methods of data analysis to achieve unprecedented spatial resolution and precision of multiscale measurements. Within the CRF we collaborate with Jonathan Frank, who applies advanced imaging diagnostics to turbulent flames, and with Joe Oefelein, who performs high fidelity large-eddy simulations (LES) of our experimental flames in order to gain greater fundamental understanding of the dynamics of multi-scale flow-chemistry interactions.

### Recent Progress

#### Multi-mode Combustion in Inhomogeneous Piloted Jet Flames

We have made significant progress during the past year in our investigation of multi-mode combustion in partially premixed jet flames with inhomogeneous inlets. This work, conducted in collaboration with the University of Sydney, uses a version of the Sydney/Sandia piloted burner that includes an additional central tube within the main tube (Figure 1a). The central tube can deliver either fuel or air and can be recessed a variable distance,  $L_r$ , to control the degree of fuel-air mixing upstream of the jet exit. Overall flame stability, as indicated by the measured blowoff velocity, is significantly enhanced at an optimal recess distance of 75 mm (Figure 1b). Initial experiments revealed near-stoichiometric mixtures at the edge of the exiting jet, adjacent to the

pilot flame, such that there is a stratified-premixed mode of combustion near the base of the jet flame. The resulting additional heat release augments the stabilizing effect of the pilot. This is followed by rapid transition to diffusion-dominated combustion within ten jet exit diameters (Meares et al. *Proc. Combust. Inst.* 2015, 35, 1477–1484; Barlow et al. *Combust. Flame* 2015, 162, 3516–3540).

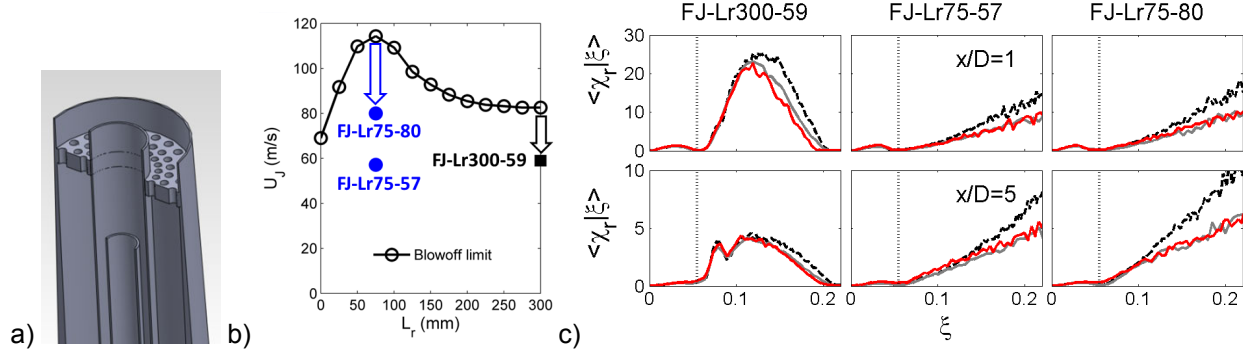


Figure 1. a) Inhomogeneous piloted burner. b) Dependence of blowoff velocity on recess distance,  $L_r$ . c) Conditional means of the 1D (radial) mixture fraction dissipation at 1 and 5 jet exit diameters downstream of the burner exit plane: red — original 0.1 mm data spacing; black — 0.02 mm spaced data with wavelet denoising; gray — high-resolution data binned by 5 to approximate the spatial filtering effect of the lower resolution measurements.

In order to further investigate this transition in the mode of combustion, we undertook a second complete set of experiments, this time applying a method of spatial oversampling and wavelet denoising and including additional radial profiles in the near-field. The denoising approach was developed for the study of thin reaction zones in premixed and stratified flames to improve both spatial resolution and precision of the Raman/Rayleigh/CO-LIF line measurements (Sweeney et al., *Combust. Flame* 2013, 160, 322–334). Figure 1c shows that the two sets of measurements of conditional scalar dissipation (1D radial contribution) are in close agreement for mixture fraction values up to at least 0.1, which includes the reaction zone. Results diverge at higher mixture fraction values, particularly in the inhomogeneous flames FJ-Lr75-57 and FJ-Lr75-80 (center and right columns). When the higher resolution data are binned by two (not shown), the effect is negligible except within the cold interior of the inhomogeneous jet flames, where the dissipation scales extend below the  $\sim 0.06$  mm optical resolution of the system. Binning by five yields results that match the original experiments. A significant conclusion from this comparison is that measurements of mixture fraction dissipation are fully resolved in all high-temperature regions of the flow, including the near-field reaction zones (Cutcher et al. *Proc. Combust. Inst.* accepted).

The joint statistics of mixture fraction and progress variable are important in flamelet-based modeling approaches for turbulent partially-premixed combustion. However, experimental data on these joint statistics are almost nonexistent, and a common simplifying assumption is that fluctuations in mixture fraction and progress variable are statistically independent. We have evaluated several progress variable definitions in the context of the present experiments, and have proposed normalized progress variable base on oxygen. The inhomogeneous and near-homogeneous flames have very different near-field behavior of the Favre average statistics of mixture fraction and progress variable. It is clear that an assumption of statistical independence is inappropriate in most regions of these flames. Further, the magnitude of the correlation

coefficient,  $R_{\xi c} = \overline{\xi^n c_0^n} / (\overline{\xi^{n2} c_0^{n2}})^{1/2}$ , on the rich side of the reaction zone ( $\xi = 0.07$ ) increases significantly through the region of combustion mode transition, changing from roughly -0.2 to roughly -0.8, and then decreases again as the probability of local increases farther downstream.

With these new experiments, we have achieved the first ever measurements of the cross-dissipation, which is defined for 1D measurements as  $\chi_{\xi c} = 2D(d\xi/dr)(dc/dr)$ . This had been attempted in experiments on the Cambridge/Sandia stratified flames. However, effects of differential diffusion and residual noise on measured gradients in mixture fraction were comparable to the gradients attributable to stratification. The present flames have large mixture fraction gradients within the region where the combustion mode changes. Figure 2 shows a single-shot example of profiles of mixture fraction, progress variable, and the corresponding 1D dissipation terms. Further work is needed to quantify uncertainties and apply conditional analysis to extract quantitative information on the evolution of the three dissipation terms,  $\chi_{\xi\xi}$ ,  $\chi_{cc}$ , and  $\chi_{\xi c}$ , through the combustion mode transition.

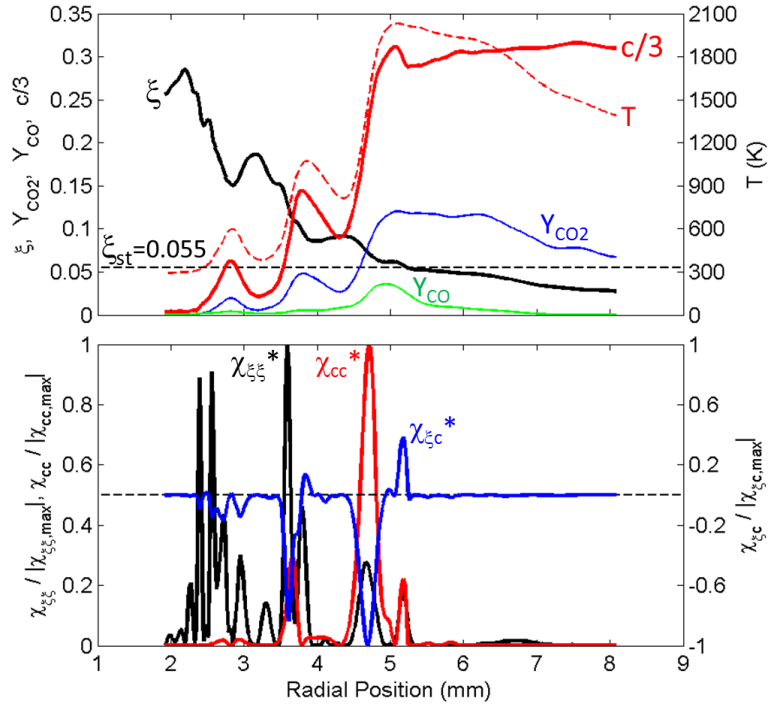


Figure 2. Single-shot example of high-resolution, wavelet-denoised radial profiles of scalars and scalar dissipation across the reaction zone in the FJ-Lr75-103 flame at  $x/D=7$ .

### Other Progress

Papers were written and submitted or accepted during the past year on turbulent stratified combustion (Kamal et al., *Combust. Flame* 2015 and 2016; Stahler et al. *Proc. Combust. Inst.* accepted), dual-resolution Raman measurements of six hydrocarbon species and twelve species overall, including  $N_2$ ,  $O_2$ ,  $H_2O$ ,  $CO_2$ ,  $CO$ ,  $H_2$ ,  $CH_4$ , DME,  $CH_2O$ ,  $C_2H_2$ ,  $C_2H_4$ , and  $C_2H_6$  (Magnotti et al. *Proc. Combust. Inst.* accepted), and scalar dissipation measurements in a piloted DME jet flame (Fuest et al. *Combust. Flame*, submitted).

### **Future Plans**

Multi-mode combustion will be a major thrust, involving further conditional analysis of data from the Sydney inhomogeneous jet flames as well as close collaboration with modeling and simulation groups. At least six groups are running simulations of these flames for collaborative comparisons at the next TNF Workshop (July, Seoul). Collaborative experiments on stratified combustion are continuing with the group at TU Darmstadt, Germany, with current efforts focused on hydrogen addition to the methane fuel and higher levels of stratification and shear-generated turbulence.

### **BES Supported Publications (2014 - present)**

Ma, B.; Wang, G.; Magnotti, G.; Barlow, R.S.; Long, M.B., Intensity-ratio and color-ratio thin-filament pyrometry: Uncertainties and accuracy, *Combust. Flame* **2014**, *161*, 908-916.

Rankin, B.A.; Magnotti, G.; Barlow, R.S.; Gore, J.P., Radiation intensity imaging measurements of methane and dimethyl ether turbulent nonpremixed and partially premixed jet flames, *Combust. Flame* **2014**, *161*, 2849–2859.

Fuest, F.; Magnotti, G.; Barlow, R.S.; Sutton, J.A., Scalar structure of turbulent partially-premixed dimethyl ether/air jet flames, *Proc. Combust. Inst.* **2015**, *35*, 1235–1242.

Meares, S.; Prasad, V.N.; Magnotti, G.; Barlow, R.S.; Masri, A.R., Stabilization of piloted turbulent flames with inhomogeneous inlets, *Proc. Combust. Inst.* **2015**, *35*, 1477–1484.

Magnotti, G.; Geyer, D.; Barlow, R.S., Interference-free spontaneous Raman spectroscopy for measurements in rich hydrocarbon flames, *Proc. Combust. Inst.* **2015**, *35*, 3765–3772.

Magnotti, G.; Barlow, R.S., Effects of high shear on the structure and thickness of turbulent premixed methane/air flames stabilized on a bluff-body burner, *Combust. Flame* **2015**, *162*, 100–114.

Barlow, R.S.; Dunn, M.J.; Magnotti, G., Preferential transport effects in premixed bluff-body stabilized CH<sub>4</sub>/H<sub>2</sub> flames, *Combust. Flame* **2015**, *162*, 727–735.

Fuest, F.; Barlow, R.S.; Magnotti, G.; Dreizler, A.; Ekoto, I.W., Sutton, J.A., Quantitative acetylene measurements in laminar and turbulent flames using 1D Raman/Rayleigh scattering, *Combust. Flame* **2015**, *162* 2248–2255.

Magnotti, G.; KC, U.; Varghese, P.L.; Barlow, R.S., Raman spectra of methane, ethylene, ethane, dimethyl ether, formaldehyde and propane for combustion applications, *JQSRT* **2015** *163*, 80–101

Barlow, R.S.; Meares, S.; Magnotti, G.; Cutcher, H., A.R. Masri, Local extinction and near-field structure in piloted turbulent CH<sub>4</sub>/air jet flames with inhomogeneous inlets, *Combust. Flame* **2015**, *162*, 3516–3540.

Kamal, M.M.; Barlow, R.S.; Hochgreb, S., Conditional analysis of turbulent premixed and stratified flames on local equivalence ratio and progress of reaction, *Combust. Flame* **2015**, *162*, 3896–3913.

Kamal, M.M.; Barlow, R.S.; Hochgreb, S., Scalar structure of turbulent stratified swirl flames conditioned on local equivalence ratio, *Combust. Flame* **2016**, (in press).

Cutcher, H.C.; Magnotti, G.; Barlow, R.S.; Masri, A.R., Turbulent Flames with Compositionally Inhomogeneous Inlets: Resolved Measurements of Scalar Dissipation Rates, *Proc. Combust. Inst.* (accepted).

Stahler, T.; Geyer, D.; Magnotti, G.; Trunk, P.; Barlow, R.S.; Dreisler, A., Multiple conditioned analysis of the Turbulent Stratified Flame A, *Proc. Combust. Inst.* (accepted).

Magnotti, G.; Barlow, R.S., Dual-Resolution Raman Spectroscopy for Measurements of Temperature and Twelve Species in Hydrocarbon-Air Flames, *Proc. Combust. Inst.* (accepted).

Fuest, F.; Barlow, R.S.; Magnotti, G.; Sutton, J.A., Scalar dissipation rates in a turbulent partially-premixed dimethyl ether/air jet flame, *Combust. Flame* (submitted).

**TNF Workshop Information:** <http://www.sandia.gov/tnf>

# Predictive Large-Eddy Simulation of Supercritical-Pressure Reactive Flows in the Cold Ignition Regime

Josette Bellan

Mechanical and Civil Engineering Department, California Institute of Technology  
Pasadena, CA 91125

[Josette.Bellan@jpl.nasa.gov](mailto:Josette.Bellan@jpl.nasa.gov)

DOE Award Number: **02\_GR-ER16107-14-00**

STRIPES award number: **SC0002679**

## I. Program Scope

This study addresses issues highlighted in the Basic Energy Needs for Clean and Efficient Combustion of 21st Century Transportation Fuels (DOE BES, 2006) under the topic of Combustion under Extreme Pressure. It is there noted that “the most basic concepts of thermal autoignition” are “based on experience and theory at near atmospheric pressures” and that “as pressure increases significantly..., many of these conceptual pictures begin to change or disappear”. It is also stated “A better description of the coupling and interaction of high pressure flow and molecular transport processes with chemistry is also necessary”, particularly because “Ignition and flame propagation of alternative and renewable fuels, as well as of the changing feed stocks of conventional fossil-based fuels, are very likely to be much different at very high pressures than under the more familiar, lower pressure conditions of current engines.” Recognizing that “Under such (*increasing pressure*) conditions distinctions between gas and liquid phases become moot, new equations of state must be used...”, it is immediately apparent that there must be “a re-examination of the basic assumptions that govern the physics and chemistry related to combustion; and the need for this type of re-examination increases as the combustion pressure increases.” This recognition is also stated under the topic of Multiscale Modeling since due to the new equations of state “The combination of unexplored thermodynamic environments and new physical and chemical fuel properties results in complex interactions among multiphase (*according to the above, the multiphase distinction becomes moot with increasing pressure*) fluid dynamics, thermodynamic properties, heat transfer, and chemical kinetics that are not understood even at a fundamental level.” From the theoretical viewpoint for “systems at high pressure, fluid dynamic time scales can be comparable to chemical time scales.” and therefore “completely diffusion-controlled reactions ... can become important”.

Thus, the objective of this study is the investigation of the coupling among thermodynamics, transport properties, intrinsic kinetics and turbulence under the high-pressure and the relatively (with respect to combustion) low-temperature conditions typical of the auto-ignition regime, with particular emphasis on the manifestation of this coupling on the effective kinetic rate. As planned, we established collaboration with Dr. Joseph Oefelein of the Combustion Research Facility at Sandia Livermore to work together towards implementing the models developed in this research into the high-pressure Large Eddy Simulation (LES) code (named RAPTOR) under development by him at Sandia.

## II. Recent Progress

This report contains results obtained during the previous year of funding. The focus of the research during this year was to (1) further analyze the temporal mixing layer turbulent high-pressure (“high-*p*”) regime reactive flow Direct Numerical Simulation (DNS) database so as to understand the mixing/turbulence/reaction coupling, and (2) explore, in an *a priori* study of the

same database, the difference in turbulent reaction-rate modeling requirements between LES and Explicitly Filtered LES (EFLES) in which highly non-linear terms are explicitly filtered. The four DNS realizations described in [iii], obtained by varying the initial Reynolds number ( $Re_0$ ), the free-stream pressure and the initial composition of the two streams were probed;

only one of the simulation was initiated with the freestream devoid of traces of  $CO_2$  and  $H_2O$  (i.e. Exhaust Gas Recirculation (EGR)). The DNS were run until each reached transition to turbulence; chemical reactions were initiated in each DNS at its respective transitional time. For the simulation at the larger  $Re_0$ , we used smaller amplitudes of the initial perturbations employed to hasten transition, so as to avoid the computation blowing up. The dissipation, i.e. the irreversible entropy

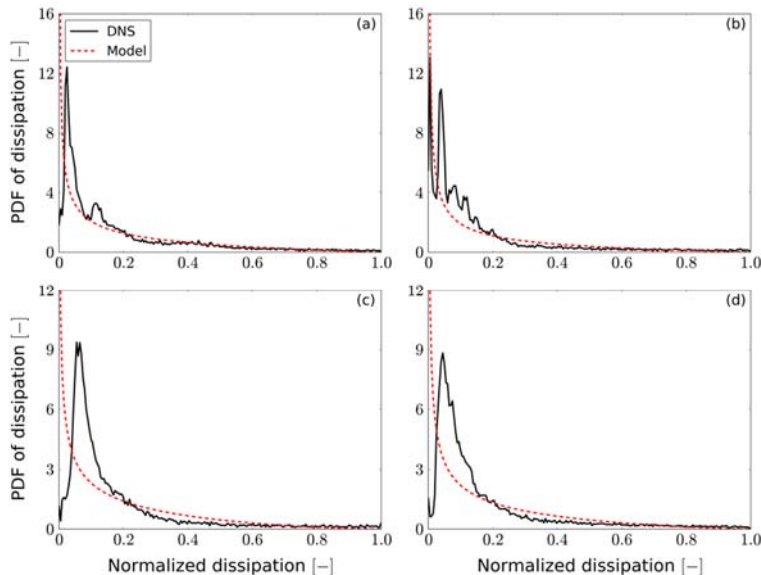


**Figure 1. Probability density function of the dissipation for the four DNS realizations compared to the log normal distribution (model) using the moments extracted from the DNS at  $t_{pp}^*$ .**

production, is a pivotal quantity in turbulence modeling: reproducing the small-scale dissipation is one of the goals of SGS modeling. Figure 1 illustrates the comparison of the dissipation to the log normal distribution computed with its moments extracted from the exact PDF: that is, the log normal is the most accurate representation obtainable using this assumed PDF. In each case, the abscissa is non-dimensionalized by the maximum for that particular realization at the peak-volumetric pressure time,  $t_{pp}^*$ . The results show that in all cases the high value range PDF is well captured by the log normal model, whereas the small-range values are very poorly modeled. Translating this information to the physical space, the regions of large dissipation are those of intense transport and/or chemical activity including the diffusion flame regions, whereas the regions of small dissipation are those of smaller fluxes and/or chemical activity. The regions of smaller fluxes could be thought to be of less interest except if trace species undergo there uphill diffusion (indeed, uphill diffusion does occur in regions of small gradients and thus create small turbulent scales. Therefore, the trends indicate that the log normal PDF could be a useful model to represent the dissipation if a good model for relatively small magnitudes and for its two moments could be developed.

The first activity in considering atmospheric- $p$  turbulent reaction rate models for application to high- $p$  turbulent combustion is to test whether the models' assumptions are satisfied by the present database. Since the existence of a mixture fraction as a conserved variable which can be found from an equation independent of other dependent variables is pivotal to flamelet-type models, this assumption was the first focus of examination. The conservation equation for the mixture fraction was written in a way to highlight the typical diffusion term under the unity Lewis number assumption and the remaining diffusion terms which are called 'correction' to the typical terms. The r.m.s. of the typical diffusion term and the correction term are displayed in Fig. 2 for the four realizations of the database. Clearly, the correction is about twice the typical diffusion term and thus cannot be neglected. For all

practical purposes, the correction term can be considered as a ‘source’ term in the mixture fraction equation since it depends on dependent variables other than the mixture fraction. A general observation is that the structural variation of the correction term in the cross-stream direction closely emulates that of the typical diffusion term. This suggests that in LES modeling one might try to develop a SGS model for these terms based on self-similarity. In conjunction with the examination of the mixture fraction, we also tested the applicability of the beta PDF for representing the statistics of the mixture fraction. To this end, the PDF was computed for each DNS at  $t_{pp}^*$  and compared to the beta PDF computed with the exact moments extracted from the DNS solution. The results show that the beta PDF approximates quite well the exact PDF in the upper part of the mixing layer where burning occurs, but it differs substantially from the exact PDF in the mixing region; a more in-depth exploration must be undertaken.

Since modeling the turbulent reaction rate for high- $p$  situations is not an easy task, we explored the possibility of the filtered turbulent reaction rate term playing a lesser role in EFLES than LES, and therefore inaccuracies in its modeling having less of an impact in the solution. To this end, we conducted an *a priori* study of the database for 3 grid-filter width and for a fixed explicit filter width. In LES, the turbulent reaction rate term is not mathematically well defined because only the implicit filter width is known, but not its shape, so the term’s relationship to the DNS reaction rate is mathematically unknown. However, in EFLES a relationship between EFLES and DNS expressions is readily available; a fact which is useful for testing models. A common feature of all EFLES analysis is that in all equations the activity of the SGS terms for the convective effect are of the same order of magnitude as that of the convective resolved terms, unlike in LES where the activity of the SGS terms is much smaller than that of the resolved terms; also the activity of the convective SGS terms decreases with increasing grid-filter width rather than increasing with increasing grid-filter width, as it is in LES. Since these were the only terms on which explicit filtering has been previously applied, we conjecture that the success of EFLES is due to these characteristics of the small scales. The impact of these results is still being analyzed.

The PI has continued the collaboration with Dr. Oefelein who will modify RAPTOR once we have developed the methodology of LES for high- $p$  flows.

### III. Future Plans

The following activities are planned:

- Propose subgrid-scale models for the filtered turbulent reaction term.

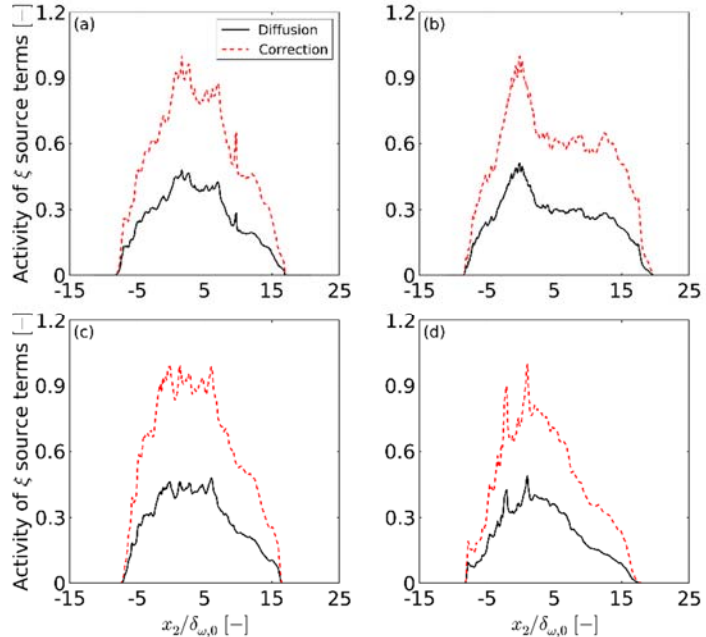


**Figure 2. Normalized activity of the correction (here denoted as ‘source’) terms in mixture fraction equation for DNS realizations at the respective  $t_{pp}^*$ .**

- Examine *a priori* their performance in LES and EFLES.

#### IV. References

- i. Borghesi, G.; Bellan, J., *Proc. of the Comb. Inst.*, 35 **2015** 1537-1547
- ii. Masi, E.; Bellan, J.; Harstad, K.; Okong'o, N. *J. Fluid Mech.* **2013**, 721, 578
- iii. Bellan, J., Direct Numerical Simulation of a high-pressure reacting temporal mixing layer, submitted 2015

#### V. Publications, presentations and submitted articles supported by this project during 2013- 2016

- [1] Masi, E., Bellan, J., Harstad, K. and Okong'o N., Multi-species turbulent mixing under supercritical-pressure conditions: modeling, Direct Numerical Simulation and analysis revealing species spinodal decomposition, *J. Fluid Mech.*, 721, 578-626, 2013
- [2] Masi, E., Bellan, J. and Harstad, K., Pressure effects from Direct Numerical Simulation of high-pressure multispecies mixing, paper 2013-0711, 51<sup>th</sup> Aerospace Sciences Meeting, Dallas, TX, 1/7-1/10, 2013
- [3] Borghesi, G. and Bellan, J., Models for the LES equations to describe multi-species mixing occurring at supercritical pressure, paper 2014-0823 presented at the 52<sup>nd</sup> Aerospace Sciences Meeting, New Harbor, MD, January 13-17, 2014
- [4] Borghesi, G. and Bellan, J., Models for the Large Eddy Simulation equations to describe multi-species mixing occurring at supercritical pressure, *Int. J. Energ. Mat. Chem. Prop.*, 13(5), 435-453, 2014
- [5] Borghesi, G. and Bellan, J., *A priori* and *a posteriori* analysis for developing Large Eddy simulations of multi-species turbulent mixing under high-pressure conditions, *Phys. Fluids.*, 27, 035117 (35 pages), 2015
- [6] Bellan, J., Possible phase formation during high-pressure multi-species jet disintegration, **Keynote Invited Lecture**, ILASS meeting, May 18-21, 2014, Portland, OR.
- [7] Bellan, J., Modeling and numerical simulations of multi-species high-pressure flows, **Invited Plenary Lecture**, 10<sup>th</sup> International Symposium on Special Topics in Chemical Propulsion, June 2-6, 2014, Poitiers, France
- [8] Bellan, J., Modeling and numerical simulations of multi-species high-pressure reactive flows, **Invited Plenary Lecture**, Summer Program of the SFBTRR40, Institute of Aerodynamics and Fluid Mechanics Technische Universität München, Garching, Germany, August 3, 2015
- [9] Bellan, J., Modeling and numerical simulations of multi-species high-pressure reactive flows, **Invited Seminar**, Purdue University, West Lafayette, IN., October 22, 2015
- [10] Bellan, J., Reduced models for the simulation of multi-scale problems in physics and chemistry, **Invited Seminar**, Cornell University, Ithaca, NY., November 17, 2015
- [11] Borghesi, G. and Bellan, J., Irreversible entropy production rate in high-pressure turbulent reactive flows, *Proc. of the Comb. Inst.*, 35, 1537-1547, 2015
- [12] Borghesi, G. and Bellan, J., *A priori* and *a posteriori* analyses of multi-species turbulent mixing layers at supercritical-*p* conditions, paper 2015-0162 presented at the 53<sup>rd</sup> Aerospace Sciences Meeting, Kissimmee, FL., January 5-9, 2015; also presented at the 9<sup>th</sup> US National Combustion Meeting, Cincinnati, OH., May 17-20, 2015
- [13] Bellan, J., Direct Numerical Simulation of a high-pressure reacting temporal mixing layer, submitted 2015
- [14] Bellan, J., The mixture fraction for high-pressure turbulent reactive flows, paper 2016-1686 presented at the 54<sup>th</sup> Aerospace Sciences Meeting, San Diego, CA, January 4-8, 2016

## Towards predictive simulations of soot formation: from surrogate to turbulence

Guillaume Blanquart  
Department of Mechanical Engineering  
California Institute of Technology  
1200 E. California Blvd., Pasadena, CA 91125

### Objectives

The combustion of hydrocarbon fuels, including kerosene, gasoline, and diesel, leads to the formation of soot particles which are known to be the source of several health problems and environmental issues.

The objective of the proposed work is to reduce the gap in the present understanding and modeling of soot formation both in laminar and turbulent flames. This effort spans several length scales from the molecular level to large scale turbulent transport. More precisely, the objectives are three fold: 1) develop a *single combined chemical and soot model* validated for all relevant components usually found in real fuel surrogates; 2) develop a framework able to *explain the complete evolution of soot particles* from cluster of PAHs to oxidation of large fractal aggregates; 3) *understand and model the interplay* between unsteady chemistry, differential diffusion, and turbulent transport.

### Recent progress

This year's focus has been placed on the numerical simulations of turbulent sooting diffusion flames. Two flames have been selected, both of which are targets for the upcoming 2016 International Sooting Flames (ISF) workshop.

#### *Atmospheric kerosene flame*

We performed one of the first Large Eddy Simulations (LES) of a turbulent sooting flame burning a kerosene surrogate (77% *n*-dodecane/ 23% *m*-xylene). The simulation is intended to reproduce a piloted turbulent diffusion flame experiment performed at Sandia Nat Labs by Shaddix et al. (**Figure 1**) and was performed with our low-Mach code and used the same modeling approaches that we used for previous simulations of a sooting ethylene/air jet diffusion flame (also from Sandia Nat Labs). First, the subfilter quantities are modeled using the dynamic Smagorinsky model, and local thermo-chemical quantities are tabulated using a flamelet/progress variable approach. Second, soot particles are described using a bivariate model, based on particle volume and surface area. The statistical evolution of soot particles is described by solving transport equations for moments of the soot Number Density Function (NDF), using the Direct Quadrature Method of Moments. In the present work a bimodal formulation for the NDF is used. Third, radiative heat losses from the gas phase and soot are also included, using the optically-thin gas assumption. The preliminary LES results are compared against the experimental data of Shaddix and Zhang (**Figure 1**). The analysis is complemented by comparisons against an analogous simulation burning ethylene. This work represents the first of a series of simulations aimed at characterizing the impact of the fraction of aromatic species in kerosene-surrogate fuels on the formation of soot.

These simulations also highlighted computational challenges associated with large density ratios in low Mach flow solvers. Improving the numerical time integration scheme will be the subject of future work.

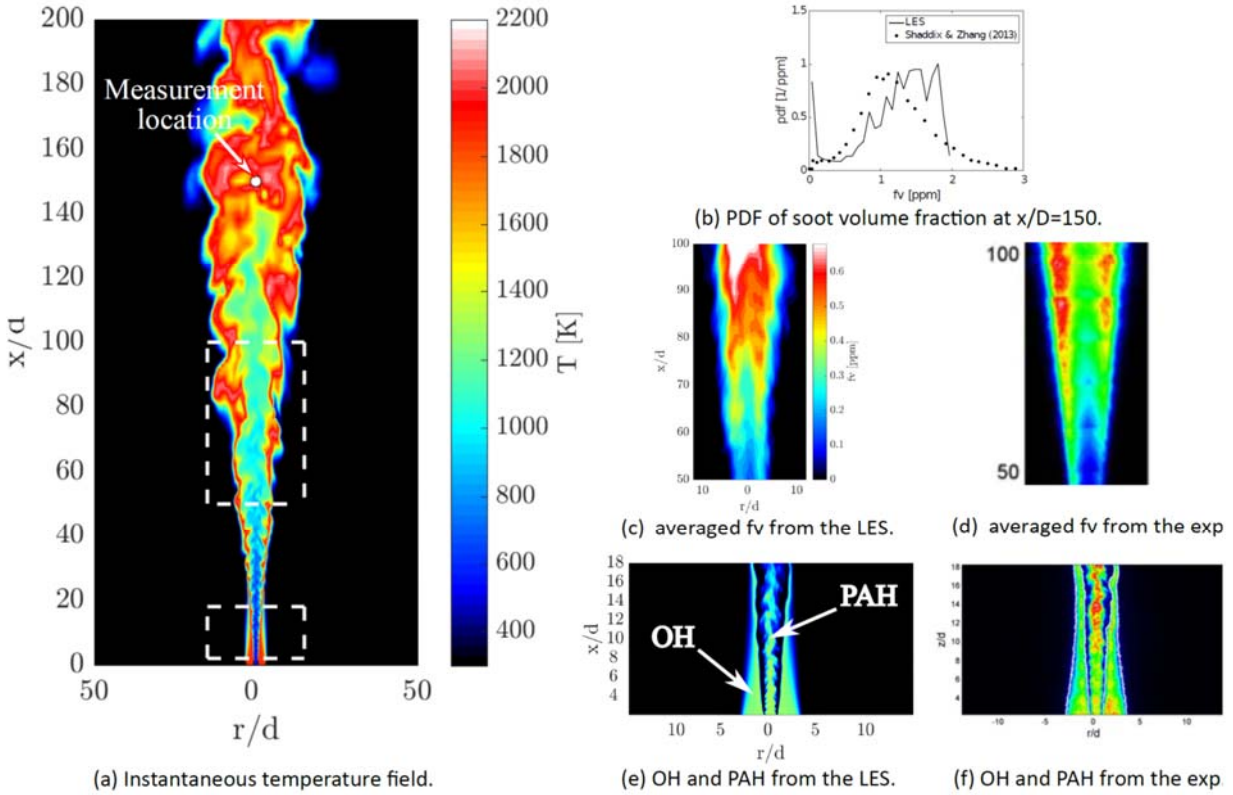


**Figure 1.** Preliminary results of an LES of a turbulent, sooting, diffusion flame of a kerosene surrogate.

### *High pressure swirled flame*

The second investigation targeted a high pressure (four atmosphere), turbulent ethylene, jet diffusion flame. This flame, investigated experimentally at the DLR in Germany, is intended to reproduce realistic flow fields and features encountered in aircraft gas turbine engines. The central piece to this burner is a complex swirler composed of multiple air and fuel streams (**Figure 2**). In contrast to most strategies relying on a body-fitted unstructured mesh, we captured the complex geometry with the use of Immersed Boundaries (IB). Once again, the same combustion and soot modeling approaches previously are being used.

### *Turbulent Lewis numbers*

The third aspect of the work performed this year focused on estimating turbulent Lewis numbers. In many combustion modeling approaches (such as in tabulated chemistry), the species Lewis numbers (ratio of heat diffusion to mass diffusion) are used as input parameters. While it is well-accepted that these Lewis numbers tend toward unity under intense turbulence, it is unclear what their values

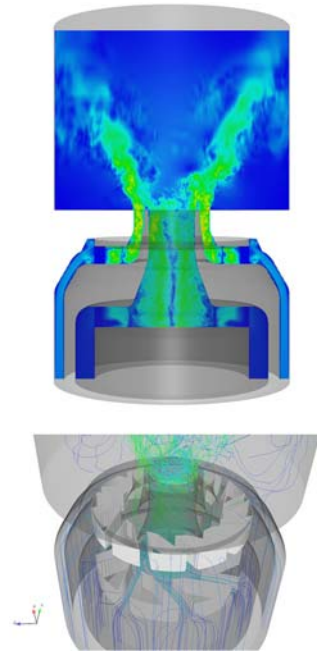


**Figure 2.** Preliminary results of an LES of a high-pressure turbulent swirled sooting ethylene flame.

are for less turbulent conditions and for heavy hydrocarbon species as found in kerosene fuels and for soot precursors (PAH species). Using incorrect Lewis numbers could lead to factors of two to three variations in soot nucleation rates. The goal of this work is to develop simple, physics-based correlation functions to relate these turbulent Lewis numbers in terms of the local Reynolds number. We developed a methodology to extract these turbulent Lewis numbers from experimental measurements of species mass fractions conditioned on mixture fraction (**Figure 3**). This approach has been applied so far to the series of Sandia B through E flames, and is being extended to a wide range of flames from the Turbulent Non-premixed Flames (TNF) workshop.

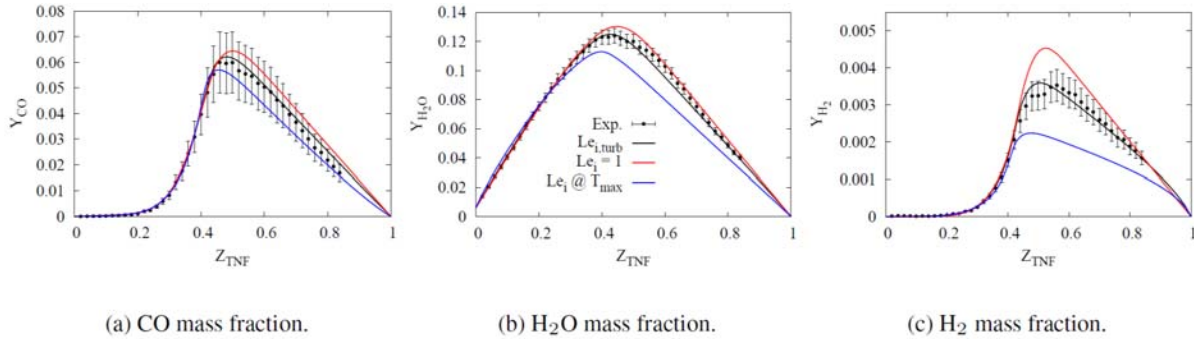


**Figure 3.** Comparison of measured species conditional mean mass fractions for Sandia flame C at  $x/D=30$ , against the flamelet solutions corresponding to turbulent Lewis numbers (black line), unity Lewis numbers (red line), and laminar Lewis numbers (blue line).

## Publications

Xuan, Y., Blanquart, G., « *Effects of aromatic chemistry-turbulence interactions on soot formation in a turbulent non-premixed flame* », Proc. Comb. Inst. (2015).

Burali, N., Xuan, Y., Blanquart, G., « *Assessment of the constant non-unity Lewis number assumption in chemically-reacting flows* », Combust. Theory Model. (2016).

Burali, N., Blanquart, G., « *Characterization of the sooting behavior of a turbulent jet flame burning a kerosene surrogate fuel* », Int. Symp. Comb. (2016), Work in Progress Poster.

Burali, N., Blanquart, G., « *A model for the turbulent Lewis numbers in turbulent non-premixed flames* », Int. Symp. Comb. (2016), Work in Progress Poster.



# Dynamics of Product Branching from Radical Intermediates in Elementary Combustion Reactions

Laurie J. Butler

The University of Chicago, The James Franck Institute  
929 E 57<sup>th</sup> St, CIS E 211, Chicago, IL 60637  
L-Butler@uchicago.edu

## I. Program Scope

While the total rate constant for many elementary reactions is well-characterized, understanding the product branching in complex reactions presents a formidable challenge. To gain an incisive probe of such reactions, our experiments investigate the dynamics of the product channels that arise from transient radical intermediates along the bimolecular reaction coordinates. Our work<sup>1-7</sup> uses the methodology developed in my group in the last fifteen years, using both imaging and scattering apparatuses. The experiments generate a particular isomeric form of an unstable radical intermediate along a bimolecular reaction coordinate and study the branching between the ensuing product channels of the energized radical as a function of its internal rotational and vibrational energy under collision-less conditions.

The experiments use a combination of: 1) measurement of product velocity and angular distributions in a crossed laser-molecular beam apparatus, with electron bombardment detection in my lab in Chicago or 2) with tunable vacuum ultraviolet photoionization detection at Taiwan's National Synchrotron Radiation Research Center (NSRRC), and 3) velocity map imaging using state-selective REMPI and single photon VUV ionization of radical intermediates and reaction products. We also employ tunable VUV photoionization detection in our imaging apparatus, using difference frequency four-wave mixing to produce photoionization light tunable from 8 to 10.8 eV. The first year of the present funding started Jan. 1, 2016, but during the no-cost extension before that date we were able to complete a detailed study of the competing unimolecular dissociation channels of vibrationally excited  $\text{CH}_2\text{CH}_2\text{ONO}$  radicals. This work has just been published<sup>6</sup> and is described in Section II.A below. The data evidence two channels predicted by conventional transition state theory,  $\text{NO}_2$  + ethene and  $\text{NO}$  + oxirane, and also a non-IRC product channel to form  $\text{HNO}$  + vinoxy. We also completed, after three years of work, our study of the energetic onset of the  $\text{H}$  + ketene product channel of vinoxy radicals.<sup>7</sup> By photodissociating 2-chloroacetaldehyde at 157 nm, we were able to produce nascent vinoxy radicals dispersed by internal energy with well-characterized rotational angular momenta and vibrational energies. The vibrational energy ranges from just below the isomerization barrier that leads, through acetyl, to  $\text{CH}_3$  +  $\text{CO}$  products to energies well above the barrier to the  $\text{H}$  + ketene product channel. This work, also just published,<sup>7</sup> is described in Section II.B below. It offers a new benchmark for the relative energies of the  $\text{H}$  + ketene transition state and the isomerization barrier that leads to  $\text{CH}_3$  +  $\text{CO}$  products. That work also introduces an accurate way to account for the velocity-dependent rotational angular momentum of the nascent vinoxy radicals in using RRKM theory to predict the product branching and the measured onset of the  $\text{H}$  + ketene product channel. We hope this will be of use to investigators studying radical intermediates produced photolytically.

## II. Recent Progress

### A. Unimolecular Dissociation Channels of the $\text{CH}_2\text{CH}_2\text{ONO}$ Radical

While the photodissociation of  $\text{BrCH}_2\text{CH}_2\text{ONO}$  at 351 nm results in fission of the weak (39 kcal/mol) O-NO bond,<sup>2</sup> at 193 nm a significant fraction of the molecules undergo C-Br

bond photofission.<sup>3</sup> The C-Br photofission channel gives vibrationally excited  $\text{CH}_2\text{CH}_2\text{ONO}$  radicals, allowing us to study the competition between two unimolecular dissociation channels predicted by statistical transition state theory,  $\text{NO}_2$  + ethene and an  $\text{NO}$  + oxirane, and to discover a third dissociation channel, a non-IRC pathway to  $\text{HNO}$  + vinoxy, shown in green in Figure 1. The traditional transition state for that channel is too high in energy (32.1 kcal/mol) for that channel to be significant, so we postulate a non-IRC pathway that begins with the  $\text{NO}$  moiety beginning to depart from oxirane, but extracting an H atom en route. The angular distribution of the  $\text{HNO}$  product is sideways scattered with respect to the velocity of the  $\text{CH}_2\text{CH}_2\text{ONO}$  radical, supporting this presumed dynamics. The experiment detected the vinoxy co-product at both parent ion,  $m/z = 43$ , and at the  $\text{CH}_3^+$  daughter ion from dissociative photoionization. Prior

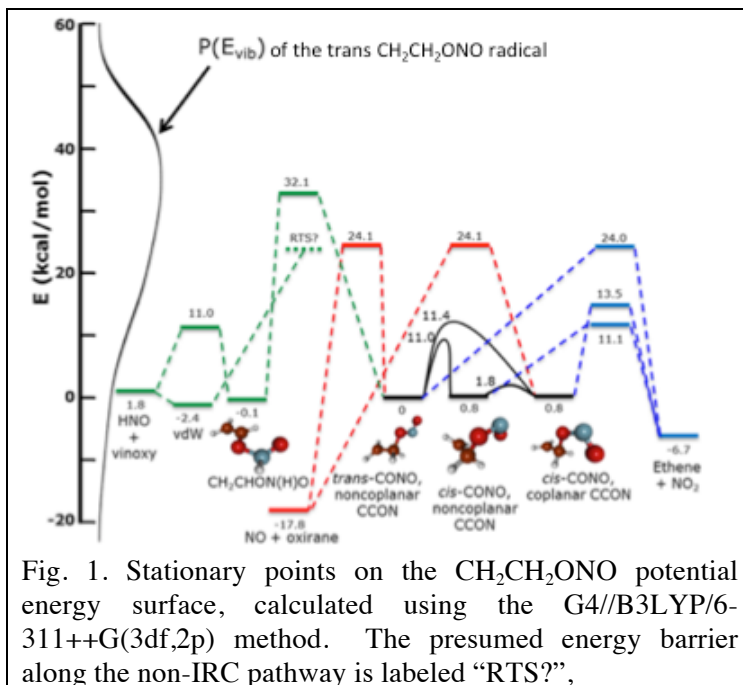


Fig. 1. Stationary points on the  $\text{CH}_2\text{CH}_2\text{ONO}$  potential energy surface, calculated using the G4//B3LYP/6-311++G(3df,2p) method. The presumed energy barrier along the non-IRC pathway is labeled “RTS?”.

work by D. Osborn in our program and S.-H. Lee at the NSRRC had detected vinoxy at the  $\text{CH}_3^+$  daughter ion, with an appearance energy of about 10.2 eV, but had not detected vinoxy at parent ion. We hope to interest Bowman’s group in developing a global PES for  $\text{CH}_2\text{CH}_2\text{ONO}$  to assess this non-IRC pathway and the other two product channels, as his group and others have investigated a roaming channel that produced  $\text{HNO}$  from a closed-shell species, nitromethane.

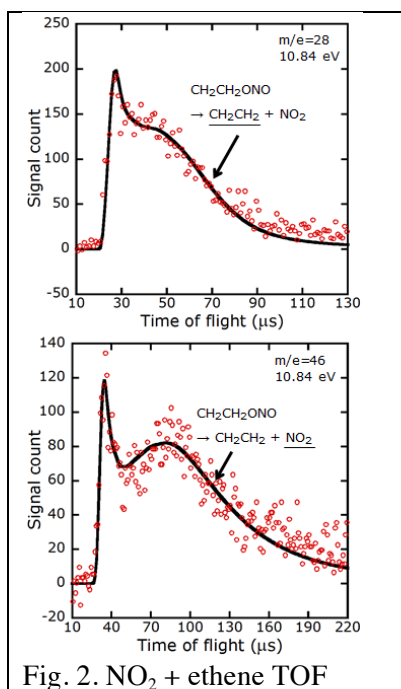


Fig. 2.  $\text{NO}_2$  + ethene TOF

The dominant product channel from the  $\text{CH}_2\text{CH}_2\text{ONO}$  radical is  $\text{NO}_2$  + ethene, as might be expected from the low barriers in blue in Figure 1. Figure 2 shows this data. Some of the momentum-matched  $\text{NO}_2$  products undergo secondary photodissociation, as observed in prior work on nitromethane and on 2-bromo-2-nitropropane.

We also detected an  $\text{HNO}$  photoelimination channel from  $\text{BrCH}_2\text{CH}_2\text{ONO}$  upon excitation at 193 nm that competed with O-NO photofission and C-Br photofission. We have not yet been able to determine the branching ratios to the  $\text{HNO}$  product channels. Although the  $\text{HNO}$  photoionization spectrum has been measured, no one has been able to determine the absolute photoionization cross section. Our preliminary attempts at doing so with ethyl nitrite photodissociation were unsuccessful.

## B. Onset of Branching to H + Ketene from Vinyoxy Radicals

Because of its importance in combustion, the vinyoxy radical  $\text{CH}_2\text{CHO}$  has been the subject of many theoretical and experimental studies, several by investigators in our program. Neumark and Osborn studied the competition between the H + ketene and  $\text{CH}_3 + \text{CO}$  product channels when vinyoxy is prepared in the  $\tilde{B}$  state, and Matsika and Yarkony have characterized the excited state conical intersections and avoided crossings that facilitate internal conversion to the ground electronic state. It has been a challenge, however, to prepare nascent vinyoxy radicals at energies that span the predicted barrier to H + ketene and the isomerization barrier to acetyl which leads to the  $\text{CH}_3 + \text{CO}$  products. The only such study, one from my group by Miller et al in 2004, surprisingly did not detect any branching to the H + ketene product channel, despite the two barriers being predicted to differ by only a couple kcal/mol. At that time we suggested that nonadiabatic recrossing might be inhibiting the dissociation to H + ketene, but that hypothesis was not born out by later theoretical work.

To gain an incisive probe of the onset of the H + ketene product channel, we used the photodissociation of chloroacetaldehyde  $\text{CH}_2\text{ClCHO}$  at 157 nm.<sup>7</sup> This wavelength accesses excited states largely repulsive in the C-Cl bond, so allows us to accurately model the angular momentum distribution and vibrational energy of the nascent vinyoxy radicals, as they are dispersed by the recoil velocity imparted from the C-Cl photofission. Using a velocity map imaging apparatus, we measured the speed distribution of the recoiling chlorine atoms,  $\text{Cl}(^2\text{P}_{3/2})$  and  $\text{Cl}(^2\text{P}_{1/2})$  to determine the distribution of kinetic energy imparted to the Cl + vinyoxy fragments. From this we derive the internal energy and angular momentum distribution of the nascent vinyoxy radicals. The vinyoxy radicals are mostly formed in the  $\tilde{A}$  state, but are assumed to undergo rapid internal conversion to the ground electronic state. Vinyoxy radicals formed with enough vibrational energy to surmount the isomerization barrier to acetyl go on to dissociate to  $\text{CH}_3 + \text{CO}$ . However, our data shows the onset of the H + ketene product channel is at significantly higher energies than that predicted using statistical transition state theory and the G4 barriers. To analyze the data, we developed a model for the branching between the two channels that takes into account the change in rotational energy en route to the products. The model uses RRKM rate constants at the correct sums and densities of vibrational states while accounting for angular momentum conservation. The model predicts the portion of the C-Cl bond fission  $P(E_T)$  that produces dissociative vinyoxy radicals, then predicts the branching ratio between the H + ketene and  $\text{CH}_3 + \text{CO}$  product channels at each  $E_T$ . We find that the predicted portion of the  $P(E_T)$  that produces H + ketene products best fits the experimental portion (that we derive by taking advantage of conservation of momentum) if we use a barrier height for the H + ketene channel that is  $4.0 \pm 0.5$  kcal/mol higher than the isomerization barrier en route to  $\text{CH}_3 + \text{CO}$  products. This result is shown in Figure 3. The statistical prediction for the

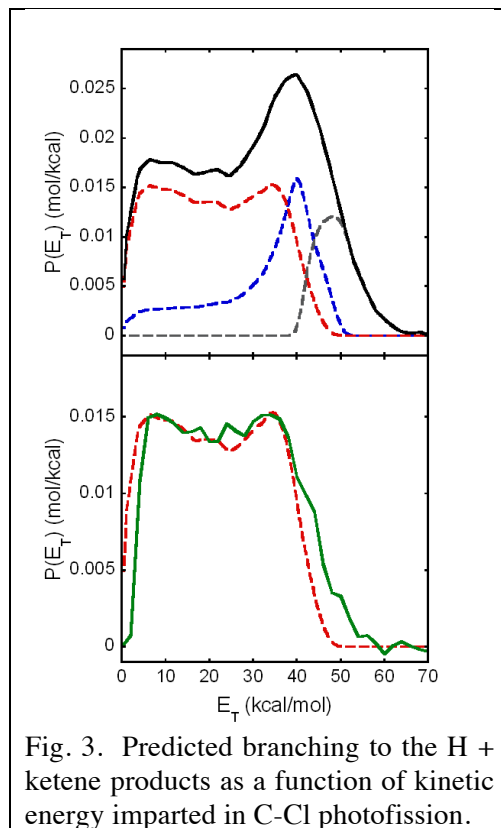


Fig. 3. Predicted branching to the H + ketene products as a function of kinetic energy imparted in C-Cl photofission.

product branching from vinyoxy radicals is shown in the top frame, with C-Cl photofission events (total shown in black line) that produce stable vinyoxy radicals shown in grey, and at lower  $E_T$ 's, producing vinyoxy radicals with correspondingly higher vibrational energy, ones that dissociate to  $\text{CH}_3 + \text{CO}$  in blue and to  $\text{H} + \text{ketene}$  in red. The measured recoil velocities of the ketene products, converted to C-Cl photofission  $E_T$  and shown in green in the lower frame, allows us to determine the distribution of vinyoxy radicals that dissociate to  $\text{H} + \text{ketene}$ . The agreement shown between the predicted (red) distribution and the measured (green) distribution is only achieved if the barrier to  $\text{H} + \text{ketene}$  is raised by over 2 kcal/mol from that predicted by G4 methods. We are pursuing coupled cluster calculations with John Stanton.

### III. Future Work

We just took data at the NSRRC on a radical intermediate in the  $\text{OH} + \text{propene}$  reaction. Our prior studies<sup>3,4</sup> of this reaction were limited because the photolytic precursor at 193 nm was a 70/30 mixture of 1-bromo-2-propanol (producing the  $\text{C}_3\text{H}_6\text{OH}$  radical intermediate from OH addition at the center carbon) and 2-bromo-1-propanol (producing the radical intermediate from OH addition at the end carbon). Our new experiments use a pure sample of 2-chloro-1-propanol for a photolytic precursor for the radical intermediate when OH adds to the end carbon of propene, the 1-hydroxy-2-propyl radical intermediate. This allowed us to isolate the reaction products from this radical intermediate, so provides a selective test of the predictions from theoretical studies of the product channels from the  $\text{OH} + \text{propene}$  reaction.

### III. Publications Acknowledging DE-FG02-92ER14305 (2013 or later)

1. Effects of high angular momentum on the unimolecular dissociation of  $\text{CD}_2\text{CD}_2\text{OH}$ : Theory and comparisons with experiment, B. G. McKown, M. Ceriotti, C. C. Womack, E. Kamarchik, L. J. Butler, and J. M. Bowman, *J. Phys. Chem. A* **117**, 10951-63 (2013).
2. Imaging and scattering studies of the unimolecular dissociation of the  $\text{BrCH}_2\text{CH}_2\text{O}$  radical from  $\text{BrCH}_2\text{CH}_2\text{ONO}$  photolysis at 351 nm, L. Wang, C. -S. Lam, R. Chhantyal-Pun, M. D. Brynteson, L. J. Butler, and T. A. Miller, *J. Phys. Chem. A*, **118**, 404-416 (2014).
3. Radical Intermediates in the Addition of OH to Propene: Photolytic Precursors and Angular Momentum Effects, M. D. Brynteson, C. C. Womack, R. S. Booth, S.-H. Lee, J. J. Lin, and L. J. Butler, *J. Phys. Chem. A* **118**, 3211-3229 (2014).
4. Predicting the effect of angular momentum on the dissociation dynamics of highly rotationally excited radical intermediates, M. D. Brynteson and L. J. Butler, *J. Chem. Phys.* **142**, 054301 (2015). (Joint funding with NSF.)
5. Two HCl-Elimination Channels and Two CO-Formation Channels Detected with Time-Resolved Infrared Emission upon Photolysis of Acryloyl Chloride [ $\text{CH}_2\text{CHC}(\text{O})\text{Cl}$ ] at 193 nm, P.-W. Lee, P. G. Scrape, L. J. Butler, and Y.-P. Lee, *J. Phys. Chem. A*, DOI 10.1021/jp512376a (2015).
6. Dissociation Pathways of the  $\text{CH}_2\text{CH}_2\text{ONO}$  Radical:  $\text{NO}_2 + \text{Ethene}$ ,  $\text{NO} + \text{Oxirane}$  and a non-Intrinsic Reaction Coordinate  $\text{HNO} + \text{Vinyoxy}$  Pathway, P. G. Scrape, T. D. Roberts, S.-H. Lee and L. J. Butler, *J. Phys. Chem. A*, in press (2016).
7. The Onset of  $\text{H} + \text{Ketene}$  Products from Vinyoxy Radicals Prepared by Photodissociation of Chloroacetaldehyde at 157, Chow-Shing Lam, Jonathan D. Adams, and Laurie J. Butler, *J. Phys. Chem. A*, in press (2016).

## Imaging Chemical Dynamics and Spectroscopy.

David W. Chandler  
Combustion Research Facility  
Sandia National Laboratory  
Livermore, CA 94551-0969  
Email: chand@sandia.gov

### **Program Scope:**

My research focuses on the field of chemical dynamics of gas phase molecular species. I define chemical dynamics as the detailed study of the motion of molecules and atoms on inter- or intramolecular potential energy surfaces in order to learn about the details of the surface as well as the dynamics of their interactions. We have tested bimolecular potential energy surfaces by the careful study of collisional energy transfer processes in crossed molecular beam arrangements utilizing Velocity Mapped Ion Imaging techniques. Last year we reported on the collision induced dissociation of vibrationally excited  $\text{NO}_2$ . This year we report on an extension of this study and a new study utilizing Velocity Mapped Ion Imaging to image spectroscopy with MHz resolution. We have also continued to work on a new multi-frequency cavity ring down spectrometer that will provide multiplexed spectroscopy with the resolution of the etalon used for the cavity ring down measurement.

### **Chemical Dynamics Progress Report: NO + NO<sub>2</sub> collisional energy transfer:**

Over the last few years we have been exciting atoms and molecules into transient excited states at the crossing of two particle beams and observing the scattering induced by collisions at the crossing point of the beams. Our first project was studying elastic collisions of Kr atoms [1], then we studied the rotational energy transfer dynamics of NO (A) with atomic partners [2,3] and have recently published a study of vibrationally excited  $\text{NO}_2$ . We did this by monitoring the dissociation of the  $\text{NO}_2$  after a single collision with an Ar atom. The collision induces translational to rotation and translation to vibration energy transfer. These ro-vibrationally hot molecules then dissociate producing NO (X,  $J < 15$ ) state molecules and a ground state O atom. By measuring the velocity distribution of each of the NO(X, J) states produced and the dissociation branching ratio of  $\text{NO}_2$  into each rotational state of the NO as a function of  $\text{NO}_2$  internal energy we are able to determine the shape of the Energy Transfer Function, P(E) for this very vibratonally hot molecule.[4]

In order to eliminate the complication of the dissociating  $\text{NO}_2$  molecule and still obtain the shape of the energy transfer function from a hot  $\text{NO}_2$  molecule in collision with NO molecule we have taken a new approach. We vibrationally excite  $\text{NO}_2$  a few hundred wavenumbers below the dissociation energy and scatter NO( $J=0.5, 1.5$ ) from the hot  $\text{NO}_2$ . Any NO changing rotational state but going faster than an elastically scattered NO would have had to gain energy from the vibrationally hot  $\text{NO}_2$ . Measurement of this velocity distribution is a direct measure the shape of the collisional energy transfer function for NO +  $\text{NO}_2$  (Hot). The first step is to study the collisional energy transfer of NO( $J = 0.5, 1.5$ ) +  $\text{NO}_2$  (Cold). We use velocity mapped ion imaging to detect the NO after an NO -  $\text{NO}_2$  collision. The NO is ionized to  $\text{NO}^+$  using 1+1' REMPI. The ions were then accelerated to a position sensitive ion detector, and the image collected on a CCD camera. We collected images with NO in  $J = 9.5-15.5$ . NO + He does not

produce images at  $J = 9.5$  or higher. Therefore, we can observe  $\text{NO} + \text{NO}_2$  (cold) without any complications from the carrier gas of the  $\text{NO}_2$ .

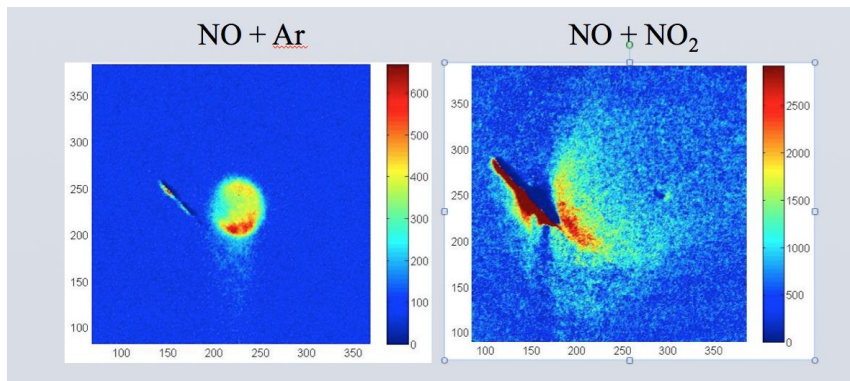


Figure 1. Image of  $\text{NO}(j=15.5)$  after collision with Ar (left) and with  $\text{NO}_2$  (right).  $\text{NO}_2$  was seeded in Helium and the NO was seeded in Ar. The center-of-mass collision energy was  $\sim 450 \text{ cm}^{-1}$  for NO collision with Ar and  $\sim 1400 \text{ cm}^{-1}$  of energy for NO collision with  $\text{NO}_2$ .

In Figure 1 is shown an image of  $\text{NO}(j=15.5)$  scattered from  $\text{NO}_2$ . The image can be inverse Abel transformed and the differential cross section and the velocity distribution can then be extracted. The DCS's are all highly forward scattered, but the distribution broadens as the NO rotational state increases. The velocity distributions also broaden, suggesting that, as expected, more highly rotationally excited states of NO are correlated with more rovibrational excitation in the  $\text{NO}_2$  collider. While some structure was observed in the rotational distribution, it is not obviously correlated with vibrational excitation (as the bend of  $\text{NO}_2$  is at  $749 \text{ cm}^{-1}$ ). Next we will excite the  $\text{NO}_2$  to a vibrationally excited state and record images subtracting out the  $\text{NO} + \text{NO}_2(\text{cold})$  background images.

### Imaging Spectroscopy with Velocity Mapped Ion Imaging:

The ability to measure the velocity of neutral atoms and molecules with a precision of several meter/sec provides an opportunity to measure subtle perturbations on electronic state spectroscopy with high resolution. Using Velocity Mapped Ion Imaging we are able to measure perturbations of electronic states such as broadening and magnetic and electric field splittings. We call this technique Doppler Imaged State Spectroscopy. We demonstrate this ability utilizing the  $5s[3/2]_2 \rightarrow 5p[5/2]_3$  cycling transition at 811.5 nm in metastable Kr atoms to investigate the saturation broadening caused by Rabi cycling on a resonant transition with MHz resolution. In addition we investigate the lifetime broadening associated with ionization from the cycling states and the Zeeman splitting of the states. As it is now possible to measure velocities to  $\sim 1 \text{ m/s}$  with VMII this represents measurement of a Doppler shift of  $\sim 1 \text{ MHz}$  for this Kr transition and represents the resolution limit that is possible with this technique. We have measured saturation broadening, lifetime broadening and Zeeman splitting with this imaging technique. Figure 2 shows the scheme and the image one obtains by retro-reflecting 811.5 laser beam 60 MHz detuned from the  $5s[3/2]_2 \rightarrow 5p[5/2]_3$  transition through the thermal sample. This laser becomes part of the REMPI process and therefore impacts the Doppler components that are ionized. The separation between the peaks in Fig.2c provides a measure of the laser detuning, the width of the peaks provides information on the saturation of the transition and the lifetime of the states.

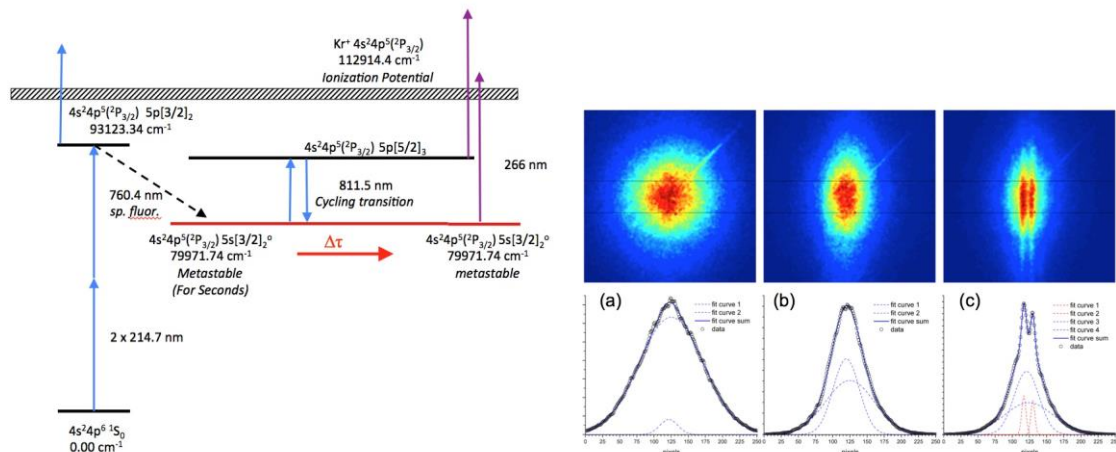


Fig 2. Scheme for producing metastable Kr  $5s[3/2]_2^o$  by two-photon excitation followed by 760.4 nm emission from the ground state of Kr utilizing a pulsed 214.7 nm laser beam. A 1 MHz resolution 811.5 nm laser beam is used to optically cycle the population utilizing the  $5s[3/2]_2^o \rightarrow 5p[5/2]_3$  transition. The broadening of the lines due to the lifetime shortening associated with the Rabi cycling brings different Doppler components into resonance. A 266-nm pulsed laser beam is used to ionize the Kr atoms from both the  $5s[3/2]_2^o$  and the  $5p[5/2]_3$  states. (a) Ion Image of Kr ions with no time delay between the 214 nm two-photon excitation laser beam and the 266-nm ionization laser beam, (b) an image of Kr Ion Image with a 10 microsecond delay between the 214 two-photon excitation laser beam and the 266-nm ionization beam with no 811.5 nm CW laser present, (c) Kr Ion Image with 10 microsecond delay between the 214 nm two-photon excitation laser beam and the 266-nm ionization laser beam with 811.5 nm laser present but detuned by 60 MHz from the line center of the transition. The 811.5 signal enhancement shown in panel(c) is centered about zero velocity as expected

We have recently begun the study of the alignment ground state molecules by moderate laser intensities. Alignment effects in non-linear optics cause distortion of the signals and calculations of polarizabilities of electronic excited states of hydrogen offer a perfect setting to study alignment as a function of rotational and vibrational state. We use one laser to excite a specific rotational and vibrational level of the  $H_2$  (E,F) state. From this state we use an intense 532-nm laser beam to align, dissociate the  $H_2$  and ionize the H atom product fragment. Measurement of the angular distribution of the  $H^+$  provides direct information on the alignment of the  $H_2$ (EF) state molecule. Preliminary results indicate that calculations of the polarizability of the E,F state are incorrect by over two orders of magnitude.

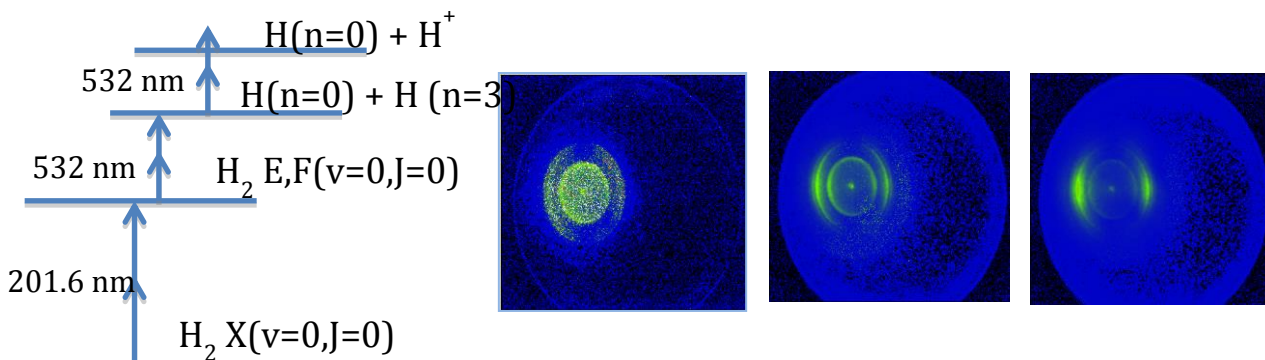


Figure 3. Schematic of experiment where a single rovibrational level of  $H_2$  is excited and then aligned and dissociated. Images representing low (532-nm laser intensity =  $1.27E^{+11}$  W/cm<sup>2</sup>), intermediate (532-nm laser intensity =  $4.80E^{+13}$  W/cm<sup>2</sup>) and high laser intensity (532-nm laser intensity =  $1.96E^{+14}$  W/cm<sup>2</sup>) are shown.

## **Present and Future work:**

### **Chemical Dynamics:**

We are building a merged molecular beam scattering apparatus such that two, short (30 microsecond initial opening time), velocity-chirped beams will collide with approximately 7 degrees of angle between the beams. With this arrangement we believe we can scan the velocity distribution of the collisions between about 5 cm<sup>-1</sup> of collision energy and 100 cm<sup>-1</sup> of collision energy. We will first investigate collisions with NO as a collision partner. Calculations on OH + H<sub>2</sub> and He as well as NH + He are also predicted to show significant resonance behavior. The energetic location of the resonances is a very stringent test of the long-range part of the potential energy surface for the collision partners and will be compared to theory. We will then move to reactive systems involving small barriers such as O(<sup>1</sup>D) + CH<sub>4</sub>. In the area of photochemistry, we will continue our study of single-quantum-state selected molecules interacting with moderately powered laser pulses for the understanding of alignment and photon/molecule interactions.

### **Spectroscopy:**

We have developed a new type of frequency-comb spectrometer using two etalons of slightly different path lengths. By measuring the interference between the outputs of the two etalons one can determine the absorption of molecules within the etalon cavities. We are continuing the development of this spectrometer and after attempting to extend this spectrometer to the near IR we have begun a new effort. We are simplifying the apparatus utilizing a single etalon containing an AR coated wave plate. This arrangement will provide two different free spectral Ranges for the same cavity for light of different orientations to the crystal axis allowing us to perform dual etalon spectroscopy with a single etalon. We will also continue to explore the use of imaging techniques to image spectroscopy, in particular to monitor Rabi cycling.

### **References:**

- 1) Cold Atoms by Kinematic Cooling, J.J. Kay, J. Klos, M. H. Alexander, K. E. Strecker, D. W. Chandler, Phys. Rev. A Vol.82 (3), 032709 (2010)
- 2) Direct Angle Resolved Measurements of Collision Dynamics with Electronically Excited State Molecules: NO(A<sup>2</sup>S<sup>+</sup>)+Ar, J. J. Kay, G Paterson, M. L. Costen, K. E. Strecker, K.G. McKendrick, D. W. Chandler., J Chem. Phys. 134, 091101 (2011)
- 3) Collisions of Electronically Excited Molecules: Differential Cross-Sections for Rotationally Inelastic Scattering of NO(A<sup>2</sup>Σ<sup>+</sup>) with Ar and He.: J. J. Kay, J. D. Steill, J. Klos, G. Paterson, M. L. Costen, K. E. Strecker, K. G. McKendrick, M. H. Alexander and D. W. Chandler, Molecular Physics 00268976.2012.670283. (2012)
- 4) Determination of the collisional energy transfer distribution responsible for the collision induced dissociation of NO<sub>2</sub> with Ar. J. D. Steill, A. W. Jasper and D. W. Chandler, Chem. Phys. Lett. Vol. 636 P 1-14 (2015).

### **Publications 2014-2016:**

- 1) Rotational Alignment of NO (A<sup>(2)</sup>Σ<sup>+</sup>) from Collisions with Ne: Steill, J. D., Kay J. J., Paterson G., Sharples T. R., Klos J., Costen M. L., Strecker K. E., McKendrick K. G., Alexander M. H., Chandler D. W., J. of Phys. Chem. Vol 117 (34), 8163-8174 (2014).
- 2) Determination of the collisional energy transfer distribution responsible for the collision induced dissociation of NO<sub>2</sub> with Ar. J. D. Steill, A. W. Jasper and D. W. Chandler, Chem. Phys. Lett. Vol. 636 P 1-14 (2015).
- 3) Imaging Spectroscopy: A novel use of Velocity Mapped Ion Imaging, Guzman J. Culberson L. Strecker K. E. Steill J. D. and Chandler D. W. Submitted to J. Chem. Phys. (2016).

## Petascale Direct Numerical Simulation and Modeling of Turbulent Combustion

Jacqueline H. Chen (PI) Yuki Minamoto and Giulio Borghesi  
Sandia National Laboratories, Livermore, California 94551-0969  
Email: [jhchen@sandia.gov](mailto:jhchen@sandia.gov)

### Program Scope

In this research program we have developed and applied massively parallel three-dimensional direct numerical simulation (DNS) of building-block, laboratory scale flows that reveal fundamental turbulence-chemistry interactions in combustion. The simulation benchmarks are designed to expose and emphasize the role of particular phenomena in turbulent combustion. The simulations address fundamental issues associated with ‘chemistry-turbulence’ interactions that underly practical combustion in engines for power generation and transportation: high pressure multi-stage autoignition, extinction and reignition, premixed and stratified flame propagation in intense shear-driven turbulence, lifted flame stabilization assisted by cool flame ignition, preferential diffusion effects on stabilization of reactive jets in crossflow, and flashback of premixed flames in boundary layers. In addition to the new understanding provided by these simulations, the DNS data are used to develop and validate predictive mixing and combustion models required in Reynolds-Averaged Navier Stokes (RANS) and large-eddy (LES) simulations.

### Recent Progress

In the past year, computer allocations from a DOE Innovative and Novel Computational Impact on Theory and Experiment (INCITE) grant have enabled us to perform several petascale three-dimensional DNS of turbulent flames with detailed chemistry. These DNS studies focused on multi-regime, multi-stage autoignition and premixed combustion to elucidate: 1) flame stabilization of a turbulent lifted dimethyl ether jet flame in the presence of low-temperature ignition, 2) velocity and scalar spectra in turbulent premixed flames, and 3) turbulent mixing effects on n-dodecane autoignition with negative temperature coefficient reactions. Highlights of our accomplishments in the past year and future directions are summarized below.

#### *Stabilizing a turbulent lifted di-methyl ether jet flame with negative temperature coefficient reactions [1]*

A three-dimensional direct numerical simulation (DNS) of a turbulent lifted dimethyl ether (DME) slot jet flame was performed at a moderate pressure of 5 bar to study interactions between chemical reactions with low-temperature heat release (LTHR), negative temperature coefficient (NTC) and shear generated turbulence in a jet in a heated coflow. By conditioning on mixture fraction, local reaction zones and local heat release rate, the turbulent flame is shown to exhibit a “pentabrachial” structure that was observed for a laminar DME lifted flame with NTC reactions and low-temperature heat release [2]. The propagation characteristics of the stabilization and triple points are also investigated. Potential stabilization points, which exhibit preferred temperature and mixture fraction conditions exhibit autoignition characteristics with large reaction rate and negligible diffusion. The stabilization point which coincides with the most upstream samples forming the potential stabilization points for each spanwise location shows passive flame structure with large diffusion. The propagation speed along the stoichiometric surface is compared with the asymptotic value obtained from theory. At stoichiometric conditions, the asymptotic and averaged DNS values of flame displacement speed deviate by a factor of 1.7. However, if the effect of low-temperature species on the local flame speed increase is accounted for, these two values become comparable. This suggests that the two-stage ignition influences the triple point propagation speed through enhancement of the laminar flame speed in a flow configuration where abundant low-temperature ignition intermediates are provided by the high-velocity jet.

#### *Dissipation spectra for velocity and reactive scalars in turbulent premixed flames [3]*

Dissipation spectra for velocity and reactive scalars - temperature and fuel mass fraction - for turbulent premixed flames were studied using DNS data of two canonical flame configurations: a temporally evolving lean hydrogen-air planar jet flame (PTJ) and a statistically stationary planar lean methane-air flame (SP). The dissipation spectra collapse when normalized by the corresponding Favre

mean dissipation rate and a cutoff length scale even though the raw spectra vary by orders of magnitude. However, the normalized spectra deviate significantly from the model spectrum of Pope [4] which is based on the classical ideas for constant density turbulence. This deviation is particularly pronounced for the high wavenumber dissipative range where a universal scaling is expected, unlike the previous studies of turbulent non-premixed combustion where good agreement with the model spectrum was reported. In the PTJ cases the dissipation spectra peak at the wavenumber corresponding to the laminar thermal thickness, consistent with a plateau in energy spectra at the same wavenumber reported in an earlier study [5]. In the SP case the peak in the dissipation spectra occurs at a lower wavenumber than that corresponding to the thermal thickness. However, in the SP case, a clear deviation in the spectra from an exponential roll-off shape is observed at the higher wavenumber corresponding to the Zeldovich thickness. While it is clear that the chemical reactions have a strong influence on the velocity and reactive scalar gradients and hence their dissipation, as manifested by the spectra, the scaling laws for this influence are still unknown, with possible dependencies on Damköhler and Karlovitz numbers, and density ratio which we will derive from dimensional analysis and assess with a parametric DNS study.

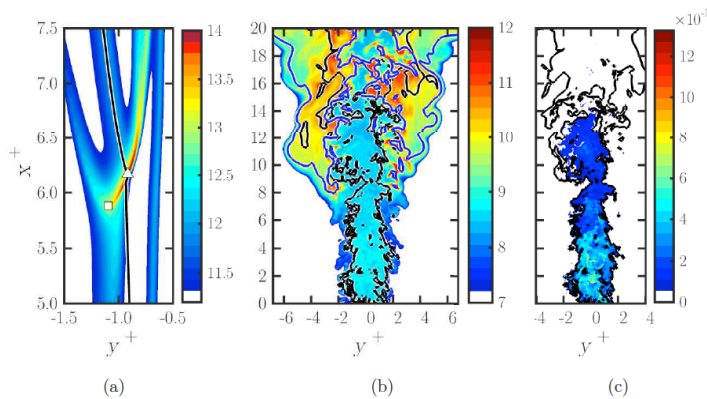


*Figure 1:* The logarithmic heat release rate field of a laminar pentabrachial flame, Ref. [2] (a). The square indicates the location of the stabilization point while the triangle indicates the location of the triple point. Instantaneous stoichiometric mixture fraction (black) and  $Y_{OH} = 0.2 Y_{OH,max}$  (blue) iso-contour lines denoting high temperature flame overlaid on the logarithm of heat release rate (b) and methoxymethyl-peroxy mass fraction,  $Y_{CH_3OCH_2O_2}$  as a low-temperature heat release marker (c) from a turbulent lifted DME jet flame in the spanwise mid plane [1].

#### Direct Numerical Simulation investigation of turbulent n-dodecane /air mixing layer autoignition [6]

A direct numerical simulation of a turbulent, self-igniting temporal mixing layer between n-dodecane and diluted air was performed to understand the influence of low-temperature chemistry on the transient dynamics of two-stage ignition. The jet parameters were selected to provide an ignition Damköhler number of 0.4, a value representative of conditions found in diesel spray flames. Chemical reactions were described by a 35-species reduced mechanism [7], including both low- and high-temperature reaction pathways of n-dodecane. Spatial inhomogeneities in the mixture composition were found to strongly affect low-temperature chemical reactions in turbulent mixtures of air and n-dodecane undergoing spontaneous ignition. High values of scalar dissipation redistribute some of the heat generated at early times in lean mixtures toward richer regions, resulting in significant low-temperature reactions occurring across a wide range of mixture compositions. However, the faster propagation of low-temperature reactions in mixture fraction space by flame propagation and diffusional processes is insufficient to compensate for the higher heat and radical losses from the ignition kernel at high values of scalar dissipation, thus leading to a longer hot-flame ignition delay time as the scalar dissipation rate increases.

#### **Future Work:**

##### Multi-Stage ignition and transition to partially-premixed flame propagation

In studying the spontaneous ignition of a two-dimensional turbulent mixing layer between diluted dimethyl ether and air, Krisman et al. [8] found that cool flame autoignition at fuel rich locations occurs

earlier than in homogeneous reactor calculations; additionally, it was observed that, as a consequence of fast propagation of the cool flame in mixture fraction space, hot flame ignition occurred first in mixture pockets with a composition much richer than the most reactive mixture fraction, and at times comparable to the minimum ignition delay time, or even shorter. We plan to further investigate the diffusional processes associated with low-temperature ignition and cool flame propagation and their influence on hot flame ignition for a range of diesel fuels exhibiting different octane sensitivities. We plan to also study the transition from hot flame ignition to the establishment of a turbulent lifted flame, including the role of edge flame propagation affected by NTC reactions.

#### References:

1. Y. Minamoto and J. H. Chen, (2016) "DNS of a turbulent lifted di-methyl ether jet flame," in press *Combustion and Flame*.
2. A. Krisman, E. R. Hawkes, M. Talei, A. Bhagatwala, J. H. Chen, (2015) "Tribrachial, tetrabrachial and pentabrachial structures in dimethyl ether edge-flames at NTC conditions," *Proc. Combust. Inst.* 35(1): 999-1006.
3. H. Kolla, X. Zhao, J. H. Chen, N. Swaminathan (2016) "Velocity and reactive scalar dissipation spectra in turbulent premixed flames," in press *Combustion Science and Technology*.
4. S.B. Pope, *Turbulent Flows*, Cambridge University Press, Cambridge, 2000.
5. H. Kolla, E. R. Hawkes, A. Kerstein, N. Swaminathan, J. H. Chen, "On velocity and reactive scalar spectra in highly turbulent premixed flames," *Journal of Fluid Mechanics* (2014) 754:456-487.
6. G. Borghesi and J. H. Chen, (2016) "A DNS investigation of turbulent n-dodecane/air mixing layer autoignition," Western States Section of the Combustion Institute Spring 2016 Meeting, March 21-22, 2016.
7. T. Lu, <http://www.engr.uconn.edu/~tlu/mechs/mechs.htm>. Accessed: 2010-09-30.
8. A. Krisman, E. R. Hawkes, M. Talei A. Bhagatwala, J. H. Chen, (2017) "A DNS of a cool-flame affected autoignition in diesel engine-relevant conditions," in press *Proc. Combust. Inst.*, 36.

#### BES Publications (2014-2016)

1. A. Gruber, P. Salimath, J. H. Chen, "Direct numerical simulation of laminar flame-wall interaction for a novel H<sub>2</sub>-selective membrane / injector configuration" *Intl Journal of Hydrogen Energy* (2014) 39:5906-5918.
2. A. Bhagatwala, T. Lu, and J. H. Chen, "Direct numerical simulations of HCCI/SACI with ethanol," *Combustion and Flame* (2014) 161:1826-1841.
3. A. Krisman, J. Tang, E. R. Hawkes, D. Lignell, and J. H. Chen, "A DNS evaluation of mixing models for transported PDF modelling of turbulent nonpremixed flames," *Combustion and Flame* (2014)161:2085-2106.
4. Y. Xin, C. S. Yoo, J. H. Chen, C. K. Law, "A DNS study of self-accelerating cylindrical hydrogen-air flames with detailed chemistry," *Proc. Combust. Inst.*, 35 (2015) 753-760.
5. A. Bhagatwala, T. Lu, H. Shen, J. Sutton, J. H. Chen, "Numerical and experimental investigation of turbulent DME jet flames," *Proc. Combust. Inst.*, 35 (2015) 1157-1166.
6. A. Krisman, E. R. Hawkes, M. Talei, A. Bhagatwala, J. H. Chen, "Tribrachial, tetrabrachial and pentabrachial structures in dimethyl ether edge-flames at NTC conditions," *Proc. Combust. Inst.* 35, (2015) 999-1006.
7. A. Gruber, A. Kerstein, D. Valiev, H. Kolla, J. H. Chen, "Modelling of Mean Flame Shape During Premixed Flame Flashback in Turbulent Boundary Layers," *Proc. Combust. Inst.*, 35 (2015) 1485-1492.
8. R. A. C. Griffiths, J. H. Chen, H. Kolla, R. S. Cant, W. Kollmann, "Three-dimensional topology of turbulent premixed flame interaction," *Proc. Combust. Inst.*, 35 (2015) 1341-1348.
9. Chan, W. L., Kolla, H., Chen, J. H., Ihme, M., "Assessment of model assumptions and budget terms of the unsteady flamelet equations for a turbulent reacting jet-in-crossflow," *Combustion and Flame* (2014) 161:2601-2613.
10. Bansal, G., Mascarenhas, A. and Chen, J. H., "Direct numerical simulation of autoignition in stratified dimethyl-ether (DME)/Air turbulent mixtures," *Combustion and Flame* (2015) 162:688-702.
11. Kolla, H., Hawkes, E. R., Kerstein, A. R., Swaminathan, N., Chen, J. H., "On velocity and reactive scalar spectra in highly turbulent premixed flames," *Journal of Fluid Mechanics* (2014) 754:456-487.
12. Lyra, S., Wilde, B., Kolla, H., Seitzman, J., Lieuwen T., Chen, J. H., "Structure and stabilization of hydrogen-rich transverse jets in a vitiated turbulent flow," *Combustion and Flame*, (2015) 162:1234-1248.
13. Scholtissek, A., Chan, W. L. Xu, H., Hunger, F., Kolla, H., Chen, J. H., Ihme, M., Class, A., "A multi-scale asymptotic analysis of flamelet equations including tangential diffusion effects for laminar and turbulent flames," *Combustion and Flame* (2015) 162:1507-1529.

14. S. Kim, M. B. Luong, J. H. Chen, C. S. Yoo, "A DNS study of the ignition of lean PRF/air mixtures with temperature inhomogeneities under high pressure and intermediate temperature," *Combustion and Flame*, (2015) **162**:717-726.
15. C. Bruno, V. Sankaran, H. Kolla and J. H. Chen, "Impact of multi-component diffusion in turbulent combustion using direct numerical simulations," *Combustion and Flame*, (2015) **162**(11):4313-4330.
16. R. Sankaran, E. R. Hawkes, C. S. Yoo, and J. H. Chen, "Response of flame thickness and propagation speed under intense turbulence in spatially developing lean premixed methane-air jet flames," *Combustion and Flame*, (2015), **162** (9): 3294-3306.
17. Y. Minamoto, H. Kolla, R. W. Grout, A. Gruber, and J. H. Chen, "Effect of fuel composition and differential diffusion on flame stabilization in reacting syngas jets in turbulent cross-flow," *Combustion and Flame*, (2015) **162**(10): 3569-3579.
18. Z. Jozefik, A. R. Kerstein, H. Schmidt, S. Lyra, H. Kolla, J. H. Chen, "One-dimensional turbulence modeling with comparison to DNS," *Combustion and Flame* (2015), **162**: 2999-2015.
19. S. Karami, E. R. Hawkes, M. Talei, and J. H. Chen, "Mechanisms of flame stabilization at low lifted height in a turbulent lifted slot-jet flame," *J. Fluid Mech.* (2015) **777**:633-689.
20. H. S. Bak, S. R. Lee, J. H. Chen, and C. S. Yoo, "A numerical study of the diffusive-thermal instability of opposed nonpremixed tubular flames," *Combustion and Flame* (2015), **162**:4612-4621.
21. Bhagatwala, A., Sankaran, R., Kokjohn, S., Chen, J. H., (2015) Numerical investigation of spontaneous flame propagation in RCCI conditions, *Combustion and Flame*, **162**(9): 3412-3426.
22. Zhao, X., Bhagatwala, A., Chen, J. H., Haworth, D. C., Pope, S. B., (2016) "An a priori DNS study of the shadow-position mixing model," *Combustion and Flame*, **165**:223-245.
23. Karami, S., Hawkes, E. R., Talei, M., Chen, J. H. (2016) "Edge flame structure in a turbulent lifted flame: a direct numerical simulation study," in press *Combustion and Flame*.
24. Gao, Y., Shan, R., Lyra, S., Li, C., Wang, H., Chen, J. H., Lu, T., (2016) "A lumped-reduced reaction model for combustion of liquid fuels," *Combustion and Flame*, **163**:437-446.
25. Y. Gao, H. Kolla, J. H. Chen, N. Swaminathan, and N. Chakraborty, (2016) "A comparison of scalar dissipation rate transport between simple and detailed chemistry based on direct numerical simulations," in press *Combustion Theory and Modeling*.
26. H. Kolla, X. Zhao, J. H. Chen, N. Swaminathan (2016) "Velocity and reactive scalar dissipation spectra in turbulent premixed flames," in press *Combustion Science and Technology*.
27. Y. Minamoto and J. H. Chen, (2016) "DNS of a turbulent lifted di-methyl ether jet flame," in press *Combustion and Flame*.
28. F. Salehi, M. Talei, E. R. Hawkes, A. Bhagatwala, J. H. Chen, S. Kook, (2016) "Doubly conditional moment closure modeling for HCCI with temperature inhomogeneities," submitted to *Proc. Combust. Inst.*, 36.
29. A. Krisman, E. R. Hawkes, M. Talei A. Bhagatwala, J. H. Chen, (2016) "A DNS of a cool-flame affected autoignition in diesel engine-relevant conditions," submitted to *Proc. Combust. Inst.*, 36.
30. H. Wang, E. R. Hawkes, B. Zhou, J. H. Chen, Z. Li, M. Alden, (2016) "A comparison between DNS and experiment of the turbulent burning velocity-related statistics in a turbulent methane-air premixed jet flame at high Karlovitz number," submitted to *Proc. Combust. Inst.*, 36.
31. S. Karami, M. Talei, E. R. Hawkes, and J. H. Chen, (2016) "Local extinction and reignition mechanism in a turbulent lifted flame: a DNS study," submitted to *Proc. Combust. Inst.*, 36.
32. E. S. Richardson and J. H. Chen, (2016) "Analysis of turbulent flame propagation in equivalence ratio-stratified flow," submitted to *Proc. Combust. Inst.*, 36.
33. M. Kuron, Z. Ren, H. Zhou, E. Hawkes, J. Tang, J. H. Chen, and T. Lu, (2016) "Performance of transported PDF mixing models in a turbulent premixed flame," submitted to *Proc. Combust. Inst.*, 36.
34. H. Wang, E. R. Hawkes, and J. H. Chen, (2016) "A Direct Numerical Simulation study of flame structure of an experimental high Karlovitz CH<sub>4</sub>/air flame," submitted to *Combustion and Flame*.
35. H. Wang, E. R. Hawkes, and J. H. Chen, B. Zhou, M. Li, M. Alden, (2016) submitted to "Petascale direct numerical simulation of a high Ka laboratory premixed jet flame," submitted to *J. Fluid Mech. Rapids*.
36. Pouransari, H. Kolla, J. H. Chen, and A. Mani, (2016) "Spectral analysis of energy transfer in turbulent flows laden with heated particles," submitted to *J. Fluid Mech.*
37. H. Wang, E. R. Hawkes, and J. H. Chen, (2016) "Turbulence-flame interactions in DNS of a laboratory high Karlovitz premixed turbulent jet flame," submitted to *Physics of Fluids*.
38. S. Lyra, H. Kolla, and J. H. Chen, (2016) "Counterflow H<sub>2</sub>/air premixed flames under intense turbulence and strain," submitted to *Intl. Journal of Hydrogen Energy*.

# Dynamics and Energetics of Elementary Combustion Reactions and Transient Species

## Grant DE-FG03-98ER14879

Robert E. Continetti (rcontinetti@ucsd.edu)

Department of Chemistry and Biochemistry, University of California San Diego  
9500 Gilman Drive, La Jolla, CA 92093-0340

## I. Program Scope

An important goal for combustion chemists is the development of first-principles approaches towards the calculation of potential energy surfaces and the dynamics of molecular collisions for combustion-relevant systems. The research program described here centers on experimental studies of transient neutral species and collision complexes, with the goal of providing benchmarks for theoretical studies of fundamental elementary reactions relevant to combustion phenomena. The experimental approach makes use of kinematically complete measurements of dissociative photodetachment (DPD) processes that anionic precursors undergo to provide a novel measure of the dynamics of unimolecular and bimolecular reactions. Photoelectron-photofragment coincidence (PPC) studies like these can be used to sample the chemical dynamics over a wide range of internal and configurational energies in a single experiment, providing a rigorous test of potential energy surface and dynamics calculations. Examples of the interplay between theory and experiment that can be provided in this manner were shown in the experimental-theoretical study reported on the  $F + H_2O \rightarrow HF + OH$  reaction in collaboration with Hua Guo and co-workers, (DOE Pub. 2), as well as a collaboration with Al Wagner and colleagues extending in a more quantitative fashion our quasi-1D model for the deep tunneling in that system and applying it to *ab initio* HOCO potential energy surfaces (DOE Pub. 5). Experimentally, the last year was spent bringing the PPC spectrometer back on-line following required maintenance beginning in December 2014 as well as commissioning of a cryogenic octupole accumulator trap (COAT) in the ion source to allow buffer gas cooling of polyatomic anions ultimately to temperatures  $< 10$  K. These efforts have been successful, and will be illustrated by a discussion of measurements of the dramatic effect anion temperature has in the UV photodetachment and photodissociation (388 nm, 3.2 eV) of the ozonide anion,  $O_3^-$ . In addition, further developments in the analysis of the  $F + CH_3OH \rightarrow HF + CH_3O$  reaction will be discussed. Manuscripts on isotopologs of  $F + H_2O$ , the effects of vibrational excitation in that system and with studies of the spectroscopy and dynamics of the propiolyl radical,  $HC_2CO_2$ , are also anticipated to be published this year. In the following sections, recent progress will be reviewed in more detail, followed by a brief discussion of future work.

## II. Recent Progress

### A. Transition State Dynamics of the $F + HOCH_3 \rightarrow HF + OCH_3$ Reaction

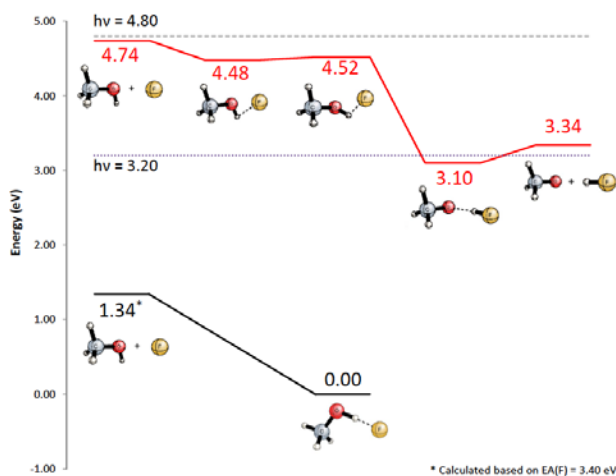


**Figure 1.** Calculated energetics for the  $F + CH_3OH \rightarrow HF + OCH_3$  reaction and the  $F^-(CH_3OH)$  anion at the CCSD(T)/aug-cc-pVTZ level of theory.

The exothermic reactions of fluorine atoms with small molecules, beginning with the  $F + H_2$  reaction, have provided a rich ground for the development of multidimensional potential energy surfaces and theories of chemical reaction dynamics. Extending these studies to higher dimensionality, our recent study of the  $F + H_2O \rightarrow HF + OH$  reaction<sup>1</sup> represents a system with six degrees of freedom at the frontier of both quantum chemistry and quantum dynamics calculations.<sup>2-6</sup> We have now further extended these efforts to higher dimensionality systems by carrying out PPC studies on  $F^-(CH_3OH)$ , nominally producing the  $F(CH_3OH)$  complex in the vicinity of the submerged barrier on the  $F + CH_3OH \rightarrow HF +$

OCH<sub>3</sub> potential energy surface. This system, with 7 atoms and 15 degrees of freedom, remains beyond the limit of full-dimensionality quantum dynamics calculations, but is a tractable system for high accuracy electronic structure calculations, as illustrated by the recent work by Schaefer and co-workers.<sup>7</sup> The energetics of photodetachment in this system as well as important stationary points on the neutral potential energy surface are shown in Figure 1. These energetics were provided through a collaboration with Agarwal and Schaefer who have carried out high level calculations (CCSD(T)/aug-cc-pVTZ) at a consistent level of theory for both the anionic and neutral complexes including zero-point-energy corrections.<sup>8</sup> Figure 1 shows that at a photon energy of 4.80 eV there is sufficient energy to access both reactant (barely) and product channels as well as the submerged barrier separating the entrance and exit channel van der Waals complexes.

PPC measurements on F<sup>-</sup>(CH<sub>3</sub>OH) at photon energies of 4.80 and 3.20 eV allowed studies of both stable and dissociative neutral complexes. Complexes that are stable on the timescale of the the 8.4 μs flight time from the interaction region to the neutral particle detector, or dissociate with

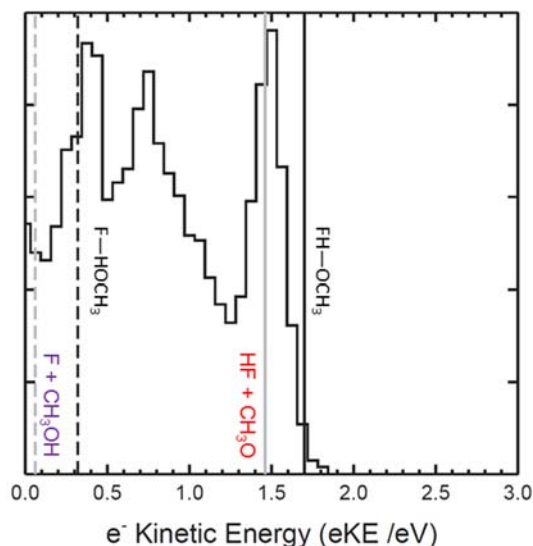


**Figure 2.** Photoelectron spectrum of the stable ( $e^- + 1$  neutral) channel at 4.80 eV (258 nm). The black vertical lines indicate the ZPE corrected, calculated EAs for the entrance (dashed) and exit (solid) complexes. The grey vertical lines correspond to the ZPE corrected, calculated KEmax for dissociation to either reactants (dashed) or products (solid) where products are formed in their vibrational and rotational ground states.

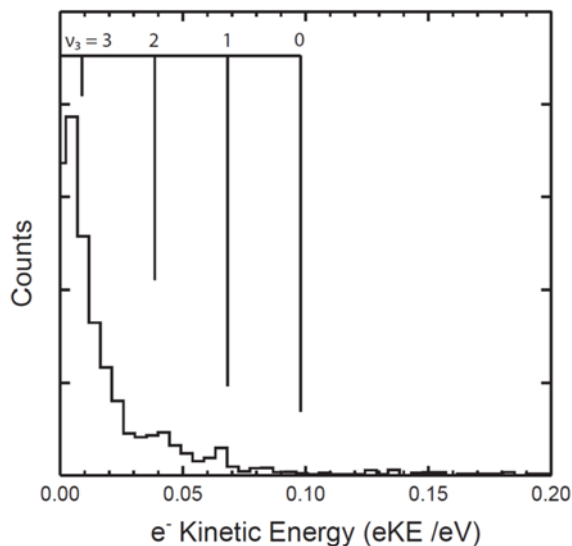


**Figure 3.** Threshold photoelectron spectrum of the stable ( $e^- + 1$  neutral) channel at 3.20 eV (388 nm). Features associated with a progression in  $v_3$  in the FH-OCH<sub>3</sub> entrance channel complex are indicated by the comb.

exceedingly small kinetic energy release, are shown in Figure 2 at a photon energy of 4.80 eV. The prominent peaks at 1.5 eV and 0.4 eV in this spectrum are assigned to the exit channel (FH—OCH<sub>3</sub>) and (tentatively) the entrance channel (F—HOCH<sub>3</sub>) van der Waals complexes, respectively. The assignment of the peak near 0.75 eV is likely a long-lived metastable complex (a vibrational Feshbach resonance) in the FH( $v=2$ )-OCH<sub>3</sub> exit channel van der Waals complex, similar to the F + H<sub>2</sub>O reaction. The energetics in Figure 1 are in excellent agreement with the observed exit channel complex, while the results for the entrance channel complex peak at greater energy than predicted. We are continuing to work with the Schaefer and Stanton groups to resolve the reason for this discrepancy. It is possible that this feature corresponds to another Feshbach resonance, but beam energy dependence measurements (not shown here) indicate that the state is long-lived like the exit channel complex feature peaking at eKE = 1.5 eV. Figure 3 shows a threshold photoelectron spectrum for the system recorded at a photon energy of 3.20 eV. The leading comb shows the theoretically predicted adiabatic EA for the system, and the series of features indicated by the comb are consistent with a progression in  $v_3 = 241$  cm<sup>-1</sup>, as calculated by Schaefer and co-workers, an FH-OCH<sub>3</sub> stretching mode coupled with an OCH<sub>3</sub> rock. These experiments would obviously benefit from a higher resolution

photoelectron spectrum, such as the slow electron velocity map imaging (SEVI) of Neumark and co-workers.

## B. Cryogenic Octupole Accumulator Trap (COAT) – Cooling of Ozonide Anion, $O_3^-$

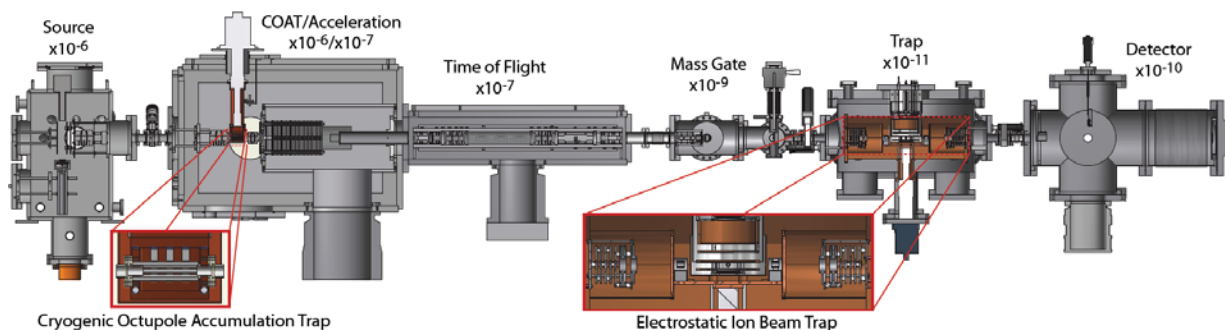


**Figure 4.** The current configuration of the photoelectron-photofragment coincidence spectrometer, showing addition of a Wiley-McLaren pulsed discharge ion source for loading the new buffer-gas cooling cryogenic octupole accumulator trap (COAT), which is then used to inject ions into the electrostatic ion beam trap (EIBT) for PPC measurements.

We have recently completed commissioning of a new cryogenic octupole accumulation trap (COAT) providing the ability to collisionally cool precursor anions, as well as the ability to heat them through energetic collisions with helium buffer gas. We are currently able to achieve a trap temperature of 18 K with a trapping time greater than 80 ms and can accumulate ions over several pulses from the Wiley-McLaren style ion source. For the demonstration of the capabilities of COAT,

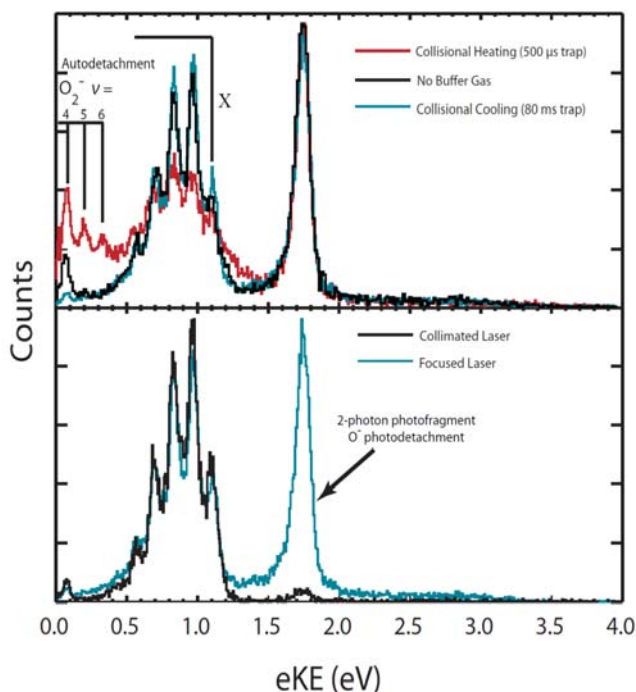


**Figure 5.** The top panel shows the photoelectron spectrum for  $O_3^-$  under three different trapping conditions within COAT leading to controlled heating (red) and cooling (blue) of precursor anions via buffer gas compared to the ion internal excitation from supersonic expansion alone (black). The bottom panel shows the peak at 1.74 eV eKE is a result of a 2-photon process involving photodetachment of the  $O^-$  photodissociation product.

we have examined the photochemistry of the  $O_3^-$  anion at 388 nm. In the near UV,  $O_3^-$  exhibits both direct photodetachment as well as two photofragmentation channels as shown by the data in Figure 5. Of particular interest is the autodetachment channel of  $O_2^- X^2\Pi$  which is predicted to be governed by a Feshbach resonance in the  $^2A_2$  excited state of  $O_3^-$ .<sup>9</sup> The onset for autodetachment after photofragmentation occurs when the product  $O_2^-$  contains  $v \geq 4$ . As Figure 6 shows, only  $v=4$  is energetically accessible from cold  $O_3^-$  precursor anion at 388 nm. Collisional heating is achieved by colliding the anions with the buffer gas at a high energy while trapping within COAT for a short period of time (500  $\mu$ s), ejecting them from the trap before they thermalize with the cold buffer gas. The photofragmentation of the internally excited  $O_3^-$  anion allows access to  $O_2^-$  products with  $v = 5$  and 6 quanta of vibrational excitation in addition to increasing the probability of 4 quanta of excitation in  $O_2^-$ . Increasing the trapping time to 80 ms gives the ions time to thermalize with the cold buffer gas resulting in removal of the  $v = 5$  and  $v = 6$  autodetachment signal with significant reduction in the  $v = 4$  channel as shown in the collisionally cooled traces in Figure 5. Now

that we have demonstrated our capability to influence the internal excitation of the anion precursor in a controlled manner, we look forward to beginning to examine larger polyatomic systems. This effort is motivated by our recent study of the photodetachment of tert-butoxide with both non-deuterated and deuterated precursors,  $(\text{CH}_3)_3\text{CO}^-$  and  $(\text{CD}_3)_3\text{CO}^-$ , as reported in DOE pub. 6. Those experiments revealed a DPD channel, involving the loss of a methyl radical. An examination of the energetics for this channel showed it could only be the result of two possible reaction pathways: from the carbanion isomer, (a)  $(\text{CH}_3)_2\text{COHCH}_2^- + h\nu \rightarrow \text{CH}_3 + \text{CH}_3\text{COHCH}_2$  or tert-butoxide, (b)  $(\text{CH}_3)_3\text{CO}^- + h\nu \rightarrow \text{CH}_3 + (\text{CH}_3)_2\text{CO}$  (acetone). It was concluded, with support from Franck-Condon simulations, that pathway (b) was observed as result of non-Boltzmann internally excited tert-butoxide anion precursors characterized by temperatures up to 1400K along critical C-C stretching modes. With the new COAT, we should be able to effectively quench vibrational and rotation excitation prior to injection into the EIBT and eliminate these kinds of pernicious hot band phenomena.

### C. Future Work

In the coming months, with the PPC spectrometer now back on-line, we look forward to examining a range of systems, including the  $\text{O} + \text{CH}_4 \rightarrow \text{OH} + \text{CH}_3$  radical-radical reaction, by photodetachment of  $\text{O}^-(\text{CH}_4)$ , as well as other systems including  $\text{OH}-\text{C}_2\text{H}_2$ ,  $\text{OH}-\text{C}_2\text{H}_4$  and the  $\text{OH} + \text{NH}_3$  system. These efforts will be assisted by the implementation of the dual pulsed valve ion source configuration recently described by Lineberger and co-workers,<sup>10</sup> enabling the synthesis of a wide range of anionic complexes as precursors to systems of combustion interest.

### D. DOE-supported publications by this project 2013-2016

1. A.W. Ray, B.B. Shen, B.L.J. Poad and R.E. Continetti, *State-resolved predissociation dynamics of the formylxyl radical*, Chem. Phys. Lett. **592**, 30-35 (2014).
2. R. Otto, J. Ma, A.W. Ray, J.S. Daluz, J. Li, H. Guo and R.E. Continetti, *Imaging dynamics on the  $F + \text{H}_2\text{O} \rightarrow \text{HF} + \text{OH}$  potential energy surfaces from wells to barriers*, Science, **343**, 396-399 (2014).  
DOE BES Highlight <http://science.energy.gov/bes/highlights/2014/bes-2014-10-d/>
3. R. Otto, A.W. Ray, J.S. Daluz and R.E. Continetti, *Direct IR excitation in a fast ion beam: Application to  $\text{NO}^-$  photodetachment cross sections*, EPJ Techniques and Instrumentation **1**:3 (2014).
4. A.F. Wagner, R. Dawes, R.E. Continetti and H. Guo, *Theoretical/experimental comparison of deep tunneling decay of quasi-bound  $\text{H}(\text{D})\text{OCO}$  to  $\text{H}(\text{D})+\text{CO}_2$* , J. Chem. Phys. **141**, 054304 (2014).
5. C.J. Johnson, R. Otto and R.E. Continetti, *Spectroscopy and dynamics of the  $\text{HOCO}$  radical*, Phys. Chem. Chem. Phys. **16**, 19091-19105 (2014).
6. B.B. Shen, B.L.J. Poad and R.E. Continetti, *Photoelectron-photofragment coincidence studies of the tert-butoxide anion  $(\text{CH}_3)_3\text{CO}$ , the carbanion isomer  $(\text{CH}_3)_2\text{CH}_2\text{COH}$  and corresponding radicals*, J. Phys. Chem. A **118**, 10223-10232 (2014).

### E. References

1. Otto, R.; Ma, J.; Ray, A. W.; Daluz, J. S.; Li, J.; Guo, H.; Continetti, R. E., *Science* **2014**, *343*, 396-399.
2. Li, G.; Zhou, L.; Li, Q.-S.; Xie, Y.; Schaefer, H. F., *Phys. Chem. Chem. Phys.* **2012**, *14*, 10891-10895.
3. Li, J.; Dawes, R.; Guo, H., *J. Chem. Phys.* **2012**, *137*, 094304.
4. Li, G.; Li, Q.-S.; Xie, Y.; Schaefer, H. F., *J. Phys. Chem. A* **2013**, *117*, 11979-11982.
5. Nguyen, L.; Li, J.; Dawes, R.; Stanton, J. F.; Guo, H., *J. Phys. Chem. A* **2013**, *117*, 8864-8872.
6. Li, J.; Jiang, B.; Guo, H., *J. Chem. Phys.* **2013**, *138*, 074309.
7. Feng, H.; Randall, K. R.; Schaefer, H. F., *J. Phys. Chem. A* **2015**, *119*, 1636-1641.
8. Agarwal, J.; Schaefer, H. F., private communication, **2015**.
9. Mann, J. E.; Troyer, M. E.; Jarrold, C. C., *J. Chem. Phys.* **2015**, *142*, 124305.
10. Lu, Y.-J.; Lehman, J. H.; Lineberger, W. C., *J. Chem. Phys.* **2015**, *142*, 044201.

## Vibrational Dynamics and Dissociation of Ground- and Excited-State Clusters

F.F. Crim  
Department of Chemistry  
University of Wisconsin–Madison  
Madison, Wisconsin 53706  
fcrim@chem.wisc.edu

Our research investigates the chemistry of vibrationally excited molecules. The properties and reactivity of vibrationally energized molecules are central to processes occurring in environments as diverse as combustion, atmospheric reactions, and plasmas and are at the heart of many chemical reactions. The goal of our work is to unravel the behavior of vibrationally excited molecules and to exploit the resulting understanding to determine molecular properties and to control chemical processes. A unifying theme is the preparation of a molecule in a specific vibrational state using one of several excitation techniques and the subsequent photodissociation of that prepared molecule. Because the initial vibrational excitation often alters the photodissociation process, we refer to our double-resonance photodissociation scheme as *vibrationally mediated photodissociation*. In the first step, fundamental or overtone excitation prepares a vibrationally excited molecule, and then a second photon, the photolysis photon, excites the molecule to an electronically excited state from which it dissociates. Vibrationally mediated photodissociation provides new vibrational spectroscopy, measures bond strengths with high accuracy, alters dissociation dynamics, and reveals the properties of and couplings among electronically excited states.

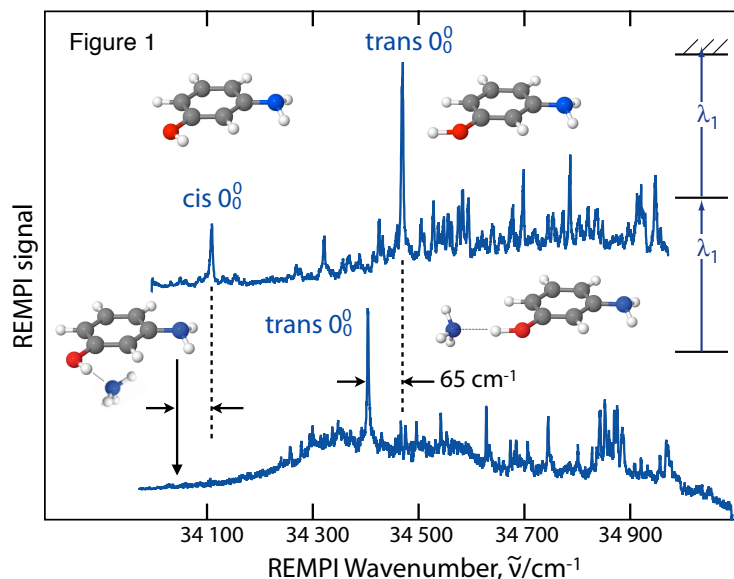
Our recent research on vibrational dynamics in clusters has produced new insights into ammonia clusters, one of the prototypical hydrogen-bonded systems. We have determined the dissociation energy of the dimer very precisely ( $660\pm 20\text{ cm}^{-1}$ ) and obtained an experimental estimate of the dissociation energy of the trimer ( $1600\pm 100\text{ cm}^{-1}$ ). The dynamics we probe show selective coupling of vibrational energy during the dissociation of the dimer. These studies have led us into new studies of ammonia-containing complexes that build on our previous investigations, and we have obtained intriguing results on vibrationally induced isomerization in the complex of ammonia with a substituted phenol. An extension of this research is now probing the excited-state dynamics of a halomethane,  $\text{CHBrCl}_2$ .

### Aminophenol-Ammonia Complexes

We studied the complex of 3-aminophenol with ammonia to understand its bond-strength and its vibrational predissociation as we move toward studying its excited-state dissociation. There are two conformers of 3-aminophenol corresponding to different orientations of the O-H bond. The structures in the top portion of Fig. 1 illustrate the slightly higher energy *cis* conformer and the lower energy *trans* conformer. The spectrum in the top of Fig. 1 is the (1+1) REMPI spectrum of 3-aminophenol with the *cis* and *trans* origins marked. [W. Y. Sohn, *et al.*, Phys. Chem. Chem. Phys. 13, 7006 (2011).] The spectrum in the bottom of the figure is that of the complex, in which the *trans* origin appears about  $65\text{ cm}^{-1}$  below that of the bare 3-aminophenol, but the *cis* isomer does not appear, possibly because of interconversion between the two conformers during the formation of the complex.

We have recently observed the influence of vibrational excitation on the complex by obtaining the REMPI spectrum after exciting the ammonia cluster (3-AP-NH<sub>3</sub>) in the OH stretching and NH stretching regions. The vibrational energy is sufficient to dissociate the cluster into its constituent 3-AP and NH<sub>3</sub> monomers, and we detect the 3-AP fragments *via* (1+1) resonance-enhanced multiphoton ionization (REMPI). The distribution of vibrational-state population of the 3-AP fragment suggests the presence of

two distinct dissociation pathways. The first dissociation channel produces a broad, unstructured predissociation feature in the REMPI-action spectrum after excitation of any of the O-H or N-H stretching vibrations, suggesting a nearly statistical dissociation pathway with strong coupling of the vibrations in the cluster during the predissociation. The second dissociation channel produces sharp features on top of the broad predissociation features, but only following excitation of the OH stretch or the symmetric NH<sub>3</sub> stretch in the cluster. This striking mode-specificity is consistent with strong coupling of these two modes to the dissociation coordinate (the O-H...N bond). The presence of clearly resolved transitions to the electronic origin and to the  $10a_0^2 + 10b_0^2$  state of the *cis*-3-AP isomer shows that vibrational excitation is driving the isomerization of the *trans*-isomer to the *cis*-isomer in the course of the dissociation of the cluster.



### Dissociation of a Halomethane , CHBrCl<sub>2</sub>

We have returned to the velocity-mapped ion imaging technique of our earlier ammonia studies to investigate the recoil energies and relative product yields in the dissociation of CHBrCl<sub>2</sub> in the range of 215 - 265 nm. The low symmetry of this molecule brings many close-lying electronic states in to play, and we are able to detect both the ground-state Br fragment and the spin-orbit excited-state Br\* fragment. The anisotropy of both channels increases with increasing wavelength, and the fractional energy released into translation increases slightly for longer wavelengths as well. However, the anisotropy of the distribution for the ground-state fragment shows a distinct minimum at intermediate wavelengths that may reflect the competition of direct and indirect dissociation on several of the intersecting surfaces.

### Future Directions

We are now in the midst of exploring the influence of vibration on the dynamics of a complex. Our future work goes in two directions. One is similar experiments in other complexes, and the other is to observe the effect of vibrational excitation and the presence of an adduct on the dissociation of electronically excited complexes. We have proven that vibrational excitation of NH<sub>3</sub> drastically alters its dissociation by changing the behavior at a conical intersection. Now we can understand that behavior in different complexes where an adduct will influence the dynamics also.

## PUBLICATIONS SINCE 2012 SUPPORTED BY DOE

A. S. Case, C. G. Heid, C. M. Western, and F. F. Crim, *Determining the dissociation threshold of ammonia trimers from action spectroscopy of small clusters*, J. Chem. Phys. **136**, 124310 (2012).

*Molecular Reaction Dynamics Across the Phases: Similarities and Differences*. F. Fleming Crim, Faraday Discussions **157**, 1 (2012).

*Vibrational Predissociation and Vibrationally Induced Isomerization of 3-Aminophenol-Ammonia*. Cornelia Heid, Wyatt Merrill, Amanda Case, and F. Fleming Crim, J. Chem. Phys. **142**, 014310 (2015).



## Annual Progress Report on project entitled “Theoretical Investigation of Kinetic Processes in Small Radicals” (ER16100)

Paul J. Dagdigian (pjdagdigian@jhu.edu),  
Department of Chemistry, The Johns Hopkins University of Maryland, Baltimore, MD 21218-2685  
Millard H. Alexander (mha@umd.edu),  
Department of Chemistry and Biochemistry, University of Maryland, College Park, MD 20742-2021

### Program Scope

Our group studies inelastic and reactive collisions of small molecules, focusing on radicals important in combustion environments. The goal is the better understanding of kinetic processes that may be difficult to access experimentally. An essential component is the accurate determination and fitting of potential energy surfaces (PESs). We use time-independent (close-coupling) methods to treat the dynamics. We have studied energy transfer (rotationally, vibrationally, and/or electronically inelastic) in small hydrocarbon radicals ( $\text{CH}_2$  and  $\text{CH}_3$ ) and the CN radical. We have made a comparison with experimental measurements of relevant rate constants for collisions of these radicals. We are calculating accurate transport properties using state-of-the-art PESs and to investigate the sensitivity to these of 1-dimensional flame simulations. Of particular interest are collision pairs involving the light H atom.

### Personnel

Millard H. Alexander, University of Maryland, Principal Investigator  
Paul J. Dagdigian, The Johns Hopkins University, Principal Investigator  
Jacek Klos, University of Maryland, Research Assistant Professor  
Lifang Ma, University of Maryland, Graduate Research Assistant (Ph.D., 2014)  
Qianli Ma, The Johns Hopkins University, Graduate Research Assistant (Ph.D., 2014)

### Recent Progress and Future Work

#### *Collisional Relaxation*

We have carried out an extensive study of the collisional relaxation of methylene ( $\text{CH}_2$ ), a system studied extensively at Brookhaven by the group of Hall and Sears. We determined determined potential energy surfaces (PES's) for the interaction of  $\text{CH}_2$  in both its ground  $X^3B_1$  and singlet excited  $a^1A_1$  electronic states with the He atom. By quantum scattering calculations we determined state-to-state integral cross sections for rotationally inelastic transitions and rate constants for total removal of given rotational levels [1,4]. The latter agreed well with the Brookhaven results. Vibrational relaxation of the bending mode of  $\text{CH}_2(X)$  in collisions with He is two orders of magnitude less efficient than rotational relaxation [14].

We also studied collision-induced internal conversion (CIIC) from the  $a$  to the  $X$  state of  $\text{CH}_2$ , a process mediated by the weak spin-orbit coupling between pairs of accidentally-degenerate rotational levels. In our use of the “gateway” model, CIIC is facilitated by coherent mixing of the scattering  $T$ -matrix elements for collisional transitions involving the few accidentally degenerate rotational states. [13]. We then used our calculated CIIC and pure-rotational rate constants in a kinetic simulation [3] of the collisional relaxation of  $\text{CH}_2(X,a)$  in collisions with He. Figure 1 presents snapshots, following the relaxation of the  $8_{18}$  mixed, nominal  $a$  state, studied at Brookhaven. Relaxation proceeds in three steps: (1) rapid equilibration of the two mixed-pair levels [ $a(0,0,0)8_{18}$  and  $X(0,2,0)9_{37}$ , in Fig. 1], (2) fast relaxation within the  $a$  state, and (3) slower relaxation among the  $X$ -state levels.

Stimulated by our theoretical work on rotational energy transfer in  $\text{CH}_3$ -He collisions [2], Orr-Ewing (Bristol, UK) applied molecular beam and velocity map imaging to the determination of differential cross sections for scattering of photolytically generated beam of  $\text{CD}_3$  with a number of collision partners. REMPI detection of the scattered  $\text{CD}_3$  allowed resolution of the rotational

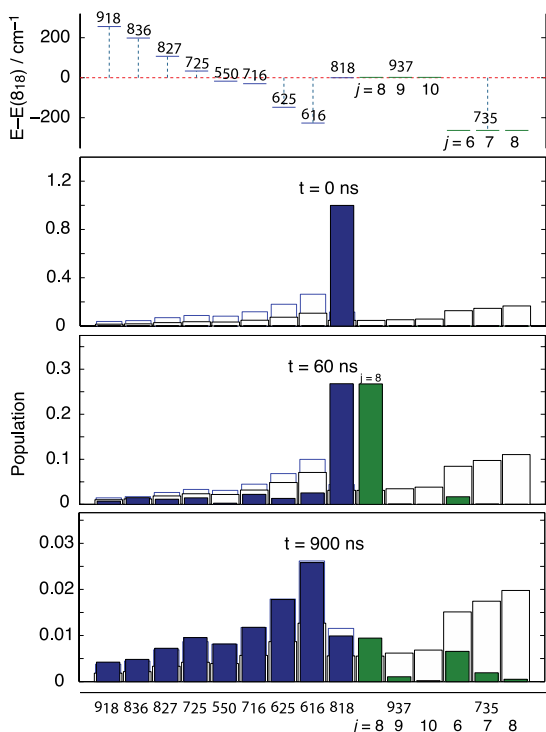


FIG. 1. Rotational distributions of selected singlet (blue) and triplet (green) levels at various times following initial population of the  $a(0,0,0)$   $8_{18}$  mixed level;  $p = 2$  Torr,  $T = 300$  K. The black rectangular empty boxes denote the relative  $T = 300$  K Boltzmann populations. The upper panel indicates the energies of the levels.

angular momentum  $n$ , but averaged over a subset of the projection quantum numbers. In a series of studies, Orr-Ewing and his group have determined differential cross sections for collisions of  $\text{CD}_3$  with He,  $\text{H}_2$ , Ar, and  $\text{N}_2$ . We have employed PES's determined by our group for the first 3 collision partners to compute differential cross sections. These agree well with experiment [9,12,16]. We find that the dynamics of collision of the symmetric top  $\text{CD}_3$  is richer than that of a diatomic. In collaborations with Orr-Ewing and van der Avoird (Nijmegen, Netherlands), we compared the scattering of  $\text{CD}_3$  with that of another (nonplanar) symmetric top  $\text{ND}_3$  [11].

We have worked with Hall and Sears on the study of rotational energy transfer (RET) of  $\text{CN}(X)$  in collisions with He and Ar [18]. These authors employed frequency modulated transient absorption in a double-resonance, depletion recovery experiment. We carried out quantum scattering calculations for RET of selected rotational levels. Our calculations agree well with measured thermal rate constants, as well as non-thermal Doppler-resolved rate constants. In the future we will investigate collisional depolarization of non-isotropic  $m$  distributions.

### Transport properties

Modeling combustion involves the prediction of the temporal and spatial dependence of the concentrations of all relevant species, as well as for the calculation of flame velocities. This requires knowledge of rate constants of all the relevant species, as well transport properties. Sensitivity analysis by several groups suggests that uncertainties in transport properties can be as significant as uncertainties in reaction rate constants. Present computational resources allow the accurate calculation of transport properties using state-of-the-art PESs. We have been computing accurate transport properties in quantum scattering calculations for collisions of various free radicals. Based on our recent work, we found that: (a) Retention of just the isotropic part of the potential results in errors in transport properties of only a few percent. (The exceptions involve species with a low-lying LUMO, such as  $\text{CH}_2(a)$  and  $\text{BH}_3$  [8].) (b) Isotropic Lennard-Jones (LJ) 12-6 potentials yield diffusion coefficients with too steep a temperature dependence. This occurs because the repulsive walls of LJ 12-6 potentials are too steep. (c) Transport property calculations with LJ potentials for radical-radical systems disagree significantly with calculations using accurate potentials.

We have concentrated on the calculation of transport properties for collision pairs involving the light H atom and have computed PESs when these are not available. We have also used these calculated properties to assess how a more accurate treatment of transport affects 1-dimensional laminar combustion simulations. In some cases accurate transport properties differ significantly from LJ estimates, as illustrated in Fig. 2 for the H-CO and H-CO<sub>2</sub> binary diffusion coefficients.

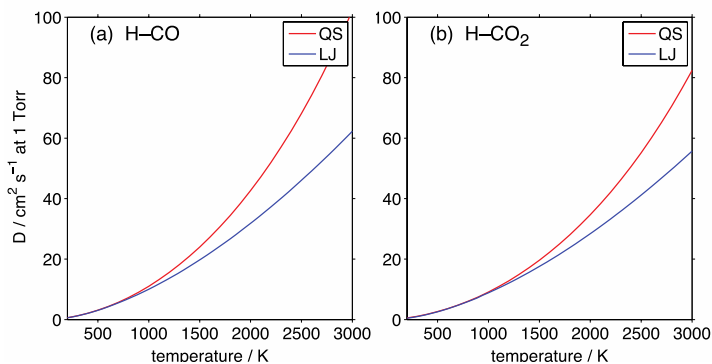


FIG. 2. Comparison of binary diffusion coefficients at 1 Torr for (a) H-CO and (b) H-CO<sub>2</sub>. QS and LJ denote quantum scattering calculations and conventional calculations with LJ (12-6) potentials, respectively.

In recent calculations, we have computed a new RCCSD(T) PES for H-N<sub>2</sub> and have computed transport properties for comparison with the previous calculations by Stallcop *et al.* [J. Chem. Phys. **97**, 3431 (1992)], who used a spherically averaged potential. We have also computed a PES for H-CH<sub>4</sub> and computed transport properties using both the full anisotropic and spherically averaged potentials.

We have extended our 1-dimensional flame simulations to the combustion of methane in both air and in oxygen. Two sets of calculations were carried out: The first set was based on the conventional parameterized LJ 12-6 potentials, while the second set incorporated exact transport properties for the available collision pairs. The calculated flame speeds as a function of the equivalence ratio are presented in Fig. 3.

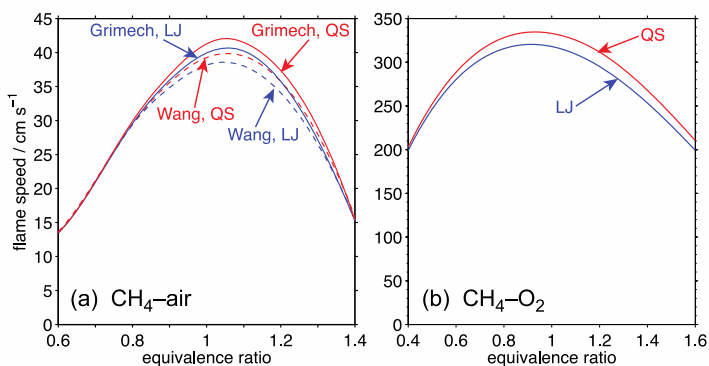


FIG. 3. Laminar flame speeds for (a) CH<sub>4</sub>-air and (b) CH<sub>4</sub>-O<sub>2</sub> at 1 atm. The blue and red curves denote calculations with LJ and accurate transport properties, respectively. Chemistry models employed for CH<sub>4</sub>-air included Grimech 3.0 (solid lines) and USC Mech 3 (dashed lines). For CH<sub>4</sub>-O<sub>2</sub> Grimech 3.0 was employed as the chemistry model.

It can be seen from Fig. 3(a) that the differences in flame speeds computed with conventional LJ and accurate transport properties are comparable to differences in flame speeds computed with different chemistry models. A sensitivity analysis indicates that for the air flame the flame speed is most strongly affected by the transport properties for H-N<sub>2</sub>, while for the O<sub>2</sub> flame the most important transport properties are for the H-CO and H-CO<sub>2</sub> collision pairs. We are interested in collaborating with modelers simulating combustion in 2 or 3 dimensions.

### Interactions with Other Groups and DOE Synergy

Alexander and Dagdigian interact closely with Hall and Sears at Brookhaven. In addition to our collaborative work on the collisional relaxation of CH<sub>2</sub>, we have collaborated on the Doppler-resolved kinetics and pressure broadening of the CN radical. We plan to compare pressure

broadening calculations on the OH  $A - X$  transition with measurements from the group of Ritchie at Oxford, UK. We collaborated with Orr-Ewing at Bristol UK on the determination of  $CD_3$  differential cross sections in collisions with a number of species. Alexander has collaborated with Chandler at Sandia Livermore on inelastic scattering of the NO radical. Dagdigian's 1-dimensional combustion simulations were facilitated by Sivaramakrishnan at Argonne.

### Publications Supported by this Project (2011-2015)

1. L. Ma, M. H. Alexander, and P. J. Dagdigian, "Theoretical investigation of rotationally inelastic collisions of  $CH_2(\bar{a})$  with helium," *J. Chem. Phys.* **134**, 154307 (13 pages) (2011)
2. P. J. Dagdigian and M. H. Alexander, "Theoretical investigation of rotationally inelastic collisions of the methyl radical with helium," *J. Chem. Phys.* **135**, 064306 (9 pages) (2011).
3. M. H. Alexander, G. Hall, and P. J. Dagdigian, "The Approach to Equilibrium: Detailed Balance and the Master Equation," *J. Chem. Educ.* **88**, 1538-1540 (2011).
4. L. Ma, M. H. Alexander, and P. J. Dagdigian, "Theoretical investigation of rotationally inelastic collisions of  $CH_2(X)$  with helium," *J. Chem. Phys.* **136**, 224306 (9 pages) (2012).
5. P. J. Dagdigian and M. H. Alexander, "Exact quantum scattering calculation of transport properties for free radicals: OH( $X^2\Pi$ )-helium," *J. Chem. Phys.* **137**, 094306 (7 pages) (2012).
6. Q. Ma, P. J. Dagdigian, and M. H. Alexander, "Theoretical study of the vibrational relaxation of the methyl radical in collisions with He," *J. Chem. Phys.* **138**, 104317 (10 pages) (2013).
7. P. J. Dagdigian, "Theoretical investigation of collisional energy transfer in polyatomic intermediates," *Int. Rev. Phys. Chem.* **32**, 229-265 (2013).
8. P. J. Dagdigian and M. H. Alexander, "Exact quantum scattering calculations of transport properties:  $CH_2(X^3B_1, a^1A_1)$ -helium," *J. Chem. Phys.* **138**, 164305 (7 pages) (2013).
9. Ondrej Tkáč, A. G. Sage, S. J. Greaves, A. J. Orr-Ewing, P. J. Dagdigian, Q. Ma, and M. H. Alexander, "Rotationally inelastic scattering of  $CD_3$  and  $CH_3$  with He: Comparison of velocity map-imaging with quantum scattering calculations," *Phys. Chem. Chem. Phys.* **140**, 4199-4211 (2013).
10. P. J. Dagdigian and M. H. Alexander, "Exact quantum scattering calculations of transport properties for the  $H_2O-H$  system," *J. Chem. Phys.* **139**, 194309 (8 pages) (2013).
11. Ondrej Tkáč, A. J. Orr-Ewing, P. J. Dagdigian, M. H. Alexander, J. Onvlee, and A. van der Avoird, "Collision dynamics of symmetric top molecules: A comparison of the rotationally inelastic scattering of  $CD_3$  and  $ND_3$  with He," *J. Chem. Phys.* **140**, 134308 (10 pages) (2014).
12. Ondrej Tkáč, Q. Ma, C. A. Rusher, S. J. Greaves, A. J. Orr-Ewing, and P. J. Dagdigian, "Differential and integral cross sections for the rotationally inelastic scattering of methyl radicals with  $H_2$  and  $D_2$ ," *J. Chem. Phys.* **140**, 204318 (12 pages) (2014).
13. L. Ma, M. H. Alexander, and P. J. Dagdigian, "Theoretical investigation of intersystem crossing between the  $a^1A_1$  and  $X^3B_1$  states induced by collisions with helium," *J. Chem. Phys.* **141**, 064312 (10 pages) (2014).
14. L. Ma, P. J. Dagdigian, and M. H. Alexander, "Theoretical investigation of the relaxation of the bending mode of  $CH_2(X)$  by collisions with helium," *J. Chem. Phys.* **141**, 214305 (4 pages) (2014).
15. P. J. Dagdigian and M. H. Alexander, "Transport cross sections for systems with deep potential wells," *J. Phys. Chem. A* **118**, 11935-11942 (2014).
16. Ondrej Tkáč, Q. Ma, M. Stei, A. J. Orr-Ewing, and P. J. Dagdigian, "Rotationally inelastic scattering of methyl radicals with Ar and  $N_2$ ," *J. Chem. Phys.* **142**, 014306 (10 pages) (2015).
17. P. J. Dagdigian, "Combustion simulations with accurate transport properties for reactive intermediates," *Comb. Flame* **162**, 2480-2486 (2015).
18. D. Forthomme, M. L. Hause, H.-G. Yu, P. J. Dagdigian, T. J. Sears, and G. E. Hall, "Doppler-resolved kinetics of saturation recovery," *J. Phys. Chem. A* **119**, 7439-7450 (2015).
19. P. J. Dagdigian, "Accurate transport properties for H-CO and H-CO<sub>2</sub>," *J. Chem. Phys.* **143**, 054303 (7 pages); erratum **143**, 159902 (1 page) (2015).

# Theory and Modeling of Multiphase Reacting Flow Dynamics in Simulations and Experiments

Rainer N. Dahms  
Combustion Research Facility, Sandia National Laboratories  
Livermore, CA 94551-0969  
[Rndahms@sandia.gov](mailto:Rndahms@sandia.gov)

## I. Program Scope

This theoretical and modeling effort on multiphase reacting flow dynamics is based on three primary objectives. The first is to establish a physically-based understanding of improved turbulent mixing and combustion models in multiphase flows. Many of the relevant fluid flow processes take place on time and length scales which are not feasible to resolve directly in simulations. Therefore, sophisticated sub-grid scale models have to be developed. This requires a comprehensive understanding of the fundamental processes of the underlying relevant phenomena. In this context, a major focus is the development of more general regimes that incorporate broader ranges of combustion modes and a more complete set of non-dimensional parameters. The second objective is to develop techniques and methods to understand data sets obtained from high-fidelity Large-Eddy simulations (Oefelein) and measurements performed in the Advanced Imaging Laboratory (Frank) and in the Turbulent Combustion Laboratory (Barlow) in a meaningful manner. The fundamental issues of comparing, validating, and understanding advanced combustion data sets will become even more important as we attempt to understand the dynamics of turbulence-flame interactions using data sets that capture the temporal evolution of turbulent flames. The third objective is to understand the implications of the conclusions obtained from well-controlled experiments in the context of advanced power and propulsion systems including gas turbines, automotive engines, and liquid rockets. This effort has to consider the poorly understood effect of elevated pressure on the fundamentals of multiphase combustion phenomena. It builds on the developed theoretical framework, which establishes a meaningful set of major scaling parameters. Combined with the identification of relevant ranges of combustion regimes and non-dimensional parameters in modern transportation and power systems, the framework will serve the general objective of this program to accelerate the development and validation of science-based, predictive computational models for turbulent combustion systems.

## II. Recent Progress

Understanding and quantifying multiphase reacting flow phenomena in fundamental experiments and modern transportation and energy systems is widely recognized as a critical research area for future combustion design. The importance to develop a basic science foundation for predictive models has been consistently highlighted over many years in a variety of industry, government, and academic forums including recent DOE workshops such as the *Workshop to Identify Research Needs and Impacts in Predictive Simulations for Internal Combustion Engines* (PreSICE),<sup>1</sup> and the *Workshop on Clean and Efficient Combustion of 21<sup>st</sup> Century Transportation Fuels*.<sup>2</sup> Liquid injection processes largely determine the mixture preparation process which ultimately governs the detailed evolution of chemical kinetic processes and their interaction with the turbulent flow field.

Understanding and control of high-pressure spray flame ignition is essential for the design of advanced combustion systems but, in practice, prediction of the low-temperature chemical reactions that lead to subsequent ignition and combustion is challenging. Specific fundamental research needs include effects

of spray mixing, detailed chemistry, and flow-chemical interactions at these conditions. Recently, Skeen et al.<sup>3</sup> provided time-resolved imaging showing how cool-flame dynamics play a significant role in high-pressure spray ignition. Simultaneous formaldehyde PLIF and high-speed schlieren imaging were applied to a spray flame ignition experiment. The measurements showed initiation of low-temperature reactions near the radial periphery of the spray, followed by rapid appearance of low-temperature reactions across the entire spray head at a position where high-temperature ignition finally occurs. Cool-flame chemistry was also found significant in fundamental droplet combustion studies mainly motivated by micro-gravity experiments performed on board the International Space Station<sup>4,5</sup>.

Recent studies aimed to develop a conceptual model for turbulent ignition in high-pressure spray flames. The model is motivated by first-principle simulations and optical diagnostics applied to high-pressure n-dodecane spray flames. The Lagrangian flamelet equations are combined with full LLNL kinetics (2755 species; 11,173 reactions) to resolve all time and length scales and chemical pathways of the ignition process at engine-relevant pressures and turbulence intensities unattainable using classic DNS. The first-principle value of the flamelet equations is established by a spectral analysis of the fully-coupled chemical and turbulent time scales. Contrary to conventional wisdom, this analysis revealed that the high Damkohler number limit, a key requirement for the validity of the flamelet derivation from the reactive Navier-Stokes equations, applies during the entire ignition process.

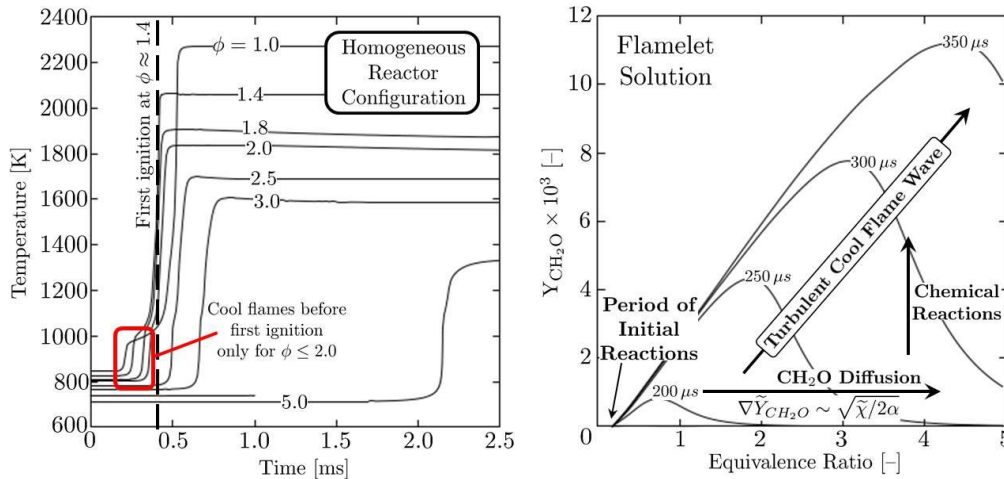


Figure 1: (Left) Temperature evolutions for various equivalence ratios using homogeneous reactor configurations. (Right) Flamelet solution shows that after the onset of initial reactions at lean mixtures, turbulence-chemistry interactions manifest in a propagating turbulent cool flame wave which triggers the formation of formaldehyde in rich mixture regions over a period of  $dt \approx 150 \mu s$  (see Dahms *et al.*<sup>6</sup>).

Figure 1 (left) shows temperature evolutions for a set of equivalence ratios using a homogeneous reactor configuration. The analysis demonstrates that only equivalence ratios  $\phi < 2$  can undergo first-stage ignition before the simulated onset of high-temperature ignition at  $\phi \approx 1.4$ . These homogeneous configurations are then extended to the flamelet equations by adding respective terms for turbulence-chemistry-interactions. Figure 1 (right) shows that after an initial formation period of  $dt \approx 190 \mu s$  of chemical activity, turbulence-chemistry-interactions manifest in a propagating turbulent cool flame wave which triggers formaldehyde formation in rich mixture regions at  $\phi > 4$  in about  $t \approx 350 \mu s$ . This time is much shorter compared to the homogeneous solutions ( $t > 2000 \mu s$ ) shown in Fig.1 (left). This quantifies the significance of turbulence-chemistry-interactions in the progress of chemical kinetics.

The significance of turbulence in the ignition mechanism is quantified in Fig. 2 (left). First-stage ignition delay is defined as the time when the early exponential rise in OH concentration ends. Second-stage ignition delay is defined using a temperature progress variable approach. Figure 2 (left) shows that

in the lean mixture, differences between homogeneous and turbulence first-stage ignition delay are diminished. Subsequently, however, and owed to the cool flame wave, turbulent first-stage ignition delay decreases, in comparison to the homogeneous reference, ever more significantly with increasing equivalence ratio. Then, high-temperature ignition over a broad range of rich equivalence ratios is initiated. The majority of the mixture is ignited by turbulent flame propagation.

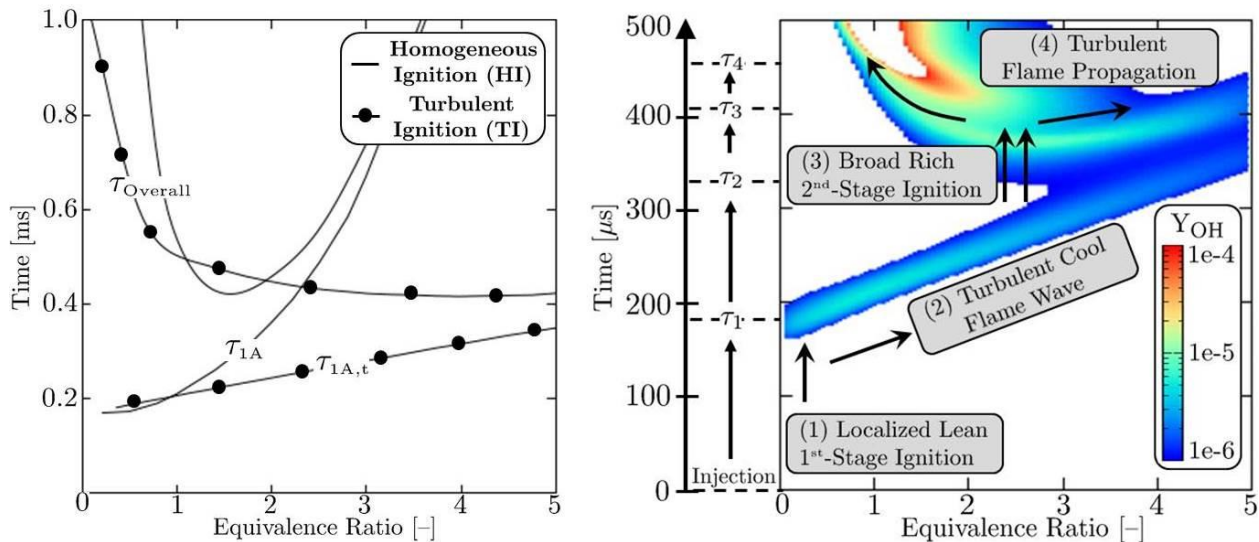


Figure 2: (Left) Homogeneous and turbulent (symbols) first-stage and second-stage ignition delay times as a function of equivalence ratio. (Right) Evolution of characteristic events and associated time scales in high-pressure spray flames (see Dahms *et al.*<sup>6</sup>).

The previous analysis allows the formulation of a conceptual model for turbulent ignition in high-pressure spray flames. Figure 2 (right) presents the evolution of this mechanism which is associated with a set of characteristic time scales. (1) Localized first-stage ignition occurs in the lean high-temperature region. (2) This initial chemical reactivity initiates a turbulent cool flame wave transporting chemical species and heat to colder and richer mixture regions which substantially increases their reactivity. (3) After cool flame wave propagation, the entire mixture is in a state of completed first-stage ignition which is succeeded by a momentary substantial decrease of chemical activity. This leads, in combination with ongoing turbulent mixing, to the formation of a quasi-homogeneous mixture characterized by large-scale stratifications in temperature and species concentration. This stage is largely responsible for the overall retard of ignition delay at high scalar dissipation rates, which forcefully counter the pathway toward thermal runaway. (4) Lastly, the formed steep gradients from high-temperature ignition result in turbulent flame propagation. It rapidly ignites the entire spray head.

### III. Future Work

All developed chemical mechanisms and performed experiments utilize a homogeneous mixture configuration. They therefore entirely neglect the presence of cool flame and hot flame waves in turbulent mixtures discovered here. The presented fundamental finding could carry immense implications for the development of more accurate chemical mechanisms for turbulent flames since the inclusion of this discovered physical complexity in simulations promises to significantly improve their predictive capabilities. The fundamental approach described above will be further developed with an emphasis on interrelated areas of research. A close collaboration between the Large-Eddy simulation program and the experimental flow research program will be maintained. A significant effort on the validation and

generalization of the proposed theory will be initiated. Such efforts include detailed comparisons to high-speed microscopic imaging at high-pressure conditions, improvements of model accuracy, and the investigation of turbulent combustion processes at elevated system pressures. The objective is to develop a predictive first-principle model framework suitable for high-fidelity combustion simulations.

#### IV. Literature Cited

1. A Workshop to Identify Research Needs and Impacts in Predictive Simulation for Internal Combustion Engines. [http://science.energy.gov/~media/bes/pdf/reports/files/PreSICE\\_rpt.pdf](http://science.energy.gov/~media/bes/pdf/reports/files/PreSICE_rpt.pdf) , 2011; Sponsored by the Office of Basic Energy Sciences, Office of Science and the Vehicle Technologies Program, Office of Energy Efficiency and Renewable Energy, U.S. Department of Energy
2. Basic Research Needs for Clean and Efficient Combustion of 21<sup>st</sup> Century Transportation Fuels. <http://www.osti.gov/scitech/servlets/purl/935428>, 2006; Report of the Basic Energy Sciences Workshop on Clean and Efficient Combustion of 21<sup>st</sup> Century Transportation Fuels, U.S. Department of Energy.
3. S.A. Skeen, J. Manin, and L.M. Pickett, “Simultaneous formaldehyde PLIF and high-speed schlieren imaging for ignition visualization in high-pressure spray flames,” *Proc. Combust. Inst.* **35**:3167-3174, 2015
4. T. Farouk and F. Dryer, “On the extinction characteristics of alcohol droplet combustion under microgravity conditions – a numerical study,” *Combust. Flame* **159**:3208-3223, 2012
5. V. Nayagam, D.L. Dietrich, P.V. Ferkul, M.C. Hicks, and F.A. Williams, “Can cool flames support quasi-steady alkane droplet burning?,” *Combust. Flame* **159**:3583-3588, 2012

#### V. BES Sponsored Publications (2013-2016)

6. R.N. Dahms, G.A. Paczko, S.A. Skeen, and L.M. Pickett, “Understanding the ignition mechanism of high-pressure spray flames,” *Proc. Combust. Inst.*, submitted.
7. R.N. Dahms, “Understanding the breakdown of classic two-phase theory and spray atomization at engine-relevant conditions,” *Phys. Fluids*, 2016. Accepted for publication.
8. R.N. Dahms. “Gradient Theory simulations of pure fluid interfaces using a generalized expression for influence parameters and a Helmholtz energy equation of state for fundamentally consistent two-phase calculations.” *J. Colloid Interface Sci.* **445**:48-59, 2015. doi: 10.1016/j.jcis.2014.12.069
9. R.N. Dahms and J.C. Oefelein, “Liquid jet breakup regimes at supercritical pressures,” *Combust. Flame*, **162**:3648-3657, 2015, doi:10.1016/j.combustflame.2015.07.004.
10. T.D. Fansler, D.L. Reuss, V. Sick, and R.N. Dahms, “Combustion instability in spray-guided stratified-charge engines: A review,” *Intl. J. Engines Res., Cyclic Dispersion Special Issue*, **16**:260-305, 2015. doi:10.1177/1468087414565675.
11. R.N. Dahms and J.C. Oefelein. “Atomization and dense fluid breakup regimes in liquid rocket engines.” *J. Propulsion Power*, **31**:1221-1231, 2015. doi:10.2514/1.B35562
12. R.N. Dahms and J.C. Oefelein. “Non-equilibrium gas-liquid interface dynamics in high-pressure liquid injection systems.” *Proc. Combust. Inst.* **35**:1587-1594, 2015. doi: 10.1016/j.proci.2014.05.155
13. R.N. Dahms and J.C. Oefelein. “On the transition between two-phase and single-phase interface dynamics in multicomponent fluids at supercritical pressures.” *Phys. Fluids* **25**, 092103, 2013. doi: 10.1063/1.4820346
14. R.N. Dahms, J. Manin, L.M. Pickett, and J.C. Oefelein. “Understanding high-pressure gas-liquid interface phenomena in diesel engines.” *Proc. Combust. Inst.* **34**:1667-1675, 2013. doi: 10.1016/j.proci.2012.06.169
15. J. Manin, M. Bardi, L.M. Pickett, R.N. Dahms, and J.C. Oefelein. “Microscopic investigation of the atomization and mixing processes of diesel sprays injected into high pressure and temperature environments.” *Fuel* **134**:531-543, 2014. doi: 10.1016/j.fuel.2014.05.060

# Bimolecular Dynamics of Combustion Reactions

H. Floyd Davis  
Department of Chemistry and Chemical Biology  
Cornell University  
Ithaca, NY 14853-1301  
hfd1@Cornell.edu

## I. Program Scope:

The aim of this research program is to better understand the mechanisms, products, and product energy disposal in elementary bimolecular reactions fundamental to combustion chemistry. Using the crossed molecular beams method, the angular and velocity distributions of neutral products from single reactive collisions are measured to gain insight into the reaction dynamics.

## II. Recent Progress:

Our DOE-supported experimental research program is now primarily conducted using a rotatable source crossed molecular beams machine with universal electron impact and single photon ionization detection using high intensity pulsed tabletop light sources developed at Cornell.<sup>1-3</sup> Using a newly-developed windowless VUV beamline, line tunable photoionization energies ranging from 9.5 to 11.9 eV are readily available. This makes it possible to carry out “soft” single photon ionization of products with ionization energies ranging from < 9.5 eV (e.g., CH<sub>2</sub>CHOH) to > 11.3 eV (e.g., HO<sub>2</sub>).

We have developed a technique for producing radiation extending to 13 eV with higher conversion efficiencies than previously reported. A description of this technique has recently appeared in *Rev. Sci. Instrum.*, involving noncollinear mixing of focused lasers in laser vaporized mercury (Hg) at room temperature.<sup>4</sup> This approach facilitates windowless operation with the short wavelength radiation spatially isolated from the residual UV and visible beams without need for lossy optical elements such as windows, lenses, and gratings.

As part of the development of molecular beam sources of ethyl, propyl and butyl radicals, we have studied the UV photodissociation of several primary, secondary and tertiary iodoalkanes.<sup>5</sup> While the photodissociation of methyl iodide (CH<sub>3</sub>I) has been studied very extensively over many decades, there have been relatively few studies of larger systems. In contrast to methyl iodide where only C-I bond fission is operable at 266 nm, we have found that HI elimination in secondary and tertiary compounds forming the corresponding alkene plays an important role. A review of the literature dating back to the 70's<sup>6</sup> indicates that in all studies except one,<sup>7</sup> HI elimination was not considered in iodoalkane photochemistry.

Since our detector mass resolution is sufficiently high to discriminate between I (m/e = 127) and HI (m/e = 128), the competing channels can be studied unambiguously using electron impact and VUV ionization. For primary 3- and 4- carbon iodoalkanes, C-I fission is the exclusive channel with dominant production of I\* and highly anisotropic product angular distributions similar to those for CH<sub>3</sub>I. Using various VUV ionization schemes, TOF spectra can be recorded for either the I or I\* products, making it possible to derive internal energy distributions of radicals correlated to each I atomic state. For secondary and tertiary iodoalkanes, the angular and velocity distributions for the

HI molecular elimination products are very similar to those for I. Because the same velocity distributions are observed for HI products ionized using electron impact, 10 eV photons (only capable of ionizing HI ( $v > 3$ ), and 12 eV photons, the HI is produced primarily in  $v > 3$ .<sup>5</sup>

### III. Future Plans:

We plan to extend our studies of alkyl iodide photolysis to wavelengths other than 266 nm in order to gain insight into the wavelength dependence of the HI:I branching ratios.

Our studies indicate that pyrolysis of azo compounds and photolysis of alkyl iodides are the cleanest sources of intense beams of alkyl radicals. We are currently using these sources in experimental studies of photodissociation reactions and bimolecular reactions.

For 1- and 2-propyl radicals, it is well-established that H atom elimination plays an important role in the UV photodissociation dynamics. However, C-C bond fission is actually the most thermodynamically favorable channel. Using soft VUV photoionization detection, we are able to study the C-C bond fission channels from photolysis of the propyl and butyl radical isomers with unprecedented sensitivity. For studies of the isomer-specific bimolecular reactions of alkyl radicals, our primary focus is on reactions of C<sub>2</sub>H<sub>5</sub> and the two C<sub>3</sub>H<sub>7</sub> isomers with O<sub>2</sub>. We are also studying the bimolecular reactions of alkenes such as C<sub>2</sub>H<sub>4</sub> and C<sub>3</sub>H<sub>6</sub> with OH. All of these systems are of particular interest because different product isomers, e.g., enols vs. aldehydes in the OH + alkene reactions (which can be distinguished from their ionization energies) are believed to be produced.

### IV. References (Numbers 1-4 are publications since 2013 citing DOE support):

1. D.R. Albert and H.F. Davis "Experimental Studies of Bimolecular Reaction Dynamics Using Pulsed Tabletop VUV Photoionization Detection", invited perspective article, *Phys. Chem. Chem. Phys.* **15**, 14566-14580 (2013).
2. High-Intensity Coherent Vacuum Ultraviolet Source Using Unfocussed Commercial Dye Lasers, D.R. Albert, D.L. Proctor, and H.F. Davis, *Rev. Sci Instrum.* **84**, 063104 (2013).
3. Crossed Molecular Beam Studies of Phenyl Radical Reactions with Propene and 2-Butene, D.R. Albert, M. A. Todt, and H.F. Davis, *J. Phys. Chem. A* **117**, 13967-13975 (2013).
4. High Intensity VUV and XUV Production by Noncollinear Mixing in Laser Vaporized Media, M.A. Todt, D.R. Albert and H. F. Davis, *Rev. Sci. Instrum.*, accepted for publication.
5. Dynamics of HI elimination from the UV Photodissociation of Alkyl Iodides, M. A. Todt and H. F. Davis, *J. Chem. Phys.*, in preparation.
6. Excited Fragments from Excited Molecules: Energy partitioning in the Photodissociation of Alkyl Iodides, S.J. Riley and K.R. Wilson, *Faraday Disc. Chem. Soc.* **53**, 132 (1972).
7. Excited State Photochemistry of Iodoalkanes, P.L. Ross and M.V. Johnston, *J. Phys. Chem.* **99**, 4078 (1995).

## Exploration and validation of chemical-kinetic mechanisms

Michael J. Davis

Chemical Sciences and Engineering Division  
Argonne National Laboratory  
Argonne, IL 60439  
Email: davis@tcg.anl.gov

The focus of the work is on exploration and theoretical validation of chemical-kinetic mechanisms, combining global sensitivity analysis with the exploration of the characteristics of the sensitivity analysis over physical and chemical parameters. An effort on reaction pathway analysis has also been undertaken. Another focus of the work is the use of methods of numerical analysis, statistics, and signal processing for studying chemical kinetics and dynamics.

### Recent Progress

Four areas have shown noticeable progress in the last year. The reaction pathway analysis work continues in collaboration with Skodje and his group. A second area is the further development of sparse regression for doing global sensitivity analysis. This methodology has been extended beyond the  $l_1$ -penalized regression used previously into  $l_0$  methods, as well as subset selection methods. Computer programs have been written to study these methods. A third area is the implementation of regression diagnostics into the research program. So far this has been used for global sensitivity analysis, but will be extended to other forms of fitting in the next year. The fourth area of progress is the development and calibration of small-sample size global sensitivity analysis in collaboration with Liu and Sivaramakrishnan, which has led to a preprint [13], now discussed. The goal of this work is to accurately implement global sensitivity for engine simulations, extending our earlier study [5]. Engine simulations are costly and limiting the number of simulations needed for accurate numbers is important.

A series of simulations were undertaken for a mixture of n-heptane and methylbutanoate under constant pressure conditions, as discussed in several of the publications listed (e.g, 10 and 13). These mixtures ignite and the ignition delay time of the simulations are fit to the following:

$$\tau^{(1)}(\{u_i\}) = \sum_{i=1}^{n_r} \sum_{k=1}^p a_{ik} u_i^k \quad (1a)$$

$$\tau^{(2)}(\{u_i\}) = \sum_{i=1}^{n_r} \sum_{k=1}^p a_{ik} u_i^k + \sum_{j=1}^{n_r} \sum_{m=1}^{m_s} \{b_{jm}\}^s Q^{(s)}(u_{j_1}, u_{j_2}) \quad (1b)$$

The cross terms, the  $Q$ 's in Eq. (1b), are quadratic, cubic, or quartic. These functions are used to calculate the global sensitivity coefficients. Model selection determines the specific form of the model, based on the leave-one-out cross-validation (loocv) error. The loocv error is an out-of-sample error that is used to avoid overfitting, most often observed as unwanted oscillations in the fitted function.

Figure 1 demonstrates several features of the fitting procedure. Two models are studied in the top row, a linear model based on Eq. (1a) ( $k=1$ ) and a quadratic model with interaction terms based on Eq. (1b) with  $m_s = 2$ . The least squares and loocv errors are shown in both panels

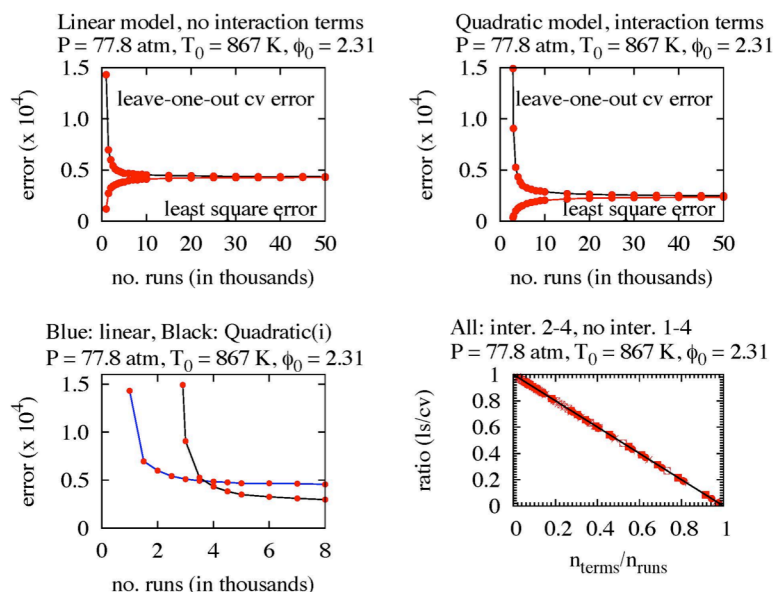


Fig. 1. The top row compares the loocv error and the least squares error for the linear and quad/int models as a function of the number of runs. The bottom left panel shows a comparison between the two errors up to sample sizes of 8000. The plot on the bottom right shows that the ratio of least squares and loocv error is nearly linear over a range of sample sizes and models.

as a function of the number of constant pressure simulations used in the calculations. The generic behavior shown in the two plots is that the least squares error increases and the loocv error decreases as the number of runs increases. These panels also demonstrate that the error tends to be smaller for the quadratic model with interaction terms, especially as the number of runs gets large. However, at small sample sizes the linear model can have a smaller loocv

Table 1: Location of the top 10 reactions as a function of sample size and model type

cmp <sup>a</sup>	2900 <sup>b</sup>	5000 <sup>b</sup>	50000 (4) <sup>c</sup>	50000 (1) <sup>c</sup>	$S_i^d$	reaction <sup>e</sup>
1	1	1	1	1	0.1479	C7H15O2-2=C7H14OOH2-4
2	3	3	2	2	0.0633	C7H15O2-4=C7H14OOH4-2
3	2	2	3	3	0.0580	C7H14OOH2-4O2=NC7KET24+OH
4	6	4	4	4	0.0452	NC7H16+HO2=C7H15-3+H2O2
5	4	5	5	5	0.0359	C7H14OOH4-2O2=NC7KET42+OH
6	13	7	6	6	0.0307	C7H14OOH1-3O2=NC7KET13+OH
7	8	6	7	7	0.0285	C7H15O2-3=C7H14OOH3-5
8	7	8	8	8	0.0258	C7H14OOH3-5O2=NC7KET35+OH
9	5	9	9	9	0.0185	MB+OH=H2O+MB3J
10	27	10	10	11	0.0162	C7H15O2-2=C7H14OOH2-5

<sup>a</sup> The nth reaction in terms of GSA ordering for the sample size of 50,000 with quad/int model

<sup>b</sup> Columns 2 and 3 show orderings for sample sizes of 2900 and 5000 for the quad/int model

<sup>c</sup> Quartic/int and linear model orderings for sample sizes of 50,000.

<sup>d</sup> GSA coefficient for the quad/int model with sample size of 50,000

<sup>e</sup> Reaction for the quad/int, 50,000 case.

error as demonstrated in the bottom left plot. The bottom right panel of Fig. 1 demonstrates that the ratio of least squares and loocv error lies on a line over a large range of sample sizes and for a range of models. The symbols on the plot show results for seven models: linear through quartic without interaction terms and quadratic through quartic for models with interaction terms.

The behavior shown in the plot on the bottom right of Fig. 1 is common. In linear least

regression the relationship between the fitted values of the ignition delay times and the numerical values can be written in matrix form:  $\tau_{\text{fit}} = H\tau$ , which leads to the relationship evident in the bottom right panel of Fig. 1,  $E(l_s)/E(l_{\text{ocv}}) \approx 1 - n_{\text{term}}/n_{\text{run}}$  [13].  $H$  is known as the hat matrix.

The errors shown in Fig. 1 indicate that simple models may have lower fitting errors than more complex models. However, the real test of these small samples is how they order the global sensitivities. Table 1 shows several examples of the assignment of reactions for different sample sizes and different models. The second column of Table 1 indicates that a sample size of 2900 may be too small to give accurate assignments, but a sample size of 5000 does quite well for the 10 most sensitive reactions. The samples are drawn randomly and we have found that there are fluctuations in the accuracy, depending on what sample is drawn of a particular size, leading us to adopt a calibration strategy based on finding small samples which are accurate over a range of conditions [13]. Because our goal is to accurately implement global sensitivity analysis for these simulations, the range of conditions studied is based on engine simulations [5].

The calibration is summarized in Fig. 2. The first two plots in the top row show how the accuracy of the assignments vary for a sample size of 3500, compared to one of size 50,000, which is accurate for this range of reactions. The straight line on these show the accurate assignments and the bars show the root-mean-square error averaged over the 50 conditions

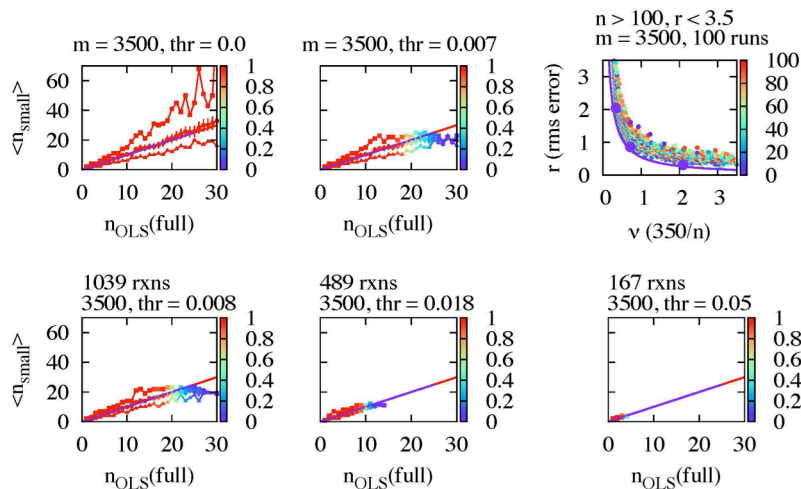


Fig. 2. The top row shows two assignment curves for two values of the threshold. The top right panel shows a trade-off plot for many thresholds. The bottom row shows assignment plots along the Pareto front (blue curve in top right panel) corresponding to the large dots.

both panels indicates. When no threshold is set all reactions are selected (left top), but the error tends to be high. Setting a threshold reduces the error, but eliminates reactions (middle top). The first situation leads to false positives and the second to false negatives, indicating that there is a trade off, explored in the plot on the upper right.

The dots on the plot in the upper right show results for a set of 100 random draws of size 3500, with the rms error, the ordinate in the plot, calculated for a number of values of the cut-off threshold. The abscissa is proportional to the inverse of the number of reactions selected. The blue curve shown on the top right plot estimates the edge of the dotted region and is analogous to a Pareto front in multi-objective optimization [13]. The front shows the best tradeoff between false positives (upper left portion of the curve) and false negatives (lower right).

The plots in the bottom row of Fig. 2 show results along the Pareto front. The three points on the front in the top right panel are the positions along the front for the plots in the bottom row. The utility of the Pareto front is that it shows explicitly the trade-off, which is

studied. The jagged lines above and below show the maxima and minima assignments for the set of 50. The plot on the upper left includes all reactions and the plot in the middle shows only those reactions whose sensitivity coefficients are above 0.007, reducing the large fluctuations in the maxima and minima significantly. However, using a threshold reduces the number of reactions selected, as the color-coding on

evident in the plots in the bottom row. Any point along the curve is a good trade-off, but we prefer the point near the knee region of the front, the middle point, which is a common choice of researchers. We prefer this region, as movement in either direction can severely increase false positives or false negatives. The knee-region example in the middle bottom selects an average of more than nine reactions for each physical condition (489/50). The plot shows that selection is accurate over the range of conditions for reactions whose sensitivity coefficient is greater than the threshold value of 0.018. The sample is a near-optimal choice for size 3500 to use to calculate global sensitivity analysis for engine simulations with the indicated threshold.

### Future Plans

The calibration discussed in this abstract for ordinary least squares regression will be extended to sparse regression. It is anticipated that we can accurately calibrate samples sizes as low as 600 with this method. The hat matrix discussed above can be used to calculate leverages for each point in a least squares fit [13]. These leverages will be used in the fitting of potential energy surfaces with Jasper (SNL) and for analysis of Active Tables with Ruscic (ANL). In addition, best subset selection will be tested for fitting in both cases. A new direction for research will be initiated using tracking, estimation, and inference to study kinetic modeling.

### Publications

1. W. Liu, R. Sivaramakrishnan, M. J. Davis, S. Som, D. E. Longman and T. F. Lu, "Development of a reduced biodiesel surrogate model for compression ignition engine modeling", Proc. Combust. Inst. 34 401-409 (2013).
2. D. D. Y. Zhou, R. T. Skodje, W. Liu, and M. J. Davis, "Multi-Target Global Sensitivity Analysis of n-Butanol Combustion", Proceedings of the 8<sup>th</sup> US National Technical Meeting of the Combustion Institute, University of Utah (2013).
3. W. Liu, S. Som, D. D. Y. Zhou, R. Sivaramakrishnan, D. E. Longman, R. T. Skodje, and, M. J. Davis, "The Role of Individual Rate Coefficients in the Performance of Compression Ignition Engine Models", Proceedings of 8<sup>th</sup> US National Technical Meeting of the Combustion Institute, University of Utah (2013).
4. D. D. Y. Zhou, M. J. Davis, and R. T. Skodje, "Multi-Target Global Sensitivity Analysis of n-Butanol Combustion", J. Phys. Chem. A 117, 3569-3584 (2013).
5. S. Som, W. Liu, D. D. Y. Zhou, G. M. Magnotti, R. Sivaramakrishnan, D. E. Longman, R. T. Skodje, and M. J. Davis, "Quantum Tunneling Affects Engine Performance", J. Phys. Chem. Lett 4, 2021-2025 (2013).
6. Y. Pei, R. Shan, S. Som, T. Lu, D. E. Longman, and M. J. Davis, "Global Sensitivity Analysis of a Diesel Engine Simulation with Multi-Target Functions", Proceedings of the Society of Automotive Engineers (SAE) World Congress, 2014, SAE Paper 2014-01-1117.
7. S. Bai, D. Zhou, M. J. Davis, and R. T. Skodje, "Sum over Histories Representation for Chemical Kinetics", J. Phys. Chem. Lett., 6, 183-188 (2015).
8. D. M. A. Karwat, M. S. Wooldridge, S. J. Klippenstein, and M. J. Davis, "Effects of New Ab Initio Rate Coefficients on Predictions of Species Formed during n-Butanol Ignition and Pyrolysis", J. Phys. Chem. A 119, 543-551 (2015).
9. Y. Pei, M. J. Davis, L. M. Pickett, S. Som, "Engine Combustion Network (ECN): Global sensitivity analysis of Spray A for different combustion vessels", Combustion and Flame 162, 2337-2347.
10. S. Som, Z. Wang, G. M. Magnotti, W. Liu, R. Sivaramakrishnan, and M. J. Davis, "Application of Sparse Sensitivity Analysis to Detailed Chemical Kinetics in High Fidelity Compression-Ignition Engine Simulations", Proceedings of the 9<sup>th</sup> US National Technical Meeting of the Combustion Institute (2015).
11. F. G. Sen, A. Kinaci, B. Narayanan, S. K. Gray, M. J. Davis, S. K. R. S. Sankaranarayanan, and M. K. Y. Chan, "Towards Accurate Prediction of Catalytic Activity in IrO<sub>2</sub> Nanoclusters Via First Principles-Based Variable Charge Force Field", J. Mater. Chem A 3, 18970-18982 (2015).
12. S. Bai, M. J. Davis, and R. T. Skodje, "The Sum Over Histories Representation for Kinetic Sensitivity Analysis: How Chemical Pathways Change When Reaction Rate Coefficients Are Varied", J. Phys. Chem A 119, 11039-11052 (2015).
13. M. J. Davis, W. Liu, and R. Sivaramakrishnan, "Global Sensitivity Analysis with Small Sample Sizes: Ordinary Least Squares Approach", to be submitted.

# Vibrational Spectroscopy of Transient Combustion Intermediates Trapped in Helium Nanodroplets (DE-FG02-12ER16298)

Gary E. Douberly

University of Georgia, Department of Chemistry, 1001 Cedar St., Athens, GA 30602-1546

## **Program Scope**

The objective of this research is to isolate and stabilize transient intermediates and products of prototype combustion reactions. This will be accomplished by Helium nanodroplet isolation (HENDI) spectroscopy, a novel technique where liquid helium nanodroplets freeze out high energy metastable configurations of a reacting system, permitting infrared spectroscopic characterizations of products and intermediates that result from hydrocarbon radical reactions with molecular oxygen and other small molecules relevant to combustion environments. A major aim of this work is to directly observe the elusive hydroperoxyalkyl radical (QOOH) and its oxygen adducts (O<sub>2</sub>QOOH), which are important in low temperature hydrocarbon oxidation chemistry.

## **Recent Projects**

### **Infrared Laser Stark Spectroscopy of Hydroxymethoxycarbene in Helium Nanodroplets**

As part of our ongoing spectroscopic study of hydroxycarbenes, hydroxymethoxycarbene (CH<sub>3</sub>O $\ddot{C}$ OH) was produced *via* pyrolysis of monomethyl oxalate and subsequently isolated in helium nanodroplets. Infrared laser spectroscopy revealed two rotationally resolved *a,b*- hybrid bands in the OH-stretch region, which were assigned to *trans,trans*- and *cis,trans*- rotamers. Stark spectroscopy of the *trans,trans*- OH stretch band provided the *a*-axis inertial component of the dipole moment, namely  $\mu_a = 0.62(7)$  D. The computed equilibrium dipole moment agrees well with the expectation value determined from experiment, consistent with a semi-rigid CH<sub>3</sub>O $\ddot{C}$ OH backbone computed *via* a potential energy scan at the B3LYP/cc-pVTZ level of theory, which reveals substantial conformer interconversion barriers of  $\approx 17$  kcal/mol.

## **On the Stark Effect in Open Shell Complexes Exhibiting Partially Quenched Electronic Angular Momentum: Infrared Laser Stark Spectroscopy of OH-C<sub>2</sub>H<sub>2</sub>, OH-C<sub>2</sub>H<sub>4</sub>, and OH-H<sub>2</sub>O**

Rovibrational Stark spectra of several hydroxyl radical containing complexes were measured in helium droplets. An effective Hamiltonian model was developed to account for the Stark effect in these systems, which all exhibit partial quenching of electronic angular momentum quantized along the OH bond axis. The spherical tensor operator formalism was employed so as to arrive at the most general solution, in which the permanent dipole moment has projections on all three inertial axes. Formula for transition intensities were given for *a*-, *b*-, and *c*-type bands measured with either parallel or perpendicular laser polarization configurations. For these open-shell complexes, a Coriolis interaction of the form  $\hat{J}_a(\hat{l}_a + \hat{s}_a)$  lifts the  $\pm\omega$  degeneracy associated with the electronic angular momentum of the OH radical. This dramatically reduces the effect of the inertial asymmetry in these complexes, and in the absence of angular momentum quenching, all rotational levels exhibit a pseudo-first-order Stark effect. In the presence of angular momentum quenching, a subset of levels is parity doubled (levels in the  $(P = \frac{1}{2}, \omega = +\frac{3}{2})$  manifold), removing the degeneracy responsible for the linear Stark effect. Stark splitting of these parity doubled levels is consistent with the quadratic Stark effect expected for non-degenerate levels of a closed-shell asymmetric top. For the *T*-shaped OH-C<sub>2</sub>H<sub>2</sub> complex, predictions of *a*- and *b*-type bands for a variety of Stark field strengths are in excellent agreement with experiment.

## **Two-center Three-electron Bonding in ClNH<sub>3</sub> Revealed via Helium Droplet Infrared Laser Stark Spectroscopy: Entrance Channel Complex along the Cl + NH<sub>3</sub> → ClNH<sub>2</sub> + H Reaction**

Pyrolytic dissociation of Cl<sub>2</sub> in a newly developed, continuous-wave, SiC pyrolysis furnace was employed to dope helium droplets with single Cl atoms. Sequential addition of NH<sub>3</sub> to Cl-doped droplets leads to the formation of a complex residing in the entry valley to the substitution reaction, Cl + NH<sub>3</sub> → ClNH<sub>2</sub> + H. Infrared Stark spectroscopy in the NH stretching region reveals symmetric and antisymmetric vibrations of a C<sub>3v</sub> symmetric top. Frequency shifts from NH<sub>3</sub> and dipole moment measurements are consistent with a ClNH<sub>3</sub> complex containing a relatively strong two-center three-electron (2c-3e) bond. The nature of the 2c-3e bonding in

ClNH<sub>3</sub> was explored computationally and found to be consistent with the complexation-induced blue shifts observed experimentally. Computations of interconversion pathways reveal nearly barrierless routes to the formation of this complex, consistent with the absence in experimental spectra of two other complexes, NH<sub>3</sub>Cl and Cl–HNH<sub>2</sub>, which are predicted in the entry valley to the hydrogen abstraction reaction, Cl + NH<sub>3</sub> → HCl + NH<sub>2</sub>.

### **Ongoing Work and Future Plans**

#### **Infrared Laser Spectroscopy of the *n*-propyl and *i*-propyl Radicals: Stretch-bend Fermi Coupling in the Alkyl CH Stretch Region**

The *n*-propyl and *i*-propyl radicals were generated in the gas phase via pyrolysis of *n*-butyl nitrite (CH<sub>3</sub>(CH<sub>2</sub>)<sub>3</sub>ONO) and *i*-butyl nitrite (CH(CH<sub>3</sub>)<sub>2</sub>CH<sub>2</sub>ONO), respectively. Nascent radicals were promptly solvated by a beam of He nanodroplets, and the infrared spectra of the radicals were recorded in the CH stretching region. Several previously unreported bands are observed between 2800 and 3150 cm<sup>-1</sup>. The CH stretching modes observed above 2960 cm<sup>-1</sup> are in excellent agreement with anharmonic frequencies computed using second-order vibrational perturbation theory. However, between 2800 and 2960 cm<sup>-1</sup>, the spectra of *n*- and *i*-propyl radicals become congested and difficult to assign due to the presence of multiple anharmonic resonances. Computations employing a local mode Hamiltonian reveal the origin of the spectral congestion to be strong coupling between the high frequency CH stretching modes and the lower frequency bending/scissoring motions. The most significant coupling is between stretches and bends localized on the same CH<sub>2</sub>/CH<sub>3</sub> group. This work is being carried out in collaboration with Henry F. Schaefer at the University of Georgia and Edwin L. Sibert at the University of Wisconsin-Madison. A manuscript describing this work is currently in preparation.

Now that we have a complete assignment of the CH stretch region of the propyl radical spectra, experiments are currently being carried out to study the outcome of the sequential pick-up and reaction between propyl and O<sub>2</sub> within helium droplets. While we expect to observe the formation of propylperoxy radicals, in principle, this is the first system we have studied in which the hydroperoxypropyl radical (QOOH) is accessible via a submerged barrier below the reactant asymptote.

### Publications acknowledging DOE support (2013-present):

1. Paul L. Raston, Tao, Liang and Gary E. Douberly, "Infrared Spectroscopy and Tunneling Dynamics of the Vinyl Radical in  $^4\text{He}$  Nanodroplets" *Journal of Chemical Physics*, **138**, 174302 (2013). Published: May 7, 2013.
2. Paul L. Raston, Jay Agarwal, Justin M. Turney, Henry F. Schaefer III and Gary E. Douberly, "The Ethyl Radical in Superfluid Helium Nanodroplets: Rovibrational Spectroscopy and Ab Initio Computations" *Journal of Chemical Physics*, **138**, 194303 (2013). Published: May 21, 2013.
3. Alexander M. Morrison, Paul L. Raston and Gary E. Douberly, "Rotational Dynamics of the Methyl Radical in Superfluid  $^4\text{He}$  nanodroplets" *Journal of Physical Chemistry A* **117**, 11640-11647 (2013). Published: November 21, 2013.
4. Christopher P. Moradi, Alexander M. Morrison, Stephen J. Klippenstein, C. Franklin Goldsmith and Gary E. Douberly, "Propargyl +  $\text{O}_2$  Reaction in Helium Droplets: Entrance Channel Barrier or Not?" *Journal of Physical Chemistry A* **117**, 13626-13635 (2013). Published: December 19, 2013.
5. Christopher M. Leavitt, Christopher P. Moradi, Bradley W. Acrey and Gary E. Douberly, "Infrared Laser Spectroscopy of the Helium-Solvated Allyl and Allyl Peroxy Radicals" *Journal of Chemical Physics* **139**, 234301 (2013). Published: December 21, 2013.
6. Christopher M. Leavitt, Christopher P. Moradi, John F. Stanton and Gary E. Douberly "Communication: Helium Nanodroplet Isolation and Rovibrational Spectroscopy of Hydroxymethylene" *Journal of Chemical Physics* **140**, 171102 (2014). Published: May 5, 2014.
7. Bernadette M. Broderick, Laura McCaslin, Christopher P. Moradi, John F. Stanton and Gary E. Douberly "Reactive Intermediates in  $^4\text{He}$  Nanodroplets: Infrared Laser Stark Spectroscopy of Dihydroxycarbene" *Journal of Chemical Physics* **142**, 144309 (2015). Published: April 14, 2015.
8. Christopher P. Moradi and Gary E. Douberly "On the Stark Effect in Open Shell Complexes Exhibiting Partially Quenched Electronic Angular Momentum: Infrared Laser Stark Spectroscopy of  $\text{OH-C}_2\text{H}_2$ ,  $\text{OH-C}_2\text{H}_4$ , and  $\text{OH-H}_2\text{O}$ " *Journal of Molecular Spectroscopy* **314**, 54-62 (2015). Published: June 22, 2015.
9. Bernadette M. Broderick, Christopher P. Moradi and Gary E. Douberly "Infrared Laser Stark Spectroscopy of Hydroxymethoxycarbene in  $^4\text{He}$  Nanodroplets" *Chemical Physics Letters* **639**, 99-104 (2015). Published: September 7, 2015.
10. Christopher P. Moradi, Changjian Xie, Matin Kaufmann, Hua Guo and Gary E. Douberly "Two-center Three-electron Bonding in  $\text{ClNH}_3$  Revealed via Helium Droplet Infrared Laser Stark Spectroscopy: Entrance Channel Complex along the  $\text{Cl} + \text{NH}_3 \rightarrow \text{ClNH}_2 + \text{H}$  Reaction" *Journal of Chemical Physics*, (2016), Accepted: April 5, 2016.

# Spectroscopic and Dynamical Studies of Highly Energized Small Polyatomic Molecules

Robert W. Field  
Massachusetts Institute of Technology  
Cambridge, MA 02139  
[rwfield@mit.edu](mailto:rwfield@mit.edu)

## I. Program Scope

The fundamental goal of the program is to develop the experimental techniques, diagnostics, interpretive concepts, spectrum-assignment strategies, and pattern-recognition schemes needed to reveal and understand how large-amplitude motions are encoded in the vibration-rotation energy level structure of small, gas-phase, combustion-relevant, polyatomic molecules. We are focusing our efforts on unimolecular isomerization in the prototypical acetylene system, including the *cis*  $\rightleftharpoons$  *trans* conformational isomerization on the  $S_1$  excited state surface and the acetylene  $\rightleftharpoons$  vinylidene isomerization on the  $S_0$  ground electronic surface. Work has been extended to characterization of atmospherically relevant molecules such as  $SO_2$ .

## II. Recent Progress

### A. Spectroscopic characterization of isomerization transition states

We have recently demonstrated a method to extract transition state energies and properties from a characteristic pattern found in frequency-domain spectra of isomerizing systems.<sup>2</sup> The characteristic pattern is a dip in the spacings (the effective frequencies,  $\omega^{\text{eff}}$ ) of the barrier-proximal vibrational levels. The effective frequency dip is modeled by a semi-empirical formula as a function of energy,  $\bar{E}$ , defined as the midpoint energy for each vibrational interval:

$$\omega_{\text{eff}}(\bar{E}) = \omega_0 \left(1 - \frac{\bar{E}}{E_{TS}}\right)^{\frac{1}{m}}, \quad (1)$$

where  $\omega_0$  is the effective frequency at  $\bar{E}=0$  for the vibrational progression being analyzed,  $E_{TS}$  is the energy of the transition state, and  $m$  is a barrier shape parameter. The transition state energy can be determined from the experimentally observed  $\omega^{\text{eff}}$  by using Eq. (1). The effective frequency dip can also be used as a simple way to distinguish between vibrational modes that are actively involved in the isomerization process and those that are passive bystanders.

Our method has been applied to the *cis-trans* conformational change in the  $S_1$  state of  $C_2H_2$  and the bond-breaking HCN-HNC isomerization. Figure 1 shows plots of  $\omega_3^{\text{eff}}$  and  $\omega_6^{\text{eff}}$  for the  $3^n 6^2$ ,  $3^n 4^2$ , and  $3^n$  series of  $S_1$   $C_2H_2$ , where Eq. (1) is used to fit the observed data. The derived barrier height is found to be within 1% of the *ab initio* value (4979  $\text{cm}^{-1}$ ). It is also evident from Figure 1 that the  $3^n 6^2$  levels experience the effects of the barrier most strongly, whereas the  $3^n 4^2$  and  $3^n$  levels are completely uninfluenced by it. A combination of *trans*-bending ( $\nu_3$ ) and *cis*-bending ( $\nu_6$ ) motion is required to access the transition state geometry, also consistent with *ab initio* calculations. Torsional motion,  $\nu_4$ , which is an alternative but higher-energy pathway for *cis-trans* isomerization, is found to be unimportant for the  $S_1$  *cis-trans* conformational change.

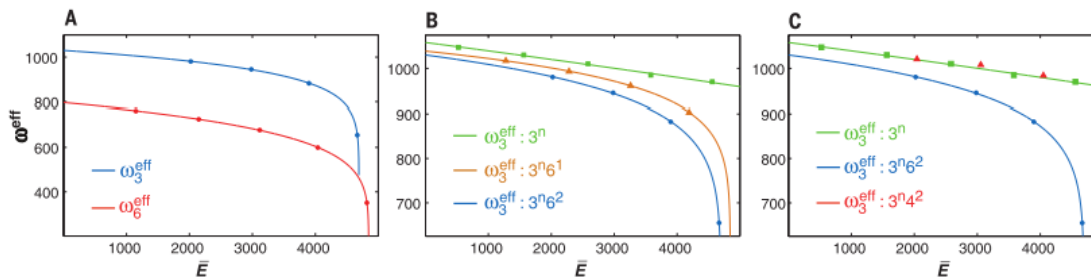


**Figure 1.** The  $\omega^{\text{eff}}$  analysis for  $S_1$   $C_2H_2$ . Equation 1 is used to fit the data points in all three subfigures. (A) Experimental  $\omega^{\text{eff}}$  for the  $3^n 6^2$  levels.  $\omega_3^{\text{eff}}$  is obtained directly from the progression of  $3^n 6^2$  levels, and  $\omega_6^{\text{eff}}$  is derived from the  $3^n 6^2$  and  $3^n 6^1$  levels at a given  $\nu_3$ . (B) Experimental  $\omega_3^{\text{eff}}$  for the  $3^n 6^2$  levels as compared to  $\omega_3^{\text{eff}}$  for other progressions with varying quanta of  $\nu_6$ . (C)  $\omega_3^{\text{eff}}$  plots for the  $3^n$ ,  $3^n 4^2$ , and  $3^n 6^2$  progressions. Notice that there is no frequency dip for  $3^n$  or  $3^n 4^2$ .

## B. Multi-photon visible fluorescence detected action spectroscopy on the $S_1(\tilde{A}^1A_u)$ state of $C_2H_2$

Detailed analysis of  $S_1$  acetylene system has led to essentially complete assignment of the vibrational and rotational structure up to  $4500\text{ cm}^{-1}$  above the zero-point level of the  $\tilde{A}$  state. Two difficulties arise when assignments are continued to higher energies. The first difficulty is the severe perturbations in the rotational K-structure of the vibrational levels (K-staggering) as a result of cis-trans tunneling. The second difficulty is that acetylene predissociation sets in roughly  $1100\text{ cm}^{-1}$  below the top of the barrier. The decrease in fluorescence quantum yield greatly limits the utility of the conventional laser-induced fluorescence (LIF) scheme, which is based on detection of fluorescence from the  $S_1$  levels.

We have developed a sensitive, easy-to-implement method of collecting spectra of predissociated levels of  $S_1$  acetylene. Our new scheme is based on detection of visible fluorescence that is a result of multi-photon excitation of acetylene (resonantly through single rovibronic  $S_1$  levels). The new detection scheme is not subject to decreases in fluorescence quantum yield of  $S_1$  levels that lie above the predissociation limit, and scattered laser light can be easily eliminated by a long-pass filter with a cutoff in the visible range. For the predissociated levels of  $S_1 C_2H_2$ , our technique has significantly improved the signal-to-noise ratio of the spectra compared to the conventional laser-induced fluorescence technique (Figure 2). The new method is also easier to implement than various H-atom detection schemes (routes we had previously pursued), which involve one additional laser of different wavelength than the excitation wavelength. Based on the power dependence and lifetime of the fluorescence signals, electronically excited  $C_2H$  and/or  $C_2$  fragments are the likely emitters of the detected visible fluorescence.

We have applied our new technique to record spectra of the ungerade vibrational levels of  $S_1 C_2H_2$  (via IR-UV double resonance excitation) in the region near the top of the isomerization barrier,  $>1000\text{ cm}^{-1}$  above the onset of  $S_1$  predissociation. The improved detection sensitivity of our new scheme has allowed us to observe and assign lines from several previously unobserved bands. We are continuing to work on complete assignments of all features.

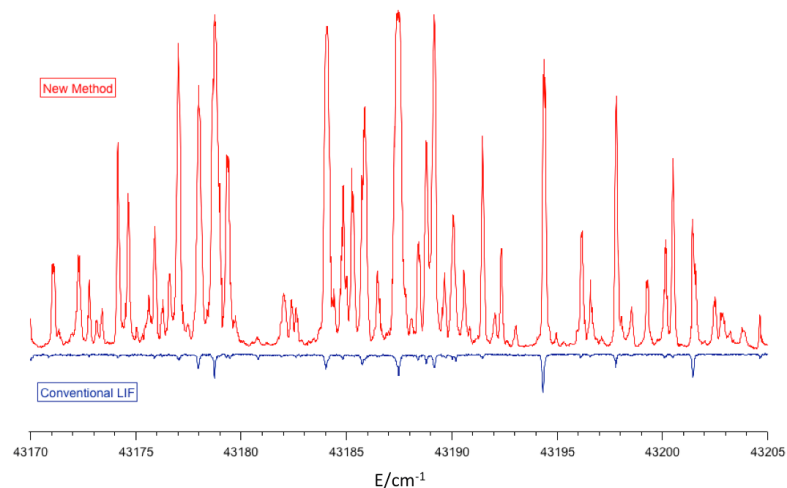


**Figure 2.** Comparison of the signal-to-noise ratio of our new multi-photon visible fluorescence detection scheme (upward red trace) and the conventional LIF scheme (downward blue trace)

## C. Spectroscopic characterizations of $SO_2 \tilde{C}^1B_2$ state

The  $SO_2 \tilde{C}^1B_2$  state has a double-well structure along the antisymmetric stretch direction on the potential energy surface (PES), so it prefers non-equivalent bond lengths ( $C_s$  geometry). In the report from last year, we reported the first direct observation (via IR-UV double-resonance) of the low-lying odd ( $b_2$ ) levels.<sup>1(a)</sup>

With the new high-resolution data, we determine a new internal coordinate quartic force field for the  $\tilde{C}$  state of  $SO_2$ .<sup>1(b)</sup> Many of the experimental observables not included in the fit, such as the Franck-Condon intensities and the Coriolis-perturbed effective  $C$  rotational constants of highly anharmonic  $\tilde{C}$  state vibrational levels, are well reproduced using our force field. Because the two stretching modes of the  $\tilde{C}$  state are strongly coupled via the Fermi-133 interaction, the vibrational structure of the  $\tilde{C}$  state is analyzed in a Fermi-system basis set (the Kellman-mode basis), constructed in this work via partial diagonalization of the vibrational Hamiltonian. By diagonalizing the vibrational Hamiltonian in the Kellman-mode basis, the vibrational characters of all vibrational levels can be determined unambiguously (Figure 3). We have shown that the bending mode cannot be treated separately from the coupled stretching modes, particularly at vibrational energies of more than  $2000\text{ cm}^{-1}$ . Based on our force field, the structure of the Coriolis interactions in the  $\tilde{C}$  state of  $SO_2$  is also discussed. We demonstrate that the alternating trends in the rotational constants of levels in the vibrational progressions of the symmetry-breaking mode (which correlates to the antisymmetric stretch in the normal mode basis) are manifestations of the presence of a double-well

on the  $\tilde{C}$  state PES.

The third paper of the series discusses the diabatic state origin of unequal bond lengths in the  $\text{SO}_2$   $\tilde{C}$   $^1\text{B}_2$  state.<sup>1(c)</sup> The measured staggering pattern is consistent with a vibronic coupling model for the double-minimum, which involves direct coupling of the diabatic  $^1\text{B}_2$  ( $\tilde{C}$ ) state to the bound  $^2^1\text{A}_1$  state and indirect coupling with the repulsive  $^3^1\text{A}_1$  state (Figure 4). The degree of staggering in the symmetry-breaking mode increases with quanta of bending excitation, consistent with the approach along the  $\tilde{C}$  state PES to a conical intersection with the  $^2^1\text{A}_1$  surface at a bond angle of  $\sim 145^\circ$ . Our work demonstrates the usefulness of low-lying vibrational level structure, where the character of the wavefunctions can be relatively easily understood, to extract information about the nature of dynamically important PES crossings that occur at much higher energy.

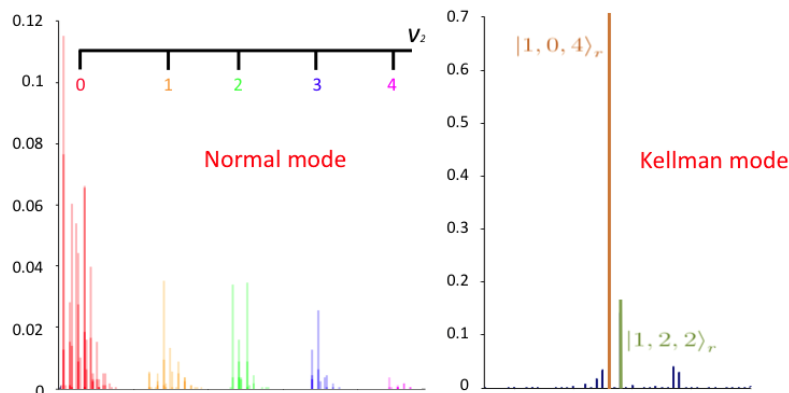


**Figure 3.** Basis state distribution of the eigenstate at  $2394\text{ cm}^{-1}$  in normal-mode (left panel) and Kellman-mode (right panel) representations. The vertical axis represents the squares of the mixing coefficient of a specific basis state. In the normal-mode representation, basis states within each color-coded cluster belong to one value of  $v_2$ , and within each cluster, basis states are ordered according to quantum number  $v_1$  followed by  $v_3$ . The eigenstate character is more broadly distributed among basis states in the normal-mode representation than in the Kellman-mode representation. While it is impossible to identify a dominant basis state in the normal-mode representation, two dominant basis states are easily identified in the Kellman-mode basis.

### III. Future Work

We plan to apply our high-sensitivity detection scheme to study the gerade symmetry vibrational states of acetylene in the energy region near the top of the cis-trans isomerization barrier. In particular, we are going to utilize hot band transition via the  $S_0$   $v_4''=1$  state to probe the currently missing  $K=0$  and 2 gerade levels in this energy region (only  $K=1$  levels are directly accessible from the ground vibrational state). The observation of a complete rotational  $K=0-2$  manifold is essential for secure vibrational assignments and the identifications of the cis-bent interloper states. The ultimate goal is to understand the spectroscopic signatures of isomerization (such as the frequency dip that we have discovered), and to be able to further characterize the transition state, e.g. the width of the isomerization barrier.

In addition, we are becoming better equipped to fully understand the  $S_0$  electronic potential energy surface of acetylene. Using recently published Franck-Condon studies of the  $\tilde{A}-\tilde{X}$  transitions, along with our improved knowledge of the shape of the  $S_1$  surface, we are in a better position to observe and characterize the acetylene  $\rightleftharpoons$  vinylidene isomerization on the  $S_0$  electronic surface, using the stimulated emission pumping technique.

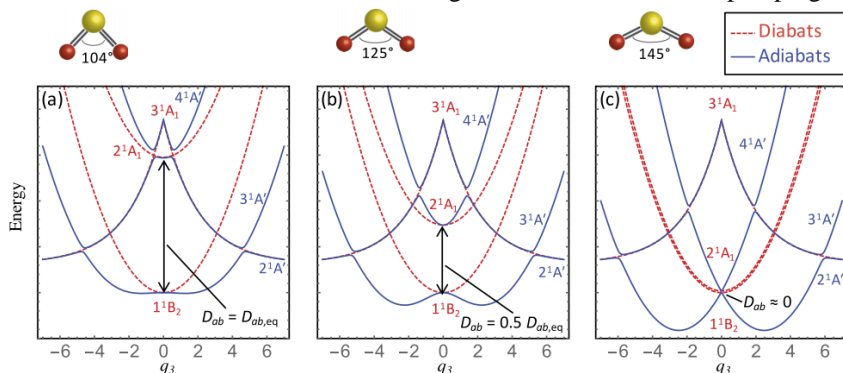


**Figure 4.** The  $q_3$ -mediated vibronic interaction between the  $^1\text{B}_2$  ( $\tilde{C}$ ) state and the  $^2^1\text{A}_1$  state at different bond angles. Interaction with the repulsive  $^4^1\text{A}'$  state is also included. The two bound potential energy surfaces cross via a conical intersection that occurs at a bond angle of  $\sim 145^\circ$ , but the crossing is avoided at  $C_s$  geometries. Therefore, as the bond angle increases, the energy denominator for the vibronic interaction decreases and the effective barrier in the  $\tilde{C}$  state adiabatic potential energy surface (and thus the degree of staggering) increases.

#### IV. Publications supported by this project 2014–2016

- (a) G. B. Park, J. Jiang, R. W. Field. "Observation of  $b_2$  symmetry vibrational levels of the  $\text{SO}_2 \tilde{C}^1\text{B}_2$  state: Vibrational level staggering, Coriolis interactions, and rotation-vibration constants", (Accepted for publication in *J. Chem. Phys.*)  
(b) J. Jiang, G. B. Park, R. W. Field. "The rotation-vibration structure of the  $\text{SO}_2 \tilde{C}^1\text{B}_2$  state explained by a new internal coordinate force field", (Accepted for publication in *J. Chem. Phys.*)  
(c) G. B. Park, J. Jiang, R. W. Field. "The origin of unequal bond lengths in the  $\tilde{C}^1\text{B}_2$  state of  $\text{SO}_2$ : Signatures of high-lying potential energy surface crossings in the low-lying vibrational structure", (Accepted for publication in *J. Chem. Phys.*)
- J. H. Baraban, P. Bryan Changala, G. C. Mellau, J. F. Stanton, A. J. Merer and R. W. Field, "Spectroscopic Characterization of Transition states", *Science* **350**, 1338-1342 (2015)
- R. W. Field, "Spectra and Dynamics of Small Molecules, Alexander von Humboldt Lectures" Springer Heidelberg, 2015.
- R. Fernando, C. Qu, J. Bowman, R. W. Field, and A. Suits, "Does Infrared Multiphoton Dissociation of Vinyl Chloride Yield Cold Vinylidene?" *J. Phys. Chem. Lett.* **6**(13), 2457 (2015).
- A. H. Steeves, H. A. Bechtel, J. H. Baraban, R. W. Field, "Communication: Observation of local-bender eigenstates in acetylene," *J. Chem. Phys.* **143**, 071101 (2015)
- G. B. Park, R. W. Field. "Edge effects in chirped-pulse Fourier transform microwave spectra", *J. Mol. Spectroscopy.* **312**, 54-57 (2015)
- C. C. Womack, M.-A. Martin-Drumel, G. G. Brown, R. W. Field, M. C. McCarthy, "Observation of the smallest Criegee intermediate  $\text{CH}_2\text{OO}$  in the gas phase ozonolysis of ethylene", *Science Advances* **1**(2), e1400105 (2015)
- P. B. Changala, J. H. Baraban, A. J. Merer, R. W. Field, "Probing *cis-trans* isomerization in the  $S_1$  state of  $\text{C}_2\text{H}_2$  via H-atom action and hot band-pumped IR-UV double resonance spectroscopies," *J. Chem. Phys.* **143**, 084310 (2015).
- G. B. Park, J. H. Baraban, A. H. Steeves, R. W. Field "Simplified Cartesian basis model for intrapolyad emission intensities in the bent-to-linear electronic transition of acetylene." *Journal of Physical Chemistry A*, **2015**, 857 (2015).
- K. Prozument, Y. V. Suleimanov, B. Buesser, J. M. Oldham, W. H. Green, A. G. Suits, R. W. Field, "A signature of roaming dynamics in the thermal decomposition of ethyl nitrite: Chirped pulse rotational spectroscopy and kinetic modeling" *J. Phys. Chem. Lett.* **5**(21), 3641-3648 (2015).
- C. Abeysekera, L. Zack, G. B. Park, B. Joalland, J. Oldham, K. Prozument, N. Ariyasingha, I. Sims, R. Field, and A. Suits, "A Chirped-Pulse Fourier-Transform Microwave /Pulsed Uniform Flow Spectrometer: II. Performance and applications for reaction dynamics," *J. Chem. Phys.* **141**(21), 214203 (2015).
- C. Abeysekera, B. Joalland, N. Ariyasingha, L. N. Zack, I. R. Sims, R. W. Field and A. G. Suits, "Product branching in the low temperature reaction of CN with propyne by chirped-pulse microwave spectroscopy in uniform supersonic flows," *J. Phys. Chem. Lett.* **6**(9), 1599 (2015).
- J. Oldham, C. Abeysekera, B. Joalland, L. Zack, K. Kuyanov-Prozument, I. Sims, G. B. Park, R. W. Field, and A. Suits, "A chirped-pulse Fourier-transform microwave pulsed uniform flow spectrometer: I. The low-temperature flow system," *J. Chem. Phys.* **141**(15), 154202 (2014).
- G. B. Park, C. C. Womack, A. R. Whitehill, J. Jiang, S. Ono, R. W. Field. "Millimeter-wave optical double resonance schemes for rapid assignment of perturbed spectra, with applications to the  $\tilde{C}^1\text{B}_2$  state of  $\text{SO}_2$ ", *J. Chem. Phys.* **142**, 144201 (2014).
- (a) G. B. Park. "Full dimensional Franck-Condon factors for the acetylene  $\tilde{A}^1\text{A}_u-\tilde{X}^1\Sigma_g^+$  transition. I. Method for calculating polyatomic linear—bent vibrational intensity factors and evaluation of calculated intensities for the *gerade* vibrational modes in acetylene," *J. Chem. Phys.* **141**, 134304 (2014).  
(b) G. B. Park, J. H. Baraban, R. W. Field. "Full dimensional Franck-Condon factors for the acetylene  $\tilde{A}^1\text{A}_u-\tilde{X}^1\Sigma_g^+$  transition. II. Vibrational overlap factors for levels involving excitation in *ungerade* modes." *J. Chem. Phys.* **141**, 134305 (2014).
- (a) P. B. Changala. "Reduced dimension rovibrational variational calculations of the  $S_1$  state of  $\text{C}_2\text{H}_2$ . I. Methodology and implementation." *J. Chem. Phys.* **140**, 024312 (2014).  
(b) P. B. Changala, J. H. Baraban, J. F. Stanton, A. J. Merer, R. W. Field. "Reduced dimension rovibrational variational calculations of the  $S_1$  state of  $\text{C}_2\text{H}_2$ . II. The  $S_1$  rovibrational manifold and the effects of isomerization." *J. Chem. Phys.* **140**, 024313 (2014).
- K. Prozument, G. B. Park, R. G. Shaver, A. K. Vasiliou, J. M. Oldham, D. E. David, J. S. Muentner, J. F. Stanton, A. G. Suits, G. B. Ellison, R. W. Field. "Chirped-pulse millimeter-wave spectroscopy for dynamics and kinetics studies of pyrolysis reactions." *Physical Chemistry Chemical Physics*, **16**, 15739, (2014).
- C. C. Womack, K. N. Crabtree, L. McCaslin, O. Martinez Jr., R. W. Field, J. F. Stanton, M. C. McCarthy, "Gas-phase structure determination of dihydroxycarbene, the smallest stable singlet carbene," *Angew. Chem. Int. Ed.* **53**(16), 4089-4092 (2014)

# Quantitative Imaging Diagnostics for Reacting Flows

Jonathan H. Frank  
Combustion Research Facility  
Sandia National Laboratories  
Livermore, CA 94551-0969  
jhfrank@sandia.gov

## Program Scope

The primary objective of this project is the development and application of quantitative laser-based imaging diagnostics for studying the interactions of fluid dynamics and chemical reactions in reacting flows. Imaging diagnostics provide temporally and spatially resolved measurements of species, temperature, and velocity distributions over a wide range of length scales. Multi-dimensional measurements are necessary to determine spatial correlations, scalar and velocity gradients, flame orientation, curvature, and connectivity. Current efforts in the Advanced Imaging Laboratory focus on studying the detailed structure of both isolated flow-flame interactions and turbulent flames. The investigation of flow-flame interactions is of fundamental importance in understanding the coupling between transport and chemistry in turbulent flames. These studies require the development of imaging diagnostic techniques to measure key species in the hydrocarbon-chemistry mechanism as well as mixture fraction, reaction rates, dissipation rates, and the velocity field. Diagnostic development includes efforts to extend measurement capabilities to a broader range of flame conditions and combustion modes and to perform three-dimensional measurements of the velocity field. A major thrust continues to be the development and application of diagnostic capabilities for measuring the temporal evolution of turbulent flames using high-repetition rate imaging techniques. Recent studies have focused on understanding the interaction between flames and the structure of turbulent flows using three-dimensional measurements of the velocity field.

## Recent Progress

### *Tomographic PIV measurements of vorticity-strain rate interactions in turbulent jet flames*

We are using tomographic particle image velocimetry (TPIV) measurements to understand the dynamics and structure of interactions between turbulent flows and flames. The TPIV technique provides volumetric, three-component velocity measurements that enable determination of key fluid dynamic quantities such as vorticity and strain rate. In turbulent combustion, strain rate fluctuations affect the heat release rate and play a central role in the dynamics of flame extinction and re-ignition. In turn, heat release introduces changes in density, viscosity, and diffusivity that can have important effects on the fluid dynamics. The vorticity and strain rate in turbulent flows are intrinsically coupled. Recently, we investigated the effects of heat release on the vorticity and strain rate fields in turbulent partially-premixed methane-air jet flames. Heat release from combustion changes the morphology of the vorticity and strain rate fields as well as the production rates of vorticity and strain. The morphological effects are apparent in comparisons of single-shot measurements of the vorticity and strain rate fields in an isothermal air jet, a flame with localized extinction ( $C_{LP}$ ), and a flame with an intact reaction zone (C) shown in Fig. 1a. Structures of elevated vorticity and strain rate are represented by isosurfaces for  $\omega = 3.0\langle\omega\rangle$  and  $|s| = 2.6\langle|s|\rangle$ , respectively. In flame C, elongated structures of high vorticity and strain rate are predominantly concentrated in overlapping regions of the jet

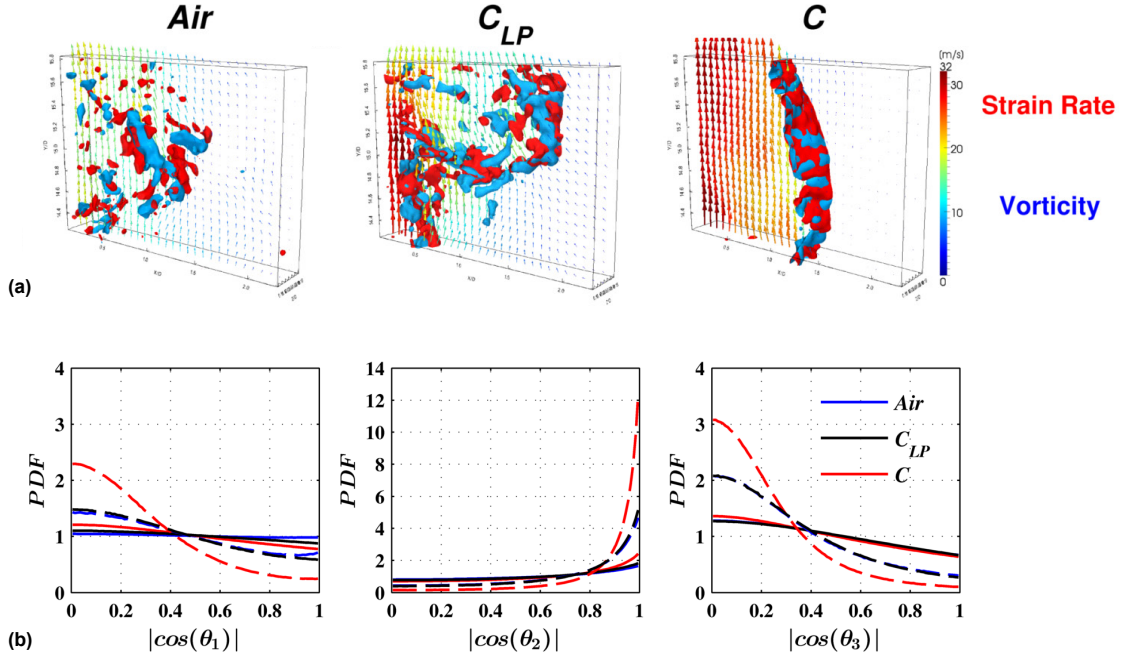


Fig. 1: (a) Isosurfaces of strain rate (red) and vorticity (blue) for  $|s| = 2.6\langle|s|\rangle$  and  $\omega = 3.0\langle\omega\rangle$  from single-shot measurements in an air jet, flame  $C_{LP}$ , and flame C. Jet axis is near the left edge of the probe volume. Velocity vectors are plotted in the central plane (1 out of 36 vectors plotted). (b) Probability density functions of the alignment angle between  $\omega$  and each of the strain rate eigenvectors,  $s_1$ ,  $s_2$ , and  $s_3$ . Solid lines: unconditional PDFs, dashed lines: conditional PDFs for  $\omega > 12000 \text{ s}^{-1}$ .

that tend to coincide with contours of the flame reaction zone. In contrast, the air jet has structures of high vorticity and strain rate that are more fragmented and less tightly overlapped than in flame C. These structures are distributed between the core of the jet and the coflow. The localized extinction in flame  $C_{LP}$  results in vorticity and strain rate fields that are a combination of structures in the air jet and the fully burning flame C.

A statistical analysis of the orientation of the vorticity,  $\omega$ , with respect to the eigenvectors of the strain rate tensor (principal strain axes),  $s_1$ ,  $s_2$ , and  $s_3$ , reveals the preferential alignment that is induced by the flame. Figure 1b shows PDFs of  $|\cos(\theta_i)|$  for the three flow conditions, where  $\theta_i$  is the angle between the vorticity vector and the  $i^{\text{th}}$  eigenvector. The plots include unconditional PDFs and PDFs conditioned on elevated vorticity for  $\omega > 12,000 \text{ s}^{-1}$ . The preferential alignment of vorticity with the axis of intermediate strain rate,  $s_2$ , is evident in the PDFs of  $|\cos(\theta_2)|$ , which all have peaks at  $|\cos(\theta_2)| = 1$ . The peak of the unconditional PDF of  $|\cos(\theta_2)|$  for flame C is higher than that of the air jet or flame  $C_{LP}$ , showing that stable combustion enhances the preferential alignment of  $\omega$  and  $s_2$ . The PDF for flame  $C_{LP}$  shows very little alignment enhancement relative to the air jet, suggesting that the localized extinction in flame  $C_{LP}$  reduces the preferential alignment of vorticity and strain towards that of a non-reacting jet. The PDFs of  $|\cos(\theta_2)|$  conditioned on  $\omega > 12,000 \text{ s}^{-1}$  have significantly larger peak values than the unconditional PDFs, indicating that the preferential  $\omega$ - $s_2$  alignment is particularly prevalent in regions of large vorticity. In addition, the enhancement of  $\omega$ - $s_2$  alignment due to the heat release in flame C is substantially greater for large values of vorticity.

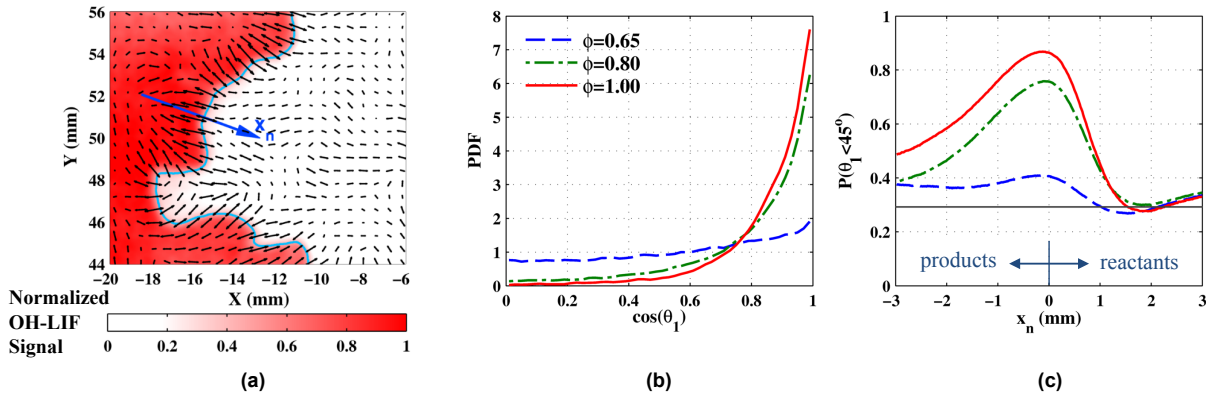


Fig. 2: (a) Single-shot measurement of extensive strain rate eigenvectors and OH-LIF image in a turbulent premixed methane-air flame. Blue contour indicates the flame front location. (b) PDFs of extensive strain rate eigenvector alignment with the flame-normal direction at the flame front ( $x_n = 0$ ) for three equivalence ratios. (c) Flame-normal conditional probabilities for  $\theta_1 < 45$  deg. as a function of the flame-normal coordinate,  $x_n$ . Black line represents a random angular distribution.

### ***Impact of heat release on strain rate field of turbulent premixed flames***

We have investigated the local vorticity-strain coupling near the flame front of turbulent premixed methane-air Bunsen flames. In contrast to the turbulent partially-premixed jet flames in which flow shear plays a significant role in the vorticity-strain alignment, the turbulent premixed flames exhibit a different preferential alignment near the flame front. Figure 2a shows a single-shot OH-LIF measurement along with the projection of the extensive strain rate eigenvectors in the OH-LIF imaging plane. The eigenvectors along the flame front tend to be oriented nearly orthogonal to the flame contour but are more scattered in the regions away from the flame front. These observations are reflected in the PDFs of the angle between the extensive strain rate eigenvectors and the flame-normal direction,  $\theta_1$ , at the flame front shown in Fig. 2b. For premixed flames with equivalence ratios from  $\phi = 0.65$  to 1.0, the alignment PDFs have a peak at  $\cos(\theta_1) = 1$ , indicating that the  $s_1$ -eigenvectors are preferentially aligned with the flame normal. This alignment is strongest for  $\phi = 1.0$  and weakest in the leanest flame  $\phi = 0.65$ .

The dependence of this preferential strain rate alignment on the distance from the flame front is shown in Fig. 2c. The probabilities of orientations with  $\theta_1 < 45$  deg. are plotted as a function of the flame-normal coordinate,  $x_n$ , extending 3 mm on each side of the flame front. For reference, a line at  $P(\theta_1 < 45^\circ) = 29\%$  indicates the corresponding probability for a randomly oriented three-dimensional vector field. For all the flames, the extensive strain rate alignment probability is largest in the reaction zone near  $x_n = 0$  mm and decreases with distance in the reactant and product regions. The extent of this preferential orientation is most pronounced for the  $\phi = 1.0$  flame and decreases for the lean flames in concert with the decrease in the heat release parameter and Damköhler number. For  $x_n > 1.5$  mm,  $P(\theta_1 < 45^\circ)$  is comparable to that of a random vector field. Overall, the probability distributions of the leanest flame exhibit a relatively small deviation from that of a randomly distributed vector field, and the flame front has a weak impact on the orientation of the eigenvectors across the 6 mm region straddling the flame front. Investigations are underway to extend the understanding of these differing effects of the flame on the turbulence to a broader range of conditions.

## Future Plans

The investigation of the structure and dynamics of flow-flame interactions in turbulent non-premixed, premixed, and stratified modes of combustion will remain a major thrust in our research program. In the near term, we plan to expand our understanding of the effects of combustion on the strain rate and vorticity fields in flames with and without localized extinction. Our planned high-speed imaging effort includes optimization of TPIV analysis and further evaluation of uncertainties, methods for noise reduction, and efficient methods for analyzing large sets of imaging data. We are pursuing a joint experimental and computational investigation of turbulent counterflow flames with high-fidelity LES calculations performed by J. Oefelein. This collaboration will include the development of a framework for comparing measurements and simulations of turbulent flame dynamics as well as the use of LES to generate synthetic TPIV data for uncertainty analysis and improvements in data processing.

Plans for advancing diagnostic capabilities include applications of a custom burst-mode laser for imaging at rates of 100 kHz. We also plan to develop the capability for joint velocity and temperature measurements using PIV and 2-D CARS in collaboration with C. Klierer. In collaboration with R. Barlow, we plan to improve quantification of CH<sub>2</sub>O-LIF measurements to understand effects of formaldehyde transport in turbulent DME flames with localized extinction.

## BES-supported publications and submitted journal articles (2014-present)

B. Coriton, A.M. Steinberg, J.H. Frank, "High-speed tomographic PIV and OH PLIF measurements in turbulent reactive flows," *Exp. Fluids*, **55**, 1-20 (2014).

J.H. Frank, A. Sharvorskiy, H. Bluhm, B. Coriton, E. Huang, D.L. Osborn, "In-situ soft x-ray absorption spectroscopy of flames," *Appl. Phys. B*, **117**, 493-499 (2014).

B. Coriton, J.H. Frank, "High-speed tomographic PIV measurements of strain rate intermittency and clustering in turbulent partially premixed jet flames," *Proc. Combust. Inst.*, **35**, 1243-1250 (2015).

B. Coriton, M. Zendejdel, S. Ukai, A. Kronenburg, O.T. Stein, S-K Im, M. Gamba, J.H. Frank, "Imaging measurements and LES-CMC modeling of a partially-premixed turbulent dimethyl ether/air jet flame," *Proc. Combust. Inst.*, **35**, 1251-1258 (2015).

A.M. Steinberg, B. Coriton, J.H. Frank, "Influence of combustion on principal strain rate transport in turbulent premixed flames," *Proc. Combust. Inst.*, **35**, 1287-1294 (2015).

J. Weinkauff, P. Trunk, J. H. Frank, M.J. Dunn, A. Dreizler, B. Böhm, "Investigation of flame propagation in a partially premixed jet by high-speed stereo PIV and acetone PLIF," *Proc. Combust. Inst.*, **35**, 3773-3781 (2015).

S. Popp, F. Hunger, S. Hartl, D. Messig, B. Coriton, J. H. Frank, F. Fuest, C. Hasse, "LES flamelet-progress variable modelling and measurements of a turbulent partially-premixed dimethyl ether jet flame," *Combust. Flame*, **162**, 3016-3029 (2015).

B. Coriton, J.H. Frank, "Experimental study of vorticity-strain rate interaction in turbulent partially premixed jet flames using tomographic particle image velocimetry," *Phys. Fluids*, **28**, 025109 (2016).

B. Coriton, J.H. Frank, A. Gomez, "Interaction of turbulent premixed flames with combustion products: Role of stoichiometry," *Combust. Flame*, Submitted.

B. Coriton, J. H. Frank, "Impact of heat release on strain rate field in turbulent premixed Bunsen flames," *Proc. Combust. Inst.*, Submitted.

G. Neuber, A. Kronenburg, O. T. Stein, M. J. Cleary, B. Coriton, J. H. Frank, "Sparse-Lagrangian MMC modelling of the Sandia DME (D-F) jet flames," *Proc. Combust. Inst.*, Submitted.

M. Kamal, B. Coriton, R. Zhou, J. H. Frank, S. Hochgreb, "Scalar dissipation rate and scales in swirling turbulent premixed flames," *Proc. Combust. Inst.*, Submitted.

# Computer-Aided Construction of Chemical Kinetic Models

William H. Green  
Department of Chemical Engineering  
Massachusetts Institute of Technology  
Cambridge, MA 02139  
whgreen@mit.edu

## I. Program Scope

The combustion chemistry of even simple fuels can be extremely complex, involving hundreds or thousands of kinetically significant species. The most reasonable way to deal with this complexity is to use a computer not only to numerically solve the kinetic model, but also to construct the kinetic model in the first place. Because these large models contain so many numerical parameters (e.g. rate coefficients, thermochemistry) one never has sufficient data to uniquely determine them all experimentally. Instead one must work in “predictive” mode, using theoretical values for many of the numbers in the model, and as appropriate refining the most sensitive numbers through experiments. Predictive chemical kinetics is exactly what is needed for computer-aided design of combustion systems based on proposed alternative fuels, particularly for early assessment of the value and viability of proposed new fuels. It is also very helpful in other fuel chemistry problems, and in understanding emissions and environmental chemistry. Our research effort is aimed at making accurate predictive chemical kinetics practical; this is a challenging goal which necessarily includes a range of science advances. Our research spans a wide range from quantum chemical calculations on individual molecules and elementary-step reactions, through the development of improved rate/thermo calculation procedures, the creation of algorithms and software for constructing and solving kinetic simulations, the invention of methods for model-reduction while maintaining error control, and finally comparisons with experiment. Many of the parameters in the models are derived from quantum chemistry, and the models are compared with experimental data measured in our lab or in collaboration with others.

## II. Recent Progress

### A. Elucidating Interesting Chemistry

#### 1. Hydrocarbon ignition

Together with Stephen Klippenstein, Michael Burke, and Franklin Goldsmith we have made a significant advance in understanding phase 1 ignition, which we find is actually is two stages: an exponential growth phase we call stage 1A, followed by a more complicated phase where the chemistry is nonlinear that we call stage 1B. Both stages are sensitive to only a handful of reactions, suggesting that it may be possible to understand and model low-temperature ignition without recourse to the very large kinetic models used currently, and indeed for pure alkanes we are able to write simple analytical expressions for ignition delay in terms of a few rate parameters.[10] We are currently pursuing a similar approach to understand phase 2 ignition chemistry, and exploring how to use this insight to construct relatively simple but still accurate models for the ignition of fuel blends. If successful, this has the potential to lead to a much more useful and accurate rating system for the ignition of fuel blends than the simple “octane” and “cetane” numbers used currently.

#### 2. Vinyl radical chemistry and formation of aromatic rings

For several years we have been measuring and computing the chemistry of vinyl radical ( $C_2H_3$ ), which is the key species at the branch point between clean combustion (to  $CO_2$ ) and soot formation.

Recently we directly measured the rate coefficient for vinyl + butadiene, a proposed route to benzene formation, which is an order of magnitude slower than published estimates, but in good agreement with our computed rate coefficient.[9] We have recently probed the vinyl + acetylene system using flash photolysis with photoionization mass spectrometry detection. This system is quite interesting, since the initial  $C_4H_5$  adduct reacts with acetylene to form benzene. However, the fact that several reactions are running with similar rates makes it difficult to extract the rate coefficients unambiguously.

We also recently theoretically studied the recombination of cyclopentadienyl radicals, which forms naphthalene ( $C_{10}H_8$ ). We found that at many conditions the  $C_{10}H_{10}$  adduct lives long enough to react with another radical, so the dominant overall reaction is not  $2 C_5H_5 \rightarrow C_{10}H_8 + H + H$  (as sometimes assumed in the literature) but instead  $3 C_5H_5 \rightarrow C_{10}H_8 + C_5H_6 + H$ . Because the former reaction converts unreactive radicals into reactive H atoms, but the latter sequence net consumes radicals, the kinetic consequences of this change are significant.

### 3. Criegee Intermediate Chemistry

In recent years we measured and computed several reactions of the smallest Criegee Intermediate  $CH_2OO$ . [1,2,12] We recently measured the T-dependence of the rate coefficients for  $CH_2OO$  additions to C=O double bonds ( $CH_2OO + CH_3CHO$  and  $CH_2OO +$  acetone) [12], and previously we measured the T-dependence of the analogous additions to C=C double bonds.[1] The transition state structures for all of these reactions are similar, so as expected they all have similar A factors. However, the additions to C=C have normal Arrhenius T dependence, while the additions to C=O have inverse T dependence, Fig.1. We interpret this as being due to the fact that the transition states for the  $CH_2OO$  additions to C=O double bonds are significantly submerged (i.e. the saddle point energy lies below the energy of the reactants), causing  $E_a$  to be negative.

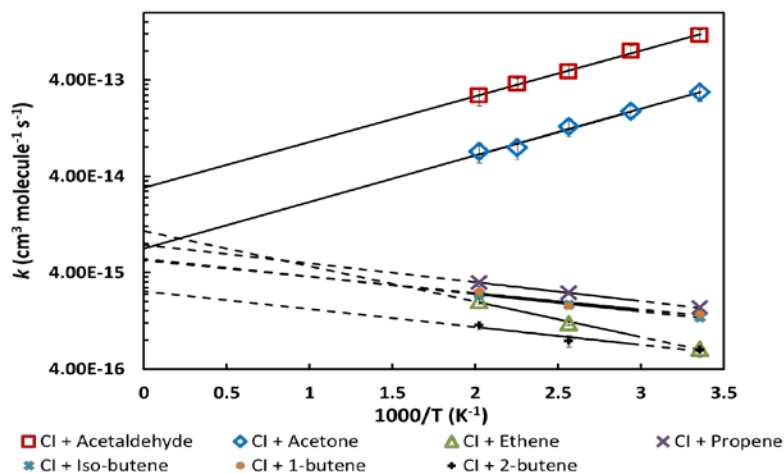


Fig. 1 Arrhenius plot for  $CH_2OO$  ("CI") addition to carbonyls and alkenes.

### B. Methodology for Computer-Aided Kinetic Modeling

A major focus of this research project continues to be the development of advanced methods for automatically constructing, reducing, and solving combustion simulations. We are constantly adding functionality and additional types of chemistry to the open-source Reaction Mechanism Generator (RMG) software package. We very recently developed a completely new version of this software package written in Python, and including a more flexible representation of molecules, allowing it to better handle ionic species and biradicals.[11] We have also significantly improved how the software handles fused cyclics

and cyclization reactions. The new “RMG-Py” also includes some organosulfur and organonitrogen chemistry. We have also developed a very convenient website <http://rmg.mit.edu> which includes many tools for estimating rate coefficients and thermochemistry, with comparisons to values in popular databases.

This computer-aided kinetic modeling approach is now being used to model a wide range of chemical systems, for examples see [a,b,c,d,5,6,7,8]. We continue to distribute the mechanism construction software to many research groups, and to train and support the new users. In the past two years researchers from several US universities plus Belgium, China, Denmark, France, Israel, Japan, United Arab Emirates, and Saudi Arabia have visited my group for training in how to use the RMG software. Several companies are also now using the software, not just energy and petrochemical companies but also other industries including computer chip manufacturers and producers of personal care products. Developers outside of my research group have begun to add functionality to this open-source software; among the most active developers are researchers at Northeastern University and the University of Ghent. These independently funded external efforts leverage the funding provided by this program.

### C. Quantum Calculations of Reaction Rates and Thermochemistry

Historically, the accuracy of rate and equilibrium calculations for combustion were almost always limited by the uncertainties in the computed potential energy surface, due to the need to use approximate electronic structure methods and small basis sets. Modern quantum chemistry methods, such as explicitly-correlated coupled-cluster methods (e.g. CCSD(T)-F12) have made it practical to significantly reduce these errors in computed PES's and molecular enthalpies. As the energy calculations improve, we find that the accuracy of our equilibrium and rate calculations is now often limited by other aspects of the overall calculation. This has led us (and many others, including Don Truhlar and Stephen Klippenstein) to invest significant efforts in improving on the traditional rate and thermochemistry computation methodology, which is based on several approximations which are not really accurate.

We are currently working on methods for more accurately handling coupled hindered rotors. This is particularly important for molecules with more than one oxygen-containing functional group, e.g. ketohydroperoxides and species in or derived from biofuels. One interesting line of work is computing the partition functions for these species using path integral methods evaluated by RPMD (e.g. using a modified version of our RPMDRate software.[e])

## III. References

- a. Enoch E. Dames, Andrew S. Rosen, Brian W. Weber, Connie W. Gao, Chih-Jen Sung, and William H. Green, “A detailed combined experimental and theoretical study on dimethyl ether / propane blended oxidation”, *Combustion & Flame* (2016, accepted).
- b. Adam G. Carr, Caleb A. Class, Lawrence T.C. Lai, Yuko Kida, Tamba E. Monroe, and William H. Green, “Supercritical Water Treatment of Crude Oil and Hexylbenzene: An Experimental and Mechanistic Study on Alkylbenzene Decomposition”, *Energy & Fuels*, **29**, 5290–5302 (2015).
- c. Nick M Vandewiele, Gregory R Magoon, Kevin Marcel Van Geem, Marie-Françoise Reyniers, William H Green, Guy B Marin, “Kinetic Modeling of Jet-Propellant 10 Pyrolysis”, *Energy & Fuels* **29**, 413-427 (2015).
- d. Joshua W. Allen, Connie Gao, Shamel S. Merchant, Adam M. Scheer, Subith S. Vasu, Oliver Welz, J.D. Savee, David L. Osborn, Changyoul Lee, Stijn Vranckx, Z. Wang, Fei Qi, Ravi X. Fernandes, William H. Green, M.Z. Hadi, Craig A. Taatjes, “Concerted Development of Biofuel Production and Utilization: A Coordinated Investigation of Diisopropyl Ketone, a Prototypical Biofuel”, *Combustion & Flame* **161**, 711-724 (2014).
- e. Y.V. Suleimanov, J.W. Allen, and W.H. Green, “RPMDrate: bimolecular chemical reaction rates from ring polymer molecular dynamics”, *Comp. Phys. Comm.* **184**(3), 833-840 (2013).

#### IV. Publications and submitted journal articles supported by BES 2014-2016

1. Zachary J. Buras, Rehab M.I. Elsamra, Amrit Jalan, Joshua E. Middaugh, and William H. Green, "Direct Kinetic Measurements of Reactions between the Simplest Criegee Intermediate  $\text{CH}_2\text{OO}$  and alkenes", *Journal of Physical Chemistry A* **118**, 1997-2006 (2014).
2. Zachary J. Buras, Rehab M.I. Elsamra, and William H. Green, "Direct Determination of the Simplest Criegee Intermediate ( $\text{CH}_2\text{OO}$ ) Self Reaction Rate", *Journal of Physical Chemistry Letters* **5**, 2224-2228 (2014).
3. Y. Li, Yury V. Suleimanov, William H. Green, and Hua Guo, "Quantum Rate Coefficients and Kinetic Isotope Effect for the Reaction  $\text{Cl} + \text{CH}_4 \rightarrow \text{HCl} + \text{CH}_3$  from Ring Polymer Molecular Dynamics", *Journal of Physical Chemistry A* **118**, 1989-1996 (2014).
4. Gonzalez-Lavado, J.C. Corchado, Y.V. Suleimanov, W.H. Green, J. Espinosa-Garcia, "Theoretical Kinetics Study of the  $\text{O}(^3\text{P}) + \text{CH}_4/\text{CD}_4$  Hydrogen Abstraction Reaction: The Role of Anharmonicity and Quantum Mechanical Effects", *J. Chem. Phys. A* **118**, 3243-3252 (2014).
5. Kirill Prozument, Yury V. Suleimanov, Beat Buesser, James M. Oldham, William H. Green, Arthur G. Suits, and Robert W. Field, "A signature of roaming dynamics in the Thermal Decomposition of Ethyl Nitrite: Chirped-Pulse Rotational Spectroscopy and Kinetic Modeling", *Journal of Physical Chemistry Letters* **5**, 3641-3648 (2014).
6. Yury V. Suleimanov, Wendi J. Kong, Hua Guo, and William H. Green, "Ring-polymer molecular dynamics: Rate coefficient calculations for energetically symmetric (near thermoneutral) insertion reactions ( $\text{X} + \text{H}_2 \rightarrow \text{HX} + \text{H}(\text{X} = \text{C}(^1\text{D}), \text{S}(^1\text{D}))$ )", *Journal of Chemical Physics* **141**, 244103 (2014).
7. A. Fridlyand, S.S. Goldsborough, K. Brezinsky, S.S. Merchant, and W.H. Green, "Influence of the Double Bond Position on the Oxidation of Decene Isomers at High Pressures and Temperatures", *Proceedings of the Combustion Institute* **35**, 333-340 (2015).
8. Connie W. Gao, Aäron Vandeputte, Nathan W. Yee, William H. Green, Robin E. Bonomi, Gregory R. Magoon, Hsi-Wu Wong, Oluwayemisi O. Oluwole, David K. Lewis, Nick M. Vandewiele, and Kevin Van Geem, "JP-10 combustion studied with shock tube experiments and modeled with automatic reaction mechanism generation", *Combustion & Flame* **162**, 3115-3129 (2015).
9. Zachary J. Buras, Enoch E. Dames, Shamel S. Merchant, Guozhu Liu, Rehab M.I. Elsamra and William H. Green, "Kinetics and Products of Vinyl + 1,3-Butadiene, a Potential Route to Benzene" *Journal of Physical Chemistry A* **119**, 7325-7338 (2015).
10. Shamel S. Merchant, C. Franklin Goldsmith, Aäron G. Vandeputte, Michael P. Burke, Stephen J. Klippenstein, and William H. Green, "Understanding low-temperature first-stage ignition delay: Propane", *Combustion & Flame* **162**, 3658-3673 (2015).
11. Connie W. Gao, Joshua W. Allen, William H. Green, and Richard H. West, "Reaction Mechanism Generator: Automatic Construction of Chemical Kinetic Mechanisms", *Computer Physics Communications* (2016, accepted).
12. Rehab M.I. Elsamra, Amrit Jalan, Zachary J. Buras, Joshua E. Middaugh, and William H. Green, "Temperature and Pressure Dependent Kinetics of  $\text{CH}_2\text{OO} + \text{CH}_3\text{COCH}_3$  and  $\text{CH}_2\text{OO} + \text{CH}_3\text{CHO}$ : Direct Measurements and Theoretical Analysis", *International Journal of Chemical Kinetics* (submitted).

# Gas-Phase Molecular Dynamics: High Resolution Spectroscopy and Collision Dynamics of Transient Species

Gregory E. Hall  
Chemistry Department, Brookhaven National Laboratory  
Upton, NY 11973-5000  
[gehall@bnl.gov](mailto:gehall@bnl.gov)

## Program Scope

This research is carried out as part of the Gas-Phase Molecular Dynamics program in the Chemistry Department at Brookhaven National Laboratory. Chemical intermediates in the elementary gas-phase reactions involved in combustion chemistry are investigated by high resolution spectroscopic tools. Production, reaction, and collisional energy transfer processes are investigated by transient, double resonance, polarization and saturation spectroscopies, with an emphasis on technique development and connections with theory.

## Recent Progress

### A. Ground state energy transfer in collisions of CN (X)

Our study of ground state CN radical collisions with rare gases has been extended with Doppler-resolved saturation transfer measurements and depolarization measurements. A tunable ns dye laser is used to bleach selected rotational states of a thermalized sample of CN radicals, while probing the saturation and recovery of the bleached state, or the transfer of saturation to a different rotational state through collisional energy transfer. By using a frequency modulated continuous probe laser for transient absorption, the recovery kinetics can be recorded as a function of Doppler detuning as well as probe polarization, giving access to a highly detailed measurement of speed-dependent kinetics and depolarization for the single and multiple-collision relaxation processes. The linewidth of the pulsed dye laser is sufficient to saturate the full Doppler width of a transition. The Doppler-resolved kinetics then depends on both the speed dependence of the relaxation and the velocity randomizing collisions that tend to re-establish Maxwell-Boltzmann velocity distributions, perturbed by coupling to the non-equilibrium state distribution. It is this same competition that plays a key role in the interpretation of collisional narrowing in the lineshapes of pressure broadened lines. Sub-Doppler bleach and probe experiments described below aim to separate these two effects definitively in the CN + rare gas systems for which accurate quantum scattering calculations are available for comparison.

### B. Photodissociation Dynamics in NO-Rare gas complexes

The central challenge of molecular dynamics is to understand chemical events in terms of the multi-dimensional surfaces of potential energy that encode the atomic and molecular forces at play. Photodissociation is a particularly simple example, for which the initial configuration of atoms and total energy and angular momentum are more constrained than in a full reactive collision, and only the final bond-breaking event is important. Comparisons of experimental and theoretically computed photoproduct state distributions, branching ratios, angular distributions, and polarization properties constitute a detailed validation of theory that underpins the enterprise of molecular dynamics and establishes the range of validity for the various approximations often needed to make the complex calculations tractable.

The weakly bound complex of the free radical NO with rare gases undergoes a particularly simple type of molecular photodissociation, producing electronically excited NO (*A*) and an unbound rare gas atom when excited at energies slightly above the energy of the *A-X* transition in diatomic NO. The spherically averaged interaction potentials for NO-Ar at the right depict excitation to a repulsive region of the upper state, prior to fragmentation. This apparent simplicity made it surprising to find dramatic energy-dependent variations in the fragment angular distributions as well as the rotational state distributions, when comparing NO-He, NO-Ne and NO-Ar in recent experiments by Australian colleagues at Flinders University. High quality potential energy surfaces for interaction of rare gases with ground and excited states of NO are available and have been tested against scattering and bound-state spectroscopic studies elsewhere, encouraging us to model these photodissociation systems with two-dimensional time-dependent wavepacket calculations performed by BNL colleague H.-G. Yu. The calculations account very well for the excitation spectra, including resonance structures close to the dissociation threshold, and experimental rotational state distributions, which display a rotational rainbow structure in the case of NO-Ar and NO-Ne, but not in the case of NO-He. The effects of different excited state potential energy surfaces can be readily visualized in these low-dimensional calculations. The distinctive and unexpected energy-dependent variation in the NO angular distributions can be qualitatively explained with an approximate Franck-Condon model in an axial recoil limit. A future, rigorous quantum mechanical treatment will require methods that include the rotational coordinates and the electronic degeneracy of the floppy ground state complex, as well as a dynamical treatment that does not rely on the axial recoil approximation. The simplicity of a  $^1S$  atom and a  $^2\Sigma$  state of the vibrationally inactive diatomic co-fragment removes most other complexity from the problem. This is a continuing collaboration with H.-G. Yu in our group and external theoretical and experimental collaborators.

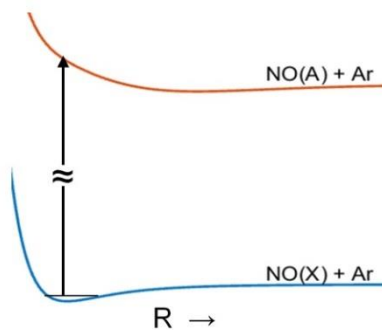


**Fig. 1. Spherically averaged NO-Ar potentials**

## Future Work

### A. Intersystem crossing in CH<sub>2</sub> induced by O<sub>2</sub> ( $^3\Sigma_g^-$ )

The collision-induced intersystem crossing (ISC) between singlet *a* and triplet *X* states of CH<sub>2</sub>, induced by nonreactive singlet collision partners is dominated by a gateway state mechanism involving a few pairs of accidentally perturbed rotational levels with mixed singlet/triplet character. Interaction of triplet O<sub>2</sub> with singlet CH<sub>2</sub> can proceed by a spin-allowed mechanism, not dependent on accidental perturbations. The complicated potential surfaces of CH<sub>2</sub>O<sub>2</sub> furthermore connect multiple low-energy product channels including energetically accessible singlet and triplet states of the Criegee intermediate. We have measured quenching kinetics of selected rotational states of singlet CH<sub>2</sub> in samples containing controlled mixtures of Ar, O<sub>2</sub> and ketene (a photolytic precursor for CH<sub>2</sub>), in order to investigate the reversible ISC process. In the absence of O<sub>2</sub>, the relaxation is double exponential, with distinguishable kinetics for *ortho* and *para* states of CH<sub>2</sub>, a mark of the stronger coupling of *para* states with the more nearly isoenergetic (030) vibrational level of the X  $^3B_2$  state of CH<sub>2</sub>. The interaction of singlet CH<sub>2</sub> with

molecular  $O_2$  accesses an excited triplet state of  $CH_2O_2$ , which intersects the lowest triplet surface, leading nonreactively to  $O_2 + \text{triplet } CH_2$ . The initial decay rate of selected rotational states of  $CH_2$  is accelerated by  $O_2$ , but the relative amplitude of the slow decay is also enhanced by  $O_2$ , suggesting a continued role for reversible population of vibrationally excited triplet  $CH_2$  in the overall mechanism. A spectroscopic search for infrared probe transitions suitable for monitoring vibrationally excited triplet methylene, a key species in the non-thermal kinetics, has not so far produced a useful diagnostic to complement the singlet and perturbed singlet transitions. The measured singlet  $CH_2$  kinetics nonetheless constrains the interpretation of the intersystem crossing process in the presence and absence of molecular oxygen. Further work on this system is in progress.

## B. Sub-Doppler saturation recovery in CN radicals

The competition between elastic, velocity-changing collisions and rotationally inelastic collisions plays a key role in the collisional dephasing that is responsible for pressure broadening and collisional narrowing. The physically distinct processes of Dicke narrowing (optical velocity diffusion) and speed-dependent relaxation can each account for a phenomenological narrowing of isolated spectral lines in comparison to a Voigt reference for pressure broadening. Sub-Doppler saturation recovery kinetics provides a direct, time-domain probe of the governing collision dynamics, in a system amenable to high-quality quantum scattering calculations for comparison.

A thermal sample of  $CN(X)$  radicals is produced by collisional relaxation following photolysis in low pressure flow cell, and interrogated by a frequency modulated probe laser, tuned to a selected rotational line in the  $A-X$  (1-0) band. A  $2 \mu\text{s}$  pulse, electro-optically chopped from a fixed frequency cw bleach laser, partially saturates a narrow velocity group of each ground-state hyperfine level within a selected rotational line of the  $CN$   $A-X$  (2-0) band. When a single sideband of the scanning probe laser interrogates the corresponding velocity group of the same hyperfine level on a different rotational transition, the transient double-resonance signal is observed, as illustrated in Fig 2. The depletion reaches a steady-state amplitude during the bleach pulse, and relaxes to near zero after the bleach pulse is extinguished, with a recovery rate that scales with the total pressure. Scanning the probe laser and recording the amplitude of the steady-state bleach signal yields a characteristic hyperfine sub-Doppler saturation spectrum, as shown in Fig 3. The arrow in the spectrum indicates the frequency in the probe laser scan where the illustrated transient signals of Fig. 1 were extracted. The collisional

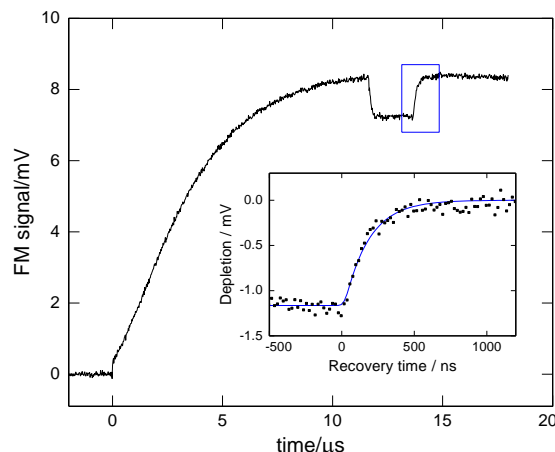


**Fig. 2. CN transient FM signal with saturation and recovery. Inset: recovery kinetics**

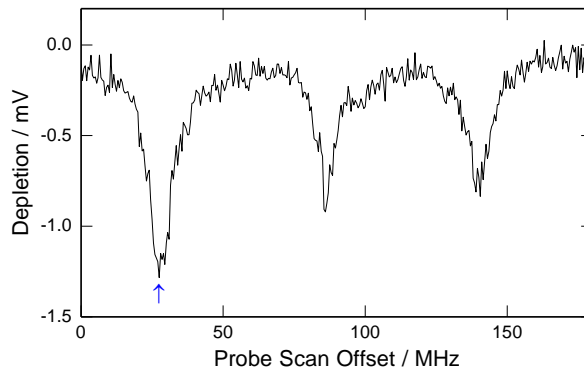


**Fig. 3. Two color sub-Doppler saturation spectrum: bleach (2-0)  $R_1(4)$ ; probe (1-0)  $R_1(4)$**

recovery rate is found to decrease with detuning from the center of the saturation maxima, characterizing the time-dependent broadening of the saturation line shape after the bleach pulse is shut off. The velocity-independent component of the recovery is known from the rotationally inelastic rates measured in the broadband saturation recovery experiments, while the broadening of the saturation lineshape during collisional relaxation is caused by the small angle elastic scattering that dominates the velocity changing collision processes. If elastic collisions were to occur with a large scattering angle, the Doppler shift would change enough to remove molecules from the restricted spectral region of observation as effectively as an inelastic collision. Calculations show, however, that very few elastic CN+Ar collisions suffer deflection angles greater than about 5°, limiting the effectiveness of optical diffusion as a line narrowing mechanism in this system. Comparisons of the experimental measurements with Monte Carlo modeling of multiple collisions are in progress, using calculated ratios of elastic to inelastic cross sections and elastic differential cross sections for selected rotational states and selected velocity groups.

### Publications supported by this project since 2014

- Collinear two-color saturation spectroscopy in CN A-X (1-0) and (2-0) bands, D. Forthomme, C. P. McRaven, T. J. Sears, and G. E. Hall, *J. Molec. Spectrosc.* **296**, 36-42 (2014). <http://dx.doi.org/10.1016/j.jms.2013.12.006>
- Frequency Comb-Referenced Spectroscopy in the  $\nu_1 + \nu_3$  Region of Acetylene, M.J. Cich, D. Forthomme, G.E. Hall, C.P. Mcraven, T.J. Sears, S. Twagirayezu, *The 13th Biennial HITRAN Conference (HITRAN13), Harvard-Smithsonian Center for Astrophysics, Cambridge, MA, USA, 23-25 June, 2014.* <http://dx.doi.org/10.5281/zenodo.11181>
- Frequency-comb referenced spectroscopy of  $\nu_4$ - and  $\nu_5$ -excited hot bands in the 1.5  $\mu\text{m}$  spectrum of C<sub>2</sub>H<sub>2</sub> S. Twagirayezu, M. J. Cich, T. J. Sears, C. P. McRaven, G. E. Hall, *J. Molec. Spectrosc.* **316**, 64-71 (2015). <http://dx.doi.org/10.1016/j.jms.2015.06.010>
- Doppler-Resolved Kinetics of Saturation Recovery, D. Forthomme, M. L. Hause, H.-G. Yu, P. J. Dagdigian, T. J. Sears and G. E. Hall, *J. Phys. Chem. A* **119** 7439-7450 (2015). <http://dx.doi.org/10.1021/acs.jpca.5b00628>
- Application of the Hartmann–Tran profile to precise experimental data sets of <sup>12</sup>C<sub>2</sub>H<sub>2</sub>. Forthomme, M. J. Cich, S. Twagirayezu, G. E. Hall and T. J. Sears, *J. Quant. Spectrosc. Rad. Trans.* **165** 28-37 (2015). <http://dx.doi.org/10.1016/j.jqsrt.2015.06.013>
- Rotational and angular distributions of NO products from NO-Rg (Rg = He, Ne, Ar) complex photodissociation, H. L. Holmes-Ross, R. J. Valenti, Hua-Gen Yu, G. E. Hall and W. D. Lawrance, *J. Chem. Phys.* **144**, 044309 (2016). <http://dx.doi.org/10.1063/1.4940690>

# Flame Chemistry and Diagnostics

Nils Hansen

*Combustion Research Facility, Sandia National Laboratories, Livermore, CA 94551-0969*

Email: nhansen@sandia.gov

## SCOPE OF THE PROGRAM

In this program, we seek to understand the detailed chemistry of combustion through a unique scheme of diagnostics development and experimental studies of simple flames. Our goal is to provide reliable experimental data on the chemical composition of laboratory-scale model flames and reactors through state-of-the-art diagnostics. The experiments are designed to serve as benchmarks for the development and validation of detailed chemical kinetic models. In particular, we study the composition of laminar premixed flames, which are stabilized on a flat-flame burner under a reduced pressure of ~15-30 Torr, of laminar opposed-flow diffusion flames at low and atmospheric pressure, and of a jet-stirred reactor that is also operated near atmospheric pressure. We employ mass spectrometry and our experimental data in the form of species identification and quantification serve as stringent tests for the development and validation of any detailed chemical kinetic mechanisms. Over the past years, the overall objective of this program has been to elucidate the chemistry of soot precursors and the formation of unwanted byproducts in incomplete combustion in flames fueled by hydrocarbons and oxygenates. Studying this complex combustion chemistry with an unprecedented level of detail requires determining the chemical structures and concentrations of species sampled from sooting or nearly-sooting model flames. Using the jet-stirred reactor we study the low-temperature oxidation chemistry of selected hydrocarbon and oxygenated fuels.

## PROGRESS REPORT

**Dimethyl ether (DME) Low-Temperature Oxidation in a Jet-Stirred Reactor:** In collaboration with the groups of Jasper (Sandia), Leone (Berkeley), Yu (Princeton), Sarathy (KAUST), Dagaut (Orleans), Taatjes (Sandia), and Kohse-Höinghaus (Bielefeld) we reported last year the detection and identification of the keto-hydroperoxide hydroperoxymethyl formate (HPMF) and other partially oxidized intermediate species arising from the low-temperature (540 K) oxidation of dimethyl ether (DME). In an extension of this work, we now determined temperature dependent mole fractions of seventeen elusive intermediates and compared them to up-to-date kinetic modeling results. Special emphasis was paid towards the validation and application of a theoretical method for determining unknown photoionization cross sections for hydroperoxide species. This approach enabled a scientifically-based quantification of the keto-hydroperoxide  $\text{HOOCH}_2\text{OCH}_2\text{O}$  and revealed new opportunities for the development of a next-generation DME combustion chemistry model.

**Investigating Repetitive Reaction Pathways for the Formation of Polycyclic Aromatic Hydrocarbons in Combustion Processes:** Covering the range from  $C_6H_6$  to  $C_{16}H_{10}$  intermediates, we analyzed repetitive hydrogen-abstraction and methyl- and acetylene-addition pathways in flame-sampled mass spectra from atmospheric-pressure opposed-flow flames fueled by *n*-butane, *i*-butane, and *i*-butene. The data suggest that repetitive methyl addition reactions onto aromatic species lead to alkyl side chains that can undergo dehydrogenation or cyclization reactions to form  $-C_2H_3$  and  $-C_2H$  side chains or cyclopenta-fused ring structures. The importance of the methyl addition sequences, which generally appeared to be consistent over the investigated range, seems to be enhanced when the reactions allow for the formation of additional ring structures, *e.g.*, when  $-C_2H$  side chains are present to form indene-like structures. Acetylene additions onto aromatic species, with the exception of benzene as a reactant, are more efficient than methyl addition reactions. As a consequence, the reaction sequences towards particle nucleation should be newly inspected in light of these findings.

## OUTLOOK

**Low-Temperature Oxidation in a Jet-Stirred Reactor:** We will continue to explore the reaction network of low-temperature oxidation processes by using the above mentioned jet-stirred reactor with molecular-beam sampling capabilities. Our work on DME will be complemented with efforts to provide new insights into the oxidation of diethyl ether and tetrahydrofuran. New information in the form of species identification and mole fraction profiles is critically needed to improve their respective combustion chemistry models. Future work will also focus on the low-temperature oxidation of the *n*- and *neo*-pentane isomers. Preliminary mass spectra were recorded and the data reduction, *i.e.* species identification and quantification, is currently in progress.

**Experimental Studies on the Molecular-Growth Chemistry of Soot Precursors in Combustion Environments:** PAH formation chemistry will be studied by analyzing the detailed chemical structures of laminar, premixed or opposed-flow flames. The data is expected to provide guidance and benchmarks needed to improve and test theoretical models describing soot-formation chemistry with predictive capabilities. Work on flames fueled by 1,3-butadiene and the  $C_5$  fuels *n*-pentane, 1-pentene, and 2-methyl-2-butene is currently in progress. In order to provide experimental evidence that benzene is not necessarily the “*first aromatic ring*” in molecular-growth chemistry and that larger aromatics can be formed without going through benzene, it is planned to study the flames of 1- and 2-butyne. Fuel consumption and aromatic precursor formation should in both cases be initiated by H-abstraction reactions, thus leading to the  $CH_3CCCH_2$  and the  $CHCCHCH_3$  radical, both of which can be interpreted as methyl-substituted propargyl radicals. Assuming, they can undergo similar reactions as the propargyl radical, it is likely, that large amounts of toluene (via a reaction with propargyl) and *o*-xylene are formed

(via a recombination reaction with another  $C_4H_5$  radical). To test this hypothesis, isomer-resolved measurements are planned that allow for identifying the  $C_4H_5$ ,  $C_7H_8$ , and  $C_8H_8$  isomers. We plan to investigate the chemical composition of these flames by flame-sampling mass spectrometry with electron ionization (EI), resonance-enhanced multiphoton ionization (REMPI), single-photon VUV ionization, and gas chromatography (GC/MS). We plan to expand our work on opposed-flow flames to  $C_3$  fuels (allene, propyne, propene, and propane), that are all convenient sources of propargyl radicals; these flames should allow us to elucidate contributions of the propargyl radical towards the formation of five-membered (like indene) and six-membered ring structures (like naphthalene) via reactions with phenyl and benzyl type radicals.

### **PUBLICATIONS ACKNOWLEDGING BES SUPPORT 2013-PRESENT**

1. C. K. Westbrook, B. Yang, T. A. Cool, N. Hansen, K. Kohse-Höinghaus, "Photoionization Mass Spectrometry and Modeling Study of Premixed Flames of Three Unsaturated  $C_5H_8O_2$  Esters", *Proc. Combust. Inst.*, **2013**, 34(1), 443-451.
2. A. W. Jasper and N. Hansen, "Hydrogen-Assisted Isomerizations of Fulvene to Benzene and of Larger Cyclic Aromatic Hydrocarbons", *Proc. Combust. Inst.*, **2013**, 34(1), 279-287.
3. S. A. Skeen, B. Yang, H. A. Michelsen, J. A. Miller, A. Violi, N. Hansen, "Studies of Laminar Opposed-Flow Diffusion Flames of Acetylene at Low Pressures with Photoionization Mass Spectrometry", *Proc. Combust. Inst.*, **2013**, 34(1), 1067-1075.
4. N. J. Labbe, V. Seshadri, T. Kasper, N. Hansen, P. Oßwald, K. Kohse-Höinghaus, P. R. Westmoreland, "Flame Chemistry of Tetrahydropyran as a Model Heteroatomic Biofuel", *Proc. Combust. Inst.*, **2013**, 34(1), 259-267.
5. S. A. Skeen, H. A. Michelsen, K. R. Wilson, D. M. Popolan, A. Violi, N. Hansen, "Near-Threshold Photoionization Mass Spectra of Combustion-Generated High-Molecular-Weight Soot Precursors", *J. Aerosol Sci.*, **2013**, 58(1), 86-102.
6. N. Hansen, S.S. Merchant, M. R. Harper, W. H. Green, "The Predictive Capability of an Automatically Generated Combustion Chemistry Mechanism: Chemical Structures of Premixed *iso*-Butanol Flames", *Combust. Flame*, **2013**, 160(11), 2343-2351.
7. N. Hansen, S. A. Skeen, H. A. Michelsen, K. R. Wilson, K. Kohse-Höinghaus, "Flame Experiments at the Advanced Light Source: New Insights into Soot Formation Processes", *J. Vis. Exp.*, **2014**, 87, e51369, doi:10.3791/51369
8. F. N. Egolfopoulos, N. Hansen, Y. Ju, K. Kohse-Höinghaus, C. K. Law, F. Qi, "Advances and Challenges in Experimental Research of Combustion Chemistry in Laminar Flames", *Prog. Energy Combust. Sci.*, **2014**, 43(1), 36-67.
9. S. M. Sarathy, P. Oßwald, N. Hansen, K. Kohse-Höinghaus, "Alcohol Combustion Chemistry", *Prog. Energy Combust. Sci.*, **2014**, 44(1), 40-102.
10. J. Krüger, J. Koppmann, P. Nau, A. Brockhinke, M. Schenk, N. Hansen, U. Werner, K. Kohse-Höinghaus, "From Precursors to Pollutants: Some Advances in Combustion Chemistry Diagnostics", *Eurasian Chem. Technol. J.*, **2014**, 16(2-3), 91-105.
11. A. Nawdiyal, N. Hansen, T. Zeuch, L. Seidel, F. Mauß, "Experimental and Modelling Study of Speciation and Benzene Formation Pathways in Premixed 1-Hexene Flames", *Proc. Combust. Inst.*, **2015**, 35(1), 325-332.
12. N. Hansen, M. Braun-Unkhoff, T. Kathrotia, A. Lucassen, B. Yang, "Understanding the Reaction Pathways in Premixed Flames Fueled by Blends of 1,3-Butadiene and n-Butanol", *Proc. Combust. Inst.*, **2015**, 35(1), 771-778.
13. A. Lucassen, S. Park, N. Hansen, S.M. Sarathy, "Combustion Chemistry of Alcohols: Experimental and Modeled Structure of a Premixed 2-Methylbutanol Flame", *Proc. Combust. Inst.*, **2015**, 35(1), 813-820.

14. M. Schenk, N. Hansen, H. Vieker, A. Beyer, A. Gölzhäuser, K. Kohse-Höinghaus, "PAH Formation and Soot Morphology in Flames of C<sub>4</sub> Fuels", *Proc. Combust. Inst.*, **2015**, 35(2), 1761-1769.
15. D. Felsmann, K. Moshhammer, J. Krüger, A. Lackner, A. Brockhinke, T. Kasper, T. Bierkandt, E. Akyildiz, N. Hansen, A. Lucassen, P. Oßwald, M. Köhler, G.A. Garcia, L. Nahon, P. Hemberger, A. Bodi, T. Gerber, K. Kohse-Höinghaus, "Electron Ionization, Photoionization and Photoelectron/Photoion Coincidence Spectroscopy in Mass-Spectrometric Investigations of a Low-Pressure Ethylene/Oxygen Flame", *Proc. Combust. Inst.*, **2015**, 35(1), 779-786.
16. K. O. Johansson, J. Y. W. Lai, S. A. Skeen, K. R. Wilson, N. Hansen, A. Violi, H. A. Michelsen, "Soot Precursor Formation and Limitations of the Stabilomer Grid", *Proc. Combust. Inst.*, **2015**, 35(2), 1819-1826.
17. K. Moshhammer, A. Lucassen, C. Togbé, K. Kohse-Höinghaus, N. Hansen, "Formation of Oxygenated and Hydrocarbon Intermediates in Premixed Combustion of 2-Methylfuran", *Z. Phys. Chem.*, **2015**, 229(4), 507-528
18. H. Selim, S. Mohamed, A. Lucassen, N. Hansen, S. M. Sarathy, "Effect of the Methyl Substitution on the Combustion of Two Methylheptane Isomers: Flame Chemistry Using VUV Photoionization Mass Spectrometry", *Energy Fuels*, **2015**, 29(4), 2696-2708.
19. O. P. Korobeinichev, I. E. Gerasimov, D. A. Knyazkov, A. G. Shmakov, T. A. Bolshova, N. Hansen, C. K. Westbrook, G. Dayma, B. Yang, "An Experimental and Kinetic Modeling Study of Premixed Laminar Flames of Methyl Pentanoate and Methyl Hexanoate", *Z. Phys. Chem.*, **2015**, 229(5), 759-780.
20. K. Moshhammer, A. W. Jasper, D. M. Popolan-Vaida, A. Lucassen, P. Dievart, H. Selim, Hatem, A. J. Eskola, C. A. Taatjes, S. R. Leone, S. M. Sarathy, Y. Ju, P. Dagaut, K. Kohse-Höinghaus, N. Hansen, "Detection and Identification of the Keto-Hydroperoxide (HOCH<sub>2</sub>OCHO) and other Intermediates during Low-Temperature Oxidation of Dimethyl Ether", *J. Phys. Chem. A*, **2015**, 119(28), 7361-7374.
21. I. W. Ekoto, S. A. Skeen, R. R. Steeper, N. Hansen, "Detailed Characterization of Negative Valve Overlap Chemistry by Photoionization Mass Spectrometry", *SAE International Journal of Engines*, **2015**, 9 (2015-01-1804), 20159013.
22. W. Sun, N. Hansen, C. K. Westbrook, F. Zhang, G. Wang, K. Moshhammer, C. K. Law, B. Yang, "An Experimental and Kinetic Modeling Study on Dimethyl Carbonate (DMC) Pyrolysis and Combustion", *Combust. Flame*, **2016**, 164(2), 224-238.
23. Z. Wang, L. Zhang, K. Moshhammer, D. M. Popolan-Vaida, V. S. B. Shankar, A. Lucassen, C. Hemken, C. A. Taatjes, S. R. Leone, K. Kohse-Höinghaus, N. Hansen, P. Dagaut, S. M. Sarathy, "Additional Chain-Branching Pathways in the Low-Temperature Oxidation of Branched Alkanes", *Combust. Flame*, **2016**, 164(2), 386-396.
24. N. Hansen, M. Schenk, K. Moshhammer, K. Kohse-Höinghaus, "Investigating Repetitive Reaction Pathways for the Formation of Polycyclic Aromatic Hydrocarbons in Combustion Processes", *Combust. Flame*, submitted.
25. W. Sun, B. Yang, N. Hansen, K. Moshhammer, "The Influence of Dimethoxy Methane (DMM)/Dimethyl Carbonate (DMC) Addition on Premixed Ethane/Oxygen/Argon Flame", *Proc. Combust. Inst.*, submitted.
26. K. Moshhammer, L. Seidel, Y. Wang, H. Selim, S. M. Sarathy, F. Mauss, N. Hansen, "Aromatic Ring Formation in Diffusive 1,3-Butadiene Flames", *Proc. Combust. Inst.*, submitted.
27. Z. Wang, S. Y. Mohamed, L. Zhang, K. Moshhammer, D. M. Popolan-Vaida, V. S. B. Shankar, A. Lucassen, L. Ruwe, N. Hansen, P. Dagaut, S. M. Sarathy, "The Importance of Third O<sub>2</sub> Addition in 2-Methylhexane Auto-Oxidation", *Proc. Combust. Inst.*, submitted.
28. I. Gerasimov, D. A. Knyazkov, N. Hansen, A. G. Shmakov, O. P. Korobeinichev, "Photoionization Mass Spectrometry and Modeling Study of a Low-Pressure Premixed Flame of Ethyl Pentanoate (Ethyl Valerate)", *Proc. Combust. Inst.*, submitted.
29. T. Tao, W. Sun, B. Yang, N. Hansen, K. Moshhammer, C. K. Law, "Investigation of the Chemical Structures of Laminar Premixed Flames Fueled by Acetaldehyde", *Proc. Combust. Inst.*, submitted.
30. M. Braun-Unkhoff, N. Hansen, T. Methling, K. Moshhammer, B. Yang, "The Influence of iso-Butanol Addition to the Chemistry of Premixed 1,3-Butadiene Flames", *Proc. Combust. Inst.*, submitted.
31. L. Ruwe, K. Moshhammer, N. Hansen, K. Kohse-Höinghaus, "Consumption and Hydrocarbon Growth Processes in a 2-Methyl-2-Butene Flame", *Proc. Combust. Inst.*, submitted.

# Theoretical Studies of Potential Energy Surfaces

Lawrence B. Harding  
Chemical Sciences and Engineering Division  
Argonne National Laboratory, Argonne, IL 60439  
harding@anl.gov

## Program Scope

The goal of this program is to calculate accurate potential energy surfaces for both reactive and non-reactive systems. Our approach is to use state-of-the-art electronic structure methods (CASPT2, MR-CI, CCSD(T), etc.) to characterize multi-dimensional potential energy surfaces. Depending on the nature of the problem, the calculations may focus on local regions of a potential surface or may cover the surface more globally. A second aspect of this program is the development of techniques to fit multi-dimensional potential surfaces to convenient, global, analytic functions suitable for use in dynamics calculations. A new part of this program is the use of diffusion Monte-Carlo calculations to obtain high accuracy, anharmonic zero point energies for molecules having multiple minima.

## Recent Progress

### Diffusion Monte-Carlo for High Accuracy Anharmonic Zero Point Energies

The accuracy of electronic structure calculations has now reached the point where a significant remaining source of error in calculated heats of formation is in the zero point energy. In the past, high accuracy predictions of thermochemical properties have typically employed spectroscopic perturbation theory or vibrational configuration interaction calculations to obtain estimates of anharmonic corrections to the zero point energy. Both of these methods rely on normal coordinate, force field expansions that are not appropriate for species in which the zero point wavefunction spans multiple minima, as is often the case for radicals relevant to combustion. We have recently embarked on a program to address this issue using diffusion Monte-Carlo methods<sup>1</sup> to obtain high accuracy predictions of anharmonic, zero point energies for combustion related species. This year we completed calculations on the hydroxymethyl ( $\text{CH}_2\text{OH}$ ) radical, an important combustion species having four equivalent minima connected by two equivalent pairs of transition states with energies of 140 and 1700  $\text{cm}^{-1}$

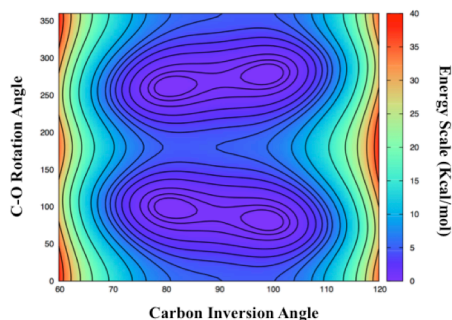


Figure 1. Contour plot of the internal rotation and inversion modes of the  $\text{CH}_2\text{OH}$  radical.

above the minimum, see Figure 1. The lower energy pair of saddle points correspond to inversion of the carbon center, while the higher energy saddle points correspond to rotation about the CO bond. The key to success here will be the ability to obtain accurate, full dimensional, analytic fits to the potential energy surfaces in the vicinity of the minima. Our calculations have demonstrated that a simple Taylor series expansion in the  $N_{\text{atom}}*(N_{\text{atom}}-1)/2$  internuclear distance coordinates can yield remarkably accurate fits. Figure 2 shows the results of quadratic (left) and

quartic (right)  $R_{ij}$  fits to this potential surface. Note that both of these are full dimensional fits from which we are showing the same two dimensional slice as shown in Figure 1. Both fits are to

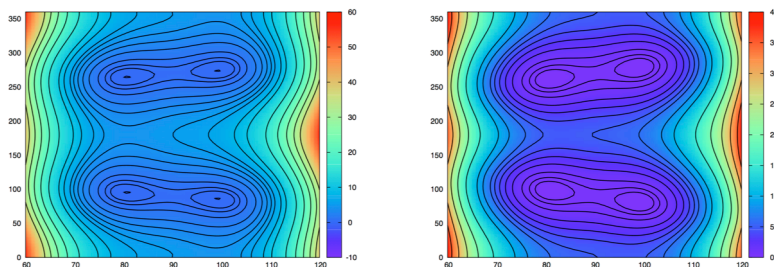


Figure 2. Contour plot of the internal rotation and inversion modes of the  $\text{CH}_2\text{OH}$  radical for quadratic (left) and quartic (right)  $R_{ij}$  fits.

100,000 ab initio, CCSD(T)/cc-pVTZ calculations spanning an energy range of  $4000\text{ cm}^{-1}$ . The quadratic fit consists of 66 terms while the quartic fit consists of 1001 terms. The striking result here is that even the quadratic  $R_{ij}$  fit yields a qualitatively correct topology for these two, low frequency, rotation/inversion modes, having four equivalent minima separated by two pairs of equivalent saddle points. The root mean square error of the quadratic fit is  $135\text{ cm}^{-1}$  presumably owing largely to the neglect of anharmonicities in the other coordinates. On the scale of these plots the quartic fit is indistinguishable from the ab initio surface, with a root mean square error of  $7\text{ cm}^{-1}$ . A second quartic fit to a 60,000 point subset covering a smaller energy range of  $1500\text{ cm}^{-1}$  yields a root mean square error of just  $1.5\text{ cm}^{-1}$ . Diffusion Monte-Carlo calculations on both quartic surfaces yield identical (to within the  $\pm 2\text{ cm}^{-1}$  statistical uncertainty) zero point energies. The zero point energy obtained in these calculations is more than  $100\text{ cm}^{-1}$  higher than the best previous calculations<sup>2</sup>.

### Roaming Mechanisms for Decomposition of Criegee Intermediates:

A recent study of Lin and coworkers<sup>3</sup> proposed a novel mechanism for the decomposition of Criegee intermediates. This new pathway involves the partial cleavage of the OO bond followed by a roaming like reorientation and then insertion into one of the CH bonds. For the case of the simplest Criegee intermediate this leads directly to the formation of formic acid. Previous studies concluded that the lowest pathway for decomposition of Criegee intermediates begin with a sequential ring-closing and re-opening forming the methylenebisoxo biradical which can then isomerize or decompose by a number of competing pathways. The energetics of the new pathway appear physically unrealistic, having a roaming-type saddle point that lies 38 kcal/mol below the corresponding bimolecular asymptote,  $\text{O}(^1\text{D})+\text{H}_2\text{CO}$ . We have shown that the analysis suffered from an inconsistent combination of spin-restricted calculations for the asymptote and spin unrestricted calculations for the saddle point. Consistent calculations on both the asymptote and the saddle point indicate that the saddle point is, as expected, within 1 kcal/mol of the asymptote or more than 30 kcal/mol above the dioxirane path. For this reason the new pathway will not compete with the well-known dioxirane pathways.

### Roaming Mechanisms for Decomposition of Aldehydes:

Recently reported photodissociation experiments on ethyl aldehyde<sup>4</sup> and acetaldehyde<sup>5</sup> have been interpreted to indicate that the roaming mechanism is more important for ethyl aldehyde than for acetaldehyde and that there is a second distinct roaming mechanism for the decomposition of

acetaldehyde. Several years ago we characterized roaming saddle point for the series acetaldehyde, ethyl aldehyde, iso-propyl aldehyde and tert-butyl aldehyde, showing that the roaming saddle points become more energetically favorable as the size of the molecule increases. So, for example, in acetaldehyde the roaming saddle point is predicted to lie 1.0 kcal/mole below the tight saddle point, whereas in ethyl aldehyde this difference increases to 2.7 kcal/mole. This difference continues to grow as the size of the aldehyde increases, however for iso-propyl aldehyde a second roaming mechanism appears leading to methane plus acrolein instead of propane plus CO. Preliminary results suggest that this second roaming mechanism is the lowest energy decomposition path for iso-propyl aldehyde.

As noted above, recent photodissociation experiments<sup>5</sup> indicate two distinct roaming mechanisms for acetaldehyde, both leading to the same products, CH<sub>4</sub>+CO. The original roaming mechanism begins with partial cleavage of the CC bond. Then the nascent HCO and CH<sub>3</sub> fragments reorient themselves and the methyl fragment abstracts the HCO hydrogen. The new mechanism is thought to involve a hydrogen atom roaming around a CH<sub>3</sub>CO core to abstract the methyl radical. We have examined the long-range H+CH<sub>3</sub>CO interaction potential and do indeed find a roaming-type saddle point for this process. However, not only is the energy of this saddle point substantially above the original methyl roaming saddle point but there is a second, hydrogen atom, roaming-type saddle point in which the hydrogen atom abstracts another hydrogen atom from the CH<sub>3</sub>CO fragment leading to ketene plus H<sub>2</sub>. This H-CH<sub>3</sub>CO→H<sub>2</sub>+H<sub>2</sub>CCO roaming saddle point is also predicted to lie below the H-CH<sub>3</sub>CO→CH<sub>4</sub>+CO roaming saddle point.

### Future Plans

We plan to extend our diffusion Monte-Carlo calculations to larger, more complicated systems, continue studies of R+O<sub>2</sub> reactions including <sup>3</sup>CH<sub>2</sub>+O<sub>2</sub> and quantify the branching ratios for some of the new roaming mechanisms discussed above.

**Acknowledgement:** This work was performed under the auspices of the Office of Basic Energy Sciences, Division of Chemical Sciences, Geosciences and Biosciences, U.S. Department of Energy, under Contract DE-AC02-06CH11357.

### References:

- (1) A. B. McCoy, *Int. Rev. Phys. Chem.* **25**, 77-107 (2006).
- (2) A. V. Marenich, J. E. Boggs, *J. Chem. Phys.* **119**, 10105-10114 (2003).
- (3) T.-N. Nguyen, P. Raghunath, M. C. Lin, *J. Chem. Phys.* **142**, 124312 (2015).
- (4) P.-Y. Tsai, K.-C. Hung, H.-K. Li and K.-C. Lin, *J. Phys. Chem. Lett* **5**, 190 (2014)
- (5) K. L. K. Lee, M.S. Quinn, A. T. Maccarone, K. Nauta, P. L. Houston, S. A. Reid, M. J. T. Jordan and S. H. Kable, *Chem. Sci.* **5**, 4633 (2014)

### PUBLICATIONS (2013 - Present):

#### A Quantitative Explanation for the Apparent Anomalous Temperature Dependence of OH + HO<sub>2</sub> → H<sub>2</sub>O + O<sub>2</sub> through Multi-Scale Modeling

M. P. Burke, S. J. Klippenstein, L. B. Harding, *Proc. Comb. Inst.* **34**, 547-555 (2013)

**Unconventional Peroxy Chemistry in Alcohol Oxidation: The Water Elimination Pathway**

O. Welz, S. J. Klippenstein, L. B. Harding, C. A. Taatjes, J. Zador  
J. Phys. Chem. Letters **4**, 350-354 (2013)

**Rate Constant and Branching Fraction for the NH<sub>2</sub> + NO<sub>2</sub> Reaction**

S. J. Klippenstein, L. B. Harding, P. Glarborg, Y. Gao, H. Hu, P. Marshall  
J. Phys. Chem. A **117**, 9011 (2013)

**Predictive Theory for the Addition Insertion Kinetics of <sup>1</sup>CH<sub>2</sub> Reacting with Unsaturated Hydrocarbons**

D. Polino, S. J. Klippenstein, L. B. Harding, Y. Georgievski  
J. Phys. Chem. A **117**, 12677-12692 (2013)

**Comparison of Multireference Configuration Interaction Potential Energy Surfaces for H + O<sub>2</sub> → HO<sub>2</sub>: The Effect of Internal Contraction**

L. B. Harding, S. J. Klippenstein, H. Lischka, R. Shepard  
Theoretical Chemical Accounts **133**,1429 (2013)

**Secondary Channels in the Thermal Decomposition of monomethylhydrazine (CH<sub>3</sub>NHNH<sub>2</sub>)**

P. Zheng, S. J. Klippenstein, L. B. Harding, H. Sun, C. K. Law  
RSC Advances **4**, 62951 (2014)

**Electronic States of the Quasilinear Molecule Propargylene (HCCCH) from Negative Ion Photoelectron Spectroscopy**

D. L. Osborn, K. M. Vogelhuber, S. W. Wren, E. M. Miller, Y.-J. Lu, A. S. Case, L. Sheps, R. J. McMahon, J. F. Stanton, L. B. Harding, B. Ruscic, W. C. Lineberger  
J. Amer. Chem. Soc. **136**, 10361 (2014)

**Predictive A Priori Pressure-Dependent Kinetics**

A.W. Jasper, K. M. Pelzer, J. A. Miller, E. Kamarchik, L. B. Harding, S. J. Klippenstein  
Science **346**, 1212 (2014)

**Resolving Some Paradoxes in the Thermal Decomposition Mechanism of Acetaldehyde**

R. Sivaramakrishnan, J. V. Michael, L. B. Harding, S. J. Klippenstein  
J. Phys. Chem. A **119**, 7724-7733 (2015)

**Thermal Dissociation and Roaming Isomerization of Nitromethane: Experiment and Theory**

C. Annesley, J. Randazzo, S. J. Klippenstein, L. B. Harding, A. Jasper, Y. Georgievski, B. Ruscic, R. S. Tranter, J. Phys. Chem. A **119**, 7872-7893 (2015)

**Comment on “A Novel and Facile Decay Path of Criegee Intermediates by Intramolecular Insertion Reactions Via Roaming Transition States” [J. Chem. Phys. **142**, 124312 (2015)]**

L. B. Harding and S. J. Klippenstein, J. Chem. Phys. **143**, 167101-1 / 167101-2 (2015)

## Theory of Electronic Structure and Chemical Dynamics

*Martin Head-Gordon, William H. Miller, and Eric Neuscamman*

Chemical Sciences Division, Lawrence Berkeley National Laboratory and  
Department of Chemistry, University of California, Berkeley, California 94720.

[mhg@cchem.berkeley.edu](mailto:mhg@cchem.berkeley.edu), [millerwh@berkeley.edu](mailto:millerwh@berkeley.edu), [eneuscamman@berkeley.edu](mailto:eneuscamman@berkeley.edu)

**Scope of the Project:** To expand knowledge of transient species such as radicals relevant to combustion chemistry and other areas including catalysis, new theoretical methods are needed for reliable computer-based prediction of their properties. The two main areas of relevant theory are electronic structure methods and techniques for chemical dynamics. Within electronic structure theory, focus centers on the development of new density functional theory methods and new wave function theories. Examples of current activity include the introduction of combinatorial design strategies for density functionals, and a new accurate wavefunction approach for electronic excited states. In chemical dynamics, recent progress and planned activity centers on the development of tractable semi-classical dynamics approaches that can address non-adiabatic processes. The focus is on turning semi-classical theory into a practical way of adding quantum effects to classical molecular dynamics simulations of large, complex molecular systems. Newly developed theoretical methods, as well as existing approaches, are employed to study prototype radical reactions, often in collaboration with experimental efforts. These studies help to deepen understanding of the role of reactive intermediates in diverse areas of chemistry. They also sometimes reveal frontiers where new theoretical developments are needed in order to permit better calculations in the future.

### Recent Progress

Due to length limitations, only a selection of projects can be summarized here.

*High Accuracy Targeting of Excited States.* Neuscamman and co-workers have developed a rigorous framework for efficiently generalizing the quantum variational principle to excited states. Made possible by their advances in quantum Monte Carlo methods, this excited variational principle (EVP-QMC) allows an approximate wave function ansatz to be fully optimized for an individual excited state, greatly increasing accuracy compared to typical approaches today that require sharing elements of the wave function between different states. An initial demonstration of EVP-QMC in the difficult and combustion-relevant case of the carbon dimer showed the method to be competitive in accuracy with the best available theoretical benchmarks despite using a much simpler wave function. Indeed, its multi-Slater Jastrow ansatz required less than 100 variables to match or exceed the accuracy of the 4,000-variable coupled cluster ansatz and the million-variable density matrix renormalization group. Perhaps most importantly, the EVP-QMC has proven highly accurate for double as well as single excitations. This should be compared to equation-of-motion coupled cluster, which is the current “high accuracy” standard for single excitations but which is unreliable for double excitations.

*Density functionals.* Head-Gordon and co-workers have been seeking the limit of transferable accuracy that can be achieved with generalized gradient approximations (GGA’s), or meta-GGA’s, which are the basis of semi-local functionals. To achieve high accuracy, non-local density-based corrections for long-range dispersion interactions are added, as well as the option of non-local range-separated hybrid (RSH) treatment of exact exchange. They introduced a novel “survival of the most transferable” (SOMT) procedure to achieve this goal. SOMT is a combinatorial design protocol that involves training a very large numbers of functionals using a fraction of the data, and then selecting the functional that performs best on the remaining data (with the fewest parameters). In 2014, this approach was used to create a new range-separated hybrid van der Waals corrected GGA functional. The functional, named  $\omega$ B97X-V, contains only 10 parameters (e.g. versus 15 for the conventionally designed 2008 functional,  $\omega$ B97X-D) yet reduces RMS errors in non-bonded interactions by about 40% relative to  $\omega$ B97X-D, while matching its performance for thermochemistry. A partial search of the vastly larger (rank  $> N_A!$ ) meta-GGA functional space led to the creation of the B97M-V

functional in 2015, which has only 12 adjustable parameters (vs 34 for M06-L, which is in the same class). On some 5000 test cases, B97M-V reduces to reduce the RMS errors of the best existing alternative meta-GGAs by nearly 30% for thermochemistry and nearly 50% for non-bonded interactions. To follow on, a still-better functional is just being finished, which is an RSH version of B97M-V. This functional,  $\omega$ B97M-V, should provide substantially improved thermochemistry and barrier heights, as well as reduced sensitivity to self-interaction errors.

*Semi-classical dynamics.* It has been well established for many years that semi-classical (SC) theory provides a very good description of essentially *all* quantum effects in molecular dynamics, and the outstanding challenge has been to what extent one can implement it efficiently enough to make it routinely useful. Recent progress by Miller included the most accurate and efficient approach to date for implementing the SC initial value representation (IVR) for molecular dynamics. The key to the efficiency is in use of a time-dependent Monte Carlo sampling function for evaluating the phase space average over initial conditions of classical trajectories that are the ‘input’ to the SC theory. Efforts were also begun at finding a general and dynamically consistent way for treating the electronic and nuclear degrees of freedom in non-adiabatic processes by classical molecular dynamics. The two essential steps for this are (1) to find a consistent way for describing the electronic (as well as nuclear) degrees of freedom by classical mechanics (currently by the Meyer-Miller (MM) ‘electronic oscillator’ model), and (2) to be able to extract quantum state information for the electronic states from such a description, where the ‘symmetrical quasi-classical’ (SQC) model was used. Both of these approaches have a long history but have never been used in concert before in this way. They have given remarkably good results for a series of standard non-adiabatic problems, even being able to describe ‘quantum coherence’ effects within a standard classical MD simulation. The most recent applications of the SQC/MM approach are to the treatment of so-called “site-exciton” non-adiabatic models, which are frequently used to simulate photo-induced electronic excitation transfer in light-harvesting pigment complexes. For a 2-state model, simulated over the 8 different parameter regimes, the SQC/MM-simulated decay of the initial electronic excitation agrees remarkably well with the reference results over all 8 parameter regimes considered. The SQC/MM approach has also been applied to a more challenging 7-state model of the well-known Fenna-Mathews-Olson (FMO) pigment complex with reasonable agreement. It is worth noting that the atomistic/trajectory-based nature of the SQC/MM approach makes it more generally applicable than the reference technique in the above studies. Therefore since SQC/MM can be applied to more realistic harmonic (or even anharmonic) bath models, it has the potential to more accurately model excitation transfer dynamics in complex environments.

*Computational studies of chemical properties and reactivity.* (i) In collaboration with experimental measurements from the Ahmed and Leone groups at LBNL, the photodissociation of glycerol has been explored. The key intermediate is a triplex between vinyl alcohol radical cation, water and formaldehyde. (ii) A joint study of the radical-neutral association reactions between ethylene radical cation and neutral ethylene, acetylene cation and acetylene, and mixed association, is just finished, in collaboration with experimental measurements from the Ahmed group.

**Future Plans:** (i) High Accuracy Targeting of Excited States: Current efforts focus on extending EVP-QMC to the variational optimization of an entire linear response function, rather than just an ansatz, in order both to improve accuracy and to make the method more black-box. Crucially, this approach has a cost very similar to optimizing the ansatz itself through a careful application of finite difference techniques. Formal analysis as well as preliminary results for this linear response form of EVP-QMC suggest an accuracy in single excitations on par with equation-of-motion coupled cluster (currently the gold standard), but with a lower cost-scaling and an algorithm that parallelizes more easily onto modern supercomputer architectures. (ii) Density functionals: Extensive comparative benchmarking of the new functionals against existing functionals is an important pre-requisite for their broader use in the future. It is essential to establish their strengths and weaknesses relative to other modern density functionals. A further possible extension is to double hybrid functionals, possibly

including orbital optimization. (iii) Semiclassical dynamics: It is planned to further pursue the recent work that has proved so encouraging for having a general and robust classical simulation model for treating electronically non-adiabatic processes, including further investigation of the fundamental theoretical model, as well as to its application to specific processes. (iv) Computational studies of chemical properties and reactivity: It is planned to continue the study of radical-neutral clustering reactions, possibly also including larger polycyclic aromatic hydrocarbon species. Suitable candidates for collaborative applications of the new EVP-QMC excited state methods will also be sought.

### Recent Publications Citing DOE Support (2013-2016)

- Azar, R. J., P.R. Horn, E.J. Sundstrom, and M. Head-Gordon, "Useful Lower Limits to Polarization Contributions to Intermolecular Interactions Using a Minimal Basis of Localized Orthogonal Orbitals: Theory and Analysis of the Water Dimer" *J. Chem. Phys.*, **2013**, 138, 084102. DOI: 10.1063/1.4792434
- Bell, F., Q. N. Ruan, A. Golan, P. R. Horn, M. Ahmed, S. R. Leone, and M. Head-Gordon, "Dissociative Photoionization of Glycerol and its Dimer Occurs Predominantly via a Ternary Hydrogen-Bridged Ion-Molecule Complex" *J. Am. Chem. Soc.*, **2013**, 135, 14229- 14239. DOI: 10.1021/ja405511v
- Bandyopadhyay, B., T. Stein, Y. Fang, O. Kostko, A. White, M. Head-Gordon, and M. Ahmed, "Probing Ionic Complexes of Ethylene and Acetylene with Vacuum-Ultraviolet Radiation" *J. Phys. Chem. A*. **2016** (in press).
- Cotton, S. J. and Miller, W. H. "Symmetrical Windowing for Quantum States in Quasi-Classical Trajectory Simulations" *J. Phys. Chem. A* **2013**, 117, 7190-7194. DOI: 10.1021/jp401078u
- Cotton, S. J. and Miller, W. H., "Symmetrical Windowing for Quantum States in Quasi-Classical Trajectory Simulations: Application to Electronically Non-Adiabatic Processes" *J. Chem. Phys.* **2013**, 139, 234112.1-9. DOI: 10.1063/1.4845235
- Cotton, S. J., Igumenshchev, K. and Miller, W. H., "Symmetrical Windowing for Quantum States in Quasi-Classical Trajectory Simulations: Application to Electron Transfer" *J. Chem. Phys.* **2014**, 141, 084104.1-14. DOI: 10.1063/1.4893345
- Cotton, S. J. and W. H. Miller, "A Symmetrical Quasi-Classical Spin-Mapping Model for the Electronic Degrees of Freedom in Non-Adiabatic Processes", *J. Phys. Chem. A* **2015**, 119, 12138-12145 (2015).
- Cotton, S. J. and W. H. Miller, "The Symmetrical Quasi-Classical Model for Electronically Non-Adiabatic Processes Applied to Energy Transfer Dynamics in Site-Exciton Models of Light-Harvesting Complexes", *J. Chem. Theory Comput.* **2016** (in press).
- Goldey, M. and M. Head-Gordon, "Separate Electronic Attenuation Allows a Spin-Component Scaled Second Order Møller-Plesset Theory to be Effective for Both Thermochemistry and Non-Covalent Interactions" *J. Phys. Chem. B*, **2014**, 118, 6519-6525. DOI: 10.1021/jp4126478
- Goldey, M. B. and M. Head-Gordon, "Convergence of Attenuated Second Order Møller-Plesset Perturbation Theory Towards the Complete Basis Set Limit" *Chem. Phys. Lett.*, **2014**, 608, 249-254. DOI: 10.1016/j.cplett.2014.05.092
- Goldey, M., A. D. Dutoi and M. Head-Gordon, "Attenuated Second Order Moller-Plesset Theory: Assessment and Performance in the aug-cc-pVTZ Basis" *Phys. Chem. Chem. Phys.*, **2013**, 15, 15869-15875. DOI: 10.1039/c3cp51826d
- Goldey, M., R. A. DiStasio, Jr., Y. Shao, and M. Head-Gordon, "Shared Memory Multi Processing Implementation of Resolution-of-the-Identity Second Order Møller-Plesset Perturbation Theory with Attenuated and Unattenuated Results for Intermolecular Interactions between Larger Molecules" *Mol. Phys.*, **2014**, 112, 836-843. DOI: 10.1080/00268976.2013.869363
- Goldey, M.B., B. Belzunces, and M. Head-Gordon, "Attenuated MP2 with a long-range dispersion correction for treating non-bonded interactions", *J. Chem. Theory Comput.* **2015**, 11, 4159-4168; DOI: 10.1021/acs.jctc.5b00509
- Horn, P.R., E.J. Sundstrom, T. Baker and M. Head-Gordon, "Unrestricted Absolutely Localized Molecular Orbitals for Energy Decomposition Analysis: Theory and Applications to Intermolecular Interactions Involving Radicals" *J. Chem. Phys.*, **2013**, 138, 134119. DOI: 10.1063/1.4798224
- Huang, Y.-H., M. Goldey, M. Head-Gordon, and G. J. O. Beran, "Achieving High Accuracy Intermolecular Interactions Through Coulomb-Attenuated Dispersion Corrected Second Order Møller-Plesset Theory" *J. Chem. Theory Comput.*, **2014**, 10, 2054-2063. DOI: 10.1021/ct5002329

- Li, B., Levy, T. J., Swenson, D. W. H., Rabani, E. and Miller, W. H., “A Cartesian Quasi- Classical Model to Nonequilibrium Quantum Transport: The Anderson Impurity Model” *J. Chem. Phys.* **2013**, 138, 104110.1-6. DOI: 10.1063/1.4793747
- Li, B., Miller, W. H., Levy, T. J., and Rabani, E., “Classical Mapping for Hubbard Operators: Application to the Double-Anderson Model” *J. Chem. Phys.* **2014**, 140, 204106.1-7. DOI: 10.1063/1.4878736
- Li, B., Wilner, E. Y., Thoss, M., Rabani, E., and Miller, W. H., “A Quasi-Classical Mapping Approach to Vibrationally Coupled Electron Transport in Molecular Junctions” *J. Chem. Phys.* **2014**, 140, 104110.1-7. DOI: 10.1063/1.4867789
- Mardirossian, N., D.S. Lambrecht, L. McCaslin, S.S. Xantheas, and M. Head-Gordon, “The Performance of Current Density Functionals for Sulfate-Water Clusters” *J. Chem. Theory Comput.*, **2013**, 9, 1368-1380. DOI: 10.1021/ct4000235
- Mardirossian, N. and M. Head-Gordon “Characterizing and Understanding the Remarkably Slow Basis Set Convergence of Several Minnesota Density Functionals for Intermolecular Interaction Energies” *J. Chem. Theor. Comput.*, **2013**, 9, 4453-4461. DOI: 10.1021/ct400660j
- Mardirossian, N. and M. Head-Gordon, “ $\omega$ B97X-V: A 10 Parameter Range Separated Hybrid Density Functional Including Non-Local Correlation, Designed by a Survival of the Fittest Strategy” *Phys. Chem. Chem. Phys.*, **2014**, 16, 9904-9924. DOI: 10.1039/c3cp54374a
- Mardirossian, N., and M. Head-Gordon, “Exploring the Limit of Accuracy for Density Functionals Based on the Generalized Gradient Approximation: Local, Global Hybrid and Range-Separated Hybrids With and Without Dispersion Corrections” *J. Chem. Phys.*, **2014**, 140, 18A527. DOI: 10.1063/1.4868117
- Mardirossian, N. and M. Head-Gordon, “Mapping the genome of meta-generalized gradient approximation density functionals: The search for B97M-V”, *J. Chem. Phys.* **2015**, 142, 074111; (32 pages) <http://dx.doi.org/10.1063/1.4907719>
- Miller, W. H., “A Journey Through Chemical Dynamics” *Annu. Rev. Phys. Chem.* **2014**, 65, 1- 19. DOI: 10.1146/annurev-physchem-040513-103720
- Miller, W.H., and S. J. Cotton, Communication: Note on Detailed Balance in Symmetrical Quasi-Classical Models for Electronically Non-Adiabatic Dynamics, *J. Chem. Phys.* **2015**, 142, 131103.1-3.
- Peverati, R. and M. Head-Gordon, “Orbital Optimized Double Hybrid Density Functionals” *J. Chem. Phys.*, **2013**, 139, 024110. DOI: 10.1063/1.4812689
- Sharada, S.M, D. Stück, E.J. Sundstrom, A.T. Bell, and M. Head-Gordon, “Wavefunction stability analysis without analytical electronic Hessians: Application to orbital-optimized post-Hartree-Fock methods and VV10-containing density functionals,” *Mol. Phys.* **2015**, 113, 1802-1808. DOI:10.1080/00268976.2015.1014442CH
- Small, D. W., K. V. Lawler, and M. Head-Gordon, “Coupled Cluster Valence Bond Method: Efficient Implementation and Application to Extended Acene Oligomers” *J. Chem. Theor. Comput.*, **2014**, 10, 2027-2040. DOI: 10.1021/ct500112y
- Small, D.W., E.J. Sundstrom, and M. Head-Gordon, “A simple way to test for collinearity in spin symmetry broken wave functions: Theory and application to Generalized Hartree-Fock”, *J. Chem. Phys.* **2015**, 142, 094112 (9 pages). <http://dx.doi.org/10.1063/1.4913740>
- Stück, D. and M. Head-Gordon, “Regularized Orbital Optimized Second Order Perturbation Theory” *J. Chem. Phys.*, **2013**, 139, 244109. DOI: 10.1063/1.4851816
- Tao, G., and Miller, W. H., “Time-Dependent Important Sampling in Semiclassical Initial Value Representation Calculations or Time Correlation Functions. III. A State-Resolved Implementation to Electronically Non-Adiabatic Dynamics” *Mol. Phys.* **2013**, 111, 1987- 1993. DOI: 10.1063/1.4793747

# Laser Studies of Combustion Chemistry

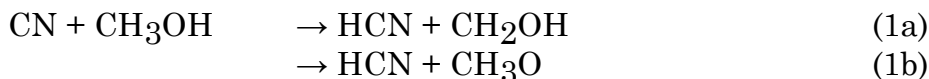
John F. Hershberger

Department of Chemistry and Biochemistry  
North Dakota State University  
NDSU Dept. 2735, PO Box 6050  
Fargo, ND 58108-6050  
john.hershberger@ndsu.edu

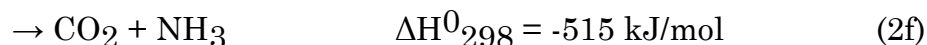
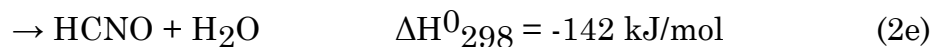
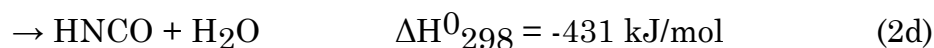
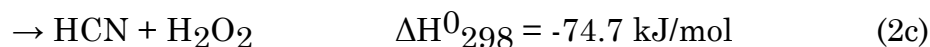
Time-resolved infrared diode laser absorption is used in our laboratory to study the kinetics and product channel dynamics of chemical reactions of importance in the gas-phase combustion chemistry of nitrogen-containing species. This program is aimed at improving the kinetic database of reactions crucial to modeling of combustion processes, with emphasis on NO<sub>x</sub> chemistry. When feasible, we perform quantitative measurement of both total rate constants and product branching ratios.

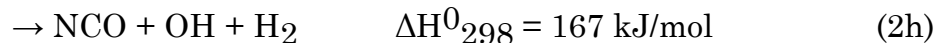
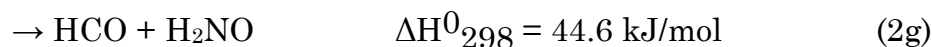
## 1) Reactions of Hydroxymethyl Radical

In a previous year's report, we noted that the CN radical primarily abstracts an alkyl hydrogen atom when it reacts with methanol:



Where we found that the yield of (1a) is ~0.8-0.9, while that of (1b) is only ~0.08. This reaction therefore represents a relatively clean source of hydroxymethyl (CH<sub>2</sub>OH), using ICN as a CN precursor at 248 or 266 nm. CH<sub>2</sub>OH can then react with NO, as follows:





One previous experimental study found a fairly high rate constant,  $2.5 \times 10^{-11} \text{ cm}^3 \text{ molecule}^{-1} \text{ s}^{-1}$ , but only at 1 atm pressure.<sup>1</sup> Another study found a lower rate constant of  $2.2 \times 10^{-12} \text{ cm}^3 \text{ molecule}^{-1} \text{ s}^{-1}$  at 0.5-1.5 Torr for the  $\text{CD}_2\text{OH} + \text{NO}$  reaction;<sup>2</sup> it is not clear whether the lower value is due to isotope effects or pressure dependence. It is therefore possible that the collisionally stabilized adduct (2a) dominates, but experimental data is scarce. Therefore, we have used transient infrared spectroscopy and ab initio calculations to study the product channels of this reaction. We initially thought that channel (2e) was likely, because it requires a single hydrogen migration from carbon to oxygen, starting with a  $\text{CH}_2(\text{NO})\text{OH}$  complex. Ab initio calculations show that this pathway involves high barriers, however, and experimentally we find no fulminic acid (HCNO) formation. We also looked for HCN, HNO,  $\text{CO}_2$ , and CO. No  $\text{CO}_2$  or CO was found; a very small transient signal for HNO was found, but is believed to originate primarily from side reactions. The HCN signal is unchanged when we compare with and without NO, indicating that it originated from (1a), not from (2c). We did quite surprisingly find, however, a strong transient signal for isocyanic acid, HNCO. Although calibration of the signal reveals that it is produced in only about 10% yield, channel (2d) is clearly active at room temperature and low pressures. This is surprising, because previously ab initio calculations do not show a low energy pathway to this product.<sup>3</sup> <sup>4</sup> Our calculations are in rough agreement that the most obvious pathway to  $\text{HNCO} + \text{H}_2\text{O}$  involves a high barrier, but after extensive searching we found a multistep pathway involving several hydrogen atom migrations that does show a low energy path to channel (2d).

## 2) CN + $\text{CH}_3\text{Br}$ Reaction

Several product channels are possible:



In a recent ab initio study, it was found that the barrier for hydrogen abstraction in this reaction was similar to that for bromine abstraction.<sup>5</sup> This implies the possibility that channel (3a) may not dominate the reaction, in contrast to the  $\text{CN} + \text{CH}_3\text{Cl}$  reaction. Reaction (3) has not previously been studied experimentally. We measured total rate constants by probing the CN radical under

pseudofirst order conditions, and quantified the yield of HCN reaction products by detection of HCN, and comparison with the reference CN+C<sub>2</sub>H<sub>6</sub> reaction, which is expected to produce HCN in unity yield. We find that this reaction is quite fast, with total rate constant  $k_3 = (2.20 \pm 0.6) \times 10^{-12} \exp(453 \pm 98/T) \text{ cm}^3 \text{ molecule}^{-1} \text{ s}^{-1}$  over the range 298-523 K. The very slight negative temperature dependence was the first indication that hydrogen abstraction may not be the dominant channel. This was then shown to be the case: direct HCN detection indicates that the yield of (3a) is only 0.12±0.02 at 298 K. Attempts to detect other products were unsuccessful: HBr is formed in negligible yield, and CH<sub>3</sub>CN and BrCN have extremely weak infrared absorption coefficients. We suspect but cannot prove that channel (3d) dominates.

### 3) CN + CH<sub>3</sub>CN Reaction

Our observation that hydrogen abstraction is only a minor channel of reaction (3) suggests a similar question for the CN + CH<sub>3</sub>CN Reaction. This reaction has a positive activation energy expected of a hydrogen abstraction mechanism, and preliminary experiments demonstrate an HCN yield of near unity. This therefore suggests that this reaction is a clean source of CH<sub>2</sub>CN radicals. Future plans include study of the CH<sub>2</sub>CN + NO (and perhaps CH<sub>2</sub>CN + O<sub>2</sub>) reactions.

### References

- (1) Pagsberg, P.; Munk, J.; Anastasi, C.; Simpson, V. J. *J. Phys. Chem.* **1989**, *93*, 5162-5165.
- (2) Nesbitt, F. L.; Payne, W. A.; Stief, L. J. *J. Phys. Chem.* **1989**, *93*, 5158-5161.
- (3) Shin, D. N.; Koh, D. J.; Kim, K. T.; Hamilton, I. P. *Catalysis Today* **2007**, *119*, 209-212.
- (4) Hu, W.-F.; He, T.-J.; Chen, D.-M. Liu, F.-C. *J. Phys. Chem. A* **2002**, *106*, 7294-7303.
- (5) Farahani, P.; Maeda, S.; Francisco, J.S.; Lundberg, M. *ChemPhysChem* **2015**, *16*, 181.

**Students/postdocs involved in project: Wenhui Feng, Erik Janssen, Mike Hodny.**

**Publications acknowledging DOE support (2012-present)**

1. “Kinetics of the O + ICN Reaction”, W. Feng and J.F. Hershberger, *J. Phys. Chem. A* 116, 4817 (2012).
2. “Product Channels of the CN + HCNO Reaction”, W. Feng and J.F. Hershberger, *J. Phys. Chem. A* 116, 10285 (2012).
3. “Experimental and Theoretical Study of the Product Channels of the C<sub>2</sub>H + NO Reaction”, W. Feng and J.F. Hershberger, *J. Phys. Chem. A* 117, 3585 (2013).
4. “Quantification of the 248 nm Photolysis Products of HCNO (Fulminic Acid)”, W. Feng and J.F. Hershberger, *J. Phys. Chem. A* 118, 829 (2014).
5. “Reaction Kinetics of CN Reactions with Alcohols”, E. Janssen and J.F. Hershberger, *Chem. Phys. Lett.* 625, 26 (2015).
6. “Reaction Kinetics of the CN Radical with Methyl Bromide”, M. Hodny and J.F. Hershberger, *Chem. Phys. Lett.* 645, 88 (2016).
7. “Product Channels in the Reaction of the Hydroxymethyl Radical with Nitric Oxide”, W. Feng, E. Janssen, and J.F. Hershberger, *J. Phys. Chem. A* 120, 1145 (2016)
8. “Product Channels in the 193 nm Photodissociation of HCNO”, W. Feng and J.F. Hershberger, *Chem. Phys.* 472, 18 (2016).

# Theoretical Methods for Pressure Dependent Kinetics and Electronically Nonadiabatic Chemistry

Ahren W. Jasper  
Combustion Research Facility, Sandia National Laboratories  
Livermore, CA 94551-0969  
ajasper@sandia.gov

## I. Program Scope

Elementary chemical kinetics calculations aid in the interpretation of experimental rate measurements and inform the development of comprehensive and detailed models of combustion. The predictive accuracy of chemical kinetics calculations is improving and is broadly approaching so-called “kinetic accuracy,” defined as a factor of  $\sim 2$  in the calculated rate coefficient. This term may be compared with the 1990s realization of “chemical accuracy” ( $\sim 1$  kcal/mol) in thermochemistry, when calculated thermochemistry began to be accurate enough to be used alongside experimental values. A similar situation has emerged in chemical kinetics thanks to ongoing improvements in computational power and theoretical methods. The principal goal of this project is to develop and validate new theoretical methods designed to broaden the applicability and improve the accuracy of theoretical chemical kinetics and to aid in the realization of kinetic accuracy for applications throughout combustion. The model developments we are presently focused on are: (1) predicting pressure dependence in elementary reactions using detailed master equation models of energy transfer informed by classical trajectories, and (2) characterizing spin-forbidden kinetics using both multistate trajectory methods and statistical theories, and (3) predicting anharmonic vibrational properties for polyatomic molecules at combustion temperatures via Monte Carlo phase space integration.

## II. Recent Progress

The accuracies of one-dimensional models for nonadiabatic transition probabilities (e.g., Landau-Zener) were tested against a full-dimensional semiclassical model for the spin-forbidden

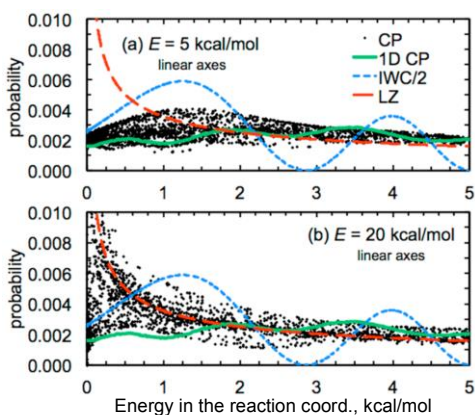


Fig. 1. Nonadiabatic transition probabilities for  $O + CO$  calculated using the 1D Landau-Zener (LZ), weak coupling (IWC), and classical path (CP) formulas, and the full-dimensional CP method.

reaction  $^3O + CO \rightarrow CO_2$  (see Fig. 1). We identified and quantified several multidimensional effects, including those associated with sampling the crossing seam, with the energy distribution in degrees of freedom orthogonal to the reaction coordinate, and with the interference of the electronic phase at multiple seam crossings. Fast electronic decoherence was shown to localize the nonadiabatic dynamics near the crossing seam. The one-dimensional models were found to have errors as large as a factor of two.

With Moshhammer and Hansen (Sandia), photoionization cross sections were calculated for 12 species using a readily applicable approach based on the frozen-core Hartree-Fock approximation, as made available by Lucchese in his ePolyScat code. First, this approach was validated against measured photoionization cross sections and found to have an average error of  $\sim 2\times$ , which likely improves on the estimates commonly used to model species with unknown

cross sections. Next, the ketohydroperoxide relevant to the low temperature oxidation of dimethyl ether was identified in a jet stirred reactor, and its mole fraction was quantified using the predicted cross section. This study demonstrated that theoretical cross sections can be useful for quantifying key intermediates, which in turn provide additional targets for testing chemical kinetic models.

With Klippenstein, Georgievskii (Argonne), and Mebel (FIU), the temperature- and pressure-dependent kinetics of several key steps in the HACA molecular growth mechanism were predicted. As part of this effort, the collision parameters (i.e., efficiencies,  $\alpha = \langle \Delta E_d \rangle$ , and effective Lennard-Jones rate parameters) required for predicting pressure dependence in the master equation were calculated using newly fitted potential energy surfaces for collisions involving small aromatic molecules and the colliders He, Ar, and N<sub>2</sub>. Similar to our previous work on saturated hydrocarbons, we found that, for a given collider, the collision parameters depended most sensitively on the chemical composition of the hydrocarbon and were relatively insensitive to the chemical arrangement. Furthermore, parameterizations of the separable pairwise functional form for the interaction potential were found to be transferable to larger aromatics. The present strategies are therefore readily applicable to the study of larger PAHs.

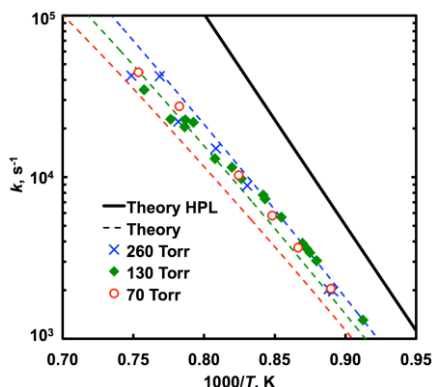


Fig. 2. Calculated and measured rate coefficients for the dissociation of 2-methyl-allyl

With Tranter (Argonne), the dissociation and the self-recombination of 2-methylallyl radicals were calculated using ab initio, transition state theory, classical trajectory, and master equation calculations. The predicted pressure- and temperature-dependent kinetics for both reactions were found to agree very well with the accompanying shock tube measurements, with, notably, no adjustments to the theory required (see Fig. 2). The observed quantitative agreement is likely somewhat fortuitous, as one might expect significant uncertainty in the partition function for the self-recombination adduct (2,5-dimethyl-1,5-hexadiene). Nonetheless, the comparisons provide yet another example of the good accuracy that can be achieved with fully a priori kinetics calculations, including trajectory-based predictions of pressure dependence.

As part of the AITSTME project (PI: Klippenstein), the spin-forbidden and spin-allowed product branching of <sup>3</sup>O + C<sub>2</sub>H<sub>4</sub> was calculated using a combination of quantum chemistry, master equation, classical trajectory, and nonadiabatic statistical theory calculations. This reaction has been widely studied, and it is known that product branching is largely controlled via the fate of the initial triplet adduct OC<sub>2</sub>H<sub>4</sub>, where intersystem crossing (ISC) to the singlet surface competes with spin-allowed bimolecular channels on the triplet surface. Here we used a Landau-Zener statistical calculation for the ISC rate (sometimes called “nonadiabatic transition state theory”) alongside conventional TST to predict the temperature-dependent branching within a single master equation calculation. Product branching immediately following ISC was determined using short-time direct classical trajectories initiated at the crossing seam. Our predicted room temperature branching agreed well with available experimental results, as well as with a previous master equation study of Vereecken, Peeters, and co-workers, who used a more approximate treatment of ISC. The two master equation studies predict different product branching at elevated temperatures, however.

The pressure-dependent unimolecular kinetics of CH<sub>4</sub> + He and C<sub>2</sub>H<sub>3</sub> + He were calculated in collaboration with Harding, Miller, and Klippenstein (Argonne). This work again involved a combination of quantum chemistry, transition state theory, classical trajectory, and master equation methods. A detailed model for the collisional energy transfer function  $P(E, J; E', J')$  was developed, which, unlike the well known single exponential down model, features: explicit angular momentum dependence, “long tail” collisions in both  $\Delta E$  and  $\Delta J$ , and nonseparability of  $\Delta E$  and  $\Delta J$ . The information required to parameterize such a model was obtained by calculating low-order moments of  $P$  using classical trajectories, against which the parameters of the model for  $P$  were optimized. Calculated rate coefficients obtained via this first-principles approach agreed with available experimental values within ~20%, which is similar to the reported accuracy of the experimental rates.

In other work,  $P(E, J; E' = 97\%$  of the dissociation threshold of NO<sub>2</sub>( $J' = 0$ ) for NO<sub>2</sub> + Ar was calculated as part of a joint theoretical/experimental study with Dave Chandler (Sandia). Both determinations of  $P$  showed biexponential (“long tail”) behavior, although the theoretical value for the

long tail range parameter ( $275\text{ cm}^{-1}$ ) was  $\sim 3\times$  larger than the experimental value. The source of this discrepancy is unclear and may be related to the calculations' neglect of excited electronic states.

We have used direct dynamics trajectories to study collisional energy transfer for  $\text{CH}_4 + \text{He}$ ,  $\text{Ne}$ , and  $\text{H}_2$ ,  $\text{C}_2\text{H}_5 + \text{He}$ , and  $\text{C}_2\text{H}_6 + \text{He}$ . These results were used to test the accuracy of the pairwise approximation for the interaction potential. We further tested the accuracy of using pairwise interaction potentials obtained for  $\text{CH}_4 + \text{M}$  for systems larger than methane, i.e., we tested the accuracy of using methane's interaction parameters as universal  $\text{C}_x\text{H}_y + \text{M}$  interaction parameters. For the saturated and lightly unsaturated systems we considered, results obtained using the universal  $\text{C}_x\text{H}_y + \text{M}$  potentials were found to agree with direct dynamics results within the statistical uncertainties of the calculations. The resulting universal potentials are very efficient relative to direct dynamics and may be used to study systems with dozens of C atoms.

We used the universal  $\text{C}_x\text{H}_y + \text{M}$  potentials to evaluate Troe's collision efficiency (and an approximation to it) for seven atomic and diatomic baths and for molecules and radicals as large as octane. In total, 266 systems were studied, including normal, branched, cyclic, and unsaturated hydrocarbon molecules, as well as hydrocarbon radicals interacting with the seven baths. These collision efficiencies are simple functions of the first moment of the energy transferred in deactivating collisions,  $\langle\Delta E_d\rangle$ . We also considered the *rotational* collision efficiency for several systems by calculating the first moment of the angular momentum transferred in deactivating collisions,  $\langle\Delta J_d\rangle$ . Trends in the collision efficiencies with respect to the bath gas, its temperature, and the size and chemical structure of the hydrocarbon target were quantified and discussed.

Several methods for predicting Lennard-Jones parameters for use as transport parameters in chemical kinetics models and for calculating collision rates in elementary kinetics were tested. The "one-dimensional minimization" method was found to be both accurate and efficient. In this method, the two interacting species are randomly oriented with respect to one another, and the interaction potential is minimized for this fixed orientation. The process is repeated for several orientations, and the resulting set of minimum energies and optimized center-of-mass separations are then averaged to obtain the Lennard-Jones parameters. Collision rates predicted using this method agree well with those based on tabulated parameters (typically within  $\sim 10\%$ ) for a wide variety of systems.

Dilute gas binary diffusion coefficients of H,  $\text{H}_2$ , and 4 n-alkanes in  $\text{N}_2$  were calculated "exactly" (but within the classical approximation) using full-dimensional classical trajectories and the  $\text{C}_x\text{H}_y + \text{N}_2$  potentials described above. The calculated diffusion coefficients were found to agree with Manion's (NIST) measured values for the n-alkanes in  $\text{N}_2$  to within a few percent. Diffusion coefficients are often approximated using Lennard-Jones parameters in combustion models, and the exact classical results were used to test the severity of this approximation for such applications. For most systems at combustion temperatures, the Lennard-Jones approximation is likely accurate within  $\sim 15\%$ . For weakly interacting systems, however, more realistic treatments of the repulsive wall are required. For systems at low temperatures, the neglect of anisotropy may introduce non-negligible errors.

### III. Future Work

We will continue the development and application of predictive models for pressure-dependent chemical kinetics. These calculations require the development of both direct dynamics and fitted potential surface strategies for accurately describing the full-dimensional target-bath systems. We will extend the types of species considered to include those with halogen and oxygen atoms. Enhanced energy transfer for halogens and alcohols has been reported, and the trajectory studies will be used to elucidate the dynamical mechanisms of these enhancements. Several applications to combustion-relevant systems will be carried out. The MCPSI method for calculating vibrational anharmonicity will continue to be applied and developed. We will focus on systems where the accuracy of existing vibrational anharmonicity approaches is not known, such as those involving constrained torsions and rings.

## V. Publications supported by this project since 2014

1. Quantification of hydroperoxymethyl formate and other elusive intermediates in low-temperature combustion of dimethyl ether. K. Moshhammer, A. W. Jasper, D. M. Popolan-Vaida, Z. Wang, V. S. B. Shankar, L. Ruwe, C. A. Taatjes, S. M. Sarathy, P. Dagaut, K. Kohse-Höinghaus, N. Hansen, *Proc. Combust. Inst.*, submitted.
2. Temperature- and pressure-dependent rate coefficients for the HACA pathways from benzene to naphthalene. A. M. Mebel, Y. Georgievskii, A. W. Jasper, and S. J. Klippenstein, *Proc. Combust. Inst.*, submitted.
3. Recombination and dissociation of 2-methyl allyl radicals: Experiment and theory. R. S. Tranter, A. W. Jasper, J. B. Randazzo, J. P. A. Lockhart, and J. P. Porterfield, *Proc. Combust. Inst.*, submitted.
4. Theoretical kinetics of  $O + C_2H_4$ . X. Li, A. W. Jasper, J. Zádor, J. A. Miller, and S. J. Klippenstein, *Proc. Combust. Inst.*, submitted.
5. Low temperature kinetics of the first steps of water cluster formation. V. Roussel, M. Capron, J. Bourgalais, A. Benidar, A. W. Jasper, S. J. Klippenstein, L. Biennier, and S. D. Le Picard, *Phys. Rev. Lett.*, in press (2016).
6. Comment on “When rate constants are not enough.” J. A. Miller, S. J. Klippenstein, S. H. Robertson, M. J. Pilling, R. Shannon, J. Zádor, A. W. Jasper, C. F. Goldsmith, and M. P. Burke, *J. Phys. Chem. A* 120, 306–312 (2016).
7. Determination of the collisional energy transfer distribution responsible for the collision-induced dissociation of  $NO_2$  with Ar. J. D. Steill, A. W. Jasper, and D. W. Chandler, *Chem. Phys. Lett.* 636, 1–14 (2015).
8. Multidimensional effects in nonadiabatic statistical theories of spin-forbidden kinetics: A case study of  $^3O + CO \rightarrow CO_2$ . A. W. Jasper, *J. Phys. Chem. A* 119, 7339–7351 (2015).
9. Kinetics of propargyl radical dissociation. S. J. Klippenstein, J. A. Miller, and A. W. Jasper, *J. Phys. Chem. A* 119, 7780–7791 (2015).
10. Thermal dissociation and roaming isomerization of nitromethane: Experiment and theory. C. J. Annesley, J. B. Randazzo, S. J. Klippenstein, L. B. Harding, A. W. Jasper, Y. Georgievskii, and R. S. Tranter, *J. Phys. Chem. A* 119, 7872–7893 (2015).
11. Detection and identification of the keto-hydroperoxide ( $HOOCH_2OCHO$ ) and other intermediates during low-temperature oxidation of dimethyl ether. K. Moshhammer, A. W. Jasper, S. M. Popolan-Vaida, A. Lucassen, P. Dievert, H. Selim, A. J. Eskola, C. A. Taatjes, S. R. Leone, S. M. Sarathy, Y. Ju, P. Dagaut, K. Kohse-Höinghaus, and N. Hansen, *J. Phys. Chem. A* 119, 7361–7374 (2015).
12. Ab initio variational transition state theory and master equation study of the reaction  $(OH)_3SiOCH_2 + CH_3 \rightarrow (OH)_3SiOC_2H_5$ . D. Nurkowski, S. J. Klippenstein, Y. Georgievskii, M. Verdicchio, A. W. Jasper, J. Akroyd, S. Mosbach, and M. Kraft, *Z. Phys. Chem.* 229, 691–708 (2015).
13. “Third-body” collision efficiencies for combustion modeling: Hydrocarbons in atomic and diatomic baths. A. W. Jasper, C. M. Oana, and J. A. Miller, *Proc. Combust. Inst.* 35, 197–204 (2015).
14. Predictive a priori pressure dependent kinetics. A. W. Jasper, K. M. Pelzer, J. A. Miller, E. Kamarchik, L. B. Harding, and S. J. Klippenstein, *Science* 346, 1212–1215 (2014).
15. First-principles binary diffusion coefficients for H,  $H_2$ , and four normal alkanes +  $N_2$ . A. W. Jasper, E. Kamarchik, J. A. Miller, and S. J. Klippenstein, *J. Chem. Phys.* 141, 124313 (2014).
16. Lennard-Jones parameters for combustion and chemical kinetics modeling from full-dimensional intermolecular potentials. A. W. Jasper and J. A. Miller, *Combust. Flame* 161, 101–110 (2014).

# Probing the Reaction Dynamics of Hydrogen-Deficient Hydrocarbon Molecules and Radical Intermediates via Crossed Molecular Beams

Ralf I. Kaiser

Department of Chemistry, University of Hawai'i at Manoa, Honolulu, HI 96822

[ralfk@hawaii.edu](mailto:ralfk@hawaii.edu)

## 1. Program Scope

The major goals of this project are to explore experimentally in crossed molecular beams experiments the reaction dynamics and potential energy surfaces (PESs) of hydrocarbon molecules and their corresponding radical species, which are relevant to combustion processes. The reactions are initiated under single collision conditions by crossing two supersonic reactant beams containing radicals and/or closed shell species under a well-defined collision energy and intersection angle. By recording angular-resolved time of flight (TOF) spectra, we obtain information on the reaction products, intermediates involved, branching ratios of competing reaction channels, reaction energetics, and on the underlying reaction mechanisms. These data are of crucial importance to comprehend the formation of two key classes of molecules in combustion processes: resonantly stabilized free radicals (RSFRs) and (substituted) polycyclic aromatic hydrocarbons (PAHs).

## 2. Recent Progress

*First*, our research program exposed that monocyclic aromatic molecules along with their corresponding radicals [benzene ( $C_6H_6$ ) / toluene ( $C_6H_5CH_3$ ) as well as the phenyl radical ( $C_6H_5$ ) / benzyl radical ( $C_6H_5CH_2$ )] can be formed as a consequence of a single collision event in the gas phase. *Second*, crossed molecular beam experiments were designed exploiting the formation of three prototype classes of (methyl substituted) polycyclic aromatic hydrocarbons (PAHs) [indene ( $C_9H_8$ ), naphthalene ( $C_{10}H_8$ ), and dihydronaphthalene ( $C_{10}H_{10}$ )]. *Third*, these studies were expanded to elucidate the formation of nitrogen-substituted aromatics [pyridine ( $C_5NH_5$ ), (iso)quinoline ( $C_9NH_7$ ), dihydro(iso)quinoline ( $C_9NH_9$ )]. *Fourth*, acetylene ( $C_2H_2$ ) reactions relevant to the hydrogen abstraction – acetylene addition mechanism (HACA) leading to bicyclic and tricyclic PAHs were investigated. *Finally*, we explored the degradation (oxidation) of monocyclic aromatic molecules: the phenyl radical. Various projects were conducted in collaboration with experimental and theoretical groups involved in DOE-BES sponsored research including Dr. Ahmed (Lawrence Berkeley National Laboratory) [P1, P11, P18-21, P24] and Prof. Mebel (Florida International University) [P1-4, P6-10, P12, P14-18, P21-23].

### 2.1. Formation of Substituted Monocyclic Aromatic Hydrocarbons

Having established that bimolecular reactions of dicarbon molecules ( $C_2(X^1\Sigma_g^+/a^3\Pi_u)$ ) and of ethynyl radicals ( $C_2H$ ) with 1,3-butadiene ( $C_2H_3C_2H_3$ ) form the phenyl radical ( $C_6H_5$ ) and benzene ( $C_6H_6$ ), respectively, under single collision conditions, we expanded these combined experimental and theoretical studies to probe potential pathways to *substituted* monocyclic aromatic molecules of fundamental importance to combustion processes: toluene ( $C_6H_5CH_3$ ) and the benzyl radical ( $C_6H_5CH_2$ ). Combining reactive scattering experiments of dicarbon molecules ( $C_2(X^1\Sigma_g^+/a^3\Pi_u)$ ) and of ethynyl radicals ( $C_2H$ ) with isoprene (2-methyl-1,3-butadiene ( $C_2H_3C_2H_2CH_3$ )) with electronic structure and RRKM calculations, our investigation reveals that the methyl group either acts as a spectator or is actively engaged in the chemistry leading eventually to the formation of toluene ( $C_6H_5CH_3$ ) and of the benzyl radical ( $C_6H_5CH_2$ ) (Figure 1). These overall strongly exoergic reactions proceed via indirect scattering dynamics without entrance barrier through complex formation via an initial addition to one of the terminal carbon atoms of isoprene followed by isomerization (ring closure, hydrogen migration) prior to hydrogen atom elimination and aromatization. These studies present the very first experimental evidence – contemplated by theoretical studies – that under single collision conditions *substituted monocyclic aromatic hydrocarbons* can be formed in a bimolecular gas phase reaction via reaction of two acyclic molecules involving cyclization processes at collision energies relevant to combustion flames.

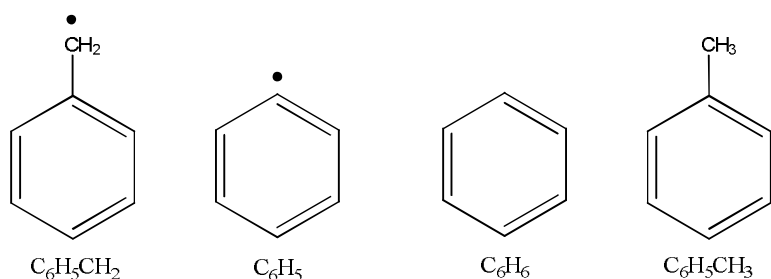


Fig. 1: Monocyclic aromatic hydrocarbons formed under single collision conditions in crossed molecular beam experiments via the reactions of dicarbon ( $C_2$ ) with isoprene ( $C_5H_8$ ), 1,3-butadiene ( $C_2H_3C_2H_3$ ) with dicarbon ( $C_2$ ), 1,3-butadiene ( $C_2H_3C_2H_3$ ) with the ethynyl radical ( $C_2H$ ), and isoprene ( $C_5H_8$ ) with the ethynyl radical ( $C_2H$ ) (from left to right): the benzyl radical, the phenyl radical, benzene, and toluene.

## 2.2. Formation of (Substituted) Bicyclic Aromatic Hydrocarbons

Considering the unique capability of our crossed molecular beams machine to untangle the energetics and dynamics of bimolecular reactions leading to prototype bicyclic polycyclic aromatic hydrocarbons (PAHs) indene ( $C_9H_8$ ), naphthalene ( $C_{10}H_8$ ), and dihydronaphthalene ( $C_{10}H_{10}$ ) via reactions of the phenyl radical ( $C_6H_5$ ) with unsaturated C3 (methylacetylene, allene) and C4 hydrocarbons (vinylacetylene, 1,3-butadiene) under single collision conditions, we expanded our studies to the next level and investigated the formation of (di)methyl-substituted PAHs with indene and naphthalene cores (Figure 2). We generated intense supersonic beams of ortho- and meta-tolyl (2- and 3-methylphenyl) radicals ( $C_6H_4CH_3$ ) via photodissociation of helium-seeded 2- and 3-chlorotoluene and probed the reactions with unsaturated C3 to C5 hydrocarbons. With the exception of methyl-substituted indene molecules, these bimolecular reactions lead to the formation of (di)methyl-substituted polycyclic aromatic hydrocarbons (PAHs) with naphthalene and 1,4-dihydronaphthalene cores in exoergic and *entrance barrier-less* reactions under single collision conditions. Most importantly, the reaction mechanism involves the initial formation of a van-der-Waals complex and addition of the phenyl-type radical to the C1 position of a vinyl-type group through a *submerged barrier*. Our investigations suggest that in the hydrocarbon reactant, the vinyl-type group must be in conjugation to a  $-C\equiv CH$  or  $-HC=CH_2$  group to form a *resonantly stabilized free radical (RSFR) intermediate*, which eventually isomerizes to a cyclic intermediate followed by hydrogen loss and aromatization with PAH formation. The barrierless formation of (dimethyl-substituted) PAHs defies conventional wisdom that PAH synthesis necessitates elevated temperatures.

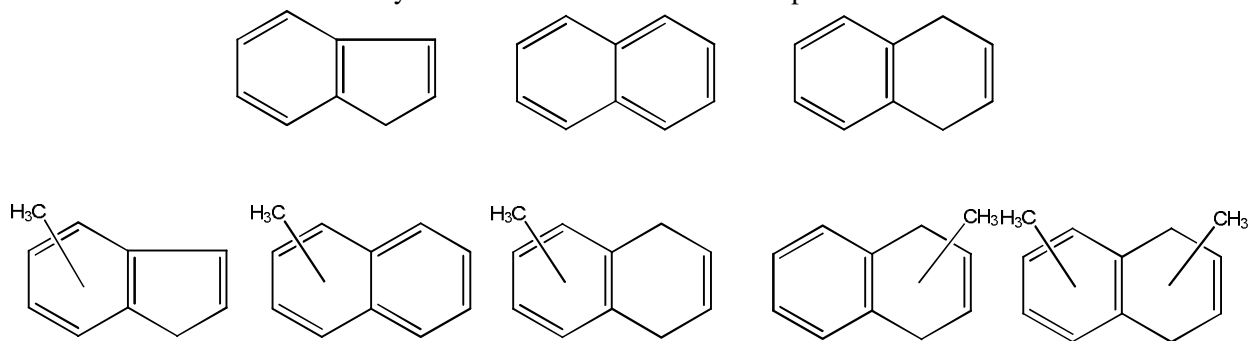


Fig. 2: Prototype polycyclic aromatic hydrocarbons (PAHs) indene, naphthalene, and dihydronaphthalene (top row) together with their (di)methylsubstituted counterparts (bottom row) formed in the reactions of phenyl-type radicals (phenyl, ortho- and meta-tolyl) with C3 to C5 hydrocarbons.

## 2.3. Acetylene Reactions Relevant to the Hydrogen Abstraction – Acetylene Addition Mechanism

Despite the popularity of the hydrogen abstraction – acetylene addition (HACA) mechanism, the underlying elementary reactions leading to PAH formation have not been verified experimentally to date under

controlled experimental conditions. Exploiting our chemical reactor to simulate combustion conditions and interrogating the supersonically cooled product via tunable vacuum ultraviolet light (ALS), we exposed for the first time that HACA-type mechanisms can produce the prototype PAHs naphthalene ( $C_{10}H_8$ ), indene ( $C_9H_8$ ), and acenaphthylene ( $C_{12}H_8$ ) via reactions of phenyl ( $C_6H_5$ ), benzyl ( $C_6H_5CH_2$ ), and naphthyl radicals ( $C_{10}H_7$ ) with acetylene ( $C_2H_2$ ) (Figure 3). However, neither anthracene ( $C_{14}H_{10}$ ) nor phenanthrene ( $C_{14}H_{10}$ ) was detected as products of the reaction of 1- and 2-naphthyl radicals with acetylene. These findings indicate that – as predicted from electronic structure calculations – the HACA mechanisms is less versatile toward the formation of more complex PAHs than previously postulated thus opening up alternative reaction pathways possibly via vinylacetylene-mediated synthesis of more complex PAHs in combustion flames.

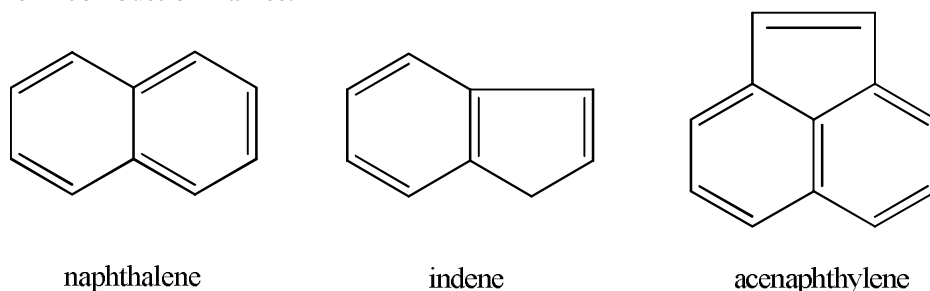


Fig. 3: Polycyclic aromatic hydrocarbons (PAHs) synthesized in the pyrolytic reactor.

### 3. Future Plans

We are planning to explore the formation of tricyclic PAHs carrying six- and five-membered rings such as anthracene/phenanthrene and fluorene under single collision conditions via reactions of bicyclic aromatic radicals like naphthyl and indenyl with C2 to C4 hydrocarbons (acetylene, methylacetylene, allene, vinylacetylene) in collaboration with Prof. Mebel. Further, we continue the elucidation of the destruction (oxidation) of PAH-based radicals such as naphthyl and indenyl in the pyrolysis reactor in collaboration with Musa Ahmed (LBNL) at the Chemical Dynamics Beamline.

### 4. Acknowledgements

This work was supported by US Department of Energy (Basic Energy Sciences; DE-FG02-03-ER15411).

### 5. Publications Acknowledging DE-FG02-03ER15411 (1/2013 – now)

**P1** A. Golan, M. Ahmed, A. M. Mebel, R.I. Kaiser, *A VUV Photoionization Study on the Formation of Primary and Secondary Products in the Reaction of the Phenyl Radical with 1,3-Butadiene under Combustion Relevant Conditions*. Physical Chemistry Chemical Physics 15, 341-347 (2013).

**P2** B.B. Dangi, D.S.N. Parker, R.I. Kaiser, A. Jamal, A.M. Mebel, *A Combined Experimental and Theoretical Study on the Gas Phase Synthesis of Toluene under Single Collision Conditions*. Angew. Chemie Int. Ed. 52, 7186-7189 (2013).

**P3** B.B. Dangi, S. Maity, R.I. Kaiser, A.M. Mebel, *A Combined Crossed Beam and Ab Initio Investigation of the Gas Phase Reaction of Dicarbon Molecules ( $C_2$ ;  $X^1\Sigma_g^+/a^3\Pi_u$ ) with Propene ( $C_3H_6$ ;  $X^1A'$ )*. The Journal of Physical Chemistry A 117 11783-11793 (2013).

**P4** D.S.N. Parker, T. Yang, R. I. Kaiser, A. Landera, A. M. Mebel, *On the Formation of Ethynylbiphenyl ( $C_{14}D_5H_5$ ;  $C_6D_5C_6H_4CCH$ ) Isomers in the Reaction of D5-Phenyl Radicals ( $C_6D_5$ ;  $X^2A_1$ ) with Phenylacetylene ( $C_6H_5C_2H$ ;  $X^1A_1$ ) Under Single Collision Conditions*. CPL 595, 230-236 (2014).

**P5** D.S.N. Parker, B. B. Dangi, R.I. Kaiser, A. Jamal, M.N. Ryazantsev, K. Morokuma, A. Korte, W. Sander, *An Experimental and Theoretical Study on the Formation of 2-Methylnaphthalene ( $C_{11}H_{10}/C_{11}H_3D_7$ ) in the Reactions of the Para-Tolyl ( $C_7H_7$ ) and Para-Tolyl-d7 ( $C_7D_7$ ) with Vinylacetylene ( $C_4H_4$ )*. The Journal of Physical Chemistry A, 118, 2709-2718 (2014).

**P6** B.B. Dangi, D.S.N. Parker, T. Yang, R.I. Kaiser, A.M. Mebel, *Gas Phase Synthesis of the Benzyl Radical ( $C_6H_5CH_2$ )*, Angew. Chemie Int. Ed. 53, 4608-4613 (2014).

- P7** D.S.N. Parker, S. Maity, B.B. Dangi, R.I. Kaiser, T. Labrador, A. M. Mebel, *Understanding the Chemical Dynamics of the Reactions of Dicarbon with 1-Butyne, 2-Butyne, and 1,2-Butadiene – Toward the Formation of Resonantly Stabilized Free Radicals*. Physical Chemistry Chemical Physics 16, 12150-12163 (2014).
- P8** B. B. Dangi, D.S.N. Parker, R.I. Kaiser, A.M. Mebel, *An Experimental and Theoretical Investigation of the Formation of C<sub>7</sub>H<sub>7</sub> Isomers in the Bimolecular Reaction of Dicarbon Molecules with 1,3-Pentadiene*, Chem. Phys. Lett. 607 92-99 (2014).
- P9** T. Yang, D.S.N. Parker, B. Dangi, R.I. Kaiser, V.V. Kislov, A.M. Mebel, *Crossed Beam Reactions of the Reaction of Phenyl (C<sub>6</sub>H<sub>5</sub>; X<sup>2</sup>A<sub>1</sub>) and D5-Phenyl Radical (C<sub>6</sub>D<sub>5</sub>; X<sup>2</sup>A<sub>1</sub>) with 1,2-Butadiene (H<sub>2</sub>CCCHCH<sub>3</sub>; X<sup>1</sup>A<sup>1</sup>)*, The Journal of Physical Chemistry A 118, 4372–4381 (2014).
- P10** B.B. Dangi, T. Yang, R.I. Kaiser, A.M. Mebel, *Reaction Dynamics of the 4-Methylphenyl Radical (C<sub>6</sub>H<sub>4</sub>CH<sub>3</sub>; p-Tolyl) with Isoprene (C<sub>5</sub>H<sub>8</sub>) - Formation of Dimethyldihydronaphthalenes*. Physical Chemistry Chemical Physics 16, 16805-16814 (2014).
- P11** D.S.N. Parker, R.I. Kaiser, T. Troy, M. Ahmed, *Hydrogen Abstraction Acetylene Addition Revealed!* Angew. Chemie Int. Edition 53, 7440-7444 (2014).
- P12** R.I. Kaiser, B.B. Dangi, T. Yang, D.S.N. Parker, A.M. Mebel, *Reaction Dynamics of the 4-Methylphenyl Radical (p-Tolyl) with 1,2-Butadiene (1-Methylallene) – Are Methyl Groups purely Spectators?* The Journal of Physical Chemistry A 118, 6181-6190 (2014).
- P13** D.S.N. Parker, B. B. Dangi, R.I. Kaiser, A. Jamal, K. Morokuma, *Formation of 6-Methyl-1,4-Dihydronaphthalene in the Reaction of the Para-Tolyl Radical with 1,3-Butadiene under Single Collision Conditions*. The Journal of Physical Chemistry A 118, 12111-12119 (2014).
- P14** R.I. Kaiser, D.S.N. Parker, A.M. Mebel, *Reaction Dynamics in Astrochemistry: Low Temperature Pathways to Polycyclic Aromatic Hydrocarbons (PAHs) in the Interstellar Medium (ISM)*. Annu. Rev. Physical Chemistry 66, 43-67 (2015).
- P15** T. Yang, L. Muzangwa, D.S.N. Parker, R. I. Kaiser, A.M. Mebel, *Synthesis of 2- and 1-Methyl-1,4-Dihydronaphthalene Isomers studied via the Crossed Beam Reactions of Phenyl Radicals (C<sub>6</sub>H<sub>5</sub>) with 1,3-Pentadiene (CH<sub>2</sub>CHCHCH<sub>3</sub>) and Isoprene (CH<sub>2</sub>C(CH<sub>3</sub>)CHCH<sub>2</sub>)*. Physical Chemistry Chemical Physics, 17, 530-540 (2015).
- P16** L.G. Muzangwa, R.I. Kaiser, T. Yang, D.S.N. Parker, A.M. Mebel, A. Jamal, K. Morokuma, *A Crossed Molecular Beam and Ab Initio Study on the Formation of 5- and 6-Methyl-1,4-Dihydronaphthalene (C<sub>11</sub>H<sub>12</sub>) via the Reaction of Meta-Tolyl (C<sub>7</sub>H<sub>7</sub>) with 1,3-Butadiene (C<sub>4</sub>H<sub>6</sub>)*. Physical Chemistry Chemical Physics 17, 7699-7706 (2015).
- P17** T. Yang, D.S.N. Parker, B. B. Dangi, R. I. Kaiser, A.M. Mebel, *Formation of 5- and 6-Methyl-1H-Indene (C<sub>10</sub>H<sub>10</sub>) via the Reactions of the Para-Tolyl Radical (C<sub>6</sub>H<sub>4</sub>CH<sub>3</sub>) with Allene (H<sub>2</sub>CCCH<sub>2</sub>) and Methylacetylene (HCCCH<sub>3</sub>) under Single Collision Conditions*. Physical Chemistry Chemical Physics 17, 10510-10519 (2015).
- P18** D.S.N. Parker, R.I. Kaiser, O. Kostko, T.P. Troy, M. Ahmed, A.M. Mebel, A.G.G.M. Tielens, *On the Synthesis of (Iso)Quinoline in Circumstellar Envelopes and Its Role in the Formation of Nucleobases in the Interstellar Medium*. The Astrophysical Journal 803-812, 53 (2015).
- P19** D.S.N. Parker, R.I. Kaiser, O. Kostko, T.P. Troy, M. Ahmed, *Unexpected Chemistry from the Reaction of Naphthyl plus Acetylene Molecules*. Angewandte Chemie – International Edition 54, 5421-5424 (2015).
- P20** D.S.N. Parker, R.I. Kaiser, O. Kostko, M. Ahmed, *Selective Formation of Indene via the Reaction of Benzyl Radicals with Acetylene* Chem. Phys. Chem. 16, 2091-2093 (2015).
- P21** D.S.N. Parker, R.I. Kaiser, T. P. Troy, O. Kostko, M. Ahmed, A.M. Mebel, *Toward the Oxidation of the Phenyl Radical and Prevention of PAH Formation in Combustion Systems*. The Journal of Physical Chemistry A 119, 7145-
- P22** T. Yang, L. Muzangwa, R.I. Kaiser, A. Jamal, K. Morokuma, *A Combined Crossed Molecular Beam and Theoretical Investigation of the Reaction of the Meta-Tolyl Radical with Vinylacetylene - Toward the Formation of Methylnaphthalenes*. Physical Chemistry Chemical Physics 17, 21564 - 21575 (2015).
- P23** A.M. Mebel, R.I. Kaiser, *Formation of Resonantly Stabilized Free Radicals via the Reactions of Atomic Carbon, Dicarbon, and Tricarbon with Unsaturated Hydrocarbons: Theory and Crossed Molecular Beams Experiments*. Int. Rev. Phys. Chem. 34, 461-514 (2015).
- P24** D.S.N. Parker, R.I. Kaiser, O. Kostko, T.P. Troy, M. Ahmed, A.H.H. Chang, *On the Formation of Pyridine in the Interstellar Medium*. Physical Chemistry Chemical Physics 17, 32000 – 32008 (2015).
- P25** D.S.N. Parker, T. Yang, B.B. Dangi, R.I. Kaiser, P.Bera, T.J. Lee, *Low Temperature Formation of Nitrogen-Substituted Polycyclic Aromatic Hydrocarbons (NPAHs) - Barrierless Routes to Dihydro(iso)quinolines*, 815, 115 The Astrophysical Journal (2015).

# Time-Resolved Nonlinear Optical Diagnostics

Christopher J. Kliewer (PI)

Combustion Research Facility, Sandia National Laboratories

P.O. Box 969, MS 9055

Livermore, CA 94551-0969

cjkliew@sandia.gov

## Program Scope

This program focuses on the development of innovative laser-based techniques for measuring temperature and concentrations of important combustion species as well as the investigation of fundamental physical and chemical processes that directly affect quantitative application of these techniques. Our development efforts focus on crossed-beam approaches such as time-resolved nonlinear wave-mixing. A critical aspect of our research includes the study of fundamental spectroscopy, energy transfer, molecular dynamics, and photochemical processes. This aspect of the research is essential to the development of accurate models and quantitative application of techniques to the complex environments encountered in combustion systems. These investigations use custom-built tunable picosecond (ps) and commercial femtosecond lasers, which enable efficient nonlinear excitation, provide high temporal resolution for pump/probe studies of collisional processes, and are amenable to detailed physical models of laser-molecule interactions.

## Recent Progress

### Quantifying spatio-thermochemical state detection through ultrabroadband coherent anti-Stokes

**Raman spectroscopy (CARS):** During the past year, we have further developed our new capabilities in ultrabroadband CARS imaging. Simultaneous measurements of high fidelity molecular thermometry and several of the major combustion species begins to address one of the most urgent needs for comparison of benchmark combustion data to combustion simulations – the determination of thermo-chemical state conditioned statistics. In the past, various dual-pump and triple-pump CARS schemes have been developed to gain simultaneous resonant signal from two or three molecular species simultaneously. In the ultrabroadband two-beam CARS technique that we have developed over the past two years, we have demonstrated the simultaneous detection of N<sub>2</sub>, O<sub>2</sub>, CH<sub>4</sub>, H<sub>2</sub>, CO<sub>2</sub>, C<sub>2</sub>H<sub>4</sub> and CO – a significant advance over previous schemes. Once the species resonances are corrected for the varying excitation efficiency of the 7 femtosecond supercontinuum source, the species mole fraction ratios may be evaluated according to Equation 1:

$$\frac{X_i}{N_2} = \sqrt{\frac{S_{X_i}}{S_{N_2}}} \times \frac{\sigma_{N_2}}{\sigma_{X_i}} \times e^{-t(1/\tau_{N_2} - 1/\tau_{X_i})} \quad (1)$$

where  $X_i/N_2$  is the molar ratio of the  $i$ -th chemical species relative to N<sub>2</sub>,  $S_{X_i}/S_{N_2}$  is the ratio of the integrated CARS signal of species  $i$  compared to N<sub>2</sub>,  $\sigma_{X_i}$  is the Raman cross section for species  $i$ ,  $t$  is the probe pulse delay time (100 ps for the concentration measurements), and  $\tau_{X_i}$  is the dephasing constant for species  $i$ . The species mole

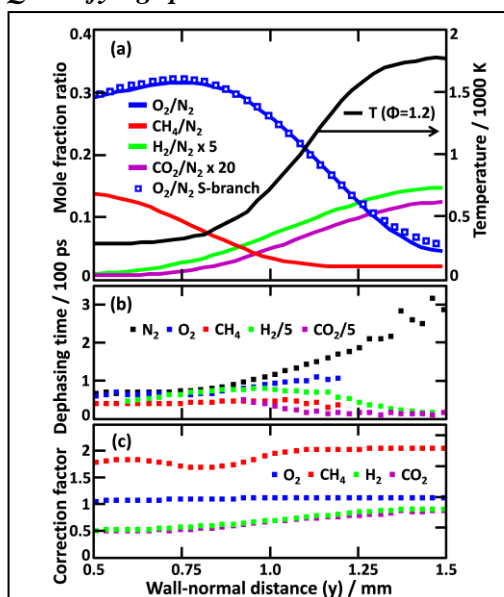
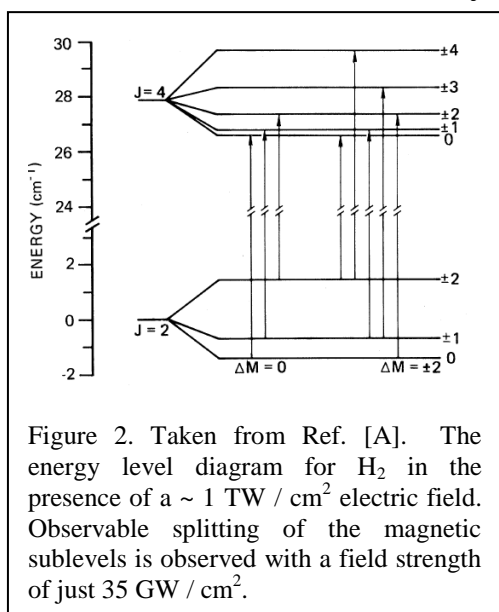


Figure 1. (a) Simultaneously measured relative species concentration measurements from 1D ultrabroadband CARS measurements taken in the quenching region of a side-wall quenching burner. (b) *In-situ* measured relative coherence dephasing rates. (c) Species-dependent correction factor to account for differential dephasing.

for the concentration measurements), and  $\tau_{X_i}$  is the dephasing constant for species  $i$ . The species mole

fraction ratio (relative to inert  $N_2$ ) is commonly employed instead of the absolute species mole fractions, due to the difficulty of detecting  $H_2O$  in CARS multiplexed techniques. The relative Raman cross sections and the dephasing constants for each species-specific transition must be obtained from the literature or measured. We have previously shown that the collisional coherence dephasing constant may be measured *in-situ* in flames with a probe delay scan technique which negates the need for a linewidth model altogether. We performed such probe delay scans during time-resolved 1D-CARS measurements in the quenching zone of a side-wall quenching burner, thereby measuring spatially dependent total collisional dephasing rates for each detected species in the wall-normal direction. With the dephasing constant known, the integrated signal intensities can be corrected for the probe delay, as shown in Figure 1. In addition, carefully calibrated gas mixtures were prepared to measure the relative differential CARS cross section for  $O_2$ ,  $CO_2$ ,  $CH_4$ , and  $H_2$ , which were found in some cases to differ substantially from the available literature values.

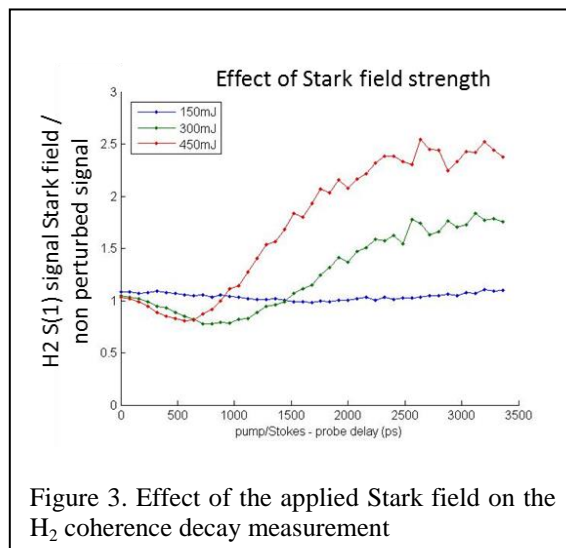
**Time-domain measurement of adiabatic strong-field effects:** In 1981, Farrow and Rahn [A]



reported the first observation of optical stark splitting of rotational Raman transitions of a molecule, demonstrated for ground state  $N_2$ . Splitting of the secondary total angular momentum quantum numbers ( $M_J$  states) could be observed even when the Stark field was of the order  $40 \text{ GW}/\text{cm}^2$  with high resolution nonlinear inverse Raman spectroscopy. The relevant energy level diagram is shown in Figure 2. For pure-rotational transitions, the interaction is based upon the polarizability anisotropy.

In the  $H_2$  molecule, transitions with energy above the  $S(0)$  line, such as the  $S(1)$  pure-rotational transition, should give rise to a similar optical stark-splitting effect with linearly polarized electric field. We have performed time-domain experiments exploring the possibility to measure such an adiabatic splitting in the time-domain as opposed to utilizing very high resolution techniques, which may yield access to an assessment of extremely small splittings of the  $M_J$  levels through polarization beating of the coherent Raman signal. The beating is because the induced splitting will be

substantially less than the bandwidth of the picosecond probe laser. In these experiments, the  $S(0)$  and  $S(1)$  pure-rotational transitions of  $H_2$  were imaged along a 1D spatial coordinate to the spectrometer and CCD camera in a 1D femtosecond pump / picosecond probe CARS experiment. A single-mode nanosecond laser at 532 nm was focused in the flow of cold  $H_2$  to create electric field strengths which varied across the CARS image from  $< 10 \text{ GW} / \text{cm}^2$  to  $> 500 \text{ GW} / \text{cm}^2$ . By delaying the probe pulse with respect to the femtosecond coherence preparation pulse, small splittings in the signal of each rotational transition should appear as a time-domain beating of the signal. The experimentally observed signal, as shown in Figure 3, shows very interesting behavior. A long timescale beating can be observed, which is indicative of a very small frequency splitting in the rotational transition, while simultaneously the coherence signal actually increases by up to a factor of 3 over the signal unperturbed by the Stark field.



## Future Work

**Development and benchmarking of a time-domain  $H_2$  S-branch CARS model.** The wide bandwidth of our recent supercontinuum based CARS measurements has allowed us to record the first complete pure rotational coherent Raman spectrum of  $H_2$  simultaneously with the pure-rotational spectrum of  $N_2$  and Q-branch detection of the other major flame species concentrations. At flame temperature, the  $H_2$  S-branch spectrum spans more than  $1000\text{ cm}^{-1}$  because of the large rotational constant. In rich and sooting flames, where significant amount of  $H_2$  are produced, a robust assessment of rotational thermometry based on a molecule other than  $N_2$  is valuable. This requires construction of the molecular model for the time-domain polarization response of  $H_2$ , incorporation into our CARS code, and verification of the assessment of temperature against a canonical burner as a standard. For this, we will employ the well characterized Wolfhard-Parker slot burner which will allow a wide span in  $H_2$  temperature, in addition to measurements in a heated cell.

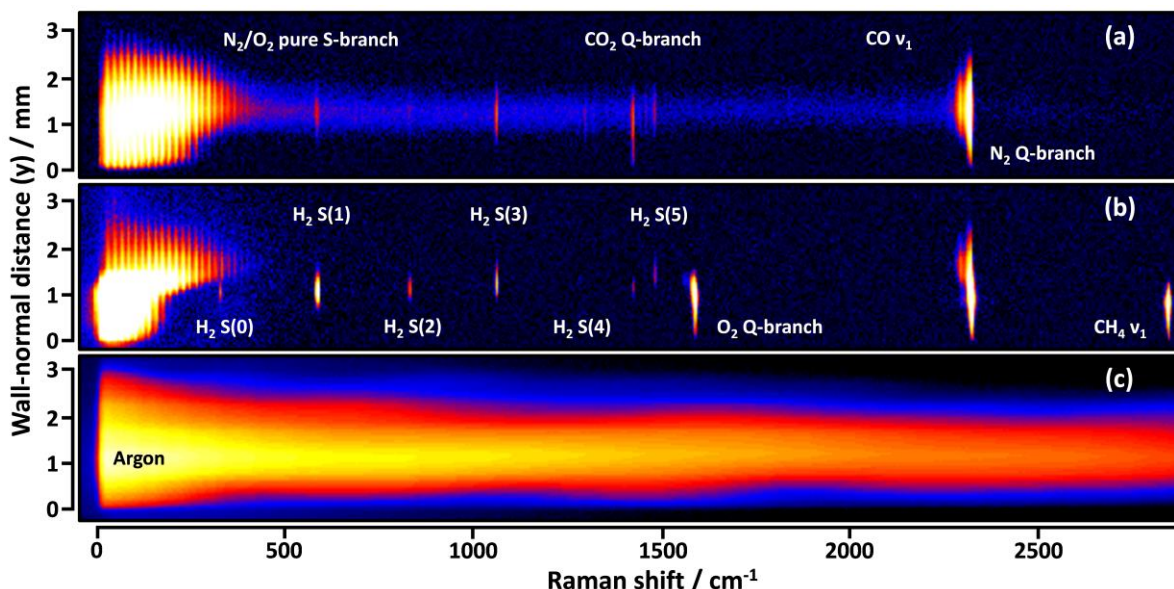


Figure 4. Measured ultrabroadband 1D-CARS image in the quenching region of a rich wall-impinging methane/air flame. Panel (a) shows the signal in the product zone. Panel (b) is an image taken prior to the quenching zone. Significant  $H_2$  is produced near the flame front and diffuses back into the reactant zone. Up to the S(5) line of  $H_2$  is observed. Panel (c) is the nonresonant signal demonstrating the broad bandwidth of interrogation.

**Multiplexing 2D-CARS with particle imaging velocimetry (PIV).** With the recent development of the first 2D-CARS measurements in our lab, our plan is to begin multiplexing the diagnostic with other techniques to gain access to joint statistics not previously attainable, such as the instantaneous thermal field and flow field obtained by combining 2D-CARS with PIV, respectively. Initial experiments will be conducted to determine if the particle scattering will interfere with the interpretation of the 2D-CARS signals, since the temperature is extracted by retrieving intensity spectra. However, since the signal is Raman shifted from the scattering frequency, it is expected that the PIV measurement will not interfere with the 2D-CARS assessment. Once this is determined, in collaboration with Dr. Jonathan Frank (CRF, Sandia), we will perform joint PIV and 2D-CARS in turbulent DME flames of current interest in Jonathan's lab. Planar CARS measurements before and after the addition of the PIV seeding particles will ensure the negligible effects of the seeding density on the combustion itself.

**Simultaneous nonresonant referencing for supercontinuum excitation.** The 7 femtosecond supercontinuum pulse used in our ultrabroadband CARS experiments is generated by focusing the

femtosecond laser output through a hollow core fiber filled with noble gas. The fiber acts as a waveguide to keep the intensity high enough for significant self-phase modulation to occur on the pulse, which has the effect of adding significant bandwidth. This bandwidth is then compressed after the fiber, allowing the generation of ultrashort pulses. Unfortunately, highly nonlinear processes occurring in the fiber are chaotic, and result in a pulse spectrum that varies substantially from shot to shot. This ultimately limits the single-laser-shot precision attainable in the multiple species measurement capability the technique enables. However, by detecting the nonresonant signal separate from the resonant signal of interest, a single-laser-shot measurement of the effective excitation profile of the laser could be achieved. This would dramatically increase the precision of ultrabroadband CARS measurements by enabling on-the-fly correction for the fluctuating excitation profile. We plan to achieve this by one of two methods: 1) polarization based separation of the resonant and nonresonant signals detected through separate spectrometer channels, or 2) using a portion of the beam to mix in a high pressure cell of argon and detect the resulting signal on a separate camera.

**Direct measurement of  $N_2$ -Fuel and  $N_2$ - $H_2O$  broadening coefficients.** With the successful development of the time-domain technique for acquiring high-accuracy S-branch broadening coefficients, demonstrated thus far for the  $N_2$ - $N_2$  and  $N_2$ - $H_2$  collisional systems, we propose to continue the collaboration with Per-Erik Bengtsson of Lund University, Sweden, to tackle the relative paucity of broadening coefficient data in the literature for air-fuel collisional systems. Initial studies will focus on the collisional broadening of  $N_2$  and  $O_2$  when perturbed by DME, ethane, ethylene, propane, and propylene. Accurate broadening models must be developed for these collisional environments, especially at elevated pressures. We will alter our current time-domain CARS code to implement these new linewidth libraries and test the validity of the model in our newly constructed high-pressure, high-temperature cell.

## References

A. Farrow, R. L., and Rahn, L. A. Optical Stark Splitting of Rotational Raman Transitions. *Phys. Rev. Lett.* **1982**, 48 (6), 395-398

## Journal publications supported by this BES project (2014-2016)

1. A. Bohlin and C. J. Kliwer, "Two-beam ultrabroadband coherent anti-Stokes Raman spectroscopy for high resolution gas-phase multiplex imaging," *Appl. Phys. Lett.* **104**, 031107 (2014).
2. A. Bohlin and C. J. Kliwer, "Diagnostic imaging in flames with instantaneous planar coherent Raman spectroscopy," *J. Phys. Chem. Lett.* **5**, 1243-1248 (2014).
3. A. Bohlin and C. J. Kliwer, "Single-shot hyperspectral coherent Raman planar imaging in the range 0-4200  $cm^{-1}$ ," *Appl. Phys. Lett.* **105**, 161111 (2014).
4. A. Bohlin, M. Mann, B.D. Patterson, A. Dreizler, C. J. Kliwer, "Development of two-beam femtosecond/picosecond one-dimensional rotational coherent anti-Stokes Raman spectroscopy: time-resolved probing of flame wall interactions," *Proc. Combust. Inst.* **35**, 3723-3730 (2015).
5. A. Bohlin and C. J. Kliwer, "Direct Coherent Raman Temperature Imaging and Wideband Chemical Detection in a Hydrocarbon Flat Flame," *J. Phys. Chem. Lett.* **6**, 643-649 (2015)
6. A. Bohlin, C. Jainski, B.D. Patterson, A. Dreizler, and C.J. Kliwer, "Multiparameter spatio-thermochemical probing of flame-wall interactions advanced with coherent Raman imaging," *Proc. Combust. Inst.*, *submitted*.
7. M. Campbell, A. Bohlin, P. Schrader, R. Bambha, C. J. Kliwer, K. Johansson, and H. Michelsen, "Design and characterization of a linear Hencken-type burner," *Rev. Sci. Instrum.*, *submitted*.

## THEORETICAL CHEMICAL KINETICS

Stephen J. Klippenstein  
Chemical Sciences and Engineering Division  
Argonne National Laboratory  
Argonne, IL, 60439  
[sjk@anl.gov](mailto:sjk@anl.gov)

### Program Scope

The focus of this program is the theoretical estimation of the kinetics of elementary reactions of importance in combustion chemistry. The research involves a combination of *ab initio* electronic structure calculations, variational transition state theory (TST), classical trajectory simulations, and master equation calculations. We apply these methods to reactions of importance in various aspects of combustion chemistry including (i) polycyclic aromatic hydrocarbon (PAH) formation, (ii) hydrocarbon oxidation, and (iii) NO<sub>x</sub> chemistry. The specific reactions studied are generally motivated by our interactions with combustion modeling efforts. We are also interested in a detailed understanding of the limits of validity of and, where feasible, improvements in the accuracy of specific implementations of transition state theory. Detailed comparisons with experiment and with other theoretical methods are used to explore and improve the predictive properties of the transition state theory based models. Dynamics simulations are performed as a means for testing the statistical assumptions, for exploring reaction mechanisms, and for generating theoretical estimates where statistical predictions are clearly inadequate. Master equation simulations are used to study the pressure dependence of the kinetics and to obtain phenomenological rate coefficients for use in kinetic modeling.

### Recent Progress

**Hydrocarbon oxidation:**  $O(^3P) + C_2H_4$ : The reaction of atomic oxygen with ethylene is an important oxidation step for many fuels and is prototypical of reactions in which oxygen adds to double bonds. For this class of reactions, decomposition of the initial adduct via spin-allowed reaction channels on the triplet surface competes with intersystem crossing (ISC) and a set of spin-forbidden reaction channels on the ground-state singlet surface. The  $^3O + C_2H_4$  reaction has been extensively studied, but previous experimental work did not provide detailed branching information at elevated temperatures, while previous theoretical studies have employed empirical and/or very approximate treatments of ISC. In collaboration with Jasper (Sandia), Zador (Sandia), and Miller the kinetics for the  $^3O + C_2H_4$  reaction was predicted with an AITSTME approach that incorporates a priori Landau-Zener statistical predictions for the ISC together with a direct classical trajectory study of the product branching directly after ISC. The theoretical predictions are in good agreement with existing experimental thermal kinetics and molecular beam studies and with past theoretical work, with the notable exception of product branching at elevated temperature. Above  $\sim 1000$  K, we predict  $CH_2CHO + H$  and  $^3CH_2 + CH_2O$  as the major products, which differs from the room temperature preference for  $CH_3 + HCO$  (which is assumed to remain at higher temperatures in some models) and from the prediction of a previous detailed ME study. These changes have important ramifications for combustion properties such as the ignition delay in  $C_2H_4$ , which is reduced by a factor of 2 to 3.

**Aromatic Radical + O<sub>2</sub>:** For aromatic radicals there is little known about the recombination kinetics, especially for the high temperatures of relevance to combustion. We

employed direct CASPT2 based VRC-TST to predict the high-pressure recombination rates for four prototypical aromatic hydrocarbon radicals: phenyl, benzyl, 1-naphthyl, and 2-naphthyl. The predicted rate coefficients are in reasonably satisfactory agreement with the limited experimental data and are expected to find utility in chemical modeling studies of PAH growth and oxidation.

**Criegee Intermediates:** There is currently considerable interest in the kinetics of Criegee intermediates (CI) due to their role as a source of OH in the atmosphere. They also arise in combustion as intermediates in low temperature radical oxidation of fuels such as dimethyl ether. In a collaboration with Lester (Penn) we explored the dissociation kinetics for syn-CH<sub>3</sub>CHOO and (CH<sub>3</sub>)<sub>2</sub>COO CI. Energy-dependent rates for unimolecular dissociation were obtained through direct time-domain experimental measurements employing pulsed tunable IR laser excitation of the CI and UV probing of the OH product. These measurements provided a novel test of our ability to predict microcanonical unimolecular dissociation rates. Remarkably, a priori tunneling corrected RRKM calculations employing potential energy surface properties evaluated with high-level thermochemical methods yielded quantitative agreement with the observations (within 10%). The conversion of these microcanonical rates to thermal rates yields reliable data for both atmospheric and combustion modeling of CI dissociation kinetics.

**Hydrocarbon Growth Studies: HACA Mechanism:** In collaboration with Mebel (Florida International), we predicted the pressure dependent thermal kinetics for various steps in the Hydrogen-Abstraction-C<sub>2</sub>H<sub>2</sub>-Addition (HACA) mechanism, which is arguably the best-known mechanism for ring growth. Introduced by Frenklach and Wang, HACA represents a repetitive sequence of two principal reaction types: the abstraction of a hydrogen atom from the reacting hydrocarbon by a radical, followed by the addition(s) of acetylene molecules to the radical site formed in the previous H-abstraction step. The production of a higher PAH, containing an extra aromatic ring in its core, can be accomplished by a ring closure ensuing the C<sub>2</sub>H<sub>2</sub> addition(s). Two alternative HACA pathways for the sequential additions of two C<sub>2</sub>H<sub>2</sub> were proposed by Frenklach et al. and by Bittner and Howard (cf. Figure 1). In Frenklach's route, the second acetylene adds to the aromatic ring activated by either a conventional or an internal hydrogen abstraction mechanism, whereas in Bittner-Howard's route, the second acetylene molecule adds directly to the product of the first addition.

Our predictions should be considerably more reliable than the early AM1-based RRKM results of Wang and Frenklach, which are employed in most current PAH/soot models. Notably, the calculations indicate strong pressure dependence for the role of the various HACA sequences. At atmospheric and lower pressures the C<sub>8</sub>H<sub>7</sub> radicals, C<sub>6</sub>H<sub>4</sub>C<sub>2</sub>H<sub>3</sub> and C<sub>6</sub>H<sub>5</sub>C<sub>2</sub>H<sub>2</sub>, cannot be stabilized above 1300 K. As a result, both the Bittner-Howard and the modified Frenklach HACA routes are inoperable under low-pressure flame conditions. However, at the

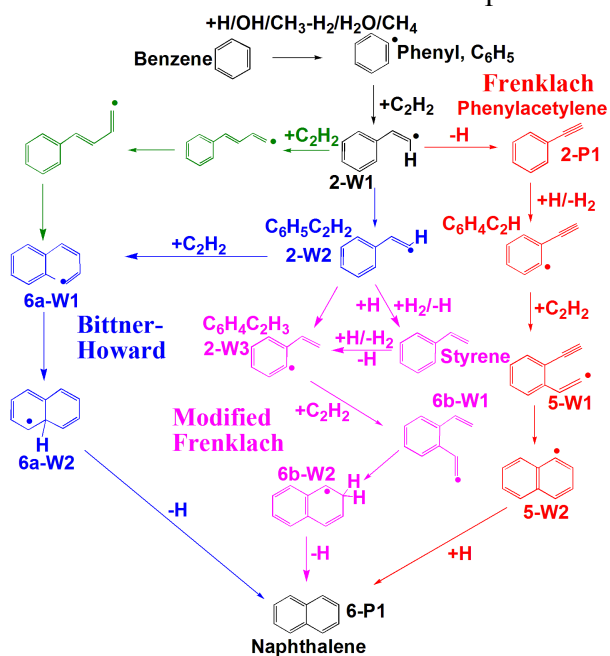


**Figure 1.** Schematic illustration of the Frenklach (red), modified Frenklach (pink), and Bittner-Howard (blue, green) HACA routes.

higher pressures of practical combustion devices (i.e., 10-100 atm) the  $C_8H_7$  species are stable enough that HACA routes may be operative. Naphthalene is predicted to be the main product of the  $C_6H_5C_2H_2 + C_2H_2$ , and  $C_6H_4C_2H_3 + C_2H_2$  reactions in the entire 500-2500 K temperature range independent of pressure (ignoring the issues related to the instability of  $C_8H_7$  species). Frenklach's original HACA route involves the  $C_6H_4C_2H + C_2H_2$  reaction, which is shown to predominantly form dehydrogenated species with a naphthalene core (naphthyl radicals or naphthynes) at  $T < 2000$  K and diethynylbenzene at higher temperatures. Overall, the results clearly indicate that one must use caution when using low-pressure flame studies to validate PAH mechanisms for use in broader ranges of pressure.

**Review Article:** We have written a lengthy review article as a companion to our upcoming plenary lecture for the International Combustion Symposium in Korea. The review highlights the success of ab initio chemical kinetics, as well as its remaining challenges, through comparisons with experiments ranging from elementary reaction kinetics studies through to global observations such as flame speed measurements. The illustrations progress from the treatment of relatively simple abstraction and addition reactions, which proceed over a single transition state, through to the complexity of multiwell multichannel reactions that commonly occur in studies of the growth of polycyclic aromatic hydrocarbons. In addition to providing high quality rate prescriptions for combustion modelers, theory will be seen to indicate various shortcomings in the foundations of chemical modeling. Future progress in the fidelity of the chemical modeling of combustion will benefit from more widespread applications of theoretical chemical kinetics and from increasingly intimate couplings of theory, experiment, and modeling.

### Future Directions

Our future work will continue to focus on the application of ab initio chemical kinetics to the prediction of the kinetics for reactions of key importance in combustion chemistry. Our various applications will continue to involve coupling with state-of-the-art electronic structure methods in collaboration with Harding and detailed comparisons with experiment as available. Currently, we are developing a code for proceeding directly from molecule specification to high accuracy rate predictions for simple reactions such as abstractions and single well radical-molecule or radical-radical additions. This code will be used to facilitate the exploration of the kinetics for large numbers of reactions in a given class.

We continue to collaborate with Mebel on a grand vision of mapping the full PAH kinetics for the first few aromatic rings. Currently we are converting numerous published detailed PES into meaningful kinetic estimates via our MESS program. Further work will explore refinements of the various AITSTME models to improve the accuracy of the predictions.

Further collaborations with Lester and Hase (Texas Tech) are planned for the analysis of the kinetics of Criegee intermediates. These studies will explore additional Criegee intermediates and will involve more detailed examinations of the pressure dependence of the kinetics including predictions of the direct decomposition fraction from trajectory determined energy distributions.

### DOE Supported Publications, 2014-Present

1. **Chemical Kinetics and Mechanisms of Complex Systems: A Perspective on Recent Theoretical Advances**, S. J. Klippenstein, V. S. Pande, D. G. Truhlar, *J. Am. Chem. Soc.* **136**, 528-546 (2014).
2. **Predictive *A Priori* Pressure Dependent Kinetics**, A. W. Jasper, K. M. Pelzer, J. A. Miller, E. Kamarchik, L. B. Harding, S. J. Klippenstein, *Science* **346**, 1212-1215 (2014).
3. **Secondary Channels in the Thermal Decomposition of Monomethylhydrazine ( $CH_3NHNH_2$ )**, P. Zhang, S. J. Klippenstein, L. B. Harding, H. Y. Sun, C. K. Law, *RSC Adv.* **4**, 62951-62964 (2014).

4. **Pressure-Dependent Branching in the Reaction of  $^1\text{CH}_2$  with  $\text{C}_2\text{H}_4$  and other Reactions on the  $\text{C}_3\text{H}_6$  Potential Energy Surface**, L.-L. Ye, Y. Georgievskii, S. J. Klippenstein, *Proc. Comb. Inst.* **35**, 223-230 (2015).
5. **The Role of Prompt Reactions in Ethanol and Methylformate Low-Pressure Flames**, N. J. Labbe, R. Sivaramakrishnan, S. J. Klippenstein, *Proc. Comb. Inst.* **35**, 447-455 (2015).
6. **Effects of New *Ab Initio* Rate Coefficients on Predictions of Species Formed During *n*-Butanol Ignition**, D. M. A. Karwat, M. S. Wooldridge, S. J. Klippenstein, M. J. Davis, *J. Phys. Chem. A* **119**, 543-551 (2015).
7. **Hydrolysis of Ketene Catalyzed by Formic Acid: Modification of Reaction Mechanism, Energetics, and Kinetics with Organic Acid Catalysis**, M. K. Louie, J. S. Francisco, M. Verdicchio, S. J. Klippenstein, A. Sinha, *J. Phys. Chem. A* **119**, 4347-4357 (2015).
8. ***Ab Initio* Variational Transition State Theory and Master Equation Study of the Reaction  $(\text{OH})_3\text{SiOCH}_2 + \text{CH}_3 = (\text{OH})_3\text{SiOC}_2\text{H}_5$** , D. Nurkowski, S. J. Klippenstein, Y. Georgievskii, M. Verdicchio, A. W. Jasper, J. Akroyd, S. Mosbach, M. Kraft, *Zeit. Phys. Chem.*, **229**, 691-708 (2015).
9. **The 2014 KIDA Network for Interstellar Chemistry**, V. Wakelam, J.-C. Loison, E. Herbst, B. Pavone, A. Bergeat, K. Beroff, M. Chabot, A. Faure, W. D. Geppert, D. Gerlich, P. Gratier, N. Harada, K. M. Hickson, P. Honvault, S. J. Klippenstein, S. D. LePicard, G. Nyman, M. Ruaud, S. Schlemmer, I. R. Sims, D. Talbi, J. Tennyson, R. Wester, *Astrophys. J. Supp.*, **217**, 20 (2015).
10. **Resolving Some Paradoxes in the Thermal Decomposition Mechanism of Acetaldehyde**, R. Sivaramakrishnan, J. V. Michael, L. B. Harding, S. J. Klippenstein, *J. Phys. Chem. A*, **119**, 7724-7733 (2015).
11. **Kinetics of Propargyl Radical Dissociation**, S. J. Klippenstein, J. A. Miller, A. W. Jasper, *J. Phys. Chem. A* **119**, 7780-7791 (2015).
12. **Global Uncertainty Analysis for RRKM/Master Equation Based Kinetic Predictions: A Case Study of Ethanol Decomposition**, L. Xing, S. Li, Z. Wang, B. Yang, S. J. Klippenstein, F. Zhang, *Comb. Flame* **162**, 3427-3436 (2015).
13. **Comment on "A Novel and Facile Decay Path of Criegee Intermediates by Intramolecular Insertion Reactions via Roaming Mechanisms"**, L. B. Harding, S. J. Klippenstein, *J. Chem. Phys.* **143**, 167101 (2016).
14. **Dimethylamine Addition to Formaldehyde Catalyzed by a Single Water Molecule: A Facile Route for Carbinolamine Formation and Potential Promoter of Aerosol Growth**, M. K. Louie, J. S. Francisco, M. Verdicchio, S. J. Klippenstein, A. Sinha, *J. Phys. Chem. A* **120**, 1358-1368 (2016).
15. **Low Temperature Kinetics of the First Steps of Water Cluster Formation**, J. Bourgalais, V. Roussel, M. Capron, A. Benidar, S. J. Klippenstein, L. Biennier, S. D. Le Picard, *Phys. Rev. Lett.* **116**, 113401 (2016).
16. **Communication: Real Time Observation of Unimolecular Decay of Criegee Intermediates to OH Radical Products**, Y. Fang, F. Liu, V. P. Barber, S. J. Klippenstein, A. B. McCoy, M. I. Lester, *J. Chem. Phys.* **144**, 061102 (2016).
17. **Theoretical Kinetics of  $\text{O} + \text{C}_2\text{H}_4$** , X. Li, A. W. Jasper, J. Zádor, J. A. Miller, S. J. Klippenstein, *Proc. Comb. Inst.* **36**, accepted for oral presentation, (2016).
18. **Temperature- and Pressure-Dependent Rate Coefficients for the HACA Pathways from Benzene to Naphthalene**, A. M. Mebel, Y. Georgievskii, A. W. Jasper, S. J. Klippenstein, *Proc. Comb. Inst.* **36**, accepted for oral presentation, (2016).
19. **Recombination of Aromatic Radicals with Molecular Oxygen**, F. Zhang, A. Nicolle, L. Xing, S. J. Klippenstein, *Proc. Comb. Inst.* **36**, accepted for oral presentation, (2016).
20. **From Theoretical Reaction Dynamics to Chemical Modeling of Combustion**, S. J. Klippenstein, *Proc. Comb. Inst.*, **36**, submitted (2016).
21. **Pressure Dependent Low Temperature Kinetics for  $\text{CN} + \text{CH}_3\text{CN}$ : Competition Between Chemical Reaction and van der Waals Complex Formation**, C. Sleiman, S. Gonzalez Rubio, S. J. Klippenstein, D. Talbi, G. El Dib, A. Canosa, *Phys. Chem. Chem. Phys.* submitted (2016).

## ARGONNE-SANDIA CONSORTIUM ON HIGH-PRESSURE COMBUSTION CHEMISTRY

Stephen J. Klippenstein (PI), Michael J. Davis, Lawrence B. Harding, Joe V. Michael,  
James A. Miller, Branko Ruscic, Raghu Sivaramakrishnan, Robert S. Tranter  
*Chemical Sciences and Engineering Division, Argonne National Laboratory, Argonne, IL, 60439*  
[sjk@anl.gov](mailto:sjk@anl.gov)

Leonid Sheps, Ahren W. Jasper, David L. Osborn, Judit Zádor, Craig A. Taatjes (PI)  
*Combustion Research Facility, Mail Stop 9055, Sandia National Laboratories*  
*Livermore, CA 94551-0969*  
[cataatj@sandia.gov](mailto:cataatj@sandia.gov)

**Program Scope:** The goal of this project is to explore the fundamental effects of high pressure (P) on the chemical kinetics of combustion and to use that knowledge in the development of accurate models for combustion chemistry at the high pressures of current and future engines. We design and implement novel experiments, theory, and modeling to probe high-pressure combustion kinetics from elementary reactions, to submechanisms, to flames. The work focuses on integrating modeling, experiment, and theory (MET) through feedback loops at all levels of chemical complexity. We are currently developing and testing the methodology for small alkanes, alcohols, and ethers as key prototype fuels. The consortium expands and enhances collaborations between Argonne's Chemical Dynamics in the Gas Phase Group and the Combustion Chemistry Group in Sandia's Combustion Research Facility.

**Recent Progress:** Ignition begins with oxidation of a fuel radical (R) to a peroxy radical (RO<sub>2</sub>), followed by decomposition or isomerization to a new carbon-centered radical (QOOH), which can decompose or undergo a second oxidation step. Decomposition of RO<sub>2</sub> and QOOH forms a relatively unreactive HO<sub>2</sub> or a single reactive OH; second O<sub>2</sub> addition can produce OH + ketohydroperoxide (KHP), which may in turn decompose to OH + oxy-radical. As a result, the degree of radical chain termination vs. chain branching in autoignition depends on the T- and P-dependent competition between unimolecular decay and second O<sub>2</sub> addition to QOOH. Our recent efforts have centered on probing these initiation reactions in the low-T autoignition regime.

*Second O<sub>2</sub> addition pathways in ether oxidation:* We explored the oxidation chemistry of dimethyl ether (DME) and tetrahydrofuran (THF), two prototypical (linear and cyclic) ethers that are also building blocks of larger promising biofuel alternatives. The O atom in ethers weakens the neighboring C-O and C-H bonds, enabling  $\beta$ -scission reactions that are not available to simple alkanes. As a result, nearly all QOOH formed in DME oxidation rapidly decomposes by C-O bond scission to OH + 2 CH<sub>2</sub>O; whereas in THF the analogous pathway leads to ring-opening and the formation of OH + butanedial. We also find strong experimental signatures of second O<sub>2</sub> addition to QOOH in both DME and THF; however, the subsequent fate of OOQOOH differs between these two cases, further highlighting the influence of molecular structure on reactivity. In DME, a second intramolecular H abstraction leads to the formation of hydroperoxymethyl formate (HPMF, analogous to KHP in butane oxidation), in agreement with earlier observations in a jet-stirred reactor. In contrast, the rigid ring structure of THF prevents the formation of KHP and instead leads to HO<sub>2</sub> elimination from OOQOOH. With help from quantum chemistry and experiments on partially-deuterated THF, we identified the relevant reaction pathway and its product, dihydrofuranyl hydroperoxide (DHF-OOH), as shown in Fig. 1. This channel outcompetes the formation of KHP and reduces radical chain-branching in THF at T < 650 K, yet pathways such as these are currently not included in low-T oxidation schemes.

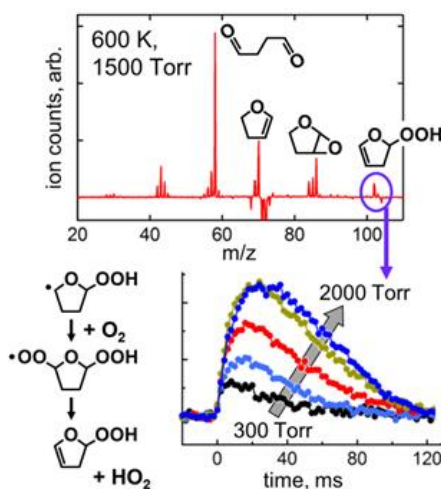


Figure 1. Top: transient photoionization mass spectrum of THF oxidation at P = 1500 Torr, T = 600 K. Bottom: time traces of 2,3-DHF-OOH, a product of second O<sub>2</sub> addition to QOOH. Bottom left: mechanism of 2,3-DHF-OOH formation.

*Development of High-Pressure Photoionization Mass Spectrometry (HP-PIMS):* Synchrotron-based multiplexed photoionization mass spectrometry for kinetics experiments has been very successful. However, high-P experiments demand increased sensitivity. In order to avoid secondary chemistry, radical concentrations must be kept no higher than  $\sim 10^{13}$  cm<sup>-3</sup>, so sample dilution must increase linearly with reactor pressure. The sensitivity of the existing apparatus has limited the range of useful accessible pressures to about 2 atm for most systems. However, within the

last year we have built a new high-pressure photoionization mass spectrometer (HP-PIMS), with a substantial increase in sensitivity compared to the earlier approach.

Chemical reactions are initiated by laser photolysis of an appropriate radical precursor in a homogeneous flow reactor in the presence of excess fuel and  $O_2$  in an inert bath at  $P$  up to 100 atm and  $T$  up to 800 K. The reaction mixture is continuously sampled through an interchangeable orifice (10 – 100  $\mu\text{m}$  diameter) into a vacuum chamber that houses a custom-built photoionization mass spectrometer. In a departure from convention, photoionization occurs only 2 mm downstream from the sampling orifice in a dense, yet already fully cooled (i.e. collisionless) part of the gas expansion. The highly divergent ion beam is extracted softly through a slit skimmer by custom electrostatic optics (without inducing additional collisions), then gently focused by custom ion guides into a pulsed reflectron TOF mass spectrometer with time resolution of 20  $\mu\text{s}$  and mass resolution  $m/\Delta m \sim 2000$ . The coupling of the continuous ion beam into the pulsed mass spectrometer is optimized by the design and operation of the ion guides, and the overall ion collection efficiency approaches 100%. Compared to the traditional approach, the high-density ionization scheme produces a factor of  $\sim 100$  increase in sensitivity, enabling sensitive, multiplexed PIMS experiments at previously inaccessible sample pressures.

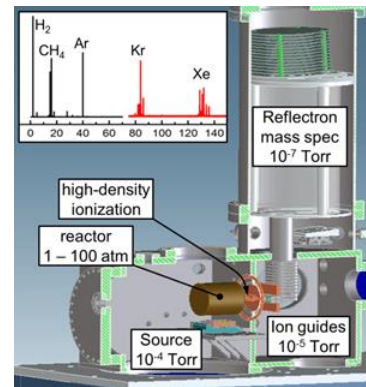


Figure 2. High-P PIMS endstation. *Inset:* calibration mass spectrum, used to obtain performance benchmarks of this apparatus.

*High-Repetition Rate miniature Shock Tube (HRRST):* The HRRST is part of a suite of instruments that have been developed under the HPCC project and operates over  $P < 100$  bar,  $600 < T < 3000$  K. The majority of experiments are conducted behind the reflected shock wave and the stable observation period has been increased to 300  $\mu\text{s}$  from 130  $\mu\text{s}$  by optimizing operation of the driver valve. The HRRST is primarily intended for use with synchrotron-based detectors. These typically produce weak signals and signal averaging is required to obtain sufficient S/N. Consequently, the HRRST is fully automated and runs at repetition rates from single shot to 4 Hz producing reproducible reaction conditions for thousands of shots. The apparatus has been run in multiple campaigns at the Advanced Photon Source (APS) and Advanced Light Source (ALS). The APS experiments primarily used x-ray absorption spectroscopy of argon to verify that well-formed shock waves with predictable, reproducible properties are created in the HRRST. However, in Dec. 2015 preliminary small angle x-ray scattering experiments were conducted at APS beamline 12-ID to examine the early stages of soot formation.

The most recent experiments at the ALS beamline 9.0.2 employed a new configuration of the HRRST, coupled by molecular beam sampling to a compact Kaesdorf mass spectrometer to obtain photoionization mass spectra with 6.667  $\mu\text{s}$  kinetic time resolution. Analysis of data from these types of experiments is discussed by Lynch et al.(14) The HRRST was operated at 1 Hz and approximately 20,000 shocks were performed per shift. At each condition (e.g. ionization energy, temperature) four hundred shocks were performed. These were binned to produce ensemble averaged mass spectra of 250-350 shocks per spectrum and standard deviations in reflected shock temperatures of  $\sim 2\%$ . Smaller standard deviations can easily be obtained by adjusting the binning criteria, at a penalty in S/N. The pyrolysis of dimethyl ether, a key species for the HPCC project, and two molecules that are routinely used as chemical thermometers (chlorocyclohexane and cyclohexene) were studied. The chemical thermometers will test that accurate rate coefficients can be extracted from these experiments. As noted below some challenges remain.

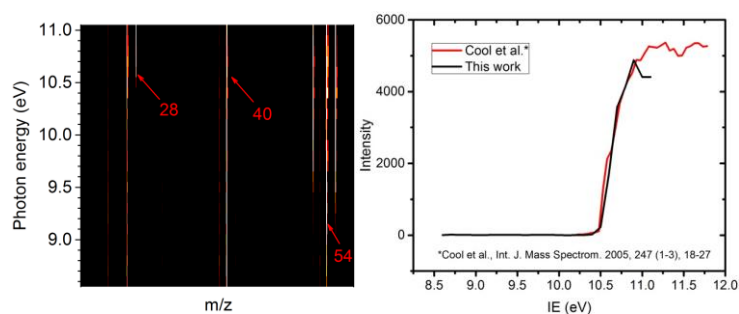


Figure 3. Ionization/mass plot for dissociation of cyclohexene ( $T_5 = 1470 \pm 30$  K;  $P_5 = 4 \pm 0.13$  bar) and PIE spectrum with 0.1 eV resolution for  $m/z$  28 ( $C_2H_4$ ).

DME and cyclohexene were studied at fixed reaction conditions and the ionization energy was scanned to obtain photoionization efficiency (PIE) spectra. Chloro-cyclohexane dissociatively ionizes, and was studied at a fixed ionization energy but over a range of reaction conditions. From the DME and cyclohexene experiments PIE spectra were obtained such as that shown in Fig. 3 for ethene. Excellent agreement with the high resolution PIE of Cool et al. is found. In addition to PIE spectra the data yield the time resolved

species concentrations from which kinetic data can be extracted. A remaining challenge to obtaining accurate rate

coefficients is that the large pressure changes within the HRRST during an experiment results in large density changes in the molecular beam entering the ion source. Consequently, even if the concentration of a species were not varying in time, the ion signal would. In conventional shock tube/MS experiments this is corrected for by normalizing the signals to an inert internal standard. However, in PIMS experiments the ionization energies of suitable standards are typically much higher than the photon energies used to produce a PIE. A promising solution that is being tested is to obtain a concentration vs. time plot of the ion signal of an inert species at sufficiently high photon energy to obtain strong signal and then use this to normalize other species measured at lower photon energies. This approach is feasible with the HRRST because signal averaging minimizes random fluctuations from successive ionization events.

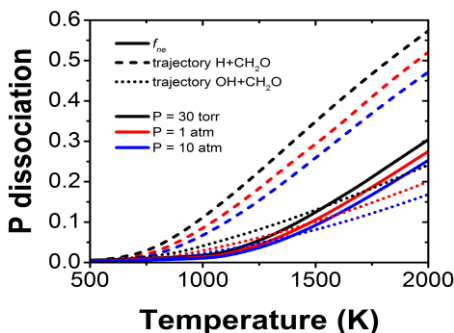


Figure 4. HCO prompt dissociation probabilities.

Fig. 4, solid lines). Additionally, these theoretical calculations indicated that prompt dissociation probabilities are enhanced when HCO is formed through exothermic abstraction reactions such as OH + CH<sub>2</sub>O and H + CH<sub>2</sub>O (dotted and dashed lines, Fig. 4).

In a companion modeling study, numerous flames of hydrocarbon and oxygenated molecules were simulated with current widely used literature kinetics models. Inclusion of our theoretically predicted prompt HCO dissociation fractions in these literature models led to an increase in the predicted flame speeds for the simulated fuels (CH<sub>4</sub>, n-C<sub>7</sub>H<sub>16</sub>, C<sub>2</sub>H<sub>4</sub>, CH<sub>3</sub>OCH<sub>3</sub>, CH<sub>3</sub>OH) by ~ 10% at 1 atm (cf. Fig. 5). Simulations of higher pressure flames (10 atm) predicted smaller enhancements in flame speeds (~ 5%). In these laminar flame speed simulations, prompt dissociation of HCO provided an additional source of H-atoms, thereby feeding chain branching reactions and promoting flame propagation in these prototypical fuels of relevance to the combustion community.

### Future Directions

We plan to continue the current experiments on DME and THF at higher pressures and temperatures, enabled by the newly-constructed HP-PIMS capability. The new high-quality THF data will be used within the HPCC framework to develop a more comprehensive mechanism for THF oxidation. We also plan to extend our efforts to increasingly complex (larger, longer-chain, and branched) hydrocarbon and oxygenated fuels.

We will also continue to pursue advances in experimental methodologies. We will re-design the flow reactor, coupled to our HP-PIMS apparatus, in order to optimize the sampling nozzle geometry and minimize heterogeneous reactions. We will also explore the possibility of using broadband cavity-enhanced transient absorption in high-pressure environments as well as coupling of HP-PIMS to other types of reactors or shock tubes. The HRRST will contribute to several core efforts of the HPCC consortium. The HRRST will be coupled to the HP-PIMS reactor, which should permit lower reagent concentrations to be used while maintaining good S/N. Several potential biofuels and intermediates in novel fuel combustion are cyclic ethers and thus, a series of experiments will be performed on molecules such as dioxanes and methylated furans to examine their pyrolytic and oxidative chemistry at elevated pressures. Additional x-ray scattering experiments are planned to refine the methodology and to allow the early stages of soot formation to be studied.

*Prompt Dissociations of Radicals:* Within combustion chemistry, open-shell radical species have always occupied a central role. In a recent theoretical study, we have shown that for a weakly bound radical such as the formyl radical (HCO), the dissociation process interferes with the collisional relaxation process and as a consequence of this it undergoes “prompt” dissociation to H + CO. When HCO is born with an initial thermal distribution, the prompt dissociation probability,  $P_{dissociation}$ , is given by  $1 - f_{ne}$  where  $f_{ne}$  is the non-equilibrium factor, which was reported in prior studies as a measure of the degree to which dissociation interferes with internal energy relaxation. We calculated that there is a significant amount of HCO prompt dissociation at the high temperatures (>1000 K) of relevance to combustion and flame chemistry (cf.

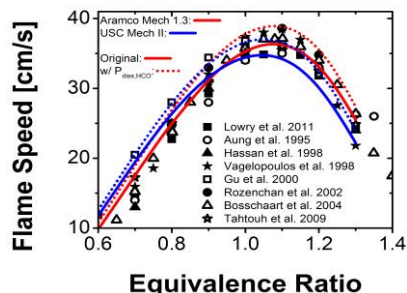


Figure 5. CH<sub>4</sub>-air flame, P = 1 atm, T<sub>u</sub> = 298 K.

Prompt dissociations are a general feature for all weakly-bound radicals. We propose to theoretically calculate prompt dissociations in other small weakly bound hydrocarbon radicals ( $C_2H_3$ ,  $C_2H_5$ ,  $CH_3O$ ,  $CH_2OH$ ,  $C_3H_5$ ,  $i-C_3H_7$ ,  $n-C_3H_7$ ,  $CH_3CO$ ,  $CH_3CH_2O$ ) and characterize their potential relevance to combustion modeling.

As a direct outcome of our recent shock tube studies that were successful in obtaining channel specific rate constants in H-atom abstractions from simple alkanes, we propose to extend this technique to obtain site-specific abstraction rate constants in simple oxygenated molecules. Furthermore, we envision that this technique will facilitate a direct probe for prompt dissociations of radicals. Abstraction using a thermal source for OH-radicals (TBHP) or O-atoms ( $O_3$ ) will be used as a means to form the radical of interest in the shock tube. H/D/O-ARAS and/or OH-multipass absorption diagnostics are then used to make time-resolved measurements of the radical decomposition.

### DOE-BES Supported Publications, 2014-Present

1. **First-Principles Binary Diffusion Coefficients for H, H<sub>2</sub>, and Four Normal Alkanes + N<sub>2</sub>**, A. W. Jasper, E. Kamarchik, J. A. Miller, S. J. Klippenstein, *J. Chem. Phys.* **141**, 124313:1-12 (2014).
2. **Photoionization Mass Spectrometric Measurements of Initial Reaction Pathways in Low-Temperature Oxidation of 2,5-dimethylhexane**, B. Rotavera, J. Zádor, O. Welz, L. Sheps, A. M. Scheer, J. D. Savee, M. A. Ali, T. S. Lee, B. A. Simmons, D. L. Osborn, A. Violi, C. A. Taatjes, *J. Phys. Chem. A* **118**, 10188-10200 (2014).
3. **UV Absorption Probing of the Conformer-Dependent Reactivity of a Criegee Intermediate CH<sub>3</sub>CHOO**, L. Sheps, A. M. Scully, K. Au, *Phys. Chem. Chem. Phys.* **16**, 26701-26706 (2014).
4. **Rate Coefficients of C<sub>1</sub> and C<sub>2</sub> Criegee Intermediate Reactions with Formic and Acetic Acid near the Collision Limit: Direct Kinetics Measurements and Atmospheric Implications**, O. Welz, A. J. Eskola, L. Sheps, B. Rotavera, J. D. Savee, A. M. Scheer, D. L. Osborn, D. Lowe, A. M. Booth, P. Xiao, M. A. H. Khan, C. J. Percival, D. E. Shallcross, C. A. Taatjes, *Ang. Chem. Int. Ed.* **53**, 4547-4550 (2014).
5. **Electronic States of the Quasilinear Molecule Propargylene (HCCCH) from Negative Ion Photoelectron Spectroscopy**, D. L. Osborn, K. M. Vogelhuber, S. W. Wren, E. M. Miller, Y. J. Lu, A. S. Case, L. Sheps, R. J. McMahon, J. F. Stanton, L. B. Harding, B. Ruscic, W. C. Lineberger, *J. Am. Chem. Soc.* **136**, 10361-10372 (2014).
6. **Predictive A Priori Pressure Dependent Kinetics**, A. W. Jasper, K. M. Pelzer, J. A. Miller, E. Kamarchik, L. B. Harding, S. J. Klippenstein, *Science* **346**, 1212-1215 (2014).
7. **High Temperature Rate Constants for H/D + n-C<sub>4</sub>H<sub>10</sub> and i-C<sub>4</sub>H<sub>10</sub>**, S. L. Peukert, R. Sivaramakrishnan, J. V. Michael, *Proc. Comb. Inst.* **35**, 171-179 (2015).
8. **Adventures on the C<sub>3</sub>H<sub>5</sub>O Potential Energy Surface: OH + Propyne, OH + Allene and Related Reactions**, J. Zádor, J. A. Miller, *Proc. Comb. Inst.* **35**, 181-188 (2015).
9. **“Third-body” Collision Efficiencies for Combustion Modeling: Hydrocarbons in Atomic and Diatomic Baths**, A. W. Jasper, C. M. Oana, J. A. Miller, *Proc. Comb. Inst.* **35**, 197-204 (2015).
10. **Toward a Quantitative Understanding of the Role of Non-Boltzmann Reactant Distributions in Low-Temperature Oxidation**, M. P. Burke, C. F. Goldsmith, Y. Georgievskii, S. J. Klippenstein, *Proc. Comb. Inst.* **35**, 205-213 (2015).
11. **Effect of Non-Thermal Product Energy Distributions on Ketohydroperoxide Decomposition Kinetics**, C. F. Goldsmith, M. P. Burke, Y. Georgievskii, S. J. Klippenstein, *Proc. Comb. Inst.* **35**, 283-290 (2015).
12. **Probing the Low-Temperature Chain-Branching Mechanism for n-Butane Autoignition Chemistry via Time Resolved Measurements of Ketohydroperoxide Formation in Photolytically Initiated n-C<sub>4</sub>H<sub>10</sub> Oxidation**, A. J. Eskola, O. Welz, J. Zádor, I. O. Antonov, L. Sheps, J. D. Savee, D. L. Osborn, C. A. Taatjes, *Proc. Comb. Inst.* **35**, 291-298 (2015).
13. **Direct Observation and Kinetics of a Hydroperoxyalkyl Radical (QOOH)**, J. D. Savee, E. Papajak, B. Rotavera, H. Huang, A. J. Eskola, O. Welz, L. Sheps, C. A. Taatjes, J. Zádor, D. L. Osborn, *Science* **347**, 643-646 (2015).
14. **Probing Combustion Chemistry in a Miniature Shock Tube with Synchrotron VUV-Photoionization Mass Spectrometry**, P. T. Lynch, M. Ahmed, T. P. Troy, R. S. Tranter, *Anal. Chem.* **87**, 2345-2352 (2015).
15. **Multi-Scale Informatics for Low-Temperature Propane Oxidation: Further Complexities in Studies of Complex Reactions**, M. P. Burke, C. F. Goldsmith, S. J. Klippenstein, O. Welz, H. Huang, I. O. Antonov, J. D. Savee, D. L. Osborn, J. Zádor, C. A. Taatjes, L. Sheps, *J. Phys. Chem. A* **119**, 7095-7115 (2015).
16. **New Insights into Low-Temperature Oxidation of Propane from Synchrotron Photoionization Mass Spectrometry and Multi-Scale Informatics Modeling**, O. Welz, M. P. Burke, I. O. Antonov, C. F. Goldsmith, J. D. Savee, D. L. Osborn, C. A. Taatjes, S. J. Klippenstein, L. Sheps, *J. Phys. Chem. A* **119**, 7116-7129 (2015).
17. **OH + 2-butene: A Combined Experimental and Theoretical Study in the 400-800 K Temperature Range**, I. O. Antonov, J. Kwok, J. Zádor, L. Sheps, *J. Phys. Chem. A* **119**, 7742-7752 (2015).
18. **Temperature and Pressure-Dependent Rate Coefficients for the Reaction of Vinyl Radical with Molecular Oxygen**, C. F. Goldsmith, L. B. Harding, J. A. Miller, S. J. Klippenstein, *J. Phys. Chem. A* **119**, 7766-7779 (2015).
19. **Direct Observation and Kinetics of a Critical Reactive Intermediate in Hydrocarbon Oxidation**, J. D. Savee, E. Papajak, B. Rotavera, H. Huang, A. J. Eskola, O. Welz, L. Sheps, C. A. Taatjes, J. Zádor, D. L. Osborn, *Science* **347**, 643-646 (2015).
20. **Understanding Low Temperature First State Ignition Delay: Propane**, S. S. Merchant, C. F. Goldsmith, M. P. Burke, S. J. Klippenstein, W. H. Green, *Comb. Flame* **162**, 3658-3673 (2015).
21. **Comment on “When Rate Constants are Not Enough” by John R. Barker, Michael Frenklach, and David R. Golden**, J. A. Miller, S. J. Klippenstein, S. H. Robertson, M. J. Pilling, R. Shannon, J. Zádor, A. W. Jasper, C. F. Goldsmith, M. P. Burke, *J. Phys. Chem. A* **120**, 306-312 (2016).
22. **Weakly Bound Free Radicals In Combustion: “Prompt” Dissociation of Formyl Radicals and Its Effect on Laminar Flame Speeds**, N. J. Labbe, R. Sivaramakrishnan, C. F. Goldsmith, Y. Georgievskii, J. A. Miller, S. J. Klippenstein, *J. Phys. Chem. Lett.* **7**, 85-89 (2016).
23. **Ramifications of Including Non-equilibrium Effects for HCO in Flame Chemistry**, N. J. Labbe, R. Sivaramakrishnan, C. F. Goldsmith, Y. Georgievskii, J. A. Miller, S. J. Klippenstein, *Proc. Comb. Inst.*, submitted, (2016).

# SPECTROSCOPY AND DYNAMICS OF REACTION INTERMEDIATES IN COMBUSTION CHEMISTRY

Marsha I. Lester  
Department of Chemistry  
University of Pennsylvania  
Philadelphia, PA 19104-6323  
milester@sas.upenn.edu

## I. Program Scope

The hydroxyl radical, a key oxidant in combustion, is generally detected by laser-induced fluorescence on the  $A^2\Sigma^+ - X^2\Pi$  band system. Sensitive, state-selective ionization detection of OH radicals offers additional advantages, and thus this laboratory is expanding its efforts to develop and apply a robust  $1+1'$  ionization scheme that combines OH A-X excitation with VUV ionization via autoionizing Rydberg states. Carbonyl oxides, important intermediates in tropospheric hydrocarbon oxidation and some combustion reactions, and related isomeric species are also being examined to determine their intrinsic stability and explore dynamical pathways.

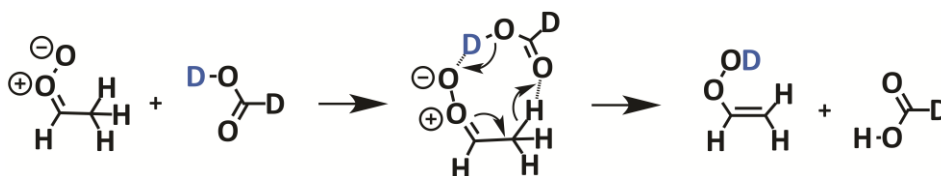
## II. Recent Progress

### A. VUV photoionization studies

Recently, we demonstrated a new  $1+1'$  resonance enhanced multiphoton ionization (REMPI) scheme for sensitive and state-selective detection of OH  $X^2\Pi$  radicals,<sup>1,2</sup> which is readily implemented using typical laboratory laser setups. UV excitation on the  $A^2\Sigma^+ - X^2\Pi$  transition is used to prepare a range of intermediate  $A^2\Sigma^+$  ( $v'=1, 2$ ) levels. Subsequent fixed-frequency VUV excitation at 118 nm (10.5 eV), generated by frequency-tripling the third harmonic of a Nd:YAG laser in Xe, accesses autoionizing OH [ $A^3\Pi, 3d$ ],  $v=0$  Rydberg states. The  $1+1'$  REMPI scheme is practical and has already been applied in this laboratory for photoionization mass spectrometry and velocity map imaging studies of OH radicals.<sup>3-5</sup>

While easy to implement, the underlying mechanism for the  $1+1'$  REMPI scheme is not as straightforward. The present study uses tunable VUV radiation to continuously scan over a broad frequency range to access OH Rydberg states with an  $A^3\Pi$  core and  $3d$  electron from specifically prepared rovibrational levels of the OH  $A^2\Sigma^+$  ( $v'=1$ ) state.<sup>6</sup> The tunable VUV is generated via two-photon resonant four-wave mixing ( $\omega_{\text{VUV}}=2\omega_1-\omega_2$ ) with  $2\omega_1$  fixed on a Kr resonance, building on analogous studies by Pratt and coworkers.<sup>7</sup> Distinct rotational and fine structure levels are observed for two newly identified OH  $^2\Pi$  Rydberg states. Spectroscopic constants are derived and several effects due to uncoupling of the spin and/or angular momentum of the Rydberg electron are identified, most notably significant  $\Lambda$ -doublet splittings. The VUV transitions exhibit a range of linewidths, indicating that the Rydberg state lifetimes due to autoionization are on the order of a picosecond. Moreover, this study demonstrates that the OH  $1+1'$  REMPI scheme is enhanced by accidental overlap of the fixed VUV radiation with rotationally resolved  $^2\Pi$  Rydberg -  $A^2\Sigma^+$  transitions, followed by ionization. The overlap of fixed VUV (118 nm) radiation with prominent lines in VUV scans also corroborates the previously reported enhancement factors for REMPI to LIF signals.<sup>2</sup> In the future, it would be highly desirable to use photoelectron imaging to unravel the ionization mechanism.

Vinyl hydroperoxide, a family of molecules with a C=COOH moiety, is predicted to be an important intermediate in many reaction pathways leading to OH radical products. The photoionization thresholds for the vinyl hydroperoxides are computed to be quite similar to other isomers, including carbonyl oxides known as Criegee intermediates, which makes separation of the isomers quite difficult by this means. We recently reported the first direct detection of stabilized vinyl hydroperoxides.<sup>8</sup> This laboratory demonstrated that a number of alkyl substituted vinyl hydroperoxides can be generated by carboxylic acid catalyzed tautomerization reactions of Criegee intermediates with  $\alpha$ -hydrogens. A doubly hydrogen-bonded interaction between the Criegee intermediate and carboxylic acid facilitates efficient hydrogen transfer through a double hydrogen shift. Deuteration of formic or acetic acid permits migration of a D atom to yield partially deuterated vinyl hydroperoxides as shown in the scheme below, which are distinguished from the CH<sub>3</sub>CHOO, (CH<sub>3</sub>)<sub>2</sub>COO, and CH<sub>3</sub>CH<sub>2</sub>CHOO Criegee intermediates by mass.



Reaction scheme for *syn*-CH<sub>3</sub>CHOO with DCOOD.

Using 10.5 eV photoionization, three prototypical vinyl hydroperoxides, CH<sub>2</sub>=CHOOD, CH<sub>2</sub>=C(CH<sub>3</sub>)OOD, and CH<sub>3</sub>CH=CHOOD, are detected directly.<sup>8</sup> Complementary electronic structure calculations by Kumar and Thompson revealed several reaction pathways, including the barrierless acid-catalyzed tautomerization reaction that they had predicted previously<sup>9</sup> as well as a barrierless addition reaction that yields hydroperoxy alkyl formate.

In collaboration with Taatjes and coworkers, we have also carried out experiments on hydroxyacetone (CH<sub>3</sub>C(O)CH<sub>2</sub>OH) formation using the multiplexed photoionization mass spectrometer at the Chemical Dynamics Beamline with tunable VUV radiation from the Advanced Light Source. Hydroxyacetone was observed as a persistent signal at *m/z* 74 at long reaction times in a flow tube after photolytically generating (CH<sub>3</sub>)<sub>2</sub>COO Criegee intermediates.<sup>10</sup> Hydroxyacetone is detected at a photoionization threshold of ca. 9.7 eV, which is considerably higher than that for the (CH<sub>3</sub>)<sub>2</sub>COO isomer. Complementary electronic structure calculations by Kumar and Thompson have revealed multiple reaction pathways for hydroxyacetone formation including unimolecular isomerization involving hydrogen atom transfer and -OH group migration as well as self-reaction of the Criegee intermediates.<sup>10</sup>

## B. Velocity map imaging studies

Recently, we utilized our new 1+1' REMPI ionization scheme for state-selective detection of OH X<sup>2</sup>Π radicals in its initial application with velocity map imaging (VMI). This initial VMI study examined the angular and velocity distributions of OH products arising from unimolecular decay of CH<sub>3</sub>CHOO, revealing the release of excess energy to internal and translational degrees of freedom as a means of elucidating the dynamical pathway(s) to products.<sup>5</sup> The more stable *syn*-conformer of the CH<sub>3</sub>CHOO Criegee intermediate was vibrationally activated using IR radiation in the CH stretch overtone region to access the transition state (TS) barrier region leading to OH products. The reaction pathway involves intramolecular 1,4 hydrogen atom transfer that results in isomerization to vinyl hydroperoxide. This is followed by O-O bond

cleavage to form OH + vinoxy products, although not via a simple barrierless O-O bond breaking process due to the presence of exit channel barriers and associated product minima.<sup>5,11</sup> The VMI experiments were complemented by quasi-classical trajectory (QCT) calculations from the TS to products by Wang and Bowman in a joint publication.<sup>5</sup>

This study focused on infrared excitation of *syn*-CH<sub>3</sub>CHOO at 6081 cm<sup>-1</sup>, which provides just enough energy to surmount or tunnel through the barrier and dissociation to OH products that are detected.<sup>12</sup> At this excitation energy, the OH products appear within the temporal resolution of the lasers ( $\leq 5$  ns).<sup>13</sup> The angular distribution of the OH products obtained using VMI is isotropic, demonstrating that dissociation occurs more slowly than the rotational period of *syn*-CH<sub>3</sub>CHOO ( $\geq 2$  ps). The total kinetic energy release (TKER) derived from the 2D image is a broad and unstructured distribution with an average TKER of 1100 cm<sup>-1</sup> or 20% of the available energy. The OH products are released with minimal excitation, indicating that most of available energy flows into internal excitation of the vinoxy products. The release of the excess energy to internal and translational degrees of freedom differs considerably from a statistical distribution, but is captured in QCT calculations initiated at critical configurations along the reaction pathway. The best agreement comes from trajectories starting at a submerged saddle point in the exit channel.<sup>5</sup>

### III. Future Work

We plan to utilize this novel OH detection scheme in VMI studies of photochemical and unimolecular reactions. Ongoing studies are examining the release of excess energy to internal and translational degrees of freedom upon IR activation and unimolecular decay of the dimethyl-substituted Criegee intermediate (CH<sub>3</sub>)<sub>2</sub>COO<sup>13,14</sup> and the hydrogen trioxy HOOO radical. The latter should provide a definitive measurement of the stability of the *trans*-HOOO species,<sup>15,16</sup> which has a weak chemical bond between the associated OH and O<sub>2</sub> components.

### IV. References

1. J. M. Beames, F. Liu, M. I. Lester and C. Murray, *J. Chem. Phys.* 134, 241102 (2011).
2. J. M. Beames, F. Liu, and M. I. Lester, *Mol. Phys.* 112, 897 (2014).
3. J. M. Beames, F. Liu, L. Lu, and M. I. Lester, *J. Chem. Phys.* 138, 244307 (2013).
4. F. Liu, J. M. Beames, A. M. Green, and M. I. Lester, *J. Phys. Chem. A* 118, 2298 (2014).
5. N. Kidwell, H. Li, X. Wang, J. M. Bowman, and M. I. Lester, *Nat. Chem.*, in press (2016).
6. A. M. Green, F. Liu, and M. I. Lester, submitted (2016).
7. H. Xu and S. T. Pratt, *J. Phys. Chem. A* 117, 9331 (2013).
8. F. Liu, Y. Fang, M. Kumar, W. H. Thompson and M. I. Lester, *Phys. Chem. Chem. Phys.* 17, 20490 (2015).
9. M. Kumar, D. H. Busch, B. Subramaniam and W. H. Thompson, *Phys. Chem. Chem. Phys.*, 16, 22968 (2014).
10. C. A. Taatjes, F. Liu, M. I. Lester, M. Kumar, W. H. Thompson, B. Rotavera, in preparation (2016).
11. T. Kurten and N. M. Donahue, *J. Phys. Chem. A* 116, 6823 (2012).
12. F. Liu, J. M. Beames, A. S. Petit, A. B. McCoy, and M. I. Lester, *Science* 345, 1596 (2014).
13. Y. Fang, F. Liu, V. P. Barber, S. J. Klippenstein, A. B. McCoy, and M. I. Lester, *J. Chem. Phys.* 144, 061102 (2016).
14. F. Liu, J. M. Beames, and M. I. Lester, *J. Chem. Phys.* 141, 234312 (2014).
15. C. Murray, E. L. Derro, T. D. Sechler, and M. I. Lester, *Acc. Chem. Res.* 42, 419 (2009).

16. S. D. Le Picard, M. Tizniti, A. Canosa<sup>1</sup>, I. R. Sims, and I. W. M. Smith, *Science* 328, 1258 (2010).

#### V. Publications supported by this project (2013-2016)

1. N. M. Kidwell, H. Li, X. Wang, J. M. Bowman, and M. I. Lester, “Unimolecular dissociation dynamics of vibrationally activated CH<sub>3</sub>CHOO Criegee intermediates to OH radical products”, *Nat. Chem.*, in press (2016).
2. H. Li, Y. Fang, N. M. Kidwell, J. M. Beames, and M. I. Lester, “UV photodissociation dynamics of the CH<sub>3</sub>CHOO Criegee intermediate: Action spectroscopy and velocity map imaging of O-atom products”, *J. Phys. Chem. A* **119**, 8328-37 (2015).
3. H. Li, Y. Fang, J. M. Beames, and M. I. Lester, “Velocity map imaging of O-atom products from UV photodissociation of the CH<sub>2</sub>OO Criegee intermediate”, *J. Chem. Phys.* **142**, 214312 (2015).
4. K. Samanta, J. M. Beames, M. I. Lester, and J. E. Subotnik, “Quantum dynamical investigation of the simplest Criegee intermediate CH<sub>2</sub>OO and its O-O photodissociation channels”, *J. Chem. Phys.* **141**, 134303 (2014).
5. J. H. Lehman and M. I. Lester, “Dynamical outcomes of quenching: Reflections on a conical intersection”, *Ann. Rev. Phys. Chem.* **65**, 537-55 (2014).
6. J. M. Beames, F. Liu, and M. I. Lester, “1+1' resonant ionization of OH radicals via the A<sup>2</sup>Σ<sup>+</sup> state: Insights from direct comparison with A-X fluorescence detection”, *Mol. Phys.* **112**, 897-903 (2014).
7. J. H. Lehman, H. Li, J. M. Beames and M. I. Lester, “Communication: Ultraviolet photodissociation dynamics of the simplest Criegee intermediate CH<sub>2</sub>OO”, *J. Chem. Phys.* **139**, 141103 (2013).
8. J. H. Lehman, H. Li and M. I. Lester, “Ion imaging studies of the photodissociation dynamics of CH<sub>2</sub>I<sub>2</sub> at 248 nm”, *Chem. Phys. Lett.* **590**, 16-20 (2013).
9. J. H. Lehman, M. I. Lester, J. Kłos, M. H. Alexander, P. J. Dagdigian, D. Herráez-Aguilar, F. J. Aoiz, M. Brouard, H. Chadwick, T. Perkins, and S. A. Seamons, “Electronic quenching of OH A<sup>2</sup>Σ<sup>+</sup> induced by collisions with Kr atoms”, *J. Phys. Chem. A* **117**, 13481-90 (2013).

# Computational Flame Diagnostics for Direct Numerical Simulations with Detailed Chemistry of Transportation Fuels

Tianfeng Lu

Department of Mechanical Engineering  
University of Connecticut, Storrs, CT 06269-3139  
tlu@engr.uconn.edu

## I. Program Scope

The goal of the proposed research is to create computational flame diagnostics based on chemical explosive mode analysis (CEMA) and bifurcation analysis to systematically detect critical flame features such as ignition, extinction and premixed and non-premixed flamelets, and to further understand the underlying physicochemical processes controlling limit flame phenomena, flame stabilization, turbulence-chemistry interactions and pollutant emissions etc. Diagnostics based on CEMA are performed for typical laminar flames and a variety of turbulent flames of transportation fuels (collaboration with J.H. Chen at Sandia and S. Som at Argonne) to extract salient physical information from the complex flow fields. CEMA is further employed to segment complex turbulent flames based on the critical flame features, such as premixed reaction fronts, and to enable zone-adaptive turbulent combustion modeling.

## II. Recent Progress

### A. Extinction of strained non-premixed flames based on CEMA diagnostics

The extinction behavior of strained non-premixed flames for ethylene-air is systematically investigated using CEMA. It was found that the competition of the chemical explosive mode (CEM) and diffusion plays a critical role in determining flame extinction, which is corresponding to the bifurcation points on the S-curve response to the flow straining.

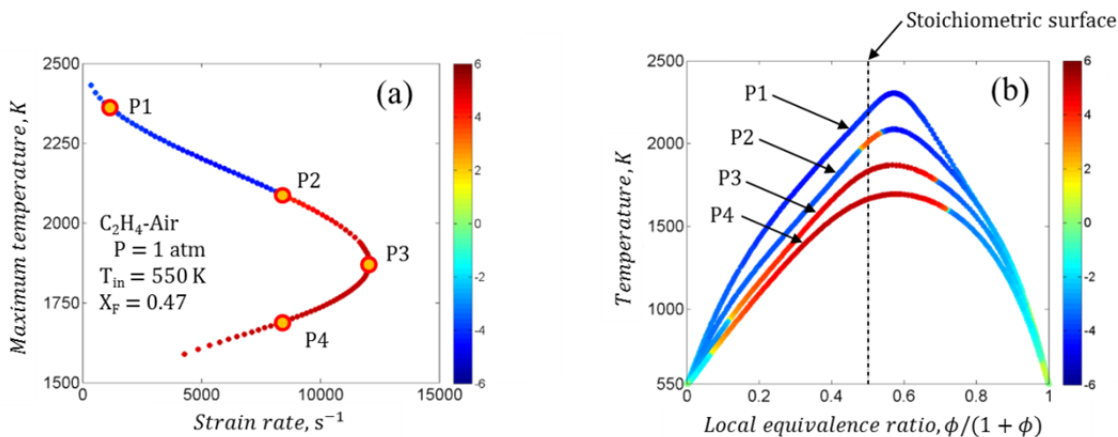


Figure 1. (a) Maximum temperature as function of strain rate in non-premixed flames of nitrogen diluted ethylene-air, and (b) temperature profiles at selected points on the S-curve in (a). Color indicates  $\text{sign}(\text{Re}(\lambda_e)) \times \log_{10}(1 + |\text{Re}(\lambda_e)|)$  at the stoichiometric surface, and  $\lambda_e$  is the eigenvalue of CEM.

This extinction mechanism is consistent with that of perfectly stirred reactors (PSR) identified in our previous studies based on bifurcation analysis [8]. In the present study of the diffusion flames, it was found that CEM first emerges at the stoichiometric surface of the non-premixed flame. This observation can be used as an indicator that the flame is approaching extinction as

shown in Fig. 1. It was further found that the crossover of the timescales of CEM and local diffusion projected to the direction of the CEM on the stoichiometric surface is an efficient and robust indicator of flame extinction for the ethylene flame, as shown in Fig. 2. This criterion for extinction of strained non-premixed flames is shown to be valid under different conditions, including different extents of fuel dilution and different inlet temperatures and was found to closely agree with the turning points on the S-curves of the ethylene flames, providing a possible diagnostic of local extinction in complex turbulent flow fields.

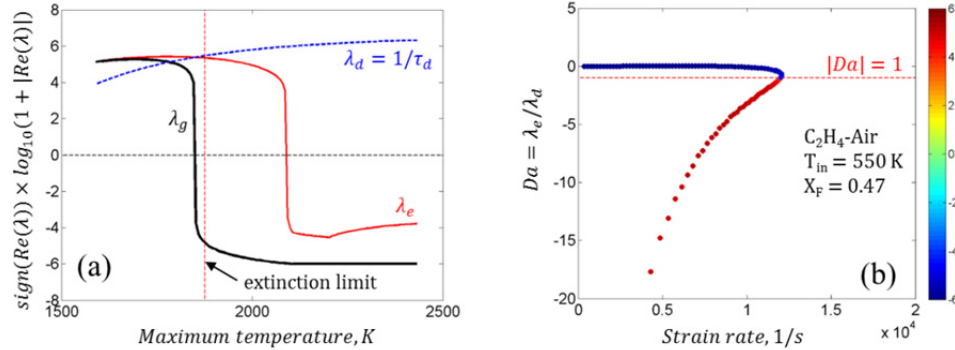


Figure 2. (a) Timescales as function of maximum temperature, (b) Damköhler ( $Da = \lambda_e/\lambda_d$ ) as function of strain rate in non-premixed counterflow flames of ethylene-air, showing that  $Da = 1$  accurately captures extinction. Color in (b) indicates  $\text{sign}(\text{Re}(\lambda)) \times \log_{10}(1 + |\text{Re}(\lambda)|)$  at stoichiometric surface.

### B. An explicit CEMA formulation for on-the-fly computational diagnostics

While CEMA can identify critical flame features in both premixed and non-premixed flames, it involves time consuming eigen-decomposition of the chemical Jacobian and thus is difficult to be applied on-the-fly in large-scale flame simulations. To address this issue, a semi-analytic explicit criterion is developed to provide an efficient and robust replacement of CEMA to predict local limit phenomena in complex flow fields. The reactions dominate the CEM are first identified by decomposing the eigenvalue, such that the reactions with negligible effects to the CEM can be eliminated. The coefficients between the reaction timescales, which can be evaluated analytically, and the CEM eigenvalue are then tabulated as function of local thermodynamic quantities, e.g. temperature and local mixture fraction. The explicit CEMA formulation is validated in large eddy simulations of non-premixed n-dodecane jet flame into heated air, as shown in Fig. 3. It is seen that the explicit CEMA formulation can accurately capture the zero-crossing of

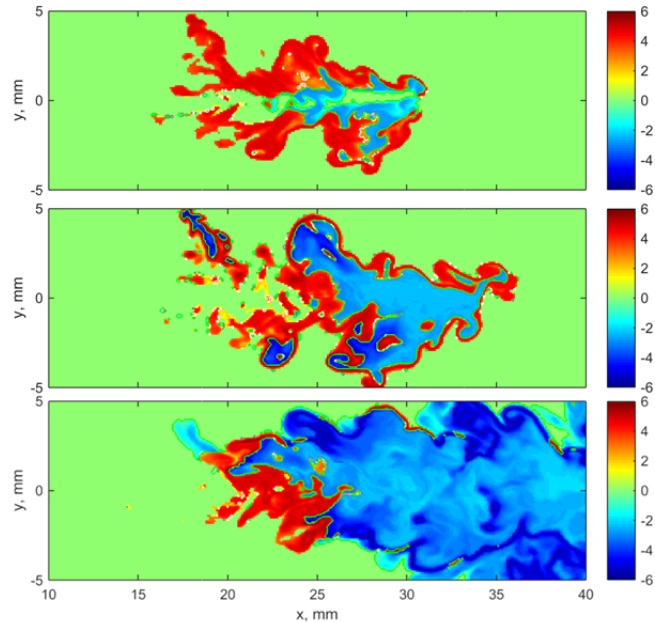


Figure 3. (a) Timescale of CEM calculated with full and semi-analytic explicit CEMA formulation, respectively, for a non-premixed n-dodecane jet into air at Spray A condition at different time. Isocontour: full CEMA, isolate: explicit formulation.

the CEM eigenvalue, which is critical for the diagnostics of limit flame phenomena, while the computational overhead of the explicit formulation is negligible compared with the overall computational cost of practical 3-D flame simulations.

### C. CEMA based zone-adaptive modeling of turbulent flames

Turbulent combustion modeling is challenging when complex flame configurations are involved, e.g. being hybrid of premixed and non-premixed. Most current models are typically specific for a particular type of flame, e.g. either premixed or non-premixed flamelet, or either auto-ignition or stirred reactors. CEMA is a reliable diagnostic to identify different flame features in complex flow fields, and it is extended to enable zone adaptive modeling for complex turbulent flames.

The zone adaptive modeling is investigated *a posteriori* in large eddy simulation of a transient lifted n-dodecane jet flame into hot air at Spray A condition. The explicit CEMA formulation was employed to identify premixed reaction fronts, and subsequently pre-ignition zone, and post-ignition zones in the flame. The premixed fronts were identified as the zero-crossing of the CEM eigenvalue, pre-ignition zones are identified by the presence of CEM and post-ignition zone was identified by the absence of CEM. Figure 4 shows the temperature isocontour obtained using full chemistry and the progress variable model, a variation of the non-premixed flamelet model, respectively, for post-ignition mixtures identified using the explicit CEMA. Accurate result was obtained using a single progress variable because CEMA accurately identifies the applicable range of the highly simplified progress variable model. Figure 5 further shows the scatter plots of temperature and CO concentration for the full solution and modeled post-ignition zone, respectively. It is seen that the scatter of post-ignition states in the full solution (blue) are accurately captured by the model (green). CEMA-based zone adaptive modeling is shown capable to integrate existing models specific to certain flame conditions by rigorous identification of the applicable zones of such models in complex flow fields.

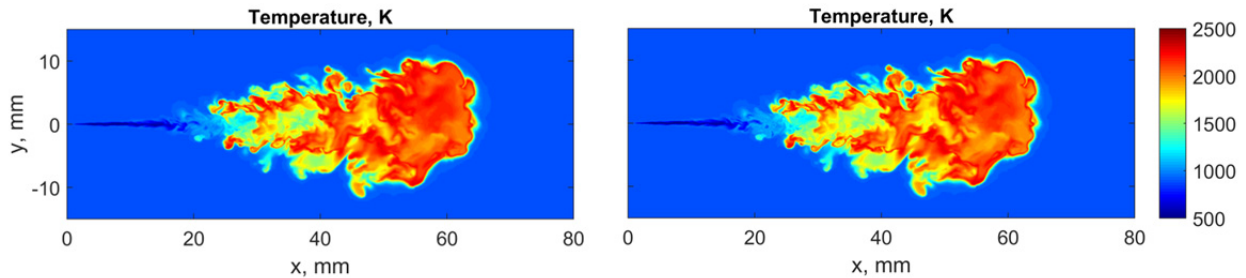


Figure 4. Temperature isocontour of a lifted n-dodecane jet flame at Spray A condition solved with full chemistry (left) and a progress variable model for the post-ignition zone identified with CEMA (right).

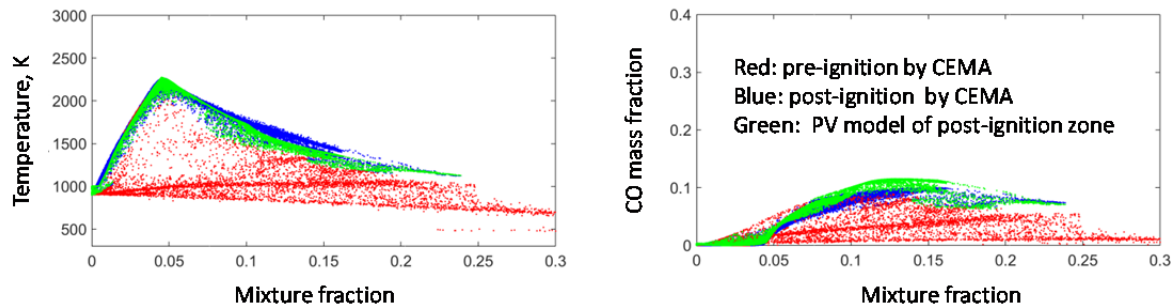


Figure 5. Scatter plots of temperature (left) and CO mass fraction (right) for the lifted n-dodecane flame in Fig. 4.

### Journal papers funded by this grant

1. M.B. Luong, Z. Luo, T.F. Lu, S.H. Chung, C.S. Yoo, "Direct numerical simulations of the ignition of lean primary reference fuel/air mixtures under HCCI condition," *Combustion and Flame*, 160 (10) 2038–2047, 2013.
2. S.M. Sarathy, S. Park, B. Weber, W. Wang, P. Veloo, A.C. Davis, C. Togbe, C.K. Westbrook, O. Park, G. Dayma, Z. Luo, M.A. Oehlschlaeger, F. Egolfopoulos, T.F. Lu, W.J. Pitz, C.J. Sung, P. Dagaut, "A comprehensive experimental and modeling study of iso-pentanol combustion," *Combustion and Flame*, 160 (12) 2712-2728, 2013.
3. Z. Ren, Y. Liu, T.F. Lu, L. Lu, O.O. Oluwole, G.M. Goldin, "The use of dynamic adaptive chemistry and tabulation in reactive flow simulations," *Combustion and Flame*, 161 (1) 127–137, 2014.
4. Z. Ren, H. Yang, T.F. Lu, "Effects of Small-Scale Turbulence on NO<sub>x</sub> Formation in Premixed Flame Fronts," *Fuel*, 115 241–247, 2014.
5. Z. Ren, C. Xu, T.F. Lu, M.A. Singer, "An Operator Splitting Scheme with Dynamic Adaptive Chemistry for Reactive Flow Simulations," *Journal of Computational Physics*, 263 19–36, 2014.
6. Z. Luo, S. Som, S.M. Sarathy, M. Plomer, W.J. Pitz, D.E. Longman, T.F. Lu, "Development and Validation of an n-Dodecane Skeletal Mechanism for Diesel Spray-Combustion Applications," *Combustion Theory and Modeling*, 18 (2) 187-203, 2014.
7. A. Bhagatwala, J.H. Chen, T.F. Lu, "Direct numerical simulations of HCCI/SACI with ethanol," *Combustion and Flame*, 161 (7) 1826-1841, 2014.
8. R. Shan, T.F. Lu, "A Bifurcation Analysis for Limit Flame Phenomena of DME/air in Perfectly Stirred Reactors," *Combustion and Flame*, 161 (7) 1716-1723, 2014.
9. M.B. Luong, T.F. Lu, S.H. Chung, C.S. Yoo, "Direct numerical simulations of the ignition of a lean biodiesel/air mixture with temperature and composition inhomogeneities at high pressure and intermediate temperature," *Combustion and Flame*, 161(11) 2878–2889, 2014.
10. A. Bhagatwala, T.F. Lu, H. Shen, J.A. Sutton, J.H. Chen, "Numerical and experimental investigation of turbulent DME jet flames," *Proceedings of the Combustion Institute*, 35(2) 1157-1166, 2015.
11. Y.X. Xin, W.K. Liang, W. Liu, T.F. Lu, C.K. Law, "A Reduced Multicomponent Diffusion Model," *Combustion and Flame*, 162(1) 68-74, 2015.
12. M.B. Luong, G.H. Yu, T.F. Lu, S.K. Chung, "Direct numerical simulations of ignition of a lean n-heptane/air mixture with temperature and composition inhomogeneities relevant to HCCI and SCCI combustion," *Combustion and Flame*, 162(12) 4566-4585, 2015.
13. Y. Pei, E.R. Hawkes, S. Kook, G.M. Goldin, T.F. Lu, "Modelling n-dodecane spray and combustion with the transported probability density function method," *Combustion and Flame*, 162(5) 2006-2019, 2015.
14. Z. Lu, L. Zhou, Z. Ren, T.F. Lu, K.H. Luo, C.K. Law, "Effects of spray and turbulence modelling on the mixing and combustion characteristics of an n-heptane spray flame simulated with dynamic adaptive chemistry," *Flow, Turbulence and Combustion*, DOI: 10.1007/s10494-015-9702-5, 2016.

# Advanced Nonlinear Optical Methods for Quantitative Measurements in Flames

Robert P. Lucht

School of Mechanical Engineering, Purdue University

West Lafayette, IN 47907-2088

Lucht@purdue.edu

## I. Program Scope

Nonlinear optical techniques such as laser-induced polarization spectroscopy (PS), resonant wave mixing (RWM), and electronic-resonance-enhanced (ERE) coherent anti-Stokes Raman scattering (CARS) are techniques that show great promise for sensitive measurements of transient gas-phase species, and diagnostic applications of these techniques are being pursued actively at laboratories throughout the world. The objective of this research program is to develop and test strategies for quantitative concentration and temperature measurements using nonlinear optical techniques in flames and plasmas. We have continued our fundamental theoretical and experimental investigations of these techniques. We have also initiated both theoretical and experimental efforts to investigate the potential of femtosecond (fs) laser systems for sensitive and accurate measurements in gas-phase media. Our initial efforts have been focused on fs CARS, although the systems will be useful for a wide range of future diagnostic techniques involving two-photon transitions. In the last two years we have demonstrated the acquisition of single-shot temperature measurements at data rates of 5 kHz in highly turbulent, swirl-stabilized methane-air flames. The fs CARS measurements exhibited high signal-to-noise ratios and temperatures were extracted from nearly every laser shot. We have spent a considerable amount of time over the last year in analyzing the data from these measurements and have two Combustion and Flames papers accepted for publication describing the measurements.

We have also extended the dynamic range of the fs CARS temperature measurement system by using a two-channel detection scheme. To test the two-channel scheme, we borrowed equipment from Andor Corp. Thanks to a supplemental funding grant from the Gas Phase Chemical Physics Program, we bought a new electron-multiplying charge-coupled device (EMCCD) camera system and imaging spectrometer, and we are now using the two-channel detection system on a routine basis.

During the previous year we performed two-color PS measurements of nitric oxide using two injection-seeded optical parametric generator/pulsed dye amplifier (OPG/PDA) systems, both operating near 452 nm. Collision-induced resonances were clearly observed with this system. The effects of different buffer gases on the generation of the collision-induced resonances were investigated and a numerical code for calculation of the two-color PS spectra developed. However, the operation of the OPG/PDA systems was very complicated, especially with the short-lived blue dyes used in the PDA, and we are now in the process of setting up a system with two dye lasers operating near 620 nm. The output of these dye lasers will be sum-frequency mixed with the 355-nm output of an injection-seeded Nd:YAG laser to produce the two tunable laser beams near 226 nm needed for the experiments.

We are investigating the physics of both fs CARS and two-color PS by direct numerical integration (DNI) of the time-dependent density matrix equations for the resonant interaction. Significantly fewer restrictive assumptions are required using this DNI approach compared with the assumptions required to obtain analytical solutions. We are concentrating on the accurate simulation of two-photon processes, including Raman transitions, where numerous intermediate electronic levels contribute to the two-photon transition strength. We have made significant progress in the last year on modeling two-color PS of atomic hydrogen, and are obtaining good agreement between experiment and modeling. We have also developed a code for the modeling of two-color PS signals, including the generation of collision-induced resonances.

## II. Recent Progress

### A. Femtosecond CARS Calculations and Experiments

The single-shot, chirped-pulse-probe (CPP) fs CARS system for temperature measurements is shown in Fig. 1. Fs CARS offers several major potential advantages compared with nanosecond (ns) CARS; i.e., CARS as usually performed with nanosecond pump and Stokes lasers. These potential advantages include an elimination of collisional effects in the signal generation and the capability of performing real-time temperature and species measurements at data rates of 1 kHz or greater as

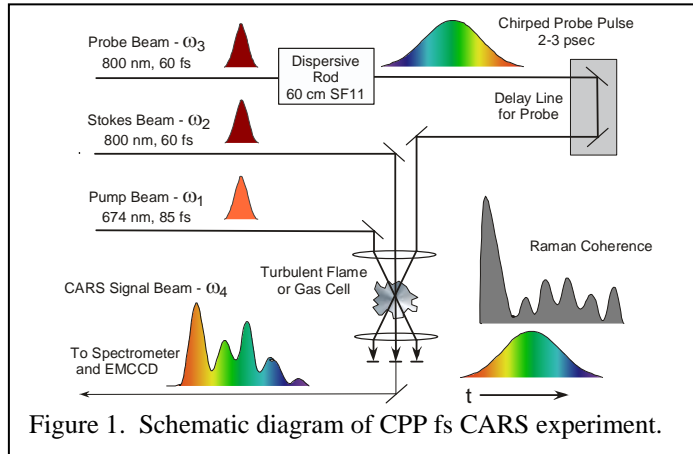


Figure 1. Schematic diagram of CPP fs CARS experiment.

Fourier-transform-limited to within a few percent. The fundamental 800-nm beam is used as the probe beam for our chirped-pulse-probe (CPP) fs CARS experiments as shown in Fig. 1. The greatly increased pulse energy of the chirped-pulse-probe beam results in a significant increase in the signal-to-noise ratio of the single-pulse measurements. During the past year we continued our analysis of single-laser-shot temperature measurements acquired at a data rate of 5 kHz in a highly turbulent, swirl-stabilized burner that has been characterized extensively at DLR Stuttgart. Measurements were performed for a so-called “stable” case and for a case with significant thermoacoustic instabilities. The CARS temperature measurements are in good agreement with previous single-shot Raman scattering measurements in the same flame. A microphone was used to record pressure pulsations in the burner. Simultaneous acoustic measurements enabled phase-synchronization of the fs CARS measurements with the thermo-acoustic pulsations in the burner. The rapid accumulation of statistically-converged datasets also supported a phase conditioned statistical analysis to study the time-evolving thermo-chemical state over the course of a thermoacoustic cycle. The CARS measurements are described in P1 and in a pair of articles accepted for publication in Combustion and Flame.

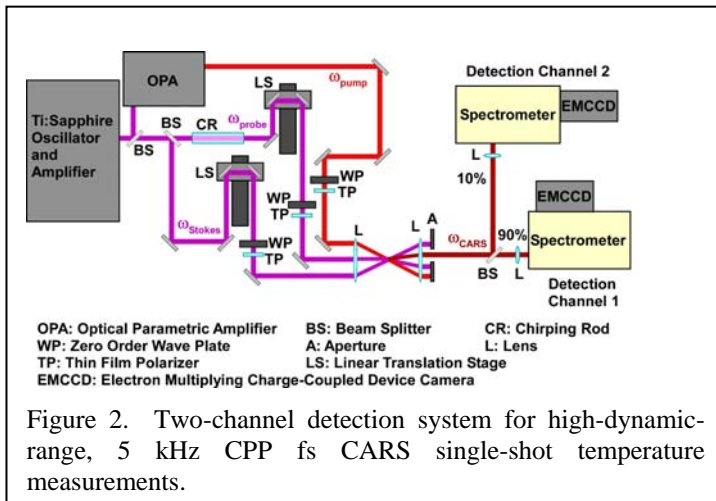


Figure 2. Two-channel detection system for high-dynamic-range, 5 kHz CPP fs CARS single-shot temperature measurements.

compared to 10-50 Hz for ns CARS. Our Coherent ultrafast laser system operates at 5 kHz with a fundamental pulse width of 60 fs and energy of over 2 mJ. The fundamental 800-nm pulse is Fourier-transform-limited to within a few percent. The fundamental 800-nm beam is used as the probe beam for our CPP fs CARS experiments. The greatly increased pulse energy of the chirped-pulse-probe beam results in a significant increase in the signal-to-noise ratio of the single-pulse measurements.

The fundamental 800-nm pulse is Fourier-transform-limited to within a few percent. The fundamental 800-nm beam is used as the probe beam for our chirped-pulse-probe (CPP) fs CARS experiments as shown in Fig. 1. The greatly increased pulse energy of the chirped-pulse-probe beam results in a significant increase in the signal-to-noise ratio of the single-pulse measurements. During the past year we continued our analysis of single-laser-shot temperature measurements acquired at a data rate of 5 kHz in a highly turbulent, swirl-stabilized burner that has been characterized extensively at DLR Stuttgart. Measurements were performed for a so-called “stable” case and for a case with significant thermoacoustic instabilities. The CARS temperature measurements are in good agreement with previous single-shot Raman scattering measurements in the same flame. A microphone was used to record pressure pulsations in the burner. Simultaneous acoustic measurements enabled phase-synchronization of the fs CARS measurements with the thermo-acoustic pulsations in the burner. The rapid accumulation of statistically-converged datasets also supported a phase conditioned statistical analysis to study the time-evolving thermo-chemical state over the course of a thermoacoustic cycle. The CARS measurements are described in P1 and in a pair of articles accepted for publication in Combustion and Flame.

The measurements in the DLR burner were quite successful in that on virtually every laser shot the signal level was high enough and the signal was clean enough such that a temperature could be determined by least squares fitting of theoretical spectra to the experimental spectra. However, in regions of the burner where cold gas pockets were present the CARS signal was high enough to saturate the EMCCD detector. To address this problem we borrowed a spectrometer and EMCCD camera

from Andor and set up a two-channel detection system featuring a 90%T/10%R beamsplitter as shown in Fig. 2. When the gas in the CARS probe volume was hot ( $>1000\text{K}$ ), the signal in detection channel 1 was analyzed to determine the temperature. When the gas in the CARS probe volume was cold ( $<1000\text{K}$ ), the signal in detection channel 2 was analyzed to determine the temperature. The experimental system and measurements in a hydrogen jet diffusion flame are discussed in paper P2. As discussed above, the measurements discussed in paper P2 were performed with equipment borrowed from Andor Corp. to test the system, and thanks to supplemental funding from this program we have now bought the needed EMCCD camera and spectrometer and have set up the two-channel detection system on a permanent basis.

We have also begun to perform CPP fs CARS measurements of fuel species. We performed measurements of methane, ethylene, and propane, and mixtures of these gases at room temperature for a range of pressures up to 8 bars. We developed a model for methane and we were able to simulate the room temperature spectra from pure methane and methane/nitrogen mixtures very well. We will continue fs CARS measurements of species such as methane, ethylene, and propane in a newly developed high-temperature, high-pressure gas cell.

### B. Development of a New High-Pressure, High-Temperature Gas Cell

During the last year we designed and fabricated a new high-temperature, high-pressure gas cell. The gas cell is depicted schematically in Fig. 3. The gas cell tube and inner flanges are fabricated from Hastelloy and is electrically heated over the central portion of the Hastelloy tube. The stainless steel window flanges are water-cooled to enable the use of elastomeric O-rings for pressure sealing. The gas cell is designed for point measurements at the center so a significant temperature gradient between the center and ends of the cell will exist. Convective flow due to the temperature gradient will be minimized using interior baffles. The cell is designed for a maximum pressure of 30 bars at the maximum center temperature of 1000 K.

### III. Future Work

We will continue to perform fs CARS experiments in our laboratory using the Coherent ultrafast laser system. Our studies of temperature measurements using CPP fs CARS will continue. We continue to investigate the effect of laser system parameters on the CPP fs CARS spectrum to improve the temperature accuracy of the technique. We will explore the potential for using CPP fs CARS for accurate concentration measurements for hydrocarbon species and other polyatomic molecules, a very hard species to measure using ns CARS. We will make full use of the high-temperature, high-pressure

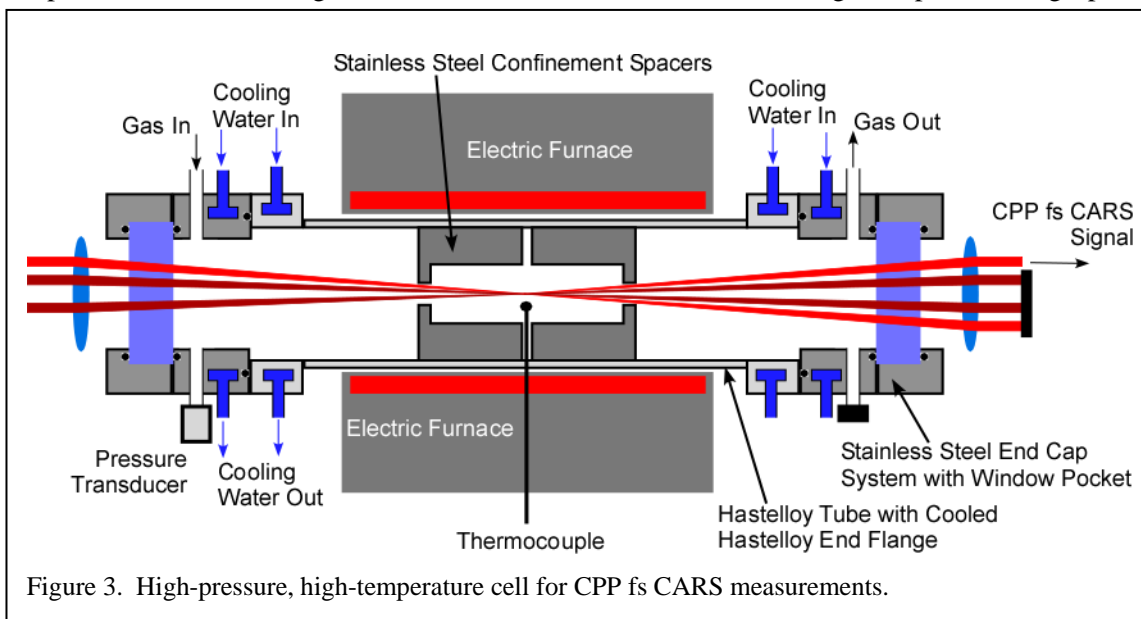


Figure 3. High-pressure, high-temperature cell for CPP fs CARS measurements.

gas cell that we have fabricated for fundamental studies of the effects of temperature and pressure on fs CARS measurements of temperature and species concentrations. We are also working with Prof. Carlo Scalo of our department to parallelize the fs CARS density matrix codes and run them on the Purdue supercomputer.

Our investigation of the physics of single-photon, two-color PS for species such as NO will continue. We have developed a new experimental apparatus for these measurements and collected extensive line shape and concentration data for atomic hydrogen, and are in the process of investigating collision-induced resonances for two-color PS of NO. We will be able to explore collisional effects on the PS and 6WM processes in much more detail using the two-dye laser system that we are currently setting up. We will continue to use the density matrix code to gain insight into the physics of the PS and 6WM processes.

In the past year we have begun to perform measurements using combined the two-beam pure rotational CARS and a three-laser, dual-pump vibrational CARS system. We have been measuring CO<sub>2</sub>, N<sub>2</sub>, and O<sub>2</sub> with the dual-pump vibrational CARS system in lean premixed methane/air pilot-stabilized flames. This work will continue throughout the next year and we will switch narrowband dye laser wavelengths for simultaneous dual-pump CARS measurements of H<sub>2</sub> and N<sub>2</sub>.

#### **IV. Refereed publications and submitted journal articles supported by this project 2014-2016**

- P1. C. N. Dennis, C. D. Slabaugh, I. G. Boxx, W. Meier, R. P. Lucht, "Femtosecond Coherent Anti-Stokes Raman Scattering Thermometry at 5 kHz in a Gas Turbine Model Combustor," *Proceedings of the Combustion Institute* **35**, 3731-3738 (2015). DOI: 10.1016/j.proci.2014.06.063
- P2. C. N. Dennis, A. Satija, and R. P. Lucht, "High Dynamic Range Thermometry at 5 kHz in Hydrogen-Air Diffusion Flame using Chirped-Probe-Pulse Femtosecond Coherent Anti-Stokes Raman Scattering," *Journal of Raman Spectroscopy* **47**, 177-188 (2016). DOI: 10.1002/jrs.4773
- P3. C. N. Dennis, C. D. Slabaugh, I. G. Boxx, W. Meier, and R. P. Lucht, "5 kHz Thermometry in a Swirl-Stabilized Gas Turbine Model Combustor using Chirped Probe Pulse Femtosecond CARS. Part 1: Temporally Resolved Swirl-Flame Thermometry," *Combustion and Flame*, accepted for publication (2016).
- P4. C. D. Slabaugh, C. N. Dennis, I. G. Boxx, W. Meier, and R. P. Lucht, "5 kHz Thermometry in a Swirl-Stabilized Gas Turbine Model Combustor using Chirped Probe Pulse Femtosecond CARS. Part 2: Analysis of Swirl Flame Dynamics," *Combustion and Flame*, accepted for publication (2016).

#### **V. PhD theses completed by students supported by this project 2014-2016**

- T1. Claresta N. Dennis, "Applications of Femtosecond Coherent Anti-Stokes Raman Scattering in Combustion," **Ph.D. Thesis**, Purdue University, West Lafayette, December 2014.

# Particle Diagnostics Development

H. A. Michelsen

Sandia National Labs, MS 9055, P. O. Box 969, Livermore, CA 94551

hamiche@sandia.gov

## I. Program Scope

Combustion processes often produce solid carbon particles, i.e., soot. These particles may be oxidized to form gas-phase species or released into the exhaust stream, where they can be coated with liquid coatings. These coatings can be comprised of any of a number of components, including unburned fuel, lube oil, sulfuric acid, water, and other combustion by-products.<sup>1</sup> The research program described here focuses on the development and use of diagnostics for soot particles in combustion environments and combustion exhaust plumes. The goal of this work is *in situ* measurements of volume fraction, size, composition, and morphology of combustion-generated particles with fast time response and high sensitivity. Measurement techniques are targeted for studies of soot formation and evolution and must be versatile enough to probe particles throughout their entire life cycle. Techniques are being developed for detection and characterization of particles in combustion environments from incipient particles that are 2-10 nm in diameter and composed of condensed large organic species to mature soot particles composed of aggregates of carbonaceous primary particles resembling polycrystalline graphite. Diagnostics are also being developed for chemical studies of growth, pyrolysis, and oxidation within combustors and characterization of inhomogeneous particles in exhaust streams.

## II. Recent Progress

Our work has focused on developing a detailed understanding of the chemical and physical mechanisms that influence the applicability of laser-based, X-ray, and mass spectrometric techniques for soot detection and characterization under a wide range of conditions. In recent work, we have developed, refined, and applied a range of diagnostic methods to investigate the formation, evolution, and oxidation of soot in atmospheric premixed flat and laminar diffusion flames.

### A. Probing Soot Chemistry Using X-Ray and Complementary Diagnostics

Measurements of soot-particle size, morphology, fine structure, and composition form the foundation for our understanding of soot formation, graphitization, and oxidation in combustors and the basis for predictive soot-chemistry models. Numerous experimental techniques have been developed to probe the evolution of these parameters, but many of these methods involve extractive sampling, which leads to large perturbations of the chemistry under investigation. There is a need for diagnostics that can be used to characterize particles formed in the combustor without resorting to extractive sampling. We have initiated a collaboration with Drs. Jon Lee and Tony Van Buuren (LLNL) to exploit X-ray techniques for *in situ* measurements of soot physical and chemical characteristics. We are using Small-Angle X-ray Scattering (SAXS) for particle size, Wide-Angle X-ray Scattering (WAXS) for particle fine structure, and spontaneous X-ray Raman Spectroscopy (XRS) for particle composition information. We are coupling these *in situ* X-ray diagnostics with complementary *in situ* laser diagnostics, such as Laser-Induced Incandescence (LII), extinction, and scattering, and *ex situ* X-ray, laser, and imaging diagnostics, such as Scanning Mobility Particle Sizer (SMPS) measurements for particle size, Transmission Electron Microscopy (TEM) for particle fine structure, and X-ray Photoelectron Spectroscopy (XPS), Near-Edge X-ray Absorption Fine-structure Spectroscopy (NEXAFS), Raman Microscopy (RM), and Aerosol Mass Spectrometry (AMS) for particle composition information. We are also collaborating with ALS beamline scientists Drs. Zhu, Hexemer, and Schaible for SAXS/WAXS, Stanford Synchrotron Radiation Lightsource (SSRL) beamline scientists Drs. Weng, Nordlund, Sokaras, and Kroll for XRS and NEXAFS, and our Sandia colleague Dr. Farid El Gabaly for XPS and RM.

We have designed and built several burners to study soot formation, graphitization, and oxidation under premixed and diffusion-controlled conditions. These burners were designed for compatibility with X-ray diagnostics, given constraints of synchrotron hutch, beam, and detector configurations. We have recorded XRS spectra *in situ* in an ethylene-fueled premixed flat flame produced by a mini-McKenna burner, a smaller version of a common research burner and in a partially premixed laminar diffusion flame produced by a linear Hencken burner.<sup>2</sup> The spectra were recorded at the carbon K edge and demonstrate features indicative of aromatic hydrocarbons. These spectra were recorded on Beamline 6-2

at the SSRL using the Si(111) monochromator, which delivers photons at  $\sim 6.5$  keV with a flux of  $2 \times 10^{13}$  photons/s and energy resolution of 0.85 eV.<sup>3</sup> The detector was a Johann-type crystal spectrometer with 40 spherically bent and diced Si(110) crystals positioned on a 1-m Rowland circle and subtending a solid angle of 1.9% of  $4\pi$  sr.<sup>3</sup> The signal was recorded on a silicon drift detector that was used to reduce background by spectrally discriminating against diffuse scatter. Because both the incident beam and signal were in the hard X-ray regime, the experiment could be performed at atmospheric pressure without excessive loss of signal. The photon energy of the incident beam was scanned, and the detection wavelength was fixed. The transition energy is recorded as the energy difference between the incident and detected photons. A photograph of the setup is shown in Fig. 1.

The most striking features in the spectra are those attributable to gas-phase CO and CO<sub>2</sub> in the flame. This result is similar to the measurements of NEXAFS spectra recorded in a low-pressure methane diffusion flame by Frank et al.<sup>4</sup> In the premixed flame, oxygen is consumed within the first 2 mm above the burner, such that there is no oxygen available to convert hydrocarbons to CO or CO to CO<sub>2</sub>. The feature corresponding to CO and CO<sub>2</sub> are constant with increasing height above the burner (HAB) above 2 mm. The underlying features of the soot particles and precursors are difficult to discern in these spectra, but there is some evidence of aromatic hydrocarbons at  $\sim 287$  eV, in the shoulder of the CO peak. This small  $\pi^*$  peak is evidence of soot or polycyclic aromatic hydrocarbons (PAHs) and is also nearly constant as a function of HAB. In contrast, in the diffusion flame, CO and CO<sub>2</sub> increase and shift towards CO<sub>2</sub> with increasing HAB as the combustion moves toward completion. In this burner the  $\pi^*$  peak is more pronounced low in the flame but decreases with increasing HAB until it disappears.

Functional group information can also be derived from XPS spectra. We recorded XPS spectra at the oxygen K edge to aid in the identification of oxygen functional groups on the surfaces of particles extracted from the premixed flat flame used for the XRS experiments. Although the XRS spectra change little with HAB, the XPS results indicate a change in the composition of the particles with position in the flame. In particular, low in the flame hydroxyl functional groups are more prevalent than they are higher in the flame, and ether groups appear to increase in prevalence with increasing height in the flame. We have combined these results with AMS measurements and simulations to develop an understanding of the role of oxygenated species in soot precursor chemistry (see below).

We have also measured small-angle X-ray scattering (SAXS) from particles in these flames in order to derive size distributions of particles without extractive sampling. A photograph of the setup is shown in Fig. 2. Analysis of the results is still in progress. These results are being coupled with *ex situ* measurements using TEM and SMPS and *in situ* measurements using LII, laser extinction, and laser scattering.

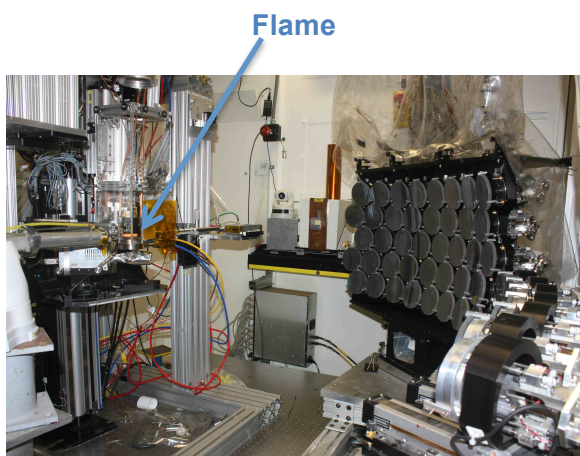


Figure 1. Photo of X-ray Raman setup at SSRL Beamline 6-2. The premixed flat flame is shown in the path of the X-ray beam, as indicated. The Johann-type crystal spectrometer is shown on the right. The drift detector is below the burner. The beam enters the hutch on the left.

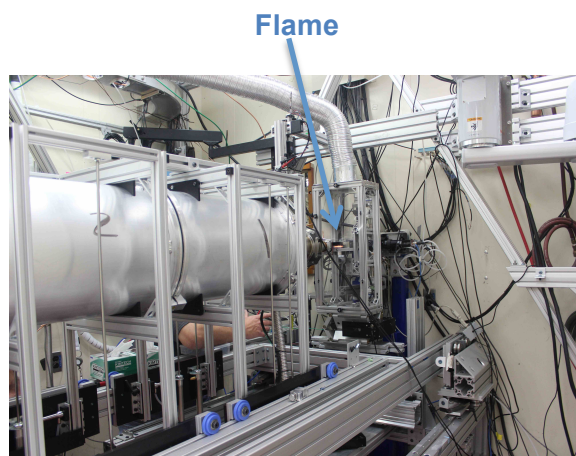


Figure 2. Photo of small-angle X-ray scattering setup at ALS Beamline 7.3.3. The premixed flat flame is shown in the path of the X-ray beam, as indicated. The detector is on the left, and the beam enters the hutch on the other side of the flame.

## B. Gaining Insight into Soot Formation through Measurements and Simulations

We are also working on a SISGR project led by Prof. Angela Violi (University of Michigan) to develop a validated predictive multiscale model to describe the chemical composition of soot nanoparticles in premixed and diffusion flames. This project closely couples experimental investigations of soot precursors and incipient particle characteristics with the development of a predictive model for the chemical composition of soot nanoparticles. The co-investigators on the project are Prof. Angela Violi for model development, Dr. Nils Hansen (Sandia) for mass spectrometry of gas-phase species, and Dr. Hope Michelsen (Sandia), in collaboration with Dr. Kevin Wilson (LBNL ALS), for aerosol mass spectrometry, coupled with other techniques for particle composition, size, and morphology measurements.

This project uses *ab initio* and probabilistic computational techniques to identify low-barrier reaction mechanisms for the formation of soot precursors and online vacuum-ultraviolet photoionization aerosol mass spectrometry and other techniques to confirm model predictions. Example VUV-AMS mass spectra are shown in Fig. 3 for soot samples extracted from the premixed flat flame described above and a counter-flow diffusion flame.

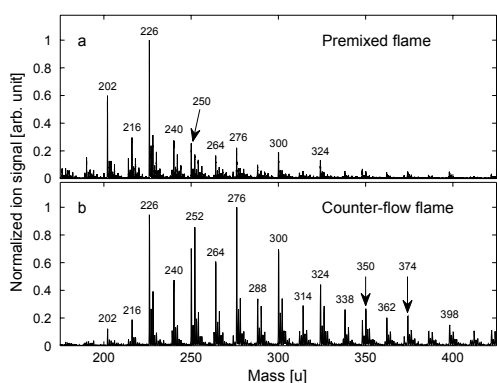


Figure 3. Aerosol mass spectra recorded at (a) an HAB of 3.4 mm in the premixed flat flame and (b) a distance from the fuel outlet of 3.0 mm in the counter-flow diffusion flame. This figure is reproduced from Johansson et al.<sup>5</sup>

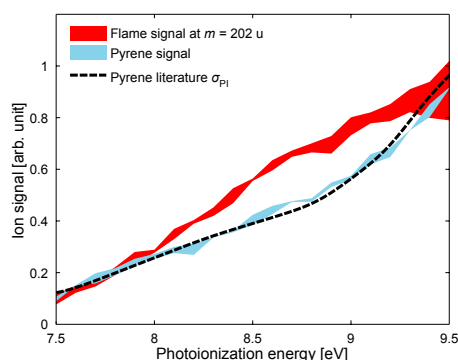


Figure 2. The red curve shows the lower and upper bounds of four separate PIE scans of the mass peak at 202 u at several HABs in the premixed flat flame. The blue curve displays the bounds for two PIE scans performed on pyrene. The dashed black shows the shape of the pyrene photoionization cross section ( $\sigma_{PI}$ ) obtained from Verstraete et al.<sup>6</sup> This figure is reproduced from Johansson et al.<sup>5</sup>

The mass at 202 u is often assumed to be the stabilomer pyrene. Figure 4 shows the ion yield at mass 202 u as a function of the VUV photon energy compared with similar measurements of the photoionization efficiency (PIE) curve for pyrene.<sup>5</sup> The disagreement between the two measurements indicates that the peak at 202 u is not solely attributable to pyrene. Our computational results suggest that pyrene is a relatively minor contributor at mass 202 u in our flame and that 86% of mass 202-u species contain at least one 5-membered ring and are products of the growth trajectories of acenaphthalene.<sup>5</sup> We have also investigated the roles of oxygenated species and radical-radical reactions in soot and soot-precursor formation.<sup>5,7</sup>

## III. Future Work

Future work will refine and expand on the X-ray measurements described above. We will continue to develop laser-based diagnostics that can be used to probe particle size, morphology, and composition and apply these *in situ* diagnostics to study soot evolution and oxidation in flames. These diagnostics will be complemented by *ex situ* diagnostics, such as AMS, TEM, and SMPS, making an effort to deploy all of these diagnostics on selected combustion systems. Our goal is to eventually apply these diagnostics to combustion systems at higher pressure with an emphasis on working with the modeling community to facilitate model development and validation.

#### IV. References

1. (a) Kittelson, D. B., Engines and nanoparticles: A review. *J. Aerosol Sci.* **1998**, *29* (5/6), 575-588; (b) Lighty, J. S.; Veranth, J. M.; Sarofim, A. F., Combustion aerosols: Factors governing their size and composition and implications for human health. *J. Air Waste Manage. Assoc.* **2000**, *50* (9), 1565-1618.
2. Campbell, M. F.; Bohlin, A.; Schrader, P. E.; Bambha, R. P.; Kliewer, C. J.; Johansson, B.; Michelsen, H. A., Design and characterization of a linear Hencken-type burner. *Rev. Sci. Instrum.* **2016**, submitted.
3. Sokaras, D.; Nordlund, D.; Weng, T.-C.; Alonso Mori, R.; Velikov, P.; Wenger, D.; Garachtchenko, A.; George, M.; Borzenets, V.; Johnson, B.; Qian, Q.; Rabedeau, T.; Bergmann, U., A high resolution and large solid angle x-ray Raman spectroscopy end-station at the Stanford Synchrotron Radiation Lightsource. *Rev. Sci. Instrum.* **2012**, *83*, 043112.
4. Frank, J. H.; Shavorskiy, A.; Bluhm, H.; Coriton, B.; Huang, E.; Osborn, D. L., In situ soft X-ray absorption spectroscopy of flames. *Appl. Phys. B* **2014**, *117*, 493-499.
5. Johansson, K. O.; Dillstrom, T.; Elvati, P.; Campbell, M. F.; Schrader, P. E.; Popolan-Vaida, D. M.; Hendersen-Richards, N. K.; Wilson, K. R.; Violi, A.; Michelsen, H. A., Radical-radical reactions, pyrene nucleation, and incipient soot formation in combustion. *Proc. Combust. Inst.* **2016**, submitted.
6. Verstraete, L.; Léger, A.; d'Hendecourt, L.; Défourneau, D.; Dutuit, O., Ionization cross-section measurements for two PAH molecules: Implications for the heating of diffuse interstellar gas. *Astron. Astrophys.* **1990**, *237*, 436-444.
7. Johansson, K. O.; Dillstrom, T.; Monti, M.; El Gabaly, F.; Campbell, M. F.; Schrader, P. E.; Popolan-Vaida, D. M.; Richards-Henderson, N. K.; Wilson, K. R.; Violi, A.; Michelsen, H. A., Toxins, carcinogens, fire, and soot: Explaining large furan and oxygenated hydrocarbon formation in flames. *Proc. Natl. Acad. Sci. U. S. A.* **2016**, submitted.

#### V. Publications and submitted journal articles supported by this project 2014-2016

1. M. F. Campbell, A. Bohlin, P. E. Schrader, R. P. Bambha, C. J. Kliewer, K. O. Johansson, and H. A. Michelsen, "Design and characterization of a linear Hencken-type burner", *Rev. Sci. Instrum.*, submitted (2016).
2. K. O. Johansson, T. Dillstrom, M. F. Campbell, M. Monti, F. El Gabaly, P. E. Schrader, D. M. Popolan-Vaida, N. K. Richards-Henderson, K. R. Wilson, A. Violi, and H. A. Michelsen, "Toxins, carcinogens, fire, and soot: Explaining large furan and oxygenated hydrocarbon formation and emission from flames", *Proc. Natl. Acad. Sci. USA*, submitted (2016).
3. H. A. Michelsen, "Probing soot formation, chemical and physical evolution, and oxidation: A review of diagnostic techniques and needs", *Proc. Combust. Inst.*, submitted (2016).
4. K. O. Johansson, T. Dillstrom, P. Elvati, M. F. Campbell, P. E. Schrader, D. M. Popolan-Vaida, N. K. Richards-Henderson, K. R. Wilson, A. Violi, and H. A. Michelsen, "Radical-radical reactions, pyrene nucleation, and incipient soot formation in combustion", *Proc. Combust. Inst.*, submitted (2016).
5. R. P. Bambha and H. A. Michelsen, "Effects of aggregate morphology and size on laser-induced incandescence and scattering from black carbon (mature soot)", *J. Aerosol Sci.* **88**, 159-181 (2015).
6. H. A. Michelsen, C. Schulz, G. J. Smallwood, and S. Will, "Laser-induced incandescence: Particulate diagnostics for combustion, atmospheric, and industrial applications", *Progress Energy Combust. Sci.* **51**, 2-48 (2015).
7. K. O. Johansson, J. Y. W. Lai, S. A. Skeen, K. R. Wilson, N. Hansen, A. Violi, and H. A. Michelsen, "Soot precursor formation and limitations of the stablomer grid", *Proc. Combust. Inst.* **35**, 1819-1826 (2015).
8. A. Nanthaamornphong, K. Morris, D. W. I. Rouson, and H. A. Michelsen, "A case study: Agile development in the Community Laser-Induced Incandescence Modeling Environment (CLiME)", *Comput. Sci. Eng.* **16(3)**, 36-46 (2014).
9. X. López-Yglesias, P. E. Schrader, and H. A. Michelsen, "Effects of soot maturity on its absorption cross section and thermal-accommodation coefficient", *J. Aerosol Sci.* **75**, 43-64 (2014).
10. N. Hansen, S. A. Skeen, H. A. Michelsen, K. R. Wilson, and K. Kohse-Höinghaus, "Flame experiments at the Advanced Light Source: New insights into soot formation processes", *Journal of Visualized Experiments (JoVE)* **87**, e51369 (2014).

# Reaction Dynamics in Polyatomic Molecular Systems

William H. Miller

Department of Chemistry, University of California, and  
Chemical Sciences Division, Lawrence Berkeley National Laboratory  
Berkeley, California 94720-1460  
millerwh@berkeley.edu

## I. Program Scope

The goal of this program is the development of theoretical methods and models for describing the dynamics of chemical reactions, with specific interest for application to polyatomic molecular systems of special interest and relevance. There is interest in developing the most rigorous possible theoretical approaches and also in more approximate treatments that are more readily applicable to complex systems.

## II. Recent Progress

Effort in earlier years focused on developing *semiclassical* (SC) theory<sup>1-3</sup> into a practical way for adding quantum mechanical effects to classical molecular dynamics (MD) simulations, which are so ubiquitously applied to all types of dynamical processes in complex molecular systems, e.g., chemical reactions in clusters, nano-structures, molecules on or in solids, bio-molecular systems, etc. More recently, however, we have been exploring how successful even simpler, *purely classical* MD approaches can be (with some judicious SC ideas incorporated), especially for the important case of *electronically non-adiabatic processes*, i.e., those which involve transitions between different electronic states. The two essential ingredients to the approach, (a) how are the electronic degrees of freedom described within a classical mechanics framework, and (b) how one identifies specific electronic states (initially and finally) within a classical picture.

The Meyer-Miller (MM) classical vibronic Hamiltonian<sup>4</sup> maps the electronic degrees of freedom (DOF) of a coupled electronic-nuclear system onto a set of classical harmonic oscillators, each oscillator representing the occupation of the various electronic states. Since the electronic as well as the nuclear DOF are thus described classically, a standard classical MD simulation treats these DOF and their interaction dynamically consistently (albeit at the level of classical mechanics). (If all these DOF were treated quantum mechanically, the MM Hamiltonian becomes a representation of the exact QM *operator* and would thus provide the exact QM vibronic dynamics.) In a recent series of papers, a symmetrical quasi-classical (SQC) windowing methodology<sup>5</sup> has been described and applied to the MM Hamiltonian in order to “quantize” these electronic DOF both initially and finally<sup>6</sup>. It was found that this approach provides a very reasonable description of non-adiabatic dynamics exhibited in a suite of standard benchmark model problems for which exact quantum mechanical (QM) results are available for comparison. Among the examples were systems exhibiting strong quantum coherence effects and systems representative of condensed-phase non-adiabatic dynamics, including some which other simple approaches have difficulty in describing

correctly (e.g., the asymmetric spin-boson problem<sup>6</sup> and the inverted regime in electron transfer processes<sup>7</sup>).

It was also discussed in these recent papers how various aspects of the SQC/MM model are appealing from a theoretical perspective<sup>8</sup>: e.g., it has a straightforward theoretical justification, and by providing an equivalent treatment of the electronic and the nuclear DOF (i.e., via classical mechanics) it is able to describe “quantum” coherence and de-coherence without resorting to any “add ons” to the theory. The (classical) time evolution of the nuclear and electronic DOF is continuous at all times (as it is QM'ly), and it gives equivalent results whether implemented in adiabatic or diabatic representations. It was also emphasized that though the equations of motion that result from the MM Hamiltonian are “Ehrenfest” — in that the force on the nuclei at any time is the coherent average of that over all electronic states — the fact that zero point energy is included in the electronic oscillators means that there is an ensemble of trajectories for each initial state (rather than only one trajectory as in the “Ehrenfest method” itself), and the population of each final electronic state is determined by the fraction of that ensemble that end up in that state. I.e., each trajectory in this ensemble contributes to only one final electronic state. The approach thus does not suffer from the well-known “Ehrenfest disease” of having all final electronic states determined by one (average) nuclear trajectory. As a result, the SQC method of quantizing the electronic DOF initially and finally leads to detailed balance being described correctly<sup>9</sup>. From a practical perspective, the SQC/MM is attractive since it is trajectory-based and can be straightforwardly incorporated within the framework of a standard classical MD simulation. One has only to add one vibrational-like DOF for each electronic state, which are propagated along with the (perhaps very many) nuclear DOF via Hamilton's equations that result from the MM Hamiltonian.

Shown below are results from the most recent applications of the SQC/MM approach to the treatment of so-called “site-exciton” non-adiabatic models, which are frequently used to simulate photo-induced electronic excitation transfer in light-harvesting pigment complexes. The first set of examples treat a 2-state model, which is shown simulated over the same 8 parameter regimes used by Ishizaki and Flemming (in their original paper<sup>10</sup>) to develop the hierarchical equations of motion (HEOM) method (which should be essentially exact for the thermal bath model employed in these systems). The plots below show that the SQC/MM-simulated decay of the initial electronic excitation agree remarkably well with the HEOM results over all 8 parameter regimes considered. Noteworthy here is that, although the HEOM technique is used as a reliable benchmark for validation, the atomistic/trajectory-based nature of the SQC/MM approach makes it more generally applicable than the HEOM technique since it can be applied to more realistic harmonic (or even anharmonic) bath models, thus having the potential to more accurately model excitation transfer dynamics in complex environments.

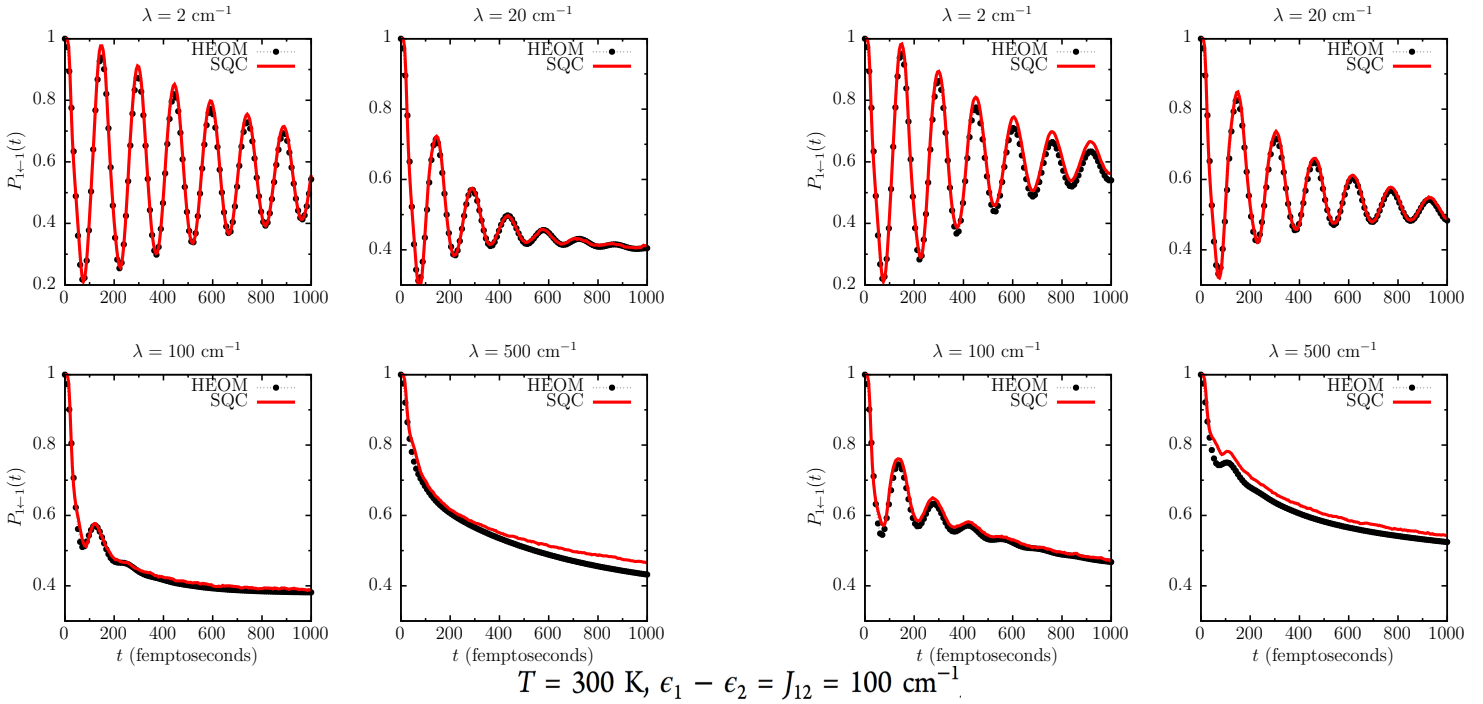
Also shown below are the results of applying the SQC/MM approach to a more challenging 7-state model<sup>11</sup> of the well-known Fenna-Mathews-Olson (FMO) pigment complex. Of the examples below, one calculation corresponds to an initial localization of the electronic excitation on pigment 1, and the other on pigment 6. For both, the SQC/MM result is shown

(left) contrasted with the benchmark HEOM calculation (right). Though there are some differences (notably some population bleed out of initial state 1 at long-time in the first example), the agreement is in general quite good—for instance, in both examples capturing (reasonably quantitatively) the transfer of the electronic excitation (from either initial pigment site 1 or 6) through the pigment complex to sites 3 and 4.

## 2-Pigment Site-Exciton Model

$$\omega_c = 53.08 \text{ cm}^{-1}$$

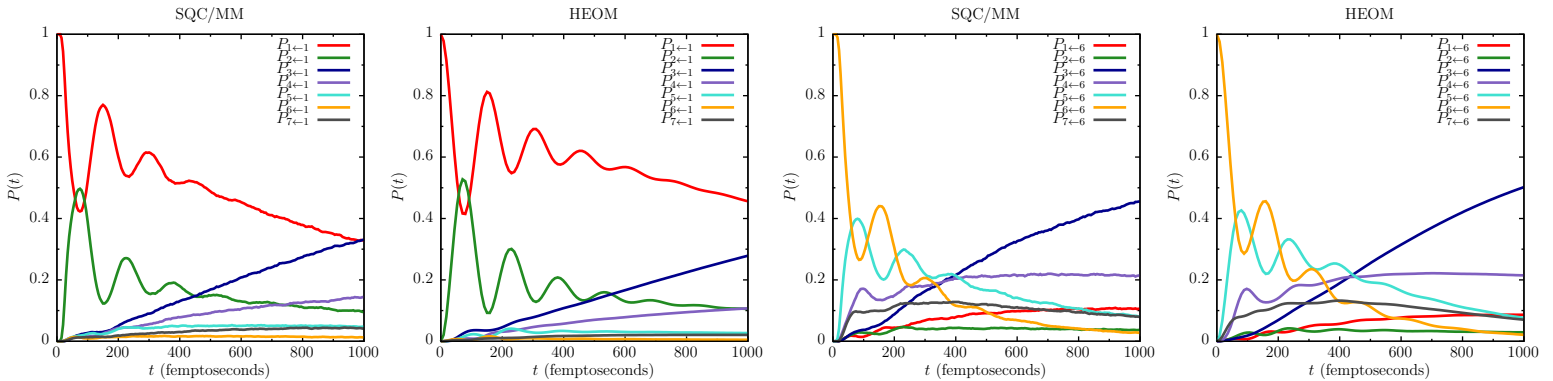
$$\omega_c = 10.61 \text{ cm}^{-1}$$



## 7-Pigment Site FMO Model

### Pigment Site 1 Initialization

### Pigment Site 6 Initialization



### III. Future Plans

Since this quasi-classical model has proved quite reliable for describing electronically non-adiabatic dynamics in these simple model problems, work is in progress to extend its application to more general and complex non-adiabatic processes.

## References

1. For reviews, see W. H. Miller, *Adv. Chem. Phys.* **25**, 69-177 (1974); **30**, 77-136 (1975).
2. W. H. Miller, *J. Chem. Phys.* **53**, 1949-1959 (1970).
3. For reviews, see W. H. Miller, (a) *J. Phys. Chem. A* **105**, 2942-2955 (2001); (b) *Proc. Natl. Acad. Sci. USA* **102**, 6660-6664 (2005); (c) *J. Chem. Phys.* **125**, 132305.1-8 (2006).
4. H. D. Meyer and W. H. Miller, *J. Chem. Phys.* **71**, 2156-2169 (1979).
5. S. J. Cotton and W. H. Miller, *J. Phys. Chem. A* **117**, 7190-7194 (2013).
6. S. J. Cotton and W. H. Miller, *J. Chem. Phys.* **139**, 234112.1-9 (2013).
7. S. J. Cotton, K. Igumenshchev and W. H. Miller, *J. Chem. Phys.* **141**, 084104.1-14 (2014).
8. S. J. Cotton and W. H. Miller, *J. Phys. Chem. A* **119**, 12138-12145 (2015).
9. W. H. Miller and S. J. Cotton, *J. Chem. Phys.* **142**, 131103.1-3 (2015).
10. A. Ishizaki and G. R. Fleming, *J. Chem. Phys.* **130**, 23411 (2009).
11. A. Ishizaki and G. R. Fleming, *Proc. Natl. Acad. Sci. USA* **106**, 17255-17260 (2009).

## IV. 2013 - 2015 DOE Publications

1. B. Li, T. J. Levy, D. W. H. Swenson, E. Rabani and W. H. Miller, A Cartesian Quasi-Classical Model to Nonequilibrium Quantum Transport: The Anderson Impurity Model, *J. Chem. Phys.* **138**, 104110.1-6 (2013).
2. G. Tao and W. H. Miller, Time-Dependent Important Sampling in Semiclassical Initial Value Representation Calculations or Time Correlation Functions. III. A State-Resolved Implementation to Electronically Non-Adiabatic Dynamics, *Mol. Phys.* **111**, 1987-1993 (2013).
3. S. J. Cotton and W. H. Miller, Symmetrical Windowing for Quantum States in Quasi-Classical Trajectory Simulations, *J. Phys. Chem. A* **117**, 7190-7194 (2013).
4. S. J. Cotton and W. H. Miller, Symmetrical Windowing for Quantum States in Quasi-Classical Trajectory Simulations: Application to Electronically Non-Adiabatic Processes, *J. Chem. Phys.* **139**, 234112.1-9 (2013).
5. W. H. Miller, A Journey Through Chemical Dynamics, *Annu. Rev. Phys. Chem.* **65**, 1-19 (2014).
6. B. Li, E. Y. Wilner, M. Thoss, E. Rabani and W. H. Miller, A Quasi-Classical Mapping Approach to Vibrationally Coupled Electron Transport in Molecular Junctions, *J. Chem. Phys.* **140**, 104110.1-7 (2014).
6. B. Li, W. H. Miller, T. J. Levy and E. Rabani, Classical Mapping for Hubbard Operators: Application to the Double-Anderson Model, *J. Chem. Phys.* **140**, 204106.1-7 (2014).
8. S. J. Cotton, K. Igumenshchev and W. H. Miller, Symmetrical Windowing for Quantum States in Quasi-Classical Trajectory Simulations: Application to Electron Transfer, *J. Chem. Phys.* **141**, 084104.1-14 (2014).
9. W. H. Miller and S. J. Cotton, Communication: Note on Detailed Balance in Symmetrical Quasi-Classical Models for Electronically Non-Adiabatic Dynamics, *J. Chem. Phys.* **142**, 131103.1-3 (2015).
10. S. J. Cotton and W. H. Miller, A Symmetrical Quasi-Classical Spin-Mapping Model for the Electronic Degrees of Freedom in Non-Adiabatic Processes, *J. Phys. Chem. A* **119**, 12138-12145 (2015).
11. S. J. Cotton and W. H. Miller, The Symmetrical Quasi-Classical Model for Electronically Non-Adiabatic Processes Applied to Energy Transfer Dynamics in Site-Exciton Models of Light-Harvesting Complexes, *J. Chem. Theory Comput.* (in press).

## Dynamics of Activated Molecules

Amy S. Mullin

Department of Chemistry and Biochemistry, University of Maryland

College Park, MD 20742

mullin@umd.edu

### I. Program Scope

The focus of my program is to investigate the microscopic mechanisms of collisional energy transfer for molecules with large amounts of internal energy. Collisional energy transfer is ubiquitous in gas-phase chemistry and affects reaction rates and branching ratios. This is particularly true for high energy molecules that are more likely to undergo chemical transformations. Currently, there are no first-principle theories of energy transfer between high energy molecules and polyatomic collision partners. A lack of fundamental knowledge results in insufficient treatments in reactive models. One goal of this research is to gain new insights into the behavior of relatively large complex molecules at high energy as they undergo quenching collisions and redistribute their energy. These data provide important benchmarks for developing new models that account for energy partitioning in molecular collisions.

We use state-resolved transient IR absorption spectroscopy to characterize the pathways responsible for the collisional relaxation of high energy molecules. Direct probing of high energy molecules is challenging due to their transient nature, poorly defined spectral signatures and high state densities. Our approach is to develop a molecular level understanding by focusing instead on the small energy-accepting bath molecules that undergo collisions with high energy molecules. We measure time-resolved population changes for individual ro-vibrational states that are induced by collisions and characterize their nascent translational energy distributions by measuring time-resolved Doppler-broadened line profiles. With this approach, we have performed a number of in-depth spectroscopic studies that provide a greater understanding of high energy molecules and their collisional energy transfer.

Two major advances have revolutionized our ability to study collisional energy transfer. About a decade ago, we developed the means to measure the transient behavior for the **full range** of rotational states for the scattered molecules.[1] Previously, energy transfer studies of this type were limited to high energy quantum states, thereby giving information just about the dynamics of the “strongest” collisions that correspond to the high-energy tail of the energy transfer distribution function. Now, we have eyes to see the nascent outcome of so-called “weak” collisions, from which we characterize the **entire energy transfer distribution** with unprecedented detail. The second major advance is the addition of two new IR light sources, a quantum cascade laser and a mid-IR OPO, that enable our measurements by virtue of their high output powers, high spectral resolution, and broad wavelength tunability.[2]

We have incorporated the new IR sources into our transient absorption spectrometers and used these instruments to investigate the state-resolved collision dynamics of a number of energy-accepting molecules including of HCl, methane (CH<sub>4</sub>) and most recently ammonia (NH<sub>3</sub>). A goal of this research is to identify the mechanisms by which different bath molecules remove energy from highly vibrationally excited molecules through collisions. For many of these studies we have used pyrazine (C<sub>4</sub>H<sub>4</sub>N<sub>2</sub>, E=38000 cm<sup>-1</sup>) as a prototype high energy molecule because of its favorable radiationless decay properties following λ=266 nm excitation. We have already characterized energy transfer from pyrazine(E) to H<sub>2</sub>O, HOD, CO<sub>2</sub> and DCl using state-resolved probing.[3-8] Our data on this combination of molecular bath gases will enable us to make direct comparisons as to how molecular structure impacts the quenching of high energy molecules from a fundamental perspective.

In the past year, we have focused our efforts on investigating the energy transfer pathways for collisions of ammonia and pyrazine(E). We first developed the necessary tools and expertise for performing transient IR measurements of ammonia using our mid-IR OPO-based transient absorption spectrometer. We then measured transient Doppler-broadened line profiles for rotational states up to

$J=22$  in the ground vibrationless state of ammonia. So far, we have found that the vibration-to-rotation/translation (V-RT) energy transfer pathway is the most probable relaxation channel. In contrast, collisions that lead to vibrational excitation of the bath (through a V-V pathway) have smaller cross sections. In the work described below, we have investigated the V-RT channel for pyrazine(E)/ammonia by measuring the translational and rotational energy distributions of the scattered ammonia in  $v=0$ , the energy transfer rate constants, and the energy transfer distribution function.

## II. Recent Progress

### A. High-resolution transient IR detection of ammonia

Ammonia has two strong absorption bands in the IR that we have used for high-resolution transient probing: the  $\nu_3$  stretch at  $3.0\ \mu\text{m}$  and the  $\nu_1$  stretch at  $2.9\ \mu\text{m}$ , as shown in Fig. 1a.  $\text{NH}_3$  has a pyramidal structure with  $C_{3v}$  symmetry and its rotational structure is that of a symmetric top with quantum numbers  $J$  and  $K$ .  $J$  describes total angular momentum and  $K$  is the projection of the total angular momentum along the  $C_{3v}$  symmetry axis. Values for  $K$  range from  $K=0$  to  $J$ . In addition, rotational states with  $K>0$  are split by inversion doubling and labeled with a or s symmetry.

We have performed transient IR measurements on ammonia states up to  $J=22$  following pulsed UV excitation of pyrazine at  $266\ \text{nm}$  under low pressure conditions of  $25\ \text{mTorr}$  (1:1 mixture of pyrazine and ammonia initially at  $300\ \text{K}$ ). Rapid radiationless decay ( $\tau=50\ \text{ns}$ ) results in pyrazine with a large amount of vibrational energy ( $E=38000\ \text{cm}^{-1}$ ). The average time between collisions is  $\sim 4\ \mu\text{s}$  and nascent population data is recorded at  $1\ \mu\text{s}$  following the UV pulse. Fig. 1b shows the transient IR absorption signal collected at line center for the  $J_K=1_0$  state of ammonia. This low energy state is well populated at  $300\ \text{K}$  and collisions with pyrazine(E) induce population depletion as seen by the negative-going slope. We observe scattering of ammonia into states that have higher rotational energy, such as the  $J_K=11_9$  state, where appearance is seen by the positive-going slope in Fig. 1c.

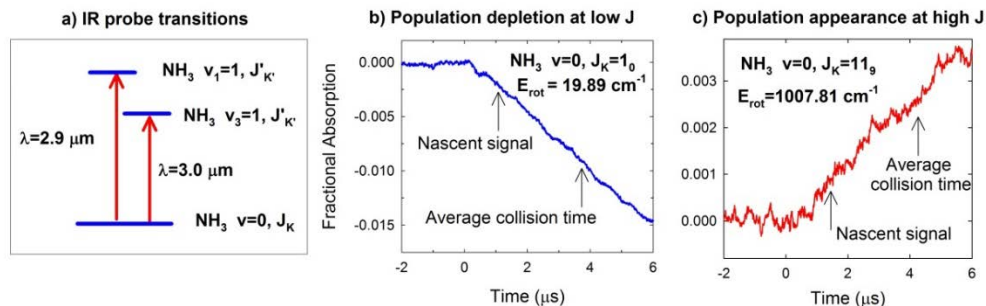


Fig. 1. a) IR probe scheme for transient measurements of  $\text{NH}_3$  ( $v=0$ ) uses  $\nu_1$  and  $\nu_3$  stretching transitions. b) Transient for  $\text{NH}_3$  ( $J_K=1_0$ ) shows population loss due to collisions with pyrazine(E). c) Transient of  $\text{NH}_3$  ( $J_K=11_9$ ) shows appearance of population.

### B. Collision dynamics of pyrazine ( $E=38000\ \text{cm}^{-1}$ ) and ammonia

Doppler-broadened transient line profiles were measured for a number of rotational states of ammonia by collecting transient absorption signals (Fig.1) as a function of IR probe wavelength. Fractional absorption signals at  $t=1\ \mu\text{s}$  for several rotational states of ammonia are plotted in Fig. 2 as a function of IR frequency shift from line center. Low energy rotational states show negative-going depletion profiles. Positive-going appearance signals grow in as the rotational energy increases. Each line profile is fit to a double Gaussian function to get amplitude and line width information for the nascent appearance and depletion populations of individual rotational states. Line widths characterize the nascent translational energy of the scattered ammonia molecules.

The energy transfer mechanism is revealed by the translational and rotational energy distributions. We find that the relative translational energy resulting from pyrazine(E)/ammonia collisions is relatively

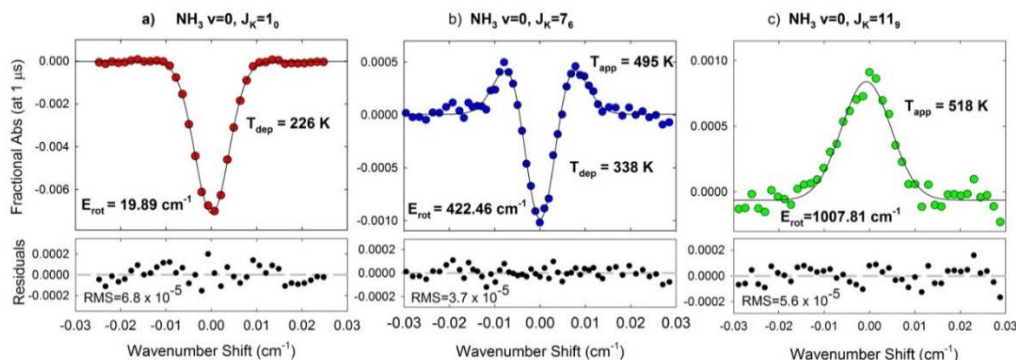


Fig. 2. Nascent Doppler-broadened line profiles for several  $J_K$  states of  $\text{NH}_3$  ( $v=0$ ) scattered from pyrazine(E) measured at  $t=1 \mu\text{s}$  following excitation of pyrazine with 266 nm light.

modest with values of  $T_{\text{rel}}=350\text{-}620$  K, as shown in Fig. 3. The translational energy does not seem to correlate with ammonia rotational energy, but there is a slight negative correlation with ammonia rotational quantum number  $J$ . No significant differences are seen for different  $K$  states with the same  $J$  value or for states with same  $J$  and different inversion symmetry. The rotational energy distribution is

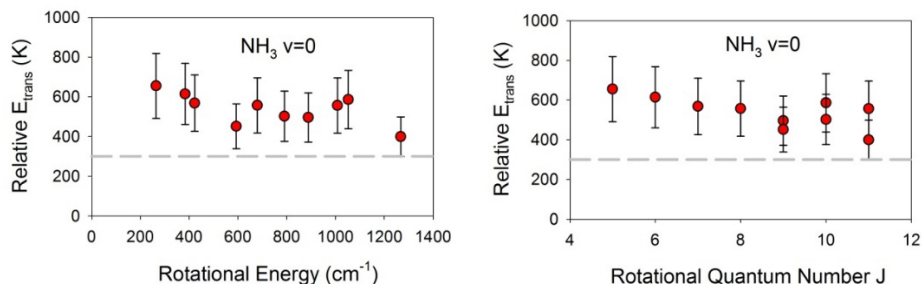


Fig. 3. Center of mass frame  $J$ -dependent translational energy for scattered ammonia ( $v=0$ ) plotted vs. a) rotational energy and b) angular momentum quantum number.

shown in Fig. 4a. Ammonia is scattered with a rotational temperature of  $T_{\text{rot}}=480$  K, showing that only modest rotational energy is gained in pyrazine(E) collisions. Absolute state-specific energy gain rate

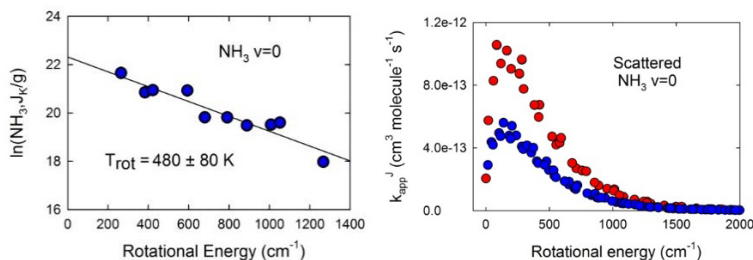


Fig. 4. a) Nascent rotational energy distribution of scattered ammonia. b) State-specific energy transfer rate constants. Integer  $K/3$  states have twice the statistical weight of other states.

constants were measured and are shown in Fig 4b. State-specific rates are summed to give a V-RT rate constant of  $k=4.1 \times 10^{-10} \text{ cm}^3 \text{ molecule}^{-1} \text{ s}^{-1}$ , which is 58% of the Lennard-Jones (LJ) collision rate. Depletion rates agree with the LJ rate, providing some confidence in its use. These results show that the V-RT pathway is the primary relaxation pathway for pyrazine(E)/ammonia collisions but suggest that V-V energy transfer plays an increasingly important role as the number of vibrational modes increases in the energy accepting bath. This topic is now under investigation. Fig. 5 shows the state-specific and summed energy transfer probability distribution functions. The average energy transfer is  $\langle \Delta E \rangle = 320 \text{ cm}^{-1}$ .

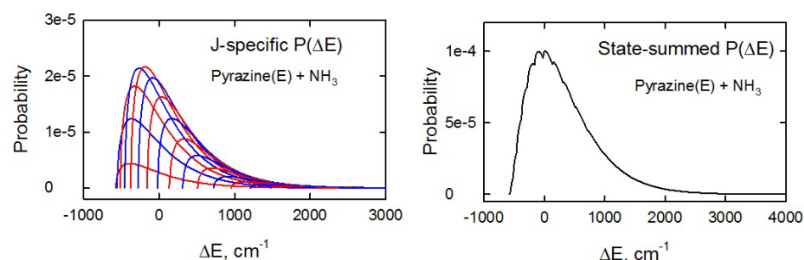


Fig. 5. Representative J-specific energy transfer distribution functions were determined for 540 ammonia states with  $J \leq 22$  and summed to yield an overall  $P(\Delta E)$  curve. The average energy transfer is  $\langle \Delta E \rangle = 320 \text{ cm}^{-1}$ .

### III. Future Work

We are now poised to make detailed comparisons for the energy transfer mechanisms of various energy-accepting bath molecules. We have seen substantial variation in the rotational and translational energy distributions for quenching by different bath molecules. We will consider how various bath properties such as moment of inertia, polarity, and structure impact the energy transfer mechanisms. Such a comparison will provide important clues for developing predictive models of energy transfer.

### IV. References

1. "Direct determination of collision rates beyond the Lennard-Jones model through state-resolved measurements of strong and weak collisions," D. K. Havey, Q. Liu, Z. Li, M. Elioff, M. Fang, J. Neudel and A. S. Mullin, *J. Phys. Chem. A* **111**, 2458-2460 (2007)
2. "Performance of a high-resolution mid-IR optical parametric oscillator transient absorption spectrometer," G. Echebiri, M. Smarte, W. Walters and A. S. Mullin, *Optics Exp.* **22**, 14885-14895 (2014).
3. "State-resolved studies of collisional quenching of highly vibrationally excited pyrazine by water: The case of the missing  $V \rightarrow RT$  supercollision channel," M. Fraelich, M. S. Elioff and A. S. Mullin, *J. Phys. Chem.* **102**, 9761-9771 (1998)
4. "Vibrational energy gain in the  $\nu_2$  bending mode of water via collisions with hot pyrazine ( $E=37900 \text{ cm}^{-1}$ ): Insights into the dynamics of energy flow" M. S. Elioff, R. Sansom and A. S. Mullin, *J. Phys. Chem. A* **104**, 10304-10311 (2000)
5. "Collisions of highly vibrationally excited pyrazine with HOD: State-resolved probing of strong and weak collisions," D. K. Havey, Q. Liu, Z. Li, M. Elioff and A. S. Mullin, *J. Phys. Chem. A* **111**, 13321-13329 (2007)
6. "Full state-resolved energy gain profiles of  $\text{CO}_2$  ( $J=2-80$ ) from Collisions with Highly Vibrationally Excited Molecules. I. Relaxation of Pyrazine ( $E=37900 \text{ cm}^{-1}$ )" D. K. Havey, J. Du and A. S. Mullin, *J. Phys. Chem. A* **114**, 1569-1580 (2010)
7. "State-resolved collisional quenching vibrationally excited pyrazine ( $E=37000 \text{ cm}^{-1}$ ) with DCl," Z. Li, E. Korobkova, K. Werner, L. Shum and A. S. Mullin, *J. Chem. Phys.* **123**, 174306 (2005)
8. "Dynamics of weak and strong collisions: Vibrationally excited pyrazine ( $E=37900 \text{ cm}^{-1}$ ) with DCl," J. Du, L. Yuan, S. Hsieh, F. Lin and A. S. Mullin, *J. Phys. Chem. A* **112**, 9396-9404 (2008)

### V. Publications supported by this project 2013-present

1. J. Du, N. A. Sassin, D. K. Havey, K. Hsu and A. S. Mullin, "Full energy gain profiles of  $\text{CO}_2$  from collisions with highly vibrationally excited molecules. II. Energy dependent pyrazine ( $E=32700$  and  $37900 \text{ cm}^{-1}$ ) relaxation" *J. Phys. Chem. A* **117**, 12104-12115 (2013)
2. G. Echebiri, M. Smarte, W. Walters and A. S. Mullin, "Performance of a high-resolution mid-IR optical parametric oscillator transient absorption spectrometer" *Optics Express* **22**, 14885-14895 (2014)
3. J. Du, D. K. Havey, S. W. Teitelbaum and A. S. Mullin, "Full energy gain profiles of  $\text{CO}_2$  from collisions with highly vibrationally excited molecules. III. 2-Methylpyridine, 2,6-dimethylpyridine and 3,5-dimethylpyridine ( $E \sim 38500 \text{ cm}^{-1}$ ) relaxation" in preparation
4. M. Smarte, G. Echebiri, W. Walters, J. Cleveland and A. S. Mullin, "Unusual isotope effects in collisions of pyrazine (E) with HCl and DCl: Evidence of strong interactions", in preparation
5. C. A. Bognar, G. Echebiri, H. Danchi and A. S. Mullin, "State-resolved energy transfer dynamics of methane with highly vibrationally excited pyrazine ( $E=37900 \text{ cm}^{-1}$ ), in preparation

# Reacting Flow Modeling with Detailed Chemical Kinetics

Habib N. Najm

Sandia National Laboratories  
P.O. Box 969, MS 9051, Livermore, CA 94551  
hnnajm@sandia.gov

## I. Program Scope

The goal of this research program is to improve fundamental understanding of reacting flow, thereby advancing the state of the art in predictive modeling of combustion. The work involves: (1) Developing numerical methods for the efficient solution of reacting flow systems of equations with detailed kinetics and transport, massively parallel codes for computing large scale reacting flow with detailed kinetics, and techniques for analysis of multidimensional reacting flow; (2) Using computations to investigate the structure and dynamics of flames using detailed chemical kinetics; (3) Developing numerical methods for uncertainty quantification (UQ) in reacting flow computations; (4) Estimation of chemical model parameters, and calibration/validation of reacting flow models, based on experimental data and computational predictions; and (5) UQ studies in computations of chemical systems and reacting flow. In the following, recent progress and future plans in this overall area are discussed.

## II. Recent Progress

### A. Statistical Inference of Reaction Rate Coefficients

We continued work on the application of our “data free inference” (DFI) algorithm to  $H_2$ - $O_2$  chemistry, focusing on the inference of a joint density on the Arrhenius parameters ( $\lambda_1 = (A_1, E_1, n_1)$ ) of the reaction (R1):  $H+O_2 \rightarrow OH+O$ , and relying on reported experimental measurements [1]. The need for DFI lies in the fact that reported measurements, as is typical, provide a partial degree of information, and do not include the full raw data behind the measurement. In recent progress, we focused on the handling of nuisance parameters in this context. Specifically, we developed means for handling nuisance parameters that are other uncertain rate constants, measured previously, and thus specified with a given density, arriving at a joint density on new and old parameters. In particular, rather than marginalizing over the density of the nuisance parameter, which is what was done earlier, we had to redesign the algorithm to arrive rather at the joint density. We applied this new construction to the inference of a joint density on  $(\lambda_1, \lambda_2)$ , where  $\lambda_2 \equiv A_2$  is the uncertain Arrhenius pre-exponential rate constant of the reaction (R2):  $OH+H_2 \rightarrow H_2+OH$ , and where the marginal density  $p(\lambda_2)$  is given.

The requisite development of the algorithm for the joint inference necessitated efficient handling of the computation for the Bayesian evidence for  $\lambda_1$ -inference, conditional on  $\lambda_2$ ,  $p(D|\lambda_2)$ , for each MCMC-sample of  $\lambda_2$ , with corresponding expense. Efficient implementation was necessary for evaluating integrals with Gauss-Hermite quadrature, including the evidence integrals. Further, we evaluated the evidence at a suitable mesh, and subsequently used its interpolation on this mesh in the context of the MCMC chain for  $\lambda_1$ .

The application of the method to the problem at hand arrived at a number of findings. To begin with, we find strong correlation in the resulting marginal posterior structure on  $\lambda_1$ , with strong pair-wise correlations among  $(\ln A_1, n_1, E_1)$ . On the other hand, we find relatively weak correlation between  $(\ln A_1, \ln A_2)$ . Forward propagation of the uncertainty on  $\lambda_1$  arrives at an uncertain  $k(T)$  that is consistent with the scatter of reported measurements, and exhibits increasing uncertainty with increasing/decreasing temperature outside the range of the data. Further, by propagating parametric uncertainty in the ignition model, we arrive at the associated characterization of the uncertain ignition delay time. We find, in particular, significant uncertainty in ignition delay. Further, the associated PDF is strongly dependent on the specified joint uncertainty structure in the parameters, such that the often relied-upon strategy of ignoring uncertainty in  $(n, E)$ , and employing only conditional uncertainty in  $\ln A$ , leads to a misleadingly small degree of uncertainty in predicted ignition delay time. Similar conclusions hold for predicted uncertainty in the solution state at any instant in time. These findings highlight the necessity for the current study, in pursuit of a self-consistent joint uncertainty structure on chemical model parameters, despite the relatively limited amount of available information in the literature.

## B. Estimation of Model Error in Chemical Models

We have continued to work on theoretical and algorithmic developments for model error estimation in Bayesian model calibration, as well as the demonstration of these algorithms in the context of chemical systems. These demonstrations have targeted the calibration of a simple chemical model against computations from a detailed kinetic model, where, for the purposes of this calibration, the latter predictions are treated as truth. Specifically, we considered the context of homogeneous constant pressure ignition of a methane-air mixture, focusing on a single quantity of interest, being the ignition delay time. We used the GRImech3.0 mechanism, and a single-step irreversible global mechanism, as the detailed and simple models respectively. We used ignition time predictions from GRImech3.0 to calibrate the 1-step model, over a range of initial temperature and equivalence ratio  $(T, \Phi)$ . This calibration involved Bayesian inference of the Arrhenius pre-exponential and activation energy coefficients of the 1-step model, with an embedded parameterization of model error using polynomial chaos expansions. The Bayesian estimation of this parameterization provided a joint density on all uncertain parameters, whose forward propagation through the calibrated 1-step model provided an uncertain prediction of ignition time with desired characteristics, over the range of  $(T, \Phi)$ . In particular, the mean of the uncertain ignition time prediction was centered on the ignition time predictions from GRImech3.0, while its standard deviation was consistent with the discrepancy between its mean and the GRImech3.0 data, both in an L2 sense. This result was robust to arbitrary increases in the amount of detailed model data used, being constrained accordingly by the construction of the underlying likelihood function employed in the Bayesian procedure. This was a key requirement of the construction. Given that no amount of data employed in this fitting would eliminate the fact of the discrepancy between the two models, due to the structural error in the 1-step model, the procedure is designed to ensure that additional data would only serve to improve the estimation of the model error discrepancy, and its corresponding predictive uncertainty, thus avoiding the erroneous conclusion of reduced predictive uncertainty with increasing data volumes, which would occur if no accounting of model error were implemented.

## C. Uncertainty Quantification in Large Eddy Simulation of Turbulent Combustion

In collaboration with J. Oefelein and G. Lacaze we have continued to work on the statistical calibration of a 2-step chemical model for n-dodecane oxidation to be used in large-eddy simulation (LES) of turbulent combustion. We used a reference detailed mechanism [2] for n-dodecane, with 255 species and 2,289 reactions as the basis for calibration. The Arrhenius parameters of one of the reactions in the 2-step model, namely the reaction step accounting for incomplete oxidation of n-dodecane into CO, were written as functions of equivalence ratio and temperature, and the parameters defining this functional dependence were the object of Bayesian inference. We have extended our previous work in this context, which relied on a conventional likelihood construction, to one which accounted for model error. The motivation was, again, the need for meaningful predictive uncertainties from the calibrated simple model, providing some estimation of the discrepancy from the detailed model predictions. In the present context, the simple model involved  $O(10)$  parameters. Accordingly, the best place for embedding the model error parameterization was not obvious. Moreover, embedding model error in all parameters is undesirable because of the associated great increase in dimensionality of the inverse problem. We have compared a range of alternative choices in this context using Bayesian evidence/marginal-likelihood, and associated model selection strategies. This identifies the particular embedding of model error that has the highest marginal likelihood for the given data. This degree of freedom exists because of the residual freedom, within the L2 fitting context, for different dependences of predictive uncertainty on initial temperature and equivalence ratio, all satisfying the requisite L2 constraints. This procedure readily found the embedding, within the trial set, that provided a profile of predictive uncertainty that is closest to that of the discrepancy between predictions from the two models. Finally, we also found negligible sensitivity to priors, so that the model selection answer was quite robust.

## D. Chemical Model Reduction under Uncertainty

We have continued our work on the application of computational singular perturbation (CSP) based chemical model reduction methods in a context where the starting model has uncertain parameters. We demonstrated the technique in the context of simplification of an n-butane mechanism with  $O(10^3)$  uncertain reaction rates. The performance of reduced mechanisms was analyzed in terms of *a posteriori* average errors combining both stochastic and deterministic dimensions. Results highlight the joint roles of conventional CSP importance-index thresholds and probabilistic thresholds in determining the simplified mechanism. They also highlight the limitations of the

technique under conditions where the deterministic CSP analysis itself is challenged as regards its capacity for monotonic control of *a posteriori* errors. Nonetheless, the more solidly expected result of monotonicity in mechanism size is indeed maintained as regards probabilistic thresholds. Broadly speaking, results demonstrate desired reliable model reduction with both dynamical and probabilistic controls.

### III. Future Plans

#### A. Global Sensitivity Analysis in Combustion

We have developed methods for global sensitivity analysis (GSA) in computational models in general, and have applied them to computational models of ignition for hydrocarbon fuel-air mixtures. Going forward there are a number of developments we are planning to explore. Getting accurate estimation of Sobol sensitivity indices, particularly higher-order ones, is a challenge, requiring typically very large numbers of samples. When the computational model is expensive, this is a serious challenge. We envision application of polynomial chaos surrogates, along with Bayesian compressive sensing, and low rank tensor decomposition methods, to provide regularized robust estimation of Sobol indices in high-dimensional expensive combustion models where the number of feasible samples is computationally-limited. We will apply these methods in both homogeneous ignition and steady 1D premixed flames with hydrocarbon fuels. We will explore a range of quantities of interest (QoIs), aside from ignition time and flame speed, including exploration of the time/space structure of ignition/flame profiles. It is of interest to explore the importance of different parameters for different structural features of an ignition or flame solution. In this context, we will treat these field-QoIs as random fields, represent them using Karhnen-Loeve expansions, and analyze the dependence of their parameterization on model parameters. Ultimately, this line of inquiry would establish, over the range of uncertainty of each parameter in the chemical model, the importance of different parameters for prediction of various aspects of flame and ignition-process structure.

#### B. Estimation of Model Error in Chemical Systems

Accounting for model error in chemical models is particularly relevant in the context where *simplified* models are used, accepting a degree of error with respect to a detailed model. For example, consider a detailed kinetic model  $M^*$  with parameters  $\lambda^*$ , and its simplification to arrive at a skeletal, yet elementary, model  $M(\lambda)$ , where  $M(\lambda) \subset M^*(\lambda^*)$ . At this point, whether this reduction was done deterministically or accounting for uncertainty, there are two viable scenarios for prediction with the simplified model going forward. The default scenario is to simply use the simplified model as-is, with the same parameter values (or associated distributions if uncertain) for its reactions as in the detailed model. The other scenario, which we propose to explore here, uses computational results from the detailed model to *recalibrate* (a relevant subset of) the parameters of the simplified model. Considering in particular our model error work, this calibration ought to be done such that the predictive uncertainty from the simplified model is consistent with its predictive error relevant to the detailed model. Doing this, we ensure that the simplified model has minimal average error on relevant QoIs, and provides meaningful predictive uncertainty in these QoIs. The key challenge in extending our model error approach in this direction is high-dimensionality of the simplified model parametric space. Given our recent work with model evidence and model selection, and relying on an initial dimensionality reduction based on GSA, we envision a practical strategy for identifying a small number of parameters where model error can be suitably embedded.

#### C. UQ in LES of Turbulent Combustion

We will continue to work with J. Oefelein and G. Lacaze towards enabling UQ in LES computations of turbulent combustion. Having calibrated the simple model for n-dodecane, with embedded model error, the path forward involves computations of turbulent combustion with LES, employing this model, and estimating uncertainties in computational predictions. One key challenge here is that, for the planned QoI, being the ignition delay time, the results depend significantly not only on the uncertain parameters of the chemical and subgrid models, but also on the particular realization of the turbulent inflow. Accordingly, the key task at hand will be dimensionality reduction in order to achieve feasible UQ results. We will rely on Karhnen-Loeve expansions for representing uncertainty in the turbulent inflow, and employ adaptive basis UQ methods for dimensionality reduction, employing random samples of model response.

## D. Statistical Inference of Reaction Rate Constants

The next steps in the DFI context for H<sub>2</sub>-O<sub>2</sub> chemistry is to move beyond the current set of two reactions, enhancing the representation of the uncertain input space one reaction at a time. This is a somewhat lengthy process, and will involve addressing experimental details and available information at each stage/reaction. However, going forward towards reactions with less importance will clearly lead to a point of diminishing returns, when the full uncertainty picture is well represented within acceptable error limits.

## E. Chemical Model Reduction under Uncertainty

We will continue working on exploring the utility of our CSP-based strategy for chemical model reduction under uncertainty. We are working towards a demonstration of the utility of the resulting simplified model, by examining its accuracy under uncertain rate constants, as compared to that available from a deterministically simplified mechanism. We will also evaluate and compare the utility of the different error-measures in providing robust reduction results. Further, we will examine the joint statistics on reaction probabilities, hoping to shed light on implicit dependences/correlations among reactions, as informed by specified tolerances on CSP/dynamical importance indices as well as probabilistic thresholds for reaction inclusion.

## F. Uncertainty Quantification in PIV of Reacting Flow

We plan to work jointly with J. Frank on the development of methods for UQ in particle imaging velocimetry (PIV) in reacting flows. Initial stages along this road will involve the statistical formulation of existing data processing methods, and their setting in an overall Bayesian framework encompassing all the relevant stages of the measurement process. The resulting construction would be most useful for providing additional information on measured flowfields, and in the larger context of experimental design.

## IV. References

- [1] D.A. Masten, R.K. Hanson, and C.T. Bowman. "Shock Tube Study of the Reaction  $\text{H} + \text{O}_2 \rightarrow \text{OH} + \text{O}$  Using OH Laser Absorption". *Journal of Physical Chemistry* 94 (1990), pp. 7119–7128.
- [2] K. Narayanaswamy, P. Pepiot, and H. Pitsch. "A chemical mechanism for low to high temperature oxidation of n-dodecane as a component of transportation fuel surrogates". *Comb. Flame* 161 (2014), pp. 867–884.

## V. BES-Supported Published/In-Press/Submitted Publications [2014-2016]

- [B1] M. Khalil, K. Chowdhary, C. Safta, K. Sargsyan, and H.N. Najm. "Inference of Reaction Rate Parameters based on Summary Statistics from Experiments". *Proc. Comb. Inst.* (2016). Submitted.
- [B2] C. Safta, M. Blaylock, J. Templeton, S. Domino, K. Sargsyan, and H. Najm. "Uncertainty Quantification in LES of Channel Flow". *Int. J. Num. Meth. Fluids* (2016). Submitted.
- [B3] L. Hakim, G. Lacaze, M. Khalil, H. Najm, and J. Oefelein. "Modeling Auto-Ignition Transients in Reacting Diesel Jets". *ASME J. Eng. Gas Turb. Power* (2016). In press.
- [B4] K. Sargsyan, H. N. Najm, and R. Ghanem. "On the Statistical Calibration of Physical Models". *International Journal for Chemical Kinetics* 47.4 (2015), pp. 246–276.
- [B5] M. Khalil, G. Lacaze, J.C. Oefelein, and H.N. Najm. "Uncertainty quantification in LES of a turbulent bluff-body stabilized flame". *Proceedings of the Combustion Institute* 35 (June 2015), pp. 1147–1156.
- [B6] X. Han and H.N. Najm. "Dynamical Structures in Stochastic Chemical Reaction Systems". *SIAM J. Appl. Dyn. Systems* 13.3 (2014), pp. 1328–1351.
- [B7] K.S. Kedia, C. Safta, J. Ray, H.N. Najm, and A.F. Ghoniem. "A second-order coupled immersed boundary-SAMR construction for chemically reacting flow over heat-conducting Cartesian grid-confirming solid". *J. Comput. Phys.* 272 (2014), pp. 408–428.
- [B8] H.N. Najm, R.D. Berry, C. Safta, K. Sargsyan, and B.J. Debusschere. "Data Free Inference of Uncertain Parameters in Chemical Models". *Int. J. for Uncertainty Quantification* 4.2 (2014), pp. 111–132.
- [B9] H.N. Najm and M. Valorani. "Enforcing Positivity in Intrusive PC-UQ Methods for Reactive ODE Systems". *J. Comput. Phys.* 270 (2014), pp. 544–569.

## Spectroscopy, Kinetics and Dynamics of Combustion Radicals

Grant No. DE-FG02-09ER16021

Annual Progress Report, David J. Nesbitt

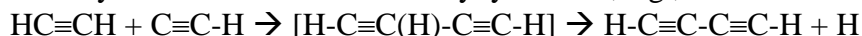
[djn@jila.colorado.edu](mailto:djn@jila.colorado.edu), April 1, 2016

*JILA, University of Colorado and National Institute of Standards and Technology, and  
Department of Chemistry and Biochemistry, University of Colorado, Boulder, Colorado*

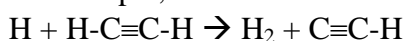
Our research program involves detailed study of the spectroscopy, kinetics and dynamics of highly reactive, transient hydrocarbon radical species of importance in combustion phenomena. The experimental approach is based on the powerfully synergistic combination of i) high resolution IR difference frequency light generation, ii) slit discharge sources for formation of jet cooled radicals, and iii) high sensitivity detection with direct laser absorption methods near the quantum shot noise limit. The crucial advantage of such methods is that such highly reactive transients can be “synthesized” at relatively high pressures/temperatures that are characteristic of combustion conditions, and yet with the resulting reactive species cooled within several mm (5-10  $\mu$ s) down to  $T \approx 10$ -15K in the slit supersonic expansion for maximal spectroscopic simplification. Selected highlights from work over the last year are summarized below.

### I. Spectroscopy/Dynamics of Polyynes: Sub-Doppler Infrared Studies of Diacetylene

Diacetylene ( $\text{H-C}\equiv\text{C-C}\equiv\text{CH}$ ) is the smallest member of the polyyne family and represents an ubiquitous species in the combustion chemistry of unsaturated hydrocarbons and fuel rich flames. What makes these linear polyynes so chemically interesting is the fact that they form readily via addition with CCH ethynyl radical, e.g.,



where the subsequent regeneration of CCH to complete the chain reaction can occur via additional H-atom abstraction, for example,

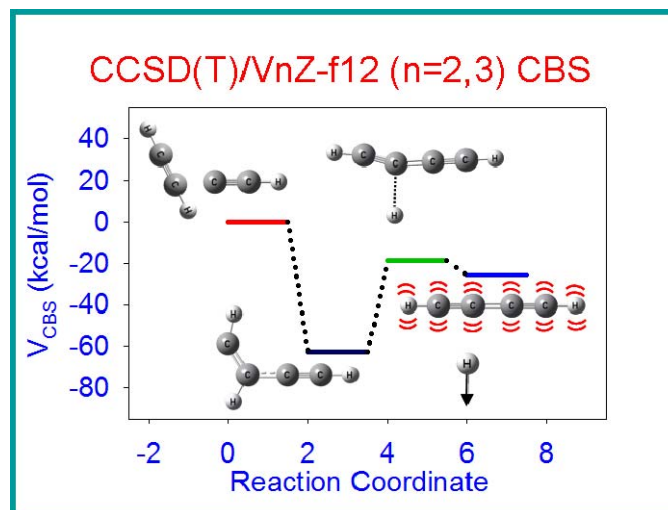


at sufficiently elevated temperatures. It is worth noting here that the intermediate  $\text{H-C}\equiv\text{C(H)-C}\equiv\text{C-H}$  species is not a high energy transition state but rather a stable radical adduct,  $\approx 63$  kcal/mol lower in energy than  $\text{HCCH} + \text{CCH}$  reactants, with little or no barrier to insertion and therefore resulting in a reaction rate constant at the near gas kinetic limit. This process can continue by subsequent exothermic attack of CCH into one of the diacetylenic  $\text{C}\equiv\text{C}$  bonds, which then can form higher order polyynes such as triacetylene, tetraacetylene, etc.. Indeed, such chain reaction kinetics are extremely rapid under non-oxidizing flame conditions at normal pressures and temperatures, which therefore makes diacetylene (as well as each of the successive polyynes) a key crucial intermediate in the formation chemistry of soot.

Despite critical importance of diacetylene in combustion phenomena, there is remarkably little spectroscopic characterization of this species at high spectral resolution. This is due to the absence of a permanent dipole moment, which makes these species completely invisible to rotational spectroscopy, augmented by the lack of sufficiently long lived electronically excited states to enable visible/UV spectroscopy. The combination of these properties makes high resolution infrared spectroscopic methods the most powerful avenue of investigation for polyynes larger than acetylene. As a first step toward detailed characterization and exploration of such species, fundamental, bending ( $\nu_6, \nu_7, \nu_8, \nu_9$ ), and CC-

stretch ( $\nu_2$ ,  $\nu_3$ ) hot band spectra in the antisymmetric CH stretch ( $\nu_4$ ) region near  $3330\text{ cm}^{-1}$  have been observed and analyzed for jet cooled diacetylene ( $\text{HC}\equiv\text{C}-\text{C}\equiv\text{CH}$ ) under sub-Doppler conditions.

Diacetylene is generated *in situ* in the throat of a pulsed supersonic slit expansion by discharge dissociation of acetylene to form ethynyl ( $\text{C}\equiv\text{CH}$ ) + H, followed by radical attack ( $\text{HC}\equiv\text{CH} + \text{C}\equiv\text{C}-\text{H}$ ) to form  $\text{HC}\equiv\text{C}-\text{C}\equiv\text{CH} + \text{H}$ . The combination of i) sub-Doppler line widths and ii) absence of spectral congestion permits rotational structure and Coriolis interactions in the  $\nu_4$  CH stretch fundamental to be observed and analyzed with improved precision. Of particular dynamical interest, the spectra reveal diacetylene formation in highly excited internal vibrational states. Specifically, multiple  $\Pi \leftarrow \Pi$  and  $\Delta \leftarrow \Delta$  hot bands built on the  $\nu_4$  CH stretch fundamental are observed, due to doubly degenerate bending vibrations [cis  $\text{C}\equiv\text{C}-\text{H}$  bend ( $\nu_6$ ), trans  $\text{C}-\text{C}\equiv\text{C}$  bend ( $\nu_7$ ), trans  $\text{C}\equiv\text{C}-\text{H}$  bend ( $\nu_8$ ) and cis  $\text{C}-\text{C}\equiv\text{C}$  bend ( $\nu_9$ )], as well as a heretofore unobserved  $\Sigma \leftarrow \Sigma$  band assigned to excitation of  $\nu_2$  or  $2\nu_3$  CC stretch. Boltzmann analysis yields populations consistent with a universally cold rotations ( $T_{rot} \approx 15 \pm 5\text{ K}$ ) and yet *superthermal* vibrations ( $T_{vib} \approx 85\text{-}430\text{ K}$ ), the latter of which is quite anomalous for the high collision densities in a slit jet expansion. In order to elucidate the physical mechanism for this excess vibrational excitation, high level *ab initio* CCSD(T) calculations have been pursued with explicitly correlated basis sets (VnZ-f12;  $n=2,3$ ) and extrapolated to the complete basis set (CBS) limit using MOLPRO quantum chemistry software. The results suggest that the extensive hot band structure observed arises from i) highly exothermic CCH + HCCH addition to yield a strongly bent HCCHCCH radical intermediate ( $\Delta H = -62.6\text{ kcal/mole}$ ), followed by ii) rapid fragmentation over a submerged transition state barrier ( $\Delta H = -18.9\text{ kcal/mole}$ ) to form vibrationally hot diacetylene + H products ( $\Delta H = -25.6\text{ kcal/mol}$ ), and consistent with crossed molecular beam studies by Kaiser and coworkers [Phys. Chem. Chem. Phys. **4**, 2950 (2002)]. Finally, RRKM fragmentation rates for this complex are calculated, which exceed collision frequencies in the slit jet expansion and suggest near unity quantum efficiency for diacetylene formation.



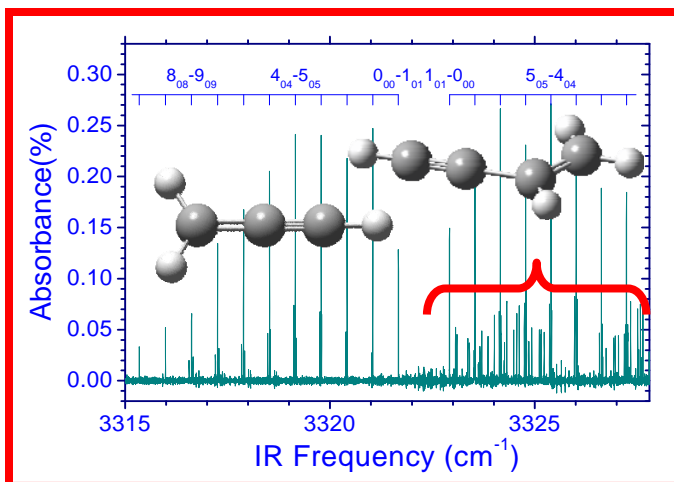
## II. Sub-Doppler Infrared Spectroscopy of Jet-Cooled Propargyl Radical ( $\text{H}_2\text{CCCH}$ )

Hydrocarbon radical species play a crucial role in a wide range of extreme chemical environments, ranging from solar photochemistry in the upper atmosphere, to high temperature kinetics of combustion flames, to synthesis of molecules in the interstellar medium. It has been suggested, for example, that highly unsaturated radicals are responsible for the initial formation of polycyclic aromatic hydrocarbons (PAH) in astronomical contexts, as well as possible carriers of the diffuse interstellar bands (DIB). In a more terrestrial venue, complex reaction mechanisms have been proposed that suggest unsaturated reactive hydrocarbon radicals to be especially important intermediates in controlling combustion efficiency, as well as triggering the formation of large aromatic molecular structures that eventual result in macroscopic “soot” carbon particulate.

The formation of large aromatic structures by sequential addition of acetylene and ethynyl radical to smaller aromatic molecules has been well studied, with specific models, e.g., hydrogen abstraction acetylene addition (HACA) to existing aromatic ring structures, receiving strong support. In light of the success of such models for predicting facile growth on aromatic species, it is therefore interesting to note that the detailed kinetics and dynamics

for formation of even the *simplest* aromatic compounds from smaller non-aromatic radical species is still not well understood. One potential pathway toward aromatic ring formation has been bimolecular reaction of two propargyl radicals ( $\text{H}_2\text{CCCH}$ ) to form phenyl radical + H at low pressures or benzene at sufficiently high pressures. The removal kinetics due to the self reaction of propargyl + propargyl has been well studied, with the aromatically stabilized product species considered in theoretical models. In particular, such efforts are beginning to highlight the importance of highly unsaturated  $\text{C}_3$  open shell species such as  $\text{H}_2\text{CCCH}$  in the early growth stages to form larger aromatic structures. This provides additional motivation for detailed high resolution spectroscopy and dynamics studies of jet cooled propargyl radical, in order to facilitate both laser based identification and absolute concentration measurements in further experimental studies of such aggregation processes.

In order to facilitate such efforts, the acetylenic CH stretch mode ( $\nu_1$ ) of propargyl ( $\text{H}_2\text{CCCH}$ ) radical has been studied at sub-Doppler resolution ( $\sim 60$  MHz) via infrared laser absorption spectroscopy in a supersonic slit-jet discharge expansion, where low rotational temperatures ( $T_{\text{rot}} = 13.5(4)$  K) and lack of spectral congestion permit improved determination of band origin and rotational constants for the excited state. For the lowest J states primarily populated in the slit jet cooled expansion, fine structure due to the unpaired electron spin is resolved completely, which permits accurate analysis of electron spin-rotation interactions in the vibrationally excited state ( $\epsilon_{aa} = -518.1(1.8)$ ,  $\epsilon_{bb} = -13.0(3)$ ,  $\epsilon_{cc} = -1.8(3)$  MHz). In addition, hyperfine broadening in substantial excess of the sub-Doppler experimental linewidths is observed due to nuclear spin-electron spin contributions at the methylenic ( $-\text{CH}_2$ ) and acetylenic ( $-\text{CH}$ ) positions, which permits detailed modeling of the fine/hyperfine structure line contours. The results are consistent with a delocalized radical spin density extending over both methylenic and acetylenic C atoms, in excellent agreement with simple resonance structures as well as *ab initio* theoretical calculations.



### III. Infrared Spectroscopy and Formation Dynamics of Jet-Cooled Triacetylene

Chemical formation and spectroscopic detection of linear polyynes ( $\text{H}(\text{CC})_n\text{H}$ ) have been issues of longstanding interest in combustion, as well as interstellar astronomy and the evolution of planetary atmospheres. In our own solar system, the chemistry of Titan's atmosphere, the largest of Saturn's moons, is known to have significant acetylene and higher polyyne content. Indeed, one distinguishing optical feature of Titan's atmosphere is an aerosol-based "haze", which gives the planet its orange-brownish color and even precluded observation of the surface until the arrival of the Cassini-Huygens spacecraft. The underlying

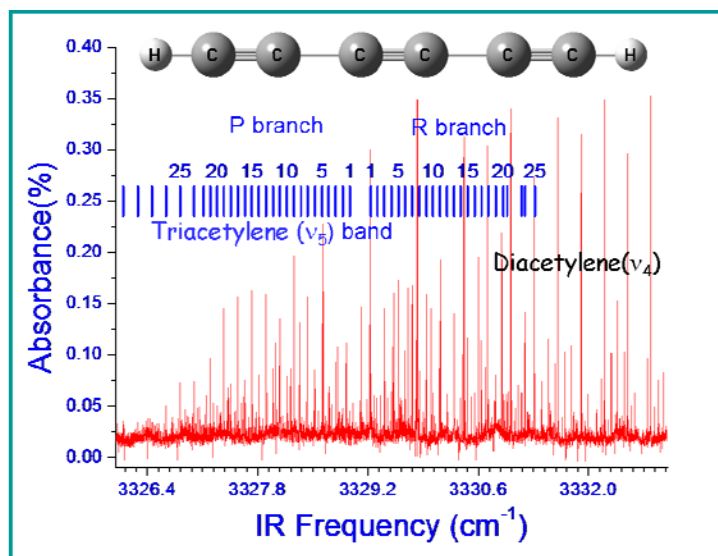
chemical process which triggers this haze formation is still not well understood, but is linked to the chemistry of similar processes in combustion for soot formation.

To help further elucidate these issues, infrared spectroscopy and formation dynamics of triacetylene have been investigated in a slit jet supersonic discharge and probed with sub-Doppler resolution ( $\approx 60$  MHz) on the fundamental antisymmetric CH stretch mode ( $\nu_5$ ). The triacetylene is generated in the throat of the discharge by

sequential attack of ethynyl radical with acetylene and diacetylene: i)  $\text{HCCH} \rightarrow \text{HCC} + \text{H}$ , ii)  $\text{HCC} + \text{HCCH} \rightarrow \text{HCCCCH} + \text{H}$ , iii)  $\text{HCC} + \text{HCCCCH} \rightarrow \text{HCCCCCCH} + \text{H}$ , cooled rapidly in the slit expansion to 15 K, and probed by near shot-noise-limited absorption sensitivity with a tunable difference-frequency infrared laser. The combination of jet cooled temperatures ( $T_{\text{rot}} = 15$  K) and low spectral congestion permits i) analysis of rotationally avoided crossings in the  $\nu_5$  band ascribed to Coriolis interactions, as well as ii) first detection of  $\nu_5$   $\Pi$ - $\Pi$  hot band progressions built on the  $\nu_{12}$  sym CC bend and definitively assigned via state-of-the-art *ab initio* vibration-rotation interaction parameters ( $\alpha_i$ ), which make for interesting comparison with recent spectroscopic studies of Doney et al. [J. Mol. Spectrosc. **316**, 54 (2015)]. The combined data provide direct evidence for significantly *non-equilibrium* populations in the CC bending manifold, dynamically consistent with a strongly bent radical intermediate and transition states for forming triacetylene product. The presence of intense triacetylene signals under cold, low density slit jet conditions provides support for i) barrierless addition of HCC with HCCCCH and ii) a high quantum yield for HCCCCCCH formation. Complete basis set (CBS) calculations for energetics (CCSD(T)-f12/VnZ-f12,  $n=2,3$ ) and frequencies (CCSD(T)-f12/VdZ-f12) are presented for both radical intermediate and transition state species, predicting collision stabilization in the slit jet expansion to be competitive with unimolecular decomposition with increasing polyynes chain length.

#### Papers published or submitted:

- 1) C.-H. Chang and D. J. Nesbitt, "Spectroscopy and dynamics of jet cooled polyynes in a slit supersonic discharge: Sub-Doppler infrared studies of diacetylene HCCCCH," J. Phys. Chem. A. DOI:10.1021/acs.jpca.5b02310 (2015). (Al Wagner, Joe Michel, Festschrift).
- 2) C.-H. Chang and D. J. Nesbitt, "Sub-Doppler Infrared Spectroscopy of Propargyl Radical ( $\text{H}_2\text{CCCH}$ ) in a Slit Supersonic Expansion," J Chem Phys. doi: 10.1063/1.4922931 (2015).
- 3) C.-H. Chang, J. Agarwal, W. D. Allen, and D. J. Nesbitt, "Sub-Doppler infrared spectroscopy and reaction dynamics of triacetylene in a slit supersonic expansion," J. Chem. Phys. 144, 074301 (2016); <http://dx.doi.org/10.1063/1.4940905>
- 4) Chih-Hsuan Chang and David J. Nesbitt, "High resolution spectroscopy of jet cooled phenyl radical: The  $\nu_1$  and  $\nu_2$   $a_1$  symmetry C-H stretching modes," (J. Chem. Phys., submitted, 2016)



## Spectroscopy and Dynamics of Free Radicals

*Stephen R. Leone and Daniel M. Neumark*

Lawrence Berkeley National Laboratory and Departments of Chemistry and Physics, University of California, Berkeley, California 94720 (510) 643-5467 [srl@berkeley.edu](mailto:srl@berkeley.edu), 510-642-3502 [dmneumark@berkeley.edu](mailto:dmneumark@berkeley.edu)

**Scope of the Project:** In this program, a diverse approach to researching processes relevant to combustion chemistry is taken by applying techniques to study radical spectroscopy and dynamics. It is motivated in part by the need to develop and refine reaction mechanisms for combustion, as more fuel variations are explored and combustion under various temperature and pressure regimes is considered. This experimental program characterizes key properties of free radicals including bond dissociation energies, orbital energetics, electron affinities, spectroscopy of low-lying electronic states, primary photochemistry, transition state regions, and reaction dynamics. Laser spectroscopic methods and vacuum ultraviolet (VUV) light from the Chemical Dynamics Beamline of the Advanced Light Source are used to selectively investigate individual processes involved in formation and reaction of radicals. These studies facilitate a detailed understanding of the role of free radicals in reaction mechanisms that govern diverse processes such as low-temperature autoignition, the oxidation of aromatic hydrocarbons, and the growth of complex molecules such as PAH's in flames. The spectroscopy and photodissociation dynamics of free radicals are using three complementary, state-of-the-art experiments. Slow Electron Velocity-Map Imaging of cryogenically cooled anions (cryo-SEVI) yields precise electron affinities, vibrational frequencies, and term values of low-lying states for radicals that are generated by negative ion photodetachment. Negative ion photodetachment also forms the basis of the fast radical beam (FRBM) instrument, in which neutral free radicals generated in this manner are photodissociated, with the kinetic energy and angular distributions of the various photofragment channels analyzed using sophisticated coincidence detection techniques. The photodissociation processes of radicals generated by flash pyrolysis are investigated using a molecular beam instrument with a rotating mass spectrometer as a detector.

### **Recent Progress:**

#### ***Jet Stirred Reactor experiments***

A high temperature (500-1100 K) jet-stirred reactor was constructed and interfaced to a sampling cone of a high-resolution time-of-flight mass spectrometer arrangement on the Sandia flame apparatus at the Advanced Light Source. This experimental arrangement presents a unique approach to monitor chemical transformations of key intermediates with tunable photoionization spectroscopy in well-defined conditions comparable to those in combustion engines. Oxidation studies of n-butane, partially deuterated n-butane, dimethyl ether, cyclohexane, 2-methylhexane and 2, 5-dimethylhexane have revealed new insights into the oxidation mechanism of these species. In addition to corroborating the observations of the ketohydroperoxide species in the oxidation of butane, the use of deuterated butane provides evidence for the Korcek mechanism of decomposition of the intermediate ketohydroperoxide species into acid, ketone and aldehyde pairs, through the observation of the partially deuterated acetone and formic acid Korcek pair. Highly oxygenated species with four and five oxygen atoms were identified in the low temperature oxidation of cyclohexane, 2-methylhexane and 2, 5-dimethylhexane, by using isotopically labeled oxygen ( $^{18}\text{O}$ ), as multifunctional molecules containing hydroperoxy and carbonyl/ether functional groups. The detection of these species suggests that a third  $\text{O}_2$  addition process might exist at combustion relevant conditions indicating the presence of previously unrevealed radical chain-branching pathways.

#### ***Femtosecond XUV Transient Absorption Experiments***

The photodissociation of halogenated hydrocarbons represents an important class of benchmark reactions in chemical reaction dynamics. Recently, femtosecond extreme ultraviolet (XUV) transient absorption spectroscopy was applied using a table-top high harmonic generation source to investigate halogenated hydrocarbons such as methyl iodide and allyl iodide to characterize the transition state region along the C-I bond dissociation coordinate. Single-photon excitation at 266 nm was used to launch the molecules in a dissociative state manifold (collectively referred to as the A-Band) via a  $n(\text{I}) \rightarrow \sigma^*(\text{C-I})$  transition. Product iodine atoms were produced both in the spin-orbit excited ( $^2\text{P}_{1/2}$ ) and

ground ( $^2P_{3/2}$ ) states, with the former as the major pathway. XUV absorption at the iodine  $N_{4/5}$  edge (45 to 60 eV) provides a direct probe of the long-lived atomic iodine products as well as the fleeting transition state region of the photodissociation reaction. Two features are observed in the case of  $CH_3I$  (at 45.6 eV and 47.4 eV, denoted transients A and B) and three features are observed in the case of allyl iodide (at 45.3 eV, 47.3 eV, and 48.4 eV, denoted transients A, B, and C, respectively) which arise from the valence-excited  $n\sigma^*$  state and are projected onto the high-lying core-excited states of the dissociating molecule via excitation of 4d(I) core-electrons. Transients A and B, which appear at similar energies in both molecules, are assigned to 4d(I) $\rightarrow n$ (I) core-to-valence transitions whereas transient C is assigned to a 4d(I) $\rightarrow \sigma^*(C-I)$  transition. By extracting temporal lineouts at these spectral positions, the transition state resonances are found to reach a maximum at  $\sim 40$  fs in case of  $CH_3I$  and  $\sim 60$  fs in case of allyl iodide, decaying to complete C-I bond-dissociation by  $\sim 90$  fs ( $CH_3I$ ) and  $\sim 145$  to 185 fs ( $C_3H_5I$ ). The results represent the shortest-lived chemical transition state observed by core-level spectroscopy to date.

In recent months, the apparatus has undergone a significant upgrade to extend the high-harmonic source energies from the XUV to the soft x-ray range up to and beyond 300 eV. These probe energies give access to the core levels of several key combustion-relevant elements, which were previously inaccessible, including the sulfur L-edge ( $\sim 160$  eV) and the carbon K-edge ( $\sim 285$  eV). This opens a wealth of possibilities for detailed characterization of hydrocarbon and thiyl radicals and corresponding chemical dynamics, utilizing the unique and powerful advantages of x-ray absorption spectroscopy with unprecedented time-resolution ( $<100$  fs) at these energies. The new setup incorporates a tunable, high-energy optical parametric amplifier that converts sub-40 fs, 800 nm pulses into sub-60 fs, 1150–2200 nm pulses, which are required for driving high harmonic generation into the x-ray regime. Additionally, a custom high-resolution, dual-grating spectrometer with a translatable CCD detector has been constructed to spectrally detect both XUV and soft x-ray wavelengths. The completed apparatus allows for both the production and highly-efficient spectral detection of broadly tunable femtosecond pulses of x-ray radiation ranging from 40 eV to  $\sim 600$  eV. Preliminary tests have demonstrated high harmonic energies up to  $\sim 310$  eV using 1300–1550 nm driving wavelengths, high quality static absorption spectra of methyl iodide to characterize the source, and, recently, and transient spectra of methyl radical at 280 eV upon 266 nm dissociation of methyl iodide. Femtosecond time-resolved pump-probe measurements at the carbon K-edge are now underway.

### ***Cryo-SEVI Spectroscopy of PAH Radicals***

The vibrational and electronic spectroscopy of gas-phase 9-, 1-, and 2-anthracenyl radicals ( $C_{14}H_9$ ) was probed by photodetachment of the corresponding cryogenically cooled anions via slow photoelectron velocity-map imaging (cryo-SEVI). The use of a newly designed velocity-map imaging lens in combination with ion cooling yields photoelectron spectra with  $<2$   $cm^{-1}$  resolution. Isomer selection of the anions was achieved using gas-phase synthesis techniques, resulting in observation and interpretation of detailed vibronic structure of the ground and lowest excited states for all three anthracenyl radical isomers. The ground state bands yielded electron affinities of 1.7155(2) eV, 1.5436(2) eV, and 1.4671(2) eV for 9-, 1-, and 2-anthracenyl respectively. Vibrational frequencies for several Franck-Condon active modes were measured and assigned for each isomer. Term energies of the first excited states of the 9-, 1-, and 2-anthracenyl radicals were found to be 1.205(6) eV, 1.515(4) eV, and 1.755(8) eV, respectively. Spectra were interpreted through comparison with *ab initio* quantum chemistry calculations, Franck-Condon simulations, and calculations of threshold photodetachment cross sections and photoelectron angular distributions.

### ***Fast Radical Beam Spectroscopy***

The photodissociation dynamics of the methyl perthiyl radical ( $CH_3SS\cdot$ ) were investigated on the fast radical beam (FRBM) instrument. Methyl perthiyl radicals were produced by photodetachment of the  $CH_3SS^-$  anion followed by photodissociation at 248 nm (5.0 eV) and 193 nm (6.4 eV). Photofragment mass distributions and translational energy distributions were measured at each dissociation wavelength. Experimental results show S atom loss as the dominant (96%) dissociation channel at 248 nm with an anisotropic angular distribution and translational energy peaking near the maximal energy available to the fragments, indicating that the dissociation occurs along a repulsive excited state. At 193 nm, S atom loss remains the major fragmentation channel, although  $S_2$  dissociation

becomes more competitive and constitutes 32% of the fragmentation. The translational energy distributions for both channels are very broad, suggesting formation of products in several excited electronic states.

### **Molecular Beam Radical Photodissociation**

The photodissociation of jet cooled benzyl radicals,  $C_7H_7$ , at 248 nm was studied using photofragment translational spectroscopy. The benzyl radical was produced by flash pyrolysis of phenylethyl nitrite. Source conditions were optimized using a recently installed electron impact ionizer in the mass spectrometer detector in which the electron energy could be tuned to as low as 7 eV. Appearance energy measurements enabled us to distinguish between  $C_7H_7^+$  ions produced from benzyl ionization as opposed to dissociative ionization of precursor molecules. Two photodissociation channels were observed,  $H + C_7H_6$  and  $CH_3 + C_6H_4$ . The translational energy distribution determined for each channel suggested that both dissociation mechanisms occur via internal conversion to the ground state followed by intramolecular vibrational redistribution and dissociation. The branching ratio between these two channels was found to be  $CH_3 + C_6H_4:H + C_7H_6 = 0.011 \pm 0.004$ . The dominance of the  $H + C_7H_6$  channel was corroborated by the branching ratio calculated using Rice-Ramsperger-Kassel-Marcus theory.

### **Future Plans:**

In future experiments, the aforementioned upgraded x-ray apparatus will be used to spectroscopically investigate hydrocarbon radicals including methyl, allyl, vinyl, and phenyl and fundamental hydrocarbon photochemical processes including internal conversion, predissociation, and ring-opening/closing reactions. Utilizing the new capabilities at carbon K-edge probing energies, the recent studies on the transition state region of alkyl halide dissociation reactions will be revisited, now from the perspective of the carbon atom, and by capturing the evolution of the alkyl radical electronic structure as the bond breaks. In complementary future experiments, the ultrafast photodissociation dynamics of  $CH_3I$  will also be explored through I 4d core-level ionization by time-resolved x-ray photoelectron spectroscopy.

The three instruments available to the second part of the effort will provide an integrated experimental platform for the study of free radical spectroscopy and dissociation experiments. During the coming year, the cryo-SEVI instrument will generate high resolution spectra for larger polycyclic aromatic hydrocarbon radicals,  $RO_2$  species, and other radicals whose photodissociation dynamics will be investigated on the FRBM and molecular beam instruments. The “soft ionization” electron impact ionizer that has recently been installed on the molecular beam instrument represents a major instrumental advance that will, by reducing dissociative ionization, facilitate the interpretation of radical photodissociation experiments. Experiments on the reactive scattering of free radicals from liquid surfaces will be explored. FRBM experiments will focus on the photodissociation of the t-butyl peroxy radical, as part of our programmatic goal to map out the spectroscopy and dissociation dynamics of radicals that play a key role in low temperature combustion and autoignition.

### **Recent Publications Citing DOE Support (2013-2016):**

- N. C. Cole-Filipiak, M. Shapero, C. Haibach-Morris, and D. M. Neumark, "Production and Photodissociation of the Methyl Perthiyl Radical", *J. Phys. Chem. A*, **in press**.
- M. L. Weichman, J. A. DeVine, D. S. Levine, J. B. Kim, and D. M. Neumark, "Isomer-specific vibronic structure of the 9-, 1-, and 2-anthracenyl radicals via slow photoelectron velocity-map imaging" *PNAS*, **113**, 1698 (2016).
- A. Bhattacharjee, A. R. Attar, and S. R. Leone, "Transition-state region in the A-band photodissociation of Allyl Iodide – A femtosecond extreme ultraviolet transient absorption study", *J. Chem. Phys.* **in press**.
- Z. Wang, L. Zhang, K. Moshhammer, D. M. Popolan-Vaida, V. S. Bhavani Shankar, A. Lucassen, C. Hemken, C. A. Taatjes, S. R. Leone, K. Kohse-Höinghaus, N. Hansen, P. Dagaut, S. M. Sarathy, "Additional chain-branching pathways in the low-temperature oxidation of branched alkanes", *Comb. and Flame* **164**, 386 (2016).
- M. Shapero, N. C. Cole-Filipiak, C. Haibach-Morris, and D. M. Neumark, "Benzyl Radical Photodissociation Dynamics at 248 nm" *J. Phys. Chem. A* **119**, 12349 (2015).

- A. R. Attar, A. Bhattacharjee, and S. R. Leone, “Direct observation of the Transition-State Region in the Photodissociation of  $\text{CH}_3\text{I}$  by Femtosecond Extreme Ultraviolet Transient Absorption Spectroscopy”, *J. Phys. Chem. Lett.*, **6**, 5072 (2015)
- D. M. Popolan-Vaida, C.-L. Liu, T. Nah, K. R. Wilson, and S. R. Leone, “Reaction of chlorine molecules with unsaturated submicron organic particles”, *Z. Phys. Chem.* **229**, 1521 (2015)
- K. Moshhammer, A. W. Jasper, D. M. Popolan-Vaida, A. Lucassen, P. Diévert, H. Selim, A. J. Eskola, C. A. Taatjes, S. R. Leone, S. M. Sarathy, Y. Ju, P. Dagaut, K. Kohse-Höinghaus, and Nils Hansen, “Detection and Identification of the Keto-Hydroperoxide ( $\text{HOCH}_2\text{OCHO}$ ) and Other Intermediates during Low-Temperature Oxidation of Dimethyl Ether”, *J. Phys. Chem. A*, **119**, 7361 (2015)
- M. L. Weichman, J. B. Kim and D. M. Neumark, “Slow Photoelectron Velocity-Map Imaging Spectroscopy of the ortho-Hydroxyphenoxide Anion”, *J. Phys. Chem. A*, DOI: 10.1021/acs.jpca.5b00768, (2015)
- M. L. Weichman, J. B. Kim, J. A. DeVine, D. S. Levine and D. M. Neumark, “Vibrational and Electronic Structure of the  $\alpha$ - and  $\beta$ -naphthyl Radicals via Slow Photoelectron Velocity-Map Imaging”, *J. Am. Chem. Soc.*, **137**, 1420, (2015)
- A. R. Attar, L. Piticco, and S. R. Leone, “Core-to-valence spectroscopic detection of the  $\text{CH}_2\text{Br}$  radical and element-specific photodissociation dynamics of  $\text{CH}_2\text{IBr}$ ”, *J. Chem. Phys.*, **141**, 164308 (2014)
- J. F. Lockyear, M. Fournier, I. R. Sims, J.-C. Guillemin, C. A. Taatjes, D. L. Osborn and S. R. Leone, “Formation of fulvene in the reaction of  $\text{C}_2\text{H}$  with 1,3-butadiene”, *Int. J. Mass. Spectrom.*, in press (2014)
- T. Nah, S. H. Kessler, K. E. Daumit, J. H. Kroll, S. R. Leone, and K. R. Wilson, “Influence of molecular structure and chemical functionality on the heterogeneous OH-initiated oxidation of unsaturated organic particles”, *J. Phys. Chem. A*, **118**, 4106 (2014)
- D. M. Popolan-Vaida, K. R. Wilson, and S. R. Leone, “Reaction of I atoms with sub-micron squalane and squalene droplets: mechanistic insights into heterogeneous reactions”, *J. Phys. Chem. A*, **118**, 10688 (2014)
- N. Cole-Filipiak, M. Shapero, B. Negru and D. M. Neumark, “Revisiting the Photodissociation Dynamics of the Phenyl Radical”, *J. Chem. Phys.*, **141**, 104307, (2014)
- M. Ryazanov, A. Harrison, G. Wang, P. Crider and D. M. Neumark, “Investigation of 3-fragment Photodissociation of  $\text{O}_3$  at 193.4 and 157.6 nm by Coincident Measurements”, *J. Chem. Phys.*, **140**, 234304, (2014)
- J. F. Lockyear, O. Welz, J. D. Savee, F. Goulay, A. J. Trevitt, C. A. Taatjes, D. L. Osborn and S. R. Leone, “Isomer Specific Product Detection in the Reaction of CH with Acrolein”, *J. Phys. Chem. A*, **117**, 11013 (2013)
- A. J. Trevitt, M. B. Prendergast, F. Goulay, J. D. Savee, D. L. Osborn, C. A. Taatjes and S. R. Leone, “Product Branching Fractions of the CH plus Propene Reaction from Synchrotron Photoionization Mass Spectrometry”, *J. Phys. Chem. A*, **117**, 6450, (2013)
- J. Bouwman, M. Fournier, I. R. Sims, S. R. Leone and K. R. Wilson, “Reaction Rate and Isomer-Specific Product Branching Ratios of  $\text{C}_2\text{H} + \text{C}_4\text{H}_8$ : 1-Butene, cis-2-Butene, trans-2-Butene, and Isobutene at 79 K”, *J. Phys. Chem. A*, **117**, 5093, (2013)
- E. R. Hosler and S. R. Leone, “Characterization of Vibrational Wave Packets by Core-Level High-Harmonic Transient Absorption Spectroscopy”, *Phys. Rev. A*, **88**, 023420, (2013)
- S. D. Chambreau, J. B. Liu, G. L. Vaghjiani, C. J. Koh, A. Golan, O. Kostko and S. R. Leone, “Thermal decomposition mechanisms of ionic liquids by direct dynamics simulations and vacuum ultraviolet photoionization mass spectrometry”, *Abstracts of Papers of the Am. Chem. Soc.*, **245**, 206-PHYS, (2013)
- T. Nah, M. Chan, S. R. Leone and K. R. Wilson, “Real Time in Situ Chemical Characterization of Submicrometer Organic Particles using Direct Analysis in Real Time Mass Spectrometry”, *Anal. Chem.*, **85**, 2087, (2013)
- T. Nah, S. H. Kessler, K. E. Daumit, J. H. Kroll, S. R. Leone and K. R. Wilson, “OH-initiated oxidation of sub-micron unsaturated fatty acid particles”, *Phys. Chem. Chem. Phys.*, **115**, 18649, (2013)
- A. W. Harrison, J. S. Lim, M. Ryazanov, G. Wang, S. Gao and D. M. Neumark, “Photodissociation Dynamics of the Thiophenoxy Radical at 248, 193, and 157nm”, *J. Phys. Chem. A*, **117**, 11970, (2013)
- N. C. Cole-Filipiak, B. Negru, G. M. P. Just, D. Park and D. M. Neumark, “Photodissociation Dynamics of the Methyl Perthiyl Radical at 248 nm via Photofragment Translation Spectroscopy”, *J. Chem. Phys.*, **138**, 054301, (2013)

# Large Eddy Simulation of Reacting Flow Physics

Joseph C. Oefelein, Anthony Ruiz, Guilhem Lacaze  
Combustion Research Facility, Sandia National Laboratories  
Livermore, CA 94551-0969  
oefelei@sandia.gov

## Program Scope

Application of the Large Eddy Simulation (LES) technique within the Diagnostics and Reacting Flows program at the CRF is based on two primary objectives. The first is to establish a set of high-fidelity first-principles computational benchmarks that identically match the geometry and operating conditions of selected experimental target flames. The second is to establish a scientific foundation for advanced model development that effectively bridges the gap between the idealized jet flame processes studied under this program and application relevant processes that exist at the device scale. The goal is to provide direct one-to-one correspondence between measured and modeled results at conditions unattainable using Direct Numerical Simulation (DNS) by performing a series of detailed simulations that progressively incorporate the fully coupled dynamic behavior of reacting flows with detailed thermodynamics, transport, chemistry, and realistic spectra of turbulence. The primary focal point is the series of flames that have been studied as part of the Experimental Reacting Flow Research program in collaboration with Barlow and Frank (see their respective abstracts). This represents a direct extension of joint activities being pursued as part of the *International Workshop on Measurement and Computation of Turbulent (Non)premixed Flames* [1] (i.e., the “TNF Workshop”). Complementary information from highly specialized LES calculations, combined with detailed laser-based measurements, provide new opportunities to understand reacting flow physics in realistic parameter spaces and for the development of accurate predictive models for turbulent combustion and related thermophysical flow processes. After achieving an adequate level of validation, results from high-fidelity LES using first-principles sub-models provide fundamental information that cannot be measured or calculated via DNS and a strong link between theory, experiments, and relevant applications. The insights gained provide a basic science foundation for the development of predictive models required for the design of advanced transportation, propulsion, and power devices.

## Recent Progress

Turbulent opposed jet experiments provide significant potential to study a wide range of flame-turbulence interactions across different combustion regimes in a highly compact and computationally simple domain. However, flow conditions generated at respective nozzle exits are extremely complex; e.g., anisotropic and transitional in nature, which potentially diminishes the utility of these configurations due to uncertainties in boundary conditions. Intrinsic bulk motions within and between the nozzles can create further uncertainties. All of these uncertainties become problematic when using the measured data to assess combustion models. Conversely, minimizing these uncertainties by including the large and complex nozzle flow passages as part of flame modeling studies negates the notion of a simple and compact computational domain. Thus, there is a need to fully characterize the turbulent flow dynamics that exist both inside and between the nozzles so that accurate and robust boundary conditions can be derived. To address this need, we have performed a detailed set of simulations to fully characterize the Yale-Sandia Turbulent Opposed Jet (TOJ) burner, which is one of the current target cases being considered as part of the TNF Workshop series (see Frank’s abstract). The goal is to investigate strategies on how to best specify the complex turbulent flow dynamics at the nozzle exits as boundary conditions in a simple and compact computational domain.

Figure 1a shows the geometry of the TOJ burner. An 80/20-percent (by volume) mixture of methane and nitrogen is injected in the fuel nozzle. Pure oxygen is injected in the oxidizer nozzle. The turbulent Reynolds number is defined as  $Re_t = u' l_t / \nu$ , where  $u'$  is the RMS velocity fluctuation on the jet centerline at the nozzle exit,  $l_t$  is the integral scale determined from the autocorrelation of the velocity fluctuation, and  $\nu$  is the kinematic viscosity. A Turbulence Generating Plate (TGP), as shown in Fig. 1b, is positioned inside each nozzle at a distance  $L$  from the nozzle exits.

Adjusting the distance  $L$  is what controls the magnitude of the turbulent Reynolds number at the nozzle exits. A turbulent Reynolds number of  $Re_t = 600$  (the “Low Turbulence” (LT) case) is obtained by placing the TGP at a position  $L_{LT} = 113$  mm. Similarly,  $Re_t = 1000$  (the “High Turbulence” (HT) case) is obtained when  $L_{HT} = 94$  mm. The volume flow rate is  $Q = 85$  SLM in both nozzles for both the LT and HT cases. Similarly, the bulk Reynolds number is  $Re_b = U_b d / \nu = 8800$ , where  $d = 12.7$  mm is the nozzle exit diameter, and the bulk velocity is  $U_b = 11.2$  m/s.

A series of LES calculations were performed over a range of resolutions to establish the characteristics of the flow dynamics at the nozzle exits. LES was performed using the RAPTOR code framework. The theoretical framework solves the fully-coupled conservation equations of mass, momentum, total-energy, and species for a chemically reacting flow. It is designed to handle high Reynolds number, high-pressure, real-gas and/or liquid conditions over a wide Mach operating range. It also accounts for detailed thermodynamics and transport processes at the molecular level. A noteworthy aspect of RAPTOR is it was designed specifically for LES using non-dissipative, discretely conservative, staggered, finite-volume differencing. This eliminates numerical contamination of the sub-models due to artificial dissipation and provides discrete conservation of mass, momentum, energy, and species, which is an imperative requirement for high quality LES. Details related to the formulation are given by Oefelein [2]. Representative case studies are given by Oefelein et al. [3–8].

Both the fuel and oxidizer streams are injected azimuthally prior to a set of honeycombs. The honeycombs then dissipate the swirling motion and straighten the flow such that it becomes laminar. To eliminate ambiguities associated with boundary conditions, the simulations performed here employ a domain that starts just downstream of respective honeycombs. The flow through the TGP is then calculated part of the interior domain. Thus, the laminar to turbulent transition is calculated directly. The velocity profile at the honeycomb exit is known to be parabolic at this location, so a Poiseuille profile is assumed consistent with laminar flow in a pipe. Note that this is the only *a priori* assumption used in the numerical setup. Surrounding each nozzle are coflowing nitrogen streams to condition the flow across the stagnation plane. These are also included in the domain. The benefit of this approach is that it allows the turbulence field to develop entirely inside of the computational domain.

Detailed analysis of results over a range of grid resolutions has confirmed that we are able to precisely match measured turbulence characteristics at respective nozzle exits. Figure 2 shows a representative result of the internal nozzle flow. Here, a volume rendering of the instantaneous enstrophy field (vorticity squared) is shown for the LT case using a grid resolution of  $d/60$ . The nonideal structure of the instantaneous turbulence generated across the TGP is observed, which highlights the importance of better quantifying the effect of these nonidealities at respective nozzle exits. A vorticity sheet is generated by acceleration of the flow through the petal-shaped hole created by the TGP. This vorticity sheet rapidly destabilizes and transforms into tube-like structures as it is convected towards the nozzle exit. Interactions between the transitional jet that emanates from the TGP and the internal recirculation zones inside the nozzles is complex and change as a function of the turbulent Reynolds number. This is due to the change in position of the TGP and its effect on the transition length relative to the nozzle exit. Thus, the converging nozzle has two effects. It recirculates some of the early formed turbulence that emanates from the TGP and thus increases its residence time.

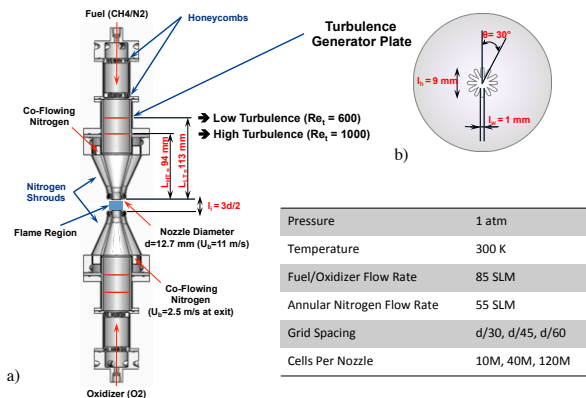


**Figure 1.** Yale-Sandia Turbulent Opposed Jet burner for the nonpremixed flame configuration. A turbulent Reynolds number of  $Re_t = 600$  (“Low Turbulence”) is obtained by placing the Turbulence Generating Plate (TGP) at a position of  $L = L_{LT} = 113$  mm, and  $Re_t = 1000$  (“High Turbulence”) by placing the TGP at  $L = L_{HT} = 94$  mm.

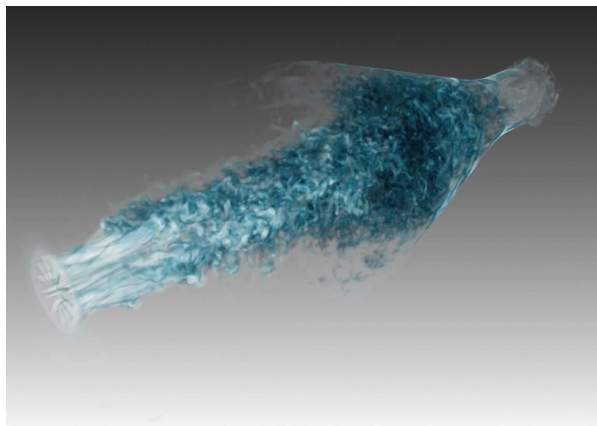


**Figure 2.** Volume rendering of the instantaneous enstrophy field (vorticity squared) showing the instantaneous structure of turbulence generated inside the TOJ nozzles (mesh resolution is  $d/60$ ).

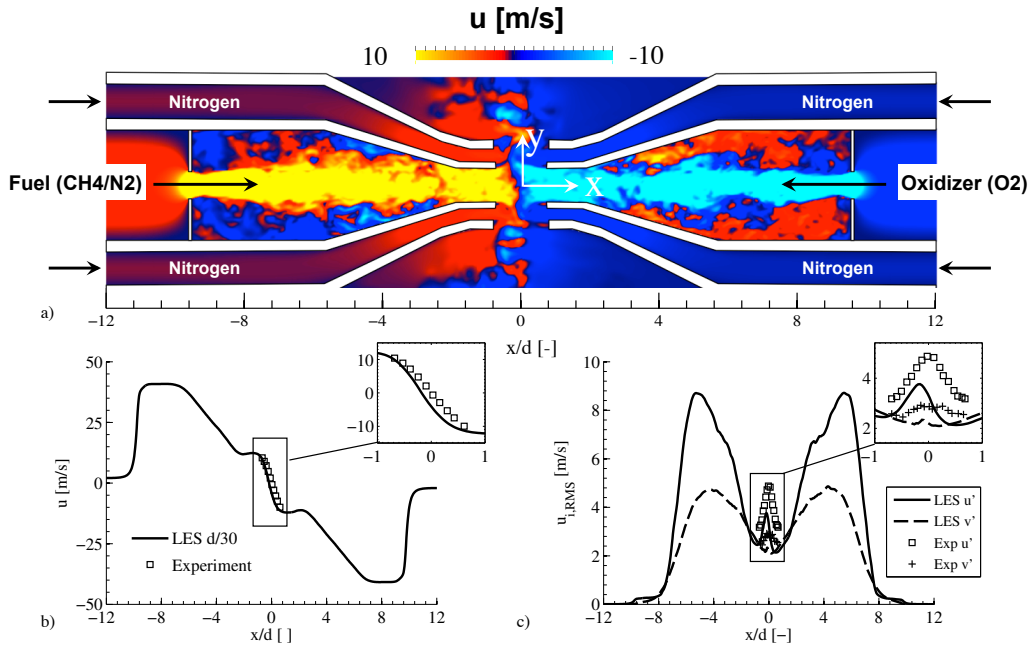


**Figure 3.** Cross-section of full TOJ configuration with three-stream flamelet model showing: a) the instantaneous axial velocity field, and b) axial profiles of mean and RMS velocity across the stagnation plane. Boundary conditions match experiment and applied with no tuned constants.

This decreases the level of anisotropy at the exit of the nozzles. However, the alignment of vortex tubes with the jet axis tends to negate this effect and thus increase anisotropy in the nozzle exit statistics as the transition length becomes shorter. Boundary conditions imposed at the nozzle exits must take these trends into account.

Having established validated solutions for the internal nozzle flow, attention was then focused on the reacting flow dynamics in the full TOJ domain. Figure 3 illustrates these counter-flow dynamics using a three-stream flamelet model to provide realistic levels of heat release. Here, two mixture fractions are transported. The first is the classical mixture fraction used to tabulate a 1D laminar counterflow flame structure. The second represents the amount of dilution by the nitrogen coflow. The goal is to verify that the simulations accurately represent the flow dynamics axially across the stagnation plane. Figure 3a shows a representative snapshot of the instantaneous axial velocity. The fuel stream is injected through the left nozzle with positive axial velocity. The oxidizer stream is injected through the right nozzle with negative axial velocity. As in the experiment, the volume flow rate is the same in both nozzles. Since pure oxygen is 10-percent denser than the methane/nitrogen fuel mixture, the momentum of the oxygen stream is larger than the fuel stream, which shifts the mean location of the stagnation plane closer to the fuel nozzle. This shift is qualitatively shown in Fig. 3a and quantitatively in Fig. 3b, and represents another important factor that must be considered in deriving approximate turbulent inflow conditions in a domain that starts at the nozzle exits. The time evolving fuel and oxidizer streams at the respective nozzle exits are biased by this shift. Similarly, heat release appears to have little impact on the mean velocity statistics at nozzle exits, but a measurable impact on RMS statistics (> 10-percent). In addition, the anisotropic nature of the turbulence emanating from respective nozzles remained anisotropic across the stagnation planes. Near the flame, this anisotropy was amplified by the shift-and-tilt motion of the stagnation plane. The precise mechanisms associated with this motion are still under investigation.

Current research is focused on how to best treat time-evolving boundary conditions at respective nozzle exits such that a one-to-one correspondence with experimental data can be established using a simple and compact computational domain (e.g., the small blue box between the nozzles in Fig. 1). The goal is to specify turbulent inflow conditions appropriate for a wide range of LES and/or DNS studies that robustly account for the geometry dependent anisotropic turbulence characteristics. It is also important that these conditions adjust appropriately as a function of the turbulent Reynolds number specified. In this regard, we are investigating the merits of methods such as the Synthetic Eddy Method that use calculated or measured distributions of the Reynolds stresses and integral scales at the nozzle exit to generate time correlated signals as inflow conditions. The precise methodology to generate these signals and robustness in their ability to reproduce important higher-order moments is currently under investigation. The ability to specify these conditions to within the variability in the experimental measurements will maximize benefits of comparisons with data for model development while significantly minimizing computational costs.

## Future Plans

We will continue to apply the approach and framework described above with emphasis on three interrelated areas of research: 1) Maintain close coordination between LES and experimental reacting flow research with emphasis on the collaborative activities of the TNF Workshop. 2) Maintain a significant effort in the development of quality assessment and uncertainty quantification (UQ) techniques for LES aimed at understanding and controlling the myriad of errors that complicate the development of predictive models. 3) Continue to develop advanced models and simulation techniques aimed at accurate prediction of flame behavior (and related flow physics) across a broad range of combustion regimes and fuels. Tasks related to research area 1 will be pursued through close collaborations with Barlow and Frank et al. following the proposed series of experiments outlined in their respective abstracts. Tasks related to research area 2 will be pursued through close collaborations with Najm et al. (e.g., see Najm's abstract). Tasks will continue to focus on advanced model development in a manner that effectively bridges the gap between the idealized jet flame processes studied under this program and application relevant processes exhibited at the device scale.

## Literature Cited

- [1] R. S. Barlow. International workshop on measurement and computation of turbulent (non)premixed flames. [www.sandia.gov/TNF](http://www.sandia.gov/TNF), 1996-Present. Sandia National Laboratories, Combustion Research Facility, Livermore, California.
- [2] J. C. Oefelein. Large eddy simulation of turbulent combustion processes in propulsion and power systems. *Progress in Aerospace Sciences*, 42(1):2–37, 2006.
- [3] J. C. Oefelein, R. W. Schefer, and R. W. Barlow. Toward validation of LES for turbulent combustion. *AIAA Journal*, 44(3): 418–433, 2006.
- [4] J. C. Oefelein. Mixing and combustion of cryogenic oxygen-hydrogen shear-coaxial jet flames at supercritical pressure. *Combustion Science and Technology*, 178(1-3):229–252, 2006.
- [5] J. C. Oefelein, V. Sankaran, and T. G. Drozda. Large eddy simulation of swirling particle-laden flow in a model axisymmetric combustor. *Proceedings of the Combustion Institute*, 31:2291–2299, 2007. Distinguished Paper Award, 2007.
- [6] T. C. Williams, R. W. Schefer, J. C. Oefelein, and C. R. Shaddix. Idealized gas turbine combustor for performance research and validation of large eddy simulations. *Review of Scientific Instruments*, 78(3):035114–1–9, 2007.
- [7] J. C. Oefelein and G. Lacaze. Low-temperature injection dynamics and turbulent flame structure in high-pressure supercritical flows. *Proceedings of the 23rd International Colloquium on the Dynamics of Explosions and Reactive Systems*, July 24–29 2011. Irvine, California.
- [8] J. C. Oefelein, R. N. Dahms, and G. Lacaze. Detailed modeling and simulation of high-pressure fuel injection processes in diesel engines. *SAE International Journal of Engines*, 5(3):1–10, 2012.

## BES Sponsored Publications (2014–Present)

- A. M. Ruiz, G. Lacaze, J. C. Oefelein, R. Mari, B. Cuenot, L. Selle, and T. Poinsot. A numerical benchmark for high-reynolds number supercritical flows with large density gradients. *AIAA Journal*, 2015. Accepted.
- R. N. Dahms and J. C. Oefelein. Liquid jet breakup regimes at supercritical pressures. *Combustion and Flame*, 162:3648–3657, 2015.
- R. N. Dahms and J. C. Oefelein. Atomization and dense-fluid breakup regimes in liquid rocket engines. *Journal of Propulsion and Power*, 31(5):1221–1231, 2015.
- A. M. Ruiz, G. Lacaze, and J. C. Oefelein. Flow topologies and turbulence scales in a jet-in-cross-flow. *Physics of Fluids*, 27(045101):1–35, 2015.
- G. Lacaze, A. Misdariis, A. Ruiz, and J. C. Oefelein. Analysis of high-pressure diesel fuel injection processes using LES with real-fluid thermodynamics and transport. *Proceedings of the Combustion Institute*, 35:1603–1611, 2015.
- M. Khalil, G. Lacaze, J. C. Oefelein, and H. N. Najm. Uncertainty quantification in LES of a turbulent bluff-body stabilized flame. *Proceedings of the Combustion Institute*, 35:1147–1156, 2015.
- R. N. Dahms and J. C. Oefelein. Non-equilibrium gas-liquid interface dynamics in high-pressure liquid injection systems. *Proceedings of the Combustion Institute*, 35:1587–1594, 2015.
- J. Manin, M. Bardi, L. M. Pickett, R. N. Dahms, and J. C. Oefelein. Microscopic investigation of the atomization and mixing processes of diesel sprays injected into high pressure and temperature environments. *Fuel*, 134:531–543, 2014.
- J. Quinlan, J. McDaniel, T. Drozda, G. Lacaze, and J. Oefelein. A priori analysis of flamelet-based modeling for a dual-mode scramjet combustor. *50th AIAA/ASME/SAE/ASEE Joint Propulsion Conference and Exhibit, Paper 2014-3743*, July 28–30 2014. Cleveland, Ohio. Best Paper Award, AIAA High Speed Air Breathing Propulsion Technical Committee, 2015.
- J. Oefelein, G. Lacaze, R. Dahms, A. Ruiz, and A. Misdariis. Effects of real-fluid thermodynamics on high-pressure fuel injection processes. *SAE International Journal of Engines*, 7(3):1–12, 2014.

## KINETICS AND DYNAMICS OF COMBUSTION CHEMISTRY

David L. Osborn

*Combustion Research Facility, Mail Stop 9055, Sandia National Laboratories*

*Livermore, CA 94551-0969*

[dlosbor@sandia.gov](mailto:dlosbor@sandia.gov)

### PROGRAM SCOPE

The goal of this program is to elucidate mechanisms of elementary combustion reactions through the use of multiplexed spectroscopy and mass spectrometry. We developed a technique known as time-resolved multiplexed photoionization mass spectrometry (MPIMS), which is used to sensitively and selectively probe unimolecular and bimolecular reactions. This work is in collaboration with Craig Taatjes, Leonid Sheps, and Judit Zádor, and has been utilized through collaboration by many scientists from other institutions in the US and abroad. The Sandia-designed MPIMS instrument utilizes tunable vacuum ultraviolet light from the Advanced Light Source (ALS) synchrotron at Lawrence Berkeley National Laboratory (LBNL) for sensitive, isomer-specific ionization of reactant and product molecules sampled from chemical reactions.

As a complementary approach, we use time-resolved Fourier transform spectroscopy (TR-FTS) to probe multiple reactants and products with broad spectral coverage ( $> 1000 \text{ cm}^{-1}$ ), moderate spectral resolution ( $0.1 \text{ cm}^{-1}$ ), and a wide range of temporal resolution (ns – ms). The inherently multiplexed nature of TR-FTS makes it possible to simultaneously measure product branching ratios, internal energy distributions, energy transfer, and spectroscopy of radical intermediates. Together with total rate coefficients, this additional information provides further constraints upon and insights into the potential energy surfaces that control chemical reactivity. Because of its broadband nature, the TR-FTS technique provides a global view of chemical reactions and energy transfer processes that would be difficult to achieve with narrow-band, laser-based detection techniques.

### RECENT PROGRESS

#### Isomer-resolved mass spectrometry

The multiplexed chemical kinetics photoionization mass spectrometer operates both at Sandia National Laboratories (using various discharge lamps to create VUV radiation), and at the Chemical Dynamics Beamline of the ALS synchrotron of LBNL. The chemical reactor is based on the Gutman design,<sup>1</sup> which allows the study of photodissociation and bimolecular reactions at pressures of 1 – 10 Torr and temperatures of 250 – 1000 K.

During the past 3-year period, we have applied this apparatus to a broad array of chemical problems, including studies of biofuel oxidation, reactions relevant to Saturn's moon Titan, the chemistry of carbonyl oxides (Criegee Intermediates), hydroperoxyalkyl radicals in autoignition chemistry, and fundamental studies of photoionization dynamics and absolute cross sections.

#### The propargyl ( $\text{H}_2\text{CCCH}$ ) + acetylene ( $\text{HCCH}$ ) reaction sequence

There has been much debate on the mechanism for the formation of the first and second aromatic ring in molecular weight growth chemistry during rich combustion. One mechanism, Hydrogen Abstraction aCetylene Addition (HACA), proposed by Frenklach and co-workers,<sup>2</sup> involves addition of acetylene to free radicals, forming a larger free radical, which may add additional acetylenes in a reaction sequence. Using time-resolved mass spectrometry, Knyazev and Slagle<sup>3</sup> studied the propargyl + acetylene reaction from 800 – 1100 K, which they described

with the following sequence of reactions:  $C_3H_3 + HCCH \rightarrow C_5H_5 (+HCCH) \rightarrow C_7H_7 (+HCCH) \rightarrow C_9H_8 + H$ . Although no isomeric information on the free radicals could be obtained, they inferred, contrary to Frenklach's assumption, that the radicals at each stage must be resonance stabilized due to their stability at such high temperatures.

We have revisited this reaction using MPIMS with tunable synchrotron radiation for isomer selectivity. Our kinetic traces are similar to Knyazev and Slagle's, confirming the same reaction sequence they assigned. At 800 K, the initial step produces two isomers of  $C_5H_5$ : the 1-vinyl propargyl radical ( $HCCCH-C_2H_3$ ), and the cyclopentadienyl radical (the most stable  $C_5H_5$  isomer). These two isomers are formed at the same rate, but vinyl propargyl reacts more rapidly with  $HCCH$  than cyclopentadienyl. By comparing 800 to 1000 K data, we know that vinyl propargyl reacts with  $HCCH$  to form a different  $C_7H_7$  isomer than in the case of cyclopentadienyl radical.

Surprisingly, the main  $C_7H_7$  radical produced from the propargyl + acetylene reaction is the tropylium (*c*- $C_7H_7$ ) isomer, not the benzyl isomer, despite the latter being more stable. This result is qualitatively consistent with recent master equation calculations of DaSilva and coworkers.<sup>4</sup> The final product is indene ( $C_9H_8$ ), a two-ring aromatic compound. This reaction sequence demonstrates a pathway to a 2-ring polycyclic aromatic hydrocarbon without any involvement of a benzene, phenyl, or benzyl intermediate.

### **The $O(^3P)$ + propyne reaction: Intersystem crossing plays a key role**

Reactions of ground state oxygen atoms with unsaturated hydrocarbons are important reactions in some regions of flames. Because the radical reactant is a triplet,  $O(^3P)$ , the initial addition occurs on the triplet surface, but intersystem crossing to the singlet surface can dramatically change the reaction outcome. We have studied this reaction at 298 K and 4 Torr, and observed five major product channels, with product branching fractions shown in parentheses:  $C_2H_3 + HCO$  (1.00),  $CH_3 + HCCO$  ( $0.35 \pm 0.11$ ),  $H + CH_3CCO$  ( $0.18 \pm 0.10$ ),  $C_2H_4 + CO$  ( $0.73 \pm 0.27$ ), and  $C_2H_2 + H_2 + CO$  ( $1.31 \pm 0.62$ ). The data is consistent with an addition-elimination mechanism, with 10% of products arising from addition to the central carbon, 89% from addition to the terminal carbon, and direct abstraction playing only a minor role ( $< 1\%$ ). Experiments with both  $d_0$  and  $d_1$ -propyne suggest that  $84 \pm 14\%$  of the observed product channels result from intersystem crossing to the lower-lying singlet potential energy surface. This dominance of the singlet surface is in stark contrast to the electronically similar reaction with acetylene, which reacts only on the initial triplet surface.

### **Absolute photoionization cross sections for benchmark species OH, $HO_2$ , $H_2O_2$ , and $H_2CO$**

A major advantage of the MPIMS approach to studying bimolecular reactions is the ability to extract quantitative product branching ratios from time-resolved signals of open- and closed-shell species. Doing so requires absolute photoionization cross sections, which are easily measured for stable molecules, but are quite challenging to measure for free radicals and cantankerous closed-shell molecules. In collaboration with Prof. Mitchio Okumura's group at Caltech, we have measured the absolute cross sections of two radicals of great importance in all types of oxidation chemistry: OH and  $HO_2$ . In addition, we have measured the cross sections of  $H_2O_2$  and  $H_2CO$ , two molecules that are difficult to produce in a pure state with known concentration, but are also ubiquitous in combustion and atmospheric chemistry. All these measurements rely on both the spectroscopy and the kinetics capabilities of MPIMS.

## Breaking through the false coincidence barrier of PEPICO (Photoelectron Photoion Coincidence Spectroscopy)

We and others have made great use of photoionization spectroscopy as a tool for quantitative chemical analysis in complex chemical environments such as flames and time-evolving chemical reactions. The technique provides an efficient method to sort a chemical mixture first by  $m/z$  ratio, and further by ionization energy and spectral shape at each  $m/z$  ratio for isomer identification. However, all techniques have their limits, and in some cases, mixtures of three or more isomers can be difficult or impossible to quantify by this technique.

Photoelectron spectroscopy would provide an improved spectral fingerprint, but for analysis of a time-evolving mixture of neutral molecules, we must use photoelectron photoion coincidence, pioneered by Tom Baer in this program, to collect such spectra. However, PEPICO (and other coincidence spectroscopies) suffer from so-called false coincidences, where electron/ion pairs that did not originate from the same neutral molecule contribute noise to the dataset. This noise limits the dynamic range of PEPICO to  $\sim 10^3$ . For our purposes of studying bimolecular chemical reactions, we often require dynamic range of  $10^5$  or better.

In collaboration with Drs. Andras Bodi and Patrick Hemberger of the Swiss Light Source, and Prof. Bálint Sztáray of the University of the Pacific, we have conceived, built, and now tested a scheme that eliminates essentially all false coincidences from PEPICO data. This advance relies on deflecting the ions using a time-varying electric field, while measuring both the time-of-flight and the spatial impact coordinates of each ion. A true coincidence (an electron/ion pair arising from the same neutral) has a predictable impact position, whereas a cation paired with an unrelated electron (a false coincidence) almost always has predicted and measured impact positions that differ. In this way, we can achieve a 2 to 3 order of magnitude improvement in dynamic range. This research is being submitted for publication.

## Future Plans

Prototype experiments for a new PEPICO spectrometer, incorporating this advance and several others, are now complete. In the next review period, we will design and build the new CRF-PEPICO spectrometer for operation at Sandia and the Advanced Light Source. It will enable better molecular fingerprints to help resolve chemical reaction mechanisms that are beyond our capabilities at present.

## BES-sponsored publications, 2014 – present

- 1) Formation and stability of gas-phase o-benzoquinone from oxidation of orth-hydroxyphenyl: a combined neutral and distonic radical study, M. B. Prendergast, B. B. Kirk, J. D. Savee, D. L. Osborn, C. A. Taatjes, K. S. Masters, S. J. Blanksby, G. da Silva, A. J. Treiff, *Phys. Chem. Chem. Phys.* **18**, 4320 (2016).
- 2) Low temperature chlorine-initiated oxidation of small-chain methyl esters: quantification of chain-terminating HO<sub>2</sub>-elimination channels, G. Muller, A. Scheer, D. L. Osborn, C. A. Taatjes, and G. Meloni, *J. Phys. Chem. A* DOI: 10.1021/acs.jpca.6b00148 (2016)
- 3) Photoelectron wave function in photoionization: plane wave or coulomb wave?, S. Gozem, A. O. Gunina, T. Ichino, D. L. Osborn, J. F. Stanton, and A. I. Krylov, *J. Phys. Chem. Lett.* **6**, 4532 (2015)
- 4) The C(<sup>3</sup>P) + NH<sub>3</sub> reaction in interstellar chemistry. I. Investigation of the product formation channels, J. Bourgalais, M. Capron, R.K.A. Kailasanathan, D. L. Osborn, K. M. Hickson, J. C. Loison, V. Wakelam, F. Goulay, and S. D. Le Picard, *Astrophys. J.*, **812**, 106 (2015).
- 5) Flow tube studies of the C(<sup>3</sup>P) reactions with ethylene and propylene, M. Capron, J. Bourgalais, R.K.A. Kailasanathan, D. L. Osborn, S. D. Le Picard, and F. Goulay, *Phys. Chem. Chem. Phys.* **17**, 23833 (2015).
- 6) Molecular weight growth in Titan's atmosphere: branching pathways for the reaction of 1-propynyl radical (H<sub>3</sub>CC≡C•) with small alkenes and alkynes, B. B. Kirk, J. D. Savee, A. J. Trevitt, D. L. Osborn, and K. R. Wilson, *Phys. Chem. Chem. Phys.* **17**, 20754 (2015).
- 7) Time- and Isomer-Resolved Measurements of Sequential Addition of Acetylene to the Propargyl Radical, J. D. Savee, T. M. Selby, O. Welz, C. A. Taatjes, and D. L. Osborn, *J. Phys. Chem. Lett.* **6**, 4153 (2015).

- 8) Multiscale Informatics for Low-Temperature Propane Oxidation: Further Complexities in Studies of Complex Reactions, M. P. Burke, C. F. Goldsmith, S. J. Klippenstein, O. Welz, H. Huang, I. O. Antonov, J. D. Savee, D. L. Osborn, J. Zador, C. A. Taatjes, and L. Sheps, *J. Phys. Chem. A* **119**, 7095 (2015).
- 9) New insights into low-temperature oxidation of propane from synchrotron photoionization mass spectrometry and multiscale informatics modeling, O. Welz, M. P. Burke, I. O. Antonov, C. F. Goldsmith, J. D. Savee, D. L. Osborn, C. A. Taatjes, S. J. Klippenstein, and L. Sheps, *J. Phys. Chem. A* **119**, 7116 (2015).
- 10) The physical chemistry of Criegee intermediates in the gas phase, D. L. Osborn and C. A. Taatjes, *Int. Rev. Phys. Chem.* **34**, 309 (2015).
- 11) Multiplexed photoionization mass spectrometry investigation of the  $O(^3P) +$  propyne reaction, J. D. Savee, S. Borkar, O. Welz, B. Sztáray, C. A. Taatjes, and D. L. Osborn, *J. Phys. Chem. A* **119**, 7388 (2015).
- 12) Low temperature (550-700 K) oxidation pathways of cyclic ketones: dominance of  $HO_2$ -elimination channels yielding conjugated cyclic coproducts, A. M. Scheer, O. Welz, S. S. Vasu, D. L. Osborn, C. A. Taatjes, *Phys. Chem. Chem. Phys.* **17**, 12124 (2015).
- 13) Synchrotron-based double imaging photoelectron/photoion coincidence spectroscopy of radicals produced in a flow tube: OH and OD, G. A. Garcia, X. F. Tang, J. F. Gil, L. Nahon, M. Ward, S. Batut, C. Fittschen, C. A. Taatjes, D. L. Osborn, and J. C. Loison, *J. Chem. Phys.* **142**, 164201 (2015).
- 14) VUV photoionization cross sections of  $HO_2$ ,  $H_2O_2$ , and  $H_2CO$ , L. G. Dodson, L. H. Shen, J. D. Savee, N. C. Eddingsaas, O. Welz, C. A. Taatjes, D. L. Osborn, S. P. Sander, and M. Okumura, *J. Phys. Chem. A* **119**, 1279 (2015).
- 15) Formation of fulvene in the reaction of  $C_2H$  with 1,3-butadiene, J. F. Lockyear, M. Fournier, I. R. Sims, J. C. Guilemin, C. A. Taatjes, D. L. Osborn, and S. R. Leone, *Int. J. Mass Spec.* **378**, 232 (2015).
- 16) Threshold photoelectron spectrum of the benzyl radical, J. D. Savee, J. Zádor, P. Hemberger, B. Sztáray, A. Bodi, and D. L. Osborn, *Mol. Phys.* **113**, 2217 (2015).
- 17) Chlorine atom-initiated low-temperature oxidation of prenyl and isoprenyl: The effect of  $C=C$  double bonds on the peroxy radical chemistry in alcohol oxidation, O. Welz, J. D. Savee, D. L. Osborn, and C. A. Taatjes, *Proc. Combust. Inst.* **35**, 401 (2015).
- 18) Direct observation and kinetics of a hydroperoxyalkyl radical (QOOH), J. D. Savee, E. Papajak, B. Rotavera, H. Huang, A. J. Eskola, O. Welz, L. Sheps, C. A. Taatjes, J. Zador, and D. L. Osborn, *Science* **347**, 643 (2015).
- 19) Photoionization Mass Spectrometric Measurements of Initial Reaction Pathways in Low-Temperature Oxidation of 2,5-Dimethylhexane, B. Rotavera, J. Zador, O. Welz, L. Sheps, A. M. Scheer, J. D. Savee, M. A. Ali, T. S. Lee, B. A. Simmons, D. L. Osborn, A. Violi, and C. A. Taatjes, *J. Phys. Chem. A* **118**, 10188 (2014).
- 20) Correction to Facile Rearrangement of 3-oxoalkyl radicals is evident in low-temperature gas-phase oxidation of ketones, A. M. Scheer, O. Welz, D. Y. Sasaki, D. L. Osborn, and C. A. Taatjes, *J. Am. Chem. Soc.* **136**, 8486 (2014).
- 21) Synchrotron photoionization study of mesitylene oxidation initiated by reaction with  $Cl(^2P)$  or  $O(^3P)$  radicals, M. Y. Ng, J. Nelson, C. A. Taatjes, D. L. Osborn, and G. Meloni, *J. Phys. Chem. A* **118**, 3735 (2014).
- 22) Probing the low-temperature chain-branching mechanism of *n*-butane autoignition chemistry via time-resolved measurements of ketohydroperoxide formation in photolytically initiated *n*- $C_4H_{10}$  oxidation, A. J. Eskola, O. Welz, J. Zador, I. O. Antonov, L. Sheps, J. D. Savee, D. L. Osborn, C. A. Taatjes, *Proc. Combust. Inst.* **35**, 291 (2015).
- 23) Influence of temperature and resonance-stabilization on the ortho- effect in cymene oxidation, B. Rotavera, A. M. Scheer, H. Huang, D. L. Osborn, and C. A. Taatjes, *Proc. Combust. Inst.* **35**, 543 (2015).
- 24) In situ soft X-ray absorption spectroscopy of flames, J. H. Frank, A. Shavorskiy, H. Bluhm, B. Coriton, E. Huang, and D. L. Osborn, *Appl. Phys. B* **117**, 493 (2014).
- 25) Electronic states of the quasilinear molecule propargylene (HCCCH) from negative ion photoelectron spectroscopy, D. L. Osborn, K. M. Vogelhuber, S. W. Wren, E. M. Miller, Y. J. Lu, A. S. Case, L. Sheps, R. J. McMahon, J. F. Stanton, L. B. Harding, B. Ruscic, and W. C. Lineberger, *J. Am. Chem. Soc.* **136**, 10361 (2014).
- 26) Low-Temperature Combustion Chemistry of Novel Biofuels: Resonance-Stabilized QOOH in the Oxidation of Diethyl Ketone, A. M. Scheer, O. Welz, J. Zádor, D. L. Osborn and C. A. Taatjes, *Phys. Chem. Chem. Phys.* **16**, 13027 (2014).
- 27) Rate Coefficients of C1 and C2 Criegee Intermediate Reactions with Formic and Acetic Acid Near the Collision Limit: Direct Kinetics Measurements and Atmospheric Implications, O. Welz, A. J. Eskola, L. Sheps, B. Rotavera, J. D. Savee, A. M. Scheer, D. L. Osborn, D. Lowe, A. M. Booth, P. Xiao, M. A. H. Khan, C. J. Percival, D. E. Shallcross, and C. A. Taatjes, *Angew. Chem.* **53**, 4547 (2014).
- 28) A coordinated investigation of the combustion chemistry of diisopropyl ketone, a prototype for biofuels produced by endophytic fungi, J.W. Allen, A.M. Scheer, C. Gao, S.S. Merchant, S.S. Vasu, O. Welz, J.D. Savee, D.L. Osborn, C. Lee, S. Vranckx, Z. Wang, F. Qi, R.X. Fernandes, W.H. Green, M.Z. Hadi, and C.A. Taatjes, *Combustion and Flame* **161**, 711 (2014).

## References

- <sup>1</sup> I. R. Slagle and D. Gutman, *J. Am. Chem. Soc.* **107**, 5342 (1985).
- <sup>2</sup> M. Frenklach, T. Yuan, and M. K. Ramachandra, *Energy Fuels* **2**, 462 (1988).
- <sup>3</sup> V. D. Knyazev and I. R. Slagle, *J. Phys. Chem. A* **106**, 5613 (2002).
- <sup>4</sup> G. da Silva, J. A. Cole, and J. W. Bozzelli, *J. Phys. Chem. A* **114**, 2275 (2010).

**Program Title:** A Theoretical Investigation of the Structure and Reactivity of the Molecular Constituents of Oil Sand and Oil Shale

**Principle Investigator:** Carol Parish

Address: Department of Chemistry, University of Richmond, Richmond, VA 23227  
cparish@richmond.edu

## **PROGRAM SCOPE**

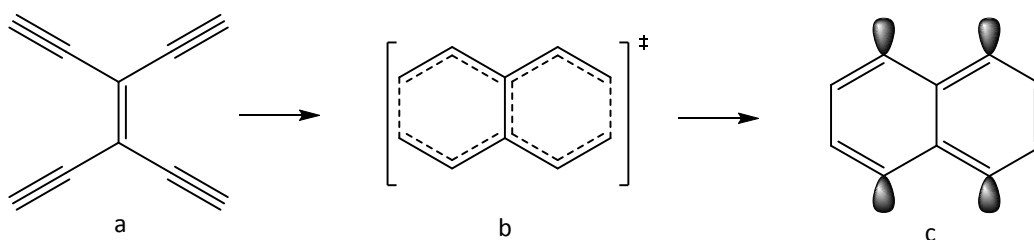
Our work focuses on the theoretical characterization of the gas phase structures, energies and reactivities of the molecular constituents of asphaltenes contained in oil sand and oil shale. Asphaltenes represent an untapped source of hydrocarbon fuel in North America; however, information about the molecular nature of these deposits has only recently become available. Theoretical and experimental evidence suggests that asphaltenes are composed of aromatic molecules that contain 4-10 fused ring cores, with alkyl chain arms extending from the core. Sulfur and nitrogen are also present. Very little is known about the reaction pathways, combustion efficiency and reactivity of these heteroaromatic species. We are currently characterizing the combustion and pyrolysis reaction channels available to asphaltene constituents such as thiophene and methyl thiophene.

## **RECENT PROGRESS - FY 2015 HIGHLIGHTS**

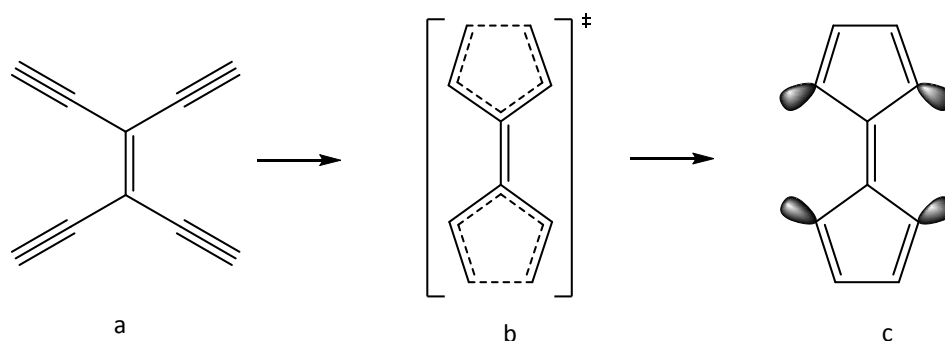
### **A Highly Correlated, Multireference Study of Aromatic Tetraradicals**

Tetradehydrobenzenes, or benzdiynes, comprise a large majority of recent efforts to characterize small organic tetraradicals. The sizable static and dynamic correlation effects in these polyradicals challenge most computational methods, and only a small body of experimental results exists for comparison. While metal complexes and large molecular systems with tetraradical character have been reported, this study focuses on small organic systems, for which a body of literature is unfortunately small. Derivatives of benzdiynes have been observed experimentally, and numerous computational studies have sought to determine the best methods for describing their physical characteristics including the identification of the most stable isomer and accurate determination of heats of formation. However, most computational work is limited to highly correlated single reference methods and unrestricted DFT, and the multireference problem still remains largely unresolved. We have utilized highly correlated, multireference quantum chemical methods to characterize the low lying electronic states of a tetradehydronaphthalene and tetradehydrofulvalene tetraradical formed by electrocyclization of tetraethynylethene. We find that that both forms of the tetraradical are stable and correspond to minima on the corresponding potential energy surface. The tetradehydronaphthalene tetraradical lies approximately 70 kcal/mol lower in energy than the fulvalene tetraradical. The barrier to a double 1,6 cyclization is substantially lower than the barrier to 1,5 double cyclization. MR results suggests a  $^1A_g$  ground state for the naphthalene tetraradical, in addition to a high-density cluster of six states near the ground state. The low spin ground state and its leading configurations imply that through bond coupling is the source

of stabilization in the singlet, which outweighs aromatic stabilizing effects that dominate the quintet. Analysis of geometries also suggests that through bond coupling has a stabilizing effect, and it likely occurs between radical centers on the same hemisphere, in addition to centers across hemispheres through the central bond. Preliminary data suggests the tetradehydrofulvalene has similar electronic properties to 2,5,7,10-tetradehydronaphthalene and a low spin ground state stabilized by through bond effects. This work is in preparation for submission to the *Journal of Physical Chemistry A*.



**Scheme 1.** 1,6 cyclization pathway of tetraethynylethene (a) through a transition state (b) to the tetradiradical product, 2,5,7,10-tetradehydronaphthalene



**Scheme 2.** 1,5 cyclization pathway of tetraethynylethene (a) through a transition state (b) to the tetradiradical product, 2,5-tetradehydrofulvalene

### Jahn-Teller Stabilization in POSS Cations: Octatert-butyl and Octachloro silsesquioxanes $\text{Si}_8\text{O}_{12}(\text{C}(\text{CH}_3)_3)_8^+$ and $\text{Si}_8\text{O}_{12}\text{Cl}_8^+$

Polyoligomeric silsesquioxanes (POSS) are molecules containing a rigid, cubic inorganic core  $\text{Si}_8\text{O}_{12}$  with Si atoms attached to organic or inorganic peripheral groups. These compounds have found many applications in polymer chemistry as they impart thermal stability when mixed with organic polymers to form nanostructured organic-inorganic hybrids. We have investigated the symmetry breaking mechanism in cubic octatert-butyl silsesquioxane and octachloro silsesquioxane monocations ( $\text{Si}_8\text{O}_{12}(\text{C}(\text{CH}_3)_3)_8^+$  and  $\text{Si}_8\text{O}_{12}\text{Cl}_8^+$ ) applying density functional theory (DFT) and group theory. Under  $O_h$  symmetry, these ions possess  ${}^2T_{2g}$  and  ${}^2E_g$  electronic states and undergo different symmetry breaking mechanisms. The ground states of  $\text{Si}_8\text{O}_{12}(\text{C}(\text{CH}_3)_3)_8^+$  and  $\text{Si}_8\text{O}_{12}\text{Cl}_8^+$  belong to the  $C_{3v}$  and  $D_{4h}$  point groups and are characterized by Jahn-Teller stabilization energies of 3959 and 1328  $\text{cm}^{-1}$ ; respectively, at the B3LYP/def2-SVP level of

theory. The symmetry distortion mechanism in  $\text{Si}_8\text{O}_{12}\text{Cl}_8^+$  is Jahn-Teller type, whereas in  $\text{Si}_8\text{O}_{12}(\text{C}(\text{CH}_3)_3)_8^+$  the distortion is a combination of both Jahn-Teller and pseudo-Jahn-Teller effects. The distortion force acting in  $\text{Si}_8\text{O}_{12}(\text{C}(\text{CH}_3)_3)_8^+$  is mainly localized on one Si-(tert-butyl) group while in  $\text{Si}_8\text{O}_{12}\text{Cl}_8^+$  it is concentrated on the oxygen atoms. In these ionic compounds, the main distortion forces acting on the  $\text{Si}_8\text{O}_{12}$  core arise from the coupling between the electronic state and the vibrational modes; identified as  $9t_{2g}+1e_g+3a_{2u}$  for the  $\text{Si}_8\text{O}_{12}(\text{C}(\text{CH}_3)_3)_8^+$  and  $1e_g+2e_g$  for  $\text{Si}_8\text{O}_{12}\text{Cl}_8^+$ . This work has been published in the *Journal of Physical Chemistry A*.

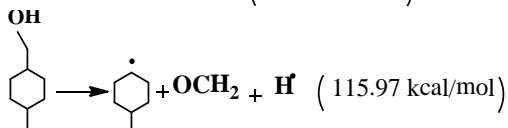
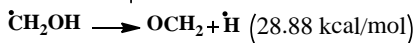
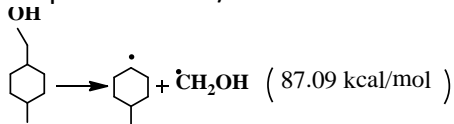
### **Ground and low-lying valence excited states of didehydrothiophene diradicals: A multireference comparison study**

High-level multireference theories (MCSCF, MRCISD, MRCISD+Q and MRAQCC at ccpVdz and ccpVtz levels) using an active space of 8 eight electrons (for 2,5DDTH) and ten electrons in eight orbitals (for all other isomers), CAS(8,8) and CAS(10,8), were employed to investigate the ground and low-lying excited states of all four didehydrothiophenes (DDTHs). Both state averaged and single state reference MCSCF wave functions were used for high symmetrical structures,  $C_{2v}$ . These computational methods consistently predict the singlet state as the ground state and with a singlet-triplet (S-T) adiabatic energy gap of 15-23 kcal/mol indicative of through bonds coupling. The 2,3-DDTH presents the highest S-T splitting energies of 23.53 kcal/mol at MRAQCC/ccpVtz. The remaining DDTHs have quite similar S-T splitting energies  $\sim 16$  kcal/mol at MRAQCC/ccpVtz. A comparison between different multireference methods reveals a competitive performance between MRAQCC and MR-CISD+Q. The lowest energy isomer is 2,3-didehydrothiophene on the basis of the computed total electronic energies (MRAQCC/ccpVtz and MRCISD+Q/ccpVtz) and the CCSD(T)/6-311++G(3df,2p) single points energies of the MRAQCC/ccpVtz optimized geometries. The 2,3-DDTH isomer has the strongest C-C bond, close to ethyne C-C triple bond. However, an examination of the electronic structure and NBO analysis show 2,3 and 2,5-DDTH to have the lowest and highest diradical character, respectively. Similar to o-benzyne, the latter can be considered a strained alkyne. In general, the singlet-triplet splitting energies of all didehydrothiophenes are smaller than in the benzyne suggesting them to be more reactive systems. This work is in preparation for submission to the *Journal of Physical Chemistry A*.

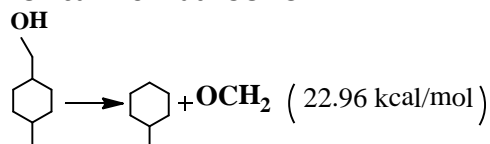
### **A First Principle Study of the Thermal Decomposition of (4-Methylcyclohexane)methanol, $\text{C}_8\text{H}_{15}\text{OH}$ – Is the Formation of Formaldehyde a Possibility?**

On January 9, 2014 (4-methylcyclohexane)methanol (4-MCHM) was inadvertently released into the Elk River in Charleston, West Virginia. Very little is known about the effect of MCHM on human health and initial news reports suggested that MCHM breaks down to form formaldehyde. We have investigated the probable initial steps of the thermal decomposition pathways of 4-MCHM and examined possible formation of formaldehyde using various quantum chemical methods such as B3LYP/6-311++G(d,p), MP2/6-311++G(d,p), CCSD(T)/6-31G(d,p), G3B3, G4, G4MP2 and CBS-QB3. For the reaction,  $^{\bullet}\text{CH}_2\text{OH} \rightarrow \text{CH}_2\text{O} + \text{H}^{\bullet}$ , the W1BD theory was also employed. The C-C bond rupture between the cyclohexane ring and the

methanol group in 4-MCHM is a predicted precursor of the thermal decomposition of 4-MCHM and requires 87 kcal/mol for bond homolysis at CS-QB3 level.



The production of formaldehyde and methylcyclohexyl arising from the decomposition of 4-MCHM is found to be endothermic ( $\Delta H_f = 115 \text{ kcal/mol}$ ) and is unlikely to occur at ambient temperature without any specific catalyst. The enthalpy of the decomposition reaction of the 4-methylcyclohexylmethanol in 4-methylcyclohexane and formaldehyde stable species is about  $23 \text{ kcal mol}^{-1}$  at 298.15K.



The total atomization energy at 0K and enthalpy of formation of 4-MCHM at 298.15K calculated at the same level of theory (CBS-QB3) amount to 2555 and -322 kcal/mol, respectively. This work is in preparation for submission to the *Journal of Physical Chemistry A*.

## FUTURE WORK

Work is currently underway to characterize the electrocyclizations of penta-, hepta- and octa-diyne as well as the ground and excited states of heteroaromatic diradicals such as thiophene, fulvene and pyrrole. We are also pursuing a complete characterization of the singlet and triplet surfaces of the electrocyclization reaction of (Z)-hexa-1,3,5-triene leading to *p*-benzyne as well as a characterization of the endo and exo-dig radical cyclization reactions.

## PUBLICATIONS

1. "Jahn-Teller Stabilization in POSS Cations", Jules Tshishimbi Muya, Arnout Ceulemans, Gopinadhanpillai Gopakumar and Carol A. Parish\*, *Journal of Physical Chemistry A*, **2015**, *119*, 4237-4243.
2. "Mechanisms for the reaction of thiophene and methylthiophene with singlet and triplet molecular oxygen," Xinli Song, Matthew G. Fanelli, Justin M. Cook, Furong Bai and Carol A. Parish\*, *Journal of Physical Chemistry A*, **2012** *116*, 4934-4946.
3. "A Mechanistic Study of the 2-Thienylmethyl + HO<sub>2</sub> Radical Recombination Reaction," Xinli Song and Carol Parish,\* *Journal of Physical Chemistry A*, **2011**, *115*, 14546-14557
4. "Pyrolysis Mechanisms of Thiophene and Methylthiophene in Asphaltenes," Xinli Song and Carol Parish,\* *Journal of Physical Chemistry A* **2011**, *115*, 2882-2891.

# Chemical Kinetic Modeling of Combustion Chemistry

William J. Pitz, Charles K. Westbrook  
Lawrence Livermore National Laboratory, Livermore, CA 94550  
pitz1@llnl.gov

## 1. Program Scope

We develop chemical kinetic reaction mechanisms to describe the combustion of hydrocarbons and other related fuels, including fuels derived from biomass. These mechanisms are validated through comparisons between computations and experimental results in carefully controlled laboratory-scale facilities including shock tubes, laminar flames, stirred reactors, and rapid compression machines. After validation, these mechanisms are then used to understand more complex combustion phenomena in practical engines and other combustion systems. We determine particularly sensitive parts of these mechanisms and provide that information to other DOE/BES researchers who can use theory and new experiments to refine the kinetic models. We try to anticipate kinetic modeling needs of the DOE combustion community, so other researchers can have accurate models to assist in their own research projects. Our kinetic mechanisms are freely available at <https://combustion.llnl.gov/> and provide a valuable service to the combustion community.

## 2. Recent Progress

Since kinetic reaction mechanisms can be large and complex, we try to identify specific reaction classes that can apply to many different types of fuel molecules. Some examples of reaction classes include H-atom abstraction, radical decomposition, addition of O<sub>2</sub> to hydrocarbon radicals, alkyl and alkylperoxy radical isomerization; current models consider nearly 30 reaction classes. When this project began in about 1980, very few of the reaction classes, especially those dealing with complex radical isomerization and addition reactions of O<sub>2</sub> to alkyl and related radical species, had been studied using either chemical theory or direct laboratory experiments, so most of these important reaction classes had to use estimated rates, usually based on similar but sometimes not very close chemical analogies. In the past few years, new theory, new experiments, and new kinetic modeling approaches have greatly improved the accuracy of these kinetic models. In many cases, our publications of kinetic models and modeling results stimulated new attention for others to contribute new theoretical and experimental studies that were extremely useful, and this type of exchange accelerates the development of more accurate and powerful kinetic models.

### A. Reaction rate rules for alkane fuels

Reaction rates in the alkylperoxy radical isomerization pathways have received an enormous amount of excellent kinetic theory attention in the past 3-5 years, requiring us to revise thoroughly all of the low temperature reaction rates and reaction pathways. In particular, in the past two years we have done a complete renovation of the low temperature kinetics of saturated hydrocarbons and produced much improved agreement between computed and experimental observations. This work is in collaboration with Prof. Curran at the NUIG and Prof. Sarathy at KAUST and will be continued into the next year to complete the renovation of our n-alkane (n-decane to n-eicosane), branched alkanes (2-methyl hexane to 2-methyl nonadecane), and primary reference fuels (PRF) (iso-octane, iso-cetane) that are an important part of the legislated quality

controls of engine fuels. At first, we had assumed that the reaction rate rules governing low temperature alkylperoxy radical isomerization and cool flame pathways, depended only on the transition state ring size and the C-H bonds being broken and formed, but the new theory studies, combined with inaccurate model predictions, led to a conclusion that the overall structure of the fuel molecule plays a stronger role in determining the reaction rate rules than previously believed, and the new rules are now being implemented into our new kinetic models.

### B. Reaction rate rules for multiple fuel classes and Octane Sensitivity

We extended our past studies of weak, allylic C-H bonds in the small olefin fuel 2-methyl 2-butene [1] to study the kinetics of classes of weak C-H bonds in a wide variety of other hydrocarbon fuels. Specifically, we have discovered that benzylic bonds in alkyl benzenes, as well as C-H bonds adjacent to the OH group in alcohol fuels, and C-H bonds adjacent to the alkyl ester group in biodiesel and other alkyl ester fuels have the same effect as allylic C-H bonds in olefin fuels of inhibiting low temperature cool flame reactivity. We have traced this macroscopic effect to the theoretical phenomenon of electron delocalization in these fuel molecules, which then produces resonance stabilization in the hydrocarbon radical species produced via H atom abstraction from these fuels. This work has shown that such weak bonds encourage rapid H atom abstraction, but the resulting hydrocarbon radicals are too stable to react at low temperatures, in contrast with hydrocarbon fuels like n-heptane that react very rapidly via cool flame kinetics and radical isomerization reactions. We have been able to relate this phenomenon to Octane Sensitivity, where a fuel has a high Research Octane Number (RON) but a surprisingly low Motored Octane Number (MON), resulting in a high Octane Sensitivity  $S$ , defined as  $RON - MON = S$ . A high Octane Sensitivity has unusual advantages for use under “boosted” operating conditions, where fuel is injected into a Spark-Ignition (SI) engine at elevated intake pressures to increase power production in that engine. Fuels with zero or low Sensitivity will respond to boosted fuel injection with engine knock, but fuels with considerable Octane Sensitivity can withstand such elevated intake pressures without knocking. We have coordinated our kinetic model development and analysis with colleagues at Sandia National Laboratories, initiating further theoretical studies by Dr. Judit Zador and Dr. David Osborne of SNL to compute new reaction pathways and reaction rates of key elementary reactions that we identified in our kinetic modeling studies. We also collaborated with engine design studies of Dr. Magnus Sjoberg at SNL to provide a computer model to use our detailed kinetic mechanisms to predict fuel Octane Numbers for engine designers who would like to design fuels and engines together to enhance performance and limit emissions. The composite kinetic model used for this study [2] represents the largest, most comprehensive such reaction mechanism produced to date and offers enormous potential for further use by our group and many others on complex fuel analysis and practical applications. This collaborative effort will continue in the coming year.

### C. Reaction rate rules for cyclohexanes and cyclo-benzenes

Our ongoing detailed kinetic modeling studies of the important class of alkyl benzene hydrocarbon fuels, including toluene (methyl benzene) [3], n-propyl benzene [4] and n-butyl benzene [5] were utilized in the above analyses of octane sensitivity and their contributions to ignition and combustion in engines. In this process, we found again that the presence of the aromatic ring produces a sufficiently different electronic environment that most or all of the low temperature radical isomerization and many other kinetic classes required new reaction rate rules. In similar studies on cycloalkanes, specifically cyclopentane [6], new reaction class rules

were required to be able to produce the low degree of low temperature kinetic behavior that is observed in experiments, and we found that, in contrast with aromatic fuels of similar size and complexity, the cycloalkanes do not appear to show electron delocalization that would contribute to octane sensitivity. Instead, in the case of cyclopentane, it suppresses low temperature chemistry because its six-membered ring alkylperoxy (RO<sub>2</sub>) isomerization reactions are relatively slow compared to other hydrocarbons that exhibit significant low temperature chemistry.

### 3. Future Plans

We plan to continue developing kinetic mechanisms for fuels important for energy production in modern engines, including conventional reciprocating engines as well as promising next-generation engine and gas turbines, and using these models to address practical combustion problem. We welcome the contributions of more fundamental scientists and engineers who can help us refine the current and upcoming kinetic models to improve their functionality.

### References

1. Paper 4 below.
2. Westbrook, C. K., Mehl, M., Pitz, W. J. and Sjöberg, M., "Chemical Kinetics of Octane Sensitivity in a Spark Ignition Engine," *Combustion and Flame* (2016), submitted.
3. Paper 1 below.
4. Paper 14 below.
5. Paper 15 below.
6. Paper 2 below.

### Published papers in 2014 to 2016

1. Zhang, Y., Somers, K., Mehl, M., Pitz, W. J., Cracknell, R. and Curran, H. J., "Probing the Antagonistic Effect of Toluene as a Component in Surrogate Fuel Models at Low Temperatures and High Pressures. A Case Study of Toluene/Dimethyl Ether Mixtures," *Proceedings of the Combustion Institute* (2016), accepted.
2. Al Rashidi, M. J., Thion, S., Togbé, C., Dayma, G., Mehl, M., Dagaut, P., Pitz, W. J., Zádor, J. and Sarathy, S. M., "Elucidating Reactivity Regimes in Cyclopentane Oxidation: Jet Stirred Reactor Experiments, Computational Chemistry, and Kinetic Modeling," *Proceedings of the Combustion Institute* (2016), accepted.
3. Sarathy, S. M., Kukkadapu, G., Mehl, M., Javed, T., Ahmed, A., Naser, N., Tekawade, A., Kosiba, G., Abbad, M. A., Singh, E., Park, S., Rashidi, M. A., Chung, S. H., Roberts, W. L., Oehlschlaeger, M. A., Sung, C.-J. and Farooq, A., "Compositional Effects on the Ignition of Face Gasoline Fuels," *Combustion and Flame* (2016), accepted.
4. Westbrook, C. K., Pitz, W. J., Mehl, M., Glaude, P. A., Herbinet, O., Bax, S., Battin-Leclerc, F., Mathieu, O., Petersen, E. L., Bugler, J. and Curran, H. J., "Experimental and Kinetic Modeling Study of 2-Methyl-2-Butene: Allylic Hydrocarbon Kinetics," *Journal of Physical Chemistry A* 119 (28) (2015) 7462-7480.
5. Mehl, M., Herbinet, O., Dirrenberger, P., Bounaceur, R., Glaude, P.-A., Battin-Leclerc, F. and Pitz, W. J., "Experimental and Modeling Study of Burning Velocities for Alkyl Aromatic Components Relevant to Diesel Fuels," *Proc. Combust. Inst.* 35 (2015) 341-348.

6. Goldsborough, S. S., Johnson, M. V., Banyon, C., Pitz, W. J. and McNenly, M. J., "Experimental and Modeling Study of Fuel Interactions with an Alkyl Nitrate Cetane Enhancer, 2-Ethyl-Hexyl Nitrate," *Proc. Combust. Inst.* 35 (1) (2015) 571–579.
7. Nakamura, H., Curran, H., Córdoba, A. D. P., Pitz, W. J., Dagaut, P., Togbé, C., Sarathy, S. M., Mehl, M., Agudelo, J. and Bustamante, F., "An Experimental and Modeling Study of Diethyl Carbonate Oxidation," *Combust. Flame* 162 (4) (2015) 1395–1405.
8. Kukkadapu, G., Kumar, K., Sung, C.-J., Mehl, M. and Pitz, W. J., "Autoignition of Gasoline Surrogates at Low Temperature Combustion Conditions," *Combustion and Flame* 162 (5) (2015) 2272-2285.
9. Korobeinichev, O.P., Gerasimov, I.E., Knyazkov, D.A., Shmakov, A.G., Bolshova, T.A., Hansen, N., Westbrook, C.K., Dayma, G., and Yang, B., "An Experimental and Kinetic Modeling Study of Premixed Laminar Flames of Methyl Pentanoate and Methyl Hexanoate", *Z. Phys. Chem.* 229 (5) (2015) 759-780.
10. Kumar, K., Zhang, Y., Sung, C.-J. and Pitz, W. J., "Autoignition Response of N-Butanol and Its Blends with Primary Reference Fuel Constituents of Gasoline," *Combustion and Flame* 162 (6) (2015) 2466-2479.
11. Burke, U., Pitz, W. J. and Curran, H. J., "Experimental and Kinetic Modeling Study of the Shock Tube Ignition of a Large Oxygenated Fuel: Tri-Propylene Glycol Mono-Methyl Ether," *Combustion and Flame* Propylene Glycol Mono-Methyl Ether," *Combustion and Flame* 162 (7) (2015) 2916–2927.
12. Li, S., Sarathy, S.M., Davidson, D.F., Hanson, R.K., and Westbrook, C.K., "Shock tube and modeling study of 2,7-dimethyloctane pyrolysis and oxidation", *Combust. Flame* 162 (5) (2015) 2296-2306.
13. Wagnon, S.W., Karwat, D.M.A., Wooldridge, M.S., and Westbrook, C.K., "Experimental and Modeling Study of Methyl trans-Hexenoate Autoignition", *Energy & Fuels* 28, 7227-7234 (2014).
14. Darcy, D., Nakamura, H., Tobin, C. J., Mehl, M., Metcalfe, W. K., Pitz, W. J., Westbrook, C. K. and Curran, H. J., "A High-Pressure Rapid Compression Machine Study of n-Propylbenzene Ignition," *Combust. Flame* 161 (1) (2014) 65-74.
15. Nakamura, H., Darcy, D., Mehl, M., Tobin, C. J., Metcalfe, W. K., Pitz, W. J., Westbrook, C. K. and Curran, H. J., "An Experimental and Modeling Study of Shock Tube and Rapid Compression Machine Ignition of n-Butylbenzene/Air Mixtures," *Combust. Flame* 161 (1) (2014) 49-64.
16. Darcy, D., Nakamura, H., Tobin, C. J., Mehl, M., Metcalfe, W. K., Pitz, W. J., Westbrook, C. K. and Curran, H. J., "An Experimental and Modeling Study of a Surrogate Mixtures of n-Propyl- and n-Butylbenzene in n-Heptane to Simulate n-Decylbenzene Ignition," *Combust. Flame* 161 (6) (2014) 1460-1473.
17. Sarathy, S. M., Javed, T., Karsenty, F., Heufer, A., Wang, W., Park, S., Elwardany, A., Farooq, A., Westbrook, C. K., Pitz, W. J., Oehlschlaeger, M. A., Dayma, G., Curran, H. J. and Dagaut, P., "A Comprehensive Combustion Chemistry Study of 2,5-Dimethylhexane," *Combust. Flame* 161 (6) (2014) 1444–1459.
18. Weber, B. W., W. J. Pitz, M. Mehl, E. J. Silke, A. C. Davis and C.-J. Sung (2014). "Experiments and Modeling of the Autoignition of Methylcyclohexane at High Pressure." *Combust. Flame* 161 (8) (2014).

# INVESTIGATION OF NON-PREMIXED TURBULENT COMBUSTION

Grant: DE-FG02-90ER14128

Stephen B. Pope & Perrine Pepiot  
Sibley School of Mechanical & Aerospace Engineering  
Cornell University, Ithaca, NY 14853  
s.b.pope@cornell.edu, pp427@cornell.edu

## 1 Scope of the Research Program

The underlying theme of this work is the development of computational approaches which allow our detailed knowledge of the chemical kinetics of combustion to be applied to the modeling and simulation of combustion devices. The principal modeling approaches used are large-eddy simulation (LES) to describe the flow and turbulence, and particle-based probability density function (PDF) methods to treat the turbulence-chemistry interactions. Research is currently focused on the development and validation of a pre-partitioned adaptive chemistry (PPAC) approach for use in LES-PDF simulations, in which individual particles evolve according to a reduced set of kinetic equations tailored for their specific compositions, thereby significantly reducing both the time and memory required for a computation with a given kinetic mechanism, and enabling affordable computations with significantly more detailed chemistry descriptions.

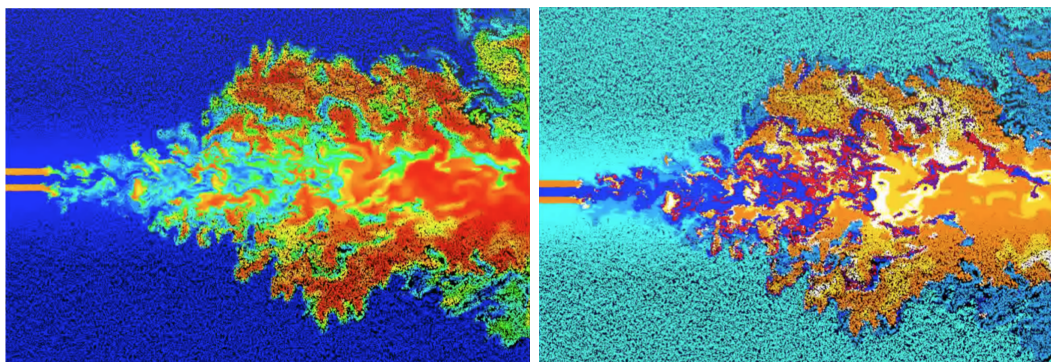
## 2 Recent Progress - An Adaptive Methodology to Implement Detailed Chemistry in LES/PDF

The principal research results from this program are described in the publications listed in Section 4. We have developed a pre-partitioned adaptive chemistry (PPAC) methodology tailored to LES/PDF simulations, in which each particle is assigned a specialized reduced representation and chemical model tailored to their individual composition. Instead of performing chemical reduction at runtime to determine the optimal set of equations to use for a given particle, an analysis of the composition space region likely accessed during the turbulent flow simulation is conducted first, in order to *a priori* partition the composition space into a user-specified number of regions. Suitable reduced chemical representations and chemical models are then identified for each region. This is done automatically using the Directed Relation Graph with Error Propagation (DRGEP) method, extended to simultaneously eliminate non-important species and reactions. In the LES/PDF simulation, a computational particle evolves according to, and carries only the variables present in the reduced representation corresponding to the composition space region it belongs to, thereby simultaneously reducing both the CPU time and memory cost of the simulation. This region is identified using a low-dimensional binary tree search algorithm, thereby keeping the run-time overhead associated with the adaptive approach to a minimum.

A preliminary assessment of the PPAC methodology in LES/PDF has been conducted in NGA [1] using a two-dimensional piloted methane/air flame configuration similar to Sandia Flame D. The PDF solver, directly integrated into NGA, is adapted from [2] in order to conveniently account for the multiple chemical models required by the adaptive approach. The chemical kinetic model for methane oxidation, with 38 species, is taken from [3]. To serve as reference for accuracy

and timing purposes, the flame is first simulated with the detailed chemical kinetics and without adaptive chemistry, until a statistically stationary state is reached. Gas phase compositions are then randomly sampled from the particle field, and fed to the PPAC pre-processing algorithm to generate a partition of the composition space, along with appropriate reduced representations and reduced kinetic models. All tests are carried out with  $N_R = 10$  regions. The accuracy of the reduced models is controlled by a single reduction error threshold  $\varepsilon$ . The flame simulation is restarted from a statistically stationary state with PPAC turned on, and the results are compared to those obtained in the reference, non-adaptive case.

Figure 1 illustrates the instantaneous distribution of reduced representations (and therefore models) used by the PDF particles throughout the domain. Figure 1(a) shows the particles colored according to their temperature, while Fig. 1(b) shows them colored according to the reduced representation they are carrying, with one unique color associated with each of the  $N_R$  representations. The main observation is that, for this case, clear regions can be identified, over which a single model, and therefore, a specific chemistry, dominates. For example, as expected, particles in the surrounding cold air co-flow all carry the same reduced representation and evolve according to the same reduced kinetic model containing a very small number of species and no reactions.



(a) Particles colored according to their temperature. (b) Particles colored according to their reduced representation and chemical model (one color per representation).

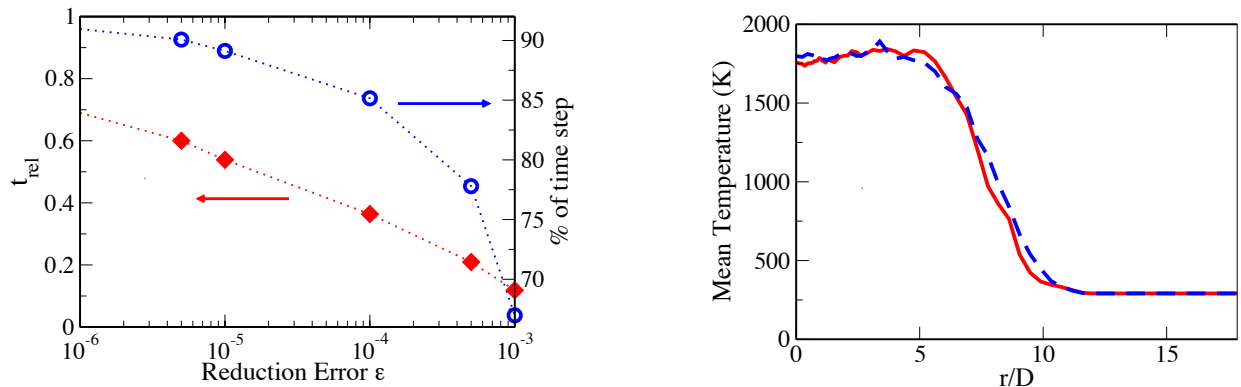
Figure 1: Particle field in the LES/PDF adaptive simulation of a two-dimensional piloted methane/air flame. PPAC with an error threshold of  $\varepsilon = 10^{-4}$  is used.

A comprehensive assessment of the performance of the PPAC strategy must combine accuracy and computational savings. For that purpose, the simulation described above was carried out several times, with varying reduction error thresholds  $\varepsilon$ . Note that changing  $\varepsilon$  does not change the partition of the composition space into regions, but only the level of reduction (and therefore, accuracy) of the kinetic models generated for each region. Figure 2(a) shows some timing comparisons between the adaptive and non-adaptive, or reference, simulations, plotted as function of the reduction error threshold  $\varepsilon$ :

- The red diamonds (left axis) provide the ratio between the time spent in integrating the chemistry in the adaptive simulations and the time spent integrating the chemistry in the reference case ( $t_{\text{rel}}$ ). We observe that even with very low reduction error thresholds, integrating the chemistry in adaptive simulations only require around 60% of the time spent in the reference case. This is due to the ability of the PPAC strategy to correctly identify compositions, for

example in the co-flow, that can be considered as chemically inert, and eliminating the need of integrating the chemical source terms for those compositions without introducing inaccuracies. As  $\varepsilon$  increases, the size of the reduced models decreases, thereby decreasing chemistry CPU costs by an order of magnitude at  $\varepsilon = 10^{-3}$ .

- The blue circles (right axis) show the percentage of time per time step spent in chemistry-related routines. Without PPAC or any additional acceleration strategy such as In-Situ Adaptive Tabulation, 90% of the computational time is spent integrating the chemical equations. This percentage decreases significantly as adaptivity is used, reaching less than 70% for  $\varepsilon = 10^{-3}$ . We expect ISAT to further decrease this contribution.



(a) Timing comparisons between non-adaptive and adaptive simulations for varying error thresholds  $\varepsilon$ : ratio between the time spent in integrating the chemistry in the adaptive simulations and the time spent integrating the chemistry in the reference case (red diamonds, left axis), and percentage of the time per time step spent in chemistry-related routines for the adaptive simulations (blue circle, right axis).

(b) Radial profiles of mean temperature at the  $x/D = 45$  axial location. Comparison between the non-adaptive, detailed chemistry simulation (red, solid line) and the PPAC simulation with an error threshold  $\varepsilon = 10^{-4}$  (blue, dashed line).

Figure 2: Preliminary assessment of PPAC performance in LES/PDF simulation of a 2D flame.

To relate timings and accuracy, Figure 2(b) displays a comparison between the adaptive and non-adaptive mean temperature profile at  $x/D = 45$  downstream of the nozzle, collected over one flow-through time, showing very good agreement between the two, and thereby demonstrating the limited impact of model reduction and adaptive approach on the temperature predictions.

### 3 Future Plans

The work in the near future will focus on further performance assessment and optimization of the PPAC adaptive strategy in LES/PDF using larger chemical kinetic mechanisms.

### 4 Publications from DOE Research 2013-2016

1. R.R. Tirunagari, M.W.A. Pettit, A.M. Kempf, S.B. Pope (2015) "A Simple Approach for Specifying Velocity Inflow Boundary Conditions in Simulations of Turbulent Opposed-Jet Flows", *Flow, Turb. Combust.*, submitted for publication.
2. R.R. Tirunagari, S.B. Pope (2015) "LES/PDF for Premixed Combustion in the DNS Limit", *Combust. Th. Model.*, submitted for publication.

3. R.R. Tirunagari, S.B. Pope (2016) “Characterization of extinction/re-ignition events in turbulent premixed counterflow flames using strain-rate analysis”, *Proc. Combust. Inst.*, accepted.
4. R.R. Tirunagari, S.B. Pope (2016) “An Investigation of Turbulent Premixed Counterflow Flames using Large-Eddy Simulations and Probability Density Function Methods”, *Combust. Flame* 166, 229–242.
5. Y. Liang, S. B. Pope, and P. Pepiot (2015) “An adaptive methodology for the efficient implementation of combustion chemistry in particle PDF methods”, *Combust. Flame* 162, 3236–3253.
6. M. Mehta, R. O. Fox, and P. Pepiot. (2015) “Reduced chemical kinetics for the modeling of TiO<sub>2</sub> nanoparticle synthesis in flame reactors”, *Ind. Eng. Chem. Res.* 54, 5407–5415.
7. K. Narayanaswamy, P. Pitsch, and P. Pepiot (2015) “A chemical mechanism for low to high temperature oxidation of methylcyclohexane as a component of transportation fuel surrogates”, *Combust. Flame*, 162, 1193–1213.
8. Pope, S. B. (2014) “The determination of turbulence-model statistics from the velocity-acceleration correlation”, *J. Fluid Mech.* 757, R1, DOI:10.1017/jfm.2014.563.
9. Pope, S. B. and R. Tirunagari (2014) “Advances in probability density function methods for turbulent reactive flows”, In *Proceedings of the Nineteenth Australasian Fluid Mechanics Conference*. RMIT University, Melbourne.
10. Popov, P. and S. B. Pope (2014) “Large eddy simulation/probability density function simulations of bluff body stabilized flames”, *Combust. Flame* 161, 3100–3133.
11. K. Narayanaswamy, P. Pepiot, and P. Pitsch (2014) “A chemical mechanism for low to high temperature oxidation of *n*-dodecane as a component of transportation fuel surrogates”, *Combust. Flame*, 161, 866–884.
12. Hiremath, V., S. R. Lantz, H. Wang, and S. B. Pope (2013) “Large-scale parallel simulations of turbulent combustion using combined dimension reduction and tabulation of chemistry”, *Proc. Combust. Inst.* 34, 205–215.
13. Hiremath, V. and S. B. Pope (2013) “A study of the rate-controlled constrained-equilibrium dimension reduction method and its different implementations”, *Combust. Theory Modelling* 17, 260–293.
14. Pope, S. B. (2013) “A model for turbulent mixing based on shadow-position conditioning”, *Phys. Fluids* 25, 110803.
15. Pope, S. B. (2013) “Small scales, many species and the manifold challenges of turbulent combustion”, *Proc. Combust. Inst.* 34, 1–31.
16. Ren, Z., G. M. Goldin, V. Hiremath, and S. B. Pope (2013) “Simulations of a turbulent non-premixed flame using combined dimension reduction and tabulation for combustion chemistry”, *Fuel* 105, 636–644.

## References

- [1] O. Desjardins, G. Blanquart, G. Balarac, and H. Pitsch. *J. Comput. Phys.*, 227 (2008) 7125–7159.
- [2] H. Wang and S. B. Pope. *Proc. Combust. Inst.*, 33 (2011) 1319–1330.
- [3] G. Esposito and H.K. Chelliah, *Combust. Flame*, 158 (2011) 1477–489.

## OPTICAL PROBES OF ATOMIC AND MOLECULAR DECAY PROCESSES

S.T. Pratt  
Building 200, B-125  
Argonne National Laboratory  
9700 South Cass Avenue  
Argonne, Illinois 60439  
E-mail: spratt@anl.gov

### PROGRAM SCOPE

The study of molecular photoabsorption, photoionization, and photodissociation dynamics can provide considerable insight into how energy and angular momentum flow among the electronic, vibrational, and rotational degrees of freedom in isolated, highly energized molecules. This project involves the study of these dynamics in small molecules, with an emphasis on understanding the mechanisms of intramolecular energy flow and determining how these mechanisms influence decay rates and product branching ratios. Such studies also shed light on related collision processes such as dissociative recombination, providing a connection between spectroscopy and dynamics. In recent years, one focus of the project has been trying to understand the factors that determine and influence photoabsorption and photoionization cross sections, as well as dissociative ionization processes. The experimental approach combines a variety of laser-based techniques, including nonlinear methods to generate tunable vacuum ultraviolet light, and double-resonance methods to prepare selected excited states of the species of interest. The detection methods include mass spectrometry, photoion- and photoelectron-imaging, and high-resolution photoelectron spectroscopy, which are used to characterize the decay processes of the selected excited states. In addition, synchrotron-based photoabsorption spectroscopy is now being used to provide high resolution spectra both above and below the ionization threshold, and synchrotron photoelectron-photoion coincidence experiments are being performed to characterize autoionization processes in small molecules and radicals. Finally, experiments enabled by the new vuv and x-ray free electron laser sources are being explored.

### RECENT PROGRESS

Over the past year we have performed experiments both in the laboratory at Argonne and at synchrotron facilities, in particular, the Soleil Synchrotron. We have also spent a significant amount of time analyzing results from earlier experiments.

#### *High-Resolution Photoabsorption Studies of Alkynes*

We have continued our project to study the photoabsorption spectra of a series of alkyne molecules using the Fourier-transform vacuum-ultraviolet spectrometer at the Soleil Synchrotron facility. This past year we worked on the analysis of the data for the butynes, pentynes, and hexynes, with an emphasis on the shape resonances observed just above threshold for the internal alkynes (i.e., 2-butyne, 2-pentyne, and 2- and 3-hexyne). As illustrated in Figure 1 for the hexynes, while these resonances can be quite strong in the internal alkynes, they are not present in the 1-alkynes. Qualitative arguments based on the nature of the highest occupied molecular orbitals and calculations on 2-butyne suggest that the relevant HOMOs have significant  $l = 3$  character, and that the shape resonance has  $l = 4$  or  $g$  character. New calculations were performed on the other alkynes to determine if this behavior extended to the larger molecules. Unfortunately, while the initial calculations showed that there was significant  $l = 4$  character in the outgoing partial waves, the presence of the shape resonances for the internal alkynes was not at all obvious. However, this past year it was realized that because these species had two nearly degenerate ionization channels (2-butyne has higher symmetry and the two channels are degenerate), and that a single-channel calculation was not sufficient to describe the photoionization process. Subsequently, two-channel calculations were performed that not only show interference between the ionization channels, but also clearly show the expected shape resonance behavior. These results have now been published in the Journal of Physical Chemistry A. Because the effects of the near-threshold shape resonance will also extend below the ionization threshold, we are continuing to work on the analysis of the bound state

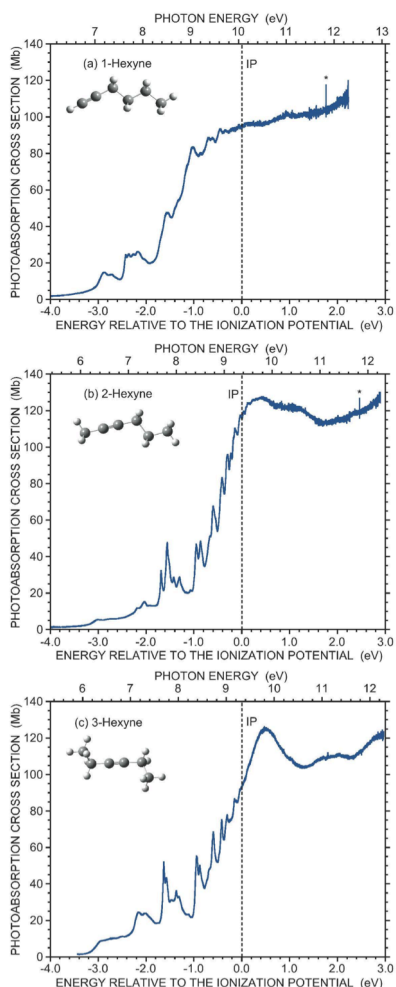


Figure 1. The photoabsorption spectra of 1-, 2-, and 3-hexyne. The latter two show a strong shape resonance feature just above the ionization threshold, while 1-hexyne does not. section just above threshold shows significant contributions from  $\ell = 3$  and 4 partial waves, which is consistent with the presence of the corresponding states in the bound portion of the spectrum. The box corresponds to  $n = 3$  levels with vibrational excitation in the  $\text{C}\equiv\text{C}$  stretching mode.

Optical Physics Group. The data from these experiments was analyzed over the past year, and provide insight into the time evolution of the electronic and nuclear structure and dynamics as the molecule fragments following inner-shell excitation of the Xe atom. A manuscript describing these results is under review at Nature Communications. The experiments also produced additional x-ray pump/x-ray probe data on  $\text{N}_2$  and  $\text{O}_2$ , and these data are also being analyzed. However, it is expected that additional experiments will be required to fully characterize the electronic processes involved in the fragmentation of these molecules. In the past year, I also collaborated with Katherine Reid (Nottingham) and David Holland (Daresbury) on synchrotron-pump/laser-probe experiments at SOLEIL. In these experiments, we hoped to selectively excite Rydberg states of  $\text{NO}$  and  $\text{NH}_3$ , and probe the photoionization dynamics of

spectra of these alkynes. In the future, we will also explore the effects of substitutions and branching of the alkynes on the intensity and positions of the shape resonances.

We have also used our laboratory vuv-photoelectron imaging apparatus to record photoelectron images of all of the linear butynes, pentynes, and hexynes. While the photoelectron spectra of these species have been reported previously, our spectra were recorded much closer to the ionization threshold, where we could focus on the bands corresponding to the ground electronic state of the cation. In addition, these images provide information on the photoelectron angular distributions, which provide additional insight into the photoionization process. These data are currently under analysis.

#### *Photoionization studies and photoionization cross sections*

The propargyl radical is one of the simplest resonance stabilized radicals and plays an important role in a wide range of applications. The near-threshold photoionization spectrum of propargyl is also of considerable interest because it shows a number of intense, relatively sharp features produced by autoionization of Rydberg states converging to electronically excited states of the cation [see, for example, T. Zhang et al. *J. Chem. Phys.* 124, 074302 (2006)]. These resonances have not yet been assigned. This past year, my collaborators and I had beamtime at SOLEIL to attempt to record a higher resolution spectrum of propargyl along with photoelectron spectra for some of the more intense features. Unfortunately, the pyrolysis source we were using was not sufficient to produce an improved spectrum. In subsequent discussions, however, J. C. Loison (Universite Bordeaux) showed us that a new flow source he had developed based on fluorine abstraction reactions was capable of a much improved propargyl beam. We hope to return to SOLEIL with him this year to use this source to record the spectrum of interest. In addition, we hope to extend these studies to several butynyl radicals. We are hoping to see if the near-threshold shape resonances observed in the internal alkyne molecules are also observed in the corresponding radicals.

#### *Pump-probe experiments at the Linac Coherent Light Source (LCLS) and SOLEIL*

In 2014, I collaborated on an x-ray pump/x-ray probe study of  $\text{XeF}_2$  at the LCLS with the Argonne Atomic, Molecular, and

these excited states with the laser. Unfortunately, the initial experiments on these molecules were unsuccessful. However, we did perform analogous experiments on atomic Kr, and studied the dependence of the photoelectron angular distributions on the intermediate states, the ionic final states, and the polarizations of the pump and probe beams. These results have been analyzed and published in Physical Review A. Based on this experience, we intend to revisit the molecular experiments in the near future.

## FUTURE PLANS

I will continue to perform new experiments at SOLEIL on the photoabsorption of small- to medium-sized molecules and radicals, and to perform new experiments on the photoionization of radicals produced with the fluorine abstraction source. I am currently waiting to hear the status of our collaboration's most recent beamtime requests. I will also work to complete the analysis of the high-resolution photoionization and photoelectron imaging data on N<sub>2</sub>.

In the coming year, I intend to go back to measurements of the absolute photoionization cross sections of some hydrocarbon radicals using photodissociation and vuv photoionization imaging. In particular, we are interested in extending our work on the propargyl radical to larger alkynyl radicals. This work will complement experiments at SOLEIL on the relative photoionization cross sections of the same radicals and on the photoabsorption spectra of some of the radical precursors.

New laboratory experiments will be initiated on the photoionization dynamics of small molecules, with an effort to provide a more complete description of the exchange of angular momentum between the photoion and photoelectron. In particular, my work with Reid and Holland at SOLEIL has suggested a new approach to performing experiments involving the circular dichroism of photoelectron angular distributions (CDAD). These experiments were first developed in the 1980s, but were extremely challenging given the electron spectrometers of the day. We will now explore the possibility of gaining the same information by using photoelectron imaging techniques with circular polarized pump and probe beams in our laboratory at Argonne. The simplicity of the imaging technique and the ability to record full angular distributions very quickly should allow us to maximize the potential of the CDAD approach. Initial experiments are planned for mid-FY2016.

I will continue to collaborate with Christian Jungen on theoretical models of vibrational autoionization and dissociative recombination in polyatomic molecules and, in particular, on using results from *ab initio* photoionization calculations to try to characterize the importance and interactions among the bound Rydberg states of the alkynes and related molecules. This past year we used Robert Lucchese's K matrix from calculations of the photoionization cross section in 2-butyne to extract quantum defects for the bound Rydberg states. In particular, we were interested in how the introduction of *f* and *g* states at  $n = 4$  and  $5$ , respectively, perturb the  $n = 4$  and higher members of the Rydberg series with  $l < 3$ . The standard expectation is that Rydberg states with  $l > 3$  will be non-penetrating, and thus have little effect on the states with lower  $l$ . However, the near threshold shape resonance in 2-butyne and the other internal alkynes suggests that the higher- $l$  states may be more penetrating than generally expected, and will thus be expected to perturb the lower- $l$  states more significantly. If this effort is successful, it would provide a new approach to connecting the continuum and bound-state portions of photoabsorption and photoionization spectra.

I will also continue to explore the potential of free-electron laser sources to characterize the intramolecular dynamics of highly excited molecules. I participated in two new proposals for beamtime at the LCLS, both focusing on small molecules. The first will use x-ray/x-ray pump-probe techniques and photoelectron spectroscopy to study the electron and nuclear dynamics in CO. The second will use similar pump-probe techniques, but focus on the mass spectra and ion kinetic energies to characterize the intramolecular dynamics in systems like N<sub>2</sub>, O<sub>2</sub>, and CO<sub>2</sub>. I am also currently developing a proposal with Reid and Holland for beamtime at the FERMI FEL, which is seeded (narrow bandwidth) and operates in the vacuum ultraviolet. These experiments will focus on medium-sized molecules and involve two-color excitation, with a conventional laser for one step and the FEL for the other step.

## ACKNOWLEDGEMENTS

This work was performed in collaboration with Hong Xu and Ananya Sen. Work at Soleil was performed in collaboration with S. Boyé-Péronne and B. Gans (Institut des Sciences Moléculaires d'Orsay), D. M. P. Holland (STFC, Daresbury), U. Jacovella (ETH-Zürich), R. R. Lucchese (Texas A&M), E. F. McCormack (Bryn Mawr College) and N. de Oliveira (Soleil). Work on dissociative recombination was performed in collaboration with Ch. Jungen (Laboratoire Aime Cotton). This work was supported by the U.S. Department of Energy, Office of Science, Office of Basic Energy Sciences, Division of Chemical Sciences, Geosciences, and Biological Sciences under contract No. DE-AC02-06CH11357.

## DOE-SPONSORED PUBLICATIONS SINCE 2014

1. S. T. Pratt  
CHARGE TRANSFER GOES THE DISTANCE  
*Science* **345**, 267-268 (2014).
2. U. Jacovella, D. M. P. Holland, S. Boyé-Péronne, D. Joyeux, L. E. Archer, N. de Oliveira, L. Nahon, R. R. Lucchese, Hong Xu, and S. T. Pratt  
HIGH-RESOLUTION PHOTOABSORPTION SPECTRUM OF JET-COOLED PROPYNE  
*J. Chem. Phys.* **141**, 114303 (14 pages) (2014).
3. S. T. Pratt and Ch. Jungen  
GENERAL FEATURES OF THE DISSOCIATIVE RECOMBINATION OF POLYATOMIC MOLECULES  
*EPJ Web of Conf.* **84**, 04001 (5 pages) (2015).
4. Hong Xu and S. T. Pratt  
PHOTODISSOCIATION OF METHYL IODIDE VIA SELECTED VIBRATIONAL LEVELS OF THE  $\tilde{B}$  ( $^2E_{3/2}$ ) $6s$  RYDBERG STATE  
*J. Phys. Chem. A*, **119**, 7548-7558 (2015).
5. U. Jacovella, D. M. P. Holland, S. Boyé-Péronne, B. Gans, N. de Oliveira, D. Joyeux, L. E. Archer, R. R. Lucchese, Hong Xu, and S. T. Pratt  
HIGH-RESOLUTION VACUUM-ULTRAVIOLET PHOTOABSORPTION SPECTRA OF 1-BUTYNE AND 2-BUTYNE  
*J. Chem. Phys.* **143**, 034304 (14 pages) (2015).
6. S. J. Klippenstein and S. T. Pratt  
A TRIBUTE TO LAWRENCE B. HARDING, JOE V. MICHAEL, AND ALBERT F. WAGNER FOR THEIR 100 YEARS OF COMBUSTION KINETICS STUDIES AT ARGONNE  
*J. Phys. Chem. A*, **119**, 7075-7077 (2015).
7. U. Jacovella, D. M. P. Holland, S. Boyé-Péronne, B. Gans, N. de Oliveira, K. Ito, D. Joyeux, L. E. Archer, R. R. Lucchese, Hong Xu, and S. T. Pratt  
A NEAR-THRESHOLD SHAPE RESONANCE IN THE VALENCE SHELL PHOTOABSORPTION OF LINEAR ALKYNES  
*J. Phys. Chem. A*, **119**, 12339-12348 (2015).
8. N. Saquet, D.M.P. Holland, S.T. Pratt, D. Cubaynes, X. Tang, G. A. Garcia, L. Nahon, and K.L. Reid  
EFFECT OF ELECTRONIC ANGULAR MOMENTUM EXCHANGE ON PHOTOELECTRON ANISOTROPY FOLLOWING THE TWO-COLOUR IONIZATION OF KRYPTON ATOMS  
*Phys. Rev. A* (in press).
9. A. Piçon, C. S. Lehmann, C. Bostedt, A. Rudenko, A. Marinelli, T. Osipov, D. Rolles, N. Berrah, C. Bomme, M. Bucher, G. Doumy, B. Erk, K. Ferguson, T. Gorkhover, P. J. Ho, E. P. Kanter, B. Krässig, J. Krzywinski, A. A. Lutman, A. M. March, D. Moonshiram, D. Ray, L. Young, S. T. Pratt, and S. H. Southworth  
HETERO-SITE-SPECIFIC ULTRAFast INTRAMOLECULAR DYNAMICS  
*Nature Commun.* (submitted).

# Chirped-Pulse Fourier Transform Millimeter-Wave Spectroscopy for Dynamics and Kinetics Studies of Combustion-Related Reactions

Kirill Prozument  
Chemical Sciences and Engineering Division  
Argonne National Laboratory  
Argonne, IL 60439  
[prozument@anl.gov](mailto:prozument@anl.gov)

## 1. Scope of the Program

I am developing a new program to use microwave and millimeter-wave rotational spectroscopy to probe stable and reactive species relevant to combustion chemistry, and to use this capability to study reaction dynamics and kinetics. Rotational spectroscopy is known for its unsurpassed resolution and precision in determining molecular structure. The program will be based on chirped-pulse Fourier transform millimeter-wave (CP-FTmmW) spectroscopy<sup>1-4</sup>, which is rapidly revolutionizing the field of molecular spectroscopy. The CP-FTmmW spectroscopy is capable acquiring ~10 GHz wide rotational spectra with sub-MHz resolution in several microseconds with meaningful relative intensities of the transitions of multiple reaction products. The technique is nearly universal (applicable to all polar species) chemical tool that is conformer- and state-specific, quantitative and non-destructive, and suitable for studies of stable and transient species. The versatility of the CP-FTmmW technique is sufficient to allow its application to a wide range of experiments in reaction dynamics and kinetics.

## 2. Previous Work

### a. Argonne chirped-pulse Fourier transform millimeter-wave spectrometer

The chirped-pulse Fourier transform millimeter-wave spectrometer for W-band (75–100 GHz spectral region) from BrightSpec Company that has a number of unique capabilities was installed and tested at Argonne. The combination of the Argonne BrightSpec spectrometer and the fast oscilloscope is capable of acquiring, in 5 microseconds, 11 GHz of spectral range within the W-band. This broadband mode of operation is similar to that of the original CP millimeter-wave spectrometer developed by the PI and coworkers.<sup>3</sup> The broadband mode will be instrumental in recording rotational spectra of rapid processes, such as fast reactions in the flow tube reactor, or passage of photoproducts in a supersonic jet expansion. The rotational transitions of multiple reaction products can be detected with meaningful relative intensities, which can be converted to the relative abundance of the species given that the rotational temperature ( $T_r$ ) can be determined. With the exception of small linear or diatomic molecules, the number of detected transitions is usually sufficient to infer the  $T_r$  from the spectrum.

When slower processes are under investigation, high duty cycles with long averaging times are available. Under these conditions the CP technique can, in principle, reach staggering  $\sim 10^5$  dynamic ranges (signal-to-noise ratio, S/N) while acquiring up to  $10^5$  resolution elements (detection channels). However, the broadband mode of operation described above will face the limitations related to the speed with which the data can be digitized and processed by even fastest

oscilloscopes. Furthermore, the onset of spurious lines of different nature can be observed in the spectrum. To overcome these obstacles, the segmented chirped-pulse spectroscopy was developed<sup>5</sup> and implemented in our spectrometer as the High Dynamic Range (HDR) mode. In the HDR regime the narrow-band chirps polarize the molecular rotational transitions in small 30 MHz segments of the 75–110 GHz band and the fast digitizer acquires the free induction decays (FIDs) from those segments, one after another. The spurious lines caused by mixing of the molecular lines with the local oscillator frequencies and with each other are, for the most part, left out of the narrow 30 MHz detection windows.

In the case of periodic processes with intermediate duty cycles, yet another approach is required. BrightSpec in collaboration with the PI has developed a new regime of the spectrometer termed synchronized (or sync-) HDR, in which the consecutive acquisition of 30 MHz segments is time-gated. With the shortest 133 microsecond acquisition on-time, the sync-HDR mode is applicable to relatively fast periodic processes while retaining the advantages of the HDR mode.

## b. Pyrolysis of acetone

One of the proposed directions of this program is utilizing the pulsed flash pyrolysis reactor<sup>6</sup> to study combustion-related chemistry in complex mixtures. The preliminary results of the first flash pyrolysis measurement using the sync-HDR mode of the Argonne chirped-pulse spectrometer are shown in Figure 1. Acetone molecules containing 50% normal acetone,  $\text{CH}_3\text{COCH}_3$  and 50% fully deuterated acetone,  $\text{CD}_3\text{COCD}_3$ , entrained in argon carrier gas, are introduced to the pulsed flash pyrolysis reactor with a backing pressure of about 1 bar.

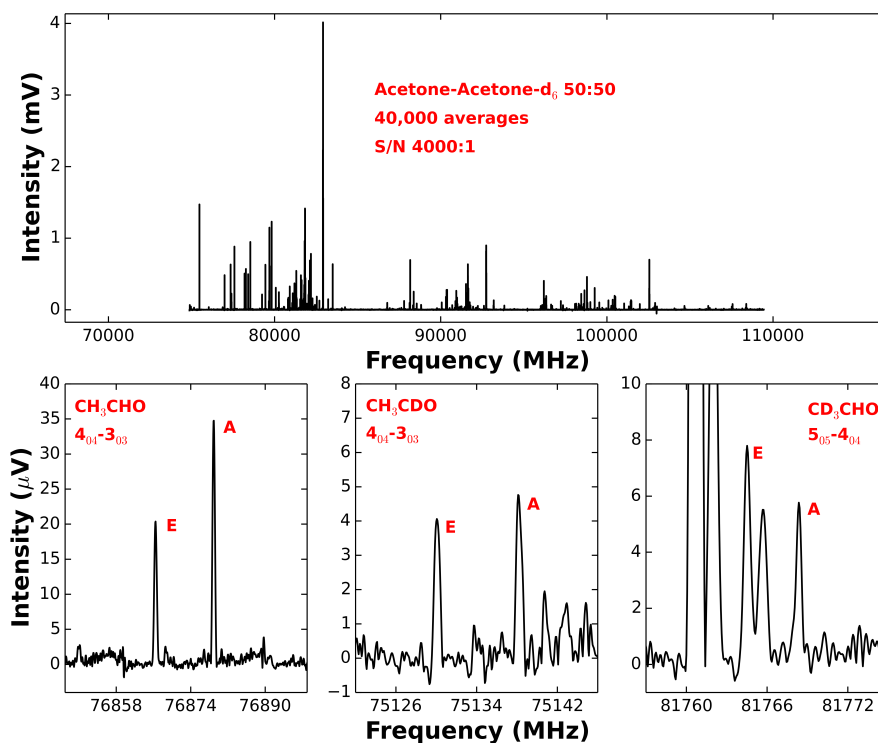


Figure 1. Pyrolysis of acetone (50%  $\text{CH}_3\text{COCH}_3$  and 50%  $\text{CD}_3\text{COCD}_3$ ) studied by chirped-pulse Fourier transform millimeter-wave spectroscopy. Acetaldehyde  $\text{CH}_3\text{CHO}$ ,  $\text{CH}_3\text{CDO}$  and  $\text{CD}_3\text{CHO}$  are observed as the pyrolysis products.

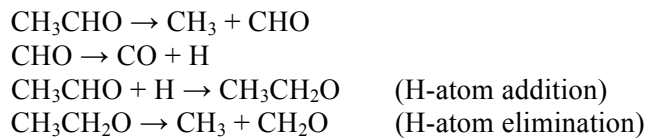
The acetone precursor is observed at S/N ~ 4000 after approximately 3 hours of averaging (upper panel of Fig. 1). When heating the nozzle to 1800 K the transitions of acetaldehyde are observed (lower panels of Fig. 1). One of the explanations for the appearance of acetaldehyde in the pyrolysis of acetone may be H-atom addition/elimination reactions that are discussed in the next section. Other products observed are ketene and propyne. We are working on building a model that will describe the chemistry leading to the observed pyrolysis products.

### 3. Future Work

Some previous results by the PI and other members of the Argonne Chemical Dynamics group suggest importance of the H-atom addition/elimination reactions in combustion-related and other reactions in the gas phase.<sup>7-8</sup>

We propose investigation of the pyrolysis of aldehydes and ketones using the chirped-pulse rotational spectroscopy aimed at understanding the properties, and quantifying the contribution of the H-atom addition/elimination reactions. The first two systems that we are planning to study are acetone and acetaldehyde. The initial pyrolysis results that were recently obtained by the PI in the newly built laboratory at Argonne, described in the previous section, suggest that applying chirped-pulse rotational spectroscopy to these studies is a promising direction. An important aspect of our investigation will be the effort to characterize<sup>9</sup> the thermodynamic conditions in the miniature SiC tube that we are using as our flash pyrolysis reactor. The branching between the reaction pathways and the final products that we detect with the CP spectrometer are expected to be affected by the temperature and pressure distributions inside the reactor. Once the conditions of the reactor are characterized and can be controlled, we expect a better agreement between the experimentally measured product branching ratios and kinetic modeling for known reactions and a greater predictive power of the method for new chemical dynamical effects.

Expanding our initial studies of the pyrolysis of acetone, pyrolysis of acetaldehyde, CH<sub>3</sub>CHO, will be investigated. It can involve the following reactions:



The CHO, CH<sub>3</sub>CH<sub>2</sub>O, and CH<sub>2</sub>O products and reactive intermediates can be detected and quantified with CP spectroscopy. Investigation of formaldehyde, CH<sub>2</sub>O, product would require expanding the spectrometer to the E-band (60 – 90 GHz) spectral region. We are going to investigate what role does keto-enol isomerization play in the pyrolysis of acetaldehyde. Similar classes of reactions can be investigated for acrolein, CH<sub>2</sub>CHCHO, and propanal. Preliminary results in acetone, CH<sub>3</sub>CH<sub>3</sub>CHO, are described in the previous section.

Recently, the PI has demonstrated that a combination of the CP spectroscopic measurement of products' branching ratios with accurate kinetic modeling is a powerful approach to studying dynamical effects in chemical reactions.<sup>6, 10</sup> A signature of roaming dynamics in the thermal decomposition of ethyl nitrite in a flash pyrolysis reactor was observed and rationalized.<sup>10</sup> We propose investigation of the importance of roaming reactions at the conditions that are relevant to combustion. One of the questions that remains open and can be addressed in our experimental program is the pressure dependence of branching into roaming reaction channels. We plan to devise a version of the reactor in which the pressure in the reactor can be varied, in a controlled way, by an order of magnitude or more, approximately from 0.2 to 2 bar.

Expanding beyond the studies of roaming dynamics, we propose investigating other chemical dynamics phenomena using the CP spectroscopy. As noted by Al Wagner and Stephen Klippenstein, a potentially important for creating reliable predictive models effect that is not presently well-understood is energy redistribution from the energized molecules proceeding through their transition states into the reaction products.<sup>11</sup> Vibrational energy partitioning into various products may either initiate consecutive reactions or relax into the bath molecules depending on the gas pressure and properties of the reactions' transition states. In the Argonne chirped-pulse spectrometer coupled with splash pyrolysis reactor the aforementioned dynamical effects will be reflected in the measured reaction products branching ratios. Accurate kinetic modeling that will be performed in collaboration with Raghu Sivaramakrishnan, Stephen Klippenstein and other members of the Argonne Chemical Dynamics group will guide our intuition in understanding the chemical dynamics beyond the experimental results.

## References

1. Brown, G. G.; Dian, B. C.; Douglass, K. O.; Geyer, S. M.; Shipman, S. T.; Pate, B. H. A Broadband Fourier Transform Microwave Spectrometer Based on Chirped Pulse Excitation. *Rev. Sci. Instrum.* **2008**, *79* (5), 053103.
2. Dian, B. C.; Brown, G. G.; Douglass, K. O.; Pate, B. H. Measuring Picosecond Isomerization Kinetics via Broadband Microwave Spectroscopy. *Science* **2008**, *320* (5878), 924-928.
3. Park, G. B.; Steeves, A. H.; Kuyanov-Prozument, K.; Neill, J. L.; Field, R. W. Design and Evaluation of a Pulsed-Jet Chirped-Pulse millimeter-Wave Spectrometer for the 70-102 GHz Region. *J. Chem. Phys.* **2011**, *135* (2), 024202.
4. Prozument, K.; Colombo, A. P.; Zhou, Y.; Park, G. B.; Petrovic, V. S.; Coy, S. L.; Field, R. W. Chirped-Pulse Millimeter-Wave Spectroscopy of Rydberg-Rydberg Transitions. *Phys Rev Lett* **2011**, *107* (14), 143001.
5. Neill, J. L.; Harris, B. J.; Steber, A. L.; Douglass, K. O.; Plusquellic, D. F.; Pate, B. H. Segmented Chirped-Pulse Fourier Transform Submillimeter Spectroscopy for Broadband Gas Analysis. *Opt. Express* **2013**, *21* (17), 19743-19749.
6. Prozument, K.; Park, G. B.; Shaver, R. G.; Vasiliou, A. K.; Oldham, J. M.; David, D. E.; Muentner, J. S.; Stanton, J. F.; Suits, A. G.; Ellison, G. B.; Field, R. W. Chirped-pulse millimeter-wave spectroscopy for dynamics and kinetics studies of pyrolysis reactions. *Phys Chem Chem Phys* **2014**, *16* (30), 15739-15751.
7. Sivaramakrishnan, R.; Michael, J. V.; Harding, L. B.; Klippenstein, S. J. Resolving Some Paradoxes in the Thermal Decomposition Mechanism of Acetaldehyde. *J Phys Chem A* **2015**, *119* (28), 7724-7733.
8. Prozument, K.; Vasiliou, A. K.; Shaver, G. R.; Park, G. B.; Muentner, J. S.; Stanton, J. F.; Ellison, G. B.; Field, R. W. Bimolecular pyrolysis reactions studied by chirped-pulse millimeter-wave spectroscopy. In *International Symposium on Molecular Spectroscopy*, Columbus, OH, 2013.
9. Guan, Q.; Urness, K. N.; Ormond, T. K.; David, D. E.; Ellison, G. B.; Daily, J. W. The properties of a micro-reactor for the study of the unimolecular decomposition of large molecules. *Int Rev Phys Chem* **2014**, *33* (4), 447-487.
10. Prozument, K.; Suleimanov, Y. V.; Buesser, B.; Oldham, J. M.; Green, W. H.; Suits, A. G.; Field, R. W. A Signature of Roaming Dynamics in the Thermal Decomposition of Ethyl Nitrite: Chirped-Pulse Rotational Spectroscopy and Kinetic Modeling. *J Phys Chem Lett* **2014**, *5* (21), 3641-3648.
11. Labbe, N. J.; Sivaramakrishnan, R.; Goldsmith, C. F.; Georgievskii, Y.; Miller, J. A.; Klippenstein, S. J. Weakly Bound Free Radicals in Combustion: "Prompt" Dissociation of Formyl Radicals and Its Effect on Laminar Flame Speeds. *J Phys Chem Lett* **2016**, *7* (1), 85-89.

## Photoinitiated Reactions of Radicals and Diradicals in Molecular Beams

Hanna Reisler

Department of Chemistry, University of Southern California

Los Angeles, CA 90089-0482

reisler@usc.edu

### Program Scope

Open shell species such as radicals, diradicals and excited electronic states are central to reactive processes in combustion and environmental chemistry. Our program is concerned with photoinitiated reactions of radicals, carbenes, and other open shell species. The goal is to investigate the detailed dynamics of dissociation of species in which multiple pathways participate, including molecular rearrangements, and compare them with high-level calculations. Studies include unimolecular reactions on the ground state as well as photodissociation dynamics on excited Rydberg and valence states that involve multiple potential energy surfaces.

### Recent Progress

#### Photodissociation of Highly Vibrationally Excited CO<sub>2</sub>

One of the goals of our renewed DOE grant is to characterize the gas phase dissociation of hydroxycarbenes on the ground and excited electronic states. These radicals have been produced before by flash pyrolysis of  $\alpha$ -keto carboxylic acids, albeit not in a molecular beam. The pyrolysis of glyoxylic acid, for example, generates CO<sub>2</sub> and HCOH, and our first step is to investigate the behavior of these products at the high temperatures required for pyrolysis (~ 1000 K).

We noticed that CO<sub>2</sub>, which is expected to be transparent at wavelengths >190 nm, in fact absorbs at >225 nm when heated. Experiments with 1-5% CO<sub>2</sub> in He demonstrated that, indeed, CO<sub>2</sub> does not absorb when unexcited; however, when heated in the SiC tube attached to the pulsed valve it absorbs at much longer wavelengths and dissociates to CO + O. A literature search provided the explanation: Hanson and coworkers demonstrated that there was a large red-shift in absorption for vibrationally excited CO<sub>2</sub>, which absorbs even at >300 nm with sufficient internal energy.<sup>1-4</sup> Because the ground state of CO<sub>2</sub> is linear and the lowest excited electronic states (singlet and triplet) are bent, Franck-Condon factors involving the zero-point levels of the ground and excited states are vanishingly small. Vibrationally excited CO<sub>2</sub>, on the other hand, can absorb at much longer wavelengths. Hanson and coworkers quantified their findings by estimating the average internal energy that CO<sub>2</sub> must possess in order to absorb at specific wavelengths. At 230 nm this was estimated at ~1 eV.<sup>3</sup> The influence of such hot band absorption on the dissociation dynamics of CO<sub>2</sub> has not been investigated.

The flash pyrolysis nozzle installed in our pulsed molecular beam apparatus allows for changing the temperature continuously by varying the heat supplied to the SiC tube. We need to bear in mind, however, that the material exiting the nozzle is then cooled by supersonic expansion to an unknown degree, and therefore the final internal energy of the reactants cannot be characterized by a temperature. Nevertheless, the final vibrational energy distribution depends on the degree of heating inside the SiC tube.

The first indication of absorption that we detected was with 230 nm excitation, giving rise to CO fragments that were monitored by 2+1 REMPI spectroscopy via the B(<sup>1</sup> $\Sigma^+$ ) state in a one-color pump and probe experiment. No CO was observed without heating, whereas as heating

was increased, CO products began to appear with increasing intensity. The relative populations of  $v=2$  increased at higher heating, while CO in  $v=1$  did not change as much (see an example in Fig. 1).

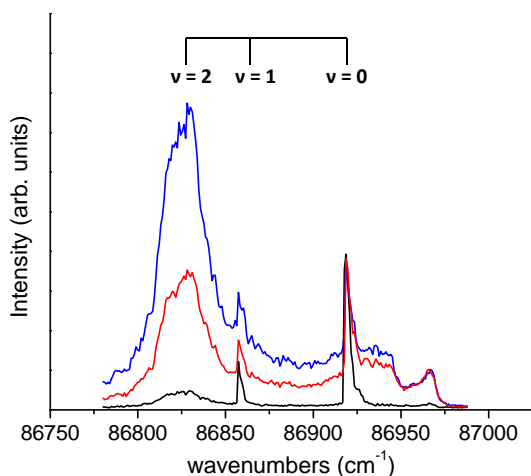


**Fig. 1:** Spectrum of  $\text{CO}(X^1\Sigma^+)$  products recorded by 2+1REMPI with low (black), medium (red), and high (blue)  $\text{CO}_2$  heating.

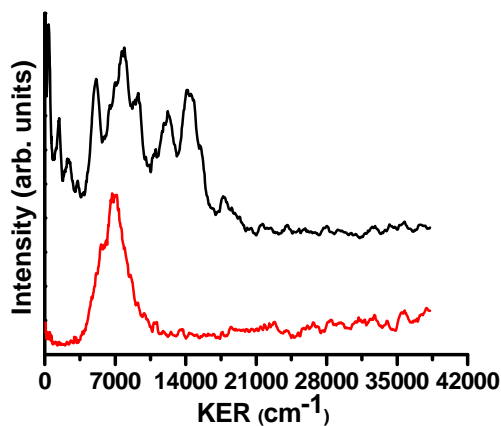


**Fig. 2.** KER plots of  $\text{CO}(X^1\Sigma^+;v=0)$  obtained with high (top) and low (bottom) heating.

Images of the CO product in several rovibrational states were obtained using time-sliced velocity map imaging. Images obtained when monitoring  $\text{CO}(v=0)$  in low rotational states are shown in Fig. 2. Similar images were obtained when monitoring low and high rotational levels of  $v=0$  under the same heating conditions. The thermochemical threshold for  $\text{CO}(v=0) + \text{O}(^3\text{P})$  production is  $\sim 44,000 \text{ cm}^{-1}$ , and excitation of cold  $\text{CO}_2$  with 230 nm ( $43,480 \text{ cm}^{-1}$ ) provides  $\sim 500 \text{ cm}^{-1}$  less energy than required by the thermochemistry. However, as noted above, all the *absorbing* molecules must have significant internal energy (greater than  $\sim 4000 \text{ cm}^{-1}$ ), and can dissociate. Thus, the kinetic energy release (KER) derived from images of  $\text{CO}(v=0)$  provides in essence a measure of the internal energies of the absorbing  $\text{CO}_2$  molecules. At high heating, this internal energy can exceed  $20,000 \text{ cm}^{-1}$ , as seen in the upper trace of Fig. 2.

The series of peaks at the lowest KEs in the upper trace of Fig. 2 can be energetically correlated with the  $\text{CO} + \text{O}(^1\text{D})$  channel, which requires an additional  $\sim 16,000 \text{ cm}^{-1}$  of energy. Experiments carried out at lower heating support this interpretation (Fig. 2, lower trace). These images show that the highest and lowest parts of the kinetic energy distribution (KED) decrease with decreased heating, demonstrating that they are both correlated with highly internally excited  $\text{CO}_2$ . With low heating, the KER plot is constrained on the low and high KE sides by the minimum  $\text{CO}_2$  internal energy required for absorption at 230 nm and the maximum internal energy achieved by heating, respectively.

It is impossible to convert the KEDs to  $\text{CO}_2$  internal energy distributions, because the long wavelength absorption cross-sections increase so sharply with internal energy. Thus, the KEDs provide only an estimate of the internal energies that can be achieved by heating. The structures reflect the lumpy nature of the  $\text{CO}_2$  vibrational energies, which are organized in polyad-like clumps.

We have also obtained images of  $O(^3P)$  and  $O(^1D)$  and their dependence on heating. The KED derived from the  $O(^1D)$  image obtained at 205 nm is shown in Fig. 3, and it confirms the interpretation derived from the KEDs of  $CO(v=0)$ . The  $O(^3P, ^1D)$  KEDs show no discernible structure, as each is pair-correlated with many rovibrational states of CO. In addition, direct monitoring of  $CO_2$  using 3+1 REMPI confirms that  $CO_2$  in excited bending and stretching states reaches the interaction region of our imaging apparatus when heating the SiC tube.

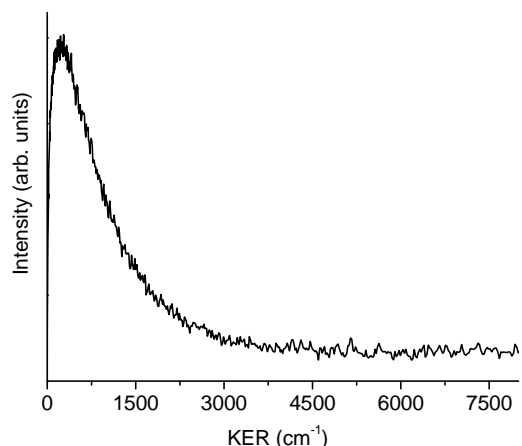


**Fig. 3:** KED derives from an image of  $O(^1D)$  obtained at 205 nm with high heating of the SiC tube.

While the above interpretation of the  $CO v=0$  and  $O(^3P, ^1D)$  images is reasonable, other results are still puzzling. For example, images recorded for  $CO v=1$  and  $v=2$  with high heating of the SiC tube gave KEDs that were limited to only a narrow range of kinetic energies centered around  $5000 \text{ cm}^{-1}$ , with FWHM of about  $1000 \text{ cm}^{-1}$ . We may rationalize this observation by envisioning the opening of a competitive pathway at high heating with adiabatic transfer of internal energy from  $CO_2$  to  $CO$ , but more theoretical work on the dissociation of vibrationally excited  $CO_2$  is needed.

### Future Work

We plan to elucidate the effect of vibrational excitation on  $CO_2$  photodissociation dynamics by using vibrationally-mediated photodissociation. It is well known that several singlet and triplet states of  $CO_2$  are located near the bright singlet state, and these states interact by conical intersections and spin-orbit couplings with other singlet and triplet states, including the ground state. Theoretical calculations identify multiple surface intersections,<sup>5-9</sup> but experimental studies are needed to distinguish among dissociation mechanisms. For example, conical intersections are predicted to be strongest for  $CO_2$  with bent and asymmetric stretch excitations, and hence state specific effects are expected. We have also initiated work on the state-specific dissociation and isomerization of HCOH on the ground and electronic excited states. We plan next to characterize  $CO_2$  and HCOH as products of the UV photolysis of glyoxylic acid.

### References

1. Jensen, R. J.; Guettler, R. D.; Lyman, J. L., *Chem. Phys. Lett.* **1997**, 277 (4), 356-360.
2. Schulz, C.; Koch, J. D.; Davidson, D. F.; Jeffries, J. B.; Hanson, R. K., *Chem. Phys. Lett.* **2002**, 355 (1-2), 82-88.

- Oehlschlaeger, M. A.; Davidson, D. F.; Jeffries, J. B.; Hanson, R. K., *Chem. Phys. Lett.* **2004**, 399 (4–6), 490-495.
- Oehlschlaeger, M. A.; Davidson, D. F.; Jeffries, J. B., *Appl. Opt.* **2005**, 44 (31), 6599-6605.
- Spielfiedel, A.; Feautrier, N.; Cossart-Magos, C.; Chambaud, G.; Rosmus, P.; Werner, H. J.; Botschwina, P., *J. Chem. Phys.* **1992**, 97 (11), 8382-8388.
- Schmidt, J. A.; Johnson, M. S.; Schinke, R., *Proc. Natl. Acad. Sci. USA* **2013**, 110 (44), 17691-17696.
- Grebenshchikov, S. Y., *J. Chem. Phys.* **2013**, 138 (22), 224106 and 224107.
- Jasper, A. W., Dawes, R., *J. Chem. Phys.* **2013**, 139, 154313.
- Zhou, B.; Zhu, C.; Wen, Z.; Jiang, Z.; Yu, J.; Lee, Y.-P.; Lin, S. H., *J. Chem. Phys.* **2013**, 139 (15), 154302.

### **Publications, 2013-2016**

- M. Ryazanov and H. Reisler, “Improved sliced velocity map imaging apparatus optimized for H photofragments”, *J. Chem. Phys.* 138, 144201 (2013).
- C. Rodrigo, C. Zhou, and H. Reisler, “Accessing multiple conical intersections in the 3s and 3p<sub>x</sub> photodissociation of the hydroxymethyl radical”, *J. Phys. Chem. A (Wittig Festschrift)* 117, 12049-12059 (2013).
- C.P. Rodrigo, S. Sutradhar, and H. Reisler, “Imaging studies of excited and dissociative states of hydroxymethylene produced in the photodissociation of the hydroxymethyl radical”, *J. Phys. Chem. A (Yarkonly Festschrift)*, 118(51), 11916-11925 (2014).

## Active Thermochemical Tables

Branko Ruscic  
Chemical Sciences and Engineering Division, Argonne National Laboratory,  
9700 South Cass Avenue, Argonne, IL 60439  
ruscic@anl.gov

### Program Scope

The *spiritus movens* of this program is the need to provide the scientific community with accurate and reliable thermochemical information on chemical species that are relevant in combustion, or play prominent roles in related post-combustion environmental chemistry. Detailed knowledge of thermodynamic parameters for a broad array of stable and ephemeral chemical species is pivotal to chemistry and essential in many industries. In particular, the availability of accurate, reliable, and internally consistent thermochemical values is a *conditio sine qua non* in kinetics, reaction dynamics, formulation of plausible reaction mechanisms, and construction of predictive models of complex chemical environments. Furthermore, the availability of accurate thermochemical values has historically been the prime driver for steady advancement of increasingly sophisticated electronic structure theories.

The focus of this program is on bringing substantial innovations to the field of thermochemistry through the development of new methodologies, and utilizing them to systematically improve both the quality and quantity of available thermochemical data relevant to energy-producing processes. In order to achieve the stated goals, this program has developed a novel approach that is centered on analyzing and optimally utilizing the information content of *all available* thermochemically relevant determinations. The aim is not only to dynamically produce the best currently possible thermochemical parameters for the targeted chemical species, but also to allow efficient updates with new knowledge, properly propagating its consequences through all affected chemical species, as well as to provide critical tests of new experimental or theoretical data, and, when possible, to develop pointers to additional determinations that are most likely to efficiently improve the overall thermochemical knowledge base. In order to provide a broad perspective of this area of science, the effort of this program is synergistically coordinated with related experimental and theoretical efforts within the Gas-Phase Chemical Dynamics Group at Argonne.

### Recent Progress

Over the past year we have continued the development of various aspects of Active Thermochemical Tables (ATcT). ATcT are a new paradigm for developing accurate and reliable thermochemical values for stable and reactive chemical species. Enthalpies of formation, are - with very few exceptions - not directly measured quantities, but are intrinsically defined via complex manifolds involving intertwined dependencies, where determinations (such as reaction enthalpies, equilibrium constants, bond dissociation energies) simultaneously involve several chemical species, and thus define the desired quantity of the target species only *relative* to other species. Extracting the enthalpies of formation from intertwined dependencies was historically considered to be an intractable complication, forcing the adoption of a simplified *sequential* approach of inferring the enthalpies of formation one at the time (A begets B, B begets C, etc.), which produces static sets of values that are plagued by hidden progenitor-progeny relationships and are thus impossible to update with new knowledge without introducing serious inconsistencies. The success of ATcT is rooted in treating the intertwined dependencies as a network of simultaneous relationships that is amenable to mathematical and statistical manipulation. This effectively converts the originally intractable problem into an asset that drives a quantum leap in the quality and reliability of the resulting thermochemistry. The Thermochemical Network (TN) represent a system of qualified constraints that need to be simultaneously satisfied to produce a set of enthalpies of formation that correctly reflect the knowledge content of the TN in its entirety, providing that the individual uncertainties associated with the determinations present in the TN are realistic. Because of the unavoidable presence of determinations with “optimistic” uncertainties (i.e. erroneous determinations), ATcT first performs an iterative analysis, which isolates them and brings the TN to self-consistency. Once the latter is achieved, ATcT proceeds to solve the TN simultaneously for all species included.

We are currently working on ver. 1.122 of the ATcT TN, which by now includes > 1400 species, interlinked by >20,000 determinations. As mentioned preliminarily in last year's abstract, this version has been exploited to generate the best currently available 0 K and 298 K thermochemistry for  $\text{CH}_n$ ,  $n = 4 - 0$  (methane, methyl, methylene, methylidyne, and carbon atom),  $\text{C}_2\text{H}_n$ ,  $n = 6 - 0$  (ethane, ethyl, ethylene, ethylidene, vinyl, ethylidyne, acetylene, vinylidene, ethynyl, and ethynylene),  $\text{COH}_n$ ,  $n = 4 - 0$  (methanol, hydroxymethyl, methoxy, formaldehyde, hydroxymethylene, formyl, isoformyl, and carbon monoxide), as well as  $\text{OH}_n$ ,  $n = 2 - 0$  (water, hydroxyl, oxygen atom), and carbon dioxide. The related paper, which is now published, provides all possible sequential bond dissociation energies for three prototypical fuels: methane, ethane, and methanol, and details interesting insights into bonding patterns that can be gained from highly accurate thermochemical values, including a purely thermodynamical proof that the recent claims about the quadruple bond in  $\text{C}_2$  do not withstand scrutiny, and confirms that the primary bonding contribution in  $\text{C}_2$  is due to a suspended  $\pi$  bond, akin to an acetylenic  $\pi$  bond without the skeletal C-C  $\sigma$  bond, while the contributions of the  $\sigma$  and 'inverted'  $\sigma$  bonds (proposed in the quadruple bonding scheme) are at most marginal. One important background activity during this project, which we felt to be necessary in order to prepare ATcT for producing as accurate values as possible, was in correcting the ubiquitous RRHO partition functions for the relevant species to non-rigid-rotator anharmonic-oscillator (NRRAO) partition functions. In ATcT, these are obtained by incorporating first- (NRRAO1) or second-order (NRRAO2) anharmonic corrections to the initial RRHO partition functions (which are already based on fundamentals), and are further corrected for effects of rotation-vibration interaction, centrifugal distortion, Darling-Dennison and Fermi resonances, as well as the Strip-Kirkwood correction, and combined with direct counts at lowest temperatures. For internal rotors or inversions the corrections are typically obtained by direct counts of the corresponding levels. The effects of anharmonicity can be rather pronounced, particularly at higher temperatures relevant in combustion. The consequences of the ATcT thermochemistry for these fundamental combustion species, including both the latest thermochemistry and the NRRAO partition functions, are currently being probed in actual combustion models in collaboration with R. Sivaramakrishnan. Preliminary tests indicate that the new ATcT thermochemistry has a very significant effect on combustion modeling. One key reaction that is clearly affected is the recombination of methyl with a hydrogen atom to form methane, and changes in its high-temperature equilibrium constant cascade down the relevant chemical mechanisms, impacting methylene and other species, ultimately causing, for example, changes in methane-air flame speeds of 20-30%.

With additional modifications and expansions, ver. 1.122 of the ATcT TN was used in our recent study of the  $\text{HCN} \leftrightarrow \text{HNC}$  equilibrium. This equilibrium is a textbook case of isomerization, and is relevant in many areas, ranging from combustion ( $\text{NO}_x$  reduction processes) to astrochemistry. In this study, performed in collaboration with researchers at the University of Texas at Austin (J. Stanton, T. L. Nguyen, and J. H. Baraban), we were able to (once again) highlight the ability of ATcT to clearly distinguish between the 'right' and the 'wrong' thermochemical value, and conclusively show that a recently proposed value for the energy gap between the two isomers ( $5705 \pm 20 \text{ cm}^{-1}$ ), ostensibly obtained from high-level MRCI composite computations and used to readjust astrophysical spectral lists, is too high by at least 1.4 kcal/mol and highly unlikely to be correct in spite of the extremely high accuracy claim. This was accomplished by performing several rounds of statistical hypothesis testing via the ATcT machinery. The resulting ATcT recommendation ( $5212 \pm 30 \text{ cm}^{-1}$ ) was finalized by incorporating a new HEAT-456QP computation ( $5236 \pm 50 \text{ cm}^{-1}$ ).

On the front of disseminating the ATcT values, including interim results for species that have not been yet completely 'finalized', we have continued to maintain and expand our website, ATcT.anl.gov. We have now released the last completed version of results (ver. 1.118). One of the novelties in the just released version is the search functionality, based on the full ATcT Species Dictionary. While the addition of the latter functionality superficially appears like a simple insertion of a search bar toward the top of the page, in reality it required a complete overhaul of the website, from what used to be a web table that was generated from the ATcT results by decorating the relevant data with HTML tags, to a fully database driven web content. We were originally hoping that this development might be achieved as a graduate student project through the Practicum Program within the Masters Program in Computer Science

at the University of Chicago, which includes graduates with chemistry majors, but after several semesters we had no takers, and were ultimately forced to accomplish this development with our own forces. Once the current developmental version of the TN 1.122 is wrapped up, we will populate the website with the corresponding results. The transition to a database-driven website opens the door for including other relevant information. One of the targets that we are currently working on is the per-species provenance analysis (which is typically very distributed in ATcT, sometimes over a hundred or more relevant determinations), providing that we can sort out how to better interpret the results obtained from variance decomposition, how to efficiently and automatically generate the needed information automatically for every species, and how to systematize and store the huge amount of data thusly generated.

One extremely interesting activity was the collaboration with the IUPAC Task Group on Standard Electrode Potentials. The Task Group, which became aware of the ATcT approach to thermochemistry, sought to utilize our approach for establishing their IUPAC recommendations. One peculiarity of their data sets (which is rather pervasive in electrochemistry) is that the information content is virtually completely in terms of free energy relationships, but with essentially zero information about entropy (and thus enthalpy). This required some retooling of the ATcT machinery, but the final results demonstrate rather flamboyantly (in the shape of a formal IUPAC Report) that ATcT is fully capable of operating in all areas of thermochemistry, including aqueous and condensed phases.

We also have a number of ongoing national and international collaborations. One such collaboration, with P. Glarborg at DTU and with the Italian team at the Politecnico di Milano, involves a continuation of our previous work on inhibition of flames by bromine- and chlorine-containing species, now extended to chlorine-containing species in the presence of carbon-containing fuels. A related collaboration with P. Glarborg focuses on the role of NO<sub>x</sub> species in combustion. With G. Bacskay (U. Sydney) and K. Peterson (WSU) we are working on developing very-high-accuracy computational results for I and Br-containing species. With M. Pilling (Leeds) we have a current collaboration on atmospherically-relevant processes. Finally, we have several combustion-related collaborative topics with J. Stanton and T. L. Nguyen (U. Texas Austin) and G. B. Ellison (Boulder), including, *inter alia*, a number of resonantly stabilized radicals that appear to play important roles in the initial stages of soot formation.

### **Future Plans**

Future plans of this program pivot around further development and expansion of the Active Thermochemical Tables approach, continuing to provide accurate thermochemistry, and driving targeted thermochemically-relevant theoretical and experimental investigations of radicals and transient species that are intimately related to combustion and post-combustion atmospheric processes. A significant part of the effort during the forthcoming period will be devoted to continued ‘finalization’ and dissemination of the resulting ATcT thermochemistry. A crucial component of the ‘finalization’ of results for groups of related chemical species consists of testing and analyzing their TN dependencies (in part by using the newly developed variance/covariance decomposition approach) as well as enhancing the accuracy of their partition functions (by gradually replacing them with fully corrected NRRAO partition functions), and, when suggested by ATcT analyses, adding new high-quality results (either virtual, *i.e.* computational, or actual, *i.e.* experimental) to coerce the resulting thermochemistry toward stable, ‘release quality’ values. This iterative process frequently results in an expansion of the number of species that are described by the current TN, which is an added benefit. Another important component in the future plans is the continuation of the current effort of designing and producing a computer-generated web site that will display the current ATcT thermochemistry, as well as the pertinent metadata, with rigorous archival capability. One interesting set of pertinent metadata relates to sufficiently documenting the provenance for each thermochemical value, which entails a variance decomposition analysis for every chemical species. Finally, a significant long-term component of future progress consists in developing the next generation of ATcT software. This will be based on a new version of the ATcT kernel, with the aim of making the software not only streamlined and more efficient, but also allowing sufficient flexibility that will enable the adoption and utilization of emerging computing technologies as they are becoming available.

This work is supported by the U.S. Department of Energy, Office of Basic Energy Sciences, Division of Chemical Sciences, Geosciences, and Biosciences, under Contract No. DE-AC02-06CH11357.

### Publications resulting from DOE sponsored research (2013 – present)

- *Active Thermochemical Tables enthalpies of formation based on ver. 1.110 of the Thermochemical Network*, B. Ruscic, <http://atct.anl.gov/Thermochemical%20Data/version%201.110/> (2013)
- *Prompt NO formation in flames: The influence of NCN thermochemistry*, E. Goos, C. Sickfeld, F. Mauss, L. Seidel, B. Ruscic, A. Burcat, and T. Zeuch, *Proc. Comb. Inst.* **34**, 657-666 (2013), DOI: 10.1016/j.proci.2012.06.128
- *Active Thermochemical Tables: Water and Water Dimer*, B. Ruscic, *J. Phys. Chem. A* **117**, 11940-11953 (2013), DOI: 10.1021/jp403197t
- *Extended Third Millennium Ideal Gas and Condensed Phase Thermochemical Database for Combustion with updates from Active Thermochemical Tables*, E. Goos, A. Burcat, and B. Ruscic (2014); (includes complete ATcT values ver. 1.112); progressive updates are currently available at <http://burcat.technion.ac.il/dir/> and mirrored at <http://garfield.chem.elte.hu/Burcat/burcat.html>
- *Improved Accuracy Benchmarks of Small Molecules Using Correlation Consistent Basis Sets*, D. Feller, K. A. Peterson, and B. Ruscic, *Theor. Chem. Acc.* **133**, 1407/1-16 (2014), DOI: 10.1007/s00214-013-1407-z
- *Active Thermochemical Tables: Dissociation Energies of Several Homonuclear First-Row Diatomics and Related Thermochemical Values*, B. Ruscic, D. Feller, and K. A. Peterson, *Theor. Chem. Acc.* **133**, 1415/1-12 (2014), DOI: 10.1007/s00214-013-1415-z
- *Uncertainty Quantification in Thermochemistry, Benchmarking Electronic Structure Computations, and Active Thermochemical Tables*, B. Ruscic, *Int. J. Quantum Chem.* **114**, 1097-1101 (2014), DOI: 10.1002/qua.24605
- *Electronic States of the Quasilinear Molecule Propargylene (HCCCH) from Negative Ion Photoelectron Spectroscopy*, D. L. Osborn, K. M. Vogelhuber, S. W. Wren, E. M. Miller, Y.-J. Lu, A. S. Case, L. Sheps, R. J. McMahon, J. F. Stanton, L. B. Harding, B. Ruscic, and W. C. Lineberger, *J. Am. Chem. Soc.* **136**, 10361-10372 (2014), DOI: 10.1021/ja5039984
- *Active Thermochemical Tables enthalpies of formation based on ver. 1.112 of the Thermochemical Network*, B. Ruscic, <http://atct.anl.gov/Thermochemical%20Data/version%201.112/> (2015)
- *High-Temperature Chemistry of HCl and Cl<sub>2</sub>*, M. Pelucchi, A. Frassoldati, T. Faravelli, B. Ruscic, and P. Glarborg, *Combust. Flame* **162**, 2693-2704 (2015), DOI: 10.1016/j.combustflame.2015.04.002
- *IUPAC Technical Report: Standard Electrode Potentials Involving Radicals in Aqueous Solution: Inorganic Radicals*, D. A. Armstrong, R. E. Huie, W. H. Koppenol, S. V. Lyman, G. Merényi, P. Neta, B. Ruscic, D. M. Stanbury, S. Steenzen, and P. Wardman, *Pure Appl. Chem.* **87**, 1139-1150 (2015), DOI: 10.1515/pac-2014-0502
- *Active Thermochemical Tables: Sequential Bond Dissociation Enthalpies of Methane, Ethane, and Methanol and the Related Thermochemistry*, B. Ruscic, *J. Phys. Chem. A* **119**, 7810-7837 (2015), DOI: 10.1021/acs.jpca.5b01346
- *Thermal Dissociation and Roaming Isomerization of Nitromethane: Experiment and Theory*, C. J. Annesley, J. B. Randazzo, S. J. Klippenstein, L. B. Harding, A. W. Jasper, Y. Georgievski, B. Ruscic, and R. S. Tranter, *J. Phys. Chem. A* **119**, 7872-7893 (2015), DOI: 10.1021/acs.jpca.5b01563
- *On the HCN – HNC Energy Difference*, T. L. Nguyen, J. H. Baraban, B. Ruscic, and J. F. Stanton, *J. Phys. Chem. A* **119**, 10929–10934 (2015), DOI: 10.1021/acs.jpca.5b08406
- *Active Thermochemical Tables enthalpies of formation based on ver. 1.118 of the Thermochemical Network*, B. Ruscic, (including: *A functionality to search online the ATcT Species Dictionary*, D. H. Bross), <http://atct.anl.gov/Thermochemical%20Data/version%201.118/> (2016)

# GAS-PHASE MOLECULAR DYNAMICS: HIGH RESOLUTION SPECTROSCOPY AND COLLISION DYNAMICS OF TRANSIENT SPECIES

Trevor J. Sears  
Department of Chemistry, Brookhaven National Laboratory  
Upton, NY 11973-5000  
[sears@bnl.gov](mailto:sears@bnl.gov)

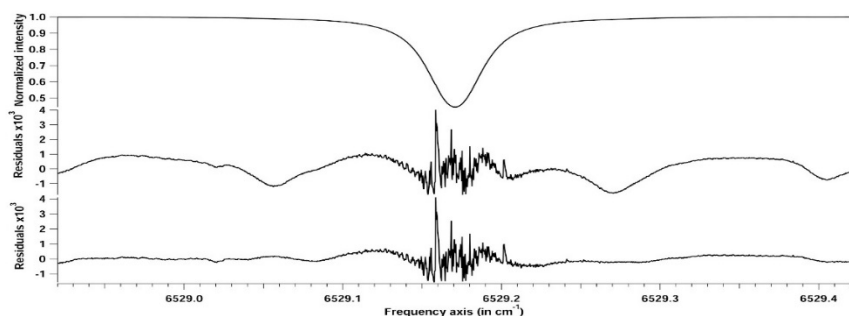
## Program Scope

This research is carried out as part of the Gas-Phase Molecular Dynamics program in the Chemistry Department at Brookhaven National Laboratory. High-resolution spectroscopic methods, augmented by theoretical and computational work, are used to investigate the structure, collision dynamics and chemical behavior of intermediates in the elementary gas-phase reactions involved in combustion chemistry. There is an emphasis on new technique development with the aim of improving both the sensitivity and resolution of spectroscopic measurements.

## I. Recent Progress

### A. Precision Line Shape Measurements

As the accuracy and precision of laboratory data continues to increase and the requirements for species profile extraction from spectroscopic remote sensing measurements become more stringent, a recent IUPAC report has recommended the adoption of a new standard model for representing line shape data, [Tennyson et al. (IUPAC Technical Report). *Pure Appl. Chem.* 2014;86(12):1931–43.]. The measurements we have made on self- and nitrogen-broadened line shapes for the  $P_e(11)$  line of the  $\nu_1 + \nu_3$  band of acetylene, using a frequency comb-stabilized laser spectrometer, provide an excellent test case for the proposed new standard. We have used the proposed Hartmann–Tran profile (HTP) line shape model in a multispectrum fitting to the data which included information recorded at temperatures between 125 K and 296 K and at pressures between 4 and 760 Torr. Also, new, sub-Doppler, frequency comb-referenced measurements of the positions of multiple underlying hot band lines have been made [see below]. We found these underlying lines significantly affect the  $P_e(11)$  line profile at temperatures above 240 K and poorly known frequencies previously introduced errors into the line shape analyses. A parameter uncertainty analysis was carried out using a Monte Carlo method based on the estimated pressure, transmittance and frequency measurement errors. From the analyses, the  $P_e(11)$  line strength was found to be  $1.2014(50)$  cm. molecule<sup>-1</sup> at 296 K, with the standard deviation in parenthesis. A reduced form of the HTP, equivalent to the Quadratic Speed Dependent Voigt profile (SDVP), was most appropriate because the additional parameters included in the full HTP were not well determined. In this work, we also derived expressions for analytic lineshape derivatives and wrote a lineshape fitting code in Matlab for the HTP both of which have been made available to the scientific community.

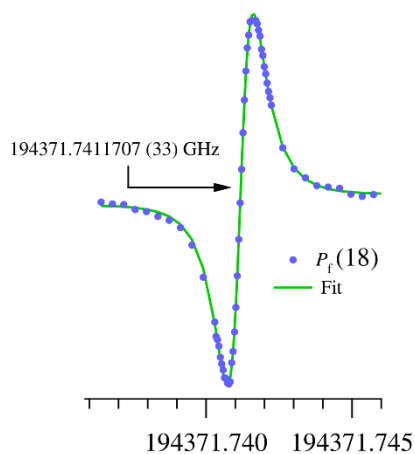


The figure shows the recorded line profile (top panel), the observed – calculated residuals derived using the best fit HTP parameters but without the hot-band and other weak underlying features included, center panel, and finally, (bottom panel) the residuals

after correctly accounting for the underlying features. Note the 1000× expansion of the lower two panels.

## B. Sub-Doppler Rest Frequency Measurements

We have measured Doppler-free rest frequencies for  $\nu_4$  - and  $\nu_5$  -excited hot bands in the  $\nu_1 + \nu_3$  band region of the spectrum of acetylene using saturation dip spectroscopy with an extended cavity diode laser referenced to a frequency comb. These measurements were made because accurate line profile models for the strong lines in this band require that the positions of weaker, underlying, lines be well known. The frequency accuracy of the measured transitions, as judged from line shape model fits and comparison to known frequencies in the  $\nu_1 + \nu_3$  band itself, is between 3 and 22 kHz in approximately 200 THz, *i.e.* a relative precision of close to  $10^{11}$ . This is some three orders of magnitude improvement on the accuracy and precision of previous line position estimates that were derived from the analysis of, Doppler-limited, high-resolution Fourier transform infrared absorption spectra. In the figure, a sample of the data shows the measurement for the  $P_f(18)$  line in the  $\nu_4$  hot band with an estimated measurement uncertainty of 3.3 kHz at 194372 GHz. The line width is dominated by uncertainty caused by the (short) transit time of the sample



molecules though the probe laser beam. The line center was estimated from a fit to an assumed derivative of the transmission lineshape based on this broadening mechanism and the figure shows the points as the data and the line as the model fit.

The measurements provide the necessary information on the rest frequencies, but they also give very accurate numbers for the upper state energy levels involved in the spectroscopic transitions. These levels lie within the dense manifold of background vibration-rotation levels belonging to combinations of lower frequency vibrations. These background levels are spectroscopically dark: they cannot be easily accessed by spectroscopic transitions from the normally populated levels in the molecule. However, their presence can be inferred from small perturbations in the observed energy levels for the spectroscopically bright levels accessed here. The perturbations are evidenced by small energy level shifts, which are detectable by the new data, but not previously observable. By providing a window to the weakly perturbing background levels, the data can calibrate models for the vibration-rotation structure of acetylene.

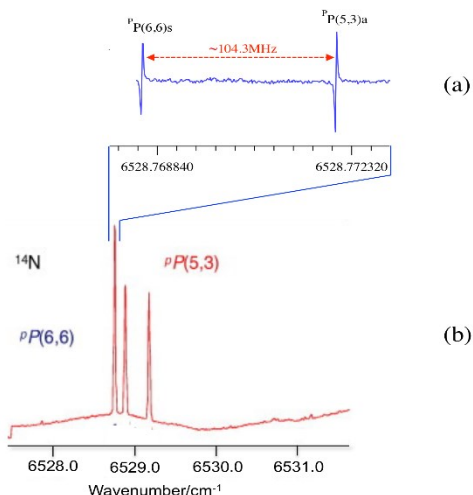
## II. Current and Future Work

### A. Near-IR Spectrum of CCH

The CCH radical is an intermediate of significant importance in combustion and the prototype for the intermediates invoked in models for the build-up of polyaromatic (PAH) species on the way to soot in fuel rich environments. More recently, identical intermediates have been proposed in mechanisms for the synthesis of single-walled carbon nanotubes by low-temperature catalyzed chemical vapor deposition. Reflecting its ubiquity in reaction systems involving unsaturated hydrocarbons, there have been large numbers of spectroscopic studies reported. The spectrum at infrared and near-infrared wavelengths is complicated by the presence of a low-lying  $^2\Pi$  state at approximately  $3000\text{ cm}^{-1}$  that splits due to the Renner-Teller effect, resulting in three vibronically-coupled low-lying potential energy surfaces. The near infrared spectrum above  $5500\text{ cm}^{-1}$  has not previously been observed in the gas phase, but theory and a low temperature matrix spectra agree that the strongest bands in the IR and near-IR lie close to  $7100\text{ cm}^{-1}$  in a region ideal for spectroscopic remote sensing. We have measured transient near-IR absorption spectra in this region and find three distinct strong vibronic bands that we have rotationally assigned. This work is currently being written up for publication. In the future, we plan to search for the spectrum of the related phenyl-substituted radical in an expansion cooled source. Other new and ongoing radical spectroscopy projects include searches for combination band transitions in methyl,  $\text{CH}_3$ , and the near-IR spectra of several other small hydrocarbon species.

## B. Comb-Referenced Rest Frequency Measurements of Ammonia

Ammonia is a non-planar symmetric top molecule with a large amplitude inversion vibrational mode. The



inversion motion is associated with a double-well potential with an effective barrier height of 2200 cm<sup>-1</sup>. Tunneling through the barrier leads to the well-known inversion splittings in the zero point and higher vibrational levels of the molecule. Further, the spins of the three equivalent protons result in two distinct spin states of the molecule, ortho ( $I_H=3/2$ ) and para ( $I_H=1/2$ ) each associated with a distinct set of rotational levels. These characteristics together with its practical importance have made ammonia a prototype molecule for spectroscopic study. Current interest in the near-infrared spectrum is driven by a desire to understand the level couplings and the observed rotational structure on the way to developing a useful spectroscopic sensor for remote sensing applications. In this spectral region, there exist multiple overtone and combination bands and even the most recent

analyses of Doppler-resolved spectra have 75% of the lines unassigned. An example of the problems is shown in the figure, panel (b), [Lees et al. *J. Molec. Spectrosc.*, **251**, 241-251 (2008)]. The left-hand line in this spectrum was postulated to consist of two distinct rotation vibration transitions, but they were totally overlapped in the Doppler-limited spectrum. Sub-Doppler, comb-referenced measurements in our laboratory (panel (a)) easily resolve the pair. Slower scans through the sub-Doppler lines show partially resolved <sup>14</sup>N and <sup>1</sup>H hyperfine structure. This hyperfine structure is characteristic for each rotational transition, therefore confirming or denying tentative assignments from analysis of lower resolution data. Among approximately 20 measurements, one particular transition, <sup>p</sup>P(5,4)<sub>a</sub> of the  $\nu_1+\nu_3$  band, has a hyperfine structure that does not match the predictions based on the known hyperfine structure of the lowest inversion levels. This indicates that the upper level in the transition is perturbed in some way that affects the nuclear spin structure. One exciting possibility is coupling between ortho and para levels because a level of the required symmetry does lie close to the upper state level involved. Confirmation of this hypothesis requires more measurements, which are planned for the near future.

## III. Publications supported by this project since 2014

Collinear two-color saturation spectroscopy in CN A-X (1-0) and (2-0) bands, D. Forthomme, C. P. McRaven, T. J. Sears, and G. E. Hall, *J. Molec. Spectrosc.* **296**, 36-42 (2014)  
<http://dx.doi.org/10.1016/j.jms.2013.12.006>

Frequency Comb-Referenced Spectroscopy in the  $\nu_1 + \nu_3$  Region of Acetylene, M.J. Cich, D. Forthomme, G.E. Hall, C.P. McRaven, T.J. Sears, S. Twagirayezu, *The 13th Biennial HITRAN Conference (HITRAN13), Harvard-Smithsonian Center for Astrophysics, Cambridge, MA, USA*, 23-25 June, 2014., <http://dx.doi.org/10.5281/zenodo.11181>

Doppler-Resolved Kinetics of Saturation Recovery, D. Forthomme, M. L. Hause, H.-G. Yu, P. J. Dagdigian, T. J. Sears, and G. E. Hall, *J. Phys. Chem. A* **119**, 7439-7450 (2015).  
<http://dx.doi.org/10.1021/acs.jpca.5b00628>.

Application of the Hartmann-Tran profile to precise experimental data sets of <sup>12</sup>C<sub>2</sub>H<sub>2</sub> D. Forthomme, M.J. Cich, S. Twagirayezu, G.E. Hall, T.J. Sears, *Journal of Quantitative Spectroscopy & Radiative Transfer* **165** (2015) 28-37. <http://dx.doi.org/10.1016/j.jqsrt.2015.06.013>

Frequency-comb referenced spectroscopy of  $\nu_4$  and  $\nu_5$  hot bands in the  $\nu_1 + \nu_3$  combination band of C<sub>2</sub>H<sub>2</sub>, S. Twagirayezu, M. J. Cich, T. J. Sears, C. P. McRaven, and G. E. Hall, *J. Molec. Spectrosc.* **316** 64-71 (2015). <http://dx.doi.org/10.1016/j.jms.2015.06.010>

Photo-assisted intersystem crossing: The predominant triplet formation mechanism in some isolated polycyclic aromatic molecules excited with pulsed lasers, P. M. Johnson, and T. J. Sears, *J. Chem Phys.*, **143**, 045305 (2015). <http://dx.doi.org/10.1063/1.4926925>

Further investigation of g-factors for the lead monofluoride ground state, L. V. Skripnikov, A. N. Petrov, A. V. Titov, R. J. Mawhorter, A. L. Baum, T. J. Sears, and J.-U. Grabow, *Phys. Rev. A* **92**, 032508 (2015),

# Theoretical Studies of Potential Energy Surfaces and Computational Methods

Ron Shepard

Chemical Sciences and Engineering Division,  
Argonne National Laboratory, Argonne, IL 60439  
[email: shepard@tcg.anl.gov]

**Program Scope:** This project involves the development, implementation, and application of theoretical methods for the calculation and characterization of potential energy surfaces (PES) involving molecular species that occur in hydrocarbon combustion. These potential energy surfaces require an accurate and balanced treatment of reactants, intermediates, and products. This difficult challenge is met with general multiconfiguration self-consistent field (MCSCF) and multireference single- and double-excitation configuration interaction (MR-SDCI) methods. In contrast to the more common single-reference electronic structure methods, this approach is capable of describing accurately molecular systems that are highly distorted away from their equilibrium geometries, including reactant, fragment, and transition-state geometries, and of describing regions of the potential surface that are associated with electronic wave functions of widely varying nature. The MCSCF reference wave functions are designed to be sufficiently flexible to describe qualitatively the changes in the electronic structure over the broad range of molecular geometries of interest. The necessary mixing of ionic, covalent, and Rydberg contributions, along with the appropriate treatment of the different electron-spin components (e.g. closed shell, high-spin open-shell, low-spin open-shell, radical, diradical, etc.) of the wave functions are treated correctly at this level. Further treatment of electron correlation effects is included using large-scale multireference CI wave functions, particularly including the single and double excitations relative to the MCSCF reference space. The recent focus has included the development and application of the Graphically Contracted Function (GCF) method.

**Recent Progress:** ELECTRONIC STRUCTURE CODE MAINTENANCE, DEVELOPMENT, AND APPLICATIONS: A major component of this project is the development and maintenance of the COLUMBUS Program System. The COLUMBUS Program System computes MCSCF and MR-SDCI wave functions, MR-ACPF (averaged coupled-pair functional) energies, MR-AQCC (averaged quadratic coupled cluster) energies, spin-orbit CI energies, analytic energy gradients, and nonadiabatic coupling. Geometry optimizations to equilibrium and saddle-point structures can be done automatically for both ground and excited electronic states. The COLUMBUS Program System is maintained and developed collaboratively with several researchers including Russell M. Pitzer (Ohio State University), Thomas Mueller (Jülich Supercomputer Center, Germany), and Hans Lischka (Tianjin University, China, University of Vienna, Austria, and Texas Tech University). The nonadiabatic coupling and geometry optimization for conical intersections is done in collaboration with David R. Yarkony (Johns Hopkins University). The distributed development effort and software coordination uses an svn repository of source code. The parallel sections of the code are based on the single-program multiple-data (SPMD) programming model with explicit

<p>This work was performed under the auspices of the Office of Basic Energy Sciences, Division of Chemical Sciences, Geosciences, and Biosciences, U.S. Department of Energy, under contract number DE-AC02-06CH11357.</p>
--

message passing using the portable MPI library, and the portable Global Array Library (distributed from PNNL) is used for data distribution. The COLUMBUS codes incorporate several of the newer language features of F90 and later in order to facilitate future development and maintenance efforts. Development versions of the single-facet and multifacet GCF methods are included within the COLUMBUS repository.

**GRAPHICALLY CONTRACTED FUNCTION METHOD:** We have developed a novel expansion basis for electronic wave functions [see *J. Chem. Phys.* **141**, 064105 (2014) and references therein]. In this approach, the wave function is written as a linear combination of *graphically contracted functions* (GCF), and each GCF in turn is formally equivalent to a linear combination of configuration state functions (CSFs) that comprise an underlying full-CI linear expansion space of dimension  $N_{\text{CSF}}$ . The CSF coefficients that define the GCFs are nonlinear functions of a smaller number of essential variables  $N_{\varphi} \ll N_{\text{CSF}}$ . The initial implementation of the GCF method relied on the nonlinear basis dimension  $N_{\text{GCF}}$  to extend the wave function flexibility and to converge molecular properties toward the full-CI limit. We have now implemented an alternative, and potentially more efficient, approach to enhance the wave function flexibility that consists of allowing multiple partially contracted wave functions to be associated with each Shavitt graph node within each GCF. The initial approach is now called the single-facet GCF (SFGCF) method, and this new approach is called the multifacet GCF (MFGCF) method. All of the properties and algorithms previously developed for the SFGCF method are being implemented within the MFGCF code: state-averaging, Hamiltonian matrix construction, one- and two-particle reduced density matrix (RDM) construction, Slater determinant overlaps, graph density computation and display, and spin-density matrix computation. Additionally, algorithms have been developed to merge multiple SFGCF and multiple MFGCF basis functions into a single MFGCF. SFGCF expansions with 10 to 20 GCFs have been shown to approach the full-CI PES to within chemical accuracy (1 kcal/mole or better), and this accuracy can also be achieved by increasing the facet counts within the MFGCF expansion to the range  $f_{\text{MAX}} \approx 4$  to 10. The GCF method is formulated in terms of spin eigenfunctions using the Graphical Unitary Group Approach (GUGA) of Shavitt, and consequently it does not suffer from spin contamination or spin instability. This is an important feature for the study of radicals and excited states that occur in hydrocarbon combustion. The GCF method scales much better with orbital basis function dimension and with the number of electrons than traditional high-level electronic structure methods. No intrinsic restrictions are imposed on the orbital occupations, and in particular there are no artificial excitation-level or occupation restrictions with respect to a reference function or reference space; in this sense, the method is more correctly characterized as a multiconfigurational method rather than a multireference method. Because the wave function is a linear combination of GCF basis functions rather than a single expansion term, this allows the method to be used for both ground and excited electronic states, the increased wave function flexibility leads to higher accuracy, and this expansion form facilitates the computation of transition moments, nonadiabatic coupling, and other properties that at present can only be computed reliably with multireference and multiconfigurational approaches.

The individual CSF coefficients within a MFGCF are given by an ordered product of rectangular arc factor arrays.

$$x_k = \alpha_{tail,j(1;k)} \alpha_{j(1;k),j(2;k)} \alpha_{j(2;k),j(3;k)} \cdots \alpha_{j(N_{orb}-1;k),head}$$

This means that it is formally a *matrix product state* (MPS), and the resulting wave function corresponds to a linear combination of such MPSs. A feature of MPS expansions is that a redundancy exists in the representation due to identities of the form

$$\begin{aligned} x_k &= \alpha_{tail,j(1;k)} (\alpha_{j(1;k),j(2;k)} \mathbf{B}_{j(2;k)}) (\mathbf{B}_{j(2;k)}^{-1} \alpha_{j(2;k),j(3;k)}) \cdots \alpha_{j(N_{orb}-1;k),head} \\ &= \alpha_{tail,j(1;k)} \tilde{\alpha}_{j(1;k),j(2;k)} \tilde{\alpha}_{j(2;k),j(3;k)} \cdots \alpha_{j(N_{orb}-1;k),head} \end{aligned}$$

where  $\mathbf{B}_j$  is some arbitrary nonsingular square transformation matrix associated with node  $j$  of the Shavitt graph, and  $\tilde{\alpha}_{j,j'}$  are the transformed arc factors. Because the CSF coefficient  $x_k$  is unchanged by this transformation of adjacent sets of arc factors, the representation in terms of the elements of the arc factor arrays is redundant (or overdetermined). The arc factor matrices  $\alpha$  associated with a given upper node may be collected into a partitioned matrix  $\mathbf{Q} \in \mathbb{R}^{m \times n}$  with  $m \geq n$ , and, without loss of flexibility in the wave function,  $\mathbf{Q}$  may be restricted to be orthogonal,  $\mathbf{Q}^T \mathbf{Q} = \mathbf{1}$ . Indeed, this restriction eliminates certain numerical instabilities that would otherwise occur. Further, the transformation matrices  $\mathbf{B}_j$  may also be taken to be orthogonal. With these restrictions, the arc factor matrices  $\mathbf{Q}$  may be restricted to be elements of a Grassmann manifold, and the minimal number of essential parameters  $\{\phi\}$  may be used to specify all of the nontrivial variations allowed within each GCF for the purposes of wave function optimization. Four different possible essential parametrizations of orthogonal matrices that comprise the Grassmann manifold, with  $N_\phi = (m-n)n$ , and the more general Stiefel manifold, with  $N_\phi = mn - n(n+1)/2$ , were considered in *J. Phys. Chem. A* **119**, 7924 (2015): the exponential representation, the Householder reflector representation, the Givens rotation representation, and the rational Cayley transform representation. For these parametrizations, the properties of the  $\mathbf{Q}(\phi)$  mapping, the  $\phi(\mathbf{Q})$  mapping, and the chain rule transformations of the form

$$\frac{\partial E}{\partial \phi_k} = \sum_{i=1}^m \sum_{j=1}^n \frac{\partial E}{\partial Q_{ij}} \frac{\partial Q_{ij}}{\partial \phi_k} \quad ; k = 1 \dots N_\phi$$

were compared. After considering the computational efficiency, the numerical stability, continuity, the need to compute smooth mappings for both  $\mathbf{Q}(\phi)$  and  $\phi(\mathbf{Q})$ , and the efficiency of the chain rule transformation, the Householder reflector representation was chosen for the initial implementation of the MFGCF method. However, the other parameterizations also have some interesting features that could prove beneficial to other chemical applications in which the elements of square or rectangular orthogonal matrices need to be parameterized in terms of the minimal number of essential variables. For example, when an interpolation of the form  $\phi(s) = \phi_0 + s\Delta$  for scalar  $s$  is imposed for the essential variables, then all of the above orthogonal parameterizations result in smooth but generally distinct mappings of the orthogonal matrix  $\mathbf{Q}(s) \equiv \mathbf{Q}(\phi(s))$ . This property may be used in interpolation, extrapolation, and optimization algorithms involving  $\mathbf{Q}(s)$  and on its properties, including the energy  $E(\mathbf{Q}(s))$ .

**Future Plans:** Our MFGCF implementation has so far used single-headed Shavitt graphs appropriate for describing individual molecular states with a given number of electrons, with a particular spin state, and that belong to a particular point group irreducible representation (irrep). We will generalize this in several respects including the ability to state-average over multiple irreps, the ability to average states described with multiheaded Shavitt graphs, and the ability to allow multiple facets for the head nodes. These generalizations will allow the computation of Hamiltonian matrix elements corresponding to states with different numbers of electrons, different spin values, and different irreps simultaneously with only a relatively small increase in effort over the current single-state approach, allowing multistate calculations to approach the efficiency of the current single-state calculations. With these generalizations, the computation of transition properties is facilitated by the fact that all states are described with the same set of arc factors.

**Publications:**

- “The Multiradical Character of One- and Two-Dimensional Graphene Nanoribbons,” F. Plasser, H. Pašalić, M. H. Gerzabek, F. Libisch, R. Reiter, J. Burgdörfer, T. Müller, R. Shepard, and H. Lischka, *Angewandte Chemie International Edition* **52**, 2581-2584 (2013).
- “Der Multiradikalcharakter ein- und zweidimensionaler Graphen-Nanobänder,” F. Plasser, H. Pašalić, M. H. Gerzabek, F. Libisch, R. Reiter, J. Burgdörfer, T. Müller, R. Shepard, and H. Lischka, *Angewandte Chemie* **125**, 2641-2644 (2013).
- “Graphically Contracted Function Electronic Structure Method,” R. L. Shepard, G. Gidofalvi, and S. R. Brozell, *Abstracts of Papers of the American Chemical Society* **246**, 159-PHYS (2013).
- “Comparison of Multireference Configuration Interaction Potential Energy Surfaces for  $H+O_2 \rightarrow HO_2$ : The Effect Of Internal Contraction,” L. B. Harding, S. J. Klippenstein, H. Lischka, and R. Shepard, *Theor. Chem. Acc.* **133**, 1429 (2014).
- “Wave Function Analysis with Shavitt Graph Density in the Graphically Contracted Function Method,” G. Gidofalvi, S. R. Brozell, and R. Shepard. *Theor. Chem. Acc.* **133**, 1512 (2014).
- “Wave function analysis with Shavitt graph density in the graphically contracted function method,” G. Gidofalvi, S. Brozell, R. Shepard, *Abstracts of Papers of the American Chemical Society* **248**, 450-COMP (2014).
- “The Multifacet Graphically Contracted Function Method. I. Formulation and Implementation,” R. Shepard , G. Gidofalvi, and S. R. Brozell. *J. Chem. Phys.* **141**, 064105 (2014).
- “The Multifacet Graphically Contracted Function Method. II. A General Procedure for the Parameterization of Orthogonal Matrices and its Application to Arc Factors,” R. Shepard , G. Gidofalvi, and S. R. Brozell. *J. Chem. Phys.* **141**, 064106 (2014).
- “The Representation and Parametrization of Orthogonal Matrices,” R. Shepard, S. R. Brozell, and G. Gidofalvi. *J. Phys. Chem. A* **119**, 7924-7939 (2015).
- “Shavitt Memorial Festschrift Collection,” *Theor. Chem. Acc.* (2016). ISSN: 2194-8666, ISSN 2194-8674 (electronic). Edited by R. Shepard, T. H. Dunning, Jr., and R. M. Pitzer.

# Mechanisms and Models for Combustion Simulations

Raghu Sivaramakrishnan

Chemical Dynamics Group, Chemical Sciences & Engineering Division

Argonne National Laboratory, Argonne, IL 60439

[raghu@anl.gov](mailto:raghu@anl.gov)

## I. Program Scope

Mechanisms describing the combustion chemistry of even simple fuels can be complex involving a myriad of unimolecular and bimolecular elementary steps. The primary scope of this program is to develop and validate detailed chemical kinetics mechanisms and models for use in combustion simulations.

The kinetics models will be developed on the basis of a consistent framework incorporating theoretical predictions, experimental measurements, and evaluations of elementary reaction rate coefficients including feedback loops between them. The detailed models will subsequently be used for simulations of data from reactors, shock-tubes, rapid compression machines, and flames, the aim being the validation of the mechanistic and kinetic aspects of these models over practical combustion regimes.

## II. Recent Progress

### A. Anharmonic Thermochemistry for the $\text{CH}_3$ Radical Impacts Combustion Simulations

In an attempt to resolve discrepancies for the small molecule kinetics in our methanol mechanism development efforts, the available literature kinetics data for the  $\text{H} + \text{CH}_3 (+\text{M}) = \text{CH}_4 (+\text{M})$  reaction has been re-analyzed over a wide temperature range (300-4300 K), in collaboration with my postdoc Nicole Labbe. There are numerous reports of kinetics studies for this reaction summarized in the most recent Baulch et al.<sup>1</sup> compilation. However, direct studies for the kinetics of this reaction are limited to the recombination measurements by Brouard et al.<sup>2</sup> (300-600 K), and the shock-tube methane dissociation measurements by Kiefer and Kumaran<sup>3</sup> (2700-4300 K), Davidson et al.<sup>4</sup> (1800-2300 K), and Sutherland et al.<sup>5</sup> (1700-2100K). Given the extended range of temperatures, adequate fits to both sets of recombination and dissociation data require accurate thermochemistry. Anharmonic corrections to the partition functions are a necessary prerequisite to calculate accurate thermochemistry over such extended temperature ranges. While these corrections are accounted for<sup>6</sup> in the thermochemistry of  $\text{CH}_4$ , the most recent IUPAC<sup>7</sup> recommendation for the thermochemistry of the  $\text{CH}_3$  radical relies on RRHO partition functions. Using the Active Thermochemical Tables<sup>8</sup> approach, Ruscic has provided updated thermochemistry including anharmonic corrections for the  $\text{CH}_3$  radical to enable accurate fits to the available literature kinetics for the  $\text{H} + \text{CH}_3 (+\text{M}) \rightarrow \text{CH}_4 (+\text{M})$  reaction. Interestingly, in the updated anharmonic thermochemistry, specific heat capacities ( $C_p$ ) for the  $\text{CH}_3$  radical are significantly lower than RRHO based thermochemistry at  $T > 1000$  K. Additionally, Ruscic has also provided us with the thermochemistry for all  $\text{HO}_x$  and  $\text{CH}_x$  species over extended temperature ranges and an analysis of these also reveals significant differences in  $C_p$  for  $^3\text{CH}_2$  from the IUPAC<sup>7</sup> recommendation.  $\text{CH}_3$  and  $^3\text{CH}_2$  are important species in combustion chemistry, particularly so for  $\text{CH}_4$  combustion. A preliminary simulation of a  $\text{CH}_4$ -air flame (Figure 1) using literature kinetics models<sup>9,10</sup> (USC Mech II and Aramco) with the updated  $\text{CH}_3$  and  $^3\text{CH}_2$  thermochemistry leads to ~ 10% increase in flame speeds in the fuel-rich part of the flame. Updating the kinetics for  $\text{H} + \text{CH}_3 (+\text{M}) \rightarrow \text{CH}_4 (+\text{M})$  along with the thermochemistry for  $\text{CH}_3$  and  $^3\text{CH}_2$  in USC Mech II leads to a notable 25-30% increase (solid lines in Fig. 1) in predicted flame speeds relative to the predictions from the original models (dashed-dotted lines in Fig. 1). Updated  $\text{CH}_3$  thermochemistry not only affects the  $\text{H} + \text{CH}_3 (+\text{M}) \rightarrow \text{CH}_4 (+\text{M})$  equilibrium but also has a cascading effect on the equilibria for  $\text{CH}_3 + \text{CH}_3 \rightarrow \text{C}_2\text{H}_6$ ,  $\text{CH}_3 + \text{CH}_3 \rightarrow \text{C}_2\text{H}_5 + \text{H}$ ,  $\text{CH}_3 + \text{O}_2 \rightarrow \text{CH}_3\text{O}_2$ , and numerous other reactions relevant to combustion chemistry. In collaboration with Ruscic we plan to initiate studies on the impact of the revised  $\text{CH}_3$  thermochemistry for kinetics measurements (notably  $\text{CH}_3 + \text{CH}_3$ ) and combustion simulations.

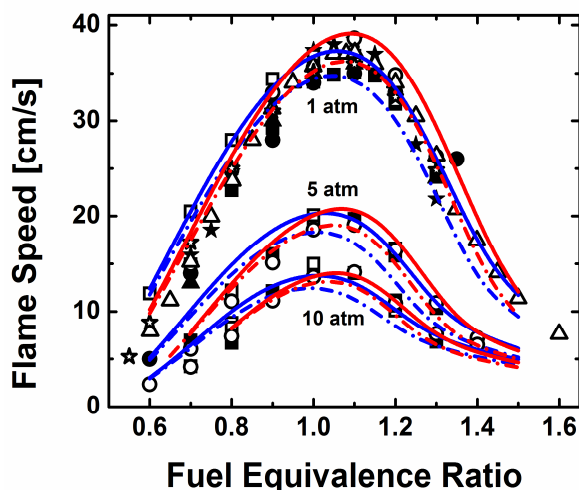


Figure 1:  $\text{CH}_4$ -air flames,  $T_u = 298\text{K}$ . Symbols – Data, Red Lines – Aramco Model<sup>10</sup>, Blue Lines – USC Mech II<sup>9</sup>. Dashed Dotted Lines - Raw Models, Solid Lines - Models updated with  $\text{CH}_3$  thermo and  $\text{H} + \text{CH}_3 = \text{CH}_4$  evaluation from present work.

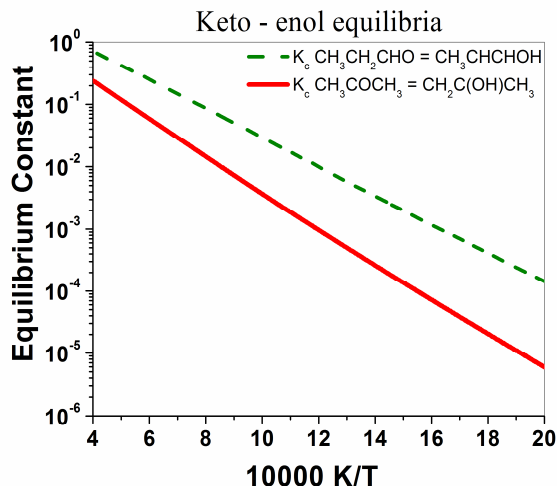


Figure 2: Keto-enol equilibria.

### B. Simulating Pyrolysis Chemistry in Micro-Tubular Reactors

Recent studies using micro-tubular reactors<sup>11,12</sup> coupled with a variety of diagnostics have been used to probe the high temperature pyrolytic chemistry of organic molecules. These experiments offer access to conditions similar to those in laminar premixed flames; i. e. low-pressures and high-temperatures, which can emphasize the role of bimolecular addition-elimination reactions. In prior work with J. V. Michael, L. B. Harding, and S. J. Klippenstein, we have conclusively demonstrated<sup>13</sup> the role of keto-enol tautomerizations and radical-molecule addition-elimination reactions to explain product observations<sup>11</sup> from  $\text{CH}_3\text{CHO}$  pyrolysis using a micro-tubular reactor.

Theory/Modeling studies in progress on  $\text{H} + \text{CH}_3\text{CHO}$  and  $\text{H} + \text{CH}_3\text{COCH}_3$  also indicate that addition-eliminations can occur in these reactions to form  $\text{CH}_2\text{O}$  and  $\text{CH}_3\text{CHO}$  respectively. While addition-elimination to form  $\text{CH}_2\text{O}$  has been predicted<sup>14</sup> to be a minor process in  $\text{H} + \text{CH}_3\text{CHO}$ , the addition process in  $\text{H} + \text{CH}_3\text{COCH}_3$  to form  $\text{CH}_3\text{CH}(\text{O})\text{CH}_3$  radical has a lower barrier than abstraction. Using the results from prior<sup>13,14</sup> and ongoing theoretical studies, we have initiated simulations to interpret micro-tubular experiments on these bimolecular reactions by Proszument and collaborators. Recent CFD studies by Barney Ellison and John Daily<sup>15</sup> indicate that the centerline temperatures in these micro-tubular reactors may be substantially lower (by 200-300 K) than the maximum wall temperatures. This suggests that some of the pyrolytic chemistry occurs at lower temperatures (800-1200 K). Consequently fuel radicals and other stable radicals persist and under such conditions bimolecular reactions are probably more facile at removing these radicals than unimolecular reactions. Preliminary simulations indicate that apart from keto-enol and addition-elimination reactions, radical-radical addition-eliminations also influence these measurements. In particular, our ongoing simulations indicate that observations of  $^{13}\text{CH}_2\text{O}$  in 0.1%  $^{13}\text{CH}_3^{13}\text{CHO}$ , 0.1%  $\text{CH}_3\text{ONO}$  (H-atom source) experiments in the micro-tubular reactor is due to  $\text{H}^{13}\text{CO} + \text{H}^{13}\text{CO} \rightarrow ^{13}\text{CH}_2\text{O} + ^{13}\text{CO}$  at low temperatures (1000 K). At higher temperatures (>1200K),  $\text{H} + ^{13}\text{CH}_3^{13}\text{CHO} \rightarrow ^{13}\text{CH}_3 + ^{13}\text{CH}_2\text{O}$  is the dominant source for  $^{13}\text{CH}_2\text{O}$ . Additionally, the importance of keto-enol tautomerization in  $\text{CH}_3\text{CHO}$  suggests that these isomerizations may also play a role in simulating the pyrolytic chemistry of other ketones and aldehydes. Figure 2 shows the keto-enol equilibria for acetone and propanal and it is evident that the enol form should be considered in simulations of high temperature experiments. Preliminary simulations indicate that the source for  $\text{C}_3\text{H}_6$  in shock-tube pyrolysis<sup>16</sup> of  $\text{CH}_3\text{CH}_2\text{CHO}$  is  $\text{H} + \text{CH}_3\text{CHCHOH} \rightarrow \text{C}_3\text{H}_6 + \text{OH}$ , a reaction not considered in the simulations by Lifshitz et al.<sup>16</sup>

### C. Thermal Decompositions of Xylyl radicals

In collaboration with J.V. Michael, S.J. Klippenstein, and C. Cavallotti (Politecnico Milano), we have initiated a joint experiment-theory study of *o*-xylylbromide dissociation as a source for *o*-xylyl radicals and the subsequent dissociation kinetics of *o*-xylyl. The high sensitivity H-atom ARAS detection technique was used to obtain quantitative measurements of the H-atom yields and rate constants for *o*-xylyl decomposition ( $1267\text{ K} \leq T \leq 1597\text{ K}$ ;  $P \sim 0.3\text{-}1.0\text{ atm}$ ). The results from these studies and comparisons to earlier studies are discussed in terms of two processes; *o*-xylyl  $\rightarrow$  H + *o*-xylylene and *o*-xylyl  $\rightarrow$  non-H-atom channel. The experimental data have been subsequently compared with the results of a computational investigation performed in collaboration. The full PES is composed of 20 wells connected by 37 transition states. Master equation simulations were performed to determine channel specific rate constants for the decomposition of *o*-, *m*-, and *p*-xylyl for a wide range of temperatures and pressures. The simulations predict that the main products of decomposition are *o*-xylylene + H, *p*-xylylene + H, styrene + H, phenyl + C<sub>2</sub>H<sub>4</sub> and fulvenallene + CH<sub>3</sub>, with H channels accounting for about 80% of the decomposition products. It was also found that *ortho-meta-para* isomerization is a fast process, with a rate that is competitive with that of decomposition. The theoretical analysis also helped clarify the decomposition kinetics of the *o*-xylylbromide precursor. A publication describing these joint experiment/theory studies is nearing submission.

### D. A detailed analysis of methanol combustion kinetics

In collaboration with N.J. Labbe, S.J. Klippenstein, and the group of Y. Ju (Princeton University), an updated model for methanol combustion was developed. Initial simulations indicated that methanol (as the dominant intermediate from methylformate) and its sub-set mechanisms required a substantial update. In particular, the methanol model includes new theoretical kinetics predictions for OH + CH<sub>3</sub>OH and decompositions of CH<sub>2</sub>OH and CH<sub>3</sub>O, with a re-analysis of the H-atom abstractions from methanol by H, CH<sub>3</sub>, HO<sub>2</sub>, and O<sub>2</sub>. Simulations with the model indicate good agreement with literature data from shock-tubes, reactors, and flames. Recommendations for methanol combustion studies are also presented.

## III. Future work

There are high-level theoretical studies<sup>17,18</sup> on the thermal dissociations of the smaller C<sub>2</sub> and C<sub>3</sub> radicals. However, such studies are lacking for the larger C<sub>4</sub> and C<sub>5</sub> radicals. In collaboration with Klippenstein, we propose to theoretically characterize the thermal dissociations of the four C<sub>4</sub>H<sub>9</sub> radical isomers, and additionally calculate prompt dissociation fractions<sup>19</sup> for inclusion in combustion modeling. In collaboration with Klippenstein and Nils Hansen (CRF-Sandia), we propose to simulate the formation of intermediates in fuel-rich flames of small alkenes/alkynes. A particular focus is on the formation and destruction of larger aromatics, and PAH's to further our understanding of soot precursor chemistry.

## IV. Acknowledgements

This work was supported by the U.S. Department of Energy, Office of Science, Office of Basic Energy Sciences, Division of Chemical Sciences, Geosciences, and Biosciences under Contract No. DE-AC02-06CH11357.

## V. References

1. D.L. Baulch, C.T. Bowman, C.J. Cobos, R.A. Cox, Th. Just, J.A. Kerr, M.J. Pilling, D. Stocker, J. Troe, W. Tsang, R.W. Walker, J. Warnatz, J. Phys. Chem. Ref. Data **2005**, 34, 757-1397.
2. M. Brouard, M.T. Macpherson, M.J. Pilling, J. Phys. Chem. **1989**, 93, 4047.
3. J.H. Kiefer, S.S. Kumaran, J. Phys. Chem. **1993**, 97, 414-420.
4. D.F. Davidson, R.K. Hanson, C.T. Bowman, Int. J. Chem. Kin. **1995**, 27, 305-308.
5. J.W. Sutherland, M. -C. Su, J.V. Michael, Int. J. Chem. Kin. **2001**, 33, 669-684.
6. A. Burcat and B. Ruscic, "Third Millennium Ideal Gas and Condensed Phase Thermochemical Database for Combustion with Updates from Active Thermochemical Tables", Joint Report: ANL-05/20, Argonne National Laboratory, Argonne, IL, USA, and TAE 960, Technion - Israel Institute of Technology, Haifa, Israel (2005).

7. B. Ruscic, J.E. Boggs, A. Burcat, A.G. Csaszar, J. Demaison, R. Janoschek, J.M.L. Martin, M.L. Morton, M.J. Rossi, J.F. Stanton, P.G. Szalay, P.R. Westmoreland, F. Zabel, T. Berces, *J. Phys. Chem. Ref. Data* **2005**, 34, 573.
8. B. Ruscic, *J. Phys. Chem. A* **2015**, 119, 7810.
9. H. Wang, X. You, A.V. Joshi, S.G. Davis, A. Laskin, F. Egolfopoulos, C.K. Law, USC Mech Version II. High-Temperature Combustion Reaction Model of H<sub>2</sub>/CO/C<sub>1</sub>-C<sub>4</sub> Compounds. [http://ignis.usc.edu/USC\\_Mech\\_11.htm](http://ignis.usc.edu/USC_Mech_11.htm)
10. W.K. Metcalfe, S.M. Burke, S.S. Ahmed, H.J. Curran, *Int. J. Chem. Kin.* **2013**, 45, 638-675.
11. A. Vasiliou, K.M. Piech, B. Reed, X. Zhang, M.R. Nimlos, M. Ahmed, A. Golan, O. Kostko, D.L. Osborn, D.E. David, K.N. Urness, J.W. Daily, J.F. Stanton, G.B.; Ellison, *J. Chem. Phys.* **2012**, 137, 164308.
12. K. Prozument, Y.V. Suleimanov, B. Buesser, J.M. Oldham, W.H. Green, A.G. Suits, R.W. Field, *J. Phys. Chem. Lett.* **2014**, 5, 3641-3648.
13. R. Sivaramakrishnan, J.V. Michael, L.B. Harding, S.J. Klippenstein, *J. Phys. Chem. A* **2015**, 119, 7724-7733.
14. R. Sivaramakrishnan, J.V. Michael, S.J. Klippenstein, *J. Phys. Chem. A* **2010**, 114, 755-764.
15. Q. Guan, K.N. Urness, T.K. Ormond, D.E. David, G.B. Ellison, J.W. Daily, *Int. Rev. Phys. Chem.* **2014**, 33, 447.
16. A. Lifshitz, C. Tamburu, A. Suslensky, *J. Phys. Chem.* **1990**, 94, 2966-2972.
17. J.A. Miller, S.J. Klippenstein, *J. Phys. Chem. A* **2004**, 108, 8296-8306.
18. J.A. Miller, S.J. Klippenstein, *J. Phys. Chem. A* **2013**, 117, 2718-2727.
19. N.J. Labbe, R. Sivaramakrishnan, C.F. Goldsmith, Y. Georgievskii, J.A. Miller, S.J. Klippenstein, *J. Phys. Chem. Lett.* **2016**, 7, 85-89.

## VI. Journal articles supported by this project 2013-2016

1. S. L. Peukert, R. Sivaramakrishnan, M.-C. Su, and J. V. Michael, "High temperature rate constants for H/D + methylformate and methylacetate", *Proc. Combust. Inst.* **34**, 463-471 (2013).
2. R. Sivaramakrishnan, W. Liu, M. J. Davis, S. Som, D. E. Longman, and T. F. Lu, "Development of a reduced biodiesel surrogate model for compression ignition engine modeling", *Proc. Combust. Inst.* **34**, 401-409 (2013).
3. S. L. Peukert, R. Sivaramakrishnan, and J. V. Michael, "High temperature shock tube and theoretical studies on the thermal decomposition of dimethylcarbonate and its bimolecular reactions with H and D-Atoms", *J. Phys. Chem. A* **117**, 3718-3728 (2013).
4. S. L. Peukert, R. Sivaramakrishnan, and J. V. Michael, "High temperature shock tube studies on the thermal dissociation of O<sub>3</sub> and the reaction of dimethyl carbonate with O-atoms", *J. Phys. Chem. A* **117**, 3729-3738 (2013).
5. S. Som, W. Liu, D. D. Y. Zhou, G. M. Magnotti, R. Sivaramakrishnan, D. E. Longman, R. T. Skodje, and M. J. Davis "Quantum Tunneling Affects Engine Performance", *J. Phys. Chem. Lett.* **4**, 2021-2025 (2013).
6. N. J. Labbe, R. Sivaramakrishnan, S. J. Klippenstein, "The Role of Radical + Fuel-Radical Well-Skipping Reactions in Ethanol and Methylformate Low-pressure Flames", *Proc. Combust. Inst.* **35** (2014) 447-455.
7. R. Sivaramakrishnan, J. V. Michael, L. B. Harding and S. J. Klippenstein, "Resolving some paradoxes in the thermal decomposition mechanism of CH<sub>3</sub>CHO", *J. Phys. Chem. A* **119**, (2015) 7724-7733.
8. N. J. Labbe, R. Sivaramakrishnan, B. Ruscic, "Anharmonic Thermochemistry for CH<sub>3</sub> Influences Hydrocarbon Flame Propagation", In Preparation, *J. Phys. Chem. A* (2016).
9. N. J. Labbe, P. Dievert, X. L. Yang, R. Sivaramakrishnan, S. J. Klippenstein, Y. Ju, "A detail analysis of the kinetics of methanol combustion", In Preparation, *Comb. And Flame* (2016).
10. D. Polino, R. Sivaramakrishnan, S. J. Klippenstein, J. V. Michael, C. Cavallotti "Experimental and theoretical studies on the thermal decomposition of xylyl radicals", In Preparation, *J. Phys. Chem. A* (2016).
11. S. L. Peukert, R. Sivaramakrishnan, S. J. Klippenstein, J. V. Michael, "Shock tube and theoretical kinetics studies on the thermal decomposition of iso-propanol and it's reaction with D-atoms", In Preparation, *J. Phys. Chem. A* (2016).

# Quantum Chemistry of Radicals and Reactive Intermediates

John F. Stanton  
Institute for Theoretical Chemistry  
University of Texas  
Austin, TX 78712  
jfstanton@mail.utexas.edu

## Scope of Research

My research group works in the area of theoretical chemical physics, especially on the thermodynamic properties, spectra, and reactions of organic radicals and other transient intermediates. In addition, we are active developers of software for computational electronic structure (quantum chemistry), computational and theoretical spectroscopy, and more recently, computational chemical kinetics<sup>1</sup>. More specifically, our quantum chemistry research follows a number of paths which tend to be associated with advanced many-body methods for treating electron correlation (many-body perturbation theory and, especially, the coupled-cluster approximation), including first-principles calculations of bond energies and other thermochemical information (as well as development of methodology for such calculations), methods tailored for the analysis of molecular spectroscopy (especially for situations in which the Born-Oppenheimer approximation breaks down) and the development of *ab initio* methods and implementations that are suitable for the accurate treatment of transient organic molecules and radicals of interest to combustion science.

## Summary of Recent Accomplishments

In the past two years, we have made considerable strides towards making the highest practical realizations of coupled-cluster theory – those involving “quadruple excitations” – realistic for practical calculations on molecules of interest. This work, which was a prominent part of our last renewal proposal, is largely that of my outstanding associate D.M. Matthews. After completing the required technical infrastructure for his new NCC program, which took a few years, the rate at which new methods have been implemented efficiently since mid-2014 has been remarkable. The NCC program is a part of the CFOUR program package developed by my group and collaborators in Europe, which is freely available to the research community; this new module for very high-level calculations has already been used by members of the gas-phase chemical physics program (GPCP). It is roughly *two orders of magnitude* faster than the other well-known implementations for the coupled-cluster method known as CCSDT(Q), and is about ten times faster for the “full” CCSDTQ treatment of electron correlation. Perhaps the principal reason for its efficiency lies in the fact that it is based on a carefully planned and optimized algorithm for these calculations, rather than a product of automated code generation of the underlying theories. While faster than existing methods for these very accurate treatments of electron correlation, energy calculations at these levels of theory are not unique to NCC and CFOUR. However, in the last year, several unique developments have been made. These include analytic gradients for CCSDT(Q), a full suite of equation-of-motion coupled cluster methods (the so-called EOMIP, EOMEE and EOMEA variants) for CCSDTQ, and non-iterative corrections to the EOM-CCSD and EOM-CCSDT methods.

The NCC program has allowed us to do some previously impossible calculations. An example here is a recent calculation for glycoaldehyde (the smallest molecule to contain an aldehyde group and a hydroxyl unit), which has been done as part of an ongoing collaboration with the research group of G.B. Ellison (Boulder) on mechanisms of anaerobic pyrolysis of organic molecules. For glycoaldehyde, we have been able

---

<sup>1</sup>We have quite recently entered into a formal partnership with J.R. Barker (Michigan) in the development of the MultiWell program suite (see: <http://clasp-research.engin.umich.edu/multiwell/>), where our efforts will be focused on the semiclassical transition state theory for the computation of state-dependent reaction probabilities, as well as master equation methods. The latter is an area of recent development by my associate T.L. Nguyen, as mentioned elsewhere in this report.

to carry out thermochemical calculations with a slight modification of the HEAT protocol developed in our group. As a part of this work, two of the calculations: CCSDT with the cc-pVTZ basis and CCSD(T) with aug-cc-pVQZ (the latter comprises more than 1000 basis functions), were done with NCC. The CCSDT(Q) calculation, which is done with a small basis set in the HEAT protocol, was negligible in comparison to the large basis set CCSD(T) and CCSDT calculations. Another previously “impossible” calculation done recently is an EOMIP-CCSDTQ calculation on the propiolate anion ( $\text{HCCCCO}_2^-$ ), which is part of a collaboration with R.E. Continetti (UCSD) of the GPCP program. We believe that NCC will see rapidly increasing use in the computational community, and will allow calculations to be done at these levels of theory for a variety of chemically interesting problems.

In other work related to high-accuracy calculations of energy, we have collaborated with B. Ruscic (Argonne) of the GPCP program and firmly established the HCN/HNC energy difference, using (NCC-based) quantum chemistry calculations in conjunction with the Active Thermochemical Tables methods of Ruscic. This work helped to clarify a somewhat puzzling disagreement between two very high-level calculations done with multireference configuration interaction methods, the most of recent of which turned out to be the less accurate. Another similar application is a recent calculation of the *cis-trans* isomerization barrier for the first singlet excited state of acetylene, which was done with EOMEE-CCSDTQ and a large atomic natural orbital basis set. The result turned out to be in excellent agreement with a value determined spectroscopically in a collaboration with the group of R.W. Field (MIT) of the GPCP program, using a novel new method based on an analysis of vibrational intervals at high energies.

In other theoretical method development work, we have collaborated with the group of A.I. Krylov (USC) and produced relatively simple and useful methods for the calculation of both photodetachment and photoionization cross sections. In my group, this work was begun some time ago by my associate T. Ichino, who focused only on photodetachment. However, the project ultimately grew into a collaboration with the Krylov group, which did beautiful developments of the theory, implemented it in an easy-to-use and free computer program, and carried out rigorous testing. Due to the simpler nature of the photodetachment problem (the outgoing electron is “free” in the sense it does not have a Coulomb interaction with its former environment), a method based on Dyson orbitals and plane waves works fairly well there, but Krylov and her team have shown that forming an admixture of Coulomb and plane waves manages to work reasonably well for many photoionization examples. As use of the Advanced Light Source and photoionization in general is integral to the research mission of many in the GPCP, we believe that these methods could provide useful interpretive assistance to many experimentalists.

Finally, my associate L.T. Nguyen has continued his excellent work in chemical kinetics. He has developed a simple approximate (steady-state) treatment of the two-dimensional (energy and angular momentum) master equation (2DME), and has applied this to the ozonolysis of ethylene, a process that involves the ballyhooed Criegee intermediate. Calculations based on high-level HEAT calculations (again facilitated by NCC) using his 2DME approach have succeeded in reproducing the observed product distribution of this classic and fundamental chemical reaction for the first time.

### **Ongoing Research and Future Plans**

Work is currently underway in a number of areas. Perhaps the most important is the extension of the NCC program to treat open-shell systems, efforts that are currently being carried out by my graduate student Christopher Lopez in collaboration with Matthews. Due to the well-organized nature of the carefully planned NCC program, this should be a fairly straightforward venture once the required infrastructure is developed. This process is fairly time-consuming (a similar period preceded the current and rapid developments of NCC for closed-shell applications), but is likely to be completed by early 2017. In other theoretical work, we have spent a fair amount of time in the last six months investigating various approaches for “cheap” (non-iterative) treatments of higher excitations (triples and quadruples) in the context of EOM-CC theory, and have identified at least one method to date that works quite well. We continue to work with P.B. Changala (Boulder) on variational methods for vibrational and vibronic problems, and are currently studying the excited state of acetylene as a vibrational problem and the deliciously complex five-state interaction that governs the vibronic energy level of structure of the nitrate radical. The latter work will also extend to rovibronic analysis, as recent high-resolution experiments in Japan and by T.A. Miller (Ohio State) need to be studied and analyzed. Some other ongoing studies are: an ATcT-based analysis of some resonance stabilized radicals with Ruscic and Ellison; an investigation of semiclassical transition state theory and its performance relative to other empirical tunneling corrections with A.F. Wagner (Argonne) of the GPCP; studies of the

structure and reactivity of radicals with M.C. McCarthy (Harvard Smithsonian); the aforementioned work with Continetti on HCCCO<sub>2</sub>; and benchmarking of approximate HEAT methods for thermochemical and kinetics applications.

**Students and Postdoctoral Supported:**

T.L. Nguyen (postdoc) C.A. Lopez (student)

## References acknowledging DE-FG02-07ER15884

**D.A. Matthews and J.F. Stanton** Nonorthogonal Spin-Adaptation of High-Order Coupled-Cluster Methods. A New Implementation of Methods Involving Quadruple Excitations *J. Chem. Phys.* 142, 064108 (2015).

**L.T. Nguyen, H. Lee, D.A. Matthews, M.C. McCarthy and J.F. Stanton** Stabilization of the Simplest Criegee Intermediate from the Reaction Between Ozone and Ethylene: A High-Level Quantum Chemical and Kinetic Analysis of Ozonolysis *J. Phys. Chem. A* 119, 5524 (2015).

**T.L. Nguyen and J.F. Stanton** A Steady-State Approximation to the Two-Dimensional Master Equation for Chemical Kinetics Calculations *J. Phys. Chem. A* 119, 7627 (2015).

**T.K. Ormond, A.M. Scheer, M.R. Nimlos, D.L. Robichaud, T.P. Troy, M. Ahmed, J.W. Daily, T.L. Nguyen, J.F. Stanton and G.B. Ellison** Pyrolysis of Cyclopentadienone: Mechanistic Insights From a Direct Measurement of Product Branching Ratios, *J. Phys. Chem. A* 119, 7222 (2015).

**T.L. Nguyen, M.C. McCarthy and J.F. Stanton** Relatively Selective Production of the Simplest Criegee Intermediate in a CH<sub>4</sub>/O<sub>2</sub> Electric Discharge: Kinetic Analysis of a Plausible Mechanism *J. Phys. Chem. A* 119, 7197 (2015).

**T.K. Ormond, P. Hemberger, T.P. Troy, M. Ahmed, J.F. Stanton and G.B. Ellison** The Ionization Potential of Cyclopentadienone: A Photoelectron-Photoion Coincidence Study, *Mol. Phys.* 113, 2350 (2015).

**J.H. Baraban, P.B. Changala, G.C. Mellau, J.F. Stanton, A.J. Merer and R.W. Field** Spectroscopic Characterization of Isomerization Transition States *Science* 350, 1338 (2015).

**S. Gozem, A.O. Gunina, T. Ichino, D.L. Osborn, J.F. Stanton and A.I. Krylov** Photoelectron Wave Function in Photoionization: Plane Wave or Coulomb Wave?, *J. Phys. Chem. Lett.* 6, 4532 (2015).

**T.L. Nguyen, J.H. Baraban, B. Ruscic and J.F. Stanton** On the HCN-HNC Energy Difference *J. Phys. Chem. A* 119, 10929 (2015).



# Universal and State-Resolved Imaging Studies of Chemical Dynamics

Arthur G. Suits

*Department of Chemistry, University of Missouri, Columbia MO 65211*  
*suitsa@missouri.edu*

## I. Program Scope

The focus of this program is on combining universal ion imaging probes providing global insight, with high-resolution state-resolved probes providing quantum mechanical detail, to develop a molecular-level understanding of chemical phenomena. Particular emphasis is placed upon elementary reactions important in understanding and predicting combustion chemistry. This research is conducted using state-of-the-art molecular beam machines, photodissociation, reactive scattering, and vacuum ultraviolet lasers in conjunction with ion imaging techniques. An important advance in the group recently is the development of a unique Chirped-pulse Fourier-Transform Microwave (CP-FTMW) spectrometer coupled to a pulsed Uniform Supersonic Flow system. This “CPUF” (Chirped-pulse/Uniform Flow) approach, developed in collaboration with the Field group at MIT, affords new opportunities to study product branching and kinetics in reactions of polyatomic molecules. New directions in the use of this instrument are described below. An important development in the past year is the move of the entire group into newly renovated laboratories at the University of Missouri, Columbia.

## II. Recent Progress

Our current DOE research is directed along two major avenues. In the first, we have continued and extended our investigations of polyatomic reaction dynamics using crossed-beams with DC slice imaging. Our recent efforts have turned to focusing on fluorine atom reactions with larger hydrocarbons, contrasting them with the Cl atom reaction extensively studied in our laboratory. Secondly, we are exploring many exciting opportunities afforded by the CPUF technique to obtain detailed product branching in combustion-relevant reactions, and to use the method to explore kinetics in unprecedented detail.

### *Systematic studies of polyatomic reaction dynamics.*

In recent years we have pursued a wide range of crossed-beam imaging studies of bimolecular reactions using the F<sub>2</sub> excimer at 157nm as a “universal” probe for C<sub>3</sub> and larger hydrocarbons and related systems for which the radical products have ionization energies below 7.9 eV. We have now begun a systematic investigation of F atom reactions with a range of target molecular systems. F atoms offer a very revealing contrast to the Cl atom reactions that we and others have extensively studied in recent years. Their reactions are analogous to Cl atom reactions in many ways albeit with greatly increased exoergicity. In our initial studies, we examined the reaction dynamics of F atom with selected alkanes using crossed beam scattering with DC slice velocity map imaging, as described in last year’s abstract. More recently we have extended these studies to F atom reaction with alcohols and alkenes as described in the following.

The first series of reactions we have studied is F atoms with alkenes, extending our recent work on Cl atom reactions. Fluorine reactions with alkenes provide rich chemistry as a result of their very large variations in exoergicity for different abstraction sites, as well as the existence of strongly bound radical adducts. We studied the reaction dynamics of fluorine + 1-butene and 1-hexene via dc slice imaging in crossed beams (see Fig. 1). Addition of F atom to either  $sp^2$  carbon atom is over two eV downhill, and H abstraction even from the vinylic sites is  $> 1\text{eV}$  exoergic, while it is over  $2\text{eV}$  exoergic for the allylic sites. As a result, a substantially larger energy release to translation is seen in these systems compared to analogous Cl atom reactions and even comparing to F atom reactions with alkanes. This energy release, however, remains a small fraction of the available energy.

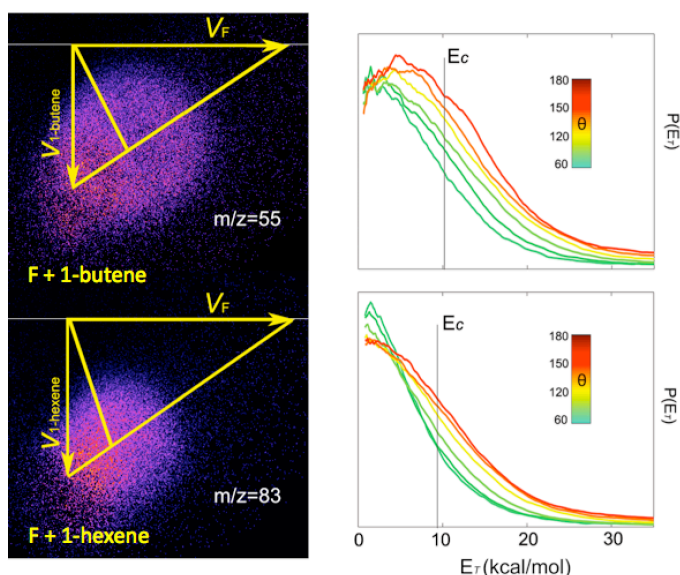


**Figure 1. Crossed-beam imaging of alkenyl radical products of F atom reactions along with angle-resolved translational energy release.**

As previous mechanistic studies suggested sharp differences in the probabilities for abstraction at alkyl H atoms vs. the hydroxyl H atom site, we will combine our results and those for selectively deuterated reactants along with further theoretical calculations of the propanol isomers to gain further insight into these reactions.

### CPUF probe of product branching in unimolecular and bimolecular reactions.

Resonant ionization methods and laser-induced fluorescence and related probes are a widely used and sensitive means of detecting reaction products, but they are limited to relatively small molecular systems for which the spectroscopy is known. Furthermore, it is extremely challenging to obtain quantitative product branching with these techniques. Even for VUV single photon ionization, determining product branching is not straightforward. The advent of the chirped-pulse microwave technique offers a compelling means of overcoming the challenges associated with these traditional techniques, at the same time offering a nearly universal probe. A key requirement for the use of rotational spectroscopy to obtain quantitative product branching is a

Oxygenated hydrocarbons are of current interest as biofuels, and these systems also offer special dynamical interest to both theory and experiment. We conducted the first crossed beam DC slice imaging study of fluorine reaction with 1-propanol. In addition to multiple reactive sites, the presence of a strongly H-bonded entrance complex and the high degree of polarities of the products and high exoergicity of the reaction make for a fascinating reaction that is challenging to interpret. We found a higher portion of collision energy goes into product translation compared with F + alkanes and Cl +

well-defined temperature. By coupling the CP-FTMW method to a uniform supersonic flow, we achieve a thermalized, low temperature environment ideal for quantifying products of photochemical or bimolecular reactions.

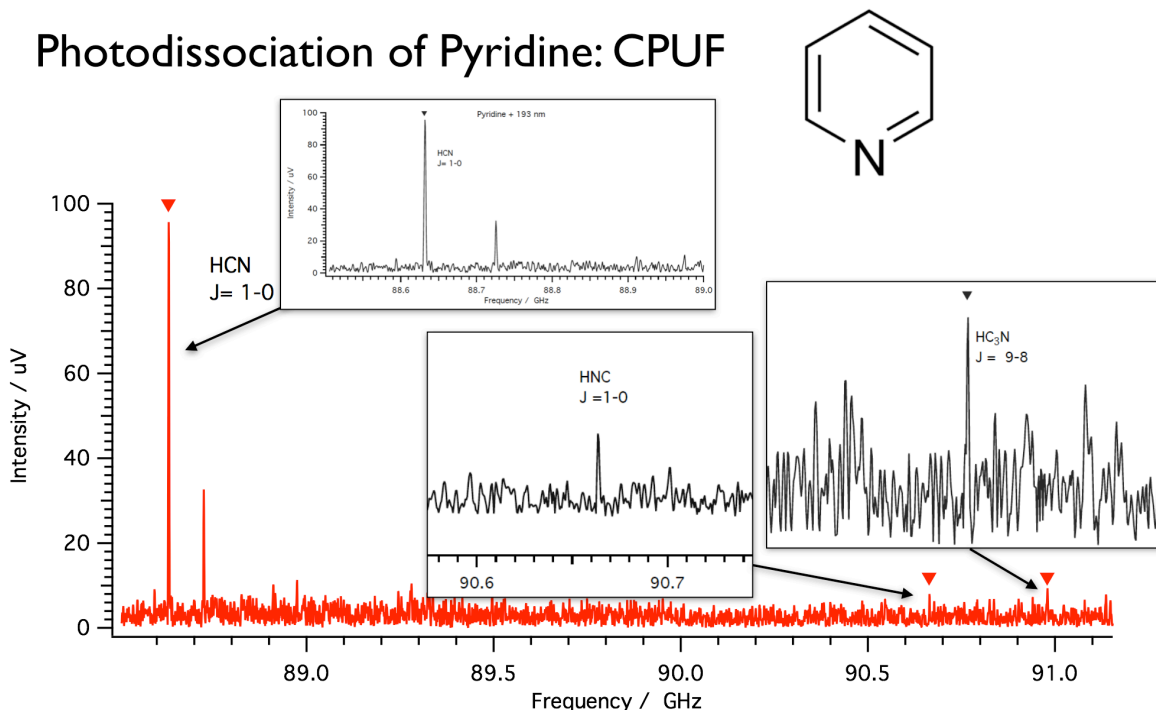


**Figure 2. mm-Wave spectra of reaction products following 193nm photodissociation of pyridine.**

In our last abstract we described initial applications of the CPUF technique to study the bimolecular reaction of CN with propyne, probing all four product channels in that reaction. We have recently applied this method to photodissociation, probing the 193nm dissociation of pyridine. Results in the W-band showing three product channels are given in Fig. 2. Strong signals at HCN and cyanoacetylene are seen. Weaker signal at HNC is detected. We expect also to see the pyridinyl radicals following H elimination and we are presently developing predicted frequencies for these, as they have not been reported in the microwave to-date. In this study we are collaborating with Alex Mebel, who has identified all the product channels and transition states and performed RRKM branching calculations. Based on the calculations, we suspect the HNC channel may be the result of two-photon excitation. We are now undertaking power dependence studies in our new laboratories to examine this as well.

### III. Future Directions

*State-resolved and universal crossed-beam DC slice imaging.* We will continue our crossed-beam imaging studies with VUV probe in our new laboratories in Missouri. Initially we will continue to explore F atom reactions with alcohols and small heterocycles. We will then move to reactions of CN and O(<sup>1</sup>D) with larger hydrocarbons. We are interested in complementary studies using the crossed-beam imaging as well as the CPUF technique to obtain detailed dynamics and accurate product branching at the same time.

Chirped-pulse mm-wave detection in uniform supersonic flows.

In addition to measuring product branching with CPUF, we can look at kinetics in unprecedented detail. We plan to couple the CPUF method to IR excitation to explore relative reactivity and kinetics of V-V energy transfer for differing modes of vibrational excitation or for conformer-specific kinetics. We have also greatly expanded our frequency coverage, down to 6 GHz and up to 140 GHz, extending the range of molecules we can study and covering several octaves.

#### IV. DOE Publications 2013-present

B. Joalland, Van Camp, R. D., Shi, Y., Patel, N., & Suits, A. G., "Crossed-Beam Slice Imaging of Cl Reaction Dynamics with Butene Isomers." *J. Phys. Chem. A.* (2013) DOI: 10.1021/jp403030s.

L. Yan, F. Cudry, W. Li, and A. G. Suits, "Isomer-Specific Mass Spectrometric Detection Via Semi-Soft Strong-Field Ionization," *J. Phys. Chem. A* (2013) DOI: 10.1021/jp403118c.

B. Joalland, Shi, Y., Patel, N., Van Camp, R., & Suits, A., "Dynamics of Cl+ Propane, Butanes Revisited: A Crossed Beam Slice Imaging Study." *Phys. Chem. Chem. Phys.* (2014) DOI: 10.1039/C3CP51785C.

B. Joalland, Y. Shi, A. G. Suits and A. M. Mebel, "Roaming dynamics in radical addition/elimination reactions," *Nature Comm.* (2014) DOI: 10.1038/ncomms5064

B. Joalland, Y. Shi, A. D. Estillore, A. Kamasah, A. M. Mebel, A. G. Suits, "Dynamics of chlorine atom reactions with hydrocarbons: Insights from imaging the radical product in crossed beams," *The Journal of Physical Chemistry A.* (2014) doi:10.1021/jp504804n (Feature Article).

F. Cudry, J. M. Oldham, S. Lingenfelter, and A. G. Suits. "Strong-Field Ionization of Flash Pyrolysis Reaction Products." *J. Phys. Chem. A* (2015) **119**, 460-467. DOI: 10.1021/jp510552a.

Y. Shi, A. Kamasah, B. Joalland, and A. G. Suits. "Crossed-Beam DC Slice Imaging of Fluorine Atom Reactions with Linear Alkanes." *J. Chem. Phys.* (2015) **142**, 184309.

# An Update on the Implementation of a Novel Multiscale Simulation Strategy for Reacting

## Flows

PI: James C. Sutherland  
Department of Chemical Engineering, The University of Utah  
Salt Lake City, UT 84112-9203  
James.Sutherland@utah.edu  
Project start date: October, 2012

### I. Lattice Based Multiscale Simulation

#### A. Introduction

Direct Numerical Simulation (DNS) of turbulent flows, particularly at high Reynolds numbers, is prohibitively expensive due to the range of length scales present. The One-Dimensional Turbulence (ODT) model is a cost effective alternative that fully resolves length scales down to the Kolmogorov length scales in a single dimension while using a stochastic model to account for turbulence. Although ODT has been shown to capture buoyant flows, stratified flows and, of most interest to us, combusting flows [1, 4, 6] accurately, it fails to capture some large scale phenomena such as vortex pairing, recirculation or three dimensional flows that cannot easily be reduced to lower dimensions such as asymmetric geometries.

We have previously proposed a new methodology to bridge the gap between Large Eddy Simulation (LES) and DNS. This methodology, termed Lattice-Based Multiscale Simulation (LBMS), creates a system of ODT models that overcomes the shortcomings of ODT at a cost significantly cheaper than DNS. Furthermore, by fully solving all governing equations at the smallest scales, all phenomena associated with turbulent combustion can be accurately captured.

#### B. Basic Formulation

The LBMS model is a lattice like structure of ODT models, as depicted in Figure 1. The governing equations take the form

$$\int_{V(t)} \frac{\partial \rho \psi}{\partial t} dV = - \int_{S(t)} \Theta_{\psi} \cdot \mathbf{n} dS + \int_{V(t)} R_{\psi} dV, \quad (1)$$

where  $\psi$  is the transported variable,  $\Theta_{\psi}$  is the flux through surface  $S$  and  $R_{\psi}$  are source terms. We solve equations for mass, momentum, internal energy, and species with an ideal gas equation of state and appropriate constitutive models for diffusive fluxes.

The fine spacing,  $\delta x_i$ , where  $i$  denotes a cartesian direction, is the resolution required for the smallest spatial structures in the flow field. The coarse spacing,  $\Delta x_i$ , is the spacing between each individual line (on the order of the integral length scale), and all lines in a given direction form a *bundle*.

Fluxes between ODT lines (*i.e.*, perpendicular to the bundle direction they are calculated on) are under-resolved due to the coarse spacing  $\Delta x_i$ . This issue is resolved in one of two ways, both of which interpolate a fully resolved flux from the bundle parallel to said flux direction to the other bundles. In the first method, flux interpolation is completed by imposing the fluxes that live on

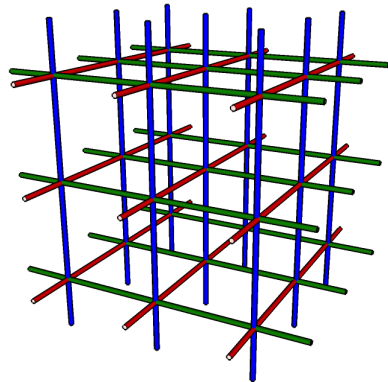


Figure 1: Representation of a 3D LBMS mesh. Each color denotes a different directional bundle. Lines are fully resolved.

other bundles. In the second, the flux is reconstructed by setting the high wave number but underresolved flux information from the bundle that is receiving the fully resolved flux to the integral of the fully resolved flux to ensure conservation across control volumes.

## II. Progress Summary

### A. Isotropic Turbulence Decay

LBMS can accurately capture the turbulent kinetic energy spectra across a range of scales as well as the appropriate decay of the total kinetic energy for isotropic turbulence. Initial conditions are created using a synthetic turbulence generator, matching the kinetic energy of experimental grid generated turbulence data [2]. Additional verification is done by comparing intermediate time steps to a traditional Large Eddy Simulation (LES) run with a dynamic Smagorinsky model. Figure 2 compares the decay of the total kinetic energy in time for LBMS, LES and the experimental data. For this case,  $N_x = N_y = N_z = 4$  coarse grid points were used with  $n_x = n_y = n_z = 512$  fine grid points ( $\Delta/\delta = 128$ ). That is, the simulation has a total of 16 ODT lines for each bundle direction, where each line has 512 points. The reference LES simulation utilized  $(\Delta_{LES}/L)^3 = 32^3$  grid points. Thus, the LBMS lattice spacing was 8 times coarser than the reference LES simulation.

This represents a significant milestone in our efforts. With a functioning isotropic turbulence decay demonstration, we have increased confidence that the formulation can adequately handle turbulent flow. As will be discussed below, we have also added species transport with detailed reaction mechanism support and are now positioned to begin examining LBMS on reacting flows.

### B. Scalability

We have previously demonstrated parallel scalability of the LBMS solver out to several thousand MPI ranks. The LBMS solver uses a task graph approach [5] that facilitates asynchronous communication to allow some overlap of communication with computation.

### C. Species Transport

Full species transport with the appropriate source terms have been implemented into the LBMS framework and coupled to the Cantera package for detailed treatment of thermochemistry. Ignition and premixed flame propagation studies have been run to ensure proper treatment of species transport and source terms.

### D. Boundary Conditions

We have implemented the Navier-Stokes Characteristic Boundary Conditions (NSCBC) treatment [7] into the LBMS framework, including the ability to pass flames through the boundaries. This is shown in Figure 3, where the OH profile of a outwardly-propagating premixed flame is shown at various times, illustrating that the flame passes through the boundary without distortion. This will allow us to simulate the reacting jet configurations that we are targeting. We also have implemented the ability to specify arbitrary boundary condition geometries.

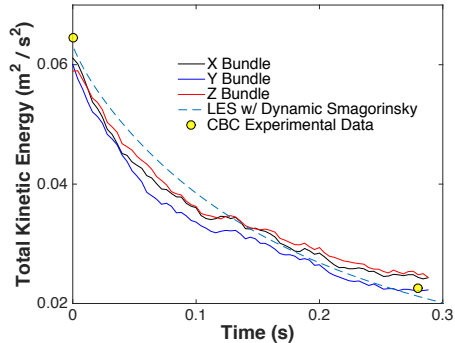


Figure 2: Total kinetic energy decay in time for each bundle with  $\Delta/\delta = 128$ .

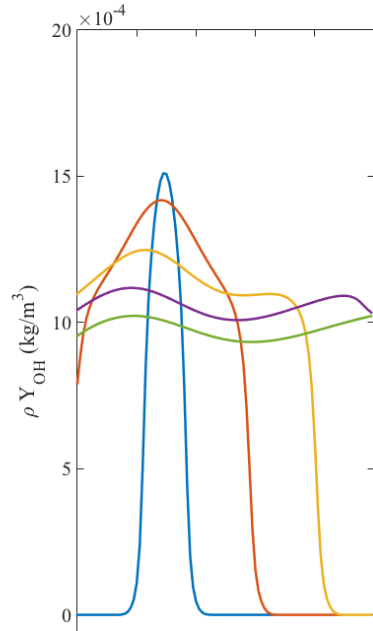


Figure 3: A flame front (indicated by OH) passing through a NSCBC boundary at various stages in time.

### III. State-Space Parameterization of Chemical Jacobian Eigenvalues

Explosive modes such as ignition and extinction are characterized by an eigenvalue of the chemical Jacobian matrix with positive real part, representing the transient instability of chain-branching chemistry and thermal feedback. This explosive eigenvalue is used in chemical explosive mode analysis (CEMA) and by a nonlinear solver known as pseudo-transient continuation ( $\Psi_{tc}$ ), or dual time-stepping. These applications require formation and eigen-decomposition of the Jacobian matrix, which are expensive operations whose cost increases exponentially with chemical mechanism size. As an alternative to directly computing the eigenvalues of the Jacobian, we have demonstrated that principal component analysis (PCA) along with nonlinear regression can provide accurate parameterization of the by a very small number of variables.

For homogeneous autoignition, the explosive regime and eigenvalue can be represented well on manifolds in two to four dimensions for a variety of initial temperatures and pressures, including both oxygen and air as oxidizers, for hydrogen, syngas, methane, ethanol and octane mechanisms. Results indicate that PCA-based models can be used for inexpensive, matrix-free eigenvalue calculation in computational flame diagnostics such as CEMA.

The implication of this work is that, for applications using CEMA, one can train a model off-line by preprocessing *e.g.*, autoignition cases and then use simple function evaluations rather than calculating the eigenvalues of the source Jacobian matrix. For application to DNS diagnostics, this can result in dramatic decrease in computational workload. Specifically, if CEMA is run at each timestep, then for explicit schemes such as those employed in Sandia's S3D DNS code, this can be up to two orders of magnitude reduction in computational time relative to a direct application of CEMA. For implicit schemes using analytic Jacobians, this can be up to one order of magnitude reduction in cost by avoiding the eigenvalue decomposition in CEMA.

This work will be submitted for publication in Combustion Theory & Modeling in April, 2016.

### IV. Future Work

#### A. Parameter Studies

Two parameters of particular importance are the eddy rate constant and the ratio of coarse to fine scales,  $\Delta/\delta$ . The eddy rate constant affects the number of eddies and thus, the transfer of momentum to thermal energy through viscous dissipation. The eddy rate constant must be tuned appropriately to ensure that the kinetic energy decay in time matches DNS, experimental or model data sets. The coarse to fine ratio,  $\Delta/\delta$ , directly affects the scale at which three-dimensional effects are directly resolved ( $\Delta$ ). Scales between  $\Delta$  and  $\delta$  are resolved along individual lines in each direction, but turbulent mixing in this range of length scales is modeled through ODT. We expect that, for isotropic turbulence, large  $\Delta/\delta$  will be feasible, but other flows involving strong recirculation such as confined jets may require somewhat smaller  $\Delta/\delta$ . This must be quantified through validation studies.

#### B. Turbulent Reacting Flow Calculations

Due to various setbacks, the appropriate boundary conditions have taken significantly longer than anticipated to implement into the LBMS methodology. The ultimate goal is still to simulate a turbulent combustive jet flow. DNS data from a CO/H<sub>2</sub> jet simulation will have conserved quantities filtered and applied as initial conditions [3]. The boundary conditions are periodic in one dimension and require Characteristic Boundary Condition treatment in the other two. A full mechanism will be applied. This case has been shown to be adequately captured by traditional ODT already. This case will allow LBMS to test its ability against a fully resolved case to capture full 3D convective diffusive interactions important in a turbulent reactive flow. More intriguing, though, is how LBMS will perform when coarsened. ODT has been shown to over-predict extinction and re-ignition properties in this case due to the lack of 3-Dimensional diffusive interactions with

the turbulence model [6]. LBMS, theoretically, should see an increase in over-prediction as the coarse to fine grid spacing,  $\Delta x_i/\delta_{x_i}$ , increases.

## V. Publications & Presentations

1. D. Cline, J. C. Sutherland, and T. Saad. Lattice based multiscale simulation. In SIAM Computational Science and Engineering Conference (poster) [www.siam.org/meetings/cse15](http://www.siam.org/meetings/cse15), March 2015.
2. J. Hutchins, D. Cline, and J. C. Sutherland. A task-parallel approach for solving PDEs on a lattice. In SIAM Computational Science and Engineering Conference (poster) [www.siam.org/meetings/cse15](http://www.siam.org/meetings/cse15), March 2015.
3. M. A. Hansen, E. Armstrong, and J. C. Sutherland, “State Space Parameterization of Chemical Eigenvalues,” in Western States Section of the Combustion Institute, 2016, pp. 1–29.
4. M. A. Hansen, E. Armstrong, and J. C. Sutherland, “State Space Parameterization of Explosive Eigenvalues for Ignition and Extinction,” *Combustion Theory & Modelling*, submitted April, 2016.

## References

- [1] Wm. T. Ashurst and Alan R. Kerstein. One-dimensional turbulence: Variable-density formulation and application to mixing layers. *Physics of Fluids*, 17(2):025107, 2005.
- [2] Stanley Corrsin and Geneviève Comte-Bellot. Simple Eulerian time correlation of full- and narrow-band velocity signals in grid-generated, isotropic turbulence. *Journal of Fluid Mechanics*, 48(2):273–337, 1971.
- [3] Evatt R. Hawkes, Ramanan Sankaran, James C. Sutherland, and Jacqueline H. Chen. Scalar mixing in direct numerical simulations of temporally evolving plane jet flames with skeletal CO/H<sub>2</sub> kinetics. *Proceedings of the Combustion Institute*, 31 I:1633–1640, 2007.
- [4] J C Hewson and A R Kerstein. Stochastic simulation of transport and chemical kinetics in turbulent CO/H<sub>2</sub>/N<sub>2</sub> flames. *Combust. Theory Modelling*, 5:669–697, 2001.
- [5] Patrick K. Notz, Roger P. Pawlowski, and James C. Sutherland. Graph-Based Software Design for Managing Complexity and Enabling Concurrency in Multiphysics PDE Software. *ACM Transactions on Mathematical Software*, 39(1):1–21, November 2012.
- [6] Naveen Punati, James C. Sutherland, Alan R. Kerstein, Evatt R. Hawkes, and Jacqueline H. Chen. An evaluation of the one-dimensional turbulence model: Comparison with direct numerical simulations of CO/H<sub>2</sub> jets with extinction and reignition. *Proceedings of the Combustion Institute*, 33(1):1515–1522, 2011.
- [7] James C. Sutherland and Christopher a. Kennedy. Improved boundary conditions for viscous, reacting, compressible flows. *Journal of Computational Physics*, 191(2):502–524, November 2003.

# Elementary Reaction Kinetics of Combustion Species

Craig A. Taatjes

*Combustion Research Facility, Mail Stop 9055, Sandia National Laboratories,  
Livermore, CA 94551-0969  
cataatj@sandia.gov*

## SCOPE OF THE PROGRAM

This program aims to develop new methods for studying chemical kinetics and to apply these methods to the investigation of fundamental chemistry relevant to hydrocarbon oxidation and combustion science. One central goal is to perform accurate measurements of the rates at which important free radicals react with each other and with stable molecules. Another goal is to characterize complex reactions that occur via multiple potential wells by investigating the formation of products. These investigations employ simultaneous time-resolved detection of multiple species in well-characterized photolytically-initiated reaction systems where multiple consecutive and competing reactions may occur. Detailed characterization of these reactions under accessible experimental conditions increases the confidence with which modelers can extrapolate to the conditions of real-world devices. This research often requires the development and application of new detection methods for precise and accurate kinetics measurements. Absorption-based techniques and mass-spectrometric methods have been emphasized, because many radicals critical to combustion are not amenable to fluorescence detection.

An important part of our strategy, especially for complex reaction systems, is using experimental data to test and refine detailed calculations (working in close cooperation with Stephen Klippenstein at Argonne and Ahren Jasper and Judit Zádor at Sandia), where the theory enables rigorous interpretation of experimental results and guides new measurements that will probe key aspects of potential energy surfaces. This methodology has been applied in our investigations of the reactions of fuel radicals with O<sub>2</sub>. The combination of rigorous theory and validation by detailed experiments has made great strides toward a general quantitative model for alkyl oxidation, and now extends to reactions of oxygenated molecules relevant to biofuel combustion and to the effects of unsaturation on the chemistry leading to autoignition. Moreover, we have increasingly aimed at producing species that are intermediates in oxidation systems (e.g., Criegee intermediates, hydroperoxyalkyl radicals) and directly probing their reaction kinetics.

## RECENT PROGRESS

We continue to apply frequency-modulation and direct absorption spectroscopy to measurements of product formation in reactions of alkyl radicals with O<sub>2</sub> and kinetics of unsaturated hydrocarbon radicals. In addition, the multiplexed photoionization mass spectrometric reactor at the Advanced Light Source (ALS), an experimental effort led by David Osborn (see his abstract), has become a major part of our investigations of low-temperature hydrocarbon oxidation chemistry. In the past year we have been largely occupied with expanding our understanding of the fundamental chemistry of carbonyl oxides (Criegee intermediates), but our attention is returning to details of reactions that are important in the ignition chemistry of biofuels, such as the reactions of molecular oxygen with fuel radicals.

**Effects of resonance stabilization on ROO and QOOH chemistry.** Last year we directly measured the kinetics of a resonance-stabilized QOOH radical,<sup>p</sup> and other work we have shown that vinylic stabilization of QOOH or ROO that occurs in ketone oxidation can steer the oxidation reaction via resonance-stabilized intermediates.<sup>1</sup> We have continued to investigate the details of ketone oxidation, following on the earlier internally funded work.

Pulsed-photolytic chlorine-initiated oxidation of diethyl ketone and partially deuterated isotopologs showed the impact of resonance stabilization on the pressure and temperature dependence of  $R + O_2$  reaction pathways. At 8 Torr, the nature of the cyclic ether + OH channel changes as a function of temperature. At 450 K, the production of OH is mainly in conjunction with formation of 2,4-dimethyloxetan-3-one, resulting from reaction of the resonance stabilized secondary  $R_S$  with  $O_2$ . In contrast, at 550 K and 8 Torr, 2-methyl-tetrahydrofuran-3-one, originating from oxidation of the primary radical ( $R_P$ ) is observed as the dominant cyclic ether product. Formation of either of these cyclic ether production channels proceeds *via* a resonance stabilized hydroperoxy alkyl (QOOH) intermediate. Little or no ketohydroperoxide (KHP) is observed under the low pressure conditions. However, at higher pressures (1 – 2 atm), a strong KHP signal appears as the temperature is increased from 450 – 500 K. Measurements on the deuterated DEK isotopologues establishes that the favored pathway produces a  $\gamma$ -KHP via resonance-stabilized alkyl, QOOH and HOOQ'OOH radicals. Several tertiary products exhibit a slow accumulation in coincidence with the observed KHP decay. The oxidation of  $d_4$ -DEK, where kinetic isotope effects disfavor  $\gamma$ -KHP formation, shows greatly reduced KHP formation and the signatures from KHP decomposition products.

In the oxidation of the cyclic ketones cyclopentanone and cyclohexanone the dominant product channel in the  $R + O_2$  reactions is chain-terminating  $HO_2$ -elimination.<sup>9</sup> The major isomeric products are the conjugated species 2-cyclopentenone and 2-cyclohexenone, respectively. The oxidation of 2-methyl-cyclopentanone is similarly dominated by  $HO_2$ -elimination. Quantum chemical calculations show that  $HO_2$ -elimination channels are energetically favored over isomerization to QOOH. The prominence of chain-terminating pathways linked with  $HO_2$  formation in low-temperature oxidation of cyclic ketones suggests little low-temperature reactivity of these species as fuels in internal combustion engines. Indeed, engine experiments have demonstrated that cyclopentanone has high knock resistance.<sup>2</sup> Oxidation reactions of three small-chain methyl esters, methyl propanoate ( $CH_3CH_2COOCH_3$ ; MP), methyl butanoate ( $CH_3CH_2CH_2COOCH_3$ ; MB) and methyl valerate ( $CH_3CH_2CH_2CH_2COOCH_3$ ; MV) show selectivity for conjugated coproducts of  $HO_2$ -elimination channels, i.e., methyl propenoate, methyl-2-butenate, and methyl-2-pentenoate, respectively. However, in MV, upon raising the temperature to 650 K, other  $HO_2$ -elimination pathways are observed that yield methyl-3-pentenoate and methyl-4-pentenoate. Cyclic ethers are observed in each of the methyl ester oxidation systems, with formation via resonance-stabilized QOOH responsible for the most prominent cyclic ether products.

**Reactions of Carbonyl Oxides.** The investigation of the reactions of carbonyl oxides, or Criegee intermediates, has also continued in the past year, in collaboration with Carl Percival (Manchester) and Dudley Shallcross and Andrew Orr-Ewing (Bristol). Partly through a new collaboration with Marsha Lester, we have interest in isomerization

reactions of Criegee intermediates. We measured the reactions of acetone oxide,  $(\text{CH}_3)_2\text{COO}$  and  $(\text{CD}_3)_2\text{COO}$  with  $\text{SO}_2$  and  $\text{NO}_2$ . The reaction with  $\text{SO}_2$  is rapid, as observed in recent experiments from other groups, and the reaction with  $\text{NO}_2$  has a similar rate coefficient to that of acetaldehyde oxide with  $\text{NO}_2$ .<sup>3</sup> The reaction of acetone oxide with  $\text{SO}_2$  produces observable  $\text{SO}_3$ , but no  $\text{NO}_3$  could be detected from the reaction with  $\text{NO}_2$ . Moreover, the other putative product of  $(\text{CH}_3)_2\text{COO}$  with  $\text{NO}_2$ , acetone, is observed to decrease with increasing Criegee intermediate removal by  $\text{NO}_2$ . Interestingly both  $\text{SO}_2$  and  $\text{NO}_2$  appear to facilitate isomerization of the acetone oxide to other isomers, perhaps the vinyl hydroperoxide 2-hydroperoxypropene.

## FUTURE DIRECTIONS

We will continue our collaboration with David Osborn and Lenny Sheps, using their photoionization mass spectrometry machines at the Advanced Light Source, and explore effects of unsaturation and oxygenation on low-temperature oxidation chemistry in coordination with Judit Zador, Ahren Jasper, and Stephen Klippenstein. Measurements of elementary oxidation reactions of representative hydrocarbon and substituted hydrocarbon molecules will continue, with a continuing goal of developing a more general understanding of ignition chemistry.

## References

1. Scheer, A. M.; Welz, O.; Zador, J.; Osborn, D. L.; Taatjes, C. A., *Phys. Chem. Chem. Phys.* **2014**, *16* (26), 13027-13040.
2. Yang, Y.; Dec, J. E.; Sjoberg, M.; Ji, C. S., *Combustion and Flame* **2015**, *162* (10), 4008-4015.
3. Taatjes, C. A.; Welz, O.; Eskola, A. J.; Savee, J. D.; Scheer, A. M.; Shallcross, D. E.; Rotavera, B.; Lee, E. P. F.; Dyke, J. M.; Mok, D. K. W.; Osborn, D. L.; Percival, C. J., *Science* **2013**, *340*, 177-180.

## Publications acknowledging BES support for CAT, 2014 –

- a. Martin Y. Ng, Jordan Nelson, Craig A. Taatjes, David L. Osborn, and Giovanni Meloni, "Synchrotron Photoionization Study of Mesitylene Oxidation Initiated by Reaction with  $\text{Cl}(^2\text{P})$  or  $\text{O}(^3\text{P})$  Radicals," *J. Phys. Chem. A* **118**(21), 3735-3748 (2014).
- b. W. G. Roeterdink, J. Bulthuis, E. P. F. Lee, D. Ding, and C. A. Taatjes, "Hexapole transmission spectrum of formaldehyde oxide," *Chem. Phys. Lett.* **598**, 96-101 (2014).
- c. D. E. Shallcross, C. A. Taatjes, and C. J. Percival, "Criegee intermediates in the indoor environment: new insights," *Indoor Air* **24**(5), 495-502 (2014).
- d. Craig A. Taatjes, Dudley E. Shallcross, and Carl J. Percival, "Research frontiers in the chemistry of Criegee intermediates and tropospheric ozonolysis," *Phys. Chem. Chem. Phys.* **16**(5), 1704-1718 (2014).
- e. Craig A. Taatjes, Dudley E. Shallcross, and Carl J. Percival, "ATMOSPHERIC CHEMISTRY: Intermediates just want to react," *Nature Chemistry* **6**(6), 461-462 (2014).
- f. Oliver Welz, Arkke J. Eskola, Leonid Sheps, Brandon Rotavera, John D. Savee, Adam M. Scheer, David L. Osborn, Douglas Lowe, A. Murray Booth, Ping Xiao, M. Anwar H. Khan, Carl J. Percival, Dudley E. Shallcross, and Craig A. Taatjes, "Rate Coefficients of C1 and C2 Criegee Intermediate Reactions with Formic and Acetic Acid Near the Collision Limit: Direct Kinetics Measurements and Atmospheric Implications," *Angew. Chemie-International Edition* **53**(18), 4547-4550 (2014).
- g. Michael P. Burke, C. Franklin Goldsmith, Stephen J. Klippenstein, Oliver Welz, Haifeng Huang, Ivan O. Antonov, John D. Savee, David L. Osborn, Judit Zador, Craig A. Taatjes, and Leonid Sheps, "Multiscale Informatics for Low-Temperature Propane Oxidation: Further Complexities in Studies of Complex Reactions," *J. Phys. Chem. A* **119**(28), 7095-7115 (2015).
- h. Leah G. Dodson, Linhan Shen, John D. Savee, Nathan C. Eddingsaas, Oliver Welz, Craig A. Taatjes, David L. Osborn, Stanley P. Sander, and Mitchio Okumura, "VUV Photoionization Cross Sections of  $\text{HO}_2$ ,  $\text{H}_2\text{O}_2$ , and  $\text{H}_2\text{CO}$ ," *J. Phys. Chem. A* **119**(8), 1279-1291 (2015).

- i. A. J. Eskola, O. Welz, J. Zador, I. O. Antonov, L. Sheps, J. D. Savee, D. L. Osborn, and C. A. Taatjes, "Probing the low-temperature chain-branching mechanism of n-butane autoignition chemistry via time-resolved measurements of ketohydroperoxide formation in photolytically initiated n-C<sub>4</sub>H<sub>10</sub> oxidation," *Proc. Combust. Inst.* 35, 291-298 (2015).
- j. Gustavo A. Garcia, Xiaofeng Tang, Jean-Francois Gil, Laurent Nahon, Michael Ward, Sebastien Batut, Christa Fittschen, Craig A. Taatjes, David L. Osborn, and Jean-Christophe Loison, "Synchrotron-based double imaging photoelectron/photoion coincidence spectroscopy of radicals produced in a flow tube: OH and OD," *J. Chem. Phys.* 142(16) (2015).
- k. Jessica F. Lockyear, Martin Fournier, Ian R. Sims, Jean-Claude Guillemin, Craig A. Taatjes, David L. Osborn, and Stephen R. Leone, "Formation of fulvene in the reaction of C<sub>2</sub>H with 1,3-butadiene," *Int. J. Mass Spectrom.* 378, 232-245 (2015).
- l. Kai Moshhammer, Ahren W. Jasper, Denisia M. Popolan-Vaida, Arnas Lucassen, Pascal Dievarti, Hatem Selim, Arkke J. Eskola, Craig A. Taatjes, Stephen R. Leone, S. Mani Sarathy, Yiguang Ju, Philippe Dagaut, Katharina Kohse-Hoeinghaus, and Nils Hansen, "Detection and Identification of the Keto-Hydroperoxide (HOCH<sub>2</sub>OCHO) and Other Intermediates during Low-Temperature Oxidation of Dimethyl Ether," *J. Phys. Chem. A* 119(28), 7361-7374 (2015).
- m. David L. Osborn and Craig A. Taatjes, "The physical chemistry of Criegee intermediates in the gas phase," *Int. Rev. Phys. Chem.* 34(3), 309-360 (2015).
- n. John Savee, Talitha Selby, Oliver Welz, Craig A. Taatjes, and David L. Osborn, "Time- and Isomer-Resolved Measurements of Sequential Addition of Acetylene to the Propargyl Radical," *J. Phys. Chem. Letters* 6, 4153-4158 (2015).
- o. John D. Savee, Sampada Borkar, Oliver Welz, Balint Sztaray, Craig A. Taatjes, and David L. Osborn, "Multiplexed Photoionization Mass Spectrometry Investigation of the O(<sup>3</sup>P) + Propyne Reaction," *J. Phys. Chem. A* 119(28), 7388-7403 (2015).
- p. John D. Savee, Ewa Papajak, Brandon Rotavera, Haifeng Huang, Arkke J. Eskola, Oliver Welz, Leonid Sheps, Craig A. Taatjes, Judit Zador, and David L. Osborn, "Direct observation and kinetics of a hydroperoxyalkyl radical (QOOH)," *Science* 347(6222), 643-646 (2015).
- q. Adam M. Scheer, Oliver Welz, Subith S. Vasu, David L. Osborn, and Craig A. Taatjes, "Low temperature (550-700 K) oxidation pathways of cyclic ketones: dominance of HO<sub>2</sub>-elimination channels yielding conjugated cyclic coproducts," *Phys. Chem. Chem. Phys.* 17(18), 12124-12134 (2015).
- r. Oliver Welz, Michael P. Burke, Ivan O. Antonov, C. Franklin Goldsmith, John D. Savee, David L. Osborn, Craig A. Taatjes, Stephen J. Klippenstein, and Leonid Sheps, "New Insights into Low-Temperature Oxidation of Propane from Synchrotron Photoionization Mass Spectrometry and Multiscale Informatics Modeling," *J. Phys. Chem. A* 119(28), 7116-7129 (2015).
- s. Oliver Welz, John D. Savee, David L. Osborn, and Craig A. Taatjes, "Chlorine atom-initiated low-temperature oxidation of prenol and isoprenol: The effect of C=C double bonds on the peroxy radical chemistry in alcohol oxidation," *Proc. Combust. Inst.* 35, 401-408 (2015).
- t. Giel Muller, Adam Scheer, David L. Osborn, Craig A. Taatjes, and Giovanni Meloni, "Low Temperature Chlorine-Initiated Oxidation of Small-Chain Methyl Esters: Quantification of Chain-Terminating HO<sub>2</sub>-Elimination Channels," *J. Phys. Chem. A* 120(10), 1677-1690 (2016).
- u. Matthew B. Prendergast, Benjamin B. Kirk, John D. Savee, David L. Osborn, Craig A. Taatjes, Kye-Simeon Masters, Stephen J. Blanksby, Gabriel da Silva, and Adam J. Trevitt, "Formation and stability of gas-phase o-benzoquinone from oxidation of ortho-hydroxyphenyl: a combined neutral and distonic radical study," *Phys. Chem. Chem. Phys.* 18(6), 4320-4332 (2016).
- v. Zhandong Wang, Lidong Zhang, Kai Moshhammer, Denisia M. Popolan-Vaida, Vijai Shankar Bhavani Shankar, Arnas Lucassen, Christian Hemken, Craig A. Taatjes, Stephen R. Leone, Katharina Kohse-Hoeinghaus, Nils Hansen, Philippe Dagaut, and S. Mani Sarathy, "Additional chain-branching pathways in the low-temperature oxidation of branched alkanes," *Combust. Flame* 164, 386-396 (2016).

# Elementary Reactions of PAH Formation

Robert S. Tranter

Chemical Sciences and Engineering Division, Argonne National Laboratory

Argonne, IL-60439

tranter@anl.gov

## I. Program Scope

This program is focused on the experimental determination of kinetic and mechanistic parameters of elementary reactions, in particular those involved in the formation and destruction of the building blocks for aromatic species. The program also encompasses dissociation of novel fuels such as ethers and cyclic species and their dissociation products that are representative of oxygenated intermediates in combustion mechanisms. Thermal sources of radicals are also investigated and characterized for use in more complex reaction systems where secondary chemistry can be significant. Recently, the scope has been increased to include thermally initiated roaming reactions. The approach involves a diaphragmless shock tube (DFST) equipped with laser schlieren (LS) and a time-of-flight mass spectrometer (TOF-MS) and low pressure, fast flow, reactor equipped with a quadrupole MS. The combination of these techniques accesses a wide range of reaction temperatures and pressures.

## II. Recent Progress

### A. Chlorobenzene pyrolysis and *o*-benzyne

Halogenated benzenes can be good thermal sources of aromatic and resonantly stabilized radicals. Previous DFST\TOF-MS\LS studies with iodobenzene and fluorobenzene respectively resulted in detailed studies of phenyl radical recombination<sup>1</sup> and the high temperature ( $T > 2100$  K) dissociation of *o*-benzyne<sup>2</sup>. A DFST\LS study of chlorobenzene pyrolysis has been conducted over 1800-2500 K and 35 - 450 Torr to generate phenyl and *o*-benzyne radicals under conditions where recombination of phenyl radicals is negligible and recombination of *o*-benzyne should be competitive with dissociation. The experimental work is complemented by theoretical investigations by Mebel, Harding and Klippenstein of  $C_6H_5Cl$  dissociation and key radical products. These results indicate that the initial dissociation of  $C_6H_5Cl$  is bond scission to  $C_6H_5 + Cl$  with a minor (<10%) roaming path to  $o-C_6H_4 + HCl$ . The agreement between the initial theoretical results and the LS experiments is satisfactory, although further refinement should resolve differences of up to a factor of 2 between the predicted and observed rate coefficients for  $T > 2100$  K. At the experimental conditions phenyl radicals readily eliminate an H-atom forming *o*-benzyne. Thus although  $C_6H_5Cl$  is not a clean source of *o*-benzyne it does provide a ready supply of the radical. Interpretation of the experimental results is further complicated by that fact that Cl is not inert but readily abstracts H-atoms. Consequently,  $Cl + C_6H_5Cl$  is a significant secondary reaction and generates a mixture of *o/m/p*- $C_6H_4Cl + HCl$ . The fates of the chlorophenyl radicals are somewhat uncertain but initial theoretical work suggests that *o*- $C_6H_4Cl$  dissociates to  $o-C_6H_4 + Cl$  providing a secondary source of *o*- $C_6H_4$ . Whereas, dissociation of *m/p*- $C_6H_4Cl$  mainly yields a rapidly equilibrated mix of *cis/trans*-hexa-1,5-diyne-3-en (*l*- $C_6H_4$ ).

The TOF-MS results show that acetylene, diacetylene and triacetylene are the main organic products and no species with masses greater than that of chlorobenzene ( $m/z$  112 and 114) were observed suggesting that recombination reactions of cyclic species are negligible. The product distributions are consistent with what might be expected based on the prior LS studies of *o*-benzyne dissociation at higher temperatures. However, Ghigo et al.<sup>3</sup> have postulated there to be a change in mechanism for dissociation of *o*- $C_6H_4$  at around 2400 K. At high temperatures they suggest a mechanism similar to that employed in the  $C_6H_5F$  study<sup>2</sup> but at lower temperatures Ghigo et al. suggest isomerization of *o*- $C_6H_4$  to *m*- $C_6H_4$  followed by ring opening to *l*- $C_6H_4$  which dissociates to  $C_4H_2 + C_2H_2$  or loses 2H to  $C_6H_2$  with the product distribution being temperature dependent. Both mechanisms produce the same products and are virtually indistinguishable to LS. However, simulations with the mechanism and rate coefficients of Ghigo et al. indicate that their rate coefficients are far too large, even when corrected for the low pressure

of the LS experiments. Initial estimates for the critical isomerization of  $o\text{-C}_6\text{H}_4 \rightarrow [m\text{-C}_6\text{H}_4] \rightarrow l\text{-C}_6\text{H}_4$  by Klippenstein are consistent with the LS profiles and along with improving the  $\text{C}_6\text{H}_4\text{Cl}$  chemistry will be the focus of future work. The simulations indicate high concentrations of benzenes are formed and using our prior estimate of the rate of  $o\text{-C}_6\text{H}_4$  recombination  $^1\text{C}_{12}\text{H}_8$  species would be expected in the TOF-MS results, but are not seen. It is unlikely that this is due to low sensitivity in the TOF-MS to  $\text{C}_{12}\text{H}_8$  (c.f.1). Instead it suggests that there is not a single dominant radical + radical/molecule reaction, but rather several which result in concentrations of multi-ring species below the detection limit of the TOF-MS. Elucidating these reaction paths will be the focus of ongoing work.

## B. Pyrolysis isomerization of $\text{C}_4\text{H}_6$ isomers

The  $\text{C}_4\text{H}_6$  isomers (1,3-butadiene, 1,2-butadiene, 1-butyne, and 2-butyne) are formed in numerous pyrolysis and combustion systems. There is a reasonable literature<sup>4-9</sup> on their initial reactions, but there is not a consistent picture of either the kinetics or mechanism. For 1,3-butadiene, 1,2-butadiene and 1-butyne isomerization can be competitive with dissociation and simulations of experiments starting with each isomer require knowledge of the chemistry of the other isomers, thereby complicating interpretation. Consequently, 350 experiments spanning all four isomers and a broad range of reaction conditions in the high temperature falloff regime have been conducted and simulated in an iterative process. Goldsmith (Brown) performed a theoretical analysis and the master equation results from this were critical for constraining the simulations. Of particular importance was the discovery of a formally direct path for dissociation of thermally excited 1,3-butadiene to  $\text{CH}_3 + \text{C}_3\text{H}_3$ . This is somewhat contradictory to the results of Hidaka et al. who suggest from single pulse shock tube experiments that isomerization of 1,3-butadiene is the dominant reaction. However, it is possible that Hidaka et al. are observing 1,2-butadiene formed by recombination of methyl and propargyl in the cooling wave of the single pulse experiments. While the theoretical results were valuable for guiding the simulations there are significant differences in the absolute values of predicted and experimental rate coefficients, e.g. Fig. 1a. These arise principally from large uncertainties in the phase space theory used and improving the theoretical predictions is the focus of ongoing work. The final mechanism provides very good simulations of all 350 experiments and as shown in Fig. 1b is capable of simulating the TOF-MS results from Kiefer et al.<sup>4</sup>

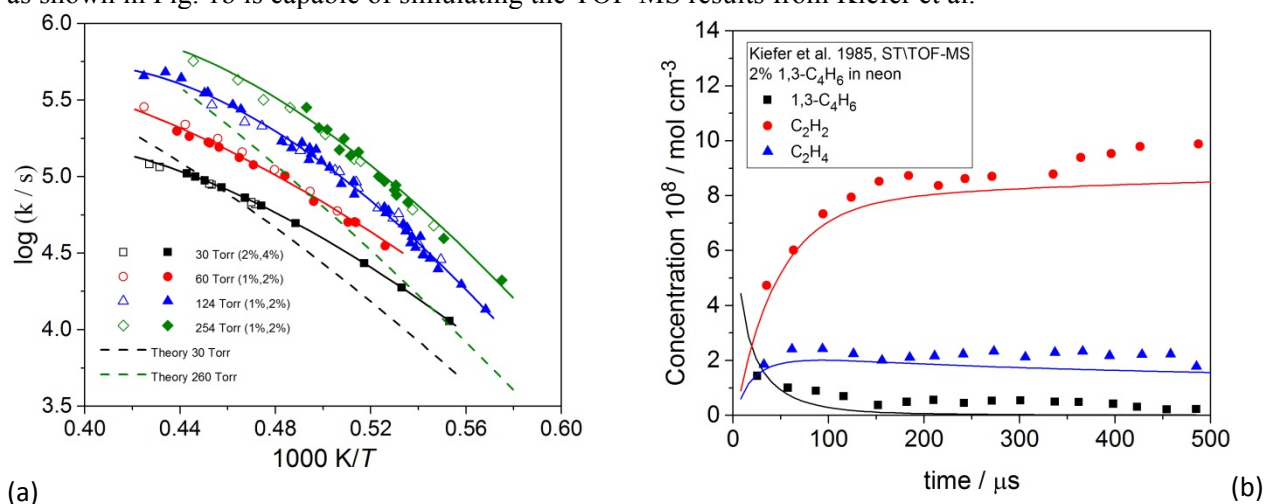


**Figure 1.** a) LS results (30- 250 Torr) for  $1,3\text{-C}_4\text{H}_6 \rightarrow \text{CH}_3 + \text{C}_3\text{H}_3$ . Solid lines are least squares fits to the experimental points. b) Simulation of shock tube/TOF-MS results from Kiefer et al.<sup>4</sup> on 1,3-butadiene pyrolysis with the mechanism from the current work. Symbols represent experiments and lines the simulations.

## C. Reactions of 2-methyl allyl radicals

Resonantly stabilized radicals such as allyl and 2-methyl allyl (2MA) play important roles in molecular growth, low temperature oxidation and inhibition of engine knock. Curran et al. have recently

demonstrated the importance of allyl radical recombination, incorporating results from DFST\LS<sup>10</sup> studies, to modeling ignition delay times from propene oxidation<sup>11,12</sup> and 2MA recombination for isobutene oxidation.<sup>13</sup> The literature on 2MA recombination is sparse, particularly in the 700 - 900 K region of interest for ignition. Consequently, recombination and dissociation of 2MA were studied in a combined LS (60 < P < 260 Torr; 770 < T < 1330 K) and theoretical effort with Jasper.<sup>14</sup> To span this temperature range two precursors for 2MA were used: 1) 2,5-dimethylhexa-1,5-diene (25DM15HD) which dissociates via scission of the weak central C-C bond, reaction (1); 2) 3-methylbut-3-enyl nitrite (C<sub>5</sub>H<sub>9</sub>ONO), synthesized from 3-methylbut-3-enol which readily eliminates NO followed by fast dissociation of the C<sub>5</sub>H<sub>9</sub>O radical, reaction (2). 25DM15HD was usable over 1090 – 1330 K and the nitrite gave access to T < 1060 K. There are no data in the literature on the high temperature dissociation of C<sub>5</sub>H<sub>9</sub>ONO and thus part of this study was to characterize its decomposition reactions.



For T < 1100 K the reverse of reaction (1) is the sole route of consumption of 2-MA. Consequently, the experiments with C<sub>5</sub>H<sub>9</sub>ONO as the precursor can be simply modelled with reactions (1) and (2) and accurate values of k<sub>1</sub> and k<sub>2</sub> are obtained. At higher temperatures dissociation of 2-MA is competitive with recombination and a more complex mechanism is necessary. After the first couple of microseconds the higher temperature LS density gradients are principally sensitive to reactions (3) and (4) and rate coefficients for both of these could be recovered. Over the experimental range k<sub>3</sub>, Fig 2a, is in falloff and the LS results are in excellent agreement with *a priori* theoretical predictions by Jasper and the limited literature. The k<sub>4</sub> are ~ a factor of 2 lower than the sole prior literature study but reasonable considering uncertainties in the prior work and differences in reaction pressure. Above 800 K k<sub>1</sub>, recombination of 2-MA, is in falloff and the pressure dependence is satisfactorily reproduced by theory, Fig. 2b.

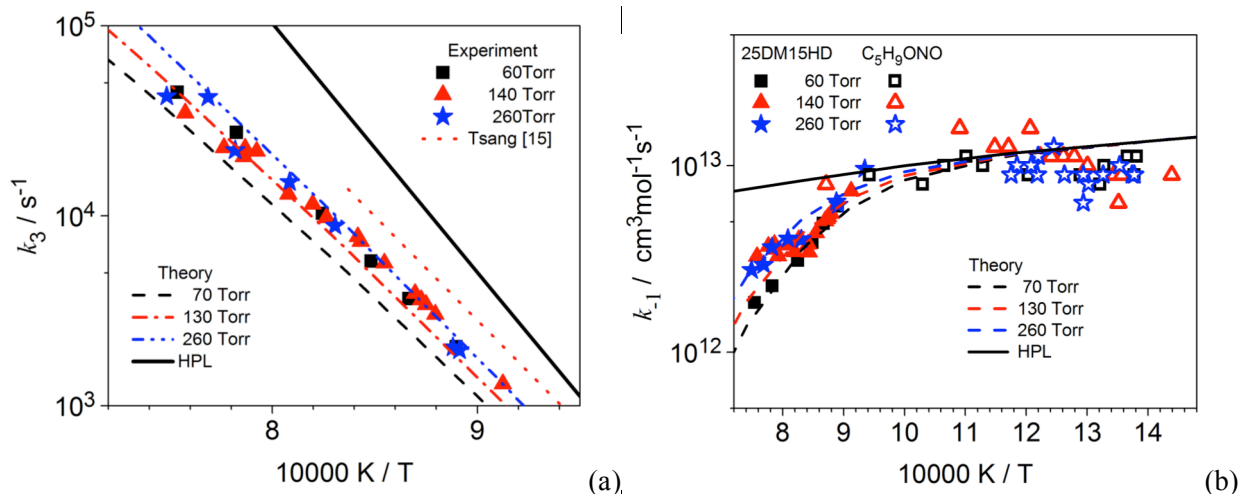


**Figure 2.** a) LS, *a-priori* theoretical results and literature<sup>15</sup> for dissociation of 2-MA. a) Comparison of

### Future Work

The DFST/TOF-MS/LS studies of aromatics and resonantly stabilized radicals are being expanded to include reactions between radicals and oxygen molecules. These represent a new application of the LS technique and initial efforts are focusing on phenyl + O<sub>2</sub>. Further investigations of PAH formation are planned with studies of the H-atom catalyzed conversion of fulvene to benzene and dimethyl fulvenes to xylenes.

### III. References

1. Tranter R. S., Klippenstein S. J., Harding L. B., Giri B. R., Yang X., Kiefer J. H., J. Phys. Chem. A **2010**, 114, 8240.
2. Lynch P. T., Annesley C. J., Tranter R. S., Proc. Combust. Inst. **2015**, 35, 145.
3. Ghigo G., Maranzana A. and Tonachini G., Phys. Chem. Chem. Phys. **2014**, 16, 23944.
4. Kiefer J. H., Wei H. C., Kern R. D. and Wu C. H., Int. J. Chem. Kinet. **1985**, 17, 225
5. Hidaka Y., Higashihara T., Ninomiya N., Masaoka H., Nakamura T., Kawano H., Int. J. Chem. Kinet **1996**, 28, 137.
6. Hidaka Y., Higashihara T., Oki T., Kawano H., Int. J. Chem. Kinet **1995**, 27, 321.
7. Hidaka Y., Higashihara T., Ninomiya N., Oshita H., Kawano H., J. Phys. Chem **1993**, 97, 1097.
8. Peukert S., Naumann C., Braun-Unkloff M., Z. Phys. Chem. **2009**, 223, 427.
9. Chambreau S. D., Lemieux J., Wang L., Zhang J., J. Phys. Chem. A **2005**, 109, 2190.
10. Lynch P. T., Annesley C. J., Aul C. J., Yang X., Tranter R. S., J. Phys. Chem. A. **2013**, 117, 4750.
11. Burke S. M., Burke U., Mc Donagh R., Mathieu O., Osorio I. et al., Combust. Flame **2015**, 162, 296.
12. Burke S. M., Metcalfe W., Herbinet O., Battin-Leclerc F., Haas F. M. et al., Combust. Flame **2014**, 161, 2765.
13. Zhou C.-W., Li Y., O'Connor E., Somers K. P., Thion S. et al. **2016**,  
doi:10.1016/j.combustflame.2016.01.021.
14. Tranter R. S., Jasper A. W., Randazzo J. B., Lockhart J. P. A., Porterfield J. P.. Recombination of 2-methyl allyl radicals: Experiment and Theory. Submitted, Proc. Combust. Inst., **2016**, 36.
15. Tsang W.. Int. J. Chem. Kinet. **1973**, 5, 929.

### IV. Publications and submitted journal articles supported by this project 2014-2016

- 1 Tranter R. S., Jasper A. W., Randazzo J. B., Lockhart J. P. A., and Porterfield J. P. 'Recombination and Dissociation of 2-Methyl Allyl Radicals: Experiment and Theory' Proc. Combust. Inst. 36 **2016** (submitted).
- 2 Randazzo J. B., Annesley C. J., Bell K., and Tranter R. S. 'A Shock Tube Laser Schlieren Study of Cyclopentane Pyrolysis' Proc. Combust. Inst. 36 **2016** (submitted).
- 3 Tranter R. S., Kastengren A. L., Porterfield J. P., Randazzo J. B., Lockhart J. P. A., Baraban J. H., and Ellison G. B. 'Measuring Flow Profiles in Heated Miniature Reactors With X-ray Fluorescence Spectroscopy' Proc. Combust. Inst. 36 **2016** (submitted).
- 4 Ossler F., Canton S. E., Seifert S., Hessler J. P., and Tranter R. S. 'Measurements of Structures and Concentrations of Carbon Particle Species in Premixed Flames by the use of *In-Situ* Wide Angle X-ray Scattering' Carbon **2016**, 96, 782-798.
- 5 Annesley C. J., Randazzo J. B., Klippenstein S. J., Harding L. B., Jasper A. W., Georgievskii Y., Ruscic B., and Tranter R. S. 'Thermal Dissociation and Roaming Isomerization of Nitromethane: Experiment and Theory' J. Phys. Chem. A **2015**, 119, 7872-7893.
- 6 Randazzo J. B., Annesley C. J. and Tranter R. S., 'Note: an improved driver section for a diaphragmless shock tube' *Rev. Sci. Instrum.* **2015**, 86, 016117
- 7 Lynch P. T., Annesley C. J. and Tranter R. S. 'Dissociation of *ortho*-Benzynes Radicals in the High Temperature Fall-off Regime' *Proc. Combust. Inst.* **2015**, 35, 145-152.
- 8 Annesley C. J., Goldsmith C. F. and Tranter R. S. 'A shock tube laser schlieren study of methyl acetate dissociation in the fall-off regime' *Phys. Chem. Chem. Phys.* **2014**, 16, 7241-7250

# **Developing a predictive model for the chemical composition of soot nanoparticles: Integrating Model and Experiment**

Lead PI: Prof. Angela Violi, University of Michigan, Ann Arbor avioli@umich.edu

Collaborating Institutions:

Combustion Research Facility - Sandia National Laboratories Livermore: PIs: Dr. H. Michelsen and Dr. N. Hansen

Lawrence Berkeley National Laboratory: PI: Dr. K. Wilson

## **Program Scope / Definition**

The goal of this project is to develop a validated predictive model to describe the chemical composition and morphology of soot nanoparticles in premixed and diffusion flames. The collaborative nature of the proposed study combines expertise in computational (Violi) and experimental (Hansen, Michelsen, and Wilson) areas to tackle the complex problem of soot nucleation and growth at the molecular level. The computational effort is tightly coupled to experimental data produced by the research groups of Michelsen and Hansen at Sandia National Laboratories and Wilson at Lawrence Berkeley National Laboratory. We have addressed several key questions concerning the formation and growth of soot nanoparticles and their precursor species with an array of state-of-the-art computational and experimental approaches. Our research provides critical insights for the development of the next generation of soot models, including those that model chemical and/or physical growth, with the capability to predict the nucleation process, and hence the number and size of nanoparticles, together with the evolution of their chemical composition. In particular, we can predict the morphologies of measured structures given their masses.

## **Recent Progress**

Recent progress has involved both experimental and theoretical investigations and the integration of these studies to gain insights on composition and morphology of nascent polycyclic aromatic hydrocarbons (PAHs) in premixed and counterflow diffusion flames. This project closely couples experimental investigations of soot precursors and incipient particle characteristics with the development of a predictive model for the chemical composition of soot nanoparticles.

The experimental group led by Dr. Michelsen studied atmospheric premixed and counterflow diffusion flames fueled by ethylene, acetylene, and methane in laboratory scale reactors. They measured and analyzed aerosol mass spectra of condensed species in the flames and extracted information on selected isomers based on vacuum ultra-violet (VUV) photoionization efficiency curves. The computational group led by Prof. Violi used these measurements to inform, constrain, and validate the methodology of our newly developed code for Stochastic NAnoParticle Simulation (SNAPS). SNAPS is an in-house software package developed for simulating gas-phase nanoparticle growth. We have implemented our software to simulate the formation and growth of nanoparticles and their precursor species, polycyclic aromatic hydrocarbons (PAHs), in high temperature flame environments with the aim of elucidating the composition of precursor molecules and ascertaining how their structures impact particle

nucleation. SNAPS, an in-house code developed in Violi group, employs a probabilistic kinetic Monte Carlo approach to generating stochastic trajectories of the growth of small gas-phase molecules in a flame environment. The governing kinetic reactions are gathered from literature and, when necessary, calculated from first principles. We have used SNAPS to model particle precursor growth in premixed and counterflow diffusion flames, in order to elucidate the chemical composition of species associated with peaks in experimentally measured aerosol mass spectra provided by Michelsen and coworkers. Because of the probabilistic nature of each growth trajectory, we rely on generating an ensemble of thousands of trajectories to produce statistically significant predictions about the likely growth pathways and final morphologies of nanoparticles. We can compare our computed number of species at each mass with mass spectra generated from experiments. For example, Figure 1 shows a very good agreement between experimentally measured and computed mass spectra for an acetylene counterflow diffusion flame at a distance of 5.75 mm from the fuel outlet. This comparison corroborates the validity of SNAPS simulations and the credibility of further detailed analysis of the simulation trajectories.

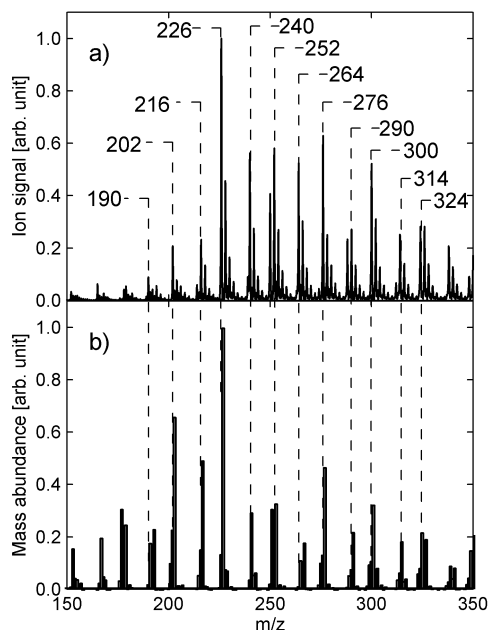


**Figure 1. (a) Experimental aerosol mass spectrum of an acetylene-argon-oxygen flame at a distance from the fuel outlet of 5.75 mm (Johansson, Lai, Skeen, Popolan-Vaida, Wilson, Hansen, Violi, and Michelsen, Proc. Comb. Inst. (35), 2015, pp. 1819-1826). (b) Computational mass spectrum (4000 trajectories) at 5.75 mm using a combination of benzene and toluene seeds according to weights proportional to the relative abundance of those species in the flame at the beginning of the SNAPS simulations. SNAPS correctly predicts the dominant masses (202, 216, 226, 240, 252, 276, 290, 300, 324, and 350 u) and less abundant masses that make up the rest of the spectrum.**

Experimental results from Michelsen's group have demonstrated non-sequential mass growth among some soot precursor molecules, i.e., that some heavier molecules appear earlier than some lighter ones in the flames. These results are not predicted by any soot formation model. More recent SNAPS modelling by Violi's group, however, have shown that non-sequential growth may be explained by radical-radical combination. Figure 2 shows some radical pairs commonly observed to combine in the simulations, yielding species at masses 266 u and 278 u. Species at these two masses typically appear before lighter ones in the experimentally studied flames. Radical-radical combination reactions bypass traditional growth pathways such as the hydrogen abstraction carbon addition (HACA) mechanism and provide rapid molecular growth. Hence, both our experimental results and our simulations show that several growth pathways have to be considered to explain soot-precursor formation and that the stabilomer species, which have had a central role in soot formation models ever since they first appeared in the literature in 1985, may not be as important as anticipated.

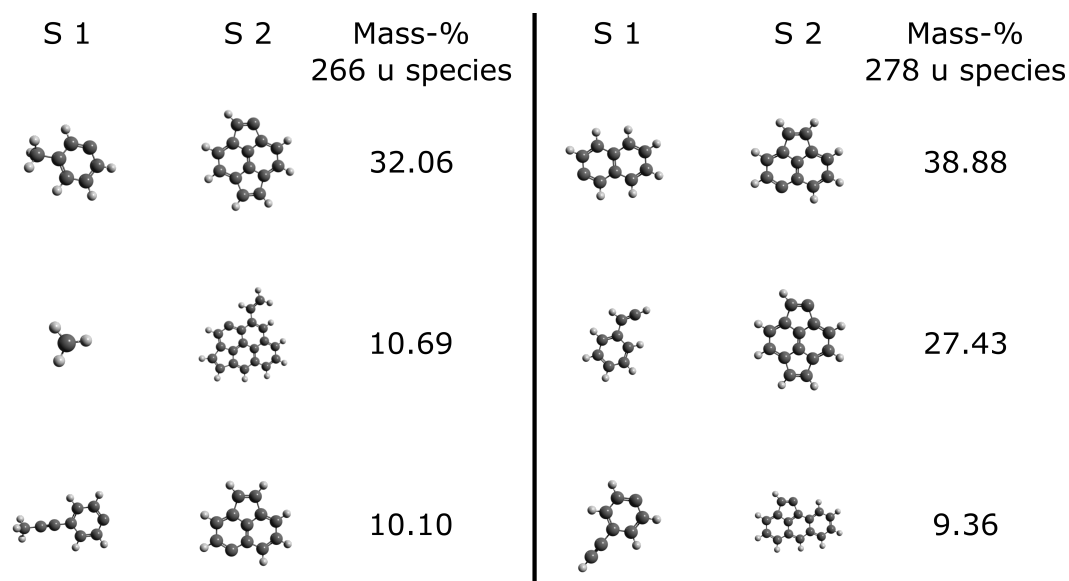


**Figure 2. Radical pairs that are predicted to combine to yield species at 266 u and 278 u.** The combination reactions of these radical pairs account for ~53% of the species predicted at 266 u and ~76% of the species predicted at 278 u. [7]

Experimental analysis compares photoionization efficiency curves of known species to those measured on sampled soot to gain information about the types of PAH species associated with soot particles. These results can be used to validate the SNAPS simulations and guide the development of a description of incipient soot formation. The experimental and computational results together elucidate molecular detail about particles involved in soot inception. In this way, we can achieve synergy between experiment and theory to further drive our collective efforts and create deeper insight into the PAH growth process. We have studied the role of pyrene in the chemical growth of soot precursors and in the particle nucleation, because pyrene is commonly used as a proxy for soot formation in combustion models. SNAPS simulations performed by Violi's group, however, showed that pyrene is not a dominating isomer among soot precursor molecules and that pyrene continues to grow to larger species as it evolves in the flame. Additionally, simulations performed by Violi's group suggest that pyrene is not prone to nucleate and form particles in a flame. Michelsen's group corroborated the simulation results by recording photoionization efficiency curves for incipient soot particles sampled from premixed and counter-flow diffusion flames, as well as from pure pyrene. By comparing the photoionization efficiency curves for the soot particles at the mass of pyrene with the photoionization efficiency curves of pure pyrene, Michelsen's group verified that pyrene is not a major contributor to incipient soot.

Recent work has focused on expanding and refining the SNAPS growth mechanism, specifically to incorporate oxygen chemistry, because Michelsen and co-workers see evidence that several of the measured PAH species in flames are in fact oxygenated; they observe peaks in mass spectra that cannot be explained when using hydrocarbon-only growth pathways in SNAPS. Violi's group has accordingly updated the SNAPS growth mechanism to account for the role oxygen plays in the growth of these species and predict the extent of oxygen inclusion in the structures of PAHs. The SNAPS mechanism has been extended to include oxygenation and oxidation

pathways; the code now accounts for oxygen chemistry through particle reactions with O, O<sub>2</sub>, OH, HO<sub>2</sub>, H<sub>2</sub>O<sub>2</sub>, H<sub>2</sub>O, CO, and CO<sub>2</sub>. The new oxygenation reactions work in parallel with the previous hydrocarbon reactions to provide a complete set of growth pathways that describe the evolution of nanoparticles and their precursors in flames. Accounting for possible oxygen addition onto the particles yields computed mass spectra in closer agreement with the mass spectra generated in experimental flames than the computed spectra produced with only carbon chemistry. These results are presently under review for publication in the Proc. Nat. Academ. Sci. USA.

We have submitted 4 manuscripts (2 accepted for oral presentation at the 36<sup>th</sup> International Symposium on Combustion) highlighting the importance of oxygenation chemistry in particle formation. The computational simulations and the experiments complement each other and have led to sustained progress and novel contributions to the field.

## Future Work

Future work will continue to involve close coupling between experimental and modeling efforts, towards further characterizing PAH growth in a variety of flame environments. These efforts will involve further experimental probing of soot precursors, searching in particular for oxygenated species predicted by simulations. The success or failure of these predictions will further enable refinement of the simulation methodology and oxygen chemistry, thus building a strong description of the beginnings of the soot-formation process.

## DOE sponsored research publications 2014-2016

1. J.Y. Lai, P. Elvati, A. Violi, "Stochastic Atomistic Simulation of Polycyclic Aromatic Hydrocarbon Growth in Combustion," *Physical Chemistry Chemical Physics* (16), **2014**, pp. 7969-7979.
2. K.O. Johansson, J.Y.W. Lai, S.A. Skeen, D.M. Popolan-Vaida, K.R. Wilson, N. Hansen, A. Violi and H.A. Michelsen, "Soot precursor formation and limitations of the stabilomer grid," *Proceedings of the Combustion Institute* (35), **2015**, pp. 1819-1826.
3. J.S. Lowe, J.Y.W. Lai, P. Elvati and A. Violi, "Towards a predictive model for polycyclic aromatic hydrocarbon dimerization propensity," *Proceedings of the Combustion Institute* (35), **2015**, pp. 1827-1832.
4. T. Dillstrom and A. Violi, "Effect of reaction mechanisms on the molecular structure of species formed in a premixed flame" *Proceedings of the Mediterranean section of the Combustion Institute*, **2015**, pp 1-10.
5. T. Dillstrom and A. Violi, "Effect of Reaction Mechanisms on the Molecular Structure of Species Formed in a Premixed Flame" *Combustion Theory & Modeling*, **2016**, in press.
6. T. Dillstrom, P. Elvati, and A. Violi, "Oxygen-driven soot formation," *Proceedings of the Combustion Institute* (36), **2016**, accepted for oral presentation.
7. K.O. Johansson, T. Dillstrom, P. Elvati, M. Campbell, P. Schrader, D. Popolan-Vaida, N. Richards-Henderson, K. Wilson, A. Violi, and H. Michelsen, "Radical-Radical Reactions, Pyrene Nucleation, and Incipient Soot Formation in Combustion," *Proceedings of the Combustion Institute* (36), **2016**, accepted for oral presentation.
8. Johansson. K.O.; Dillstrom, T.; Campbell, M.; Monti, M.; El Gabaly, F.; Schrader, P.; Popolan-Vaida, D.; Richards-Henderson, N.; Wilson, K.; Violi, A.; Michelsen, H. "Toxins, carcinogens, and fire: Explanation of large furan and hydrocarbon-oxygenate formation in flames," *Proceedings of the National Academy of Sciences*, **2016**, submitted.

# PRESSURE DEPENDENCE OF COMBUSTION REACTIONS: QUANTUM INELASTIC DYNAMICS ON AUTOMATICALLY GENERATED POTENTIAL ENERGY SURFACES

Albert Wagner  
Chemical Sciences and Engineering Division  
Argonne National Laboratory  
9700 South Cass Avenue  
Argonne, IL 60439  
Email: [wagner@anl.gov](mailto:wagner@anl.gov)

## PROJECT SCOPE

This program is aimed both at developing improved ways to automatically construct a reliable potential energy surface (PES) and at using such surfaces to understand pressure effects on relaxation and reaction processes. In this past year, opportunities in studying both inelastic relaxation at high pressures and tunneling processes in bimolecular reactions were pursued.

## RECENT PROGRES

*High Pressure Relaxation:* High pressures affect unimolecular and recombination rates and branching ratios. The pressure dependence of reaction kinetics is typically modeled by Master Equation (ME) methods that incorporate the isolated binary collision (IBC) approximate that inelastic collisions are binary events uninterrupted by collisions with other species. Since higher maximum pressures are becoming the norm in internal combustion engine design, we have developed a program to study IBC breakdown starting with an initial focus on energy relaxation.

We are using molecular dynamics simulations to study the transition in rates from low-pressure behavior where bath-gas/molecule collisions are binary to high-pressure behavior where most collisions involve multiple bath gas atoms. In collaboration with the Sewell groups (U. Missouri), we are examining the vibrational and rotational relaxation of initially excited molecules in a thermal Ar bath gas at pressures that range over two orders of magnitude from ~10 atm to ~1000 atm. With periodic boundary conditions both molecule and bath gas motion is explicitly followed. In Fig. 1, the color-coded solid lines are the computed decay of the

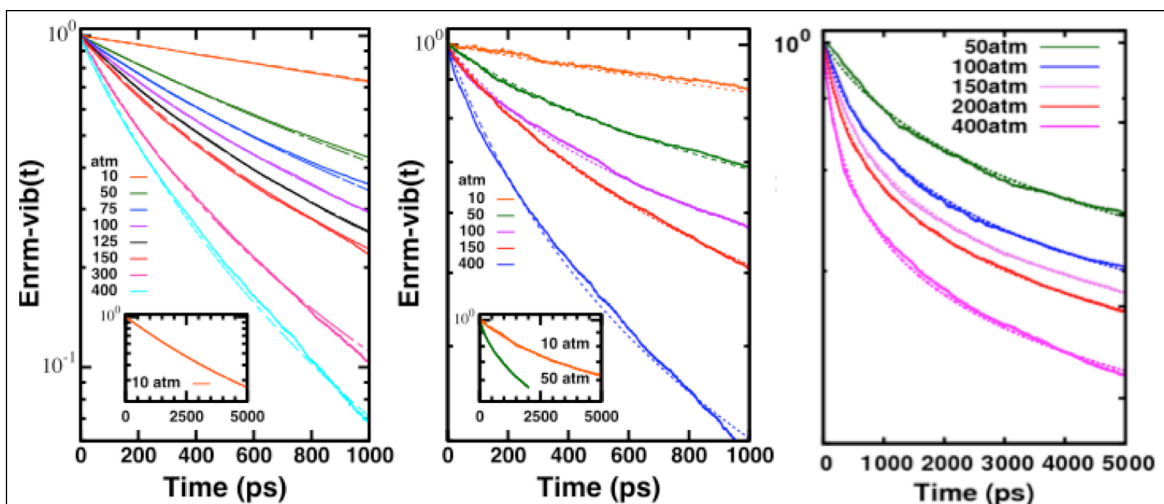


Figure 1. Solid lines color-coded by pressure are  $En_{rm-vib}(t)$  as a function of time for  $CH_3NO_2$  (left panel),  $HO_2$  (center panel), and  $OH$  (right panel). Dotted lines are LS fits (see text).

vibrational component of  $\sim 50$  kcal/mol of initial excitation in a polyatomic molecule (nitromethane),<sup>1</sup> a triatomic radical ( $\text{HO}_2$ ),<sup>2</sup> and a diatomic radical (OH) in an Ar bath (1000 atoms with periodic boundary conditions) at pressures of 10 atm to 400 atm and at 300K ( $\text{CH}_3\text{NO}_2$ , OH) or 800K ( $\text{HO}_2$ ). The initial amount of internal energy is below unimolecular dissociation for all three species. The *intramolecular* potentials used are available from the literature<sup>3</sup> and the *intermolecular* potentials are pairwise additive Exp-6 or Lennard-Jones potentials developed from combination rules applied to the homonuclear potentials.<sup>3</sup> The decay curves are ensemble averages over 1000 trajectories. In the figure Enrm-vib is the ensemble average of *excess* vibrational energy over the thermal vibrational energy all normalized to unity at zero time. The figure shows that vibrational relaxation has ns time constants. The computed decay of excess rotational energy (not shown) is  $\sim 100$ x faster.

All three systems have two important similarities: (1) the relaxation rate increases with pressure and (2) on a semi-log plot the decay curves are not straight lines, i.e., no single exponential decay. Rather the rate slows down with time. The computed decays are well fit (see dashed lines) by the Lendvay-Schatz (LS) form of  $\text{Enrm-vib}(t) = [1 - (1-m)k_i t]^{1/(1-m)}$  where  $m$  and  $k_i$  are two adjustable constants. With this form, the rate of decay at  $t = 0$  is  $k_i$  while the increase of  $m$  above 1 measures the global curvature of the decay from a straight line, single exponential decay on a semi-log plot. Plots of both parameters with Ar bath gas density are shown as the symbols in Fig. 2 with the left red axis for  $m$  and the right blue axis for  $k_i$ . The curvature  $m$  increases in going from  $\text{CH}_3\text{NO}_2$  to OH and has a relatively weak dependence on density.  $k_i$  shows a non-linear dependence on density for both  $\text{HO}_2$  and  $\text{CH}_3\text{NO}_2$ . The falloff from expected linear dependence at low densities occurs roughly at about the same density, corresponding to  $\sim 100$  atm for  $\text{CH}_3\text{NO}_2$  at 300 K and  $\sim 250$  atm for  $\text{HO}_2$  at 800 K. In contrast OH scales linearly with density over the same pressure range. The IBC approximation requires linear scaling with density, meaning that Fig. 2 shows species-dependent IBC breakdown over the range of at a few hundred atm.

The solid blue lines in Fig. 2 are based on a multiple collision model<sup>1</sup> formed by discretizing space into cells one Ar atom in size with the molecule occupying the cells required by its size. Combinatorial arithmetic can determine for a given bath gas density the probability of  $M$  cells bordering the molecule being occupied by  $N \leq M$  Ar atoms, i.e.,  $N$  Ar atoms in a single collision event. This probability plus a least-squares adjusted rate constant for a single collision

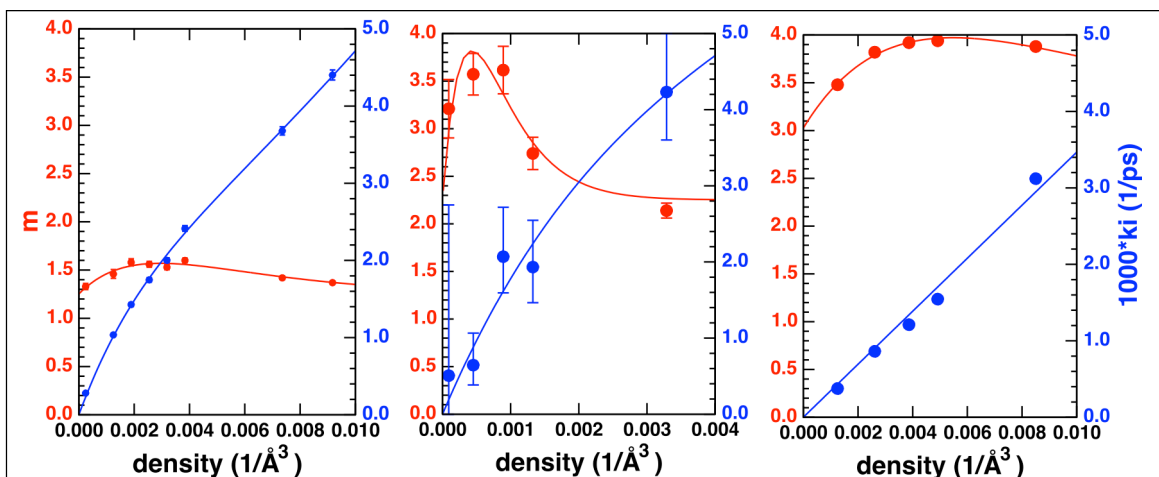


Figure 2. Plot of  $m$  (red axis) and  $k_i$  (blue axis) versus density for  $\text{CH}_3\text{NO}_2$  (left panel),  $\text{HO}_2$  (center panel), and OH (right panel). Symbols are data, lines are fits (see text).

and a least squares adjusted rate constant per Ar atom for multiple collisions lead to the blue lines in Fig. 2. For CH<sub>3</sub>NO<sub>2</sub>, the fit suggests that an N Ar atom multiple collision reduces molecular vibrational energy more efficiently than a single Ar atom collision but not N times more efficiently, i.e., a shielding effect. For OH, the results indicate that a multiple collision with N Ar atoms is just as efficient as N single Ar atom collisions, i.e., an IBC breakdown with no effective shielding. For HO<sub>2</sub>, the results are problematic because few-Ar collision events are predicted to be less efficient than even one Ar collision event. Further investigations are required.

The mechanisms behind curvature characterized by *m* are being examined on the simplest system OH/Ar. Kohno et al.<sup>4</sup> demonstrated in low pressure experiments that the vibrational relaxation rate constant of OH(*v*)/He increases exponential with *v* in accord with an exponential gap model based on the “gap” between adjacent vibrational levels being systematically reduced by anharmonicity. This approach can be converted into an alternate to the LS functional form. In this alternative form curvature is driven by the effect of anharmonicity on the relaxation rate constant – zero anharmonic effect reduces the form to single exponential decay. Preliminary results indicate that intramolecular anharmonicity drives “*m*” curvature.

*Tunneling in Bimolecular Reactions:* Most tunneling methods are based on reaction paths whose calculation is typically not readily parallelized. Miller et al.<sup>5</sup> developed an alternative approach based on readily parallelized, second order vibrational perturbation theory (VPT2) at the saddle point. This approach recognizes that the saddle point energy when expanded in various powers of the quantum numbers will have imaginary expansion coefficients connected to the quantum number for motion along the reaction path. The replacement of this quantum number by an imaginary semiclassical action leads to a quadratic expansion of the energy in the action. This leads to an expression of action as a function of energy from which an analytic, multi-dimensional, semiclassical tunneling probability can be readily obtained. This tunneling approach is labeled SCTST in the Multiwell<sup>6</sup> suite of codes for thermal kinetics. For deep tunneling substantially below the top of the barrier, the SCTST analytic formula is not qualitatively correct. To understand this, consider the bound Morse-oscillator (MO) where the dissociation energy  $D_e^{MO} = -(\hbar\omega_e)^2/(4\omega_e x_e)$ . If a diatomic molecule is not *exactly* an MO,  $D_e^{MO} \neq D_e$  and the level structure of the MO model will be qualitatively incorrect near the top of the well. Similarly, the semiclassical tunneling formula for an *inverted* MO will be qualitatively incorrect near the base of the barrier if the true barrier  $V \neq V^{MO}$ . SCTST shares the same difficulties if  $V \neq V^{MO}$ . We developed a simple modification<sup>7</sup> called iSCTST that uses a composite three-segment Eckart potential continuous everywhere in value and derivative that correctly represents in the middle segment the VPT2 properties of the saddle point and in the first and third segments the correct forward and reverse barriers. When incorporated into a semiclassical barrier penetration integral, this composite potential analytically extends the original VPT2 formula all the way to the base of the true barrier. In a recent unpublished comparison of SCTST and i-SCTST for six bimolecular reactions (O+H<sub>2</sub>, OH+CO, OH+H<sub>2</sub>, OH+OH, Cl+CH<sub>4</sub>, and F+H<sub>2</sub>O) VPT2-characterized by Nguyen/Stanton (U. Texas) and Barker (U. Michigan), SCTST was found to under-shoot (e.g., Cl+CH<sub>4</sub>), agree well (e.g., OH+OH), or over-shoot (e.g., OH+CO) the iSCTST tunneling probability with its correct barrier height.

## FUTURE PLANS

The pressure dependent studies of relaxation are continuing on multiple fronts. The suggested *k<sub>i</sub>* non-linear density dependence mechanism based on shielding in multiple collisions will be tested

by relatively inexpensive isolated N-Ar/molecule trajectory studies. The exponential gap model connecting curvature  $m$  in OH to anharmonicity will be more fully developed. For  $\text{CH}_3\text{NO}_2$  and  $\text{HO}_2$ , mode-specificity in vibrational relaxations will be examined. This can be seen as a competition between pressure-dependent, mode-specific energy transfer to the bath and pressure-independent IVR that restores equipartition of energy to the modes in the molecule. Finally increasing the initial energy of excitation will introduce direct competition of energy relaxation with isomerization and unimolecular dissociation. In collaboration with the Dawes group (Missouri Institute for Science and Technology), we are planning a study of  $\text{C}_2\text{H}_5/\text{Ar}$  with a new  $\text{C}_2\text{H}_5$  PES based on direct dynamics simulations using M05 DFT calculations.

The bimolecular tunneling studies are continuing in collaboration with the Stanton, Nguyen, and Barker team. We plan to carry out PES polyrate<sup>8</sup> calculations with various reaction-path following tunneling options on a selection of the six reactions mentioned above whose VPT2 descriptions generally compare quite favorably to kinetics measurements. We will use identical electronic structure methods for both polyrate and VPT2 descriptions. Reaction-path following methods explicitly allow the reaction bottleneck to variationally move away from the saddle point along the reaction path. Saddle-point centric VPT2 methods represent variational effects implicitly through anharmonic terms. This comparison will develop the differences.

---

<sup>1</sup> DOE-Sponsored publication #1 below.

<sup>2</sup> J. W. Perry and A. F. Wagner, *Pressure Effects on the Relaxation of an Excited Hydrogen Peroxyl Radical in an Argon Bath*, Proc. Comb. Inst. (2016) accepted for presentation.

<sup>3</sup> (a) D. C. Sorescu, B. M. Rice, and D. L. Thompson, *J. Phys. Chem. B* **104**, 8406 (2000); (b) D. Xie, C. Xu, T. Ho, H. Rabitz, G. Lendvay, S. Y. Lin, and H. Guo, *J. Chem. Phys.* **126** (2007) 074315; (c) B R. Johnson and N. W. Winter, *J. Chem. Phys.* **66**, 4116 (1977).

<sup>4</sup> N. Kohno, J. Yamashita, Ch. Kadochiku, H. Kohguchi, and K. Yamasaki, *J. Phys. Chem. A* **117**, 3253 (2013).

<sup>5</sup> Miller, W. H.; Hernandez, R.; Handy, N. C.; Jayatilaka, D.; Willets, A. *Chem. Phys. Lett.* **172**, 62 (1990).

<sup>6</sup> <http://aoss-research.engin.umich.edu/multiwell/>

<sup>7</sup> DOE-Sponsored publication #1 below.

<sup>8</sup> <http://comp.chem.umn.edu/polyrate/>

### DOE-SPONSORED PUBLICATIONS SINCE 2013

1. L. A. Rivera-Rivera, A. F. Wagner, T. D. Sewell, and D. L. Thompson PRESSURE EFFECTS ON THE RELAXATION OF AN EXCITED NITROMETHANE MOLECULE IN AN ARGON BATH, *J. Chem. Phys.* **142**, 014303 (2015).
2. A. F. Wagner, R. Dawes, R. E. Continetti, and H. Guo, THEORETICAL/EXPERIMENTAL COMPARISON OF DEEP TUNNELING DECAY OF QUASI-BOUND H(D)OCO TO H(D)+CO<sub>2</sub>, *J. Chem. Phys.* **141**, 054304 (2014)
3. A. F. Wagner, IMPROVED MULTIDIMENSIONAL SEMICLASSICAL TUNNELING THEORY, *J. Phys. Chem. A* **117**, 13089-13100 (2013).
4. J. W. Perry, R. Dawes, A. F. Wagner, and D. L. Thompson, CLASSICAL TRAJECTORY STUDY OF THE INTRAMOLECULAR DYNAMICS, ISOMERIZATION, AND UNIMOLECULAR DISSOCIATION OF HO<sub>2</sub>, *J. Chem. Phys.* **139**, 084319 (2013)
5. A. F. Wagner, L. A. Rivera, D. Bachellerie, J. W. Perry, and D. L. Thompson, A CLASSICAL TRAJECTORY STUDY OF THE DISSOCIATION AND ISOMERIZATION OF C<sub>2</sub>H<sub>5</sub>, *J. Phys. Chem. A* **117**, 11624-11639 (2013)

# Low Temperature Combustion Chemistry and Fuel Component Interactions

Margaret S. Wooldridge

Departments of Mechanical and Aerospace Engineering, University of Michigan

2350 Hayward Street, Ann Arbor, MI 48109-2121

mswool@umich.edu

## I. Program Scope

Recent research into combustion chemistry has shown that reactions at “low temperatures” (700 – 1100 K) have a dramatic influence on ignition and combustion of fuels in virtually every practical combustion system. A powerful class of laboratory-scale experimental facilities that can focus on fuel chemistry in this temperature range is the rapid compression facility (RCF), which has proven to be a versatile tool to examine the details of fuel chemistry in this important regime. Our past studies have advanced our understanding of low temperature chemistry of important fuel compounds and has identified areas of high uncertainty for further research. In particular, we have shown how factors including fuel molecular structure, the presence of unsaturated C=C bonds, and the presence of alkyl ester groups influence fuel auto-ignition and produce variable amounts of negative temperature coefficient behavior of fuel ignition. We have also reported new discoveries of synergistic ignition interactions between alkane and alcohol fuels, with both experimental and kinetic modeling studies of these complex interactions. This project focuses on further clarifying the effects of molecular structure on combustion chemistry including carbon bond saturation, through low temperature experimental studies of esters, alkanes, alkenes, and alcohols.

## II. Recent Progress

During the past year, we completed ignition and speciation studies of ethanol [1] and we expanded our hexene isomer studies to include cis forms of the isomer. All ignition delay time data were acquired using the University of Michigan (UM) RCF over a range of state and mixture conditions for each of the fuel compounds. Mass sampling and gas chromatography were applied to quantify the stable intermediates present during ignition of ethanol.

The UM RCF is an innovative and robust experimental apparatus that can be used to isolate reaction kinetics by creating uniform conditions over a broad range of temperatures ( $T = 500\text{--}3000\text{ K}$ ) and pressures ( $P = 0.5\text{--}60\text{ atm}$ ). The long test times of the UM RCF allow application of rapid gas sampling methods to simultaneously measure a large number of stable species during ignition experiments. Details on the dimensions, components and performance characterization of the UM RCF can be found in Donovan *et al.* [2]. Previous UM RCF studies have considered ignition chemistry of numerous important reference fuel compounds including iso-octane [3], n-heptane [4], n-butanol [5],  $\text{H}_2/\text{CO}$  mixtures [6],  $\text{C}_5$  esters [7,8] and the trans or linear forms of the hexene isomers [9]. UM RCF studies include continuous absolute measurements of OH radicals during iso-octane ignition [10], as well as discrete measurements of intermediate species formed during ignition for several different fuel compounds [4,5,8,11].

This report presents a brief summary of the results of the recent UM RCF speciation study of ethanol. All experiments were conducted using the UM RCF to determine ignition delay times from pressure time histories. For the ethanol studies, stoichiometric ( $\phi = 1.0$ ) mixtures were investigated

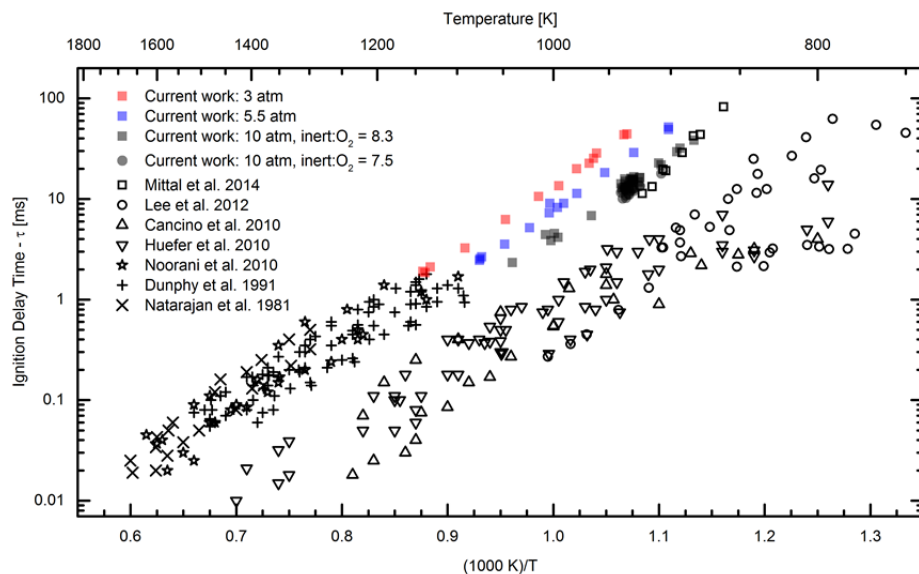


**Fig. 1.** Summary of ignition delay time data for stoichiometric mixtures of ethanol. The new ignition data from UM RCF experiments are shown as the solid symbols at pressures of 3 atm, 5.5 atm, and 10 atm with a dilution level of inert: $\text{O}_2 = 8.33:1$ , mole basis and at 10 atm with a dilution level of 7.5:1.

at 3 pressures and temperatures from 883-1141 K. Two dilution levels of buffer gas:O<sub>2</sub> were investigated for the 10 atm conditions. A summary of the measured ignition delay times are presented in **Fig. 1** and compared with previous studies of ethanol ignition. The results show the new UM RCF data fill a void that previously existed at temperatures <1200 K and pressures ≤10 atm. Additionally, the new UM RCF data are in good agreement with expected trends for pressure and temperature.

**Fig. 1** also illustrates the strength of RCF studies to study these intermediate to low temperature combustion chemistry regimes. The experimental data are compared with model predictions using the gasoline surrogate reaction mechanism from Lawrence Livermore National Laboratory (LLNL) by Mehl et al. [12], which contains a sub-mechanism for ethanol, in **Fig. 2**. The experimental data are in excellent agreement with the model predictions; consistently within the experimental uncertainties throughout the range of conditions studied.

Fast gas sampling and gas chromatography were used to quantitatively measure 12 stable intermediate species formed during the ignition delay period of each isomer at a temperature of 933 K. **Figure 3** presents the species measurements and the comparison with model predictions using the reaction mechanisms by Mehl et al. [12] and Mittal et al. [13]. In general, there is very good agreement between the experimental data and the predictions from both mechanisms, i.e. typically within the measurement uncertainties.

In **Fig. 3a**, rapid consumption of ethanol near the end of the ignition period is well represented by both kinetic mechanisms and by the concentration measurements. High concentrations of the stable intermediate species ethanal and methane are consistent with our expectations for ethanol combustion as these species are part of the primary reaction pathway for ethanol oxidation at the conditions studied. Reaction pathway analysis indicates ~72% of the ethanol reacts to produce ethanal (acetaldehyde, CH<sub>3</sub>CHO) as an early intermediate formed after hydrogen abstraction from the ethanol  $\alpha$ -carbon site by OH, H and HO<sub>2</sub>. Most of the ethanal subsequently reacts with OH, H and HO<sub>2</sub> to produce CH<sub>3</sub>CO which thermally decomposes into methyl radicals and CO. Methane and ethane are produced from branches of the main reaction pathway such as by reaction of the CH<sub>3</sub> radicals with ethanol. Ethene is the product of a  $\beta$ -scission process following hydrogen abstraction from the ethanol  $\beta$ -carbon site. For propane, propene, 1-butene, 1,3-butadiene, both reaction mechanisms predicted the experimental time histories well, typically within a factor of 2.

The results emphasize the value of bulk reactivity data (e.g. ignition delay time) and species measurements as important methods to identify and validate reaction pathways, which are particularly vital towards developing reaction rate rules for classes of fuel compounds. In particular, the results of the current work are the first species measurements for ethanol in the intermediate temperature regime for this important reference fuel compound.

### III. Future Work

Our future work includes completing ignition and speciation studies to understand the effect of cis- versus trans-isomerization on hexene combustion. This work will leverage our previous study of the trans hexene isomers. We are also continuing to explore fuel component interactions through studies of ethanol and iso-octane blends. We continue to work with Dr. Charles Westbrook to develop a more accurate understanding of the intermediates formed

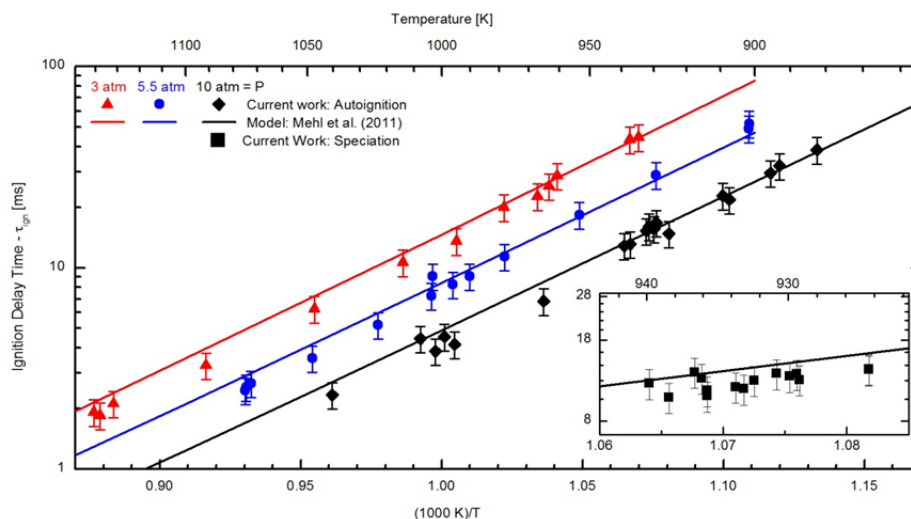


**Fig 2.** Experimental and modeling results for ethanol ignition delay time for stoichiometric conditions and dilution levels of inert:O<sub>2</sub> ratio = 8.33. Model predictions using the mechanism by Mehl et al. [12] are shown as solid lines. The inset shows ignition delay time measurements for the ethanol speciation experiments at stoichiometric conditions and dilution levels of inert:O<sub>2</sub> ratio = 7.5. The error bars represent the uncertainty in the experimental measurements of ~15%.

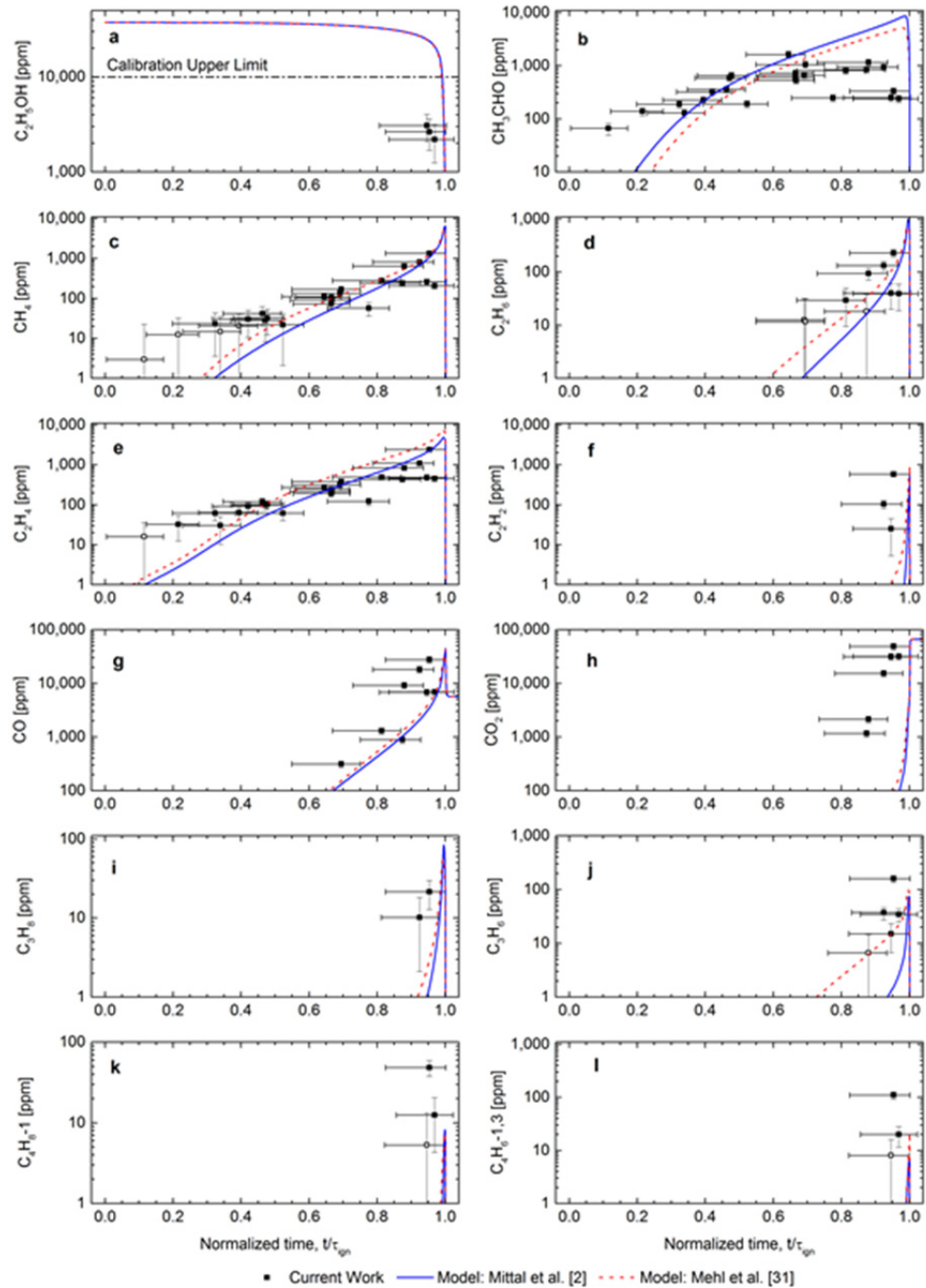


**Fig. 3.** Measured and predicted time histories of stable intermediate species produced during ethanol autoignition: a) ethanol, b) ethanal, c) methane, d) ethane, e) ethene, f) ethyne, g) carbon monoxide, h) carbon dioxide, i) propane, j) propene, k) 1-butene, l) 1,3-butadiene. Experimental measurements are presented as solid symbols and model predictions are presented as solid and dashed lines. Average conditions for the sampling experiments were  $P = 10.2$  atm,  $T = 933$  K,  $\phi = 0.99$ ,  $O_2 = 11.33\%$ , inert: $O_2 = 7.5$

during ignition of hydrocarbons and oxygenated hydrocarbons. We are also continuing our collaboration with Dr. Robert Tranter of Argonne National Laboratories to develop a high-pressure sampling valve system that will enable speciation at significantly higher pressures than we can study currently.

#### IV. References

1. Barraza-Botet, C., Wagon, S.W., Wooldridge, M.S., "An experimental study of the ignition and reaction pathways of ethanol," submitted to *Journal of Physical Chemistry A*, April 2016.
2. Donovan, M.T., He, X., Zigler, B.T., Palmer, T.R., Wooldridge, M.S., Atreya, A. (2004) *Combust. Flame* **137** 351.
3. He, X., Donovan, M.T., Zigler, B.T., Palmer, T.R., Walton, S.M., Wooldridge, M.S., Atreya, A. (2005) *Combust. Flame* **142** 266.
4. Karwat, D.M.A., Wagon, S., Wooldridge, M.S., Westbrook, C.K. (2013) *Combust. Flame* **160** 2693.
5. Karwat, D. M. A., Wagon, S., Teini, P. D., Wooldridge, M. S. (2011) *J. Phys. Chem. A* **115** 4909.
6. Walton, S.M., He, X., Zigler, B.T., Wooldridge, M.S. (2007) *Proc. Combust. Inst.* **31** 3147.
7. Walton, S.M., Wooldridge, M.S., and Westbrook, C.K. (2009) *Proc. Combust. Inst.* **32** 255.
8. Walton, S.M., Karwat, D.M., Teini, P.D., Gorny, A., Wooldridge, M.S. (2011) *Fuel* **90** 1796.
9. Wagon, S.W., Botet, C.B., Wooldridge, M.S., (2015) *J. Phys. Chem. A*, **119** 7695.
10. He, X., Zigler, B.T., Walton, S.M., Wooldridge, M.S., Atreya, A. (2006) *Combust. Flame* **145** 552.
11. He, X., Walton, S.M., Zigler, B.T., Wooldridge, M.S., Atreya, A. (2007) *Int. J. Chem. Kinet.* **39** 498.
12. Mehl, M., Pitz, W.J., Westbrook, C.K., Curran, H.J. (2011) *Proc. Combust. Inst.* **33**, 193.
13. Mittal, G., Burke, S.M., Davies, V.A., Parajuli, B., Metcalfe, W.K., Curran, H.J. (2014) *Combust. Flame*. **161** 1164.

#### V. Publications and submitted journal articles supported by this project 2011-present

1. Wagon, S. W., Botet, C.B., Wooldridge, M. S., (2015) "The Effects of Bond Location on the Ignition and Reaction Pathways of trans-Hexene Isomers," *Journal of Physical Chemistry A*, **119**, pp. 7695-7703.
2. Karwat, D. M. A., Wooldridge, M. S., Klippenstein, S. J., Davis, M. J., (2015) "Effects of New Ab Initio Rate Coefficients on Predictions of Species Formed During n-Butanol Ignition," *Journal of Physical Chemistry A*, **119**, pp. 543-551.
3. Barraza-Botet, C., Wagon, S., Wooldridge, M. S., "Ignition Measurements of Ethanol-Air Mixtures in a Rapid Compression Facility," 9<sup>th</sup> U. S. National Combustion Meeting of the Combustion Institute, May 17-20, 2015, Cincinnati, Ohio; Barraza-Botet, C., Wagon, S., Wooldridge M. S., (2014) "Ignition Delay Time Measurements and High-speed Imaging Analysis for Ethanol-Air Mixtures in a Rapid Compression Facility," Spring Meeting of the Canadian Section of the Combustion Institute, May 2014; Barraza-Botet, C., Wagon, S. W., Wooldridge, M. S., "An experimental study of the ignition and reaction pathways of ethanol," submitted to *Journal of Physical Chemistry A*, April 2016
4. Wagon, S. W., Karwat, D. M. A., Wooldridge, M. S., and Westbrook, C. K. (2014) "Experimental and Modeling Study of Methyl trans-3-Hexenoate Autoignition," *Energy and Fuels*, **28**, pp. 7227-7234.
5. Wagon, S. W., Wooldridge, M. S., (2014) "Effects of Diluent Gas Composition on Autoignition," *Combustion and Flame*, **161**, pp. 898-907.
6. Karwat, D. M. A., Wagon, S., Wooldridge, M. S., Westbrook, C. K. (2013) "Low Temperature Speciation and Chemical Kinetic Studies of n-Heptane," *Combustion and Flame* **160**, pp. 2693-2706.
7. Karwat, D. M. A., Wagon, S., Wooldridge, M. S., Westbrook, C. K., (2012) "On the Combustion Chemistry of n-Heptane and n-Butanol Blends," *Journal of Physical Chemistry A*, DOI 10.1021/jp3093 58h, **116**, pp. 12406-12421.
8. Karwat, D. M. A., Wagon, S., Teini, P. D., Wooldridge, M. S. (2011) "On the Chemical Kinetics of n-Butanol: Ignition and Speciation Studies," *Journal of Physical Chemistry A*, **115**, pp. 4909-4921.
9. Walton, S. M., Karwat, D. M., Teini, P. D., Gorny, A., and Wooldridge, M. S. (2011) "Speciation Studies of Methyl Butanoate Ignition," *Fuel*, **90**, pp. 1796-1804.

# GAS-PHASE MOLECULAR DYNAMICS: THEORETICAL STUDIES IN SPECTROSCOPY AND CHEMICAL DYNAMICS

Hua-Gen Yu (hgy@bnl.gov)

*Chemistry Department, Brookhaven National Laboratory, Upton, NY 11973-5000*

## Program Scope

The main goal of this program is the development and application of computational methods for studying chemical reaction dynamics and molecular spectroscopy in the gas phase. We are interested in developing rigorous quantum dynamics algorithms for small polyatomic systems and in implementing approximate approaches for complex ones. Our particular focus is on the dynamics and kinetics of chemical reactions and on the rovibrational spectra of species involved in combustion processes. This research also explores the potential energy surfaces of these systems of interest using state-of-the-art quantum chemistry methods, and extends them to understand some important properties of materials in condensed phases and interstellar medium as well as in combustion environments.

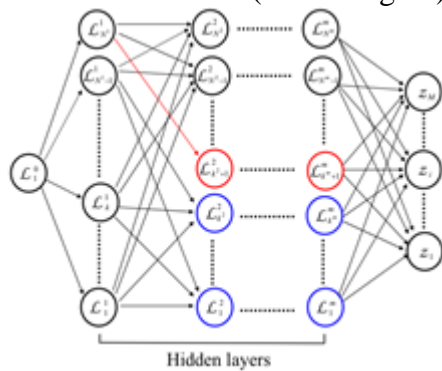
## Recent Progress

### Neural network iterative diagonalization method for the eigenvalue problems

Recently, the neural network functional has been found to be a powerful representation for electronic densities, potential energy surfaces, and vibrational wavefunctions in chemical physics. In this work, we have applied the neural network structure to develop a novel neural network iterative diagonalization method (NNiDM) to compute some eigenvalues and eigenvectors of large sparse complex symmetric or Hermitian matrices. The algorithm has a multi-layered feed-forward neural network structure (see the figure).

The artificial neurons (or nodes) are defined by a set of formally orthogonal Lanczos polynomials ( $L_j^i$ ).

The biases and weights are dynamically determined through a series of complex guided spectral transform Lanczos iterations and small matrix diagonalizations in terms of a thick restart technique. The construction of node functions starts with a random vector, and only requires the forward action of a matrix or Hamiltonian on vectors, without any training or non-linear optimization. The



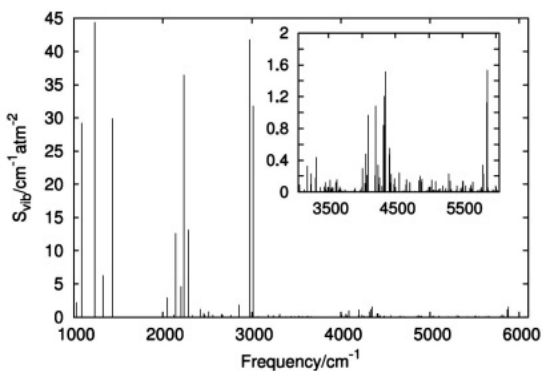
last output layer produces the desired eigenvalues and eigenvectors near a given reference value via a linear transform diagonalization approach. Since the algorithm uses the spectral transform technique, it is capable of computing interior eigenstates in dense spectral regions. In particular, the NNiDM algorithm is a universal eigensolver for complex symmetric or Hermitian matrices. The NNiDM algorithm has been applied for calculating energies, widths, and wavefunctions of two example molecules: HO<sub>2</sub> and CH<sub>4</sub>. The method is shown to retain the efficiency of other advanced iterative

diagonalization methods, but this algorithm will also produce eigenvectors with substantially reduced core memory requirements compared to other methods. Therefore, the neural network iterative diagonalization method is very attractive if both eigenvalues and eigenvectors are needed as in many layered basis contraction methods.

### Accurate quantum dynamics calculations of molecular vibrational spectra

By using the recently developed multi-layer Lanczos method, we have carried out a

rigorous variational study of the infrared (IR) vibrational spectra of both  $\text{CH}_2\text{D}_2$  and  $^{13}\text{CH}_2\text{D}_2$  isotopomers using an exact molecular Hamiltonian. All well converged 357 vibrational energy levels up to  $6100\text{ cm}^{-1}$  of  $\text{CH}_2\text{D}_2$  are obtained, together with a comparison to previous calculations and 91 experimental bands available. The calculated frequencies are in excellent agreement with the experimental results and give a root-mean-square error of  $0.67\text{ cm}^{-1}$ . The calculated IR spectra (e.g., see the left figure) provide important information for understanding the spectrum of the system, especially for those highly excited vibrational states. Based on the theoretical results, 20 experimental bands are suggested to be re-assigned. Surprisingly, an anomalous C isotopic effect is discovered in the  $\nu_5$  modes of  $\text{CH}_2\text{D}_2$ . According to our calculated IR spectra, this effect could be verified by high resolution spectroscopy. One potential band is the  $4\nu_5$  one at  $5298.72\text{ cm}^{-1}$  that shows a relative strong intensity to its neighbor bands.



*The calculated vibrational spectrum for the transitions from the vibrational ground state of  $\text{CH}_2\text{D}_2$  at  $T=298\text{ K}$ .*

Furthermore, we (in collaboration with Guo at UNM and Dawes at MUST) have also carried out full-dimensional quantum dynamics calculations of vibrational energy levels of the simplest Criegee intermediate ( $\text{CH}_2\text{OO}$ ), based on an accurate nine-dimensional permutation invariant polynomial-neural network potential energy surface. In this work, we reported about 70 converged vibrational levels, which should be very helpful for assigning experimental bands.

### Time-dependent wavepacket and classical trajectory dynamics calculations

A reduced dimension time-dependent wavepacket quantum dynamics has been carried out for molecular photodissociation in NO-rare gas complexes. The total cross sections and product rotational state distributions are calculated. The theoretical results are in good agreement with experiments by Lawrance's group at Flinders University (FU) in Australian. This work is done in collaborations with experimentalists Hall (BNL) and Lawrance (FU). In addition, together with the quantum scattering calculations of Dagdigan (JHU), we also provided theoretical assistant to explore energy transfer rates in molecular collisions such as  $\text{CN} + \text{He}/\text{Ar}$  which were measured by Hall and Sears at our GPMD group.

## Future Plans

### **Rigorous full dimensional quantum dynamics studies of molecular spectrum**

We will continue to develop and apply the multi-layer Lanczos and neural network iterative diagonalization methods for studying the ro-vibrational spectra and resonances of polyatomic molecules. One project (in collaboration with Guo at UNM) is to calculate the lowest-lying vibrational energy levels of  $\text{NH}_4^+$  ion and its deuterated isotopomers, based on the recently developed *ab initio*-based potential energy surface of  $\text{NH}_4^+$ . It was shown that this surface is very accurate. This research will focus on the prediction of highly excited vibrational states. Another on-going project is to study all bound states and some lowest-lying resonances of  $\text{N}_2\text{H}_2$  by using the NNiDM algorithm. This application will be done in collaboration with Varandas at Coimbra.

### **Time-dependent wavepacket calculations of the photodissociation of NO-Rg**

Following our previous work, this research will use a better quantum mechanical model to study the photodissociation of NO-Rg complexes. The new model will consider the electronic degeneracy of the system, photon polarizability, and rigorous dynamical treatment. Here, we are particularly interested in the property of differential cross sections that connect to the anisotropic dependence of angular distributions of product states as a function of photon energy.

### **Development of a general program for calculating vibrational spectra of polyatomic systems**

In this proposal, we aim to develop computational algorithms to accurately calculate the vibrational spectra of polyatomic molecules, and to assist experimentalists in understanding their observed spectra. For polyatomic systems beyond six-atom, the challenge in rigorous quantum dynamics calculations comes from the huge basis size arising out of high-dimensional problems. The Lanczos method is an iterative eigensolver capable of solving the eigenvalue problem of a large sparse matrix with a size up to  $N \sim 10^7$ , which might be equivalent to a chemical system with six degrees of freedom. In order to overcome this difficulty, we may try to reduce the basis size by using a compact basis set. The reduction of the basis size is the crucial idea of the sequential truncation approach widely used in direct diagonalization methods. This approach however requires too much CPU time and fast memory to be tractable for polyatomic molecules beyond five-atom molecules. During the past decade, several methods to obtain a compact basis set have been developed, e.g., the pruned basis functions.

Instead, in this proposal, we will use our recently developed ZDVR method to build a compact basis set. The ZDVR is a multi-dimensional PO-DVR method so that the ZDVR basis is very compact, which can substantially reduce the basis size. Numerical tests also demonstrated that it has the Gauss convergence speed with the basis size. Importantly, the ZDVR is a grid basis representation. As a result, the matrix representation of system Hamiltonian in ZDVR is often very sparse, which guarantees the efficiency of an iterative diagonalization method as well as the low memory requirement. The new algorithm will be called ZDVRMode.

We will apply the ZDVRMode program to study the vibrational spectra of combustion-related radicals such as vinyl ( $\text{C}_2\text{H}_3$ ) and propargyl ( $\text{C}_2\text{H}_5$ ) radicals, in collaboration with Sears and Hall in the GPMD group of BNL. They will measure the

overtones of both radicals using high-resolution near infrared spectroscopy. Currently, the Hamiltonian in normal mode coordinates has been numerically tested with propargyl radical in full dimension. The full coupled potential energy surface is used. The results obtained are very promising.

### Publications since 2013

- G. Nyman and H.-G. Yu, *Quantum approaches to polyatomic reaction dynamics*, Int. Rev. Phys. Chem., **32**, 39 (2013).
- P.P Dholabhai and H.-G. Yu, *Electronic structure and quantum dynamics of photoinitiated dissociation of O<sub>2</sub> on rutile TiO<sub>2</sub> nanocluster*, J. Chem. Phys., **138**, 194705 (2013).
- H.-G. Yu, *Origin of anomalous electronic circular dichroism spectra of [RuPt<sub>2</sub>(tppz)<sub>2</sub>Cl<sub>2</sub>]<sup>4+</sup> in acetonitrile*, J. Phys. Chem.A **118**, 5400 (2014).
- H.-G. Yu, *A complex guided spectral transform Lanczos method for studying quantum resonance states*, J. Chem. Phys. **141**, 244114 (2014).
- H.-G. Yu, *Multi-layer Lanczos iteration approach to calculations of vibrational energies and dipole transition intensities for polyatomic molecules*, J. Chem. Phys. **142**, 044106 (2015).
- H.-G. Yu, *Neural network iterative diagonalization method to solve eigenvalue problems in quantum mechanics*, Phys. Chem. Chem. Phys. **17**, 14082 (2015).
- H.-G. Yu, S. Ndengue, J. Li, R. Dawes, and H. Guo, *Vibrational energy levels of the simplest Criegee intermediate (CH<sub>2</sub>OO) from full-dimensional Lanczos, MCTDH, and MULTIMODE calculations*, J. Chem. Phys. **143**, 084311 (2015).
- H.-G. Yu, *Accurate quantum dynamics calculations of vibrational spectrum of dideuteromethane CH<sub>2</sub>D<sub>2</sub>*, J. Chem. Phys. **142**, 194307 (2015).
- D. Forthomme, M.L. Hause, H.-G. Yu, P. J. Dagdigian, T. J. Sears, and G. E. Hall, *Doppler-resolved kinetics of saturation recovery*, J. Phys. Chem. A **119**, 7439 (2015).
- H. L. Holmes-Ross; R.J. Valenti, R. J.; H.-G. Yu, G.E. Hall, and W.D. Lawrence, *Rotational and angular distributions of NO products from NO-Rg (Rg = He, Ne, Ar) complex photodissociation*, J. Chem. Phys. **144**, 044309 (2016).
- H.-G. Yu, H. Han, and H. Guo, *Full-dimensional quantum calculations of vibrational levels of NH<sub>4</sub><sup>+</sup> and isotopomers on an accurate ab initio potential energy surface*, J. Phys. Chem. A (accepted, 2016).

# Chemical Kinetics of Elementary Reactions

Judit Zádor

*Combustion Research Facility, Mail Stop 9055, Sandia National Laboratories  
Livermore, CA 94551-0969  
jzador@sandia.gov*

## I. PROGRAM SCOPE

My program focuses on the theoretical determination of rate coefficients and branching fractions of reactions in the gas-phase, mostly relevant to combustion and atmospheric chemistry, such as the formation and dissociation of radicals derived from various fuel molecules and the bimolecular reactions associated with low-temperature autoignition. I use accurate quantum chemical methods and transition-state theory in combination with time-dependent master equations<sup>i</sup> to calculate the pressure and temperature dependence of the chemical reactions. This program involves strong collaboration with experimentalists at the CRF (Craig A. Taatjes, David L. Osborn, Leonid Sheps) to achieve the accuracy and access the level of details that neither theory nor experiment could alone.

And important part of the program is that I develop methods to automatically explore reactive potential energy surfaces (PES) to systematize and significantly accelerate research in elementary chemical kinetics, and study how theoretical predictions can be made more accurate. The related code, KinBot, has been used in many of the studies outlined below.

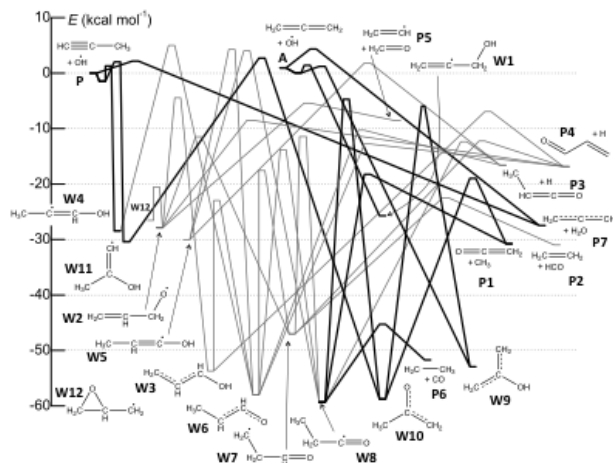
## II. RECENT PROGRESS

### A. Reactions involving the OH radical

OH radicals are the single most important chain carriers at low combustion temperatures and in the atmosphere, and alkenes are also pervasive in both environments. Between ~500 and ~800 K pressure-dependent adduct formation, backdissociation, isomerization, and simple H atom abstraction compete in OH + alkene reactions, with important implications for instance for alcohol combustion.

As a continuation of my work on the reaction of OH radicals with unsaturated molecules, in collaboration with Leonid Sheps, we studied the OH + cis/trans-2-butene reactions. We used our KinBot code to explore the relevant stationary points on the PES automatically at the CCSD(T)-F12//M06-2X level, and calculated pressure-dependent rate coefficients in a master equation framework. The calculations were supplemented with a two-transition-state model for the dynamically complex entrance channel. We also refined our previously developed methodology to analyze experimental OH-concentration–time profiles with two time scales<sup>ii</sup> and achieved an overall good agreement between theory and experiments after tuning some barriers slightly. We observed, however, larger discrepancies for the abstraction channels, pointing to remaining, and probably significant uncertainties in our approach. Our overall analysis methodology is generally applicable to other OH + alkene reactions, or even more broadly, to reactions with competing timescales.

Allene and propyne, small, doubly unsaturated molecules, play an important role in the reaction sequence contributing to molecular weight growth processes. We mapped out the stationary points and the corresponding conformational space on the corresponding C<sub>3</sub>H<sub>5</sub>O potential energy surface relevant for the OH + allene and OH + propyne reactions systematically and automatically using our KinBot software at the UCCSD(T)-F12b//M06-2X level of theory. The double unsaturation significantly increased the number of reaction pathways as shown in the



The  $C_3H_5O$  PES explored by KinBot.

complex, involving the competition of stabilization, isomerization and dissociation processes. We found that the OH addition to the central carbon of allene has a particularly interesting and complex pressure dependence, caused by the low-lying exit channel to form ketene +  $CH_3$  bimolecular products. We compared our results to a wide range of experimental data and assessed possible uncertainties arising from certain aspects of the theoretical framework. An interesting outcome of this work was that we were able to show that automated searches can find pathways that are important but were missing in previous studies.

## B. Low-temperature autoignition chemistry

The single largest experimental obstacle when studying ephemeral species such as QOOH radicals is their generation in sufficient quantities and purity. QOOH radicals are very short-lived transients in the  $R + O_2 \rightarrow ROO \rightarrow QOOH \rightarrow \text{Products}$  sequence, and, therefore, are usually present in low concentrations when starting with an alkyl radical. Previously, in collaboration with Craig Taatjes and David Osborn, we devised an experimental strategy to make QOOH radicals in an alternative way: we reacted tert-butyl hydroperoxide molecules with photolytically generated Cl atoms at room temperature.<sup>iii</sup> We could not detect the QOOH radical itself due to its rapid dissociation, but this work was the first direct determination of any QOOH kinetics providing crucial validation for theory.

In our more recent work, we studied low-temperature oxidation using cycloheptadiene precursor in photolytically initiated oxidation experiments in collaboration with David Osborn and Craig Taatjes. One of the several possible QOOH radicals has two advantageous properties: due to double resonance stabilization it is very stable (in fact, more stable than the related ROO radical), and can be detected using photoionization mass spectrometry. Our investigation yielded kinetic traces of this QOOH radical containing both its formation and decay time scales. Theory played a crucial role, as it enabled the systematic investigation and simplification of the fundamentally complex PES, provided strong support for the observed rate coefficients, and most importantly, enabled the interpretation of the measured quantities. Our calculations showed the importance of tunneling and chemical activation pathways under low-temperature combustion conditions. The results establish that resonance stabilization dramatically changes QOOH reactivity, and, hence, oxidation of unsaturated organics can produce exceptionally long-

figure on the left. Using RRKM-based 1-D master equations we calculated pressure- and temperature-dependent, channel-specific phenomenological rate coefficients for the bimolecular reactions OH + allene and OH + propyne, and for the unimolecular decomposition of the  $CH_3CCHOH$ ,  $CH_3C(OH)CH$ ,  $CH_2CCH_2OH$ ,  $CH_2C(OH)CH_2$  primary adducts, and also for the related acetyl, propionyl, 2-methylvinoxy, and 3-oxo-1-propyl radicals. The major channel of the bimolecular reactions at high temperatures is the formation propargyl +  $H_2O$ , which makes the reactions important players in soot formation at high temperatures. However, below  $\sim 1000$  K the chemistry is more

lived QOOH intermediates, which likely contribute to secondary aerosol formation in the atmosphere as well. Also, re-examination of assumed equivalences between rate coefficients for  $R + O_2$  and  $QOOH + O_2$  reactions used in many organic oxidation models might be necessary. Our work breaks fresh ground for further studies on QOOH radicals, and helps build more accurate autoignition models, which critically depend on the chemistry of these short-lived species.

We investigated several other low-temperature oxidation systems (*n*-butane, propane, 2,5-dimethyl hexane, diethyl ketone, cyclohexane, tetrahydropyrene, etc.), with varying degree of contribution from theory. For instance, we automatically generated rate coefficients for the isomerization of radicals derived from 2,5-dimethyl hexane, which were key to interpret some of the experimental results. It turned out that isomerization of the initial hexyl radicals into each other significantly alters the course of the oxidation process, and these reactions can compete with  $O_2$  addition. Similar conclusions were drawn from our study on tetrahydropyrene, where ring-opening reactions compete with  $O_2$  addition. In collaboration with S. Mani Sarathy (KAUST) we studied the low-temperature oxidation of cyclopentane. Our model correctly predicts the lowered reactivity due to the presence of the cycle that causes the suppression of certain H-transfer reactions.

Alkylperoxy chemistry plays also an important role in the degradation of organic polymers in the condensed phase. In collaboration with Kevin Leung (Sandia, NM), we investigated the degradation mechanisms of poly(3-hexylthiophene) (P3HT) theoretically and explored reaction pathways that may lead to the oxidation of the thiophene backbone as a critical step toward disrupting the polymer conjugation. We calculated barrier heights for reactions of the P3HT backbone with oxidizing agents including the hydroxyl radical (OH), hydroperoxide (ROOH), and the peroxy radical (ROO). We found that an attack of a peroxy radical on the side chain on the P3HT backbone may provide low barrier reaction pathways to photodegradation of P3HT and other similar polymers with side chains.

### C. Photoionization

In collaboration with David Osborn, Balint Sztaray (University of the Pacific) and PIs from the Paul Sherrer Institut (Switzerland) we studied the photoelectron spectrum of the benzyl radical. Using the CASPT2 electronic structure method to characterize the benzyl radical's ground and excited cationic states, both triplets and singlets, from which several contribute to the measured spectrum in the 7.0–10.5 eV range. The Franck-Condon simulations are in almost perfect agreement for the lowest singlet ( $\tilde{X}^+1A_1$ ) and triplet ( $\tilde{a}^+3B_2$ ) states, and we were able to identify most of the sharp higher energy features as well associated with state  $\tilde{A}^+1B_2$  and with possible contributions from  $\tilde{b}^+3A_1$ .

### III. NEW DIRECTIONS AND ONGOING WORK

My primary research goal for the near-term is the further development of our automated kinetics code, KinBot. There are several reaction systems where it is applied either at Sandia or in collaboration with others, exploring reactions of tetrahydrofuran, pentanol, ketohydroperoxides, and methylcyclopentane. KinBot is an expert system relying mostly on chemical rules translated into the 3-D space of molecular structures. This approach, while very efficient and quite reliable for many problems, clearly has limitations. We are exploring molecular dynamics toolsets to extend the abilities of this automated framework and also exploring the option to couple KinBot

to automated reaction generators. KinBot potentially can discover pathways that were either not known or simply not thought of in the context of combustion. It already surprised us and provided, for instance, the basis for discovering the water elimination channel in alcoholic QOOH radicals.

Other ongoing research includes the study of the photoionization mechanism of CH<sub>3</sub>OOH, where both nonstatistical and roaming dynamics play a role. We also study the effects of anharmonicity on photoionization efficiency curves for larger molecules, and develop methods to treat them within a Franck-Condon approximation.

#### IV. REFERENCES

- i. <http://chmwls.chm.anl.gov/papr/>
- ii. Kappler, C.; Zádor, J.; Welz, O.; Fernandes, R. X.; Olzmann, M.; Taatjes, C. A., *Z. Phys. Chem.* **2011**, *225*, 1271-1293.
- iii. Zádor, J.; Huang, H.; Welz, O.; Zetterberg, J.; Osborn, D. L.; Taatjes, C. A., Directly measuring reaction kinetics of QOOH – a crucial but elusive intermediate in hydrocarbon autoignition. *Phys. Chem. Chem. Phys.* **2013**, *15*, 10753-10760.

#### V. DOE SUPPORTED PUBLICATIONS, 2014-PRESENT

1. Rotavera, B.; Savee, J. D.; Antonov, I. O.; Caravan, R. L.; Sheps, L.; Osborn, D. L.; Zádor, J.; Taatjes, C. A., Influence of oxygenation in cyclic hydrocarbons on chain-termination reactions from R + O<sub>2</sub>. *Proc. Combust. Inst.*, *submitted*.
2. Li, X.; Jasper, A. W.; Zádor, J.; Miller, J. A.; Klippenstein, S. J., Theoretical kinetics of O + C<sub>2</sub>H<sub>4</sub>. *Proc. Combust. Inst.*, *submitted*.
3. Al Rashidi, M. J.; Thion, S.; Togbé, C.; Dayma, G.; Mehl, M.; Dagaut, P.; Pitz, W. J.; Zádor, J.; Sarathy, S. M., Elucidating reactivity regimes in cyclopentane oxidation: Jet stirred reactor experiments, computational chemistry, and kinetic modeling. *Proc. Combust. Inst.*, *submitted*.
4. Miller, J. A.; Klippenstein, S. J.; Robertson, S. H.; Pilling, M. J.; Shannon, R.; Zádor, J.; Jasper, A. W.; Goldsmith, C. F.; Burke, M. P., "Comment on "When rate constants are not enough" by John R. Barker, Michael Frenklach, and David M. Golden". *J. Phys. Chem. A* **2016**, *120*, 306-312.
5. Burke, M. P.; Goldsmith, C. F.; Klippenstein, S. J.; Welz, O.; Huang, H.; Antonov, I. O.; Savee, J. D.; Osborn, D. L.; Zádor, J.; Taatjes, C. A.; Sheps, L., Multi-scale informatics for low-temperature propane oxidation: Further complexities in studies of complex reactions. *J. Phys. Chem. A* **2015**, *119*, 7095-7115.
6. Antonov, I. O.; Kwok, J.; Zádor, J.; Sheps, L., OH + 2-butene: A combined experimental and theoretical study in the 300–800 K temperature range. *J. Phys. Chem. A* **2015**, *119*, 7742-7752.
7. Savee, J. D.; Zádor, J.; Hemberger, P.; Sztaray, B.; Bodi, A.; Osborn, D. L., Threshold photoelectron spectrum of the benzyl radical. *Mol. Phys.* **2015**, DOI:10.1080/00268976.2015.1021398.
8. Savee, J. D.; Papajak, E.; Rotavera, B.; Huang, H.; Eskola, A. J.; Welz, O.; Sheps, L.; Taatjes, C. A.; Zádor, J.; Osborn, D. L., Direct observation and kinetics of a critical reactive intermediate in hydrocarbon oxidation. *Science* **2015**, *347*, 643-646.
9. Eskola, A. J.; Welz, O.; Zádor, J.; Antonov, I. O.; Sheps, L.; Savee, J. D.; Osborn, D. L.; Taatjes, C. A., Probing the low-temperature chain-branching mechanism for *n*-butane autoignition chemistry via time-resolved measurements of ketohydroperoxide formation in photolytically initiated *n*-C<sub>4</sub>H<sub>10</sub> oxidation. *Proc. Combust. Inst.* **2015**, *35*, 291-298.
10. Zádor, J.; Miller, J. A., Adventures on the C<sub>3</sub>H<sub>5</sub>O potential energy surface: OH + propyne, OH + allene and related reactions. *Proc. Combust. Inst.* **2015**, *35*, 181-188.
11. Scheer, A. M.; Welz, O.; Zádor, J.; Osborn, D. L.; Taatjes, C. A., Low-temperature combustion chemistry of novel biofuels: Resonance-stabilized QOOH in the oxidation of diethyl ketone. *Phys. Chem. Chem. Phys.* **2014**, *16*, 13027-13040.
12. Sai, N.; Leung, K.; Zádor, J.; Graeme, H., First principles study of photo-oxidation degradation mechanisms in P3HT for organic solar cells. *Phys. Chem. Chem. Phys.* **2014**, *16*, 8092-8099
13. Rotavera, B.; Zádor, J.; Welz, O.; Sheps, L.; Scheer, A. M.; Savee, J. D.; Ali, M. A.; Lee, T. S.; Simmons, B. A.; Osborn, D. L.; Violi, A.; Taatjes, C. A., Photoionization mass spectrometric measurements of initial reaction pathways in low-temperature oxidation of 2,5-dimethylhexane. *J. Phys. Chem. A* **2014**, *118*, 10188-10200.

# Isomer-specific Spectroscopy and Pyrolysis of Model Aromatic Fuels

*Timothy S. Zwier*

Department of Chemistry, Purdue University, West Lafayette, IN 47907-2084  
zwier@purdue.edu

## Program Definition and Scope

The chemical complexity of hydrocarbon fuels and the fast-expanding list of potential plant-derived biofuels offer a challenge to the scientific community seeking to provide a molecular-scale understanding of their combustion. The development of accurate combustion models stands on a foundation of experimental data on the kinetics and product branching ratios of individual reaction steps. Spectroscopic tools need to continue to be developed to selectively detect and characterize the widening array of fuel components and the reactive intermediates they generate upon pyrolysis and combustion. There is growing recognition that a key component of future progress in the field is the development of detection schemes that are isomer-specific and even conformation-specific. This project uses an array of laser-based and broadband microwave methods to carry out isomer-specific and conformation-specific spectroscopy on key fuel components and the reactive intermediates formed during their pyrolysis and combustion.

## Recent Progress

### A. Toward a first principles model of the alkyl CH stretch region and its application to phenylalkanes (ref. 1, 2, 6, 8, 13, 17)

The alkyl CH stretch region of the infrared is a region rich in information content, but a challenge to assign, due to the ubiquitous presence of strong Fermi resonance mixing between the alkyl CH stretch and CH bend overtone levels. Conformational assignments based on a comparison of the observed alkyl CH stretch spectra with *ab initio* predictions of harmonic frequencies often fail in spectacular fashion due to these Fermi resonances, which shift and split bands to the point that comparison with harmonic calculations is fruitless. Working in collaboration with Ned Sibert (UW-Madison), we are developing a first-principles model of the alkyl CH stretch region built around a local mode Hamiltonian that explicitly takes into account the 2:1 Fermi resonance between the CH stretch and CH bend overtones and combination bands.

Building off earlier studies that concentrated on alkyl chains containing only CH<sub>2</sub> groups (ref. 1,2,6,8), and extension of the model to include the more complicated Fermi coupling occurring in methyl groups (ref. 13), we are currently studying the single-conformation spectroscopy of a series of phenylalkanes, C<sub>6</sub>H<sub>5</sub>-(CH<sub>2</sub>)<sub>n</sub>-CH<sub>3</sub> with n=1-9. As the prototypical member of the series, the model was first tested on ethylbenzene. In this case, spectra of partially deuterated isotopomers, particularly C<sub>6</sub>H<sub>5</sub>-CD<sub>2</sub>-CH<sub>3</sub>, provided benchmark tests of the model parameters. The extension to n-propylbenzene and n-butylbenzene provided the first conformation-specific tests of the model on alkyl chains. The model was able to account for the observed alkyl CH stretch spectra in the ground electronic state in significant detail. A manuscript describing this work has just been submitted for publication.

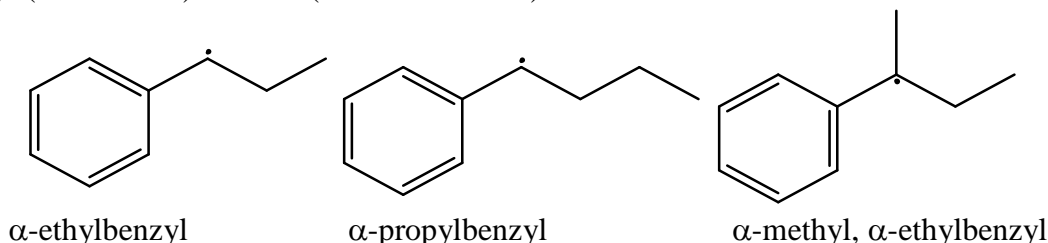
The phenylalkanes with longer alkyl chains, beginning with pentylbenzene, have LIF excitation scans that show signs of overlapping S<sub>0</sub>-S<sub>1</sub> origins for conformational minima that share the same local alkyl chain conformation near the phenyl ring. Nevertheless, high signal-to-noise scans of each unique feature in the LIF spectrum still serve as a basis for comparison with theory. In addition, beginning with n-octylbenzene, in addition to the main bands, we observe

new UV transitions that are red-shifted compared to those of shorter alkyl chains. These spectral shifts in the UV point to unique interactions of the alkyl chain with the phenyl ring, probably by folding back over the top of the ring, where dispersive interactions between the alkyl chain and phenyl  $\pi$  cloud cause the electronic frequency shift. Alkyl CH stretch spectra of these transitions show unique features that are currently under investigation with the local mode model.

Finally, we have recorded high-quality IR spectra of the entire series of n-alkylbenzenes in the excited electronic state by detecting red-shifted fluorescence that occurs following IR excitation of the  $S_1$  origin levels of the molecules.

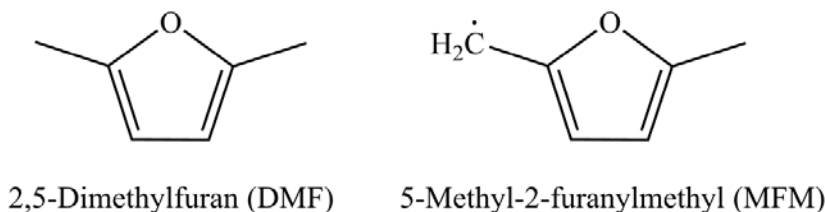
## B. Resonance-stabilized radicals (ref. 4, 6, 15, 16)

We also continue to pursue isomer-specific and conformation-specific spectroscopy of resonance-stabilized hydrocarbon radicals. Building off recently published studies of  $\alpha$ -methylbenzyl radical  $C_6H_5-\dot{C}H-CH_3$  (ref. 4), trihydronaphthyl radical, and inden-2-ylmethyl radical (ref. 6), we have recorded two-color resonant two-photon (2C-R2PI) and resonant ion-dip infrared (RIDIR) spectra of  $\alpha$ -ethylbenzyl ( $\alpha$ EtBz),  $\alpha$ -propylbenzyl ( $\alpha$ PrBz), and  $\alpha$ -methyl,  $\alpha$ -ethylbenzyl ( $\alpha$ Me $\alpha$ EtBz) radicals (structures below).



The ethyl side chain in  $\alpha$ -EtBz radical prefers an in-plane orientation, opposite to that in ethylbenzene, pointing to the effect of the radical site on the conformational preferences.  $\alpha$ PrBz radical has a sufficiently long alkyl chain to exist in more than one conformational minimum. We have used double-resonance methods to characterize the two major conformers observed. The Sibert group is applying their local mode Hamiltonian model to the alkyl CH stretch spectra of these two free radicals. A paper describing this work is in preparation (ref. 16).

The 5-methyl-2-furanylmethyl (MFM) radical is derived from 2,5-dimethylfuran (DMF) by loss of an H-atom from one of the methyl groups. DMF has properties as a biofuel that make it an attractive substitute for ethanol as a transportation fuel. Since loss of an H-atom produces a resonance-stabilized radical, it is an important first step, especially at low temperatures, for decomposition of DMF.



We have spectroscopically characterized this radical, produced in an electric discharge, under jet-cooled conditions. A well-resolved electronic spectrum is present in the visible, with an extended Franck-Condon progression involving hindered methyl internal rotation. Resonant ion-dip infrared spectra of both the ground ( $D_0$ ) and first excited ( $D_1$ ) doublet electronic states have been recorded in the alkyl CH stretch region, showing dramatic changes with electronic excitation that mirror the change in preferred orientation of the methyl group. A paper describing this work is in preparation (ref. 15).

### C. Broadband microwave spectra of intermediates formed in flash pyrolysis (ref. 10,18)

We continue to develop CP-FTMW spectroscopy as a method for characterizing the reactive intermediates formed by flash pyrolysis via a hyperthermal nozzle (or Chen nozzle). We have built a piezostack pulsed valve using the design from the Suits' group (C. Abeysekera et al., *Rev. Sci. Instr.* **85**, 116107 (2015)) that will provide dense, short gas pulses at high repetition rate, useful for pyrolysis studies. We are also working on microwave-microwave multi-resonance schemes for efficiently assigning transitions that arise from the same molecular carrier in a mixture. Finally, we are adding a VUV photoionization-TOF mass spectrometer stage to our CP-FTMW chamber that we plan to use to determine the molecular formulae of products formed by pyrolysis using 118 nm photoionization. This will help narrow our search for possible carriers of observed transitions in the microwave spectrum to species with the correct molecular formulae, adding a powerful complementary tool to this instrument.

### Future Work

- (1) We will continue our studies of long-chain alkylbenzenes in order to determine the chain length at which folded structures that bring the alkyl chain back over the phenyl ring are in competition with extended structures.
- (2) We also plan to study a series of 1,2-diaromatic ethanes to understand when  $\pi$  stacking begins to overcome steric constraints on the ethyl chain.
- (3) We will extend our CH stretch model to include alkyl chains with various prototypical functional groups.
- (4) Construction, installation, and testing of the time-of-flight section to our CP-FTMW chamber will be completed.
- (5) CP-FTMW studies of methyl butanoate, another prototypical biofuel, will be carried out both under jet cooling and at room temperature.
- (6) Pyrolysis studies of methyl butanoate, methylfuran and 2,5-dimethylfuran will also be subjects of future work.

### Publications acknowledging DOE support, 2013-present

1. Evan G. Buchanan, Jacob C. Dean, Timothy S. Zwier, and Edwin L. Sibert III, "Towards a first-principles model of Fermi resonances in the alkyl CH stretch region: Application to 1,2-diphenylethane and 2,2,2-paracyclophane", *J. Chem. Phys.* **134**, 064308 (2013).
2. Evan G. Buchanan, Edwin L. Sibert III, and Timothy S. Zwier, Ground state Conformational Preferences and CH stretch-bend coupling in a model alkoxy chain: 1,2-diphenoxyethane", *J. Phys. Chem. A* **117**, 2800-2811 (2013).
3. Evan G. Buchanan, David F. Plusquellic, and Timothy S. Zwier, "Excitonic splitting and vibronic coupling in 1,2-diphenoxyethane: Conformation-specific effects in the weak coupling limit", *J. Chem. Phys.* **138** 204313 (2013).
4. Nathanael M. Kidwell, Neil J. Reilly, Ben Nebgen, Deepali N. Mehta-Hurt, Ross D. Hoehn, Damian L. Kokkin, Michael C. McCarthy, Lyudmila V. Slipchenko, and Timothy S. Zwier, "Jet-cooled Spectroscopy of the  $\alpha$ -Methylbenzyl Radical: Probing the State-Dependent Effects of Methyl Rocking against a Radical Site", *J. Phys. Chem. A*, **117**, 13465-80 (2013).
5. Jacob C. Dean, Polina Navotnaya, Alexander P. Parobek, Rachel M. Clayton, and Timothy S. Zwier, "Ultraviolet spectroscopy of fundamental Lignin sub-units: Guaiacol, 4-methylguaiacol, syringol, and 4-methylsyringol", **139**, 144313 (2013). (16 pages)

6. Nathanael M. Kidwell, Deepali N. Mehta-Hurt, Joseph A. Korn, Edwin L. Sibert III, and Timothy S. Zwier, "Ground and Excited State Infrared Spectroscopy of Jet-Cooled Radicals: Exploring the Photophysics of Trihydronaphthyl and Inden-2-ylmethyl", *J. Phys. Chem. A* **117**, 13465–13480 (2013).
7. Jacob C. Dean, Patrick S. Walsh, Bidyut Biswas, P. V. Ramachandran, and Timothy S. Zwier, "Single-conformation UV and IR spectroscopy of model G-type lignin dilignols: the  $\beta$ -O-4 and  $\beta$ - $\beta$  linkages", *Chem. Sci.*, **5**, 1940 – 1955 (2014).
8. Edwin L. Sibert III, Nathanael M. Kidwell, and Timothy S. Zwier, "A First-Principles Model of Fermi Resonance in the Alkyl CH Stretch Region: Application to Hydronaphthalenes, Indanes, and Cyclohexane", *J. Phys. Chem. B* **118**, 8236-8245 (2014).
9. Nathan R. Pillsbury, Nathanael M. Kidwell, Benjamin Nebgen, Lyudmila V. Slipchenko, John R. Cable, David F. Plusquellic, and Timothy S. Zwier, "Vibronic Coupling in Asymmetric Bichromophores: I. Experimental Investigation of Diphenylmethane- $d_5$ ", *J. Chem. Phys.* **141**, 064316 (2014).
10. Nathanael M. Kidwell, Vanesa Vaquero-Vara, Thomas K. Ormond, Grant T. Buckingham, Di Zhang, Deepali N. Mehta-Hurt, Laura McCaslin, Mark R. Nimlos, John W. Daily, Brian C. Dian, John F. Stanton, G. Barney Ellison, and Timothy S. Zwier, "Chirped-Pulse Fourier Transform Microwave Spectroscopy coupled with a Flash Pyrolysis Microreactor: Structural Determination of the Reactive Intermediate Cyclopentadienone", *J. Phys. Chem. Lett.* **5**, 2201-07 (2014).
11. Jamie D. Young, Michael Staniforth, Jacob C. Dean, Gareth M. Roberts, Federico Mazzoni, Tolga N.V. Karsili, Michael N.R. Ashfold, Timothy S. Zwier, and Vasilios G. Stavros, "Towards Understanding Photodegradation Pathways in Lignins: The Role of Intramolecular Hydrogen Bonding in Excited States", *J. Phys. Chem. Lett.* **5**, 2138-43 (2014).
12. Jacob C. Dean, Ryoji Kusaka, Patrick C. Walsh, Florent Allais, and Timothy S. Zwier, "Plant Sunscreens in the UV-B: Ultraviolet Spectroscopy of Jet-Cooled Sinapoyl Malate, Sinapic Acid, and Sinapate Ester Derivatives", *J. Am. Chem. Soc.* **136**, 14780-95 (2014).
13. Edwin L. Sibert III, Daniel P. Tabor, Nathanael M. Kidwell, Jacob C. Dean, and Timothy S. Zwier, "Fermi Resonance Effects in the Vibrational Spectroscopy of Methyl and Methoxy Groups", *J. Phys. Chem. A* **118**, 11272-81 (2014).
14. Jacob C. Dean, Nicole L. Burke, John R. Hopkins, James G. Redwine, P.V. Ramachandran, Scott A. McLuckey, and Timothy S. Zwier, "UV Photofragmentation and IR Spectroscopy of Cold, G-type  $\beta$ -O-4 and  $\beta$ - $\beta$  Dilignol-Alkali Metal Complexes: Structure and Linkage-Dependent Photofragmentation", *J. Phys. Chem. A* **119**, 1917-32 (2015).
15. Nathanael M. Kidwell, Deepali N. Mehta-Hurt, Joseph A. Korn, and Timothy S. Zwier, "Infrared and Electronic Spectroscopy of jet-cooled 5-methyl-2-furanylmethyl Radical derived from the Biofuel 2,5-Dimethylfuran", (submitted).
16. Joseph A. Korn, Khadija Jawad, Daniel P. Tabor, Edwin L. Sibert III, and Timothy S. Zwier, "Conformation-specific Spectroscopy of Alkylbenzyl Radicals:  $\alpha$ -ethylbenzyl and  $\alpha$ -propylbenzyl radicals", (in preparation).
17. Daniel P. Tabor, Daniel M. Hewett, Sebastian Bocklitz, Joseph A. Korn, Anthony J. Tomaine, Arun K. Ghosh, Timothy S. Zwier, and Edwin L. Sibert III, "Modeling Fermi Resonance Effects in Conformation-specific Alkyl CH stretch IR Spectra of Ethyl, n-Propyl, and n-Butylbenzene", (submitted).
18. Alicia O. Hernandez, Chamara Abeysekera, Brian M. Hays, and Timothy S. Zwier, "Multi-resonant Strong Field Coherence Breaking as a Tool for Single Isomer Microwave Spectroscopy", (in preparation).

# *Participant List*



# 36<sup>th</sup> Annual Gas Phase Chemical Physics Research Meeting Participation List

<b>Last Name</b>	<b>First Name</b>	<b>Organization</b>	<b>Email</b>
Ahmed	Musahid	Lawrence Berkeley National Lab	mahmed@lbl.gov
Alexander	Millard	University of Maryland	mha@umd.edu
Allen	Wesley	University of Georgia	wdallen@uga.edu
Barlow	Robert	Sandia National Laboratories	barlow@sandia.gov
Bellan	Josette	California Institute of Technology	Josette.Bellan@jpl.nasa.gov
Blanquart	Guillaume	Caltech	g.blanquart@caltech.edu
Bunel	Emilio	Argonne National Laboratory	ebunel@anl.gov
Butler	Laurie	University of Chicago	L-Butler@uchicago.edu
Chandler	David	Sandia National Laboratories	gdecast@sandia.gov
Chen	Jacqueline	Sandia National Laboratories	jhchen50@yahoo.com
Continetti	Robert	UC San Diego	rcontinetti@ucsd.edu
Crim	Fleming	University of Wisconsin	fcrim@chem.wisc.edu
Dagdigian	Paul	Johns Hopkins University	pjdagdigian@jhu.edu
Dahms	Rainer	Sandia National Laboratories	Rndahms@sandia.gov
Davis	Michael	Argonne National Laboratory	davis@tcg.anl.gov
Davis	Harry	Cornell University	hfd1@cornell.edu
Doublerly	Gary	University of Georgia	doublerly@uga.edu
Field	Robert	MIT	rwfield@mit.edu
Frank	Jonathan	Sandia National Laboratories	jhfrank@sandia.gov
Green	William	MIT, Chemical Engineering	whgreen@mit.edu
Hall	Gregory	Brookhaven National Lab	gehall@bnl.gov
Hansen	Nils	Sandia National Laboratories	nhansen@sandia.gov
Harding	Lawrence	Argonne National Laboratory	harding@anl.gov

Harris	Alexander	Brookhaven National Laboratory	alexh@bnl.gov
Head-Gordon	Martin	LBNL/ UC Berkeley	mhg@cchem.berkeley.edu
Heard	Dwayne	University of Leeds	d.e.heard@leeds.ac.uk
Hershberger	John	North Dakota State University	john.hershberger@ndsu.edu
Hwang	Robert	Sandia National Laboratories	gdecast@sandia.gov
Jasper	Ahren	Combustion Research Facility	ajasper@sandia.gov
Kaiser	Ralf	University of Hawaii	ralfk@hawaii.edu
Kliwier	Christopher	Sandia National Labs	cjkliew@sandia.gov
Klippenstein	Stephen	Argonne National Laboratory	sjk@anl.gov
Leone	Stephen	Univ. of California and LBNL, Berkeley	srl@berkeley.edu
Lester	Marsha	University of Pennsylvania	milester@sas.upenn.edu
Lu	Tianfeng	University of Connecticut	tianfeng.lu@uconn.edu
Lucht	Robert	Purdue University	lucht@purdue.edu
Marceau	Diane	Department of Energy	diane.marceau@science.doe.gov
Mebel	Alexander	Florida International University	mabela@fiu.edu
Michelsen	Hope	Sandia National Laboratories	hamiche@sandia.gov
Miller	William	Dept of Chem UC Berkeley and LBNL	millerwh@berkeley.edu
Mullin	Amy	University of Maryland	mullin@umd.edu
Najm	Habib	Sandia National Laboratories	hnnajm@sandia.gov
Nesbitt	David	JILA/University of Colorado	djn@jila.colorado.edu
Neumark	Daniel	University of California Berkeley	dneumark@berkeley.edu
Oefelein	Joseph	Sandia National Laboratories	oefelei@sandia.gov
Osborn	David	Sandia National Laboratories	dlosbor@sandia.gov
Parish	Carol	University of Richmond	cparish@richmond.edu
Pepiot	Perrine	Cornell University	pp427@cornell.edu
Pitz	William	Lawrence Livermore National Laboratory	pitz1@llnl.gov
Pratt	Stephen	Argonne National Laboratory	stpratt@anl.gov
Prozument	Kirill	Argonne National Laboratory	prozument@anl.gov
Reisler	Hanna	University of Southern California	reisler@usc.edu
Ruscic	Branko	Argonne National Laboratory	ruscic@anl.gov
Sears	Trevor	Brookhaven National Laboratory	sears@bnl.gov
Shaddix	Christopher	Sandia National Labs	crshadd@sandia.gov

Shepard	Ron	Argonne National Laboratory	shepard@tcg.anl.gov
Sheps	Leonid	Sandia National Lab	lsheps@sandia.gov
Sisk	Wade	DOE/BES	wade.sisk@science.doe.gov
Sivaramakrishnan	Raghu	ARGONNE NATIONAL LABORATORY	raghu@anl.gov
Stanton	John	University of Texas at Austin	jfstanton@gmail.com
Suits	Arthur	University of Missouri	suitsa@missouri.edu
Sutherland	James	University of Utah	James.Sutherland@utah.edu
Taatjes	Craig	Sandia National Laboratories	cataatj@sandia.gov
Tranter	Robert	Argonne National Laboratory	tranter@anl.gov
Violi	Angela	University of Michigan	avioli@umich.edu
Wagner	Albert	Argonne National Laboratory	wagner@anl.gov
Westbrook	Charles	LLNL	westbrookck@earthlink.net
Wilson	Kevin	Lawrence Berkeley National Laboratory	krwilson@lbl.gov
Wooldridge	Margaret	University of Michigan	mswool@umich.edu
Yu	Hua-Gen	Brookhaven National Laboratory	hgy@bnl.gov
Zádor	Judit	Sandia National Laboratories	jzador@sandia.gov
Zwier	Timothy	Purdue University	zwier@purdue.edu

# *Critical Issues*



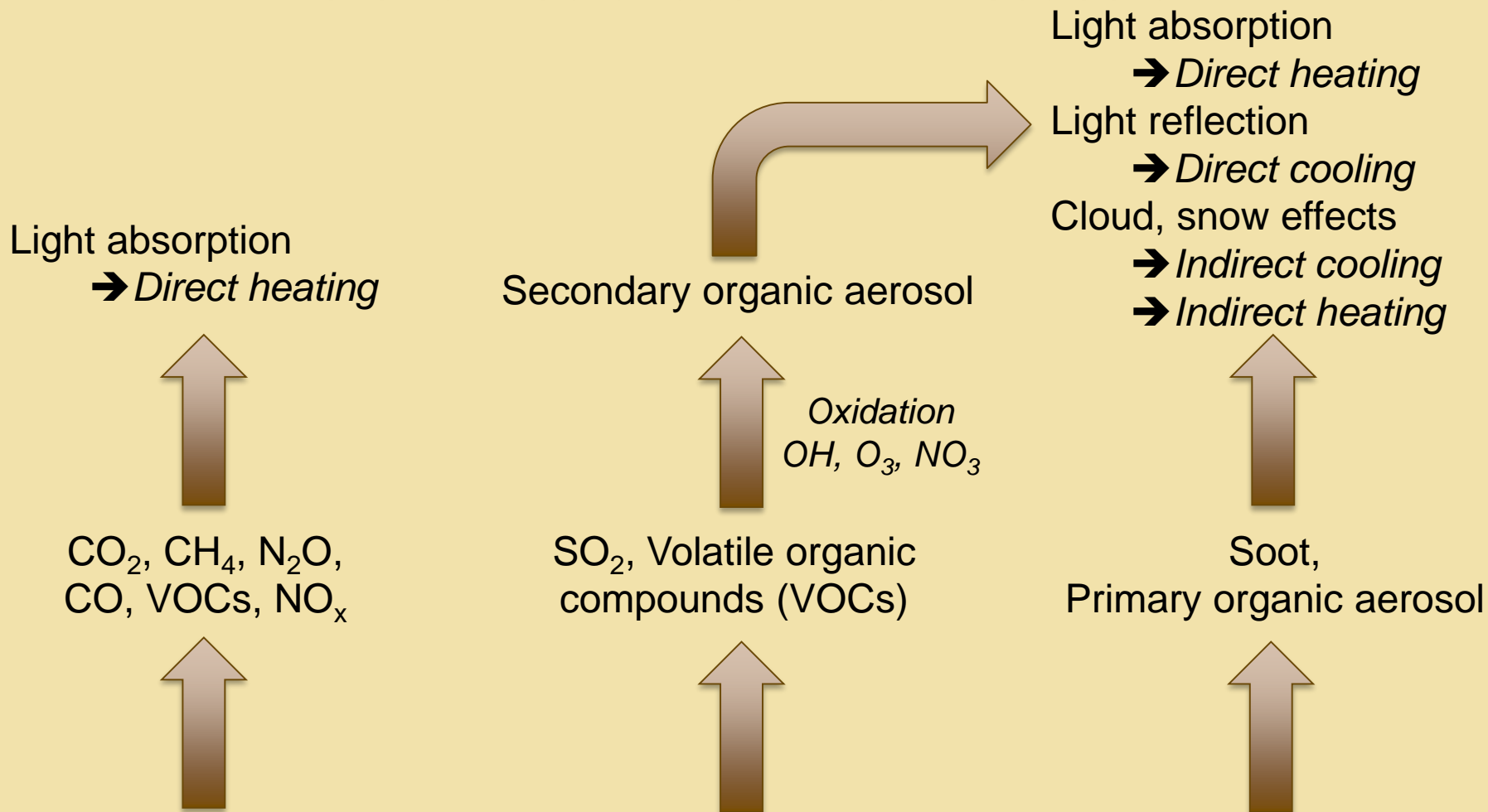
# Impact of Combustion Chemistry on Atmospheric Chemistry and Climate

## *BES Chem Sciences Panel Discussion*

- Impact of combustion emissions on climate
  - Greenhouse gases
  - Primary particulate emissions
  - Secondary aerosol formation
- Impact of combustion emissions on atmospheric chemistry
  - What comes out of the tailpipe? Conventional and biofuels?
  - What happens to combustion products exhausted into the atmosphere?
  - Coupling between chemistry and climate
- Similarities between combustion and atmospheric chemistry
  - Criegee intermediate reactions
  - QOOH chemistry
  - Different temperature & pressure, solar radiation, and time scales

# Impact of Combustion Chemistry on Climate

## BES Chem Sciences Panel Discussion



# Impact of Combustion Chemistry on Climate

## BES Chem Sciences Panel Discussion

Anthropogenic component  
from combustion

**CO<sub>2</sub>** **91%**

**CH<sub>4</sub>** **16%**

**N<sub>2</sub>O** **4%**

**CO** **100%**

**Volatile Organic Carbon** **81%**

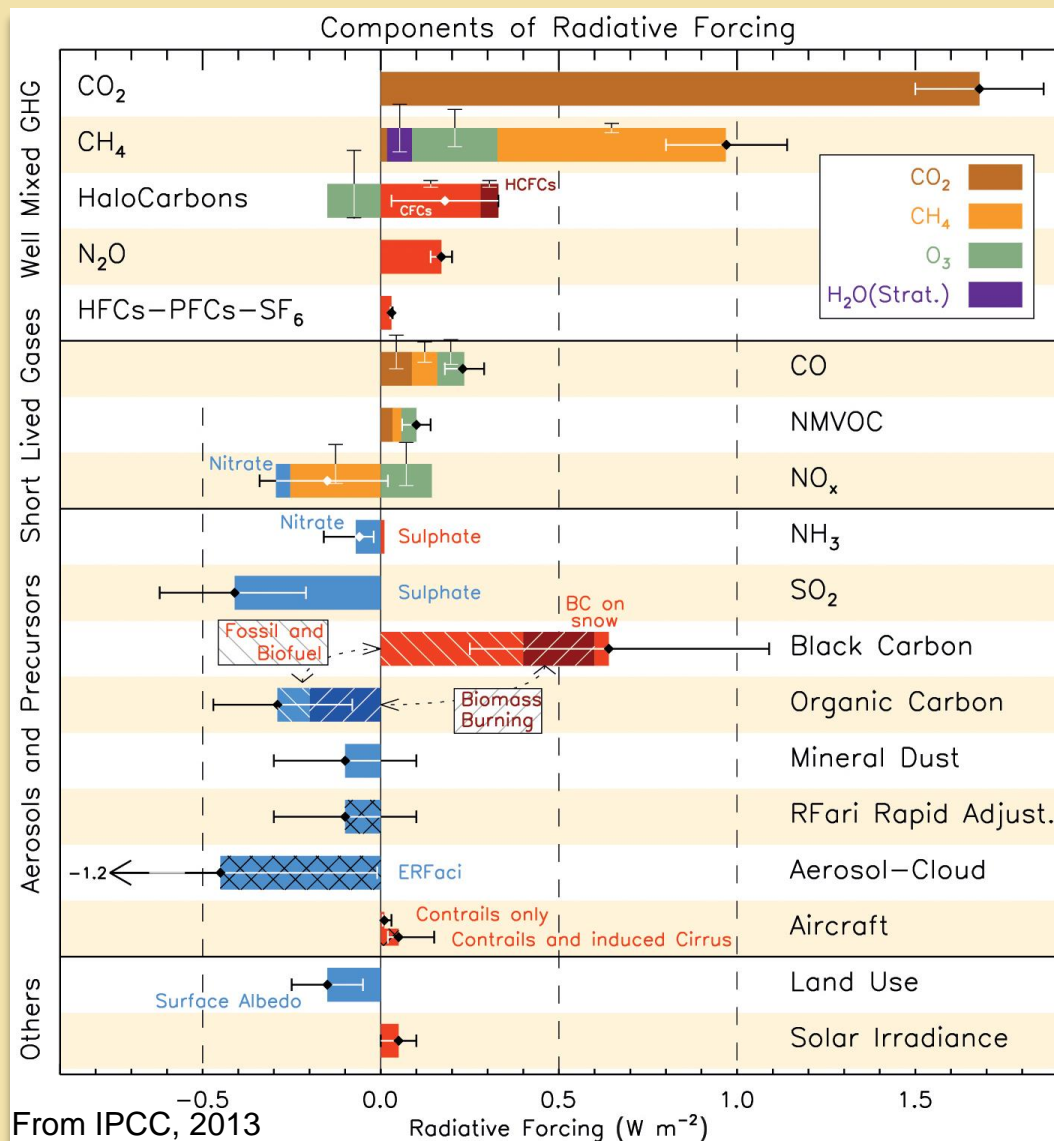
**NO<sub>x</sub>** **81%**

**SO<sub>2</sub>** **93%**

**Black Carbon** **100%**

**Organic Aerosol** **90%**

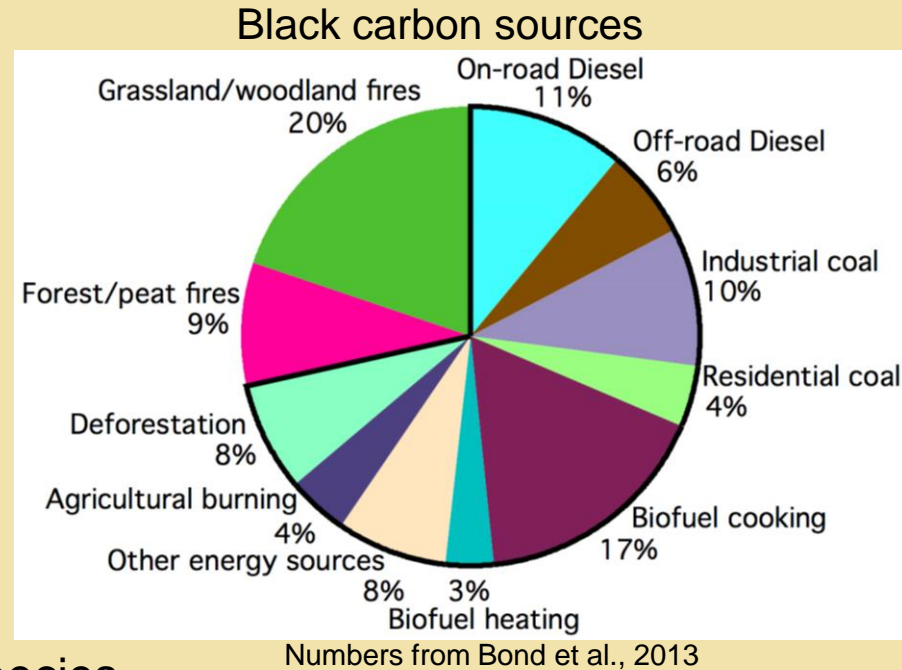
**Aircraft** **100%**



# Impact of Combustion Chemistry on Climate

## BES Chem Sciences Panel Discussion

- Impact of soot (black carbon) on climate
  - Soot absorbs light – *heating effect*
  - Soot lowers snow reflectivity - *heating*
  - Soot increases glacial melt – *heating*
  - Soot influences clouds – *heating/cooling*
  - Influence can be regional
- Other interesting facts about soot
  - Short atmospheric lifetime (~1 wk)
  - Near-term mitigation candidate
  - Can be co-emitted with aerosol-forming species
  - Can have toxic/carcinogenic adsorbates
  - Most important targets: Diesel engines, cookstoves
  - Climate effects are not well understood



# Impact of Combustion Chemistry on Climate

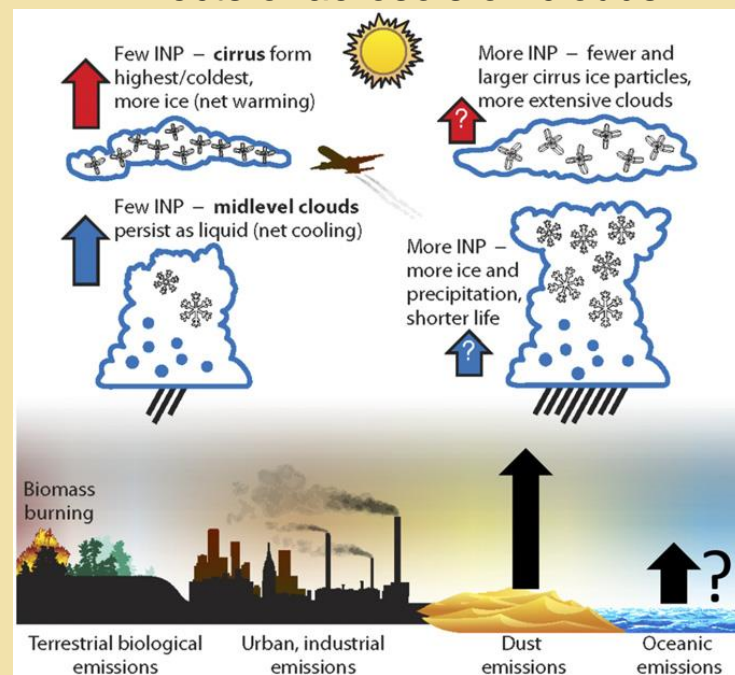
## BES Chem Sciences Panel Discussion

- Impact of organic aerosol on climate
  - OA reflects light – *cooling effect*
  - Brown carbon absorbs light – *heating effect*
  - OA influences clouds – *heating/cooling effects*
  - Influence can be regional
  - Not well understood

- Open questions

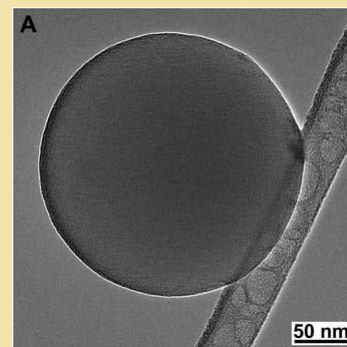
- How are these particles generated?
- What are the optical properties of BC, POA, SOA, and how do they evolve with time?
- What are the physical/chemical properties of BC, POA, SOA; how do they evolve with time?
- How do BC, POA, SOA influence cloud formation/evolution, ice nucleation, droplet size?
- What are the feedbacks and couplings?

### Effects of aerosols on clouds

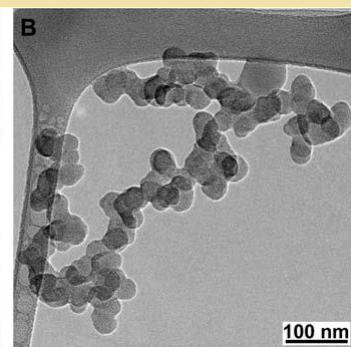


From Seinfeld et al., PNAS 113, 5785 (2016).

### Brown carbon/Tarball



### Black carbon/soot



From Alexander et al., Science 321, 833 (2008).

# DOE ASR Absorbing Aerosol Workshop

---

Held in DOE Headquarters (Germantown) on January 20 & 21, 2016

## ASR Program Managers

Ashley Williamson  
Shaima Nasiri

## Workshop Co-Chairs

Chris Cappa (U. C./Davis)  
Rao Kotamarthi (ANL)  
Art Sedlacek (BNL)

## Objectives

- Identify the underlying scientific questions regarding absorbing aerosols that limit our understanding of these species and their roles in climate-relevant radiative, thermodynamic, and dynamic processes in the atmosphere;
- Explore ways to address these questions and roles with DOE resources, including observations from the Atmospheric Radiation Measurement (ARM) facility;
- Identify measurement and modeling strategies and needs to advance our understanding of absorbing aerosol impacts

# “High-Level” Summary Themes/Issues

---

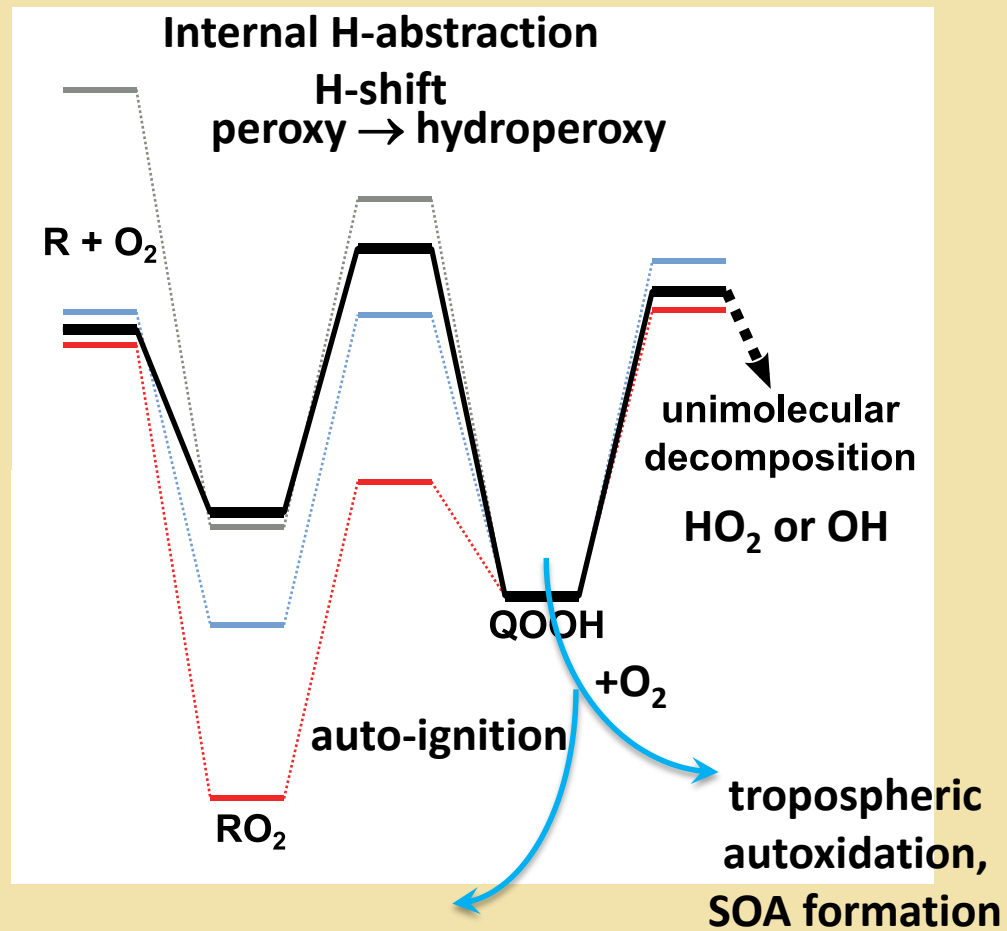
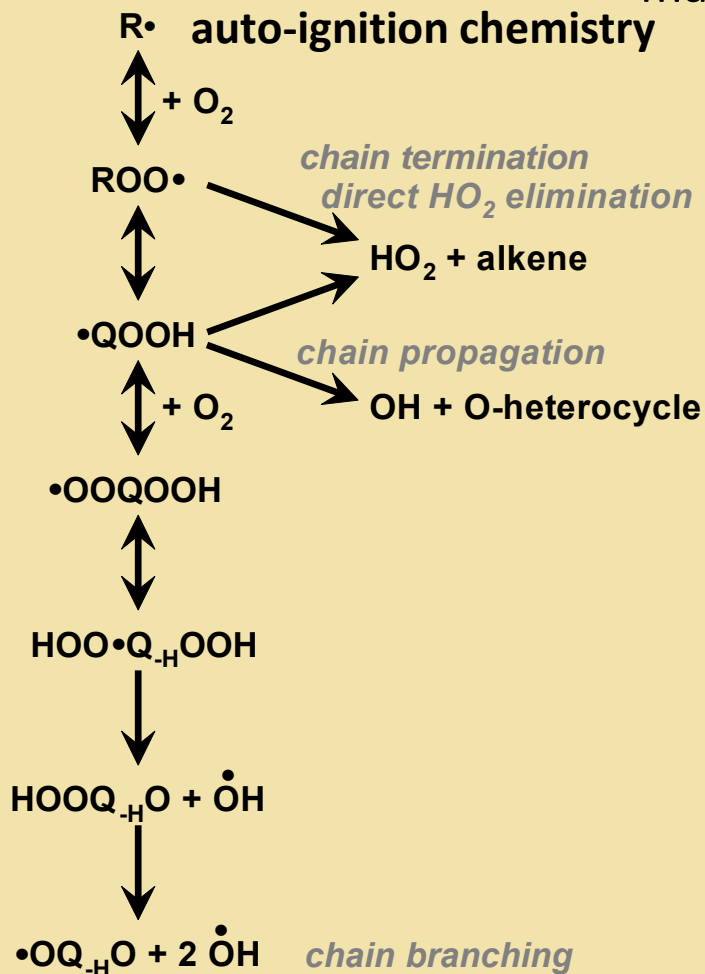
1. Coupling of the absorbing aerosol-cloud-surface system in low cloud regimes – radiative and dynamical effects
2. What are the relevant scales (time/spatial) for absorbing aerosol that affect atmospheric radiation and dynamics?
3. Biomass Burning Lifecycle – what shapes vertical and horizontal distributions of absorbing aerosol?
4. Measurements - characterizing spatial distributions of absorbing aerosol and assessing closure
5. Sensitivity studies to quantify measurement accuracy required for science questions

# Parallels between combustion and the atmosphere

QOOH and their reaction with O<sub>2</sub> lead to

Chain branching and auto-oxidation in **combustion**

Formation of low-volatility, highly oxygenated VOCS in the **atmosphere**  
 may be missing link to SOA

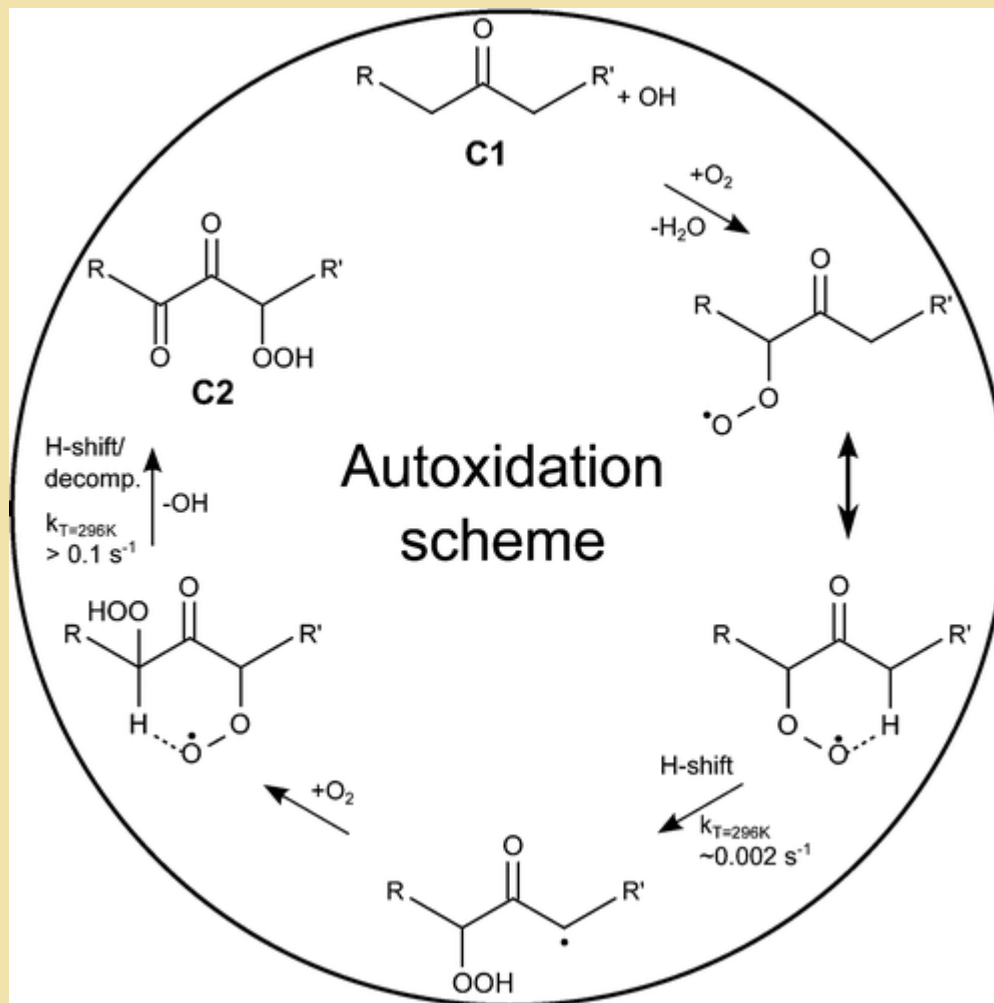


# Parallels between combustion and the atmosphere

Formation of low-volatility, highly oxygenated VOCS in the **atmosphere**

## Autoxidation of organic compounds in the atmosphere

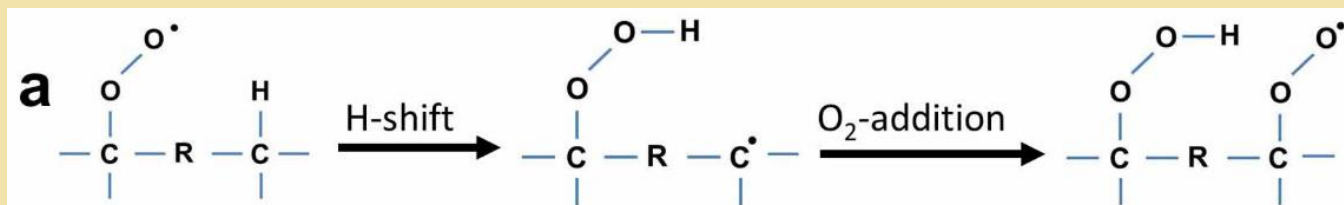
Catalytic H-shift reactions: Carbonyl compound C1 transformed to highly functionalized dicarbonyl hydroperoxide compound C2, while regenerating OH



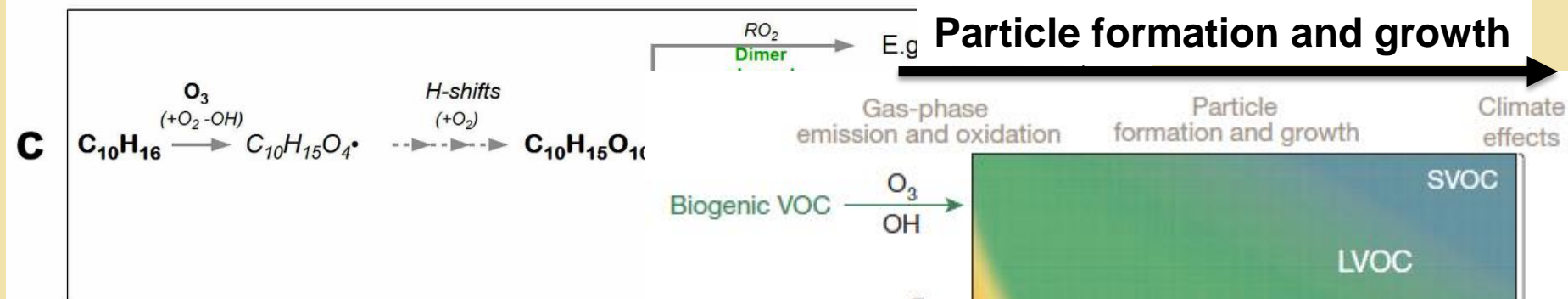
# Parallels between combustion and the atmosphere

Repeated  $RO_2$  isomerization suggested to form Extremely Low Volatility VOCs (ELVOC) that partition to form SOA

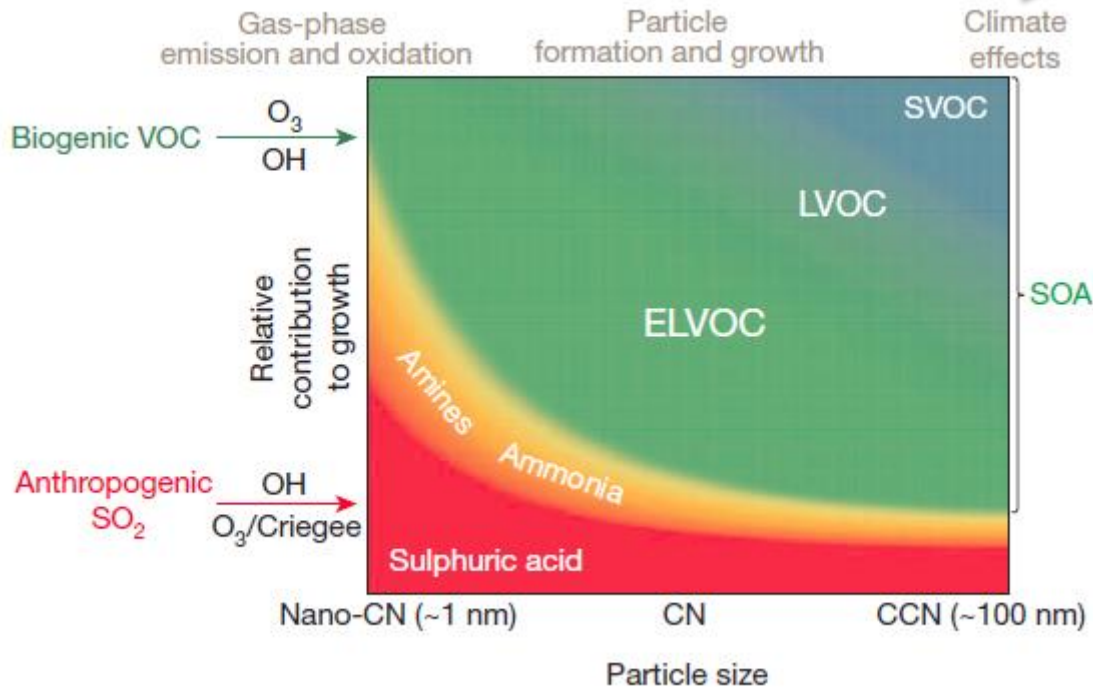
**QOOH**



$RO_2$  undergo sequential H-shifts /  $O_2$  additions that increase  $O_2$  content



Ehn et al., *Nature*, **506**, 476 (2014)



# 3 papers last week in *Science* and *Nature* on the mechanism of forming new particles in the atmosphere!

ATMOSPHERIC SCIENCE

*Nature* 26 May 2016

## Unexpected player in particle formation

CHRIS CAPPA

Three studies find that a family of organic compounds affects the formation and initial growth of atmospheric aerosol particles in clean air — with implications for our knowledge of the climate effects of aerosols. [SEE LETTERS P.521 & 527](#)

Key takeaways:

- Highly oxidized multifunctional organic compounds (HOM) drive new particle formation (nucleation) and initial growth.
- HOMs form from VOC processing by atmospheric O<sub>3</sub>, OH, and NO<sub>3</sub>.

## The role of low-volatility organic compounds in initial particle growth in the atmosphere

Jasmin Tröstl<sup>1</sup>, Wayne K. Chuang<sup>2</sup>, Hamish Gordon<sup>3</sup>, Martin Heinritzi<sup>4</sup>, Chao Yan<sup>5</sup>, Ugo Molteni<sup>1</sup>, Lars Ahlm<sup>6</sup>, Carla Frege<sup>1</sup>, Federico Bianchi<sup>1,5,7</sup>, Robert Wagner<sup>3</sup>, Mario Simon<sup>4</sup>, Katrianne Lehtipalo<sup>1,5</sup>, Christina Williamson<sup>4,8,†</sup>, Jill S. Craven<sup>9</sup>, Jonathan Duplissy<sup>5,10</sup>, Alexey Adamov<sup>3</sup>, Joao Almeida<sup>3</sup>, Anne-Kathrin Bernhammer<sup>11,12</sup>, Martin Breitenlechner<sup>11,12</sup>, Sophia Brilke<sup>4</sup>, António Dias<sup>3</sup>, Sebastian Ehrhart<sup>3</sup>, Richard C. Flagan<sup>9</sup>, Alessandro Franchin<sup>3</sup>, Claudia Fuchs<sup>1</sup>, Roberto Guida<sup>3</sup>, Martin Gysel<sup>1</sup>, Armin Hansel<sup>11,12</sup>, Christopher R. Hoyle<sup>1,13</sup>, Tuija Jokinen<sup>3</sup>, Heikki Junninen<sup>3</sup>, Juha Kangasluoma<sup>2</sup>, Helmi Keskinen<sup>5,14,†</sup>, Jaeseok Kim<sup>14,†</sup>, Manuel Krapf<sup>9</sup>, Andreas Kürten<sup>4</sup>, Ari Laaksonen<sup>14,15</sup>, Michael Lawler<sup>14,16</sup>, Markus Leiminger<sup>4</sup>, Serge Mathot<sup>3</sup>, Ottmar Möhler<sup>17</sup>, Tuomo Nieminen<sup>5,10</sup>, Antti Onnela<sup>3</sup>, Tuukka Petäjä<sup>3</sup>, Felix M. Piel<sup>4</sup>, Pasi Miettinen<sup>14</sup>, Matti P. Rissanen<sup>3</sup>, Linda Rondo<sup>4</sup>, Nina Sarnela<sup>3</sup>, Siegfried Schobesberger<sup>3,†</sup>, Kamalika Sengupta<sup>18</sup>, Mikko Sipilä<sup>3</sup>, James N. Smith<sup>14,19</sup>, Gerhard Steiner<sup>5,11,20</sup>, António Tomé<sup>21</sup>, Annele Virtanen<sup>14</sup>, Andrea C. Wagner<sup>1</sup>, Ernest Weingartner<sup>1,†</sup>, Daniela Wimmer<sup>1,5</sup>, Paul M. Winkler<sup>20</sup>, Penglin Ye<sup>22</sup>, Kenneth S. Carslaw<sup>18</sup>, Joachim Curtius<sup>4</sup>, Josef Dommen<sup>1</sup>, Jasper Kirkby<sup>3,4</sup>, Markku Kulmala<sup>3</sup>, Ilona Riipinen<sup>6</sup>, Douglas R. Worsnop<sup>5,10,22</sup>, Neil M. Donahue<sup>2,5</sup> & Urs Baltensperger<sup>1</sup>

## Ion-induced nucleation of pure biogenic particles

Jasper Kirkby<sup>1,2</sup>, Jonathan Duplissy<sup>3,4</sup>, Kamalika Sengupta<sup>5</sup>, Carla Frege<sup>6</sup>, Hamish Gordon<sup>2</sup>, Christina Williamson<sup>1,†</sup>, Martin Heinritzi<sup>1,7</sup>, Mario Simon<sup>1</sup>, Chao Yan<sup>3</sup>, João Almeida<sup>1,2</sup>, Jasmin Tröstl<sup>6</sup>, Tuomo Nieminen<sup>3,4</sup>, Ismael K. Ortega<sup>8</sup>, Robert Wagner<sup>3</sup>, Alexey Adamov<sup>3</sup>, Antonio Amorim<sup>9</sup>, Anne-Kathrin Bernhammer<sup>7,10</sup>, Federico Bianchi<sup>6,11</sup>, Martin Breitenlechner<sup>7,10</sup>, Sophia Brilke<sup>1</sup>, Xuemeng Chen<sup>3</sup>, Jill Craven<sup>12</sup>, Antonio Dias<sup>2</sup>, Sebastian Ehrhart<sup>1,2</sup>, Richard C. Flagan<sup>12</sup>, Alessandro Franchin<sup>3</sup>, Claudia Fuchs<sup>6</sup>, Roberto Guida<sup>2</sup>, Jani Hakala<sup>3</sup>, Christopher R. Hoyle<sup>6,13</sup>, Tuija Jokinen<sup>3</sup>, Heikki Junninen<sup>3</sup>, Juha Kangasluoma<sup>3</sup>, Jaeseok Kim<sup>14,†</sup>, Manuel Krapf<sup>9</sup>, Andreas Kürten<sup>1</sup>, Ari Laaksonen<sup>14,15</sup>, Katrianne Lehtipalo<sup>3,6</sup>, Vladimir Makhmutov<sup>16</sup>, Serge Mathot<sup>2</sup>, Ugo Molteni<sup>6</sup>, Antti Onnela<sup>2</sup>, Otsu Peräkylä<sup>3</sup>, Felix Piel<sup>1</sup>, Tuukka Petäjä<sup>3</sup>, Arnaud P. Praplan<sup>3</sup>, Kirsty Pringle<sup>5</sup>, Alexandru Rap<sup>5</sup>, Nigel A. D. Richards<sup>5,17</sup>, Ilona Riipinen<sup>18</sup>, Matti P. Rissanen<sup>3</sup>, Linda Rondo<sup>1</sup>, Nina Sarnela<sup>3</sup>, Siegfried Schobesberger<sup>3,†</sup>, Catherine E. Scott<sup>5</sup>, John H. Seinfeld<sup>12</sup>, Mikko Sipilä<sup>3,4</sup>, Gerhard Steiner<sup>3,7,19</sup>, Yuri Stozhkov<sup>16</sup>, Frank Stratmann<sup>20</sup>, António Tomé<sup>21</sup>, Annele Virtanen<sup>14</sup>, Alexander L. Vogel<sup>2</sup>, Andrea C. Wagner<sup>1</sup>, Paul E. Wagner<sup>19</sup>, Ernest Weingartner<sup>6</sup>, Daniela Wimmer<sup>1,3</sup>, Paul M. Winkler<sup>19</sup>, Penglin Ye<sup>22</sup>, Xuan Zhang<sup>12</sup>, Armin Hansel<sup>7,10</sup>, Josef Dommen<sup>6</sup>, Neil M. Donahue<sup>22</sup>, Douglas R. Worsnop<sup>3,14,23</sup>, Urs Baltensperger<sup>6</sup>, Markku Kulmala<sup>3,4</sup>, Kenneth S. Carslaw<sup>3</sup> & Joachim Curtius<sup>1</sup>

*Science* 27 May 2016

## New particle formation in the free troposphere: A question of chemistry and timing

F. Bianchi,<sup>1,2,3,\*</sup> J. Tröstl,<sup>1</sup> H. Junninen,<sup>3</sup> C. Frege,<sup>1</sup> S. Henne,<sup>4</sup> C. R. Hoyle,<sup>1,5</sup> U. Molteni,<sup>1</sup> E. Herrmann,<sup>1</sup> A. Adamov,<sup>3</sup> N. Bukowiecki,<sup>1</sup> X. Chen,<sup>3</sup> J. Duplissy,<sup>3,6</sup> M. Gysel,<sup>1</sup> M. Hutterli,<sup>7</sup> J. Kangasluoma,<sup>3</sup> J. Kontkanen,<sup>3</sup> A. Kürten,<sup>8</sup> H. E. Manninen,<sup>3</sup> S. Münch,<sup>8</sup> O. Peräkylä,<sup>3</sup> T. Petäjä,<sup>3</sup> L. Rondo,<sup>8</sup> C. Williamson,<sup>8,†</sup> E. Weingartner,<sup>1,†</sup> J. Curtius,<sup>8</sup> D. R. Worsnop,<sup>3,9</sup> M. Kulmala,<sup>3</sup> J. Dommen,<sup>1</sup> U. Baltensperger<sup>1,\*</sup>

- H<sub>2</sub>SO<sub>4</sub> is not needed for nucleation, this can be achieved by HOM VOCs alone.
- Different VOCs are not equally efficient at producing HOMs.

# Potential contributions from community and challenges

## *Topics funded by BER ASR in italics*

- Quantum calculations of binding energies for dimers/clusters; dimerization energies of HOMs needed to calculate evaporation rates for larger molecules
- Ion processes: ~10% of nucleation may involve ions (Galactic Cosmic rays)
- Molecular forces that determine the stability of clusters made purely from HOMs
- Condensed-phase links – chemistry in droplets (micro-reactors)
- VOC oxidation – rate-theory calculations, ab initio calculations, photodissociation cross-sections and dynamics
- Chemistry-mixing interactions
- Biomass burning fundamentals: Combustion processes tied to emissions
- *Detection of sub-nm particles before the HR-DMA can measure – link to combustion droplet work?*
- *Growth below 10 nm is crucial – study of growth – again link to combustion droplet work?*
- *Detection methodologies for black carbon and brown carbon particles*

## Panel I: Impact of Combustion Chemistry on Atmospheric Chemistry and Climate

### Panel members:

Dwayne Heard (University of Leeds, D.E.Heard@leeds.ac.uk)

Marsha Lester (University of Pennsylvania, molester@sas.upenn.edu)

Hope Michelson (Sandia National Laboratories, hamiche@sandia.gov)

Ashley Williamson (US Department of Energy/BER, Ashley.Williamson@science.doe.gov)

Ashley Williamson (US DOE, BER): his program runs the big climate models for DOE. It includes meteorological research, cloud physics, impacts of aerosols.

Hope Michelson: will give a high level overview of the climate impacts of combustion, and then we'll open up the floor for discussion.

Climate: the impacts of combustion on climate are:

- Direct emission of greenhouse gases

- Primary particulate emission (from combustors)

- Secondary aerosol formation (chemistry driven, formation in the atmosphere)

So we need to know: what comes out of the tailpipe? Is it different for conventional / biofuels?

What is the coupling between combustion and climate?

Direct emissions of GHGs directly affect radiative forcing. Soot is a primary organic aerosol (and is also called black carbon). Brown carbon (non-absorbing and reflecting species, more hydrogens than black carbon) are also emitted. The direct effect can be heating, and light reflection. Cloud and snow effects can also lead to indirect cooling or indirect heating! SOA can be formed from the VOCs emitted.

Hope shows a very interesting slide of the anthropogenic portion of CO<sub>2</sub>, CH<sub>4</sub>, etc.

The impact of black carbon on climate appears to be mostly heating, but the influences on clouds are quite uncertain and could be net heating or cooling. The influences can be regional.

Black carbon is a near-term mitigation candidate because it has an atmospheric lifetime of only ~ 1 week! Most important targets: diesel engines, cookstoves.

The impact of organic aerosols on climate is particularly important, rather uncharacterized, and could be both heating and cooling.

Open Questions:

- How are particles generated?

- What are optical properties of BC, POA, SOA, and HOW DO THEY EVOLVE WITH TIME?

- Physical chemical properties of these particles?

On a bureaucratic point, Ashley Williamson now says: we fund these open questions: we care about this and put our money into it. (This seemed a bit like defending his turf).

Ashley notes that aerosol absorption of energy at different layers in the atmosphere can affect atmospheric dynamics. Very macroscopic effects.

He recently held a workshop that had five high-level summaries / themes (Chris Cappa was one workshop coordinator). This report is not yet out.

Marsha Lester: parallels between combustion and the atmosphere.

Marsha shows the ROO ... QOOH oxidation schemes being important in both the atmosphere and combustion. The point is that the chemistry is the same or at least parallel. The second (and further) O<sub>2</sub> addition is a key current topic for quickly forming, highly oxidized, low volatility species. Three papers in Nature and Science in the last week point out that these may be the missing link to SOA.

Marsha points out the Paul Wennberg et al. paper on auto-oxidation of ketones from 2013. A second really important paper in 2014 is in Nature **506**, 476 (2014) from Ehn et al., and shows essentially the same chemistry to make ELVOC (extreme low volatility oxygenated compounds). This paper suggested that this chemistry from both biogenic and anthropogenic VOCs can impact particle formation and growth and climate effects including cloud condensation nuclei.

Dwayne Heard: When O:C ratios get larger, volatility can drop by 10 orders of magnitude. It was thought that one needed sulfuric acid present for nucleations of SOAs. But last week (May 26, 2016) three papers showed that the nucleation can be seeded and driven by the highly oxidized compounds without the need for sulfuric acid. This is a big deal.

So, how could this community contribute to areas beyond combustion?

- Binding energies for dimers / clusters

- Detection of sub-nm particles that current particle sizers cannot detect.

- Methods to study black and brown carbon

- ~10% of nucleation may involve ions (from galactic cosmic rays). The long range forces make ions great nucleators, but this physics is not well studied.

- Very little is known about the molecular forces between these highly oxygenated compounds

- Condensed phase links: chemistry in droplets, micro-reactors

- VOC oxidation using rate theory calculations, cross sections, dynamics

## **Now open up to the floor to get some discussion at 9:01 am**

Q: what is the current uncertainty in radiative forcing of aerosols compared to all radiative forcing?

A: Most aerosol effects appear to be cooling, except black carbon, which is warming, although the error bar on this 0.6 W/m<sup>2</sup> goes from 0.3 to 1.1. So the error bar is huge, but at present the IPCC chart would imply that the net effect is cooling. Dwayne points out that the error bar on the cumulative particle effects on radiative forcing reaches into positive forcing.

Q: It seems the chemical physics component of this group is well suited to contribute to many of the questions raised, via free radicals, kinetics, etc. Scientifically there is overlap and interest. But a question is the ROO radicals: are they really the same or different structures compared to combustion?

A: Dwayne points out the Master Chemical Mechanism can show you all the types of ROO in the mechanism. CH<sub>3</sub>OO is clearly a big one, and a major overlap of the exact same species as in combustion. But there are other species (likely pinene-derived ROO) that would not be present in combustion models.

Q: Hope spoke of particulates, and the US has goals to replace ~ 30% of the carbon from fossil to "renewable" carbon. The particulates could be different from this different fuel. For example, the soot may have more hydrogen in it compared to soot from fossil fuels.

A: Michelsen, you are correct that there is a lot of heterogeneity of soot structure and composition. There is an incredible variety.

Q: How many of the challenges Dwayne listed are already covered in the BER program, and where could the BES folks contribute?

A: Ashley Williams: BER doesn't support #1, doesn't support ion processes, does support particle growth, molecular forces is not directly supported by BER, not much condensed phase chemistry, not much VOC oxidation modeling. Dwayne points out that in the atmosphere there are eddies and transport on small and large scales but on slower timescales connecting chemistry with transport than in combustion. Urban canyons are a complicated environment, for example. Ashley says roughly about half of the areas on this slide are funded by BER. BER puts out targeted calls for ideas in certain subjects.

Q: I like the very first point. Mention of binding energies of dimers and clusters. But do we know that the species really are dimers, trimers, etc? How much detail do we really know about the nucleation process?

A: In these May 2016 papers, they utilize very high resolution mass spectrometers. They know the exact masses and probably the structures with these instruments, but they don't know the formation mechanisms.

Q: Martin Head Gordon: 15 years ago one could simply not compute binding energies between large species. Thanks to the BES Chemical Physics program we've developed the ways to compute non-covalent interactions quite well.

A: The mechanism of forming particles is a big deal, including ice crystals. Hope says we know a lot about the masses of these particles, but we don't necessarily know the functional groups, and those determine the chemistry. Kevin Wilson points out that the challenge is the chemical complexity. How do you model these? Explicitly with thousands of reactions? Or are there automated ways, or should we group by functional groups to simplify? This BES community is has a lot of experience with mechanism reduction, and tackling broadly complex chemical systems.

Q: To follow on an earlier point of mixing in chemistry, are there large scale processes of mixing in the atmosphere where the transport leads to rate limiting chemistry?

A: Cloud breakup is a process that is driven by turbulence, but it is hard to put into models because it is happening on such a small scale compared to grid size. Alison Tomlin at Leeds developed adaptive gridding for turbulence, and there are some people in the atmospheric community who are doing this too, similar to the LES approaches in combustion.

---

Panel 2: Bill Green

There is a strong correlation between GDP/person and energy use per person. In addition there is a strong correlation between fine particle concentration and the number of people who die each day in large cities. The anthropogenic portion of climate change will likely double as more people can afford to buy more fuel.

Most of today's combustion system was developed empirically in the 1900 – 1930s. A main strategy was to hold fuel composition constant and innovate with engines. Fuel compositions haven't changed much since the 1930s and the improvements were in the engines. Maybe it is time for the fuels to be improved. But do we know how to predict what would be an improvement?

Predictive chemistry has progressed dramatically. 1935 was TST and Hartree Fock. Such large advances have come in electronic structure that the major sources of errors may no longer be calculated energies.

So what are the challenges today?

We are still discovering reactions and chemical physics phenomena

So we know we can do these things very accurately, but we have only done them for a handful of problems. We haven't rolled it out at the level to calculate a full combustion mechanism at this same accuracy. We need better methods for handling complexity.

Large computer models

How to validate / test models?

Can machine learning / artificial intelligence help?

How can we really compare uncertainties between methods / people, and document professionally the data and the uncertainties.

Branko Ruscic: Combustion models are multiscale entities, requiring information from a number of levels.

Data from small scales like spectroscopy up to large scales like reacting flows, NEEDS TO BE CONSISTENT! Active Thermochemical Tables is a good example of this, where inconsistencies are highlighted, and extra experiments or calculations would have most impact.

So imagine if we had STACKED "ACTIVE TABLES" Imagine a kinetic database of rates that interacted with the thermochemistry. What about chemical mechanisms and reduced mechanisms tables. Each of these scales could feedback and improve on other scales. And a change in one level could propagate and impact other levels if they were linked!

Levels of automation:

Soft automation: scripting clearly repetitive tasks as an algorithm

Minimal risks; automation is interleaved with manual steps

Hard automation:

Scripting of speculative tasks

Moderate risk, errors may remain undetected; includes human intervention, some results may need to be rejected.

Extreme automation:

Aggressive attempt to algorithmically code the whole procedure

Risk is significant because there is minimal or no human intervention. It could be called mindless because it includes no human input

Intelligent Automation:

AI interleaved with algorithmic steps. Requires perspicacious definition of the problem and training of the AI.

Branko means Deep Learning when he talks about Artificial Intelligence (not earlier approaches like LM and kNN, which were not particularly successful). Deep learning is based on neural networks, is significantly more successful (speech recognition, computer vision, face recognition...). Neural networks

Judit Zador: reasons to automate and what can we automate

Habib Najm: There is not enough data to constrain models. The models are overfitted. By this he means there are too many knobs / parameters for the amount of available data. Somehow we must control complexity to reflect the amount of information we actually have in the data.

Occam's Razor gives a flavor of what Habib means. A Bayesian framework for chemical model selection could prove very valuable.

*Critical Issues Discussion:*

**Computer Augmented  
Combustion Chemistry**

by:

William H. Green (MIT Dept. of Chem. Eng.)

Branko Ruscic (ANL)

Judit Zádor (SNL)

Contributors:

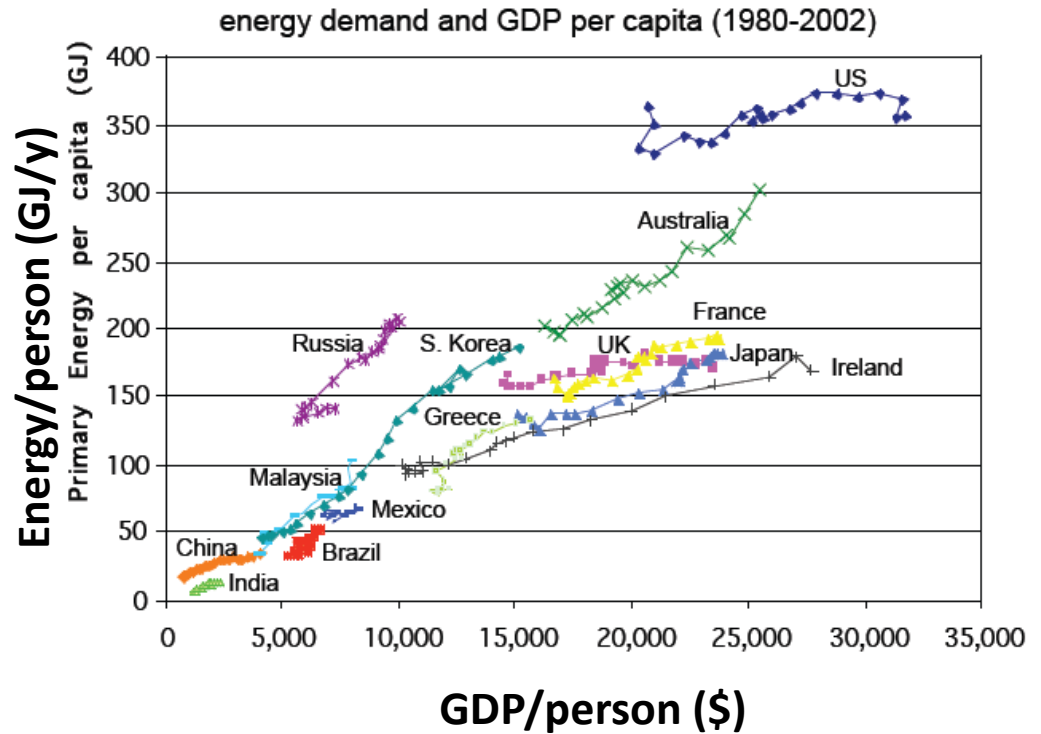
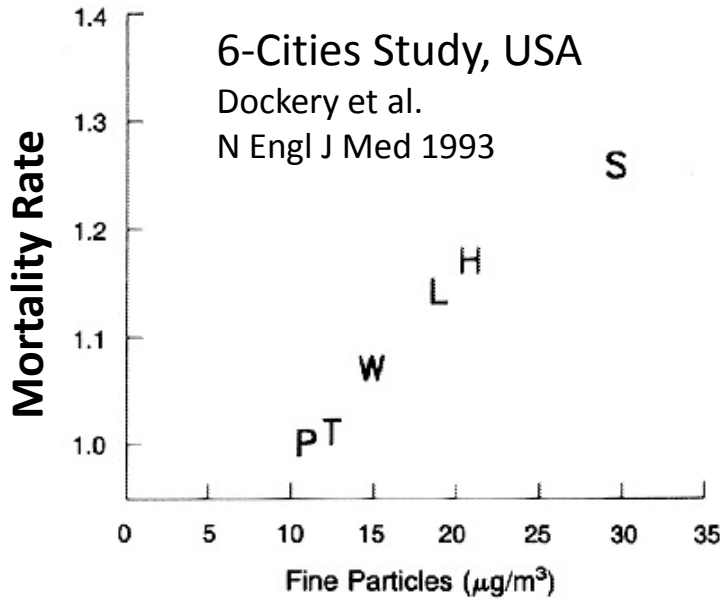
Stephen J. Klippenstein and Albert F. Wagner (ANL)

Habib N. Najm (SNL)

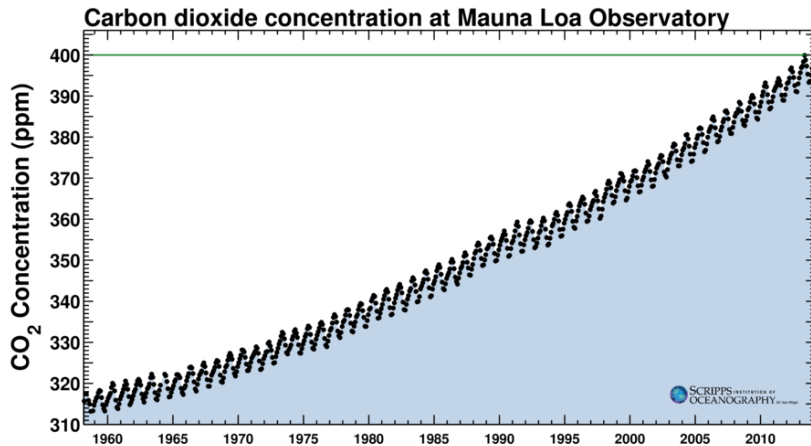
36<sup>th</sup> Annual Gas Phase Chemical Physics

Research PI Meeting

# Combustion: Boon and Bane



## Particulate Level in Air



***The importance of Scale:  
Improvements to combustion  
system have huge impacts on  
Economy, Climate, & Health.***

Much of Today's Combustion System  
was developed without benefit of  
much knowledge of Combustion  
Chemistry...

...so main strategy has been to hold  
the fuels constant and innovate with  
the engines...

...but surely the innovation rate would  
be higher if one could predict the fuel  
effects....

# Progress on Predicting Chemistry... a Timeline

- **1929 Dirac: “equations much too complicated to be soluble”**
- **1935 Transition State Theory & Hartree-Fock method formulated.**
- **1960’s DFT and Coupled-Cluster method for molecules formulated. Microcanonical TST clearly formulated: RRKM**
- **1980’s stiff ODE solvers. CHEMKIN software for multiple reactions.**
- **1988 Creation of DFT functionals usefully accurate for chemistry**
- **~1990 able to compute molecular spectra, entropies, *C<sub>p</sub>*’s *a priori*.**
- **1990’s: quantum chemistry goes mainstream. Pople & Kohn Nobel (1998). Methods for computing rates of barrierless reactions.**
- **By end of 20th century able to predict individual rate coefficients *a priori* but accuracy limited by errors in computed energies.**
- **By 2010 explicitly correlated CCSD(T)-F12 methods give accurate *a priori* energies for many molecules and transition states**

# So what are the challenges today?

- Still discovering reactions, chemical physics phenomena
- Unresolved issues with computing some types of reactions and processes.
  - How accurate are our conventional calculations?
  - Still working out how to compute collisional energy transfer, systems with multiple electronic states
- Need to apply the accurate methods at ***Scale***
  - Thousands of important reactions!
  - So many conformers and isomers!

# Need Better Methods for Handling Complexity

## + Large computer models:

- robust software for generating and solving the models
- clean well-annotated databases
- uncertainty quantification

## + How to validate/test the models? Never will be enough experimental data to determine all the rate coefficients, thermo, transport, etc.

- Better archiving of the limited experimental data we have, so easily accessible to future researchers

## + Can Machine Learning / AI help?

- Where is our Big Data going to come from: real engines and burners? From mining supercomputer simulations? From millions of quantum chemistry calculations?

# Computer Augmented Combustion Chemistry

- Combustion models are multiscale entities, requiring information from a number of levels:
  - etc.
  - Reactive Flows
  - (Reduced Chemical Mechanisms)
  - Chemical Mechanisms
  - Chemical Kinetics
  - Thermochemistry
  - Spectroscopy
  - Natural Constants
- Data at each level needs to be internally consistent
- Data also needs to be consistent across all levels



# Example: Active Thermochemical Tables

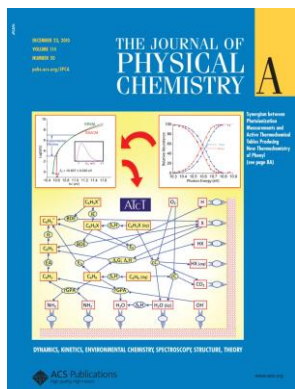
- ATcT address and resolve the deficiencies of the traditional sequential approach by constructing, statistically analyzing, and solving a Thermochemical Network (TN)

ATcT

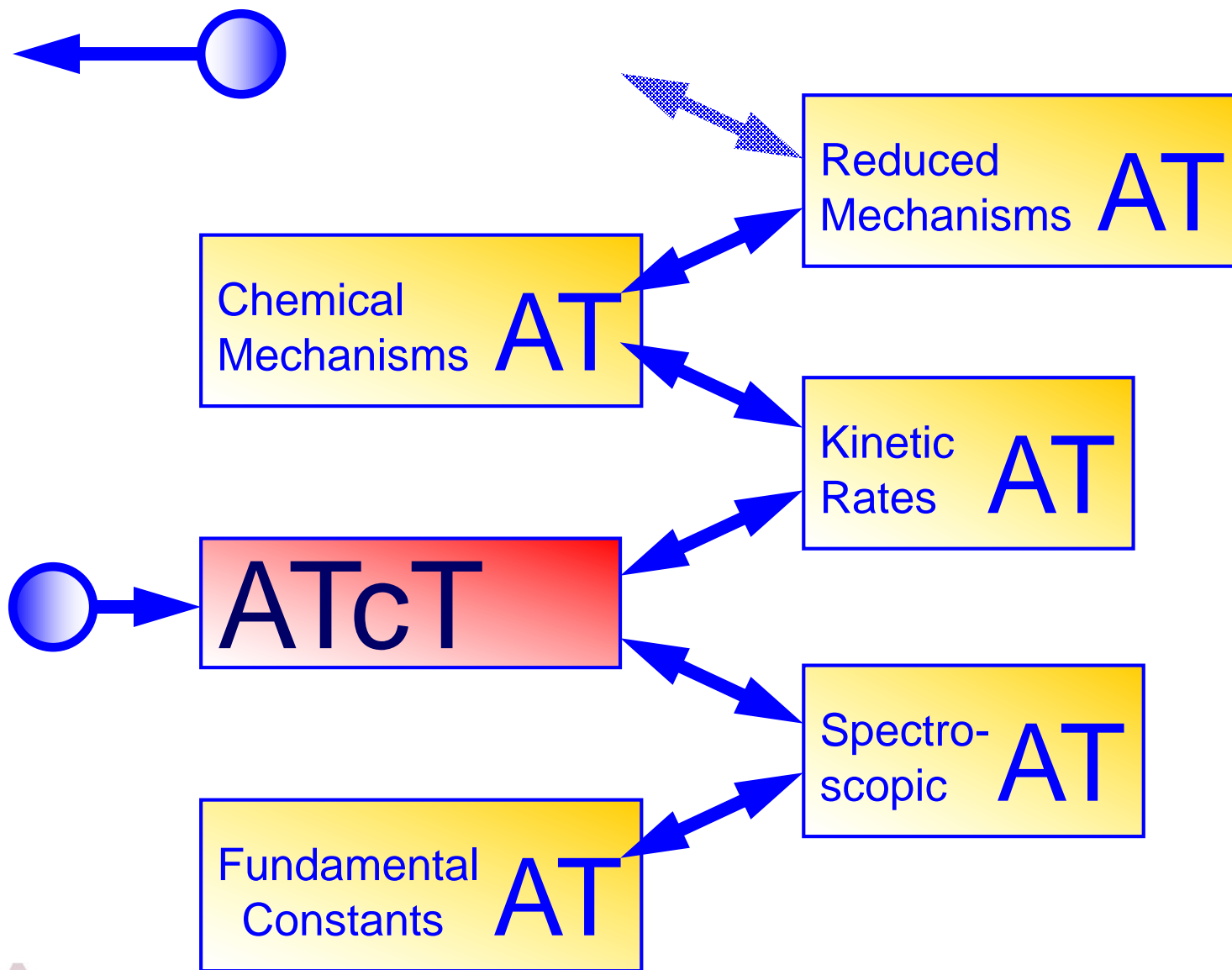
ATcT analyzes the TN for consistency and solves it simultaneously for all species by concurrently satisfying as many determinations as possible

Compared to traditional thermochemistry, the solutions have superior accuracy and robustness, because they are based on the entire knowledge content of the TN.

In the process, ATcT introduces a number of features that were never before available in thermochemistry (painless update with new info, covariance matrix, hypothesis testing, 'weak link' identification, etc.)



# The vision: stacked “Active Tables”



# Levels of Automation

## ● Soft

- Scripting clearly repetitive tasks
- Minimal risk; automation is interleaved with manual steps

## ● Hard

- Scripting of speculative tasks
- Moderate risk, errors may remain undetected;  
includes human intervention, some results may need to be rejected

## ● Extreme

- Aggressive attempt to algorithmically code the whole procedure
- Risk is significant; minimal or no human intervention

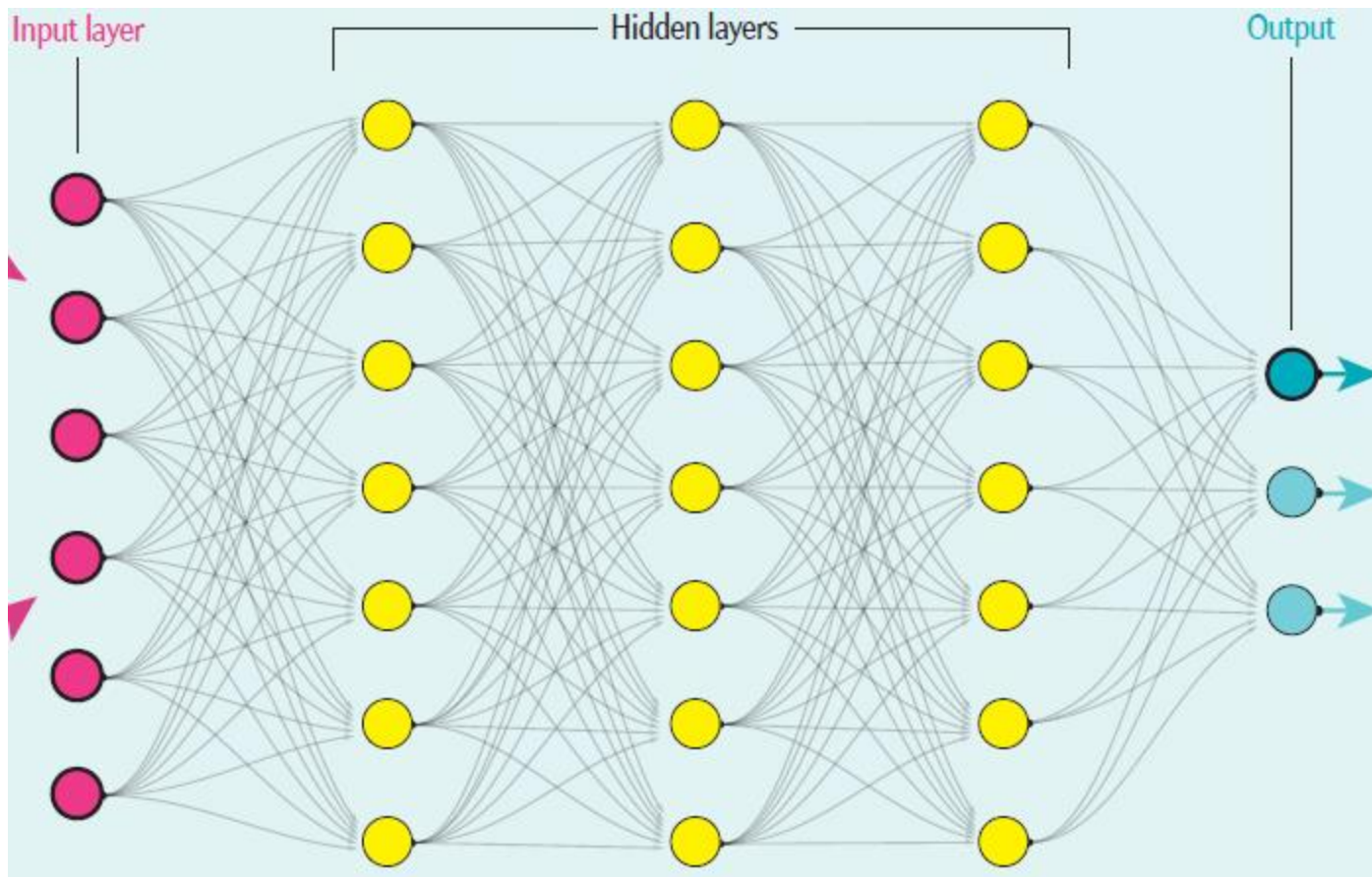
## ● Intelligent

- AI interleaved with algorithmic steps;  
AI steps require perspicacious definition of the problem,  
and extensive subsequent system training
- Risk minimal to moderate, depending on the thoroughness of training



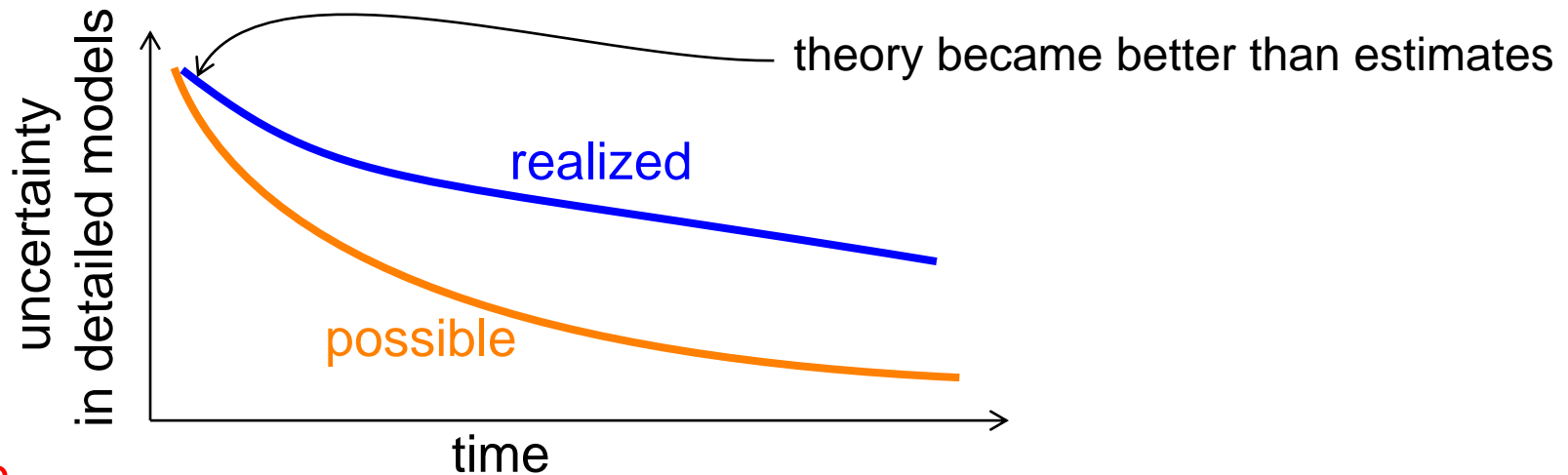
# AI: Deep Learning

- Early approaches (LM, kNN) were not particularly successful
- Deep learning, based on neural networks, is significantly more successful (speech recognition, computer vision, ...)



# Reasons to Automate

1. There are almost trivial things to automate – why do by hand if we don't have to?
2. Saving the world is hard – we should focus on the important/hard/exciting problems, and let the computer figure out the repetitive parts.
3. Reveals emergent properties – data mining. Engineering/science bridge?
4. Unused resources – gas-phase chemistry is not effectively taking advantage of large (exascale?) computers.
5. Currently very slow deployment of theoretical advances.



6. ?



# Automation in Gas-Phase Kinetics

Things “easy” to automate:

- hierarchical procedures in quantum chemistry
- conformational searches
- thermochemistry
- saddle point searches for isomerization and dissociation of not too unsaturated molecules and simple abstractions and additions
- many barrierless reactions
- ?

Difficult to automate:

- high unsaturation
- multireference problems
- excited states
- ?

Missing tools:

- metacodes
- visualization of the large datasets generated
- ?



# Massively Parallel Kinetics?

We are close to a quantum leap in gas-phase kinetics, but we have to invest into creating the tools.

We have to publish papers vs solve problems for society. How to balance this?

Should there be two pots of money?

Is accuracy a value?



# Possible Directions

1. Black box CASPT2 or similar MR method.
2. Efficient sampling of anharmonic effects, conformers, etc.
3. Robust and efficient QC schemes with IF/THEN logic.
4. Data mining of large experimental dataset? Can we use AI to connect kinetics to bulk properties?
5. “Weakest link” in kinetics ATcT style? Experiment – theory.
6. ?



# Complexity of Chemical Kinetic Models

## Problem:

- The complexity of chemical kinetic models for hydrocarbon fuels far outstrips the information available to constrain them based on experimental data
- Challenges with overfitted models :
  - Too many knobs/parameters for the amount of available data
  - Lack of robustness
  - Loss of ability to validate/invalidate hypotheses

## Need:

- Strategies for kinetic model development that take into account the degree of information in available data
- Avoid exceeding optimal complexity given available data
- A Bayesian framework for chemical model selection

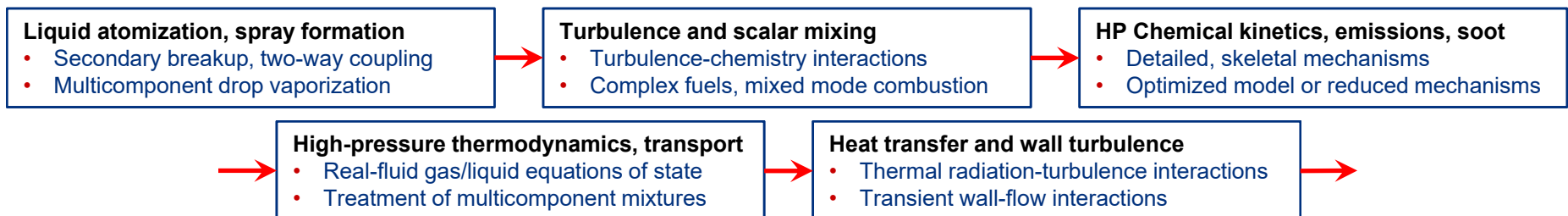
# Grand Challenge Issues on Turbulent Combustion

Josette Bellan, Tianfeng Lu and Joseph Oefelein

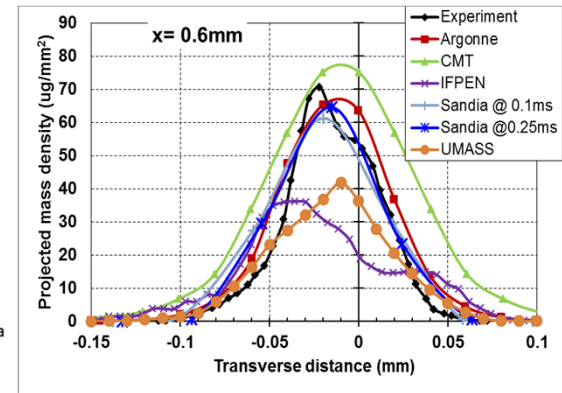
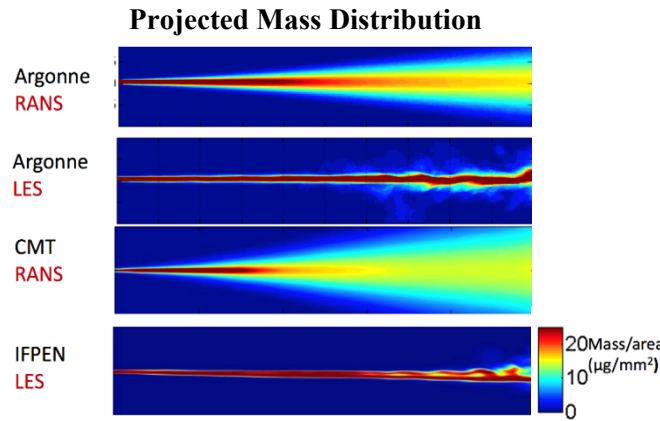
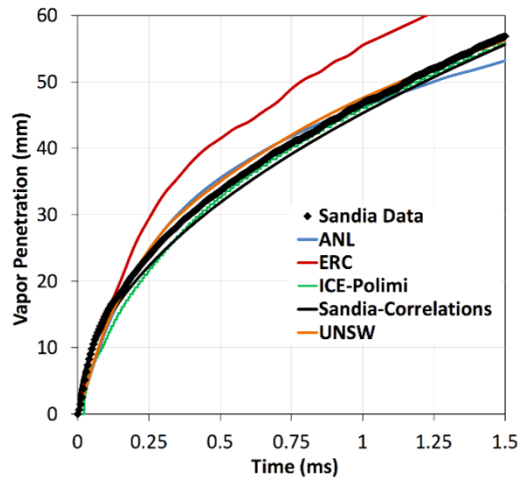
1. Modeling and simulations of high-p multi-species turbulent flows with phase formation/disappearance
2. Turbulent reaction rate models for high-p multi-species multi-reaction flows using realistic assumptions
3. Detailed experimental information allowing the discrimination among several models successfully predicting global or mean quantities.
4. Calculations of transport properties for high-pressure conditions.
5. Reduced reaction models applicable to mixtures of species over wide regimes of pressures, temperatures and equivalence ratios.
6. Coupled treatment and assessment of multiphysics models (turbulent scalar mixing and reacting flow physics with detailed thermodynamics and transport) with advanced Uncertainty Quantification for high pressure, multicomponent systems.

# Advancing predictive capabilities requires coupled treatment of multiphysics models + UQ

... at device relevant conditions

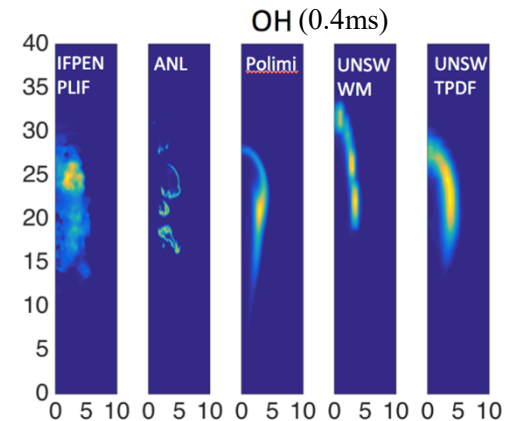
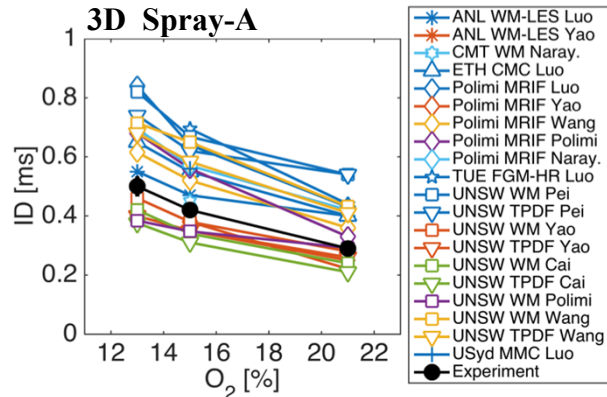
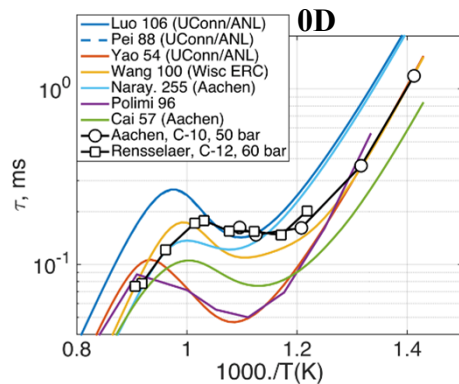


# Deficiencies in model development at real world conditions has been demonstrated for years



## Inconsistencies in non-reacting calculations observed in all ECN workshops (here ECN4)

- Correct vapor penetration but large scatter in other quantities



## Similarly, large scatter is observed in reacting calculations

- Large variability between chemical mechanisms and shock tube data, and scatter in ignition delay (ID) in Spray-A simulations

There is a distinct lack of discriminating data due to many competing effects in both models and numerical methods ...

# Grand Challenges Remaining in Combustion / Gas Phase Chemical Physics: Turbulent Reacting Flow

Josette Bellan

California Institute of Technology, Pasadena, CA, 91125

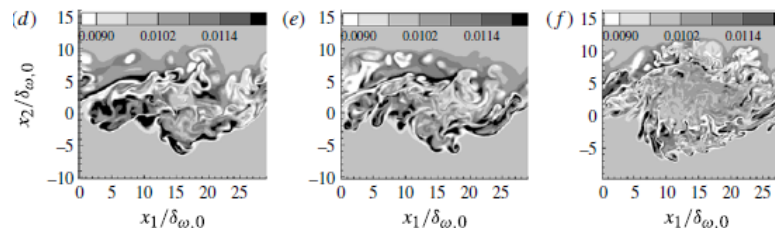
## Simulations of high-p multi-species turbulent flows with phase formation/disappearance

Phase formation/disappearance may occur due to:

- species inter-diffusion and mixing, which changes the composition
- changes in T and p

**Issues:**

1. phase identification
2. modeling aspects



Water mass fraction was initially 0.01 and uniform over the domain.

## Turbulent reaction models for high-p multi-species multi-reaction flows

Current turbulent reaction models are of 3 types (developed for single-phase low-p case):

1. PDF methods; an inter-species diffusion model (i.e. full-matrix diffusion) **missing**
2. LEM type; an inter-species diffusion model (i.e. full-matrix diffusion) **missing**
3. Mixture fraction ( $\xi$ ) based models rely on:

- a  $\xi$  conservation equation which can be solved without knowledge of other variables; **not true** for Stefan-Maxwell diffusion

- complex models having assumptions which **are most likely not valid** for high-p and/or multi-reactions, e.g. Conditional Source-term Estimation (CSE) method

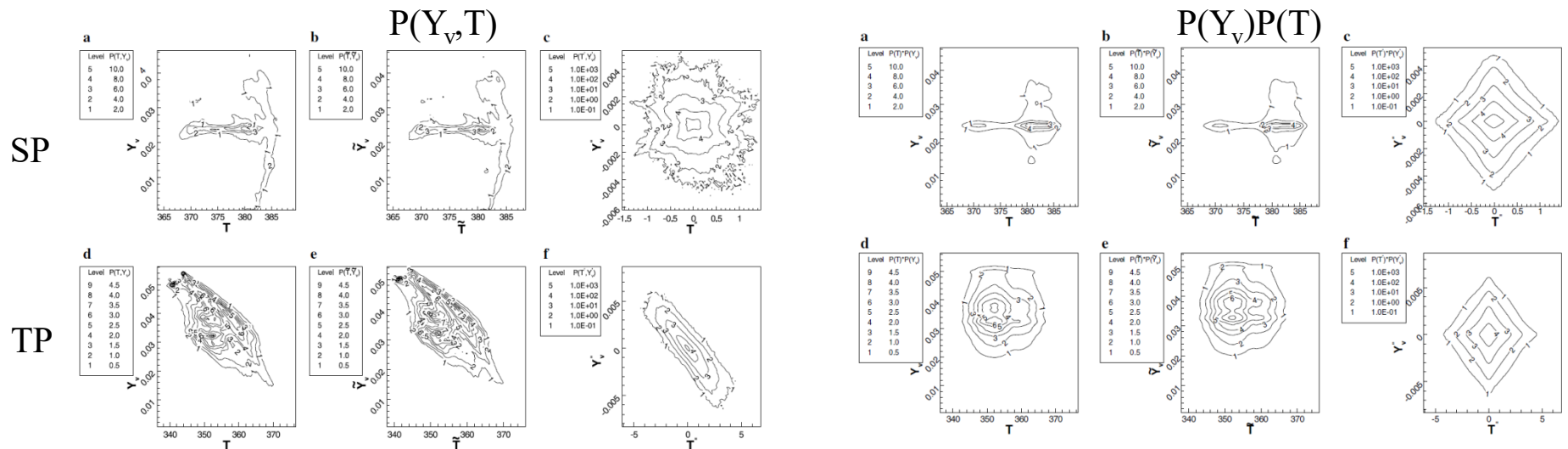
$$\langle \dot{\omega}(\rho, Y_\alpha, T) | \zeta \rangle = \dot{\omega}(\langle \rho | \zeta \rangle, \langle Y_\alpha | \zeta \rangle, \langle T | \zeta \rangle) \quad \zeta \text{ belongs to the } \xi \text{ sample space}$$

# Grand Challenges Remaining in Combustion / Gas Phase Chemical Physics: Turbulent Reacting Flow

Josette Bellan

California Institute of Technology, Pasadena, CA, 91125

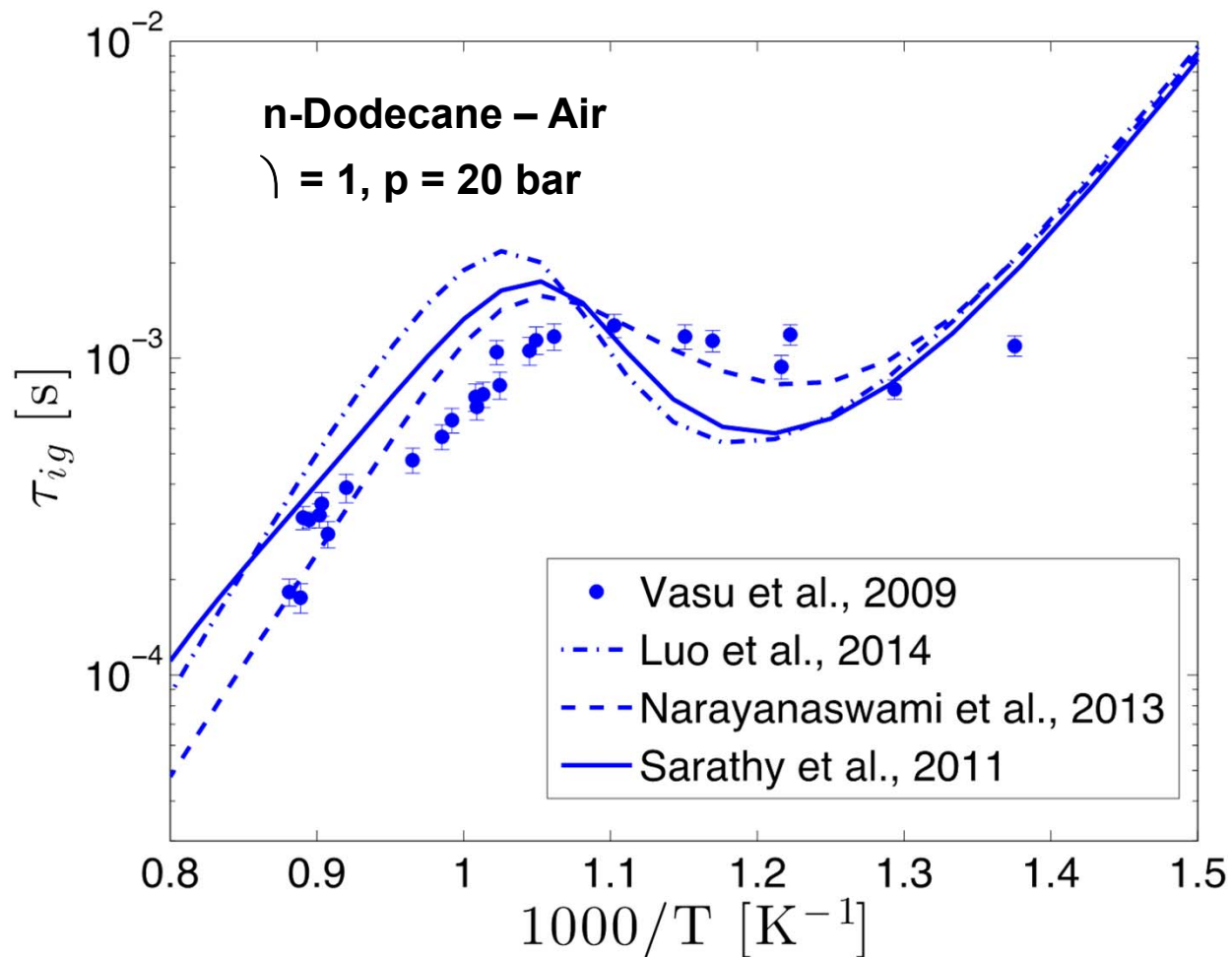
## Information affecting turbulence modeling



## Reduced kinetic mechanisms

- Have shown that elementary kinetic mechanisms can be reduced to at most 20 (and even 15) light species
  - n-heptane, n-decane, n-dodecane, n-hexadecane
  - iso-octane, iso-cetane
  - cyclohexane
  - high- $p$ ; cold ignition and hot ignition; over the entire range of  $\phi$
- Need robust computational methodologies to implement these results in LES codes
  - mixture-fraction-based models will not work for multiple reactions and when the initial fuel is not tracked

**e.g., There is wide variability between mechanisms in the prediction of key quantities**



**Significant variability between mechanisms, little development at pressures beyond 20 bar ...**

# Critical Issues in Turbulent Reacting Flows: Strongly Turbulent Flames

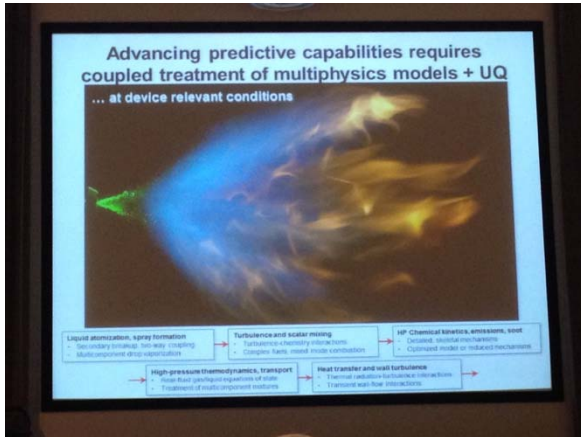
- Background
  - Combustion in turbulent flows is best understood in the limits of weak (wrinkled/corrugated flames) and strong (stirred reactors) turbulence
  - Practical combustors typically involve strongly turbulent but not well stirred flows
  - Recent direct numerical simulations (DNS) suggest the presence of small structures in strongly turbulent flames (both premixed and non-premixed), such as local ignition, extinction, flamelets and spontaneous ignition fronts
  - Small length and time scales involved: e.g.  $O(10-100)$  microns,  $O(10-100)$  microseconds
- Challenges in understanding strongly turbulent flames
  - Experimentally needs high-speed high-resolution diagnostic tools and simultaneous measurement of multiple scalars (temperature, and species concentrations)
  - DNS resolves small to intermediate sized eddies, while missing the effects of large eddies on flame structure: fully resolved device level flames may need  $O(10^{12})$  grids, state-of-the-art DNS typically involve  $O(10^9)$  grids
  - Large eddy simulations (LES) resolves large to intermediate sized eddies, while smaller structures are modeled based on speculated flame behaviors
- High resolution multi-speciation diagnostic tools + hybrid LES & DNS may provide a solution toward creating predictive models for strongly turbulent flames

## Panel Discussion - Grand Challenges Remaining in Combustion / Gas Phase Chemical Physics Turbulent Reacting Flow

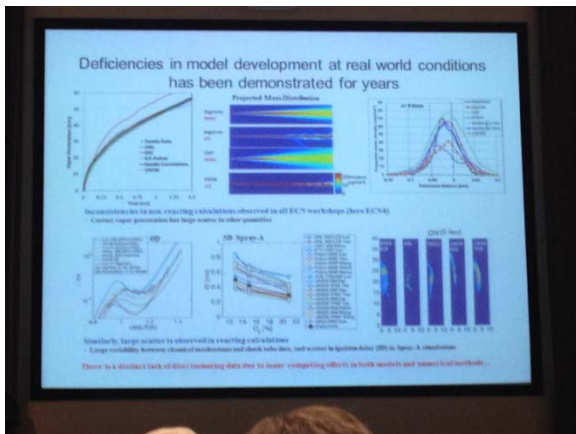
### Panelists

- Josette Bellan (California Institute of Technology)
- Tianfeng Lu (University of Connecticut)
- Joe Oefelein (Sandia National Laboratories)

### Joe Oefelein

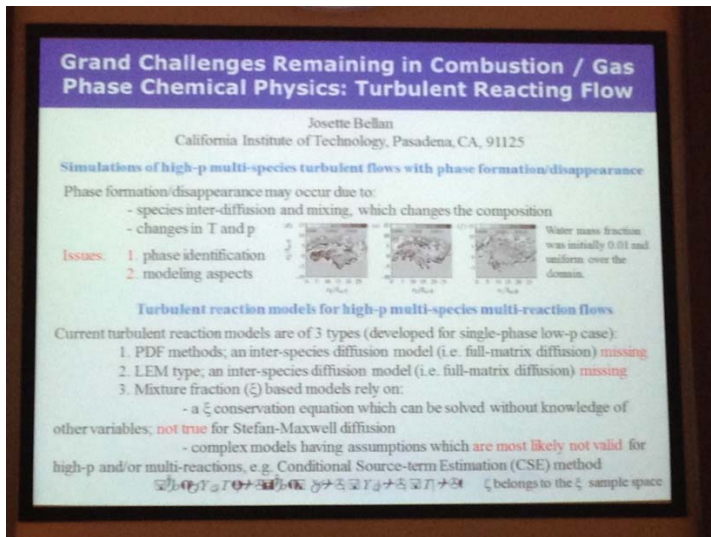


- Picture of a spray flame highlights the cascade of multiphase and reactive processes occurring during combustion, including injection of liquid fuel, atomization, evaporation, oxidation, and pollutant formation. From a modeling point of view, simulating such a complex system requires bringing together highly coupled sub-models for chemistry, mixing, transport, multiphase flows, turbulence, radiation etc., which become even more complicated at higher pressure, e.g., issues for chemistry and thermodynamics and transport, concept of spray not valid anymore, or real equation of state required instead of simpler ideal gas law.
- Every step in this cascade of processes represented by various models and sub-models boxes. The fidelity of a simulation will depend on how each sub-model is treated. Exascale computing is necessary but not sufficient: DNS of large systems are not necessarily the ultimate solution. Emphasis should be placed also on advancing modeling capabilities through multi-physics sub-model development and a rigorous workflow to develop good uncertainties associated with each sub-model. The weakest sub-model being the one dictating overall accuracy, we need to be clever in how we integrate sub-models.

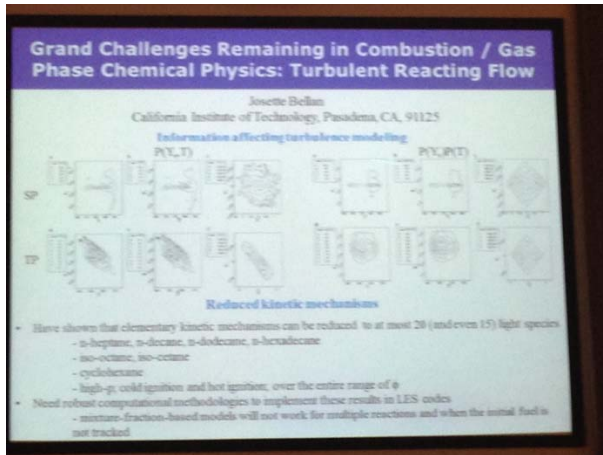


- Overview of consolidated results from the Engine Combustion Network workshop, an analog to the well-known non-premixed workshop. The large number of simulations of the same target configuration (in this case, a dodecane spray flame at condition typical of real systems), provides comparisons and outlines uncertainties: how we exploit those data and reduce the global uncertainty in the results is the real challenge. There is a distinct lack of discriminating data due to too many competing effects between sub-models and numerical methods. For example, the penetration length of fuel vapor in chamber is well captured and not that hard to match. However, there is a huge scatter in more detailed pictures of the system, such as mass distribution or ignition delay times, and no obvious rational behind the results. Chemical models that properly capture 0D homogeneous ignition can yield the worst agreement for spray ignition, and vice-versa.
- Developing predictive models has gone a long way already, but we are still hitting a wall because of the focus on individual boxes rather than their synergistic, coupled behaviors in real system simulations. There is no way we can decouple effects of various sub-models, so we need a workflow that looks at systems as a whole. We need better statistical analysis, and we need to be clever and innovative in how we combine and build synergy within our computational tools.

**Josette Bellan**

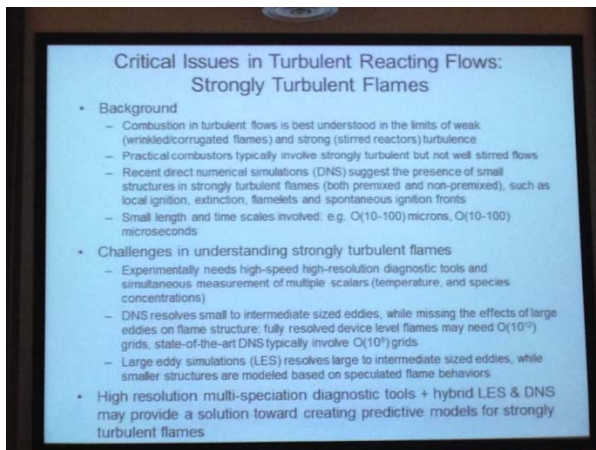


- Varying small parameters in linear problems will have very limited impact on simulation results. But with non-linear problems, small parameters can have a lot of importance! This needs to be kept in mind more than is currently done.
- In specific conditions relevant for real combustion systems, phase changes can occur in both directions due to species inter-diffusion and mixing, along with changes in temperature and pressure. This is very well known in other fields, but we don't know how to simulate that in combustion systems.
- Another challenge is developing turbulent reaction models for high pressure, multi-species multi-reaction flows. The validity of existing models at those conditions is questionable at high pressure. PDF models are beautiful because reactions are explicit, but the mixing is missing. LEM type turbulent models have the same problem: the full diffusion matrix is missing. On the other hand, mixture fraction based models, where a conserved mixing scalar can be solved without knowledge of other variables, are not valid for systems with Stefan-Maxwell diffusion. Assuming independence of the variables when deriving distributions (for the reaction rate, for example) is likely incorrect.



- Example of comparison between joint PDFs and product of marginal PDFs. For single phase, the results are not bad. However, for two-phase systems, with evaporation alone (no reaction), the results are very different across the board: DNS, LES and fluctuations. Evaporation is a correlating factor, as are non-linear equations of state: we cannot rely on existing turbulent models!
- Reduction kinetics: if you have a complex system with dominant variable (in this case, the temperature), there exists self-similarities. You can reduce the dimensionality of the system, but still need the detailed mechanisms to derive the equations. The approach allows to combine fuels, but requires the development of a robust computational methodology to be implement in LES. In particular, the fuel disappears very fast, and mixture fractions methods will not work, since the initial fuel is not tracked by the reduced models.

### Tianfeng Lu



- Typically, we look at 0D or 1D systems, or steady state configurations to develop combustion chemistry. Then we try to use it in turbulence. But story will be different because of mixing, which brings burnt products to cool fuel. In real applications, we often operate between well-stirred and weak burning regimes, where overfitting can be an issue: kinetic rates are fitted against small number of 0-D and 1-D configurations. Small scales create challenges to measuring errors. Yet, detailed chemistry should be validated in real simulations.
- There is a need for simultaneous measurements from diagnostics to be able to validate. The numerical framework in which validation is done is also important. DNS need micron-sized grids to resolve everything, which is not currently possible for device-level simulations. LES, on the other hand, uses grids as small as possible given computational constraints, and model the smallest scales. What happens locally is therefore not clear. Typically, simulations are done in the flamelet or well-stirred limits, but what in the middle is not

clear. Hybrid LES/DNS could be considered as a solution for predictive simulations of strongly turbulent flames. It would provide better feedback for detailed kinetics development.

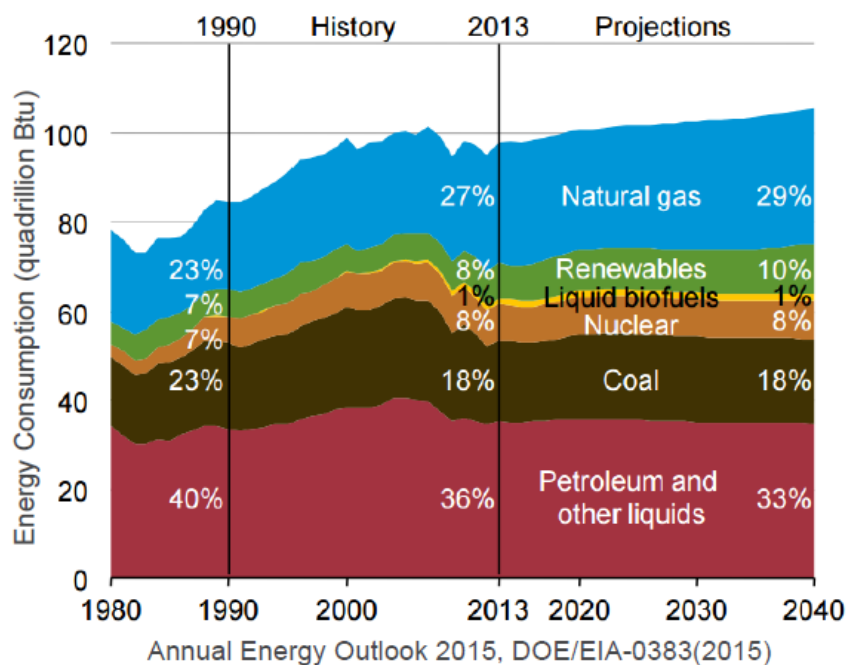
### Questions and comments from the audience

- *About reduced models: how similar are different reduced models? If there exists similarities in reducing different fuels, could we potentially create reduced models without having to start from the detailed mechanisms for each and every fuel?*
  - (Referring to similarity technique for reduced model development) How many equations you have to solve is the key aspect., but the technique does not look at reactions, only species. Reactions are taken from LLNL database, and reactions create self-similarities. Most important point in combining similarity models based on light and heavy components is to get the same light species set. Any complex system with a dominant variable has self-similarity properties.
- *It is interesting to see Workshop results showing simulations don't agree with one another. There are obviously mathematical and computer issues, but human interactions really may be key to move forward faster in resolving differences within models.*
  - The nice thing about workshops is walking in with your best simulations, and then, see the deviations. It is however difficult in workshop setting to explain why it deviating, because answering the "Why" question is very labor intensive. There is a need to formulate a way to do that. One example is the dodecane ignition case: OD vs spray ignition. The differences clearly are not just mechanism related. One option would be to use brute force computer power to figure out which one is right, what is happening with the other one.
- *On uncertainty quantification: there should be error bars on simulations. People have no clue about the uncertainties coming from each independent model.*
  - The challenge is to formulate how to do that. Can we use computer power differently? E.g. data mining, statistics etc...
- *Referring to the dodecane spray flames: The mass fraction distribution between RANS and LES are very different. Does that mean Reynolds Average techniques cannot be used for the simulation of sprays?*
  - This is unfortunately not so simple
- *Uncertainty comes from kinetics, initial conditions, and models. With a spread like that in the results, can we pinpoint where the difference is coming from?*
  - There are also numerical errors. UQ is a challenge! how do we start understanding model fidelity? This may well be the next grand challenge: understanding the contribution of sub-models to uncertainties. But the sub-models cannot be treated independently from one another, they cannot be uncoupled, since the system is non-linear! That is why it is difficult. This is exemplified in high pressure systems, where ergodicity does not hold. There is a need for a very different way to interpret simulations and experiments, since no steady state is reached!

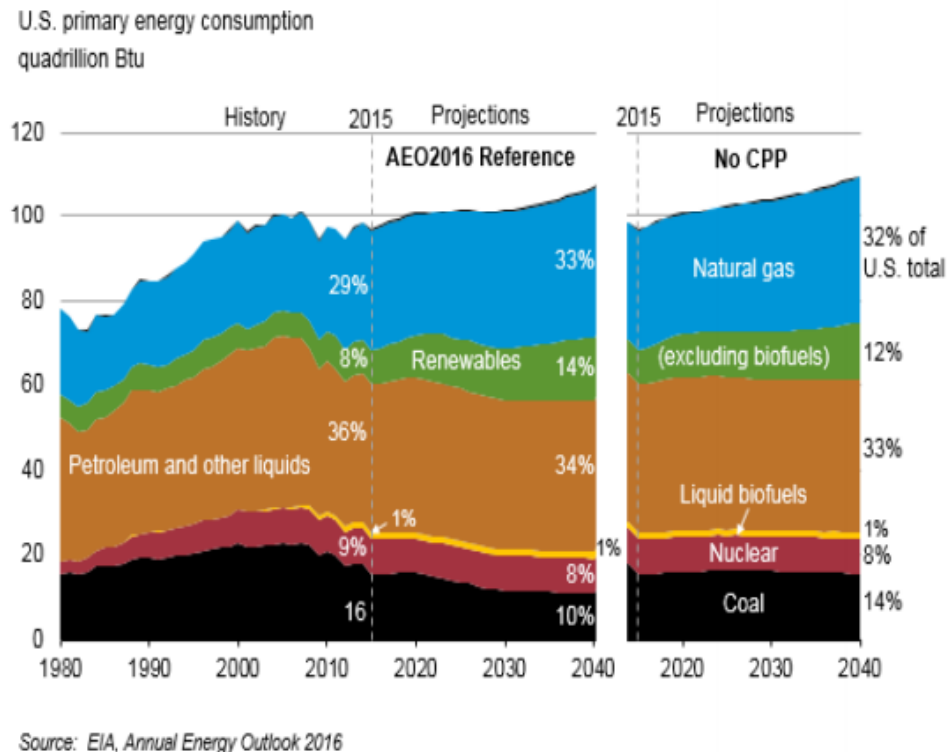
# Challenges and Opportunities: Gas Phase Chemical Physics

- Remaining Challenges?
  - Previously identified but unsolved problems
    - This meeting & previous workshops share progress, point to problems
    - Ideas and proposals at individual and lab level targeted at these goals
    - Hidden or previously neglected opportunities?
    - New methods, new insights: how many surprises can be anticipated?
- At the program level, is this a sustainable model?
  - Vulnerable to characterization as “incremental” ?
  - How does the program mesh with global carbon concern?

# Business as usual?



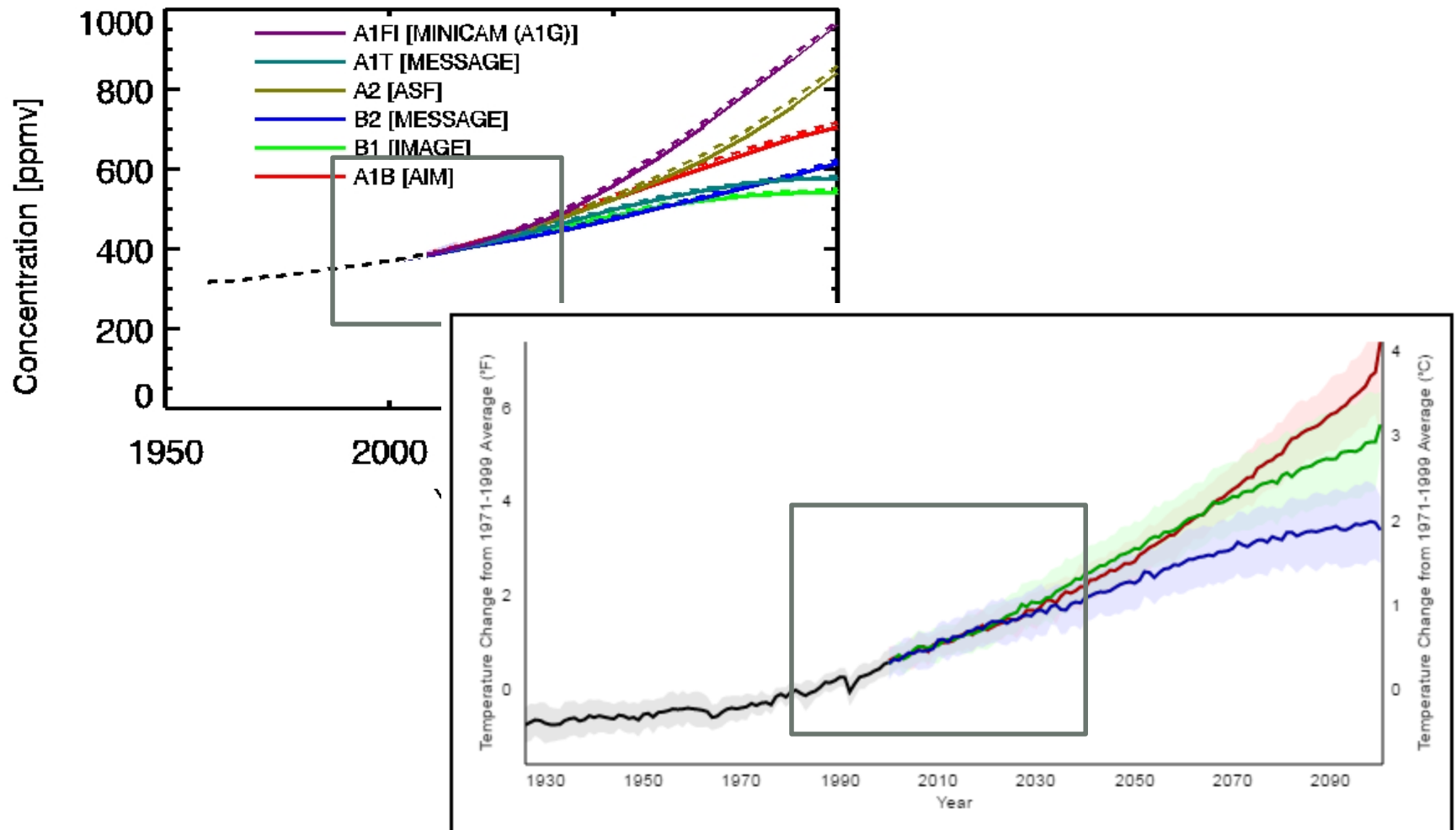
2015 Projections



2016 Revision, two scenarios

# Global

Atmospheric CO<sub>2</sub> IPCC scenarios



# Paths to competitive Chem Phys initiatives

- More clearly defined vision and justification for combustion-related research
- Diversify goals and applications to low-carbon alternatives

# COMBUSTION SYNTHESIS AND PARTICLE FORMATION

## *MAXIMIZING HIGH VALUE PRODUCTS, RATHER THAN MINIMIZING SOOT*

- Combustion synthesis is already practical for many high-value products (carbon black, fumed silica, TiO<sub>2</sub> for photocatalysts, etc.)
- Chemical mechanisms for combustion synthesis could be considerably smaller than chemical mechanisms for complex fuels
- CFD requirements should be considerably simpler than for engines
- First-principles thermochemistry and kinetic data can be generated for all important reactions
- Sensitivity and uncertainty analysis can be used for feedback-optimization of chemical mechanisms

*Predictive mechanisms for combustion synthesis will ultimately allow the optimization and control of the process, and provide a laboratory for the study of particle and aerosol formation in far-from-equilibrium environments.*

Addressing three 2008 Grand Challenges: atom- and energy-efficient synthesis, characterization and control away from equilibrium, and energy and information on the nanoscale.

Addressing three 2015 Transformative Opportunities: hierarchical architectures and beyond equilibrium matter, beyond ideal materials, and advances in modeling, algorithms, etc.

# Grand Challenges in Combustion (Leone):

**Stochastic processes in combustion (ignition, formation of aggregates,...)**

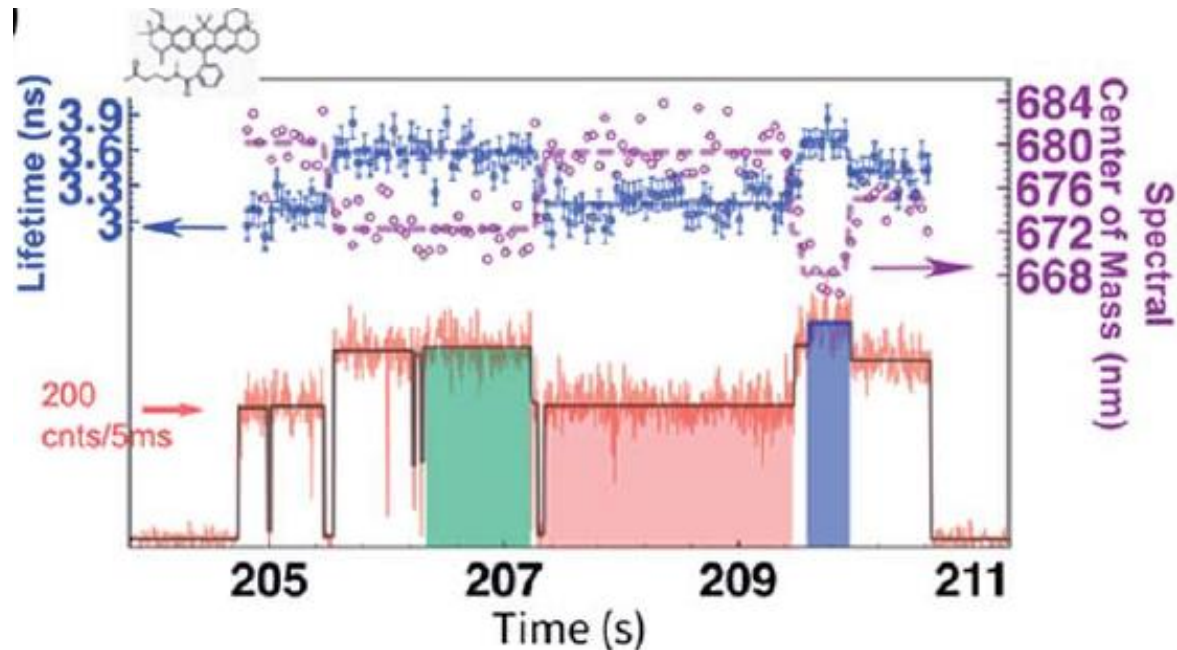
**Heterogeneous processes in combustion (spray combustion, particle formation,...)**

**Fuels reforming for higher efficiency combustion and easier greenhouse gas sequestration (also for fuel cells) – precombustion with steam or oxygen to form CO and H<sub>2</sub>, CO with steam to make more hydrogen and CO<sub>2</sub>, CO<sub>2</sub> removal. Oxyfuel, react fuel with pure oxygen, get CO<sub>2</sub> and water, CO<sub>2</sub> removal. Chemical looping combustion, metal oxide transfers oxygen to fuel, ease of removal removal of CO<sub>2</sub>.**

## Technical Advances:

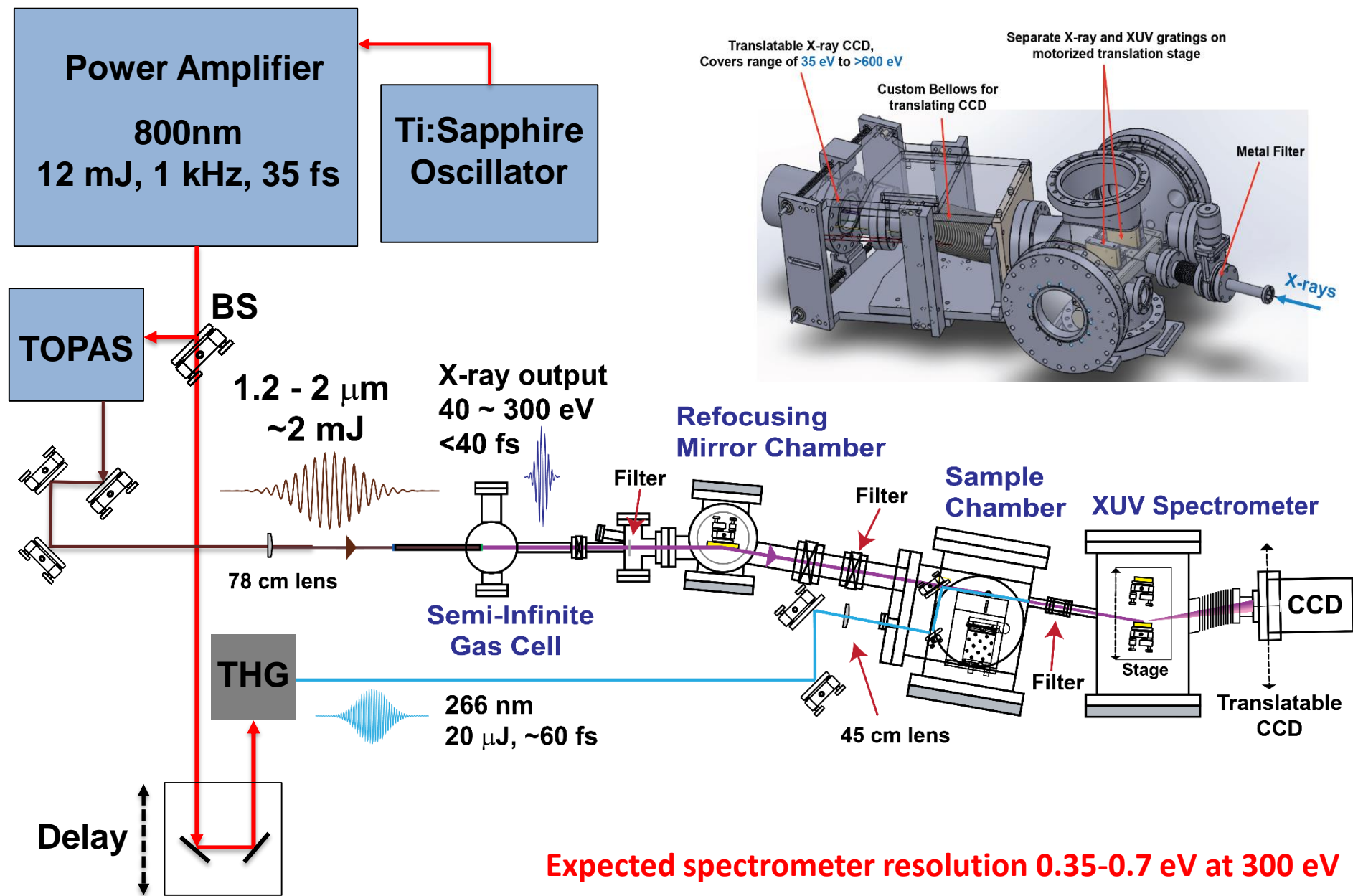
X-ray revolution in gas phase chemical physics (following slides)

How can we apply single molecule spectroscopic and kinetic approaches to combustion environment and dynamics measurements? (transport, product branches, coupled thermal diffusive, etc.)



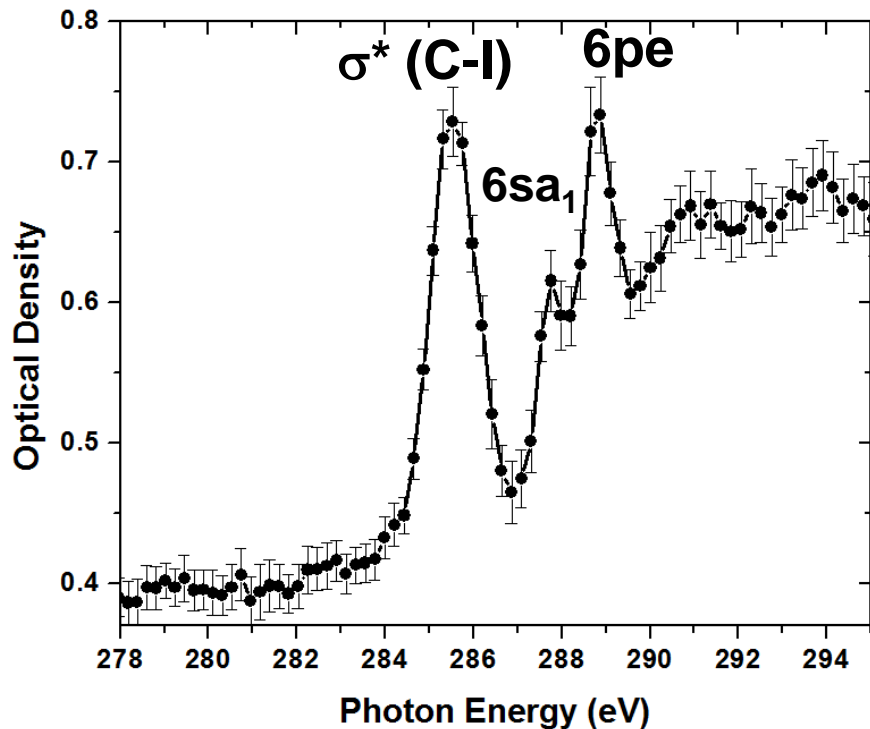
Correlated intensity-lifetime-spectral photodynamics of a single Atto647N fluorophore in solution

# X-ray Layout for Ultrafast Carbon-Edge Spectroscopy

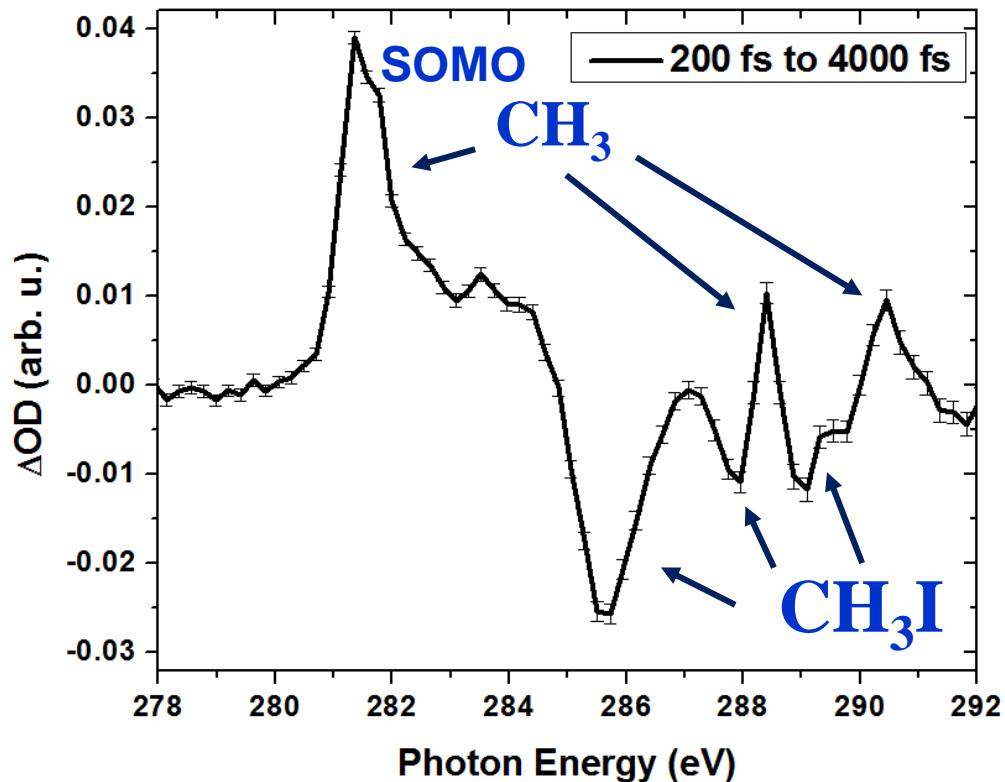


# Photodissociation of Methyl Iodide

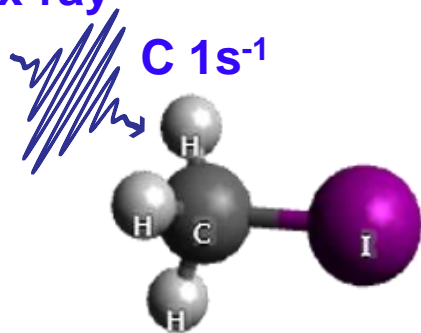
## HHG Static NEXAFS



## HHG Transient Absorption



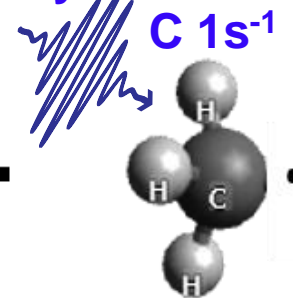
Soft x-ray



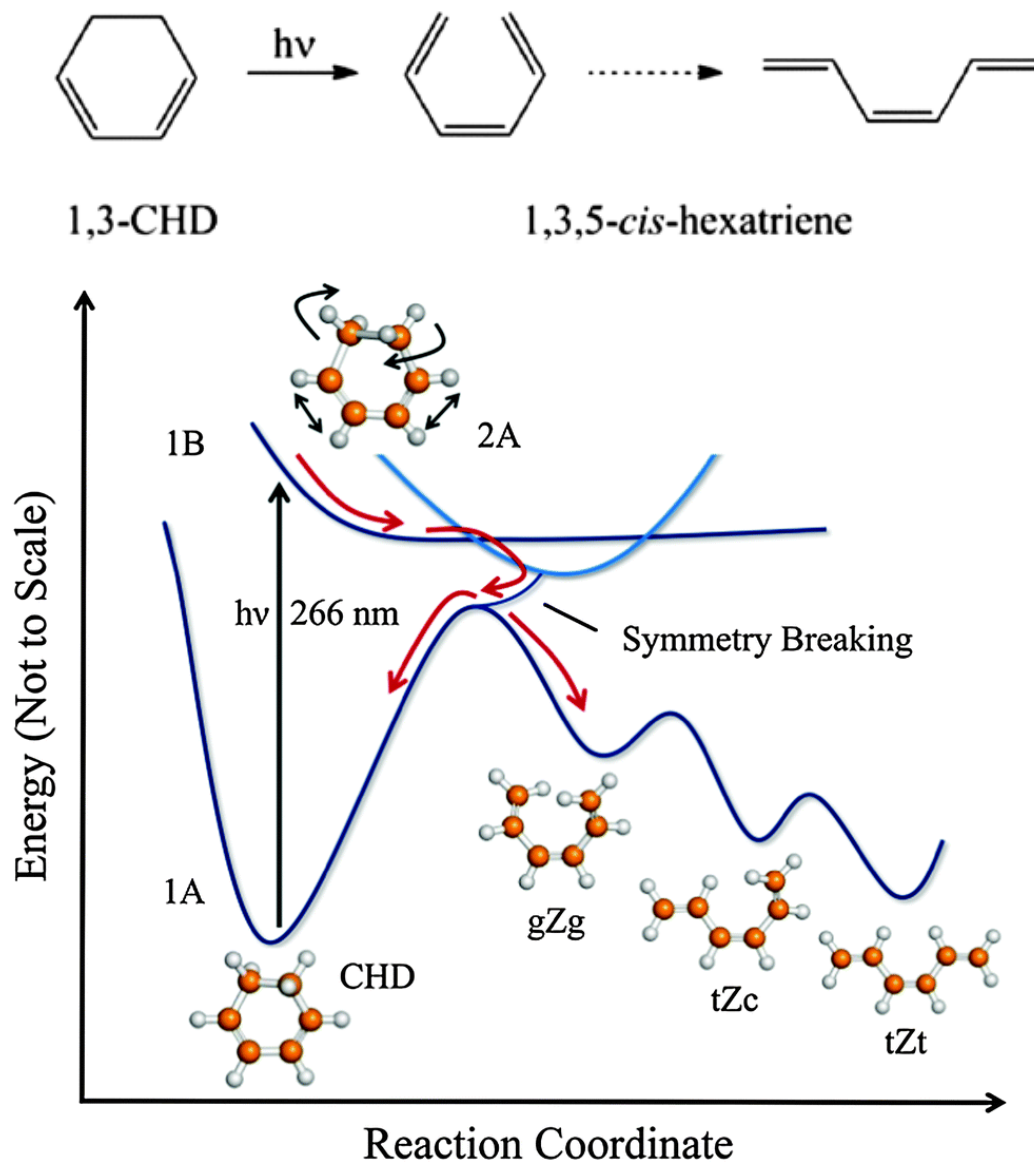
266 nm



+

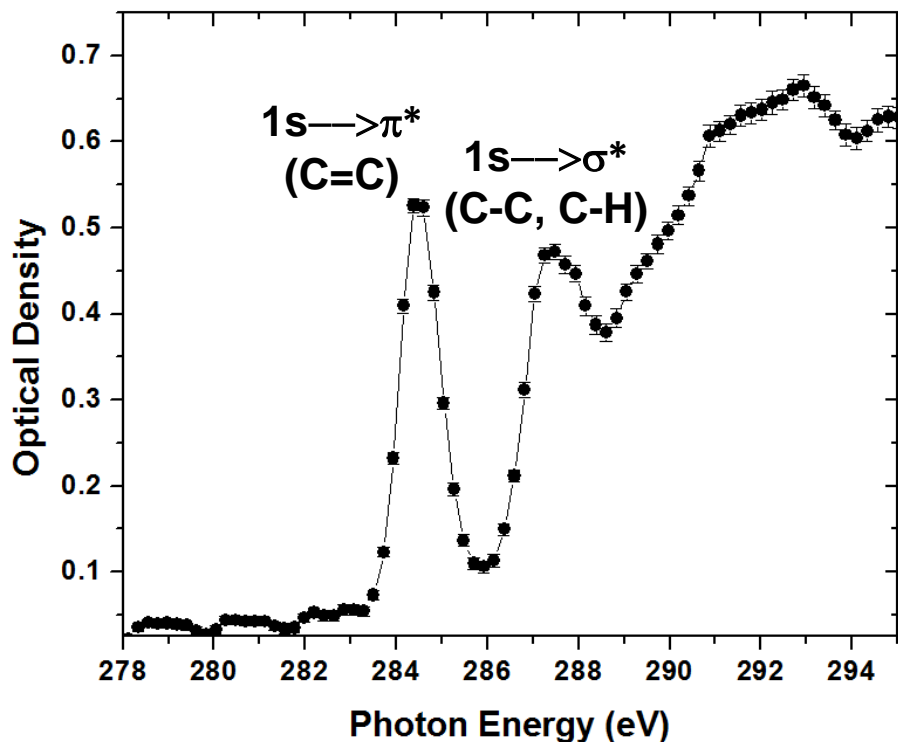


# 1,3-Cyclohexadiene Ring-Opening Reaction



# Ultrafast Photoinduced Ring-Opening of 1,3-Cyclohexadiene

## HHG Static NEXAFS of 1,3-CHD



## HHG Transient Absorption Snapshots

